Information for readers, authors and subscribers

Haematologica (print edition, pISSN 0390-6078, eISSN 1592-8721) publishes peer-reviewed papers on all areas of experimental and clinical hematology. The journal is owned by a non-profit organization, the Ferrata Storti Foundation, and serves the scientific community following the recommendations of the World Association of Medical Editors (www.wame.org) and the International Committee of Medical Journal Editors (www.icmje.org).

Haematologica publishes editorials, research articles, review articles, guideline articles and letters. Manuscripts should be prepared according to our guidelines (www.haematologica.org/information-for-authors), and the Uniform Requirements for Manuscripts Submitted to Biomedical Journals, prepared by the International Committee of Medical Journal Editors (www.icmje.org).

Manuscripts should be submitted online at http://www.haematologica.org/.

Conflict of interests. According to the International Committee of Medical Journal Editors (http://www.icmje.org/#conflicts), "Public trust in the peer review process and the credibility of published articles depend in part on how well conflict of interest is handled during writing, peer review, and editorial decision making". The ad hoc journal's policy is reported in detail online (www.haematologica.org/content/policies).

Transfer of Copyright and Permission to Reproduce Parts of Published Papers. Authors will grant copyright of their articles to the Ferrata Storti Foundation. No formal permission will be required to reproduce parts (tables or illustrations) of published papers, provided the source is quoted appropriately and reproduction has no commercial intent. Reproductions with commercial intent will require written permission and payment of royalties.

Detailed information about subscriptions is available online at www.haematologica.org. Haematologica is an open access journal. Access to the online journal is free. Use of the Haematologica App (available on the App Store and on Google Play) is free.
For subscriptions to the printed issue of the journal, please contact: Haematologica Office, via Giuseppe Belli 4, 27100 Pavia, Italy (phone +39.0382.27129, fax +39.0382.394705, E-mail: info@haematologica.org).

Rates of the International edition for the year 2020 are as following:

	Institutional	Personal
Print edition	*Euro 700*	*Euro 170*

Advertisements. Contact the Advertising Manager, Haematologica Office, via Giuseppe Belli 4, 27100 Pavia, Italy (phone +39.0382.27129, fax +39.0382.394705, e-mail: marketing@haematologica.org).

Disclaimer. Whilst every effort is made by the publishers and the editorial board to see that no inaccurate or misleading data, opinion or statement appears in this journal, they wish to make it clear that the data and opinions appearing in the articles or advertisements herein are the responsibility of the contributor or advisor concerned. Accordingly, the publisher, the editorial board and their respective employees, officers and agents accept no liability whatsoever for the consequences of any inaccurate or misleading data, opinion or statement. Whilst all due care is taken to ensure that drug doses and other quantities are presented accurately, readers are advised that new methods and techniques involving drug usage, and described within this journal, should only be followed in conjunction with the drug manufacturer's own published literature.

Table of Contents
Volume 105, Issue 11: November 2020

Articles

Letters to the Editor

Case Reports

Errata Corrige

The origin of a name that reflects Europe's cultural roots.

Ancient Greek

αἷμα [haima] = blood
αἵματος [haimatos] = of blood
λόγος [logos]= reasoning

Scientific Latin

haematologicus (adjective) = related to blood

Scientific Latin

haematologica (adjective, plural and neuter, used as a noun) = hematological subjects

Modern English

The oldest hematology journal, publishing the newest research results.
2019 JCR impact factor = 7.116

100-year-old Haematologica images: bothriocephalus and pernicious anemia

Carlo L. Balduini

Ferrata-Storti Foundation, Pavia, Italy

E-mail: CARLO L. BALDUINI - carlo.balduini@unipv.it

For over 50 years from the description of the first patients in 1887,[1] pernicious anemia has been one of the most mysterious and feared hematologic diseases. Patients almost always died after a long disease course characterized by a variable and complex clinical profile. A number of different treatment approaches, including drugs such as arsenic preparations, radiotherapy, and even splenectomy, had all proved unsuccessful. It was only in 1926 that a study by Minot and Murphy[2] radically changed the prognosis of this disease. In a study of 45 pernicious anemia patients, Minot and Murphy reported that a diet rich in liver, muscle meat, eggs and milk had been able to cure all 45 of them. This discovery not only changed patients' prognosis, but also paved the way for a long series of research initiatives to define the etiopathogenesis of pernicious anemia which ultimately led (in 1948) to the identification and purification of vitamin B12.[3,4]

But back in 1931, the etiology of pernicious anemia had still not been identified, although it was known that it frequently affected subjects with bothriocephalus infestation. Some authors suggested that there was a cause-and-effect relationship between these two conditions, but the observation that most patients with this infestation do not develop pernicious anemia convinced other clinicians that the association was purely coincidental. Edoardo Storti, then a 22-year old student of Adolfo Ferrata at the Department of Internal Medicine of the University Hospital of Pavia, who was later to become one of the most renowned Editors in Chief of Haematologica, tried to resolve this uncertainty with a very simple approach. He infected three dogs with the bothriocephalus parasite and monitored their clinical and hematologic status. After 4 months, two of the three animals developed severe organic wasting with marked macrocytic anemia. Storti concluded that bothriocephalus was responsible for their severe anemia, thus providing simple but convincing evidence in favor of the hypothesis that this tapeworm can cause pernicious anemia. The cover of this issue of Haematologica comes from one of the color tables that illustrated the paper reporting these results published in the Journal in 1931.[5]

Figure 1. Bone marrow (BM) smear from a dog with an experimental infestation with bothriocephalus. Two of the three animals used in the experiment developed severe macrocytic anemia with an abundance of BM erythroblasts. This beautiful hand-drawn color plate depicts the BM characteristics of one of them.

References

1. Osler W, Gardner W. A case of progressive pernicious anemia (idiopathic of Addison). Canadian Medical and Surgical Journal. 1877;5:385-404.
2. Minot GR, Murphy WP. Treatment of pernicious anemia by a special diet. JAMA. 1926;87:470-476.
3. Lester-Smith E. Purification of the anti-pernicious anaemia factor from liver. Nature. 1948;161:638-639.
4. Rickes EL, Brink NG, Koniusky R, Wood TR, Folkers K. Crystalline vitamin B12. Science. 1948;107:396-397.
5. Storti E. [Anemia sperimentale da Botriocefalo]. Haematologica. 1931;12:237-261.

EDITORIALS

Forward into the second century of Haematologica

Jacob M. Rowe

Department of Hematology, Shaare Zedek Medical Center, Jerusalem, Israel
E-mail: JACOB M. ROWE - rowe@rambam.health.gov.il

It is a privileged, but humbling, experience to assume the role of Editor-in-Chief of the oldest hematology journal in the world. Haematologica was first published a hundred years ago in January 1920, and since the initial foundations laid down by Adolfo Ferrata and Carlo Moreschi there has been a succession of distinguished editors and deputy editors who have taken the Journal through different generations in the advancement of the science and clinical practice of hematology. Since the Journal was first published in English in 1974, a line of distinguished editors have moved the journal through to its current position at the forefront of its field; these include Edoardo Storti, Edoardo Ascari, Mario Cazzola, Robin Foà, Jan Cools and Luca Malcovati. I am particularly grateful to Luca for the high scientific standards he has set in place for the Journal and for personally helping me prepare for my new role during these months of transition. In addition, I could certainly not do this without the guidance of Carlo Balduini, the Chairman of the Board of the Ferrata Storti Foundation who is also the Deputy Editor of the Journal, and who has spent countless hours educating me on both the exalted history of the Journal and its current thrust and focus.

Haematologica will continue to be a leading journal in the field of hematology and will strive to further the excellence of its publications. The Journal's first priority is to publish high quality studies that are novel and that will have a high impact in the international medical community. We will publish in the area of clinical practice and will continue to focus on randomized and non-randomized trials. Observational studies and meta-analyses will be considered, but the priority will always be for prospectively-designed studies that are likely to impact on current practice. In the area of basic research, we will encourage a focus on genomic and other advanced biological research areas that will evolve from the basic science to the translational areas. All articles submitted will undergo rigorous peer review designed to ensure the best papers are selected. As with all leading hematology journals, where a rigorous prioritization is in place, some very good papers cannot be published. In addition to regular articles, the Journal will also publish review articles, editorials and perspectives; these will usually be written on invitation but individual submissions can also be considered. Letters to Haematologica are high quality papers that will undergo the same standard of peer review as other types of submissions. Letters describe a novel or preliminary finding that is of major interest but not mature enough to constitute a regular article.

As I look forward to embarking on this new adventure, I am joined in partnership firstly by Jerald Radich who will be the Deputy Editor and by a very dynamic group of associate editors who will do the bulk of the peer review assignments and assessments. New members of the Editorial Board will be selected and it is hoped they will take an active part in reviewing papers and exploring new areas in which to solicit publications.

Haematologica remains committed to a rapid review procedure and we are determined to further improve this. The new website was introduced in September and is designed to facilitate the submission of articles as well as providing clear guidelines to authors. Readers are invited to experience these new features, and suggestions and observations are always welcome.

Since the recent worldwide onset of COVID-19, no area of our lives has escaped with impunity. The pandemic has affected authors, reviewers and editors alike. This, along with the proliferation of new academic outlets in hematology, both in print and digital, has presented unique challenges. We at Haematologica are committed to face these. Although primarily an on-line journal, print versions are available to libraries and for discerning individuals. The artistic cover pages from the Haematologica Atlas will continue to grace many of the issues.

The mission that I and my colleagues face is a daunting one, but one that we will meet head-on with enthusiasm, albeit with some trepidation. With quiet confidence, together we can meet the challenge.

Jacob M. Rowe
Jerusalem, Israel

Finding erythroid stress progenitors: cell surface markers revealed

Peng Ji

Department of Pathology, Feinberg School of Medicine, Northwestern University, Chicago, IL and Robert H. Lurie Comprehensive Cancer Center, Northwestern University, Chicago, IL, USA

E-mail: PENG JI - peng-ji@fsm.northwestern.edu

The constant production of red blood cells maintains the hematologic homeostasis during steady state in mammals.[1] Under stress conditions, such as bleeding or hemolysis, the increased perfusion pressure enables the switch of steady erythropoiesis to stress erythropoiesis. Research over the past few decades led to our increased understanding of the molecular mechanisms in stress erythropoiesis, especially in murine models.[2] However, finding the stress erythroid progenitor cells for detailed mechanistic investigation remains a demanding task. In this issue of *Haematologica*, Singbrant *et al.*[3] discovered cell surface markers that could aid the identification of these progenitors.

Bone marrow is the major organ that produces red blood cells in adult mammals under steady state. During stress erythropoiesis in mouse models, red cell production switches to the spleen and liver. Accumulating evidence demonstrated that bone morphogenetic protein 4 (BMP4) signaling, along with erythropoietin (Epo), Hedgehog, stem cell factor (SCF), and hypoxia, play critical roles during stress erythropoiesis.[4-8] These signaling pathways ensure a rapid response of the hematopoietic system to produce a large quantity of erythrocytes for tissue hypoxia. The erythroid progenitors responsive for stress erythropoiesis are burst-forming unit-erythroid progenitors (BFU-E) found in murine spleens. Previous reports have shown that these splenic stress BFU-E express immature cell surface marker c-Kit and low levels of erythroid markers CD71 and Ter119.[9] Further efforts were applied to expand the stress BFU-E population *in vitro* using additional markers such as CD34 and CD133.[10] However, this progenitor population is rather heterogenous with a low percentage of cells being stress BFU-E.

To identify and enrich the stress erythroid progenitors, Singbrant *et al.*[3] used an irradiation-induced anemia mouse model to mimic stress erythropoiesis. The authors previously showed that fetal erythroid BFU-E can be identified with high purity as lineage[-]cKit^{+} and CD71/CD24a^{low}Sca1^{-}CD34^{-} in mouse fetal liver.[11] Since adult stress erythropoiesis in murine models closely resembles fetal erythropoiesis, the authors determined whether splenic stress erythroid progenitors could also be enriched using these and additional markers. This approach led to the discovery that stress BFU-E could be further enriched from Lineage[-]cKit^{+}CD71/CD24a^{low} cells as CD150^{+}CD9^{+}Sca1^{-}. More than 20% of these cells produced large BFU-E colonies, which represented over 100-fold improvement of purity compared to previous methods. In addition to the identification of high purity stress BFU-E, multi-potent stress progenitors (stress-MPP) that give rise to stress BFU-E, and stress colony-forming unit-erythroid progenitors (stress-CFU-E) were also identified as CD150^{+}CD9^{+}Sca1^{+} and CD150^{+}CD9^{-}, respectively.

Using an elegant *in vivo* tracing technology with Kusabira orange (KuO) mice, the authors further demonstrated that stress-BFU-E and stress-CFU-E harbor a short-term radio-protective capacity by providing a transient wave of reconstitution in the peripheral blood and spleen. Stress-MPP follow the short-term wave and provide the multi-lineage reconstitution in the peripheral blood, spleen, and bone marrow.

Gene expressing profiling analyses further demonstrated that stress MPP and BFU-E in murine spleen express target genes of BMP, which is consistent with its role in stress erythropoiesis. The authors extended these findings by showing that mice transplanted with BMP receptor II deficient donor bone marrow cells had smaller spleens and a significant reduction in spleen cells. BMP receptor II deficient bone marrow cells also showed significantly decreased potential to form stress BFU-E from lineage[-]cKit[+] progenitors. These studies confirmed the critical role of BMP signaling in stress erythropoiesis in murine models from a genetic approach.

Interestingly, the authors also found CD150^{+}CD9^{+} BFU-E progenitors in steady-state bone marrow but not the spleen, demonstrating that these markers are useful to identify BFU-E progenitors in both steady-state and stress conditions. Previous studies indicated that steady BFU-E migrate from the bone marrow to the spleen during stress erythropoiesis to become stress BFU-E,[12] while more recent findings suggest that endogenous splenic stress BFU-E during stress erythropoiesis are distinctive from steady BFU-E.[7] The CD150^{+}CD9^{+} BFU-E progenitors Singbrant *et al.*[3] discovered in both steady state and stress conditions would be helpful to resolve this contradiction in future studies.

Using RNA sequencing and gene set enrichment analyses, the authors further revealed that steady- and stress-BFU-E exhibited a large overlap in the transcriptome. The differences are mainly in genes associated with BMP and glucocorticoid signaling, proliferation, maturation block, and erythropoiesis that are highly expressed in stress BFU-E in the spleen. The most downregulated genes in stress BFU-E include those associated with myeloid cell development and immune response. While the transcriptional landscapes of steady- and stress-BFU-E are similar, another interesting finding in this study is that there is differential chromatin accessibility in the distal elements in stress erythroid progenitors. Transcriptional regulators CTCF and ERG are significantly enriched in open chromatin regions in stress-BFU-E, indicating their potential roles in regulating stress erythropoiesis.

The findings by Singbrant *et al.*[3] provide the field with an important tool to isolate stress-BFU-E in mice. This allows researchers to investigate stress erythropoiesis in a variety of mouse model systems that mimic disease con-
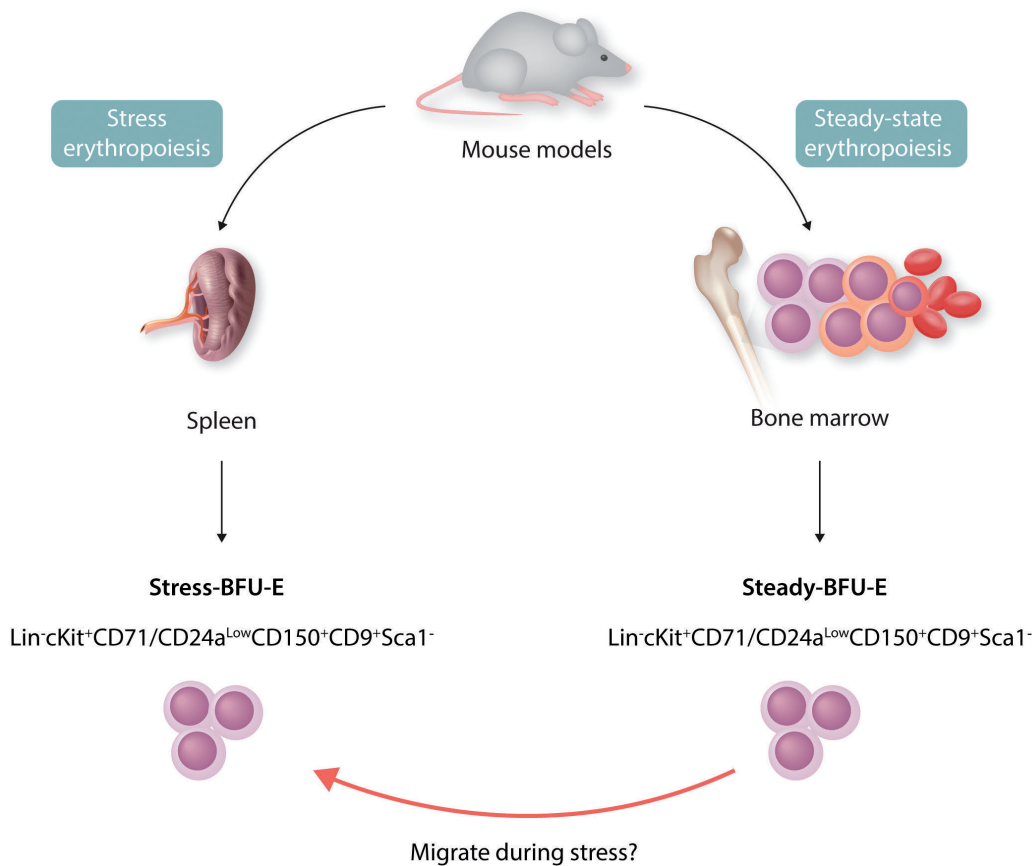
Figure 1. Schematic view of steady-state and stress erythropoiesis in mouse models. Mouse steady-state and stress erythropoiesis occur primarily in the bone marrow and spleen, respectively. Singbrant et al.[3] discovered cell surface markers that are common in steady- and stress-burst-forming unit-erythroid progenitors (BFU-E). It remains to be investigated whether and how steady-BFU-E migrate from the bone marrow to the spleen during stress.

ditions with acute anemia. With the relatively more specific markers to enrich steady- and stress-BFU-E, a detailed mechanistic investigation of erythroid lineage commitment becomes more feasible. In this aspect, Singbrant et al.[3] found that in addition to genes downstream of BMP signaling, genes that are regulated by Cbfa2t3 (also known as Eto2) were also upregulated in stress erythroid progenitors. Cbfa2t3 is a transcriptional co-repressor that maintains the primed state of erythroid progenitors and is known to be involved in stress erythropoiesis.[13,14] Future studies on how Cbfa2t3 regulates stress erythropoiesis and whether the Cbfa2t3 transcriptional corepressor complex cross talks with BMP signaling would be interesting to pursue.

One of the key remaining questions is whether these or similar markers can be used to identify human stress erythroid progenitors. The field of stress erythropoiesis relies heavily on mouse models. Several important differences are present between mouse and human. In mouse, the nature of the hypercellular bone marrow provides limited spaces for the expansion of an erythroid lineage during stress, which forces the spleen to become a major extramedullary erythropoiesis organ. However, this phenomenon is not common in humans.[15] Although studies have shown that BMP signaling is also involved in human stress erythropoiesis in vitro,[10] it is unclear whether the

same is true in vivo. Exploration of markers and signaling pathways in stress erythroid progenitors in human, or other model systems such as rats, would be the necessary next step.

References

1. Hattangadi SM, Wong P, Zhang L, Flygare J, Lodish HF. From stem cell to red cell: regulation of erythropoiesis at multiple levels by multiple proteins, RNAs, and chromatin modifications. Blood. 2011;118(24):6258-6268.
2. Bennett LF, Liao C, Paulson RF. Stress erythropoiesis model systems. Methods Mol Biol. 2018;1698:91-102.
3. Singbrant S, Mattebo A, Sigvardsson M, Strid T, Flygare J. Prospective isolation of radiation induced erythroid stress progenitors reveals unique transcriptomic and epigenetic signatures enabling increased erythroid output. Haematologica. 2020; 105(11):2561-2571.
4. Perry JM, Harandi OF, Paulson RF. BMP4, SCF, and hypoxia cooperatively regulate the expansion of murine stress erythroid progenitors. Blood. 2007;109(10):4494-4502.
5. Lenox LE, Perry JM, Paulson RF. BMP4 and Madh5 regulate the erythroid response to acute anemia. Blood. 2005;105(7):2741-2748.
6. Porayette P, Paulson RF. BMP4/Smad5 dependent stress erythropoiesis is required for the expansion of erythroid progenitors during fetal development. Dev Biol. 2008;317(1):24-35.
7. Paulson RF, Shi L, Wu DC. Stress erythropoiesis: new signals and new stress progenitor cells. Curr Opin Hematol. 2011;18(3):139-145.
8. Perry JM, Harandi OF, Porayette P, Hegde S, Kannan AK, Paulson RF. Maintenance of the BMP4-dependent stress erythropoiesis pathway in the murine spleen requires hedgehog signaling. Blood. 2009;113(4):911-918.
9. Harandi OF, Hedge S, Wu DC, McKeone D, Paulson RF. Murine ery-

throid short-term radioprotection requires a BMP4-dependent, self-renewing population of stress erythroid progenitors. J Clin Invest. 2010;120(12):4507-4519.

10. Xiang J, Wu DC, Chen Y, Paulson RF. In vitro culture of stress erythroid progenitors identifies distinct progenitor populations and analogous human progenitors. Blood. 2015;125(11):1803-1812.

11. Flygare J, Rayon Estrada V, Shin C, Gupta S, Lodish HF. HIF1alpha synergizes with glucocorticoids to promote BFU-E progenitor self-renewal. Blood. 2011;117(12):3435-3444.

12. Hara H, Ogawa M. Erthropoietic precursors in mice with phenylhy-drazine-induced anemia. Am J Hematol. 1976;1(4):453-458.

13. Chyla BJ, Moreno-Miralles I, Steapleton MA, et al. Deletion of Mtg16, a target of t(16;21), alters hematopoietic progenitor cell proliferation and lineage allocation. Mol Cell Biol. 2008;28(20):6234-6247.

14. Stadhouders R, Cico A, Stephen T, et al. Control of developmentally primed erythroid genes by combinatorial co-repressor actions. Nat Commun. 2015;6:8893.

15. Zhang J, Liu Y, Han X, et al. Rats provide a superior model of human stress erythropoiesis. Exp Hematol. 2019;78:21-34 e23.

COVID-19 and sickle cell disease

Laurel A. Menapace and Swee Lay Thein

Sickle Cell Branch, National Heart Lung and Blood Institute, National Institutes of Health, Bethesda, MD, USA

E-mail: SWEE LAY THEIN - sl.thein@nih.gov

The spread of the novel SARS-CoV-2 coronavirus (COVID-19) has resulted in widespread lockdowns and an unprecedented number of deaths globally.[1,2] The pandemic has posed unique challenges to healthcare providers involved in the care of individuals with chronic conditions, balancing maintenance of necessary care with appropriate precautions to reduce their exposure to infection. Patients with sickle cell disease (SCD) present multiple challenges due to the complexity of their condition, disease-related comorbidities, and need for frequent medical interventions. To date, there has been a paucity of published data on how COVID-19 may impact morbidity and mortality in SCD patients.

In this edition of *Haematologica*, Charkravorthy and colleagues report associated outcomes in 10 UK patients infected with SARS-CoV-2.[3] All patients had hemoglobin (Hb) SS disease with pre-existing co-morbidities, despite of this nine patients made a full recovery without receiving COVID-19 directed therapies. Five patients were hospitalized and treated supportively; two patients who had a cough and hypoxia received early preventive simple transfusions; five patients were managed at home *via* close telephone contact. Of the 10 patients, seven were female (median age of 37 years); two received hydroxyurea therapy and seven received regular blood transfusions (four exchange and three simple transfusions). Given that COVID-19 is an acute infectious pneumonia, most experts anticipated that SARS-CoV-2 infection would trigger acute chest syndrome (ACS) yet only one patient who died in this series had significant respiratory complications. The patient who died was a 54-year-old female with severe asthma, alloimmunization, and a history of delayed hemolytic transfusion reactions which prevented routine transfusion. The patient had lymphopenia, thrombocytopenia and elevated C-reactive protein (CRP), which have been identified as poor prognostic markers in COVID-19 patients.[4] The authors acknowledge that the demographic and treatment characteristics of this cohort may have influenced the observed outcomes.

This edition also includes a report of 195 cases of suspected or confirmed SARS-CoV-2 infection as captured by 10 regional centers in a real time survey over a 4-week period in the UK.[5] Patients with SCD represented the majority of cases (n=166, 85.1%) with Hb SS disease as the most common genotype (Hb SS 64.1%; Hb SC 15.4%; other genotypes 5.6%) followed by thalassemia (n=26, 13.3%) and rare inherited anemias (n=3, 1.5%). While the incidence of ACS in the SCD cohort was not specified, red cell exchange was performed in 46 patients during the course of infection. A total of eight SCD patients required mechanical ventilatory support in the setting of respiratory failure; 11 of 13 deaths attributed to COVID-19 occurred in patients with SCD. A subset analysis of 76 hospitalized SCD patients with PCR confirmed SARS-CoV-2 showed that the patient age was significantly associated with mortality, with the most deaths occurring in those aged 50 and older (n=4). The authors noted that three patients aged 20-39 years in the subset succumbed to COVID-19 although details regarding the comorbid medical conditions were not provided. Unexpectedly, mortality was higher in females and was not associated with severity of disease but observed differences were insignificant. The cases reported to date represent 1.2% of the estimated 13,655 individuals with SCD per registry data in England. There was a low incidence of infection in children (n=20) and there were no pediatric deaths. Definitive conclusions regarding COVID-19 mortality rates in SCD cannot be drawn given inherent ascertainment bias and missing data in the survey.

The mild clinical course of COVID-19 in the King's College Hospital SCD patients[3] was similarly encountered in a case series of four patients from Chicago,[6] all of whom presented with acute pain. Of the four patients, three received the usual supportive care but one patient, a 32-year-old male with Hb SS, developed ACS requiring intubation and exchange transfusion.

Two other centers reported COVID-19 pneumonia causing ACS in SCD patients. A 21-year-old male with Hb S/β⁰ thalassemia on hydroxyurea therapy presented with acute chronic left hip pain and subsequently developed a cough with progressive hypoxia and evidence of new pulmonary infiltrates during his hospital course.[7] SARS-CoV-2 PCR testing was positive during the second week of admission. In addition to antibiotic therapy, the patient was initiated
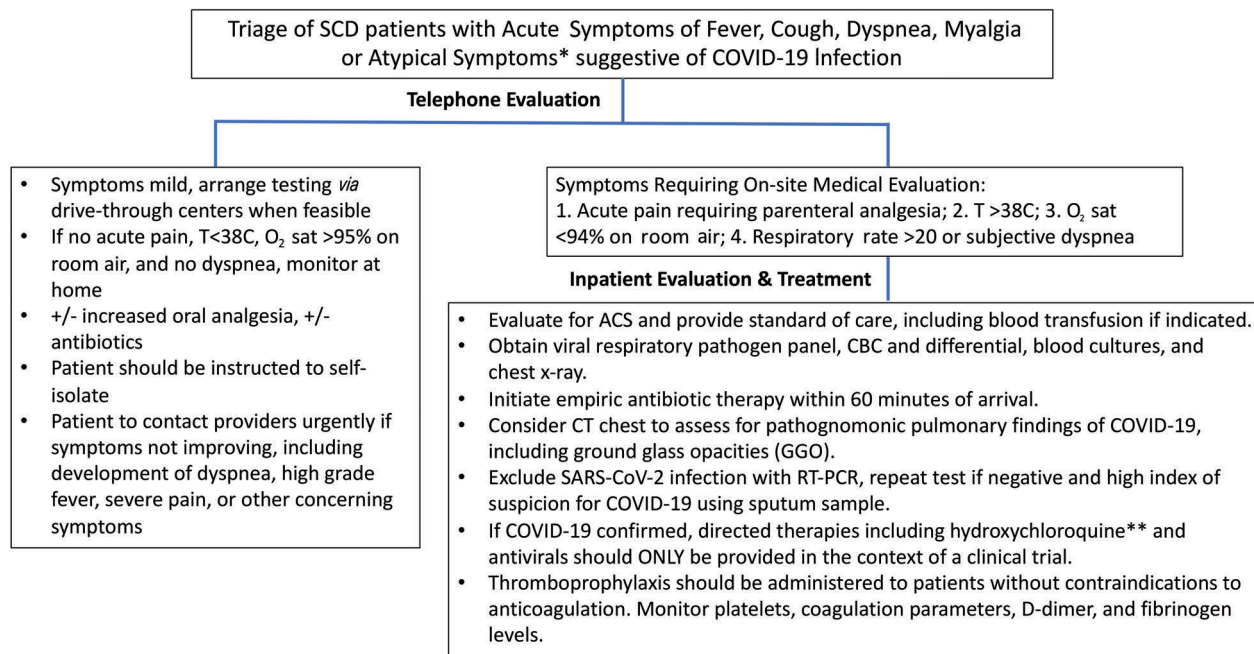
Figure 1. Triage of managing individuals with Sickle cell disease in the COVID-19 pandemic. *Loss of smell (anosmia) and taste (ageusia) and change in taste (dysgeusia) are emerging symptoms. GI symptoms (diarrhea, nausea, vomiting) with or without respiratory symptoms are reported in significant number of COVID-19 patients. **There has been conflicting evidence regarding the utility of antimalarial agents such as hydroxychloroquine[17] and the decision to utilize such therapy should take into account potential adverse effects such as ventricular arrythmias and QT prolongation common pre-existing conditions in SCD patients. Importantly, a large majority of Sickle cell disease (SCD) patients are of African descent and are at risk of drug-induced hemolysis due to concomitant G6PD deficiency. Use of hydroxychloroquine has also been associated with significant methemoglobinemia in case reports.[18] With the current lack of evidence on associated risks and complications, registries to capture global information on COVID-19 SCD cases have been established: https://covidsicklecell.org/http://eurobloodnet.eu/news/99/covid-19-infection-and-red-blood-cell-disorders. The sickle cell community can also obtain guidance on the management of individuals with SCD on the ASH website: https://www.hematology.org/covid-19/covid-19-and-sickle-cell-disease. ACS: acute coronary syndrome; CBC: complete blood count; CT: computed tomography.

on hydroxychloroquine and received exchange transfusion which reduced the Hb S level from 87.1% to 18.1%. He made a full recovery and was discharged after 16 days in the hospital.

The Amsterdam University Medical Centers reported two Hb SS patients who presented with typical acute sickle pain with no accompanying flu-like symptoms.[8] A 24-year-old male presented with acute thoracic pain in the absence of fever or dyspnea; throat and nose swabs were negative for SARS-CoV-2. Computed tomography (CT) imaging revealed bilateral pulmonary infiltrates and the patient received the presumptive diagnosis of a vaso-occlusive crisis (VOC) complicated by ACS. He received antibiotic therapy and was discharged home only to return 24 hours later with increasing pain, dyspnea, and fever. Repeat chest imaging demonstrated progression of infiltrates but radiologic findings were not consistent with COVID-19 pneumonia. A repeat PCR performed on a sputum sample was positive for SARS-CoV-2. The patient received appropriate supportive treatment and had an uneventful recovery. Patient 2, a 20-year-old female presented with an acute pain crisis. She developed transient hypoxia and subsequent SARS-CoV-2 testing was positive. Although CT imaging of the chest did not demonstrate pulmonary abnormalities, she was hospitalized for pain management and never developed respiratory symptoms or fever. We have not been informed if these patients were on hydroxyurea or regular blood transfusion programs.

Although anecdotal, a few important themes emerge from these cases – that COVID-19 might trigger a VOC without the accompanying respiratory manifestations of COVID-19, that ACS is not as common a complication as feared, and that fever was notably absent at presentation in some SCD patients,[6-8] a feature also noted among 5,700 patients admitted with COVID-19 in New York City.[9]

Are patients with SCD at greater risk for serious illness secondary to COVID-19?

Data from non-SCD cohorts have demonstrated that advanced age and the presence of medical co-morbidities including cardiovascular disease, hypertension, diabetes mellitus, and pre-existing lung disease place individuals at higher risk for developing severe complications as a result of COVID-19, including catastrophic acute hypoxic respiratory failure.[9,10] Critically ill patients can develop a cytokine storm, progressive endothelial activation with associated risk of micro- and macrothrombi, and disseminated intravascular coagulation (DIC) resulting in multi-organ failure. Marked elevations in D-dimer and prothrombin with a reduction in fibrinogen levels herald a worse prognosis and heightened risk of death in COVID-19 patients.[11]

Patients with SCD, in particular older adults, often have multiple comorbidities with progressive renal insufficiency, hypertension, and chronic lung disease including pulmonary hypertension.[12] Viral infection can trigger acute vaso-occlusive crises, including ACS which is associated with high mortality rates.[13] In this setting of multi-organ dysfunction, in particular chronic lung damage, COVID-19 could easily trigger ACS and multi-organ failure.

Underlying endothelial dysfunction and abnormal expression of procoagulants such as tissue factor could also place SCD patients at a greater risk of thromboinflammation and thrombotic events if infected with SARS-CoV-2.[14] Data from the US have shown higher rates of symptomatic infection requiring hospitalization and death in patients of African American and Hispanic ethnicity highlighting racial health disparities which impact the SCD community.[15]

Importantly, COVID-19 directed therapies such as anti-malarial agents (hydroxychloroquine or chloroquine) may confer additional risks and must be considered carefully given conflicting data regarding effectiveness.[16,17] One well known adverse effect is methemoglobinemia, particularly in individuals with concomitant G6PD deficiency. Over a 4-week period in a single health system, eight COVID-19 patients who were treated with hydroxychloroquine developed methemoglobinemia which was significant in three patients necessitating treatment with methylene blue.[18] Of note, 1 of the 3 patients who developed acute hemolysis was found to have a new diagnosis of G6PD deficiency. In this respect, hydroxychloroquine treatment presents additional risks in SCD patients in whom concomitant G6PD deficiency is not uncommon; in addition to other adverse cardiac effects including QT prolongation and ventricular arrythmias.

Strategies to optimize management of SCD patients during the COVID-19 pandemic

Hematologists caring for SCD patients have transitioned to telemedicine to reduce unnecessary exposure to SARS-CoV-2 in healthcare settings. Given asymptomatic transmission, healthcare providers should be vigilant in educating patients regarding social isolation practices in their geographic area, hand hygiene, and precautions when in public settings. Patients should be encouraged to be adherent to disease modifying therapies such as hydroxyurea to reduce the frequency of VOC episodes requiring medical attention. Laboratory monitoring for hydroxyurea and iron chelating drugs may need to be done less frequently, and when feasible, medications should be mailed or delivered to the home. Routine visits to the clinic or hospital should be avoided unless phone triage indicates acute symptoms requiring medical evaluation. Some individuals may be able to manage uncomplicated pain crises at home with optimization of oral opioid regimens and close supervision from healthcare providers. Clinical teams should develop dedicated care pathways including phone screening to assess for COVID-19 symptoms prior to a scheduled visit, clinical screening before physical entrance including temperature measurement and symptom assessment, physical distancing in waiting areas, as well as treatment in COVID-19 free clinical areas or isolation rooms. Cross-coverage of providers in the inpatient and outpatient setting should be limited and rotating clinical team schedules are encouraged to reduce the asymptomatic spread of SARS-CoV-2.

Strategies to decrease blood utilization in the setting of blood shortages

In the pandemic setting, there is a risk of severe blood shortages due not only to a decrease in donor participation but a decrease in personnel to collect and process blood. Regular blood transfusion is standard therapy for patients who have suffered an overt stroke as this offers the greatest protection from recurrence of further strokes; such patients should continue to receive transfusions in the presence of adequate blood supply. Patients with abnormal transcranial doppler (TCD) measurements may be eligible for transition to hydroxyurea therapy as per TWiTCH trial criteria for the prevention of a primary stroke.[19,20] In order to preempt the possibility of blood supply interruption, it has been suggested that all children on blood transfusion therapy for primary and secondary stroke prevention should be started on low-dose hydroxyurea (HU) therapy (fixed 10 mg/kg/day).[21] Dose escalation of HU requires frequent laboratory monitoring of peripheral blood counts which may be undesirable in areas with high rates of community spread. DeBaun emphasizes that there can only be advantages in initiating low-dose HU therapy for patients on transfusion programs for stroke prevention – low-dose HU has a minimal risk of myelosuppression, starting low-dose HU will decrease the lag time for clinical benefits if transfusions are suspended, and low-dose HU confers additional clinical benefits, such as reducing the frequency of VOC and ACS. Another approach to conserve blood during the COVID-19 pandemic is to dose-escalate hydroxyurea as this may reduce transfusion needs in SCD patients with a history of stroke.[22] Outside stroke prevention, transfusion hemoglobin thresholds may be relaxed in patients without cardiopulmonary comorbidities in the absence of acute symptoms or organ dysfunction secondary to anemia. Simple blood transfusions may be substituted for exchange regimens and Hb S goals could also be relaxed (e.g., Hb S of 40% instead of 30%).[20] Routine pre-transfusion laboratory work should be performed on the day of a scheduled transfusion to reduce unnecessary exposure to healthcare settings. Advanced planning for patients with extensive alloimmunization is necessary given that matched blood products may be difficult to source; transfusion of the least incompatible blood product with rituximab prophylaxis may be considered in emergency situations due to life-threatening anemia.[23] A triage of managing SCD patients in the COVID-19 pandemic setting is proposed in Figure 1.

Conclusions

Many unknown factors remain when considering the impact of COVID-19 in SCD patients. From published case reports, it is not clear if SCD increases the risk of SARS-CoV-2 infection. What is clear, is that fever is not always a feature, acute pain is a common presentation and COVID-19 can induce ACS but patients can recover fully with adequate supportive care. Importantly, lifesaving measures including mechanical ventilation should not be withheld from patients with SCD in the midst of this pandemic.

References

1. Fauci AS, Lane HC, Redfield RR. Covid-19 - Navigating the uncharted. N Engl J Med. 2020;382(13):1268-1269.
2. Organization WH. Coronavirus disease (COVID-19) situation summary. 2020 [cited; Available from: https://www.who.int/emergencies/diseases/novel-coronavirus-2019/situation-reports].

3. Chakravorthy S. COVID-19 in patients with sickle cell disease – a case series from a UK tertiary hospital. Haematologica. 2020;105(11):2691-2693.
4. Frater JL, Zini G, d'Onofrio G, Rogers HJ. COVID-19 and the clinical hematology laboratory. Int J Lab Hematol. 2020;42(1):11-18.
5. Telfer P. Real-time national survey of COVID-19 in hemoglobinopathy and rare inherited anemia patients. Haematologica. 2020;105(11):2651-2654.
6. Hussain FA, Njoku FU, Saraf SL, Molokie RE, Gordeuk VR, Han J. COVID-19 infection in patients with sickle cell disease. Br J Haematol. 2020;189(5):851-852.
7. Beerkens F, John M, Puliafito B, Corbett V, Edwards C, Tremblay D. COVID-19 pneumonia as a cause of acute chest syndrome in an adult sickle cell patient. Am J Hematol. 2020;95(7):E154-E156.
8. Nur E, Gaartman AE, van Tuijn CFJ, Tang MW, Biemond BJ. Vaso-occlusive crisis and acute chest syndrome in sickle cell disease due to 2019 novel coronavirus disease (COVID-19). Am J Hematol. 2020;95(6):725-726.
9. Richardson S, Hirsch JS, Narasimhan M, et al. Presenting characteristics, comorbidities, and outcomes among 5700 patients hospitalized with COVID-19 in the New York city area. JAMA. 2020;323(20):2052-2059.
10. Zhou F, Yu T, Du R, et al. Clinical course and risk factors for mortality of adult inpatients with COVID-19 in Wuhan, China: a retrospective cohort study. Lancet. 2020;395(10229):1054-1062.
11. Wu C, Chen X, Cai Y, et al. Risk factors associated with acute respiratory distress syndrome and death in patients with Coronavirus disease 2019 pneumonia in Wuhan, China. JAMA Intern Med. 2020;180(7):934-943.
12. Shet AS, Thein SL. A growing population of older adults with sickle cell disease. Clin Geriatr Med. 2019;35(3):349-367.
13. Vichinsky EP, Neumayr LD, Earles AN, et al. Causes and outcomes of the acute chest syndrome in sickle cell disease. National Acute Chest Syndrome Study Group. N Engl J Med. 2000;342(25):1855-1865.
14. Connors JM, Levy JH. Thromboinflammation and the hypercoagula-

bility of COVID-19. J Thromb Haemost. 2020;18(7):1559-1561.
15. (MMWR). CMaMWR. Hospitalization rates and characteristics of patients hospitalized with laboratory-confirmed Coronavirus disease 2019 – COVID-NET, 14 States, March 1-30, 2020. 2020 [cited; Available from: https://www.cdc.gov/mmwr].
16. Mehra MR, Desai SS, Ruschitzka F, Patel AN. Hydroxychloroquine or chloroquine with or without a macrolide for treatment of COVID-19: a multinational registry analysis. Lancet. 2020;S0140-6736(20):31180-31186.
17. Yazdany J, Kim AHJ. Use of Hydroxychloroquine and chloroquine during the COVID-19 pandemic: what every clinician should know. Ann Intern Med. 2020;172(11):754-755.
18. Naymagon L, Berwick S, Kessler A, Lancman G, Gidwani U, Troy K. The emergence of methemoglobinemia amidst the COVID-19 pandemic. Am J Hematol. 2020;95(8):E196-E197.
19. Ware RE, Davis BR, Schultz WH, et al. Hydroxycarbamide versus chronic transfusion for maintenance of transcranial doppler flow velocities in children with sickle cell anaemia-TCD With Transfusions Changing to Hydroxyurea (TWiTCH): a multicentre, open-label, phase 3, non-inferiority trial. Lancet. 2016;387(10019):661-670.
20. America SCDAo. Sickle cell disease and COVID-19: provider advisory. 2020 [cited; Available from: https://www.sicklecelldisease.org/files/sites/181/2020/03/4.10.20-MARAC-SCDAA-PROVIDER-ADVISORY-4-10-2020].
21. DeBaun MR. Initiating adjunct low dose-hydroxyurea therapy for stroke prevention in children with SCA during the COVID-19 pandemic. Blood. 2020;135(22):1997-1999.
22. Nickel RS, Margulies S, Frazer B, Luban NLC, Webb J. Combination dose-escalated hydroxyurea and transfusion: an approach to conserve blood during the COVID-19 pandemic. Blood. 2020;135(25):2320-2322.
23. Chou ST, Alsawas M, Fasano RM, et al. American Society of Hematology 2020 guidelines for sickle cell disease: transfusion support. Blood Adv. 2020;4(2):327-355.

A CD205-directed antibody drug conjugate – lymphoma precision oncology or sophisticated chemotherapy?

Damian T. Rieke[1,2] and **Ulrich Keller**[1,3]

[1]*Department of Hematology, Oncology and Tumor Immunology, Campus Benjamin Franklin, Charité - Universitätsmedizin Berlin, 12203 Berlin;* [2]*Berlin Institute of Health (BIH), 10178 Berlin and* [3]*Max-Delbrück-Center for Molecular Medicine, 13092 Berlin, Germany*

E-mail: *ULRICH KELLER - ulrich.keller@charite.de*

Precision oncology is expected to improve outcome of patients with malignant diseases by taking into account individual variability.[1] This approach is strictly linked to the availability of a targeted treatment the efficacy of which depends on the presence of a molecular alteration, i.e., a predictive biomarker. This concept has been shown to be highly successful in well-defined subgroups of patients and has led to the histology-agnostic approval of drugs in solid tumors.[2] Biomarker-stratified treatment has become first-line treatment in several solid tumors, such as non-small cell lung cancer. In many hematopoietic malignancies, including B-cell lymphomas, comparably higher cure rates and more treatment options have led to a more prognosis-oriented stratification of treatment. Here, prognostic biomarkers help to adjust treatment intensity to a cohort risk assessment.[3] Together with improved prognostication of patients, a more refined diagnosis also helps with better treatment allocation.

Therefore, diagnostic biomarkers will help with the identification of defined disease subgroups.[4] This might also correspond to differential outcome and/or response to treatment, and can therefore overlap with predictive and/or prognostic markers.

However, despite numerous advances in the understanding of cancer heterogeneity, not all diagnostic or prognostic stratifications will ultimately impact treatment and a number of patients will eventually have disease recurrence or progression. Therefore, the identification of novel treatment strategies is urgently required. The development of additional predictive biomarkers and corresponding drugs promises to improve outcome and limit toxicity. This advancement of precision oncology can be achieved in at least two ways: (i) the identification of the right treatment for given patients (as often tried in umbrella or unstratified precision oncology trials);[5] or (ii) the identification of the right patient for a given treatment (as
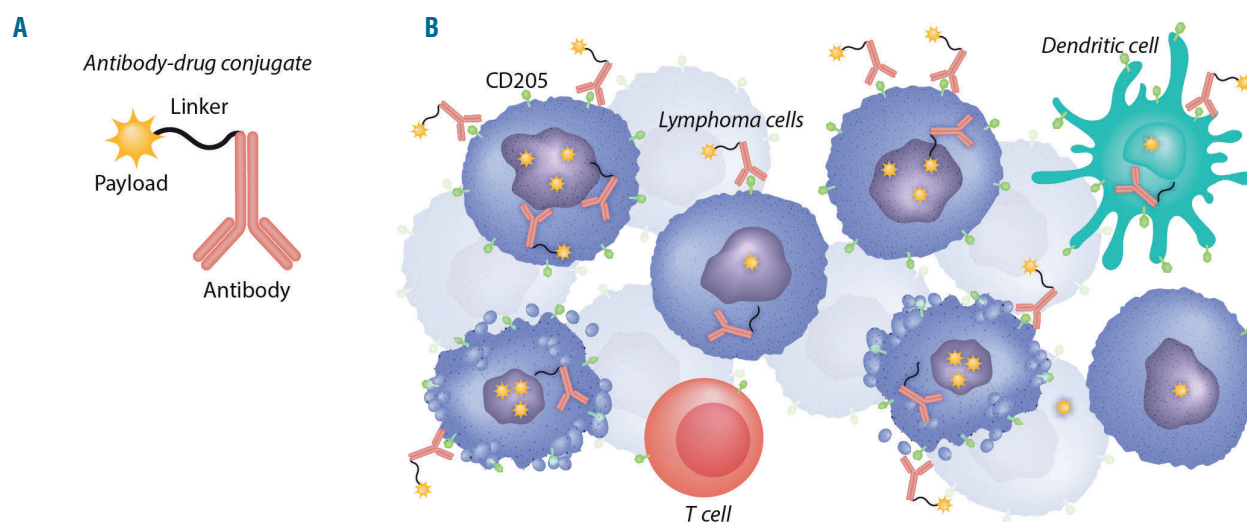
Figure 1. On- and off-target toxicities from antibody-drug conjugates (ADC) within the lymphoma microenvironment. (A) Schematic ADC, consisting of an antibody, a linker and the cytotoxic payload. Endocytosis of the ADC and linker cleavage will release the payload, resulting in cytotoxic effects. (B) On- and off-target cytotoxic effects from payload release with or without ADC internalization in a tumor microenvironment with abundant but heterogeneous expression of the target antigen. Payloads might be cleaved without endocytosis and/or permeate cell membranes to be taken up by bystander cells, thus facilitating drug efficacy even in tumor cells without adequate antigen expression. Toxic effects from microtubule-targeted compounds like maytansine on non-proliferating cells are typically reduced as compared to highly proliferating malignant cells (blue) with activated cell cycle checkpoints.

usually tried in basket trials).[2]

In this issue of *Haematologica*, Gaudio *et al.* show the efficacy of an antibody drug conjugate (ADC) targeting CD205 in lymphoma models.[6] Importantly, the efficacy of this new drug, MEN1309/OBT076, was significantly associated with cell surface expression of the target CD205 in B-cell lymphoma cell lines. Furthermore, cytotoxicity of MEN1309/OBT076 was reduced with the introduction of a competitive CD205 antibody. These findings underline the dependence of drug efficacy on target availability, suggesting the potential of CD205 expression as a predictive biomarker. In an *in vitro* screen, MEN1309/OBT076 efficacy did not depend on B-cell lymphoma subtype. Together with previous preclinical results in CD205-positive triple-negative breast, pancreatic and bladder cancer cell lines and xenografts,[7] this creates a virtual preclinical basket trial which now awaits clinical validation.

However, several questions remain to be answered for the clinical development of MEN1309/OBT076 in lymphoma. In addition to its predictive significance in preclinical models (that, as we have said, still needs to be validated in clinical trials), the biological function of CD205 is surprisingly unclear. Previous reports show that CD205 is expressed on leukocytes, mainly dendritic cells and monocytes[8,9] with a role in endocytosis and the recognition of apoptotic and necrotic cells.[10,11] The role in lymphomagenesis remains even less understood. A fusion protein involving CD205 was identified in Hodgkin lymphoma[12] but also in normal dendritic cell maturation.[10] However, improved characterization of the biological role of this protein remains vital to understanding its implications in the clinic (as a prognostic biomarker in the identification of adequate clinical settings for the introduction of a novel drug) as well as a diagnostic biomarker. If CD205 helps in defining a biologically distinct subgroup within lymphomas, this would be particularly relevant for the identi-

fication of rational combination partners, of which two, venetoclax and rituximab, showed promising signals in the study by Gaudio *et al.*[6] However, the broad expression of the antigen with a moderate to intense CD205 expression in 20-50% of tested lymphoma samples, and an overall expression of the antigen in more than 70% of samples, makes it unlikely that CD205 adequately reflects lymphoma heterogeneity, and stability of CD205 protein expression needs to be validated. Stable expression of the antigen is probably linked to continued efficacy of the drug, following the successful examples of other ADC such as brentuximab vedotin (targeting CD30),[13] polatuzumab vedotin (targeting CD79b),[14] or trastuzumab emtansine (targeting HER2).[15] Efficacy of trastuzumab emtansine could still be demonstrated despite previous HER2-directed therapies and retreatment with brentuximab vedotin showed responses in the majority of patients that had relapsed after initial response to the same drug.[16] In the work by Gaudio *et al.*,[6] a rechallenge with MEN1309/OBT076 was also sufficient to induce remission in the only xenograft model with tumor regrowth after a first dose of the ADC. These and other data support the further development of ADC as powerful tools for the targeted delivery of cytotoxic drugs. Interestingly, neither resistance to CD30-directed ADC or to HER2-directed ADC seems to be mediated by a loss of target antigen expression but rather by dysfunctional intracellular metabolism of the payload.[17,18] Again, the continued expression of CD205 even under therapeutic pressure remains to be determined and is probably linked to its biological role. Expression of the antigen is also important to predict toxicities in human trials. Even though previous work has not identified relevant toxicities in cynomolgus monkeys,[7] potential risks to humans will also depend on disease characteristics and are still to be determined in ongoing clinical trials.

Since CD205 is broadly expressed in lymphoma cells and leukocytes, target antigen expression can be expected in most tumors and/or their microenvironment. Since MEN1309/OBT076 is designed with a cleavable linker, payload release does not necessarily depend on ADC endocytosis, thus facilitating bystander killing and off-target toxicity.[19] In the case of a broadly CD205 expressing tumor microenvironment, an adequate on-tumor efficacy could therefore be expected even without adequate on-target effects and ubiquitous antigen expression on lymphoma cells (Figure 1). In this case, the novel ADC could rather act as a more sophisticated chemotherapy-delivery system and CD205 expression will not allow adequate patient selection. Even in this case, the drug might still prove useful in lymphoma therapy alone or in combination. However, the integration of this novel agent into current treatment schedules might become more difficult.

In conclusion, the work by Gaudio *et al.*[6] shows the activity of the anti-CD205 ADC MEN1309/OBT076 in preclinical CD205-positive lymphoma models that warrants further clinical investigation. The development of a biomarker-drug combination allows for a targeted application of this drug in clinical trials. However, additional preclinical and translational work is required to shed light on the role of CD205 in lymphomagenesis. This is important for the rational development of this treatment as monotherapy, but also, and in particular, as a part of combination therapy. ADC continue to be important components of tumor therapy that could sometimes find a place between precision oncology and refined chemotherapy.

References

1. Collins FS, Varmus H. A new initiative on precision medicine. N Engl J Med. 2015;372(9):793-795.
2. Drilon A, Laetsch TW, Kummar S, et al. Efficacy of larotrectinib in TRK fusion-positive cancers in adults and children. N Engl J Med. 2018;378(8):731-739.
3. Poeschel V, Held G, Ziepert M, et al. Four versus six cycles of CHOP chemotherapy in combination with six applications of rituximab in patients with aggressive B-cell lymphoma with favourable prognosis (FLYER): a randomised, phase 3, non-inferiority trial. Lancet. 2020;394(10216):2271-2281.
4. Sukswai N, Lyapichev K, Khoury JD, Medeiros LJ. Diffuse large B-cell lymphoma variants: an update. Pathology. 2020;52(1):53-67.
5. Lamping M, Benary M, Leyvraz S, et al. Support of a molecular tumour board by an evidence-based decision management system for precision oncology. Eur J Cancer. 2020;127:41-51.
6. Gaudio E, Tarantelli C, Spriano F, et al. Targeting CD205 with the antibody drug conjugate MEN1309/OBT076 is an active new therapeutic strategy in lymphoma models. Haematologica. 2020;105(11):2584-2591.
7. Merlino G, Fiascarelli A, Bigioni M, et al. MEN1309/OBT076, a first-in-class antibody-drug conjugate targeting CD205 in solid tumors. Mol Cancer Ther. 2019;18(9):1533-1543.
8. Kato M, McDonald KJ, Khan S, et al. Expression of human DEC-205 (CD205) multilectin receptor on leukocytes. Int Immunol. 2006;18(6):857-869.
9. Fukaya T, Takagi H, Uto T, Arimura K, Sato K. Analysis of DC functions using CD205-DTR knock-in mice. Methods Mol Biol. 2016;1423:291-308.
10. Butler M, Morel AS, Jordan WJ, et al. Altered expression and endocytic function of CD205 in human dendritic cells, and detection of a CD205-DCL-1 fusion protein upon dendritic cell maturation. Immunology. 2007;120(3):362-371.
11. Cao L, Shi X, Chang H, Zhang Q, He Y. pH-Dependent recognition of apoptotic and necrotic cells by the human dendritic cell receptor DEC205. Proc Natl Acad Sci U S A. 2015;112(23):7237-7242.
12. Kato M, Khan S, Gonzalez N, et al. Hodgkin's lymphoma cell lines express a fusion protein encoded by intergenically spliced mRNA for the multilectin receptor DEC-205 (CD205) and a novel C-type lectin receptor DCL-1. J Biol Chem. 2003;278(36):34035-34041.
13. Younes A, Bartlett NL, Leonard JP, et al. Brentuximab vedotin (SGN-35) for relapsed CD30-positive lymphomas. N Engl J Med. 2010;363(19):1812-1821.
14. Sehn LH, Herrera AF, Flowers CR, et al. Polatuzumab vedotin in relapsed or refractory diffuse large B-cell lymphoma. J Clin Oncol. 2020;38(2):155-165.
15. Burris HA 3rd, Rugo HS, Vukelja SJ, et al. Phase II study of the antibody drug conjugate trastuzumab-DM1 for the treatment of human epidermal growth factor receptor 2 (HER2)-positive breast cancer after prior HER2-directed therapy. J Clin Oncol. 2011;29(4):398-405.
16. Bartlett NL, Chen R, Fanale MA, et al. Retreatment with brentuximab vedotin in patients with CD30-positive hematologic malignancies. J Hematol Oncol. 2014;7:24.
17. Hunter FW, Barker HR, Lipert B, et al. Mechanisms of resistance to trastuzumab emtansine (T-DM1) in HER2-positive breast cancer. Br J Cancer. 2020;122(5):603-612.
18. Nathwani N, Krishnan AY, Huang Q, et al. Persistence of CD30 expression in Hodgkin lymphoma following brentuximab vedotin (SGN-35) treatment failure. Leuk Lymphoma. 2012;53(10):2051-2053.
19. Hoffmann RM, Coumbe BGT, Josephs DH, et al. Antibody structure and engineering considerations for the design and function of antibody drug conjugates (ADCs). Oncoimmunology. 2018;7(3):e1395127.

Splenectomy for immune thrombocytopenia: the evolution and preservation of treatment

Allison Remiker[1] and Cindy Neunert[2]

[1]Division of Pediatric Hematology, Oncology, Neuro-Oncology, and Stem Cell Transplantation, Ann & Robert H. Lurie Children's Hospital of Chicago, Northwestern University Feinberg School of Medicine, Chicago, IL and [2]Division of Pediatric Hematology/Oncology/Stem Cell Transplantation, Columbia University Medical Center, New York, NY, USA

E-mail: CINDY NEUNERT- cn2401@cumc.columbia.edu

The management of immune thrombocytopenia (ITP) has evolved over the course of the past twenty-five years as new treatments have emerged (Figure 1). Despite such advances, splenectomy remains a viable choice. In this edition of *Haematologica*, Avila *et al.* provide long-term outcomes of pediatric patients with ITP who underwent splenectomy. Using data derived from the Splenectomy Registry of the Intercontinental Cooperative ITP Study (ICIS) group, an update of outcomes of patients with primary ITP who underwent splenectomy treatment between 1997 and 2017 was analyzed.[1] Findings from this study provide important and relevant information regarding splenectomy as an effective treatment option for ITP, which in certain contexts may have improved outcomes.

Immune thrombocytopenia was first described even prior to the identification of platelets as a component of blood. Various conditions associated with purpura were described from the 11th to the 17th century.[2,3] However, it was only in 1735 that Paul Gottlieb Werlhof reported the first classical case of ITP[4] in a teenage girl with cutaneous and overt mucosal bleeding symptoms following an infectious disease. This led to the eponym of "Werlhof's Disease", which was previously used to describe ITP.[3] Over time, as microscopy technology progressed, platelets were discovered. Shortly after Bizzozero's discovery of the association between presence and function of platelets in 1881, our understanding of the pathophysiology of thrombocytopenia grew during the late 1880s.[5]

Hypotheses began to emerge regarding the pathophysiology of ITP, with respect to a state of either poor platelet production *versus* a process of peripheral platelet destruction. In the early 1900s, Marino inoculated guinea pigs with rabbit platelets producing antiplatelet antibodies, this simulated ITP in humans suggesting an immune-mediated destructive cause.[6] Years later, in 1916, Paul Kaznelson extrapolated the pathophysiology of immune-mediated hemolytic anemia to ITP and suggested that platelet destruction occurred in the spleen. This led to the first successful splenectomy in a 36-year-old woman with presumed chronic ITP, improving her platelet count from $2x10^9$/L to $500x10^9$/L.[7,8] Finally, in 1950 Dr. Harrington injected himself with blood from a woman with ITP; his platelet count immediately dropped, recovering five days later. This experiment was the first to support the concept of an anti-platelet factor in the blood.[9] Over the course of the following hundred years, knowledge of the pathophysiology of ITP has continued to expand to embrace a comprehensive recognition of the complex interactions in the immune system, in turn leading to a variety of novel treatment modalities.[2,3] Despite these advances, splenectomy has continued to stand the test of

time since it was first performed in 1916, remaining a beneficial option for this condition.

Treatment guidelines for ITP were first established through the British Paediatric Haematology Group in 1992, soon followed by American Society of Hematology (ASH) guidelines in 1996. These initial guidelines outlined expert consensus-based practice standards for the evaluation and treatment of children and adults with ITP.[10,11] Subsequently, revisions of the ASH guidelines were published in 2011, and most recently in late 2019 applying more rigorous evidence-based methodology.[12,13] Recommendations for secondary treatment for primary ITP in the original guidelines were limited to splenectomy. There were minimal data on the use of splenectomy in children, with one study demonstrating a 72% rate of complete remission.[14] Evidence of adverse effects was also insufficient, and non-specific to ITP. Both early guidelines encouraged delaying splenectomy until children had had ITP for at least 12 months and also reserved splenectomy for children with bleeding symptoms. The ASH 1996 guidelines further suggested that patients have a platelet count $<10x10^9$/L (ages 3-12 years), or 10-$30x10^9$/L with bleeding symptoms (ages 8-12 years).[10]

The next significant breakthrough in the treatment for ITP occurred with rituximab. Rituximab, a monoclonal CD20 antibody, was first used for the treatment of B-cell lymphomas in the 1980s. The first report of its use for autoimmune disease was published in 1998, and, in 2001, Stasi *et al.* reported on the first prospective trial of rituximab in adult patients with chronic ITP (n=25).[15,16] It was not until 2006, however, that the first trial was conducted in children.[17] With this new advent of successful non-surgical treatment, the 2011 ASH guidelines suggested the use of rituximab or high-dose dexamethasone as initial treatments for persistent, chronic or refractory children while it was suggested that splenectomy be used after other measures had failed, and again be delayed to at least 12 months of disease with persistence with bleeding symptoms or need for improved quality of life (HRQoL).[12] The most recent advancement in the treatment of ITP has been the development of the thrombopoietin receptor agonists (TPO-RA) following recognition of impaired thrombopoiesis and megakaryocyte apoptosis in ITP patients.[18,19] Both eltrombopag and romiplostim are now approved for children with persistent or chronic ITP who have insufficient response to corticosteroids, immunoglobulins, or splenectomy. The most recent ASH guidelines recommended both the use of TPO-RA and rituximab prior to splenectomy, based only on single arm prospective studies. The pooled evidence demonstrated a 91% response rate to splenectomy after one month, and a 77% durable response, which was
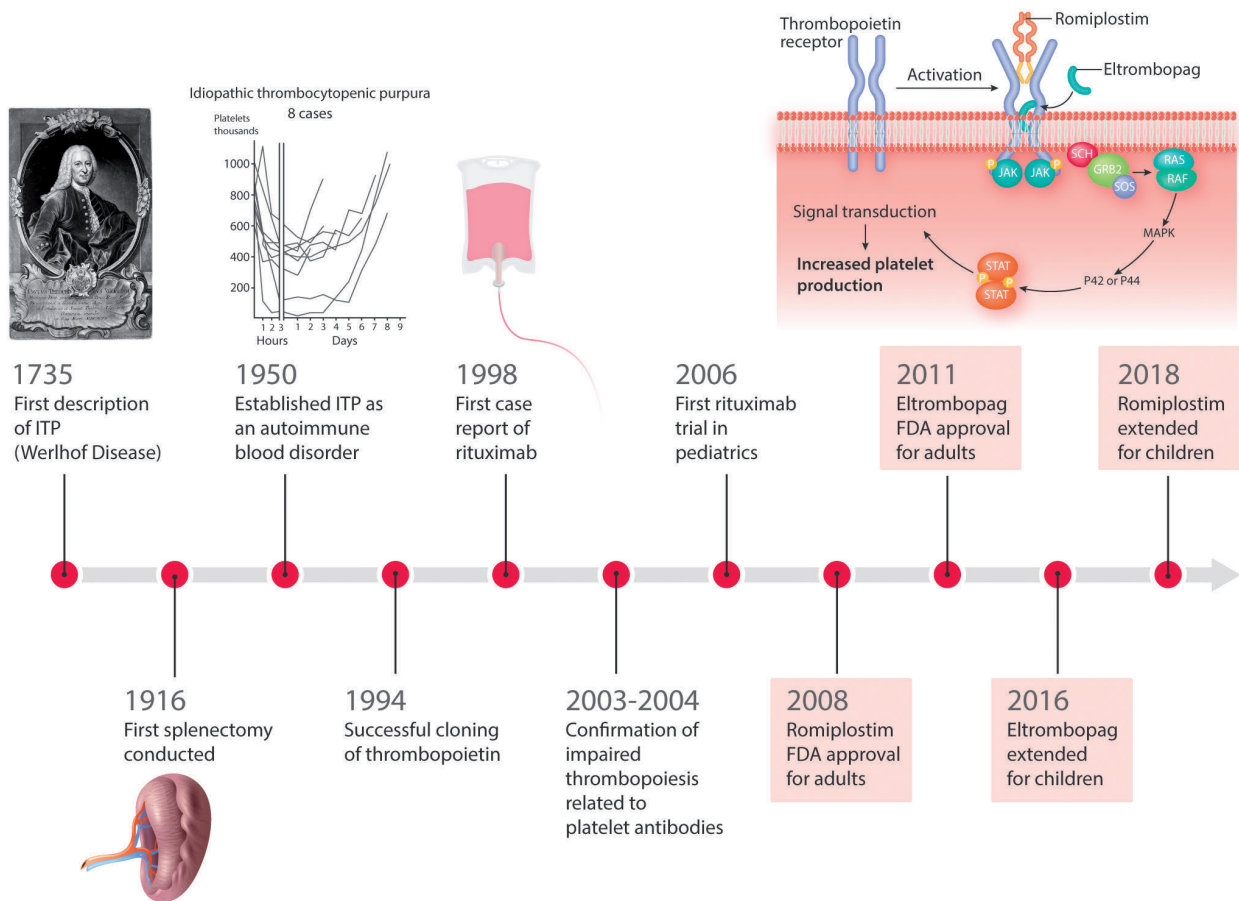
Figure 1. History of discovery and therapies for immune thrombocytopenia (ITP). FDA: US Food and Drug Administration.

superior to both alternative treatments. However, given the moderate undesirable effects associated with splenectomy, including fatal sepsis and lifelong susceptibility to bacterial infection, TPO-RA and rituximab were preferred.[13]

With the decline in the number of splenectomies performed in children with ITP, despite potential data supporting superior efficacy to alternative therapies and guidelines favoring newer more novel therapies, Avila *et al.* used the ICIS Splenectomy Registry to evaluate long-term outcomes in 239 children with ITP.[1] Analysis duration was a median of 25 months and included assessments for response and bleeding events. Interestingly, 26% of patients had splenectomies performed in the acute or persistent phase of diagnosis, which is outside the commonly recommended window per guidelines. Minimal adverse events occurred in the peri-operative window with 5% having intra-abdominal bleeding, 10% with fever, and no deaths or reports of sepsis. Of the patients followed for ≥6 months (n=168), 11% had admissions for fever and 2.7% for sepsis. Response was notable for 93% of patients achieving complete remission (CR: ≥60% of platelet counts ≥1 month post splenectomy ≥100x10^9/L) or remission (R: ≥60% of platelet counts ≥1 month post splenectomy ≥30x10^9/L). Refractoriness was seen in only 1.7% of children; however, this outcome could have been influenced by use of subsequent treatment. Predictors to achieve CR included older age of the

patient at the time of diagnosis, older age of the patient at the time of splenectomy, higher platelet counts in the first month following splenectomy, and a negative correlation with use of prior second-line therapy(ies).

These findings provide robust data in a large cohort of children who have undergone splenectomy for ITP, in particular with regard to the reported findings of an over 90% CR/R rate, with minimal adverse effects in the peri-operative period. Age in terms of a predictor for responsiveness is also a novel finding for children. As suggested by the authors, this is perhaps related to the pathophysiology of the disease in teenagers being similar to young adults, who also have improved responsiveness to splenectomy. Although the evidence provided in this study represent novel data in support of consideration of splenectomy as opposed to other forms of second-line therapy, a number of questions remain unanswered. The reason behind the selection of splenectomy and clinical decision-making was not collected, in particular regarding the indication of treatment, e.g., treatment due to bleeding symptoms, disease chronicity, or other HRQoL metrics. Splenectomy also remains the treatment of choice for emergent management of life-threatening bleeding which may be represented by a handful of cases who underwent splenectomy early in the course of their ITP in this cohort. Furthermore, the availability of alternative treatments was variable over the course of cohort enrollment (1997-2017), which possibly influenced selection of

splenectomy as treatment. The disease phase was also not defined in relation to outcomes. Additional limitations include potential selection bias related to the affiliation with the registry. In addition, the follow-up of the patients was limited to 25 months due to patient retention. It would be important to understand more long-term outcomes (i.e., decades) regarding relapse of disease in adulthood, as well as infectious risk. It may never be possible to conduct randomized trials; however, longitudinal tracking of patients requiring second-line therapy provides the opportunity for indirect comparison. Application of patient-related outcomes in prospective trials may also help to capture factors that matter to patients besides platelet count and help in decision-making.

Despite the unanswered questions and known limitations associated with a registry, the work by Avila *et al.* provides insight into the long-term outcomes associated with splenectomy in children with ITP. The authors are to be commended for the long-term follow-up and collection of data on a rare group of patients. These data give rise to an important consideration of the safe use of splenectomy to achieve remission in the majority of patients who have undergone this procedure, in spite of the decreasing numbers of patients over time in favor of therapies with presumably fewer life-long side-effects.

References

1. Aliva ML, Amiri N, Pullenayegum E, Blanchette V, Imbach P, Kühne T Long-term outcomes after splenectomy in children with immune thrombocytopenia: an update on the registry data from the Intercontinental Cooperative ITP Study Group. Haematologica. 2020;105(11): 2682-2685.
2. Freedman J, Blanchette M. Idiopathic thrombocytopenia purpura (ITP): a historical odyssey. Acta Paediatr Suppler. 1998;424:3-6.
3. Stasi R, Newland AC. ITP: a historical perspective. Br J Haematol. 2011;153(4):437-450.
4. Werlhof PG. Opera Omnia. Hanover: Helwing, 1775: 748. In: RH Major, ed. Classic descriptions of disease. 3rd ed. Springfield, IL: CC Thomas, 1965.
5. Bizzozero G. [Über einer neuen formbestandtheil der blutes und desser role bei der thrombose und der glutgerinnung]. Virchow Arch Pathol Anat Physiol. 1881;90:261-332.
6. Marino F. [Recherches sur les plaquettes du sang. Comptes Rendus des Seances de la Societe de Biologie et de Ses Filiales]. 1905;58:194-196.
7. Kaznelson P. [Verschwinden der hämorrhagischen diathese dei einem fall von "essentieller thrombopenie" (Frank) nach milzexstirpation: splenogene thrombolytische purpura]. Wiener Klinische Wochenschrift. 1916;29:1451-1454.
8. Kaznelson P. [Thrombolytische purpura]. Zeitschrift fur Klinische Medizin. 1919;87:133-164.
9. Harrington WJ, Minnich V, Hollingsworth JW, et al. Demonstration of a thrombocytopenic factor in the blood of patients with thrombocytopenic purpura. J Lab Clin Med. 1951;38(1):1-10.
10. George JN, Woolf SH, Raskob GE, et al. Idiopathic thrombocytopenic purpura: a practice guideline developed by explicit methods for The American Society of Hematology. Blood. 1996;88(1):3-40.
11. Eden OB, Lilleyman JS. Guidelines for management of idiopathic thrombocytopenic purpura. The British Paediatric Haematology Group. Arch Dis Child. 1992;67(8):1056-1058.
12. Neunert C, Lim W, Crowther M, et al. The American Society of Hematology 2011 evidence-based practice guideline for immune thrombocytopenia. Blood. 2011;117(16):4190-4207.
13. Neunert C, Terrell DR, Arnold DM, et al. American Society of Hematology 2019 guidelines for immune thrombocytopenia. Blood Adv. 2019;3(23):3829-3866.
14. Reid MM. Chronic idiopathic thrombocytopenia purpura: incidence, treatment, and outcome. Arch Dis Child. 1995;72(2):125-128.
15. Lee EJ, Kueck B. Rituxan in treatment of cold agglutinin disease. Blood. 1998;92(9):3490-3491.
16. Stasi R, Pagano A, Stipa E, et al. Rituximab chimeric anti-CD20 monoclonal antibody treatment for adults with chronic idiopathic thrombocytopenic purpura. Blood. 2001;98(4):952-957.
17. Bennett C, Rogers ZR, Kinnamon DD, et al. Prospective phase 1/2 study of rituximab in childhood and adolescent chronic immune thrombocytopenic purpura. Blood. 2006;107(7):2639-2642.
18. Neunert CE, Rose MJ. Romiplostim for the management of pediatric immune thrombocytopenia: drug development and current practice. Blood Adv. 2019;3(12):1907-1915.
19. Kim TO, Despotovic J, Lambert MP. Eltrombopag for use in children with immune thrombocytopenia. Blood Adv. 2018;2(4):454-461.

Transforming the major autoantibody site on ADAMTS13: spacer domain variants retaining von Willebrand factor cleavage activity

Marie Scully

Department of Haematology and National Institute for Health Research Cardiometabolic Programme, UCLH/UCL BRC, London, UK
E-mail: MARIE SCULLY - m.scully@ucl.ac.uk

Immune thrombotic thrombocytopenic purpura (iTTP) is an acute, rare life-threatening condition associated with antibodies to ADAMTS13, resulting in severe enzyme deficiency, failure of von Willebrand factor (VWF) cleavage, excess platelet-VWF binding and microthrombi formation, resulting in multi-organ damage. iTTP is an immune-mediated condition and antibodies to ADAMTS13 are polyclonal.[1,2] Despite this, and as replicated by a number of groups, nearly 100% of patients demonstrate a specific target region of antibody binding to the spacer domain in the N terminal region of the metalloprotease, ADAMTS13.[3-7] Antibodies can be detected in other ADAMTS 13 domains, typically the TSP 2-8 regions or CUB domains, but to a lesser degree than spacer domain antibodies. Furthermore, spacer antibodies are more likely to inhibit ADAMT13 enzyme activity, as opposed to antibodies in the C terminal region of ADAMTS13, which result in increased ADAMTS13 clearance.[8]

It has been suggested that a possible therapeutic strategy for iTTP would be an ADAMTS13 variant that would prevent antibody binding within the pathogenic region of the spacer domain. As iTTP is a polyclonal antibody response, more than one epitope may need to be considered.

In the current issue of *Haematologica*, Graça and colleagues present a detailed description of the influence of the epitope (R568/F592/R660/Y661/Y665 [RFRYY]),[9] within the spacer domain, the predominant site for autoantibody binding. The capacity for ADAMTS13 to cleave VWF with full-length mutants was reduced in varying amounts. The impact of the variants on autoantibody binding was assessed and compared to that of wild-type ADAMTS13. The comprehensive narrative concludes that non-conservative and alanine modifications of residues RFRYY, within exosite 3 of the spacer domain, were superior in preventing autoantibody binding. Importantly, selected ADAMTS13 variants maintained VWF cleavage mediated by the metalloprotease.

The spacer domain, comprising 130 amino acids, is between a cysteine-rich region and the TSP-2 repeat domain. The region is important and has two major effects. First, the binding to VWF, which is critical in ADAMTS13-mediated cleavage. The importance of spacer domain-mediated cleavage is verified by the resulting proteolytic activity involving the MDTCS compared to MDTC variants. Second, exosite 3, within the spacer domain, contains a cluster of hydrophobic residues. This specific exosite is critical in binding to the A2 region of VWF, but it is also the major epitope for ADAMTS13 autoantibodies.

Residues making up exosite 3 in the spacer domain of ADAMTS13 include Arg660, Tyr661, Tyr665,[7] Arg568 and Phe592.[10] Conservative substitution variants involve replacement of an amino acid within these residues but achieving comparable biochemical properties. A further effect of manipulation of this region is a gain-of-function ADAMTS13 variant. The effect of the gain-of-function variant, previously described, is resistance to ADAMTS13 autoantibodies and increased ADAMTS13 activity.[11] Other variants have been developed, such as alanine modifications, which resulted in reduced ADAMTS13 autoantibody binding but also diminished ADAMTS13 cleavage of VWF.

In their study published in this issue of *Haematologica*, Graça and colleagues generated 42 ADAMTS13 variants, introduced into a full-length ADAMTS13 spacer exosite 3 region. The variants included the gain-of-function fragment, truncated wild-type MDTCS and MDTSC 5x Ala variants as well as conservative, semi-conservative and non-conservative substitutions with asparagine and alanine amino acids. Initially, samples from patients were examined for autoantibody binding against these developed variants, which were compared to wild-type ADAMTS13. Concurrently, each variant was analyzed for its ability to cleave VWF.

Results re-confirmed the predominant binding of ADAMTS13 autoantibodies to the exosite 3 region of the spacer, but antibody binding to the CUB and TSP 2-8 domains was also detected. The ability of the selection of variant ADAMTS13 to resist ADAMTS13 antibody was explored.

The conservative mutants had comparable autoantibody binding, but semi-conservative variants had reduced antibody binding compared to the wild-type spacer domain of ADAMTS13. Variants containing alanine and, to a lesser extent, asparagine were the most successful at preventing ADAMTS13 antibody binding. The gain-of-function mutation only achieved a small reduction in autoantibody binding. However, the 5x Ala full-length mutant (AAAAA) had the best effect in preventing autoantibody binding. Therefore, replacing the spacer epitope with asparagine or alanine amino acids had the greatest influence in averting ADAMTS13 antibodies from binding. The variants were compared to wild-type ADAMTS 13, assessing their ability to cleave VWF. In all the cases, cleavage of VWF was reduced in comparison to the wild-type protein. However, the greatest cleavage was noted in those with conservative and some of the semi-conservative mutants. Single alanine and asparagine changes were associated with the highest ADAMTS13 cleavage activity (Figure 1). VWF cleavage was further confirmed using recombinant VWF in multimeric gels. In general, mutations associated with the lowest ADAMTS13 cleavage activity demonstrated greater antibody resistance.
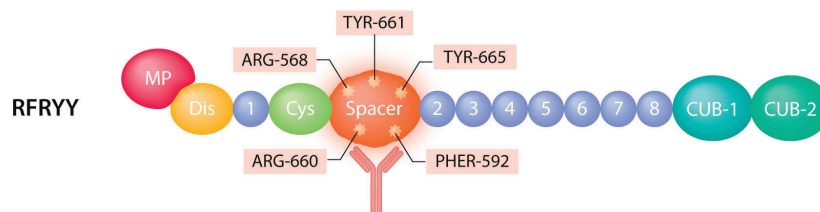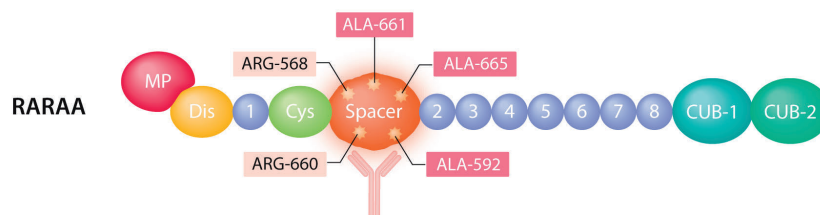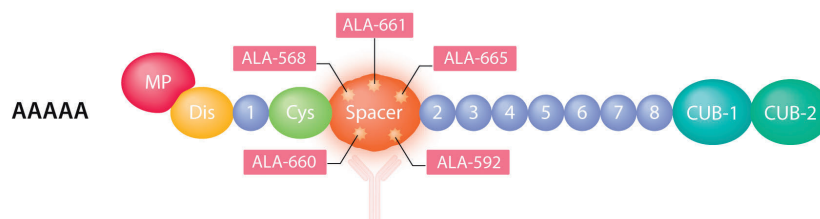
Figure 1. Effect of variants in the exosite 3 region of the spacer domain of ADAMTS13 and their impact on ADAMTS13 autoantibody binding and von Willebrand factor cleavage. The effect of wild-type (WT) ADAMTS13, with 100% ADAMTS13 autoantibody binding involving the amino acid configuration RFRRY, compared to the most productive variants (RARAA and AAAAA), which can reduce ADAMTS13 autoantibody binding but still retain von Willebrand factor (VWF) cleavage activity.

The three aromatic residues rather than the two arginine residues of exosite 3 in the spacer domain appear to have greater importance in ADAMTS 13 antibody binding. The greatest influence was noted with cumulative mutations of the aromatic residues, demonstrating the maximum effect in preventing ADAMTS13 autoantibody binding, which is achieved by re-presenting epitope loops, lowering the surface charge and reducing surface size.[9]

Current therapy for TTP aims to replace ADAMTS13, *via* plasma exchange and immunosuppression to remove autoantibodies to ADAMTS13. The main therapeutic modalities used are steroids and rituximab. Their role in reducing IgG antibody levels has been well described in both the treatment of acute TTP[12] and as prophylaxis,[13,14] usually resulting in normalization of ADAMTS13 activity. The importance of the work by Graca *et al*. is the detailed demonstration and confirmation that development of ADAMTS13 variants could be used to overcome the antibody response in iTTP, preventing autoantibodies to ADAMTS13 from binding to exosite 3 of the spacer domain but ensuring residual ADAMTS13 cleavage activity. There may be a role for these variants in future care of patients, conquering the immunological consequence of ADAMTS13 antibodies.

References

1. Furlan M, Lammle B. Aetiology and pathogenesis of thrombotic thrombocytopenic purpura and haemolytic uraemic syndrome: the role of von Willebrand factor-cleaving protease. Best Pract Res Clin Haematol. 2001;14(2):437-454.
2. Tsai HM, Lian EC. Antibodies to von Willebrand factor-cleaving protease in acute thrombotic thrombocytopenic purpura. N Engl J Med. 1998;339(22):1585-1594.
3. Klaus C, Plaimauer B, Studt JD, et al. Epitope mapping of ADAMTS13 autoantibodies in acquired thrombotic thrombocytopenic purpura. Blood. 2004;103(12):4514-4519.
4. Luken BM, Kaijen PH, Turenhout EA, et al. Multiple B-cell clones producing antibodies directed to the spacer and disintegrin/thrombospondin type-1 repeat 1 (TSP1) of ADAMTS13 in a patient with acquired thrombotic thrombocytopenic purpura. J Thromb Haemost. 2006;4(11):2355-2364.
5. Zheng XL, Wu HM, Shang D, et al. Multiple domains of ADAMTS13 are targeted by autoantibodies against ADAMTS13 in patients with acquired idiopathic thrombotic thrombocytopenic purpura. Haematologica. 2010;95(9):1555-1562.
6. Yamaguchi Y, Moriki T, Igari A, et al. Epitope analysis of autoantibodies to ADAMTS13 in patients with acquired thrombotic thrombocytopenic purpura. Thromb Res. 2011;128(2):169-173.
7. Pos W, Crawley JT, Fijnheer R, Voorberg J, Lane DA, Luken BM. An autoantibody epitope comprising residues R660, Y661, and Y665 in the ADAMTS13 spacer domain identifies a binding site for the A2 domain of VWF. Blood. 2010;115(8):1640-1649.
8. Thomas MR, de Groot R, Scully MA, Crawley JT. Pathogenicity of anti-ADAMTS13 autoantibodies in acquired thrombotic thrombocytopenic purpura. EBioMedicine. 2015;2(8):940-950.
9. Graça NGA, Ercig B, Velásquez Pereira LC, et al. Modifying ADAMTS13 to modulate binding of pathogenic autoantibodies of patients with acquired thrombotic thrombocytopenic purpura. Haematologica. 2020;105(11):2619-2630.

10. Pos W, Sorvillo N, Fijnheer R, et al. Residues Arg568 and Phe592 contribute to an antigenic surface for anti-ADAMTS13 antibodies in the spacer domain. Haematologica. 2011;96(11):1670-1677.
11. Jian C, Xiao J, Gong L, et al. Gain-of-function ADAMTS13 variants that are resistant to autoantibodies against ADAMTS13 in patients with acquired thrombotic thrombocytopenic purpura. Blood. 2012;119(16):3836-3843.
12. Scully M, McDonald V, Cavenagh J, et al. A phase 2 study of the safety and efficacy of rituximab with plasma exchange in acute acquired thrombotic thrombocytopenic purpura. Blood. 2011;118 (7):1746-1753.
13. Hie M, Gay J, Galicier L, et al. Preemptive rituximab infusions after remission efficiently prevent relapses in acquired thrombotic thrombocytopenic purpura. Blood. 2014;124(2):204-210.
14. Westwood JP, Thomas M, Alwan F, et al. Rituximab prophylaxis to prevent thrombotic thrombocytopenic purpura relapse: outcome and evaluation of dosing regimens. Blood Adv. 2017;1(15):1159-1166.

A new drug for an old concept: aptamer to von Willebrand factor for prevention of arterial and microvascular thrombosis

Agnès Veyradier[1,2]

[1]Hematology department, French National Reference Centre for Thrombotic Microangiopathies and von Willebrand disease, Hospital Lariboisière, AP-HP.Nord and [2]EA3518 Saint-Louis Research Institute, Paris University, Paris, France.

E-mail: AGNÈS VEYRADIER - agnes.veyradier@aphp.fr

Von Willebrand factor (VWF) is a large and complex multimeric glycoprotein essential for initiation of hemostasis after vascular injury. VWF is the mediator of platelet adhesion to the subendothelial collagen matrix and of platelet aggregation, especially at high shear rates of blood flow present in the microcirculation and stenotic arteries.[1] Platelet adhesion involves specific sequences of the A1 domain of VWF (VWF-A1) and the platelet receptor glycoprotein Ib (GPIb).[1] The adhesive properties of VWF are proportional to both the size of its multimers and their shear-induced unfolding, which respectively determine the number of available VWF-A1 and their swift from a cryptic to an exposed status able to bind platelet GPIb.[2] Physiologically, in order to prevent the spontaneous binding of VWF to platelets, VWF multimeric distribution is regulated by a specific-cleaving protease, ADAMTS13 (a disintegrin and metalloproteinase with thrombospondin type 1 repeats, member 13).[3] A defect in VWF (related to genetic mutations of *VWF*) causes a bleeding disorder named von Willebrand disease (VWD) while an excess of ultralarge multimers of VWF (UL VWF) (due to a severe deficiency in ADAMTS13 mostly mediated by specific auto-antibodies) causes a thrombotic microangiopathy called thrombotic thrombocytopenic purpura (TTP).[4] In addition, the interaction of VWF-A1 with platelet GPIb also contributes to arterial thrombosis present in atherosclerotic cardiovascular disease (ACD).[5] Consequently, inhibiting the binding of VWF to GPIb by specifically targeting VWF-A1, is a rational approach to decrease both arterial and microvascular thrombosis by preventing the formation of further VWF- and platelet-rich thrombi[2] in both acute ACD[5] and acute TTP[3], respectively.

In the 1990-2000s, two classes of anti-VWF-A1 therapeutic agents were developed for this purpose. On one hand, a humanized single-variable domain immunoglobulin (Nanobody®)[6,7] has recently been approved and commercialized as caplacizumab (Cablivi ™) by Ablynx, a Sanofi company (Sanofi-Aventis, Paris, France) for the treatment of acute acquired TTP in adults, on the basis of positive results in phase II and III trials.[8,9] On the other hand, several aptamers, consisting of single-stranded DNA or RNA oligonucleotides with a specific and stable three-dimensional shape able to recognize their target with high affinity and specificity, were developed and tested in animal models.[10-12] However, only the historical anti-VWF-A1 aptamer, ARC1779, developed by Archemix (Cambridge, MA, USA), was investigated in ACD[13-16] and TTP[17-21] including limited phase II studies.[16,19-21]

In this issue of *Haematologica*, Sakai K and colleagues[22] present the *in vitro* characterization of a recently developed novel aptamer to VWF-A1, TAGX-0004,[23] using an elegant and extensive structural and functional investigation in both static and dynamic conditions (platelet aggregation, shear stress-induced platelet thrombus formation, study of binding to both wild-type VWF-A1 and 16 alanine-scanning VWF-A1 mutants using an electrophoresis mobility shift assay and surface plasmon resonance, and graphic analysis of three-dimensional (3D) structure models of VWF-A1). The authors show that, *in vitro*, TAGX-0004 is able to inhibit the binding of VWF-A1 to platelet GPIb better than the historical aptamer ARC1779 and as well as the Nanobody® caplacizumab. TAGX-0004 is thus presented as a new potential therapeutic option not only in acute TTP but also in various VWF-mediated thrombotic disorders such as acute coronary syndrome (ACS) and cerebral infarction.

In terms of the biochemical properties, the comparison of TAGX-0004 with ARC1779 is solid because those aptamers were used as both monovalent entities with no polyethylene glycol (PEG). The significantly higher affinity of TAGX-0004 for VWF-A1 compared to ARC1779 is likely related to the presence of Ds, an artificial hydrophobic base, able to directly interact with a specific residue (F1366) within VWF-A1. Also, interestingly, the amino acid residues of VWF-A1 identified as binding sites for TAGX-0004 and ARC1779 by the current study did not totally overlap and some slight differences with the originally mapping of VWF-A1 binding sites for ARC1172/ARC1179 performed by Huang and colleagues[24] were also observed. Regarding the similar *in vitro* affinity for VWF-A1 measured for both TAGX-0004 and caplacizumab, the authors mention that direct comparison of an affinity of monovalent entity with
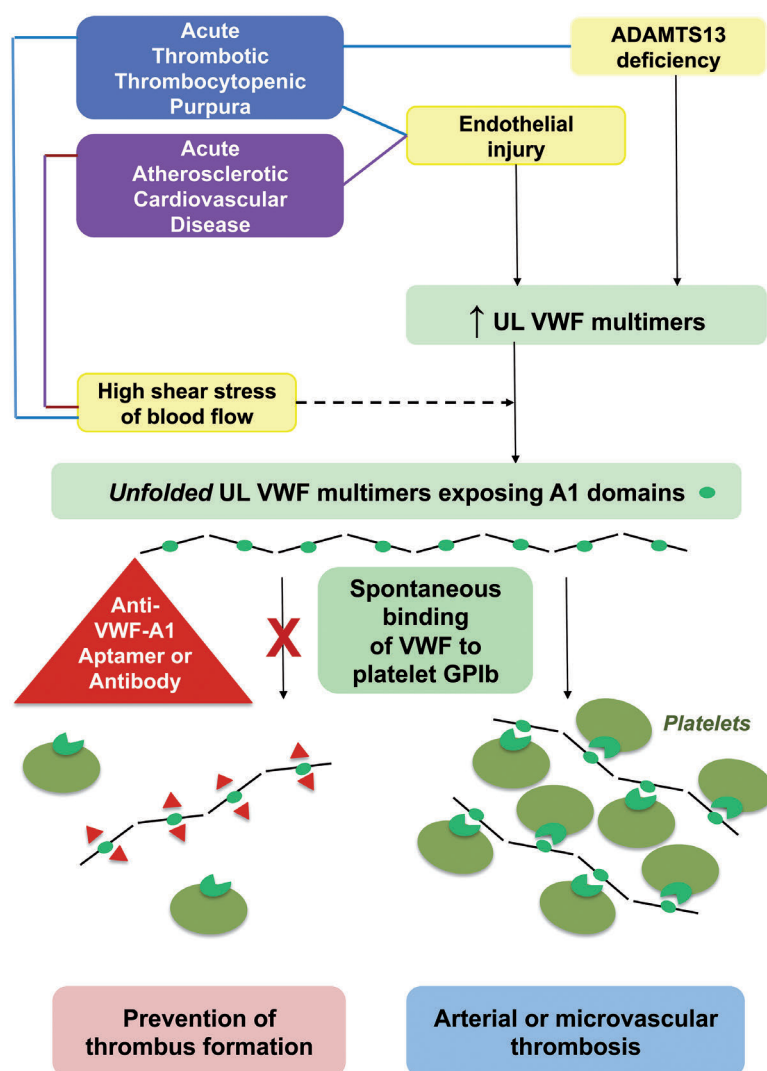
Figure 1. Von Willebrand factor–related pathophysiology for arterial and microvascular thrombosis in acute thrombotic thrombocytopenic purpura and atherosclerotic cardiovascular disease, and mechanisms for thrombus prevention by aptamers and antibodies to VWF A1 domain. VWF: von Willebrand factor; UL: ultralarge; ADAMTS13: a disintegrin and metalloproteinase with thrombospondin type 1 repeats, member 13; GPIb: glycoprotein Ib.

an avidity of bivalent entity is not straightforward, implying that this result should be considered with caution. Also, this study identified only a partial overlap of VWF-A1 binding sites for TAGX-0004 and caplacizumab, including however crucial amino acid residues (i.e., R1395 and R1399) found to be in common to all three: TAGX-0004, ARC1779 and caplacizumab.

To better consider preclinical and clinical trials' perspectives of this new anti-VWF-A1 aptamer, the historical background of both ARC1779 and caplacizumab is certainly important to recall. Since 2007, ARC1779 has been demonstrated to be efficient *in vivo* in a primate model[14] and to produce dose- and concentration-dependent inhibition of VWF activity and platelet function in a first-in-human evaluation led in healthy volunteers.[10] In addition, proof-of-concept of ARC1779 was provided in patients with VWD type 2B,[25] a genetic model of hyperadhesive VWF in which the mutated VWF-A1 exhibits a hyper-affinity for platelet GPIb leading to spontaneous binding to platelets and sometimes to thrombocytopenia. In *ex vivo* studies, ARC1779 effectively inhibited VWF activity in plasma samples of both TTP patients[18] and ACS patients.[13,15] Some clinical experiences

were first reported in three studies involving a total of 11 TTP patients.[17,19,20] Then, two randomized, double-blind, placebo-controlled phase II studies were initiated in carotid endarterectomy[16] and in acute TTP[21] but both of them underwent premature closure due to cessation of funding. The first study[16] was led in 36 patients and reported that intravenous ARC1779 reduced cerebral embolization post-carotid endarterectomy with however, a higher rate of per-operative bleeding complications in patients requiring surgery. The second study[21] led in only seven TTP patients, showed that intravenous ARC1779 (loading dose followed by daily infusion performed after each therapeutic plasma exchange [TPE]) induced a suppression of VWF activity correlated to the plasma concentration of ARC1779, apparently decreased the number of TPE to achieve a normal platelet count and was well tolerated with no bleeding complications. Despite of the latter promising results in TTP, no ARC1779 trial has been published since 2012. The caplacizumab story is significantly different. However, originally, caplacizumab was under development for the prevention of thrombosis in ACS patients undergoing percutaneous coronary intervention[6] but the development for this indication

was discontinued in favor of TTP. After proof-of-concept in a pre-clinical baboon model of acquired TTP[7] in 2012, caplacizumab rapidly emerged as a new strategy of first-line treatment of acute TTP in association with TPE and immunomodulating agents.[26,27] Caplacizumab was evaluated in two major multicenter, randomized, double-blind, placebo-controlled phase II[8] and phase III[9] trials involving 36 and 72 TTP patients and published in 2016 and 2019, respectively: intravenous and subcutaneous caplacizumab showed superiority to placebo in terms of reduction of mortality, reduction of time to platelet recovery allowing an earlier stop of TPE, prevention of formation of further microthrombi and protection of organs from ischemia.[8,9] Bleeding adverse event were common, affecting roughly half of the patients, but mostly mild or moderate and thus self-limited or resolved.[8,9] Caplacizumab approval for acute TTP was obtained in 2018 in the EU and in 2019 in the US.

Here, the authors open the door to the new anti-VWF-A1 aptamer as a promising molecule for future preclinical and clinical trials devoted to VWF-mediated thrombotic disorders, either the frequent ACD or the rare TTP.[22] They emphasize that TAGX-0004 may get an antidote as already developed for other aptamers[11,28] which may be a great advantage to control adverse bleeding events and thus to improve its main safety concern. In ischemic stroke and myocardial infarction, TAGX-0004 may be a rival of current antithrombotic and thrombolytic agents which are irreversible and associated with a significant risk of haemorrhage.[5] In addition, in contrast to antiplatelet drugs which bypass platelet adhesion and inhibit only platelet aggregation, TAGX-0004 is able to prevent the initial step of thrombus formation by inhibiting platelet adhesion and, as a consequence, also platelet aggregation. In acute TTP, TAGX-0004 may appear as a rival of caplacizumab. However, considering the complexity of TTP as a rare and life-threatening disease, several questions require specific attention during preclinical and clinical studies. First, acute TTP management relies on a mandatory concomitant use of first-line multiple targeted therapies[26,27] i.e., TPE and future recombinant ADAMTS13 as the replacement therapy for severely deficient ADAMTS13, steroids and rituximab as immunomodulators against anti-ADAMTS13 autoantibodies and now caplacizumab as an inhibitor of VWF-A1 preventing the adhesion of UL VWF to platelets. Thus, potential interactions of aptamers with ADAMTS13-replacing products and immunomodulators are unknown so far. Second, whether TAGX-0004 is able, like caplacizumab, to form a complex with VWF which clearance leads to a partial decrease of VWF antigen and coagulation factor VIII beneficial for the thrombotic atmosphere of TTP, is also unknown. Third, the superiority of TAGX-0004 to caplacizumab in terms of the bleeding risk remains to be further investigated as i) caplacizumab-associated bleeding events are mostly moderate and easily resolved,[8,9] and ii) the potential TAGX-0004 antidote constitutes an extra drug that may exhibit specific adverse events. Fourth, even if the *in vivo* half-life of TAGX-0004 is upgraded by a mini-hairpin DNA structure conferring resistance to degradation by nucleases,[22] it has to be compatible with a daily regimen adjusted to TPE. Fifth, as aptamers also have the capacity to be used as diagnostic reagents (their com-

bined therapeutics and diagnostics potential being summarized as "theranostic"),[28] the potential interference of TAGX-0004 with ADAMTS13 biologic assays crucial for therapy-driven monitoring in acute TTP[28], should also be a point of attention.

Today, aptamer technology remains one step behind the humanized monoclonal antibody research and development, mostly because antibodies biotech industry's financial investment has been highly prioritized for the last three decades. In 2020, only one aptamer targeted to vascular endothelial growth factor (Macugen/Pegaptanib sodium) has gained approval by the US Food and Drug Aminsitration for patients with age-related macular degeneration and few aptamers have successfully entered clinical trials for different therapeutic indications.[28] However, considering their advantages over antibodies (low price, small size, easy production) together with the efforts made to overcome their limitations (improvement of stability, target affinity, *in vivo* retention and corrective approaches to potential unmethylated 2'-deoxycytidine-phosphate-2'-guanine toxicity),[28] aptamers begin to slowly penetrate niche markets and bring promising therapeutic perspectives.

References

1. Matsushita T, Meyer D, Sadler JE. Localization of von Willebrand factor-binding sites for platelet glycoprotein Ib and botrocetin by charged-to-alanine scanning mutagenesis. J Biol Chem. 2000;275(15):11044-11049.
2. De Meyer SF, Vanhoorelbeke K, Ulrichts H, et al. Development of monoclonal antibodies that inhibit platelet adhesion or aggregation as potential anti-thrombotic drugs. Cardiovasc Hematol Disord Drug Targets. 2006; 6(3):191-207.
3. South K and Lane DA. ADAMTS13 and von Willebrand factor: a dynamic duo. J Thromb Haemost. 2018;16(1):6-18.
4. Sadler JE. Pathophysiology of thrombotic thrombocytopenic purpura. Blood. 2017;130(10):1181-1188.
5. Montalescot G, Philippe F, Ankri A, et al. Early increase of von Willebrand factor predicts adverse outcome in unstable coronary artery disease: beneficial effects of enoxaparin. French Investigators of the ESSENCE Trial. Circulation. 1998;98(4):294-299.
6. Ulrichts H, Silence K, Schoolmeester A, et al. Antithrombotic drug candidate ALX-0081 shows superior preclinical efficacy and safety compared with currently marketed antiplatelet drugs. Blood. 2011;118(3):757-765.
7. Callewaert F, Roodt J, Ulrichts H, et al. Evaluation of efficacy and safety of the anti-VWF nanobody ALX-0681 in a preclinical baboon model of acquired thrombotic thrombocytopenic purpura. Blood. 2012;120(17): 3603-3610.
8. Peyvandi F, Scully M, Kremer Hovinga JA, et al. Caplacizumab for acquired thrombotic thrombocytopenic purpura. N Engl J Med. 2016;374(6):511-522.
9. Scully M, Cataland SR, Peyvandi F, et al. Caplacizumab treatment for acquired thrombotic thrombocytopenic purpura. N Engl J Med. 2019;380(4):335-346.
10. Gilbert JC, DeFeo-Fraulini T, Hutabarat RM, et al. First-in-human evaluation of anti von Willebrand factor therapeutic aptamer ARC1779 in healthy volunteers. Circulation. 2007;116(23):2678-2686.
11. Nimjee SM, Lohrmann JD, Wang H, et al. Rapidly regulating platelet activity in vivo with an antidote controlled platelet inhibitor. Mol Ther. 2012;20(2):391-397.
12. Nimjee SM, Dornbos III D, Pitoc GA, et al. Preclinical development of a vWF aptamer to limit thrombosis and engender arterial recanalization of occluded vessels. Mol Ther. 2019;27(7):1228-1241.
13. Spiel AO, Mayr FB, Ladani N, et al. The aptamer ARC1779 is a potent and specific inhibitor of von Willebrand Factor mediated ex vivo platelet function in acute myocardial infarction. Platelets. 2009;20(5):334-340.
14. Diener JL, Daniel Lagassé HA, Duerschmied D, et al. Inhibition of von Willebrand factor-mediated platelet activation and thrombosis by the anti-von Willebrand factor A1-domain aptamer ARC1779. J Thromb

Haemost. 2009;7(7):1155-1162.

15. Arzamendi D, Dandachli F, Théorêt JF, et al. An anti-von Willebrand factor aptamer reduces platelet adhesion among patients receiving aspirin and clopidogrel in an ex vivo shear-induced arterial thrombosis. Clin Appl Thromb Hemost. 2011;17(6):E70-78.

16. Markus HS, McCollum C, Imray C, et al. The von Willebrand inhibitor ARC1779 reduces cerebral embolization after carotid endarterectomy: a randomized trial. Stroke. 2011;42(8):2149-2153.

17. Knöbl P, Jilma B, Gilbert JC, et al. Anti-von Willebrand factor aptamer ARC1779 for refractory thrombotic thrombocytopenic purpura. Transfusion. 2009;49(10):2181-2185.

18. Mayr FB, Knöbl P, Jilma B, et al. The aptamer ARC1779 blocks von Willebrand factor-dependent platelet function in patients with thrombotic thrombocytopenic purpura ex vivo. Transfusion. 2010;50(5):1079-1087.

19. Jilma-Stohlawetz P, Gorczyca ME, Jilma B, et al. Inhibition of von Willebrand factor by ARC1779 in patients with acute thrombotic thrombocytopenic purpura. Thromb Haemost. 2011;105(3):545-552.

20. Jilma-Stohlawetz P, Gilbert JC, Gorczyca ME, et al. A dose ranging phase I/II trial of the von Willebrand factor inhibiting aptamer ARC1779 in patients with congenital thrombotic thrombocytopenic purpura. Thromb Haemost. 2011;106(3):539-547.

21. Cataland SR, Peyvandi F, Mannucci PM, et al. Initial experience from a double-blind, placebo-controlled, clinical outcome study of ARC1779 in patients with thrombotic thrombocytopenic purpura. Am J Hematol. 2012;87(4):430-432.

22. Sakai K, Someya T, Harada K, Yagi H, Matsui T, Matsumoto M. Novel aptamer to von Willebrand factor A1 domain (TAGX-0004) shows total inhibition of thrombus formation superior to ARC1779 and comparable to caplacizumab. Haematologica. Haematologica. 2020;105 (11):2631-2638.

23. Matsunaga KI, Kimoto M, Hirao I, et al. High-affinity aptamer generation targeting von Willebrand factor A1-domain by genetic alphabet expansion for systematic evolution of ligands by exponential enrichment using two types of libraries composed of five different bases. J Am Chem Soc. 2017;139(1):324-334.

24. Huang RH, Fremont DH, Diener JL, Schaub RG, Sadler JE. A structural explanation for the antithrombotic activity of ARC1172, a DNA aptamer that binds von Willebrand factor domain A1. Structure. 2009;17(11):1476-1484.

25. Jilma-Stohlawetz P, Knöbl P, Gilbert JC, et al. The anti-von Willebrand factor aptamer ARC1779 increases von Willebrand factor levels and platelet counts in patients with type 2B von Willebrand disease. Thromb Haemost. 2012;108(2):284-290.

26. Joly BS, Vanhoorelbeke K, Veyradier A. Understanding therapeutic targets in thrombotic thrombocytopenic purpura. Intensive Care Med. 2017;43(9):1398-1400.

27. Coppo P, Cuker A, George JN. Thrombotic thrombocytopenic purpura: toward targeted therapy and precision medicine. Res Pract Thromb Haemost. 2018;3(1):26-37.

28. Kaur H, Bruno JG, Kumar A, Sharma TK. Aptamers in the therapeutics and diagnostics pipelines. Theranostics. 2018;8(15):4016-4032.

Ferrata Storti Foundation

Novel dynamic outcome indicators and clinical endpoints in myelodysplastic syndrome; the European LeukemiaNet MDS Registry and MDS-RIGHT project perspective

Theo de Witte,[1*] Luca Malcovati,[2*] Pierre Fenaux,[3] David Bowen,[4] Argiris Symeonidis,[5] Moshe Mittelman,[6] Reinhard Stauder,[7] Guillermo Sanz,[8] Jaroslav Čermák,[9] Saskia Langemeijer,[10] Eva Hellström-Lindberg,[11] Ulrich Germing,[12] Mette Skov Holm,[13] Krzysztof Mądry,[14] Aurelia Tatic,[15] António Medina Almeida,[16] Aleksandar Savic,[17] Inga Mandac Rogulj,[18] Raphael Itzykson,[3] Marlijn Hoeks,[10] Hege Gravdahl Garelius,[19] Dominic Culligan,[20] Ioannis Kotsianidis,[21] Lionel Ades,[3] Arjan A. van de Loosdrecht,[22] Corine van Marrewijk,[10] Ge Yu,[23] Simon Crouch,[23] Alex Smith[23]; on behalf of the EUMDS Registry Participants

[1]Department of Tumor Immunology - Nijmegen Center for Molecular Life Sciences, Radboud University Medical Center, Nijmegen, the Netherlands; [2]Department of Hematology Oncology, Fondazione IRCCS Policlinico San Matteo, University of Pavia, Pavia, Italy; [3]Service d'Hématologie, Hôpital Saint-Louis, Assistance Publique des Hôpitaux de Paris (AP-HP) and Université Paris 7, Paris, France; [4]St. James's Institute of Oncology, Leeds Teaching Hospitals, Leeds, UK; [5]Department of Medicine, Division of Hematology, University of Patras Medical School, Patras, Greece; [6]Department of Medicine A, Tel Aviv Sourasky (Ichilov) Medical Center and Sackler Medical Faculty, Tel Aviv University, Tel Aviv, Israel; [7]Department of Internal Medicine V (Haematology and Oncology), Innsbruck Medical University, Innsbruck, Austria; [8]Department of Haematology, Hospital Universitario y Politécnico La Fe, Valencia, and CIBERONC, Madrid, Spain; [9]Department of Clinical Hematology, Inst. of Hematology and Blood Transfusion, Praha, Czech Republic; [10]Department of Hematology, Radboud University Medical Center, Nijmegen, the Netherlands; [11]Department of Medicine, Division Hematology, Karolinska Institutet, Stockholm, Sweden; [12]Department of Haematology, Oncology and Clinical Immunology, Universitätsklinik Düsseldorf, Düsseldorf, Germany; [13]Department of Haematology, Aarhus University Hospital, Aarhus, Denmark; [14]Department of Haematology, Oncology and Internal Medicine, Warszawa Medical University, Warszawa, Poland; [15]Center of Hematology and Bone Marrow Transplantation, Fundeni Clinical Institute, Bucharest, Romania; [16]Department of Clinical Hematology, Hospital da Luz, Lisbon, Portugal; [17]Clinic of Hematology - Clinical Center of Vojvodina, Faculty of Medicine, University of Novi Sad, Novi Sad, Serbia; [18]Department of Internal Medicine, Division of Hematology, Merkur University Hospital, Zagreb, Croatia; [19]Department of Specialist Medicine, Sahlgrenska University Hospital, Göteborg, Sweden; [20]Department of Haematology, Aberdeen Royal Infirmary, Aberdeen, UK; [21]Department of Hematology, Democritus University of Thrace Medical School, University Hospital of Alexandroupolis, Alexandroupolis, Greece; [22]Department of Hematology – Cancer Center Amsterdam, Amsterdam UMC, Location VU University Medical Center, Amsterdam, the Netherlands and [23]Epidemiology and Cancer Statistics Group, Department of Health Sciences, University of York, York, UK

*TdW and LM both contributed equally as co-first authors.

Correspondence:

THEO DE WITTE,
theo.dewitte@radboudumc.nl

Introduction

Myelodysplastic syndromes (MDS) are chronic bone marrow (BM) disorders characterized by peripheral blood cytopenias, predominantly in older persons with an average age at diagnosis of 75 years.[1,2] The natural history of MDS is heterogeneous, ranging from indolent conditions to forms similar to acute myeloid leukemia (AML). In 1997, an International Prognostic Scoring System (IPSS) was established based on the percentage of BM blasts, number of cytopenias and cytogenetic characteristics.[3] In 2012, this prognostic scoring system was refined (IPSS-R) to include better categorization of cytopenias, blast cell percentage and an improved risk stratification of the cytogenetic risk groups.[4] Generally, MDS are divided into two prognostic groups: lower-risk MDS (LR-MDS) with patients from the (very) low risk or intermediate risk groups, and higher-risk MDS (HR-MDS) with patients from the (very) poor risk groups, as defined within the IPSS-R.[2]

The majority of patients with MDS (75%) have LR-MDS, which was the focus of the European LeukemiaNet MDS (EUMDS) Registry until 2017. The EUMDS Registry is a pragmatic, observational study, which has collected prospectively longi-

tudinal data from more than 2,738 patients with MDS, including 2,498 LR-MDS patients with a median age of 75 years, and a follow-up of up to 11 years, in 16 European countries plus Israel from 148 active sites (progress report as of March 1st 2020). Progression to HR-MDS/AML has occurred in 314 LR-MDS patients (13%), and 910 patients (33%) had died at time of last report. Data quality control, including monitoring of both clinical performance and data collection, has been implemented since the initiation of the EUMDS Registry. New prognostic indicators in LR-MDS have been identified as part of the MDS-RIGHT project (*https://mds-europe.eu/right*) funded by Horizon 2020, which started in May 2015 with an overarching aim of defining and implementing more (cost)-effective and safer interventions in LR-MDS.

Symptoms of anemia, the most common cytopenia in LR-MDS, accompanied by infectious or bleeding complications predominate in LR-MDS.[5] About 25% of these patients develop AML, but most patients die from complications related to progressive BM failure and worsening cytopenias, and from their negative interaction with the extra-hematologic comorbidities presented by those patients of advanced age.[6,7] Patients with LR-MDS are characterized by a notable reduction in health related quality of life (HRQoL).[8,9] Moderate to severe anemia in older individuals (>60 years) leads to increased mortality both in patients with LR-MDS and in the general population.[10,11] Likewise, anemia represents an unfavorable prognosticator in possible pre-MDS conditions at advanced age.[12] Improving response prediction will contribute to more effective and targeted use of the available health care interventions (HCI).[13]

According to the available evidence- and consensus-based therapeutic guidelines, current therapeutic interventions in LR-MDS include red blood cell transfusion (RBCT), erythropoietin stimulating agents (ESA), lenalidomide, and iron chelation therapy (ICT).[11] For ESA, a predictive model has identified a group of patients characterized by serum erythropoietin (EPO) levels <500 mU/mL and a transfusion need of <2 units RBC/month with a favorable response compared to patients with higher EPO levels and/or higher numbers of RBCT/month.[14] Treatment with lenalidomide is only recommended for a small subgroup of patients with partial loss of chromosome 5 (5q-) and RBCT-dependent anemia.[15,16]

The most frequently applied outcome parameter in this LR-MDS patient population is overall survival (OS). Analysis of the EUMDS Registry data showed that the currently available risk scoring systems, including the IPSS-R, have a better prognostic capacity for disease progression to AML as compared with OS.[2] We estimated that 58% of deaths in this population are not related to disease progression, but are attributable to non-leukemic death.[2,17] A high proportion of patients with LR-MDS have a median survival of up to 5-10 years, meaning that clinical trials, the design of which identifies survival as a primary endpoint, may result in a potentially biased assessment of the effectiveness and evidence on the appropriate use of the available interventions. Therefore, we have explored additional relevant outcome parameters in a Delphi survey, which could be used to circumvent the limited value of survival as primary endpoint in LR-MDS.[18]

Additional evidence is required to extend the existing prognostic and therapeutic response indicators in the older LR-MDS population, and to identify meaningful biological and clinical endpoints, including patient-reported outcome measures and other patient-related factors. These new endpoints may provide information on the effectiveness of the available therapeutic interventions early in the natural history of the disease. These early indicators of treatment response may drive a more effective use of those interventions currently made.

Recent studies conducted on the large population of patients with LR-MDS included in the EUMDS Registry during its first 10 years of activity allowed validation of RBCT requirement and HRQoL as independent and meaningful outcome indicators and reliable measures of response to interventions, supporting their integration in the MDS-Core Outcome Set (COS) in this patient population.[18] In addition, prospective studies based on the unbiased dataset of the EUMDS Registry allowed identification of early response determinants for targeted use of treatment modalities, including ESA, lenalidomide, and ICT.

Novel outcome indicators and meaningful early clinical endpoints in patients with lower-risk myelodysplastic syndromes

Kinetics of blood counts decrease is an independent outcome indicator in lower-risk myelodysplastic syndromes

The prognosis of LR-MDS is heterogeneous.[2] Early identification of patients at risk of rapid progression should rely on universal, affordable and non-invasive tools to gain acceptance in an older population often managed in community care centers. All current MDS prognostic scores rely on steady-state assessments of cytopenias, i.e., hemoglobin (Hb)-levels, neutrophil or platelet counts on the day of initial assessment.[19] Time-dependent prognostic scores require repeated BM examinations, raising acceptability issues in this older patient population. To circumvent this limitation, we analyzed the prognostic role of the kinetics of cytopenias during the first visit interval (6 months) following diagnosis in LR-MDS patients prospectively included in the EUMDS registry.[20] We performed a landmark analysis at the second visit, at around 6 months from diagnosis, to apply simple prognostic criteria in general clinical practice.

The results showed that a relative drop in platelets >25% at the 6-month landmark predicted shorter 5-year OS; 22% *versus* 49% in patients with platelet drop ≤ 25% (*P*<10⁻⁴), regardless of baseline IPSS-R or absolute platelet counts. Conversely, relative neutrophil drop >25% had no significant impact on OS. Subsequently, a classifier was built based on RBCT-dependency and relative platelet drop >25% at landmark. Patients with none (62%), either one of the two criteria (27%) or both criteria (11%) had 5-year OS of 53.3%, 32.7% and 9.0%, respectively (*P*<10⁻⁴) (Figure 1). Sensitivity analyses confirmed the applicability of this simple classifier even when follow-up visits were planned at any time during the first ten months after diagnosis, thus capturing most situations encountered in daily practice.[20]

Red blood cell transfusion requirement is an independent outcome indicator and freedom from transfusion a meaningful clinical endpoint in patients with lower-risk myelodysplastic syndromes

In order to extend existing outcome parameters in the older LR-MDS population,[21] RBCT administration in the LR-MDS patients enrolled in the EUMDS Registry was

evaluated with the aim of estimating the prognostic impact of regular RBCT and to validate RBCT-free survival as an early clinical endpoint in this patient population. The reference endpoint was progression-free survival (PFS), because both progression and death indicate the end of a relatively stable phase of LR-MDS.

A cohort of 1,267 patients with all relevant data available was included in this analysis. The patients were subdivided for the landmark analysis into four groups: no transfusions, >0 to <0.75 units/month (low transfusion dose), 0.75-1.75 units/month (mid transfusion dose) and >1.75 units/month (high transfusion dose). The greatest effect, compared to the non-transfused patients, occurred in patients receiving transfusions at low dose densities, since the impaired outcome of the mid and high transfusion density group was similar (Figure 2). In multivariable analysis, RBCT dose density retained statistical significance at $P<10^{-4}$.

Since treatment with ESA, lenalidomide and iron chelators may improve erythropoiesis and reduce the need for RBCT, these variables were included in the regression model. This analysis resulted in an effect for the dose density similar to the previous analyses at $P<10^{-4}$.[21] However, the dose density effect continues to increase beyond one unit per month after correction for the three interventions (ESA, iron chelation and lenalidomide) up until a dose of six units per month (Figure 3). The relative log ratios on PFS of this analysis clearly showed that the deleterious effect of transfusions already occurred at a very low transfusion burden (<3 units per 16 weeks as defined in the revised International Working Group, IWG) report, confirming the outcome of the landmark analysis (see above). It is important to realize that patients with a transfusion dose of 1-2 units per 16 weeks are considered to be untransfused in the recently revised IWG report, but are recommended to be studied in future clinical trials.[21]

Relevance of patient-reported outcomes in lower-risk myelodysplastic syndromes

Health related quality of life is an important patient-reported outcome (PRO). It provides specific information on
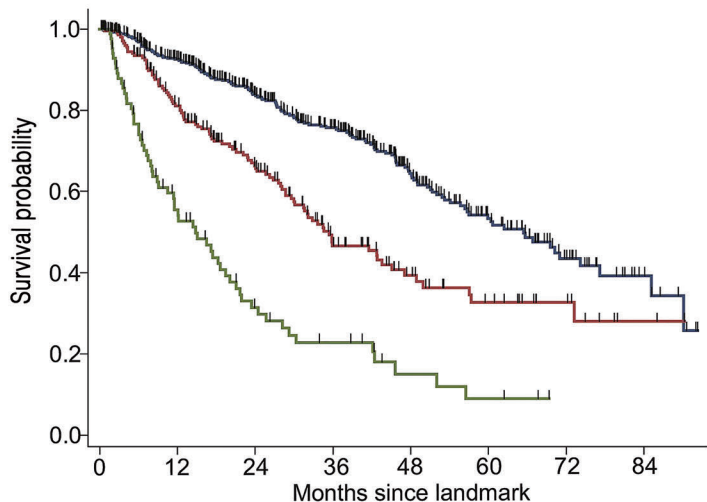
Figure 1. Kaplan-Meier plots of overall survival from landmark according to the 6-month European LeukemiaNet MDS (EUMDS) classifier based on platelet drop >25% per red blood cell transfusion (RBCT)-dependency at landmark. Black: no criteria (no platelet drop >25% or RBCT-dependency at landmark); red: either one of the two criteria; green: both criteria.
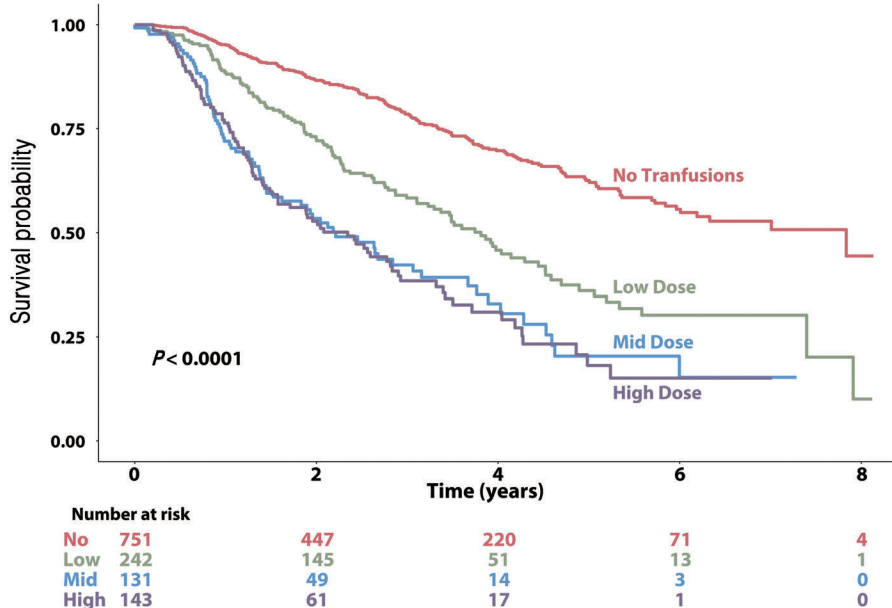
Figure 2. Kaplan-Meier plots of progression-free survival (PFS) according to transfusion status at the landmark of visit 3 (1 year after registration). Kaplan-Meier plot of PFS of patients receiving no transfusions (red line) or transfusions at a low dose density: from >0 to <0.75 units per month (green line); mid dose density: 0.75-1.75 units per month (purple line); high dose density >1.75 units per month (blue line).

older patients with chronic diseases that might not be reflected in the level of physical activity and relevant laboratory parameters, including Hb levels.[22] Preliminary data in HR-MDS patients suggest that these limitations may predict an unfavorable clinical outcome.[8] However, definitive data on HRQoL in LR-MDS are rare. This EUMDS Registry project investigated the HRQoL-profile of LR-MDS patients at time of diagnosis as compared with age- and sex-matched reference groups from the general population.[23] HRQoL was measured by the EuroQol-5 dimension (EQ-5D) score at the time of study enrolment.[24,25] Population norms were used to assess the relative HRQoL of patients in comparison to those of the average person in the community.[26]

A significant proportion of MDS patients reported moderate or severe problems in the dimensions pain/discomfort (50%), mobility (41%), anxiety/depression (38%), and usual activities (36%). Clinically meaningful restrictions in the EQ-5D index, EQ-Visual Analog Scale (VAS) were observed significantly more often in older patients and in those with a high co-morbidity burden, low Hb levels or RBCT need ($P<10^{-3}$). Relative to the EQ-5D index and EQ-VAS scores in the reference group, HRQoL was significantly lower for groups of patients with MDS who were older, female, or had increased comorbidities, low Hb-levels or RBCT dependence.[23]

Restrictions in distinct dimensions of the EQ-5D were also observed when compared with European reference populations, but this effect might (partly) be explained by the anemia in the MDS cohort, since older anemic patients in the general population also have a decreased HRQoL.[11] Low Hb levels and RBCT need were associated both with a decreased EQ-5D index and a decreased EQ-VAS after adjustment for co-variables in this EUMDS-Registry study, further supporting the use of RBCT requirement as an indicator of loss of effectiveness of interventions and worsening outcome. In addition, transfusion-free survival appeared to be a meaningful clinical endpoint in patients with lower-risk MDS, as shown in the transfusion study.[21] These findings have important implications for every-day clinical practice and the design of clinical endpoints.

Novel treatment-response indicators in lower risk myelodysplastic syndromes

Early initiation of treatment with erythropoietin stimulating agents is an important response indicator and significantly delays the onset of red blood cell transfusion dependency in patients with lower-risk myelodysplastic syndromes

Anemia of patients with LR-MDS and RBCT dependency have been associated with reduced HRQoL in several prospective trials[27,28] and with reduced survival in retrospective registry reports.[10] Current guidelines recommend ESA as first-line treatment for LR-MDS patients with symptomatic anemia.[13] In recent studies, overall response rates varied between 38% and 66%, with a median response duration of around 20 months.[29] Retrospective analyses of large multi-center cohorts from different countries compared survival in patients treated with ESA within clinical studies with untreated patients. Survival was markedly better in the group exposed to ESA with no difference in AML transformation.[30,31]

Within the EUMDS registry, the effects of ESA treatment on outcomes were explored amongst 1,696 unselected patients with anemia.[32] To overcome potential confounding by non-random allocation of ESA treatment, proportional hazards regression models comparing time-to-event outcomes in treated and untreated patients were weighted by stabilized inverse probability of treatment weights based on the propensity of a patient to receive ESA treatment. Only patients with comparable propensity scores were included in the analyses to estimate the effects of ESA treatment on outcomes. The relationship between the effects of ESA and pre-ESA treatment transfusion status was explored using this model. A non-significant beneficial effect of ESA treatment on OS was estimated from the weighted regression model comparing patients with comparable propensity scores (hazard ratio [HR] 0.82, 95% confidence interval [CI]: 0.65-1.04; $P=0.09$). A non-significant estimate of a beneficial effect of ESA treatment on progression to AML or
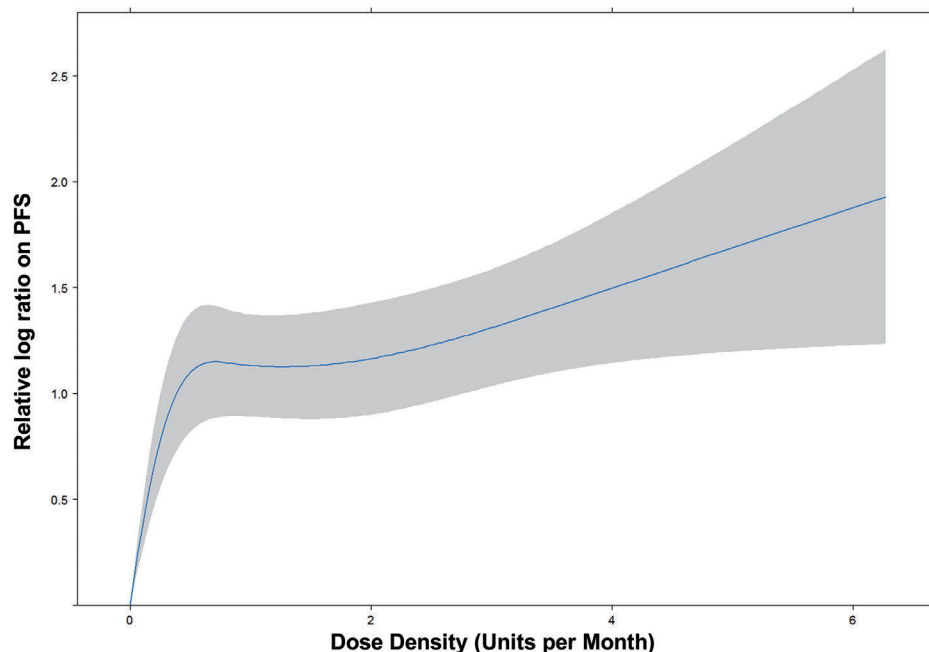
Figure 3. Influence of dose density on progression-free survival (PFS) in a multivariate regression model adjusted for treatment with either erythropoiesis-stimulating agent, iron chelation or lenalidomide. Dose density: average number of transfusions per month, calculated from start of transfusion until date of analysis.

Y-axis: Relative log ratio on PFS
X-axis: Dose Density (Units per Month)

high-risk MDS was observed (HR 0.88, CI: 0.63-1.22; *P*=0.44). Exploration of the relationship between ESA treatment and pre-treatment transfusion status revealed a larger estimated effect of ESA on survival amongst patients who had not received RBCT prior to starting ESA treatment (HR 0.71, 95%CI: 0.49-1.03; *P*=0.07) than amongst patients who had received prior RBCT (HR 0.93, 95%CI: 0.70-1.26; *P*=0.67).

Responding patients had a better prognosis, in terms of a lower risk for death (HR 0.65, 95%CI: 0.45-0.893; *P*=0.018). The effect of response on time to first post-ESA treatment transfusion was significant after stratification by pre-treatment transfusion experience. Importantly, and irrespective of response status, patients who received RBCT before starting ESA had a shorter time to their first post-treatment transfusion (median 6.1 *vs.* 23.3 months for non-transfused patients; HR 2.4, 95%CI: 1.75-3.31; *P*<10⁻⁴).

This large observational study showed that the response rate to ESA, as well as the capacity of these agents to significantly delay the onset of a regular RBCT need, is most pronounced in RBCT-naïve patients, suggesting that RBCT-naïve patients are more responsive. These results identify early initiation of ESA treatment as a relevant treatment response indicator, and suggest that ESA should be recommended as first-line treatment in LR-MDS patients with symptomatic anemia before starting regular RBCT.

Labile plasma iron levels and non-transferrin bound iron are early and clinically relevant indicators of iron toxicity and impact of iron chelation therapy on outcome in patients with lower-risk myelodysplastic syndromes receiving red blood cell transfusion

The majority of LR-MDS patients become RBCT dependent over time. With an expected survival of up to 12 years, these patients are prone to long-term accumulation of iron due to RBCT.[33] Iron overload may also occur in a fraction of MDS patients who do not receive RBCT, resulting from the stimulation of intestinal iron absorption, mediated through suppression of hepcidin production by ineffective erythropoiesis.[34] The toxic effects of iron overload in other iron loading diseases are well known, but the consequences in MDS remain to be elucidated. To this end, we evaluated erythroid marrow activity, hepcidin levels, and body iron status, including non-transferrin bound iron (NTBI) and labile plasma iron (LPI) levels over time in LR-MDS patients and their relation with disease subtype and RBCT history within the EUMDS Registry.[35]

Detectable NTBI already occurred in all patient groups at registration, with highest levels in patients with MDS and ring sideroblasts (MDS-RS). The median LPI levels were below the level of detection in all patient groups at registration, except in transfusion dependent (TD) MDS-RS patients.[35] Hepcidin levels increased with the number of transfused units, but in contrast, hepcidin levels significantly decreased over time in transfusion independent (TI) MDS-RS patients. Serum transferrin (sTfR) levels increased significantly over time in both TI and TD MDS-RS patients (*P*-values from 0.01 to <10⁻³). Both elevated NTBI and LPI levels showed a threshold effect with transferrin saturation (TSAT) rates of >70% and >80%, respectively. Elevated LPI levels occurred almost exclusively in patients with MDS-RS and/or patients, who had received RBCT. Once LPI levels are increased, survival time decreases, with greatest impact in patients who are TD (adjusted HR, 4.03, 95%CI: 0.95-17.06; *P*=0.06).

This study among LR-MDS patients showed that both treatment with RBCT and presence of ring sideroblasts increased the occurrence of the toxic iron species NTBI and LPI in serum. These data suggest that body iron accumulation and toxic iron species (NTBI and LPI) occur mainly in MDS-RS patients along the axis of ineffective erythropoiesis, characterized by elevated sTfR, low hepcidin, and increased iron levels, in some MDS subtypes, irrespective of receiving RBCT. Transfusional parenchymal iron overload, reflected by the combination of high serum ferritin levels, as well as direct iron toxicity, reflected by the presence of NTBI and LPI, was noted more frequently in MDS patients with ring sideroblasts compared to patients without ring sideroblasts. These data show that elevated LPI levels were associated with decreased survival both in the overall population of this study and in the patient groups subdivided by RBCT status. This implies that the widely used parameter TSAT cannot serve as a parameter to predict survival; however, TSAT rates can be used as a pre-screening marker to identify patients who are at risk of developing elevated LPI levels and associated poor prognosis. Finally, we could demonstrate in a limited number of patients treated with iron chelators that LPI levels decreased below detectable levels. This study suggested that NTBI and LPI may serve as early indicators of iron toxicity and as a measure for the effectiveness of iron chelation therapy in patients with lower risk MDS.

Iron overload due to RBCT is associated with increased morbidity and mortality in patients with LR-MDS.[36] Several studies have reported beneficial effects of ICT on survival and other clinical outcomes in MDS patients with iron overload.[37,38] However, valid data on the effect of ICT are limited since most studies are executed in small, selected patient groups or suffer from serious methodological problems such as confounding by indication.[38] Performing a randomized, controlled trial (RCT) for this research question is awkward, and patients included in RCT may not reflect the general LR-MDS patients, who are usually patients of advanced age with multiple chronic, complex comorbidities. In addition to the possible beneficial effects of ICT on survival, increasing evidence indicates hematologic improvement in patients during ICT.[39] Following improvement in cytopenias, transfusion independency is achieved in a minority of chelated patients.[40,41]

Results from a study conducted within the EUMDS registry on 490 non-chelated and 199 chelated patients using ICT as a time-dependent variable showed that the hazard ratio for OS was 0.50 (95%CI: 0.34-0.74) after adjusting for relevant confounding factors. Restriction of the analysis to 150 patients who were initially treated with deferasirox resulted in the adjusted HR for OS of 0.38 (95%CI: 0.24-0.60), while patients who were initially treated with deferoxamine had inferior OS compared to deferasirox treated patients (adjusted HR: 2.46, 95%CI: 1.12-5.41). The propensity-score analysis matching for all relevant variables, and a multivariate Cox proportional hazard model restricted to the deferasirox treated patients resulted in the adjusted HR for OS of 0.34 (95%CI: 0.22-0.53). An erythroid response occurred in 77 chelated patients: 61 patients had a reduction in transfusion density, and 16 patients who did not have a reduction in transfusion density became transfusion independent during at least one visit interval.

The TELESTO trial[42] is the only prospective, randomized, placebo-controlled study of ICT in MDS patients comparing deferasirox with a placebo-control group. This study

evaluated the event-free survival (EFS) (a composite outcome, including non-fatal events related to cardiac and liver function, and transformation to AML or death) and safety of deferasirox *versus* placebo in low and intermediate-1-risk MDS patients. This trial demonstrated an EFS risk reduction of 36.4% in the deferasirox arm (*P*=0.015), but the median OS in the deferasirox-treated arm did not differ (HR 0.83, 95%CI: 0.54-1.28; *P*=0.200) when compared with placebo. The results of the TELESTO study are in line with the EUMDS study, but the patients included may not represent 'real life' older MDS patients with multiple comorbidities, as reflected by the mean age of 61 years of the patients included in TELESTO study compared to the mean age of 70 years of the chelated patients in the EUMDS Registry study. Furthermore, low accrual rates and the cross-over to ICT after cessation of the placebo affected the statistical power of the TELESTO study.

Summary and concluding remarks

Available evidence suggests that in most patients with LR-MDS the risk of death is not related to disease progression but is mainly attributable to non-leukemic death.[2,17] In addition, a proportion of these patients have prolonged survival that precludes the design of clinical trials adopting OS as a primary endpoint. These challenges have resulted in potentially biased assessment of the effectiveness and appropriate use of the available interventions in this patient population. The EUMDS Registry has identified novel meaningful outcome indicators and clinical endpoints, and reliable measures of response to HCI (Figure 4).

The results of our analysis indicate that RBCT density is strongly associated with a decreased OS, even at relatively low dose densities. In addition, we observed that an early decrease in platelet count is an independent adverse prognostic indicator in LR-MDS, and combining relative platelet drop and transfusion dependency allows early identification of patients at risk of rapid progression, and may guide early therapeutic interventions, including allogeneic hematopoietic stem cell transplantation or experimental interventions. Taken together, these results indicate that regular RBCT requirement, early platelet count kinetics, and restriction in HRQoL are early independent and meaningful outcome indicators, and reliable measures of effectiveness of therapeutic interventions, evaluated in this set of studies. These findings support the integration of RBCT requirement and HRQoL in the general core outcome sets and in response criteria in patients with LR-MDS, and have important implications for clinical practice and the design of clinical endpoints. Our results strongly support the adoption of freedom from transfusion as a meaningful clinical endpoint in patients with LR-MDS.

Anemia is the main determinant of therapeutic intervention in patients with LR-MDS, and ESA are recommended as first-line treatment for patients with symptomatic anemia.[10] The observational studies within the EUMDS Registry showed that the response rate, as well as the capacity of these agents to delay the onset of a regular RBCT need, is most pronounced in RBCT-naïve patients. These results identified early initiation of treatment with ESA as a major treatment response indicator, and indicate that ESA should be recommended in LR-MDS patients with symptomatic anemia before starting regular RBCT. After the onset of RBCT dependency, patients with LR-MDS are prone to long-term accumulation of iron.[1,43] The EUMDS Registry studies provided evidence that elevated LPI levels are associated with reduced survival in RBCT
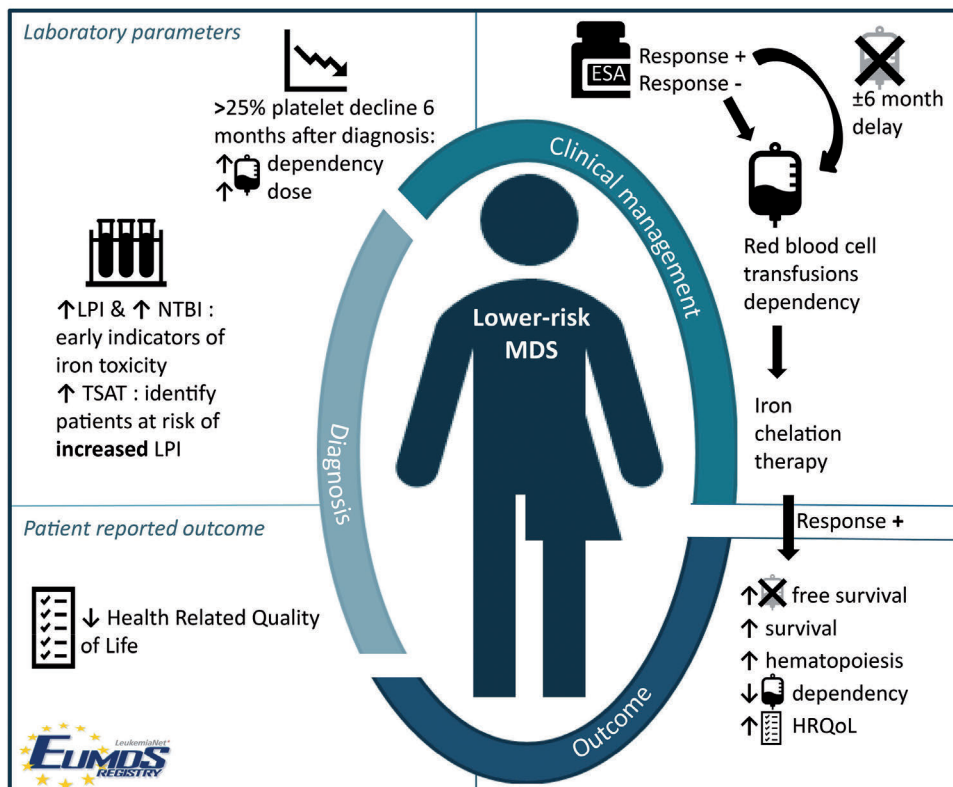
Figure 4. Overview of novel outcome indicators and clinical endpoints identified in the European LeukemiaNet myelodysplastic syndromes (EUMDS) Registry. ESA: erythropoietin stimulating agents; LPI: labile plasma iron; NTBI: non-transferrin bound iron; TSAT: transferrin saturation; HRQoL: health related quality of life.

dependent patients, whereas iron chelation therapy normalizes LPI levels. These findings suggest that NTBI and LPI may serve as early indicators of iron toxicity and a means to measure the effectiveness of iron chelation therapy in patients with LR-MDS. However, qualified NTBI and LPI are only currently available in specialized laboratories.[44]

Large observational cohorts with detailed clinical and laboratory data, like the EUMDS cohort, are the ideal framework in which to identify well defined MDS subtypes that may benefit from novel targeted treatments. An example of such a subtype is MDS with loss of parts of chromosome 5, namely del5q; these patients have a relatively favorable outcome on lenalidomide treatment. In order to identify homogeneous subsets of patients within MDS, preliminary evidence has suggested that recently identified mutations in splicing factors may recognize distinct disease entities within myeloid neoplasms.[45] Splicing modulators are now in pre-clinical testing, and are very likely to lead to the introduction of effective drugs for specific groups of MDS patients. Luspatercept, a specific inhibitor of growth and differentiation factor-11, a member of the transforming growth factor β superfamily, induced substantial improvement of anemia, especially in patients with ring sideroblasts.[46] Characterization of individual cases by new genetic markers (one of the main objectives of the MDS-RIGHT project) will allow refined classification of patients into biological subgroups that are expected to respond differently to therapeutic interventions to guide discontinuation of those interventions that are less effective or less cost-effective.

The main question is whether RCT data and retrospective cohort data in selected tertiary care centers are representative of the 'real world' data of the older patients with LR-MDS in the general population. A careful comparison of the 'real world' data and the RCT data will be needed in order to provide a clear answer to these questions. Meanwhile, the current analyses of data collected over 10 years in the EUMDS Registry provides relevant and important information which could help assess prognosis and response to standard interventions in this older patient group.

References

1. Cazzola M, Malcovati L. Myelodysplastic syndromes-coping with ineffective hematopoiesis. N Engl J Med. 2005;352(6):536-538.
2. de Swart L, Smith A, Johnston TW, et al. Validation of the revised international prognostic scoring system (IPSS-R) in patients with lower-risk myelodysplastic syndromes: a report from the prospective European LeukaemiaNet MDS (EUMDS) registry. Br J Haematol. 2015;170(3):372-383.
3. Greenberg P, Cox C, LeBeau MM, et al. International scoring system for evaluating prognosis in myelodysplastic syndromes. Blood. 1997;89(6):2079-2088.
4. Greenberg PL. Molecular and genetic features of myelodysplastic syndromes. Int J Lab Hematol. 2012;34(3):215-222.
5. Malcovati L, Porta MG, Pascutto C, et al. Prognostic factors and life expectancy in myelodysplastic syndromes classified according to WHO criteria: a basis for clinical decision making. J Clin Oncol. 2005;23(30):7594-7603.
6. Goldberg SL, Chen E, Corral M, et al. Incidence and clinical complications of myelodysplastic syndromes among United States Medicare beneficiaries. J Clin Oncol. 2010;28(17):2847-2852.
7. Della Porta MG, Malcovati L, Strupp C, et al. Risk stratification based on both disease status and extra-hematologic comorbidities in patients with myelodysplastic syndrome. Haematologica. 2011;96(3):441-449.
8. Efficace F, Gaidano G, Breccia M, et al. Prognostic value of self-reported fatigue on overall survival in patients with myelodysplastic syndromes: a multicentre, prospective, observational, cohort study. Lancet Oncol. 2015;16(15):1506-1514.
9. Efficace F, Gaidano G, Breccia M, et al. Prevalence, severity and correlates of fatigue in newly diagnosed patients with myelodysplastic syndromes. Br J Haematol. 2015;168(3):361-370.
10. Malcovati L, Della Porta MG, Strupp C, et al. Impact of the degree of anemia on the outcome of patients with myelodysplastic syndrome and its integration into the WHO classification-based Prognostic Scoring System (WPSS). Haematologica. 2011;96(10):1433-1440.
11. Wouters H, van der Klauw MM, de Witte T, et al. Association of anemia with health-related quality of life and survival: a large population-based cohort study. Haematologica. 2019;104(3):468-476.
12. Malcovati L, Galli A, Travaglino E, et al. Clinical significance of somatic mutation in unexplained blood cytopenia. Blood. 2017;129(25):3371-3378.
13. Malcovati L, Hellstrom-Lindberg E, Bowen D, et al. Diagnosis and treatment of primary myelodysplastic syndromes in adults: recommendations from the European LeukemiaNet. Blood. 2013;122(17):2943-2964.
14. Hellstrom-Lindberg E, Gulbrandsen N, Lindberg G, et al. A validated decision

model for treating the anaemia of myelodysplastic syndromes with erythropoietin + granulocyte colony-stimulating factor: significant effects on quality of life. Br J Haematol. 2003;120(6):1037-1046.

15. List A, Dewald G, Bennett J, et al. Lenalidomide in the myelodysplastic syndrome with chromosome 5q deletion. N Engl J Med. 2006;355(14):1456-1465.

16. Fenaux P, Giagounidis A, Selleslag D, et al. A randomized phase 3 study of lenalidomide versus placebo in RBC transfusion-dependent patients with Low-/Intermediate-1-risk myelodysplastic syndromes with del5q. Blood. 2011;118(14):3765-3776.

17. Della Porta MG, Malcovati L. Clinical relevance of extra-hematologic comorbidity in the management of patients with myelodysplastic syndrome. Haematologica. 2009;94(5):602-606.

18. Rochau U, Stojkov I, Conrads-Frank A, et al. Development of a core outcome set for myelodysplastic syndromes - a Delphi study from the EUMDS Registry Group. Br J Haematol. 2020 May 14. [Epub ahead of print]

19. Greenberg PL, Tuechler H, Schanz J, et al. Revised international prognostic scoring system for myelodysplastic syndromes. Blood. 2012;120(12):2454-2465.

20. Itzykson R, Crouch S, Travaglino E, et al. Early platelet count kinetics has prognostic value in lower-risk myelodysplastic syndromes. Blood Adv. 2018;2(16):2079-2089.

21. de Swart L, Crouch S, Hoeks M, et al. Impact of red blood cell transfusion dose density on progression-free survival in lower-risk myelodysplastic syndromes patients. Haematologica. 2020;105(3):632-639.

22. Stauder R, Lambert J, Desruol-Allardin S, et al. Patient-reported outcome measures in studies of myelodysplastic syndromes and acute myeloid leukemia: literature review and landscape analysis. Eur J Haematol. 2020;104(5):476-487.

23. Stauder R, Yu G, Koinig KA, et al. Health-related quality of life in lower-risk MDS patients compared with age- and sex-matched reference populations: a European LeukemiaNet study. Leukemia. 2018;32(6):1380-1392.

24. Brooks R. EuroQol: the current state of play. Health Policy. 1996;37(1):53-72.

25. Greiner W, Weijnen T, Nieuwenhuizen M, et al. A single European currency for EQ-5D health states. Results from a six-country study. Eur J Health Econ. 2003;4(3):222-231.

26. Langelaan M, de Boer MR, van Nispen RM, Wouters B, Moll AC, van Rens GH. Impact of visual impairment on quality of life: a comparison with quality of life in the general population and with other chronic conditions. Ophthalmic Epidemiol. 2007;14(3):119-126.

27. Abel GA, Efficace F, Buckstein RJ, et al. Prospective international validation of the Quality of Life in Myelodysplasia Scale (QUALMS). Haematologica. 2016;101(6):781-788.

28. Nilsson-Ehle H, Birgegard G, Samuelsson J, et al. Quality of life, physical function and MRI T2* in elderly low-risk MDS patients treated to a haemoglobin level of >/=120 g/L with darbepoetin alfa +/- filgrastim or erythrocyte transfusions. Eur J Haematol. 2011;87(3):244-252.

29. Platzbecker U, Symeonidis A, Oliva EN, et al. A phase 3 randomized placebo-controlled trial of darbepoetin alfa in patients with anemia and lower-risk myelodysplastic syndromes. Leukemia. 2017;31(9):1944-1950.

30. Jadersten M, Malcovati L, Dybedal I, et al. Erythropoietin and granulocyte-colony stimulating factor treatment associated with improved survival in myelodysplastic syndrome. J Clin Oncol. 2008;26(21):3607-3613.

31. Park S, Grabar S, Kelaidi C, et al. Predictive factors of response and survival in myelodysplastic syndrome treated with erythropoietin and G-CSF: the GFM experience. Blood. 2008;111(2):574-582.

32. Garelius HK, Johnston WT, Smith AG, et al. Erythropoiesis-stimulating agents significantly delay the onset of a regular transfusion need in nontransfused patients with lower-risk myelodysplastic syndrome. J Intern Med. 2017;281(3):284-299.

33. Shenoy N, Vallumsetla N, Rachmilewitz E, Verma A, Ginzburg Y. Impact of iron overload and potential benefit from iron chelation in low-risk myelodysplastic syndrome. Blood. 2014;124(6):873-881.

34. Ganz T. Hepcidin and iron regulation, 10 years later. Blood. 2011;117(17):4425-4433.

35. de Swart L, Reiniers C, Bagguley T, et al. Labile plasma iron levels predict survival in patients with lower-risk myelodysplastic syndromes. Haematologica. 2018;103(1):69-79.

36. Porter JB, de Witte T, Cappellini MD, Gattermann N. New insights into transfusion-related iron toxicity: implications for the oncologist. Crit Rev Oncol Hematol. 2016;99:261-271.

37. Neukirchen J, Fox F, Kundgen A, et al. Improved survival in MDS patients receiving iron chelation therapy - a matched pair analysis of 188 patients from the Dusseldorf MDS registry. Leuk Res. 2012;36(8):1067-1070.

38. Rose C, Brechignac S, Vassilief D, et al. Does iron chelation therapy improve survival in regularly transfused lower risk MDS patients? A multicenter study by the GFM (Groupe Francophone des Myelodysplasies). Leuk Res. 2010;34(7):864-870.

39. Gattermann N, Finelli C, Della Porta M, et al. Hematologic responses to deferasirox therapy in transfusion-dependent patients with myelodysplastic syndromes. Haematologica. 2012;97(9):1364-1371.

40. Angelucci E, Santini V, Di Tucci AA, et al. Deferasirox for transfusion-dependent patients with myelodysplastic syndromes: safety, efficacy, and beyond (GIMEMA MDS0306 Trial). Eur J Haematol. 2014;92(6):527-536.

41. Breccia M, Voso MT, Aloe Spiriti MA, et al. An increase in hemoglobin, platelets and white blood cells levels by iron chelation as single treatment in multitransfused patients with myelodysplastic syndromes: clinical evidences and possible biological mechanisms. Ann Hematol. 2015;94(5):771-777.

42. Angelucci E, Li J, Greenberg P, et al. Iron chelation in transfusion-dependent patients with low- to intermediate-1-risk myelodysplastic syndromes: a randomized trial. Ann Intern Med. 2020;172(8):513-522.

43. Schafer AI, Cheron RG, Dluhy R, et al. Clinical consequences of acquired transfusional iron overload in adults. N Eng J Med. 1981;304(6):319-324.

44. de Swart L, Hendriks JC, van der Vorm LN, et al. Second international round robin for the quantification of serum non-transferrin-bound iron and labile plasma iron in patients with iron-overload disorders. Haematologica. 2016;101(1):38-45.

45. Malcovati L, Karimi M, Papaemmanuil E, et al. SF3B1 mutation identifies a distinct subset of myelodysplastic syndrome with ring sideroblasts. Blood. 2015;126(2):233-241.

46. Fenaux P, Kiladjian JJ, Platzbecker U. Luspatercept for the treatment of anemia in myelodysplastic syndromes and primary myelofibrosis. Blood. 2019;133(8):790-794.

Pediatric acute lymphoblastic leukemia

Hiroto Inaba[1,2] and Charles G. Mullighan[2,3]

[1]Department of Oncology; [2]Hematological Malignancies Program and [3]Department of Pathology, St. Jude Children's Research Hospital, Memphis, TN, USA

ABSTRACT

The last decade has witnessed great advances in our understanding of the genetic and biological basis of childhood acute lymphoblastic leukemia (ALL), the development of experimental models to probe mechanisms and evaluate new therapies, and the development of more efficacious treatment stratification. Genomic analyses have revolutionized our understanding of the molecular taxonomy of ALL, and these advances have led the push to implement genome and transcriptome characterization in the clinical management of ALL to facilitate more accurate risk-stratification and, in some cases, targeted therapy. Although mutation- or pathway-directed targeted therapy (e.g., using tyrosine kinase inhibitors to treat Philadelphia chromosome [Ph]-positive and Ph-like B-cell-ALL) is currently available for only a minority of children with ALL, many of the newly identified molecular alterations have led to the exploration of approaches targeting deregulated cell pathways. The efficacy of cellular or humoral immunotherapy has been demonstrated with the success of chimeric antigen receptor T-cell therapy and the bispecific engager blinatumomab in treating advanced disease. This review describes key advances in our understanding of the biology of ALL and optimal approaches to risk-stratification and therapy, and it suggests key areas for basic and clinical research.

Introduction

Contemporary childhood ALL studies have shown improved 5-year overall survival (OS) rates exceeding 90% (Table 1).[1-9] However, OS for the St. Jude Total Therapy Study XVI (94.3%) was similar to that for the Total Therapy Study XV (93.5%) (Figure 1).[9] Therefore, with the conventional approach, the chemotherapy intensity has been raised to the limit of tolerance, and further improvements in outcomes and reduction of adverse effects will require novel therapeutic approaches. Historically, genetic factors identified by conventional karyotyping have been used to diagnose ALL and to risk-stratify children with the disease. However, the alterations thus identified, including hyper- and hypodiploidy and several chromosomal rearrangements, did not establish the basis of ALL in a substantial minority of children; nor did they satisfactorily reveal the nature of the genetic alterations driving leukemogenesis. Genomic studies have now clarified the subclassification of ALL and have demonstrated a close interplay between inherited and somatic genetic alterations in the biology of ALL. Many of these alterations have important implications for diagnosis and risk-stratification of ALL and for the use and development of novel and targeted approaches.

Heritable susceptibility to acute lymphoblastic leukemia

Several lines of evidence indicate that there is a genetic predisposition to acute lymphoblastic leukemia (ALL), at least in a subset of cases. This evidence includes the existence of: (i) rare constitutional syndromes with increased risk for ALL; (ii) familial cancer syndromes; (iii) non-coding DNA polymorphisms that subtly influence the risk of ALL; and (iv) genes harboring germline non-silent variants presumed to confer a risk of sporadic ALL. Constitutional syndromes such as Down syndrome and ataxia-telangiectasia are associated with increased risk of B-cell-ALL (with *CRLF2* rearrangement) and T-cell-ALL, respectively. Familial cancer syndromes such as Li-Fraumeni syndrome, constitutional mismatch repair deficiency syndrome, or DNA repair syndromes (e.g., Nijmegen breakage) have an increased

incidence of malignancy in general. Familial predisposition specific to leukemia is uncommon but has resulted in the identification of predisposing non-silent variants that are also observed in sporadic ALL cases, including *TP53* germline mutations and low hypodiploid B-ALL, *ETV6* variants and hyperdiploid ALL, and *PAX5* mutations and B-ALL with dicentric/isochromosome 9.[10-13] These suscep-

tibility genes are targets of somatic mutation in ALL: *ETV6* and *PAX5* are rearranged, amplified/deleted, and mutated in B-ALL,[14,15] as is *TP53* in hypodiploid ALL.[10] Germline variants of *IKZF1* are observed in familial B-ALL and immunodeficiency,[16,17] and somatic *IKZF1* alterations are enriched in Philadelphia chromosome (Ph)-positive, Ph-like, and *DUX4*-rearranged B-ALL.[18-20] *RUNX1* germline

Table 1A. Treatment results for acute lymphoblastic leukemia in major pediatric clinical trials.

Study	Years of study	Subtype	Age (y)	Patients (n)	Steroid during induction (mg/m²/day)	MTX (g/m²/dose)	Cranial irradiation	Complete remission (%)	Cumulative incidence of relapse (5y, %) (SE or 95% CI)	Death in remission (5y, %) (SE or 95% CI)	Event-free survival (5y, %) (SE or 95% CI)	Overall survival (5y, %) (SE or 95% CI)
AIEOP/BFM ALL 2000	2000-2006	B and T	1-17	3720 (randomized pts)	Pred 60 (1867 pts) /Dex 10 (1853 pts) [R]	5	HR/T /CNS3	Pred: 97.8 Dex: 97.8 (P=1.00)	Pred: 15.6 (0.8) Dex: 10.8 (0.7) (P<0.001)	Pred: 1.7 Dex: 2.3 (P=0.24)	Pred: 80.8 (0.9) Dex: 83.9 (0.9) (P=0.024)	Pred: 90.5 (0.7) Dex: 90.3 (0.7) (P=0.61)
COG AALL0232	2004-2011	B, HR	1-30	2979	Pred 60 (427 pts)/ Dex 10 (424 pts) [R] (aged 1-9 y)	HD-MTX 5 (1282 pts)/ C-MTX (1291 pts) [R]	SER/ CNS3	NA	HD-MTX: 136 pts C-MTX: 183 pts	HD-MTX: 24 pts C-MTX: 25 pts (P=0.90)	75.3 (1.1) HD-MTX: 79.6 (1.6) C-MTX: 75.2 (1.7) (P=0.008)	85.0 (0.9) HD-MTX: 88.9 (1.2) C-MTX: 86.1 (1.4) (P=0.025)
COG AALL0331	2005-2010	B, SR	1-9	5377	Dex 6	0.1 (and escalating) with or without asparaginase	CNS3	98.0	124 of 3992 pts who continued post-induction	25 of 3992 pts who continued post-induction	88.96 (0.46) (6y)	95.54 (0.31) (6y)
COG AALL0434	2007-2014	T	1-30	1562	Pred 60	HD-MTX 5 (512 pts)/ C-MTX (519 pts) [R]	IR/HR	NA	HD-MTX: 59 pts C-MTX: 32 pts	HD-MTX: 11 pts C-MTX: 8 pts	83.8 (81.2-86.4) (5y DFS) HD-MTX: 85.3 (81.0-89.5) C-MTX: 91.5 (88.1-94.8) (P=0.005)	89.5 (87.4-91.7) HD-MTX: 89.4 (85.7-93.2) C-MTX: 93.7 (90.8-96.6) (P=0.036)
DFCI ALL Consortium Protocol 05-001	2005-2010	B and T	1-18	551	Pred 40	5	CNS3/T/B with WBC ≥100k/VHR	95.5	51 of 551 total 41 of 463 pts randomized PEG: 20 of 232 Native: 21 of 231	2 of 551 total	85 (82-88) (5y DFS) PEG: 90 (86-94) Native: 89 (85-93) (P=0.58)	91 (88-93) PEG: 96 (93-98) Native: 94 (89-96) (P=0.30)
DCOG ALL10	2004-2012	B and T	1-18	778	Pred 60	5	>3y and HR who do not receive HCT	98.0	8.3 (1.0)	2.6	87.0 (1.2)	91.9 (1.0)
MRC UK ALL 2003	2003-2011	B and T	1-24	3126	Dex 6	0.02 (SR/IR), C-MTX (HR)	CNS3 (until 2009)	98.9	8.8 (7.8-9.8)	2.7 (2.1-3.3)	87.3 (86.1-88.5)	91.6 (90.6-92.6)
NOPHO ALL2008	2008-2014	B and T	1-45	1509	Pred 60 or Dex 10 (T/WBC≥100k)	5	None	91.2	10 (1)	3 (0)	85 (1)	91 (1)
SJCRH Total XVI	2007-2017	B and T	0-18	598	Pred 40	2.5 (LR), 5 (SR/HR)	None	98.7	6.6 (4.4-8.7)	2.7 (1.4-4.0)	88.2 (84.9-91.5)	94.1 (91.7-96.5)

Table 1B. Major findings in the study reports.

Study	Years of study	
AIEOP/BFM ALL 2000	2000-2006	Dexamethasone in induction resulted in less relapse but more treatment-related mortality than did prednisone. There was no survival benefit with dexamethasone except for T-ALL patients with good prednisone response.
COG AALL0232	2004-2011	5-y EFS and OS were better with HD-MTX than with C-MTX. Patients aged 1-9 y who received dexamethasone and HD-MTX had better outcomes than those in other groups.
COG AALL0331	2005-2010	SR patients had excellent outcomes. Adding intensified consolidation did not improve outcomes in patients with SR-average disease.
COG AALL0434	2007-2014	5-y DFS and OS were better with C-MTX than with HD-MTX.
DFCI ALL Consortium Protocol 05-001	2005-2010	IV PEG-asparaginase had similar toxicity and efficacy and resulted in less anxiety when compared with IM native *E. coli* asparaginase.
DCOG ALL10	2004-2012	MRD-based therapy reduction and intensification were successful.
MRC UK ALL 2003	2003-2011	MRD-based therapy reduction and intensification were successful.
NOPHO ALL2008	2008-2014	Pediatric-based protocol is tolerable and effective for young adults.
SJCRH Total XVI	2007-2017	Additional intrathecal therapy during early induction improved CNS control (any CNS relapse at 5-y: 1.5%).

AIEOP/BFM: Associazione Italiana di Ematologia e Oncologia Pediatrica/Berlin-Frankfurt-Münster; ALL: acute lymphoblastic leukemia; B: B-lineage; CI: confidence interval; CNS: central nervous system; C-MTX: Capizzi methotrexate; COG: Children's Oncology Group; DCOG: Dutch Childhood Oncology Group; Dex: dexamethasone; DFCI: Dana-Farber Cancer Institute; DFS: disease-free-survival; EFS: event-free survival; HD-MTX: high-dose methotrexate; HCT: hematopoietic cell transplantation; HR: high-risk; IM: intramuscular; IR: intermediate-risk; IV: intravenous; k.× 10³/μL; LR: low-risk; MRC UK: Medical Research Council United Kingdom; MRD: minimal residual disease; MTX: methotrexate; n: number; NA: not available; NOPHO: Nordic Society of Pediatric Hematology and Oncology; OS: overall survival; PEG: polyethylene glycol; Pred: prednisolone; pts: patients; R: randomization; SE: standard error; SER: slow early response; SJCRH: St. Jude Children's Research Hospital; SR: standard-risk; T: T-lineage; WBC: white blood cell; y: year.

mutations can lead to both T-ALL and AML, and *ETV6* variants predispose carriers to B-ALL and myelodysplasia.[21,22]

Genome-wide association studies (GWAS) have identified non-coding variants in at least 13 loci associated with ALL. The relative risk associated with each variant is typically low (corresponding to an increase of up to 1.5- or 2-fold) but cumulatively, they may result in an increase of up to 10-fold in ALL risk. Risk variants are frequently at/near hematopoietic transcription factor or tumor suppressor genes, including *ARID5B*, *BAK1*, *CDKN2A/CDKN2B*, *BMI1-PIP4K2A*, *CEBPE*, *ELK3*, *ERG*, *GATA3*, *IGF2BP1*, *IKZF1*, *IKZF3*, *USP7*, and *LHPP*.[23-25] Several variants display ancestry and ALL subtype-specific associations, such as those of *GATA3* with Hispanics and Ph-like B-ALL, *ERG* with African Americans and *TCF3-PBX1* B-ALL, and *USP7* with African Americans and T-ALL with *TAL1* deregulation.[26-28]

Finally, germline genomic analysis has identified additional susceptibility variants in sporadic hyperdiploid B-ALL (*NBN*, *ETV6*, *FLT3*, *SH2B3*, and *CREBBP*), Down syndrome-associated B-ALL (*IKZF1*, *NBN*, *RTEL1*), and T-ALL (Fanconi-BRCA pathway mutations).[29-31]

Prenatal origin of leukemia

Several lines of investigation indicate that a subset of childhood leukemia cases arise before birth.[32,33] Chromosomal translocations, particularly *ETV6-RUNX1* (*TEL-AML1*) may be detected at birth in blood spots and cord blood years before the clinical onset of leukemia, providing support for a multi-step process of leukemogenesis. This is supported by genomic analyses of monozygotic, monochorionic twins concordant for leukemia, showing genetic identity of initiating lesions and discordance for secondary genetic alterations indicating inter-twin, intrauterine transmission of leukemia.[33,34] Evidence for *in utero* origin is strongest for *KMT2A*-rearranged and *ETV6-RUNX1* ALL. Anecdotal evidence supports *in utero* origin for other subtypes of B-ALL, including hyperdiploid and *ZNF384*-rearranged leukemia.[35]

Genetics of B-cell acute lymphoblastic leukemia

B-cell acute lymphoblastic leukemia (B-ALL) is the most common form of ALL, comprising >20 subtypes of variable prevalence according to age that are associated with distinct gene expression profiles and are driven by three main types of initiating genetic alteration: chromosomal aneuploidy, rearrangements that deregulate oncogenes or encode chimeric transcription factors, and point mutations (Table 2 and Figure 2). Each subtype typically has co-occurring genetic alterations that perturb lymphoid development, cell-cycle regulation, and kinase signaling and chromatin regulation, and the genes involved and their frequency of involvement vary between subtypes.[36]

High hyperdiploidy (>50 chromosomes) is present in up to 30% of childhood ALL and is associated with mutations in the Ras pathway, chromatin modifiers such as CREBBP, and favorable outcomes.[37] Low hypodiploidy (31-39 chromosomes) is present in approximately 1% of children with ALL but in >10% of adults. It is characterized by the deletion of *IKZF2* and by near-universal *TP53* mutations, which are inherited in approximately half the cases.[10] Near haploidy (24-30 chromosomes) is present in approximately 2% of pediatric ALL and is associated with Ras mutations (particularly *NF1*) and deletions of *IKZF3*. Both low-hypodiploid and near-haploid ALL are associated with unfavorable outcomes. The prevalence of hypodiploidy may be underestimated because of the phenomenon of "masked" hypodiploidy, in which the hypodiploid genome is duplicated, leading to a hyperdiploid modal chromosome number.[10,38] Distinguishing masked-hypodiploid ALL from high-hyperdiploid ALL is important in view of the genetic (germline *TP53* alterations) and prognostic implications. Masked hypodiploidy may be suspected by the patterns of chromosomal gain (commonly diploid and tetrasomic chromosomes, rather than trisomies in high-hyperdiploid ALL) and may be formally confirmed by flow cytometric analysis of the DNA index, which commonly shows peaks for both non-masked and masked clones, and by techniques that assess loss of heterozygosity, such as SNP
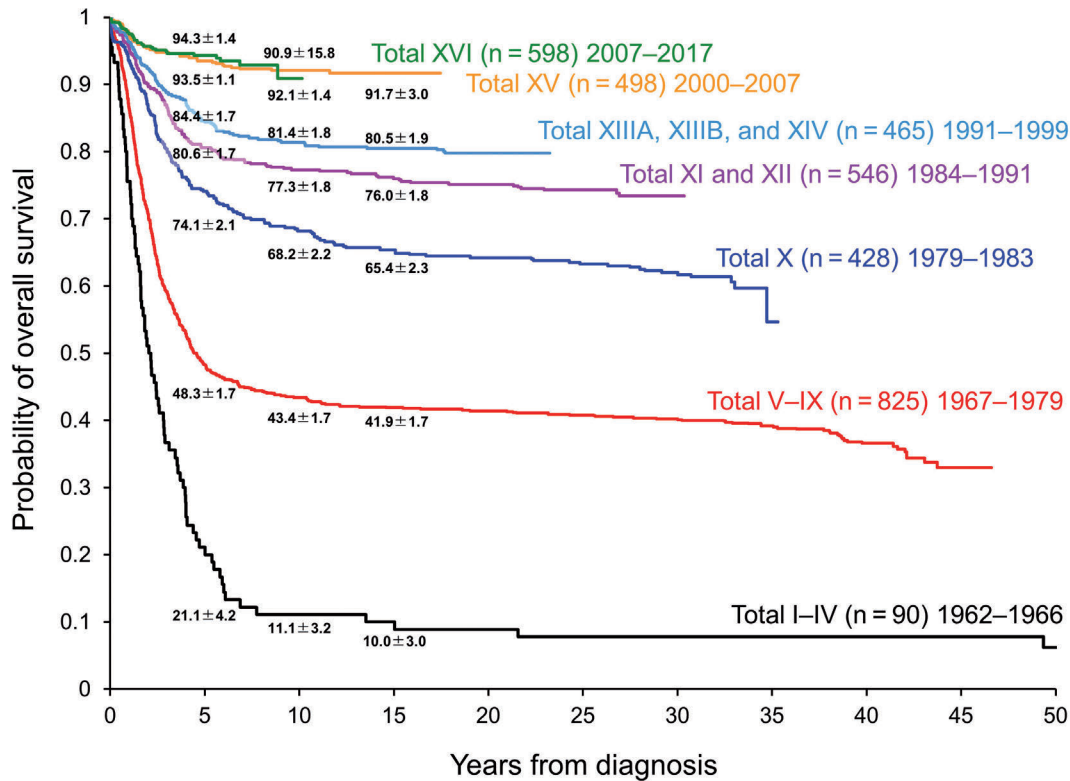
Figure 1. Change in overall survival of pediatric patients treated on the historical St. Jude Total Therapy studies.

arrays. In addition, the transcriptomic profiles and co-occurring genetic alterations (e.g., Ras pathway and *CREBBP* alterations) of near-haploid and high-hyperdiploid ALL are similar, suggesting a common origin for these entities.[15] ALL with intrachromosomal amplification of chromosome 21 (iAMP21) is most common in older children and is associated with poor prognosis, which has been improved with intensive treatment.[39]

Of the subtypes characterized by translocations, the most common in childhood B-ALL is t(12;21)(p13;q22) encoding *ETV6-RUNX1*, which is typically cryptic on cytogenetic analysis and is associated with favorable prognosis. The t(1;19)(q23;p13) translocation and variants encode *TCF3-PBX1*,[40] which is more common in African Americans and is associated with more frequent central nervous system (CNS) relapse and inferior outcomes with older,[41] but not contemporary, treatment regimens.[9] The t(9;22)(q34;q11.2) translocation results in the formation of the Philadelphia chromosome that encodes *BCR-ABL1* and is found in a subset of childhood ALL that was also associated with unfavorable outcomes, although the prognosis has now been improved with combined chemotherapy and tyrosine kinase inhibition.[42] Rearrangement of *KMT2A* (*MLL*) at 11q23 to >80 partners, most commonly t(4;11)(q21;q23) encoding *KMT2A-AFF1*, is common in infant ALL and is associated with a dismal prognosis.

Genomic analyses, particularly transcriptome sequencing, have identified multiple new subtypes not evident on cytogenetic analysis because of cryptic and/or diverse rearrangements or sequence mutations acting as driver lesions. *ETV6-RUNX1*–like ALL is characterized by a gene expression profile and immunophenotype (CD27^{+}, CD44 low/negative) similar to that of *ETV6-RUNX1* ALL.[43,44] Such patients harbor alternate gene fusions or copy number alterations in ETS-family transcription factors (*ETV6, ERG, FLI1*), *IKZF1*, or *TCF3*. *ETV6-RUNX1*–like ALL occurs almost exclusively in children (representing ~3% of pediatric ALL) and is associated with relatively favorable prognosis.[15]

Translocation of *DUX4*, encoding a double-homeobox transcription factor, to the immunoglobulin heavy-chain locus (*IGH*) is also cytogenetically cryptic and is found in 5-10% of B-ALL. The translocation results in overexpression of DUX4 protein lacking the C-terminal domain. This truncated protein binds an intragenic region of the ETS-family transcription factor *ERG* (ETS-related gene), resulting in profound transcriptional deregulation of *ERG*. This in turn commonly results in expression of a C-terminal ERG protein fragment and/or *ERG* deletion. *DUX4*-rearranged B-ALL has a distinctive gene expression profile and immunophenotype (CD2[±], CD371^{+}), and despite the deletion of *IKZF1* (otherwise an adverse prognostic factor in ALL) in approximately 40% of cases, the outcome is typically excellent.[20,45]

ZNF384 rearrangement defines a distinct group of acute leukemias that may manifest as B-ALL (often with aberrant myeloid marker expression) or B/myeloid mixed-phenotype acute leukemia (MPAL; MPO-positive leukemia). *ZNF384* rearrangement is observed in 6% of childhood B-ALL and in 48% of childhood (but notably not adult) B/myeloid MPAL.[15,46-48] *ZNF384*-like cases, often with *ZNF362* rearrangements, are also observed. Both *ZNF384* and *ZNF362* encode C2H2-type zinc-finger tran-

scription factors and are rearranged with genes encoding N-terminal transcription factors (e.g., *TAF15* and *TCF3*) or chromatin modifiers (most commonly *EP300*, but also *CREBBP*, *SMARCA2*, and *ARID1B*).[47] *ZNF384*-rearranged leukemia is associated with elevated FLT3 expression, and there are anecdotal reports of profound responses to FLT3 inhibition.[49] The lineage-ambiguous phenotype of *ZNF384*-rearranged leukemia may shift during the disease course and may result in loss of CD19 expression and failure of chimeric antigen receptor T-cell therapy.[50]

MEF2D (myocyte enhancer factor 2D)-rearranged ALL (occurring in 4% of children and up to 10% of adults with ALL) has a distinct immunophenotype (CD10-, CD38+), an older age of diagnosis (median: 14-15 years), and a poor prognosis.[51-53] The rearrangements result in increased *HDAC9* expression and sensitivity to histone deacetylase inhibitor treatment.[51]

NUTM1 (nuclear protein in testis midline carcinoma family 1) rearrangements are observed in 1-2% of childhood B-ALL, with fusion to genes encoding various transcription factors and epigenetic regulators (e.g., *ACIN1*, *BRD9*, *CUX1*, *IKZF1*, *SLC12A6*, and *ZNF618*) that drive aberrant *NUTM1* expression.[15,47] In all fusions, the NUT domain is retained, and this is hypothesized to lead to global changes in chromatin acetylation and to sensitivity to histone deacetylase inhibitors or bromodomain inhibitors. ALL with *NUTM1* rearrangements has an excellent prognosis.

Other transcription factor-driven subtypes of B-cell acute lymphoblastic leukemia

Two B-ALL subtypes have distinct alterations of the lymphoid transcription factor PAX5. PAX5-altered (PAX5alt) B-ALL accounts for 10% of childhood B-ALL, with cases featuring diverse *PAX5* alterations, including rearrangements (most commonly with *ETV6* or *NOL4L*), sequence mutations or intragenic amplification,[54] and an intermediate prognosis.[15,47] *PAX5* P80R B-ALL accounts for approximately 2% of childhood B-ALL, with cases featuring universal P80R mutation and deletion/mutation of the remaining allele,[15,47,55] mutations in Ras and *JAK2* signaling genes, and an intermediate to favorable prognosis.[15,55] A single heterozygous mutation in *IKZF1* (N159Y) defines a novel subtype of ALL (representing <1% of cases) with IKZF1 nuclear mislocalization, enhanced intercellular adhesion,[56] and expression of genes involved in oncogenesis (*YAP1*), chromatin remodeling (*SALL1*), and JAK-STAT signaling.[15,47] The *IGH-CEBPE* fusion and ZEB2 H1038R mutation are common, but not universal, events in a transcriptionally distinct form of leukemia observed in approximately 1% of cases.

Kinase-driven subtypes

Of therapeutic relevance are the two kinase-driven subtypes: Philadelphia chromosome-positive (Ph+ or *BCR-ABL1*+) and Philadelphia chromosome-like (Ph-like or *BCR-ABL1*-like) ALL. Their frequency increases with age,[57]
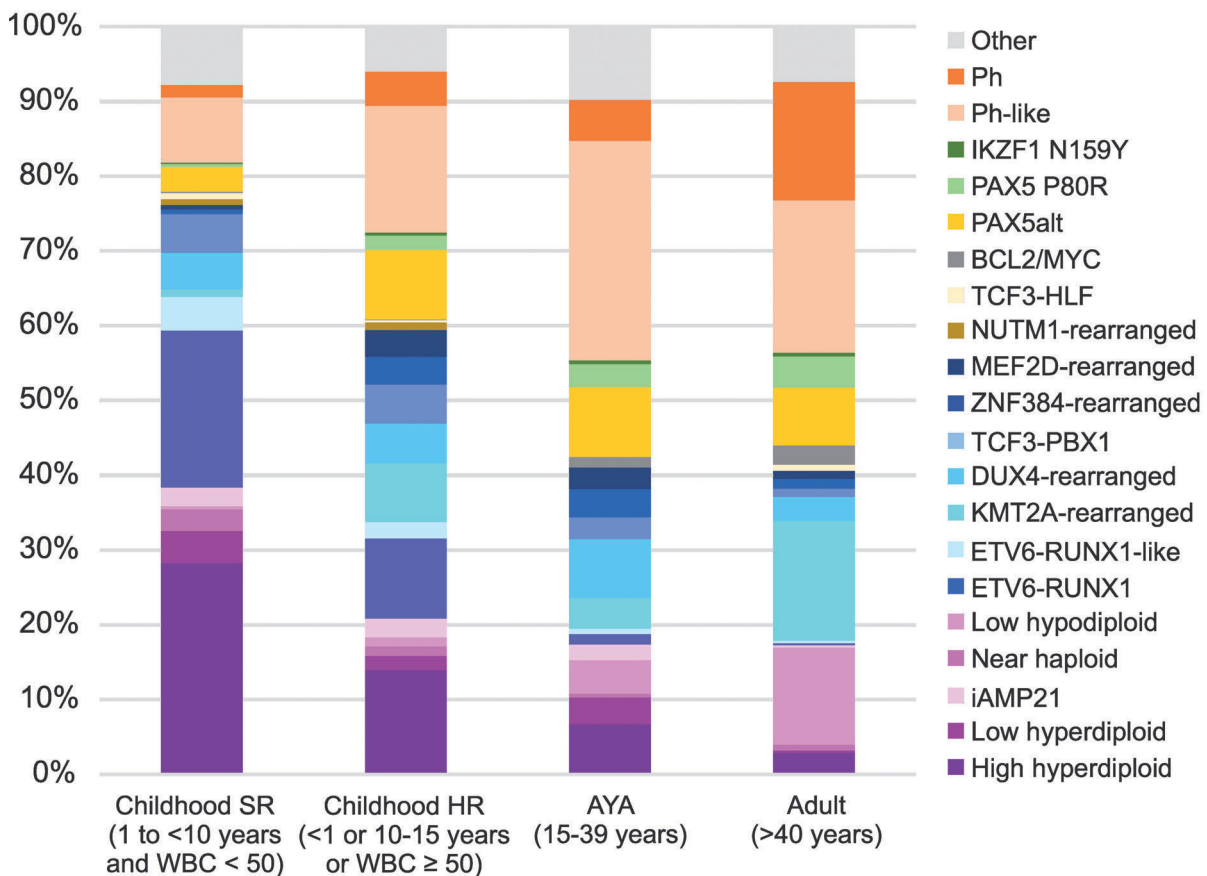
Figure 2. Distribution of B-cell acute lymphoblastic leukemia (B-ALL) subtypes within each age group. SR: standard risk; HR: high risk; WBC: white blood cell count; AYA: adolescent and young adult.

Table 2. Genetic alterations, age distribution, clinical features, and genetic-based therapy in pediatric B- and T-acute lymphoblastic leukemia.

Category	Age	Description	Potential therapeutic implications
B-cell precursor acute lymphoblastic leukemia			
Hyperdiploidy with more than 50 chromosomes	Children >> adults	Excellent prognosis; mutations in Ras signaling pathway and histone modifiers	Reduction of intensity
Near-haploid	Children-adults	24-31 chromosomes; poor prognosis; Ras-activating mutations; inactivation of *IKZF3*	BCL2 inhibitors
Low hypodiploid	Children < adults	32-39 chromosomes; poor prognosis; TP53 mutations (somatic and germline)	BCL2 inhibitors
iAMP21	Older children	Complex alterations of chromosome 21; requires high-risk therapy for good outcomes	Intensification of therapy
t(12;21)(p13;q22) encoding *ETV6-RUNX1*	Children >> adults	Excellent prognosis; cryptic rearrangement that is detectable by FISH	Reduction of intensity
ETV6-RUNX1–like	Children > adults	Absence of *ETV6-RUNX1* fusion; mutations in both *ETV6* and *IKZF1*	Reduction of intensity
t(1;19)(q23;p13) encoding *TCF3-PBX1*	Children-adults	Increased incidence in African Americans; favorable prognosis	
t(9;22)(q34;q11.2) encoding BCR-ABL1	Children << adults	Historically poor prognosis, improved with tyrosine kinase inhibitors; common deletions of IKZF1	ABL1 inhibitors, FAK inhibitors, rexinoids, BCL2 inhibitors
Ph-like	Children < adults	Kinase-activating lesions; poor outcome; potentially amenable to kinase inhibition	ABL1 inhibitors, JAK inhibitors, PI3K inhibitors, BCL2 inhibitors
CRLF2 rearranged (*IGH-CRLF2*; *P2RY8-CRLF2*)	Children < adults	Common in Down syndrome and Ph-like ALL; associated with *IKZF1* deletion and *JAK1/2* mutation	JAK inhibitors, BCL2 inhibitors
KMT2A (*MLL*) rearranged	Infants >> children-adults	Common in infant ALL; dismal prognosis; few co-operating mutations, commonly in RAS signaling pathway	DOT1L inhibitors, menin inhibitors, proteasome inhibitors, HDAC inhibitors, BCL2 inhibitors
DUX4 rearranged and *ERG* deregulated	Children-adults	Distinct gene expression profile; most have focal ERG deletions and favorable outcome despite *IKZF1* alterations	Reduction of intensity
MEF2D rearranged	Children-adults	Distinct gene expression profile; potential sensitivity to HDAC inhibition	HDAC inhibitors
ZNF384 rearranged	Children	Pro-B ALL phenotype; expression of myeloid markers; increased expression of *FLT3*	FLT3 inhibitors
PAX5alt	Children > adults	PAX5 fusions, mutation, or amplifications; intermediate prognosis	
PAX5 P80R	Children < adults	Frequent signaling pathway alterations	Kinase inhibitors
IKZF1 N159Y	Children-adults	Rare; unknown prognosis	FAK inhibitors, rexinoids
NUTM1 rearranged	Children	Exclusively in children; rare; excellent prognosis	HDAC inhibitors, bromodomain inhibitors
t(17;19)(q22;p13) encoding TCF3-HLF	Children-adults	Rare; dismal prognosis	BCL2 inhibitors
BCL2/MYC rearranged	Children << adults	Poor prognosis	
T-lineage acute lymphoblastic leukemia			
TAL1 deregulation	Children-adults	Enrichment of mutation in PI3K signaling pathway	PI3K inhibitors, nelarabine, BCL2 inhibitors
TLX3 deregulation	Children-adults	Poor prognosis; frequent co-operating mutation in ubiquitination and ribosomal genes	Nelarabine, BCL2 inhibitors
HOXA deregulation	Children-adults	Frequent mutations in JAK-STAT pathway, *KMT2A* rearrangements	JAK inhibitors, nelarabine, BCL2 inhibitors
TLX1 deregulation	Children > adults	Favorable prognosis	Nelarabine, BCL2 inhibitors
LMO2/LYL1 deregulation	Children-adults	Poor prognosis; enriched for ETP-ALL, frequent co-operating mutation in JAK-/STAT	JAK inhibitors, nelarabine, BCL2 inhibitors
NKX2-1 deregulation	Children-adults	Frequent co-operating mutation in ribosomal genes	Nelarabine, BCL2 inhibitors
NUP214-ABL1 with 9q34 amplification	Children-adults	Neutral prognosis, in contrast to kinase driven B-ALL; potentially amenable to tyrosine kinase inhibition	ABL1 inhibitors, nelarabine, BCL2 inhibitors
Early T-cell precursor ALL	Children-adults	Poor prognosis; genetically heterogeneous with mutations in hematopoietic regulators, cytokine and Ras signaling, and epigenetic modifiers	JAK inhibitors, BCL2 inhibitors

FISH: fluorescence *in situ* hybridization; ALL: acute lymphoblastic leukemia; HDAC: histone deacetylase.

and they account for 25% and 20%, respectively, of adult ALL. The prevalence of *BCR-ABL1* ALL rises progressively from <20% of ALL in adults younger than 25 years to more than half of adults aged 50-60 years, whereas the prevalence of Ph-like ALL peaks in young adulthood, and this subtype is observed in up to 25% of adults. Alterations of B-lineage transcription factor genes, particularly *IKZF1*, are a hallmark of *BCR-ABL1* ALL[18] and are a key determinant of lymphoid lineage and resistance to therapy.[56] *IKZF1* alterations are associated with poor outcome in ALL overall,[19] particularly because of the high prevalence in *BCR-ABL1* and Ph-like ALL; however, they are not associated with poor outcome in *DUX4*-rearranged ALL. This has led to the definition of "IKZF1-plus" as a marker of poor outcome in ALL, being defined by the presence of alterations in *IKZF1* and *CDKN2A/B*, *PAX5*, or pseudoautosomal region 1 (PAR1, as a surrogate for *CRLF2* rearrangement), but not *ERG* (as a surrogate for *DUX4*-rearranged ALL), commonly detected by multiplex ligation-dependent probe amplification (MLPA).[58] Although used for risk-stratification in several clinical trials, the utility of this approach is limited by the inability of MLPA to identify all cases with key high-risk (*CRLF2* rearrangement) and favorable-risk (*DUX4* rearrangements) that co-occur with *IKZF1* alterations.

Ph-like ALL has a similar transcriptional profile to Ph-positive ALL but is *BCR-ABL1* negative.[19,59] It is genetically heterogeneous with multiple rearrangements (e.g., of *CRLF2*, *ABL*-class genes, *JAK-STAT* signaling genes, *FGFR1*, and/or *NTRK3*), copy number alterations, and sequence mutations that activate tyrosine kinase or cytokine receptor signaling (Figure 3). Ph-like ALL is associated with elevated minimal residual disease (MRD) levels and/or high rates of treatment failure. The diverse genetic alterations characteristic of Ph-like ALL and its responsiveness to tyrosine kinase inhibitors (at least for *ABL*-class and *NTRK3*-rearranged ALL) have spurred the use of RNA-sequencing approaches to identify such alterations at diagnosis and direct patients to targeted therapy.[36]

Genetic basis of T-cell acute lymphoblastic leukemia

Childhood T-cell acute lymphoblastic leukemia is characterized by recurrent alterations in ten pathways, but in most cases, three pathways are deregulated: expression of T-lineage transcription factors, NOTCH1/MYC signaling, and cell-cycle control. Gene expression profiling enables classification of >90% of T-ALL into core subgroups defined by deregulation of T-ALL transcription factors as a result of rearrangement with T-cell receptor enhancers, structural variants, or enhancer mutations of *TAL1*, *TAL2*, *TLX1*, *TLX*, *HOXA*, *LMO1/LMO2*, *LMO2/LYL1*, or *NKX2-1* (Table 2).[60-62] A more recently described mechanism of deregulation is through small insertion/deletion mutations upstream of *TAL1*, which lead to a new binding motif for MYB or TCF1/TCF2 and subsequent changes in *TAL1* expression.[62,63] A similar mechanism has been described for other oncogenes in T-ALL, including *LMO2*.[64] Additional transcription factor genes, including *ETV6*, *RUNX1*, and *GATA3*, are altered by deletion or sequence mutation but are not subtype-defining.[65-67] The second core transcriptional pathway mutation found in most T-ALL cases is aberrant activation of *NOTCH1*, a critical transcription factor for T-cell development.[68] Constitutive *NOTCH1* activity, caused by activating *NOTCH1* mutations (in >75% of cases) and/or inhibitor

mutations in the negative regulator *FBXW7* (in 25% of cases), promotes uncontrolled cell growth, partly through increased *MYC* expression.[69-71] The third core alteration observed in pediatric T-ALL is deletion of tumor suppressor loci, primarily *CDKN2A/CDKN2B* (in 80% of cases) and, less commonly, *CDKN1B*, *RB1*, or *CCND3*.[62,72]

In addition to the aforementioned core alterations, T-ALL frequently involves derangement of additional transcriptional regulators (*MYB*, *LEF1*, and *BCL11B*), ribosomal function, ubiquitination through loss-of-function *USP7* mutations, RNA processing, signaling pathways, and epigenetic modifiers such as *PHF6*, *KDM6A*, and genes of polycomb repressive complex 2 (*EED*, *SUZ12*, and *EZH2*).[62] The signaling pathway most commonly activated is PI3K-AKT, through loss of negative regulation by PTEN.[73] JAK-STAT pathway activation can occur through gain-of-function mutations in *IL7R*, *JAK1*, *JAK3*, or *STAT5B* or through loss-of-function alterations in the JAK-STAT regulators *PTPN2* and *SH2B3*,[74,75] whereas mutations in RAS-MAPK signaling are less common, except in early T-cell precursor (ETP) ALL. Kinase rearrangements are observed in a minority of cases, particularly the *NUP214-ABL1* rearrangement.[76]

Genetics of relapse

The subclonal complexity of ALL is now well established, and the clonal dynamics during therapy and at relapse have been examined through genomic sequencing and single-cell analysis.[77,78] Chimeric fusions, when present, are often clonal leukemia-initiating lesions that are typically retained throughout disease progression. Alterations of signaling pathway lesions (*FLT3*, *KRAS*, *NRAS*) are often subclonal and are frequently lost or gained between diagnosis and relapse.[79]

In B-ALL, mutations in genes such as the histone acetyl transferase gene *CREBBP*, the histone methyltransferase gene *SETD2*, and the steroid receptor genes *NR3C1* and *NR3C2* are enriched at relapse.[80-83] At diagnosis, minor relapse-initiating subclones can exhibit inherent resistance to chemotherapy, even before secondary mutation acquisition.[84] Other relapse-specific mutations in *PRPS1*, *PRSP2*, *NT5C2*, or *MSH6*, each influencing thiopurine metabolism, may emerge only during therapy, being driven by selective therapeutic pressure.[81,83,85,86] These mutations confer chemotherapy resistance and might have implications for disease monitoring and therapeutic decisions.[85,86] Inherited genomic variants in specific ethnic/racial groups also contribute to relapse risk as a result of differential drug metabolism or acquisition of distinct somatic mutations.[87-89] Monitoring the dynamics of mutation clearance during induction therapy or monitoring for the emergence of relapse-associated mutations might identify patients who will benefit from early modification of therapy.

Mixed-phenotype acute leukemia

Mixed-phenotype acute leukemia (MPAL) is uncommon, representing only 2-5% of pediatric acute leukemia.[48] The 2016 World Health Organization (WHO) classification defines MPAL as acute leukemia expressing a combination of antigens not restricted to a single lineage with the following categories: B/myeloid, not otherwise specified (NOS) and T/myeloid, NOS, in addition to two genetic subgroups of MPAL: that with t(9;22)(q34.1;q11.2), *BCR-ABL1;* and that with t(v;11q23.3), *KMT2A*-rearranged.[90] Genetic characteriza-
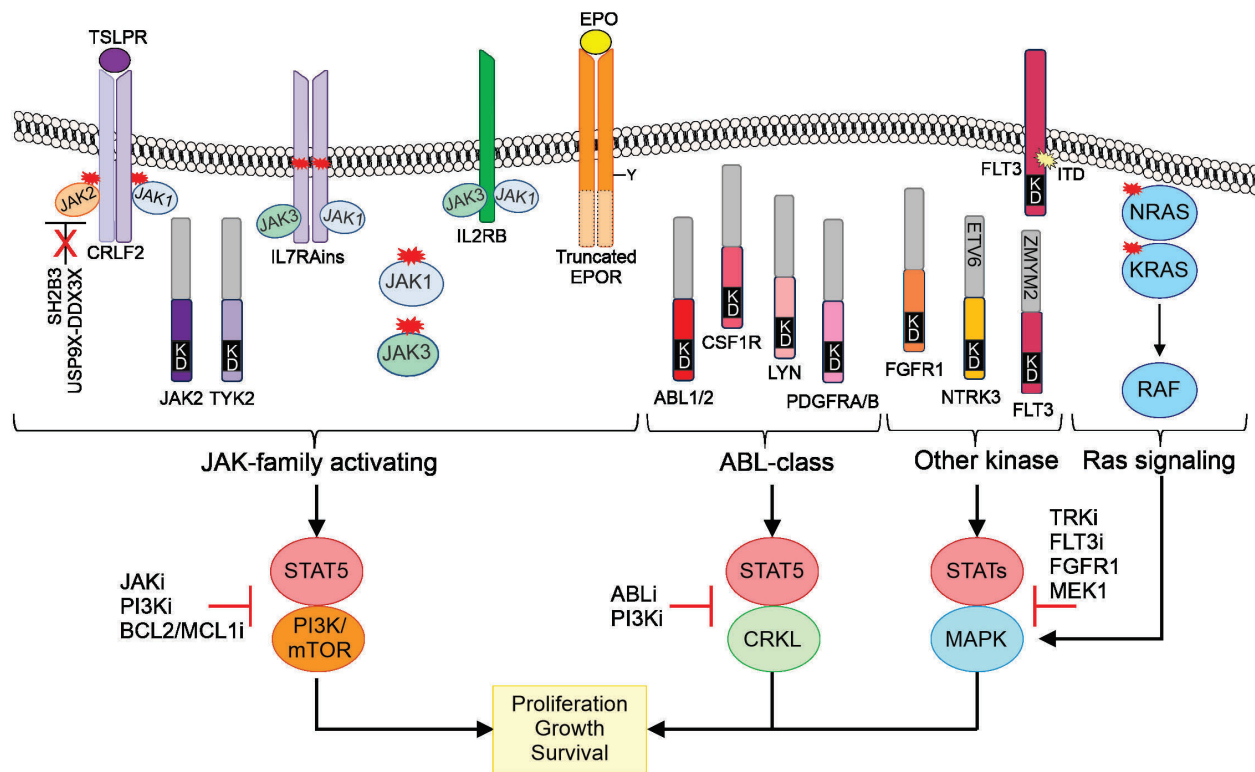
Figure 3. Kinase pathways deregulated in Philadelphia chromosome (Ph)-like acute lymphoblastic leukemia (ALL). The diverse signaling alterations observed in Ph-like ALL are grouped into JAK-STAT activating lesions (most commonly *CRLF2* rearrangement, but also *JAK* mutation and rearrangement, *IL7R* mutation, truncating rearrangements of *EPOR*, and *SH2B3* deletion/mutation), rearrangements involving ABL-class tyrosine kinases; rearrangements of genes encoding other kinases (*FGFR1*, *NTRK3*, *FLT3*), and Ras pathway mutations. Ras pathway mutations are not restricted to Ph-like ALL and are observed in other subtypes of leukemia (e.g., hyperdiploid ALL, *PAX5 P80R* ALL). They are also observed as co-mutations in a proportion of cases with *CRLF2* rearrangements. These alterations typically activate the logical downstream signaling pathway, as well as other pathways that serve as additional avenues for therapeutic intervention (e.g., PI3K, BCL2).

tion of pediatric MPAL revealed that rearrangement of *ZNF384* is common in B/myeloid MPAL and biallelic *WT1* alterations are common in T/myeloid MPAL, which shares genomic features with ETP ALL.[48] Such genetic alterations are consistent with the results of a retrospective multinational study showing that ALL-type therapy is more effective than AML- or combined-type treatment in patients with MPAL.[91] Furthermore, the immunophenotypic heterogeneity within MPAL populations is not driven by distinct genomic subclones. Such a phenotypic fate results from the acquisition of mutations in early hematopoietic progenitors with preserved myeloid and lymphoid potentials, and individual phenotypic subpopulations can reconstitute the immunophenotypic diversity.[48]

Risk assignment for treatment

Age (infant or ≥10 years), white blood cell (WBC) count at diagnosis (≥50x10^9/L), central nervous system (CNS) involvement, T-cell immunophenotype, race (Hispanic or black), and male sex have been considered clinical adverse prognostic factors (Table 3). Furthermore, certain somatic genetic alterations are significantly associated with outcome and can partly explain the clinical factors.[15] For example, patients with hyperdiploidy (>50 chromosomes or DNA index ≥1.16) and *ETV6-RUNX1* have a better prognosis and are commonly young children with low WBC counts. Conversely, patients with hypodiploidy (<44 chromosomes), Ph-positive or Ph-like ALL, *KMT2A*, *MEF2D*, or *BCL2/MYC* rearrangements, or

TCF3-HLF have worse prognoses and are more commonly adolescents or adults with higher WBC counts and/or CNS involvement.[36,92] Hispanic patients have greater incidences of Ph-like ALL with *CRLF2* fusions. Infant leukemia is strongly associated with *KMT2A* rearrangements.

Early response to chemotherapy in terms of MRD is another important prognostic factor.[93,94] MRD can be measured by flow cytometry for leukemia-specific aberrant immunophenotypes or by polymerase chain reaction (PCR) for unique immunoglobulin and T-cell receptor genes or fusion transcripts. Next-generation sequencing is more sensitive than flow cytometry or PCR for MRD detection,[95] but the superiority of this methodology for clinical application needs to be confirmed in larger studies. The relapse risk at a given MRD level differs between genetic subtypes.[93,94] Patients with favorable genetic subtypes clear MRD faster than those with high-risk genetics and T-ALL. Although patients with high-risk genetic features remain at risk for relapse even with undetectable or very low level (e.g., <0.01%) MRD at the end of induction, low-level MRD can be overcome in patients with low-risk features by subsequent treatment. Current treatment protocols incorporate clinical factors, leukemia genetics, and MRD for risk-stratification.

Treatment

Treatment of ALL comprises three phases: remission induction, consolidation (or intensification), and mainte-

Table 3. Risk factors in pediatric acute lymphoblastic leukemia

Factor	Better	Worse
Patient and clinical characteristics		
Age at diagnosis	1 to <10 years	<1 year or ≥10 years
Sex	Female	Male
Race	Caucasian, Asian	African American, Hispanic
Down syndrome	No	Yes
WBC counts at diagnosis	$<50 \times 10^9$/L	$\geq 50 \times 10^9$/L
CNS involvement at diagnosis	CNS 1	CNS 2 and CNS 3, traumatic tap with blasts
Testicular involvement	No	Yes
Immunophenotype	B-ALL	T-ALL
Cytogenetic and genetics		
	High hyperdiploidy (51-65 chromosomes)	Hypodiploidy (<44 chromosomes)
	ETV6-RUNX1: t(12;21)(p13.2;q22.1)	*KMT2A* rearrangement: t(v;11q23.3)
	NUMT1 rearrangement	*BCR-ABL1*: t(9;22)(q34.1;q11.2) (Ph+)
		BCR-ABL1-like (Ph-like)
		TCF3-HLF: t(17;19)(q22;p13)
		MEF2D rearrangement
		Intrachromosomal amplification of chromosome 21 (iAMP21)
		BCL2 or *MYC* rearrangements
Minimal residual disease		
	Negative	Positive
	Continuously decreasing and becoming negative	Increasing and/or persistently positive while monitored

WBC: white blood cell; CNS: central nervous system; ALL: acute lymphoblastic leukemia; Ph: Philadelphia chromosome.

nance (or continuation), and lasts for 2-2.5 years. Most conventional chemotherapeutic agents were developed before 1970, and the optimal dosages and schedules for combination chemotherapy were developed with dose adjustments based on tolerability, response evaluation with MRD, and individualized pharmacodynamic and pharmacogenomic studies, but with limited use of the biological features of ALL cells obtained through genomic analyses. Allogeneic hematopoietic cell transplantation (HCT) has been used for patients at very high risk. In the last decade, molecularly targeted agents and immunotherapy have emerged as novel therapeutic strategies.

Survivors treated before 1990 experienced late effects in multiple organ systems (e.g., reproductive, neurological, or gastrointestinal effects or infections), but those treated on more recent protocols have experienced predominantly musculoskeletal effects, possibly due to more intensive use of dexamethasone and asparaginase.[96] In addition, cranial radiotherapy-induced hypothalamic dysfunction has given way to impaired glucose metabolism and obesity as the use of radiotherapy has been reduced. The recent pattern of late effects could be managed by prevention or intervention as well as by rational reduction of conventional chemotherapy combined with molecularly targeted therapy and immunotherapy.

Remission-induction therapy

Remission-induction therapy consists of three drugs (glucocorticoid [prednisone or dexamethasone], vincristine, and asparaginase) or four drugs (the 3 aforementioned drugs plus anthracycline) administered over 4-6 weeks and induces complete remission (CR) in approximately 98% of pediatric patients.

Compared to prednisone, dexamethasone has a longer half-life and better CNS penetration, which improves CNS disease control.[97] In randomized studies comparing prednisone and dexamethasone, patients who received dexamethasone had better event-free survival (EFS) than did those who received prednisone at a prednisone-to-dexamethasone dose ratio of <7 (Table 1).[1,97] However, OS was similar in both arms, except in one study that found dexamethasone beneficial in patients with T-ALL who had a good prednisone-prophase response.[1] Furthermore, dexamethasone is associated with more frequent adverse effects, such as infection, bone fracture, osteonecrosis, mood/behavior problems, and myopathy. When the dose ratio was >7, there was no difference in outcomes with the two glucocorticoids.[97] Therefore, the dose, schedule, and type of glucocorticoid are determined based on the patient's age, relapse risk, and treatment phase. Bacterial infection can be reduced with prophylactic antibiotics, such as levofloxacin during neutropenia.[98,99] Alternate-week dexamethasone administration, as opposed to a continuous schedule, can reduce the risk of osteonecrosis.[100] Adding hydrocortisone to dexamethasone can reduce neuropsychological adverse effects, possibly by reducing the cortisol depletion in the cerebral mineralocorticoid receptors.[101]

Vincristine does not typically cause significant myelosuppression and is given weekly during induction therapy and as monthly or tri-monthly pulses with glucocorticoids during continuation at doses of 1.5-2.0 mg/m². However, its adverse effects include peripheral sensory and motor neuropathy, and the dose is typically capped at 2.0 mg. A GWAS in children with ALL revealed that a polymorphism within the promoter region of *CEP72* was associated with increased incidence and severity of vincristine-related peripheral neuropathy.[102]

In many countries, polyethylene glycol (PEG)-*Escherichia coli* L-asparaginase (pegaspargase) has replaced native *E. coli* L-asparaginase, compared with which pegaspargase has a longer half-life and a lower incidence of hypersensitivity. Compared with intramuscular native *E. coli* L-asparaginase, intravenous pegaspargase was similar-

ly efficacious, no more toxic, and associated with decreased patient anxiety at administration (Table 1).[5] Although pegaspargase is typically used at 1000 IU/m² to 2500 IU/m², a therapeutic drug monitoring study showed trough levels of asparaginase activity of >100 IU/L even with administration at 450 IU/m² every two weeks.[103] Interestingly, the incidence of asparaginase-related toxicities (e.g., pancreatitis, central neurotoxicity, and thrombosis) was not associated with asparaginase activity levels except in the case of liver toxicities. In a randomized study to assign non-high-risk patients to either ten continuous doses (2-week intervals) or three intermittent doses (6-week intervals) of intramuscular pegaspargase (1000 IU/m²), after receiving five doses every two weeks, asparaginase-related toxicities (hypersensitivity, osteonecrosis, pancreatitis, and thromboembolism) were significantly reduced in the latter group without compromising disease-free survival (DFS), suggesting that prolonged continuous administration of pegaspargase might not be necessary in the context of multiagent chemotherapy.[104] Most allergic reactions to pegaspargase occur after two or three doses, and are mediated by the PEG moiety and not by the L-asparaginase, possibly because of the patients' exposure to other PEG-containing products, such as laxatives and tablet coatings, before the diagnosis of ALL.[105] Although adding rituximab to ALL therapy decreased the allergic reaction to native *E. coli* L-asparaginase and improved the outcome in adults with CD20-positive Ph-negative ALL,[106] the efficacy of rituximab on PEG-related allergy is unknown. Discontinuation of planned asparaginase doses is associated with worse prognosis in high-risk patients.[107] In cases of allergy to pegaspargase or native *E. coli* asparaginase, *Erwinia* asparaginase (Erwinase) is considered an acceptable alternative. However, Erwinase is more expensive, is intermittently unavailable, and requires frequent administration because of its short half-life.[108] Universal premedication with diphenhydramine and an H2-blocker can decrease the incidence of allergic reactions,[109] and drug desensitization in patients with previous and persistent anti-PEG antibodies is feasible.[110]

Consolidation (intensification) therapy

Induction with the 3- or 4-drug regimen (the IA phase) is followed by consolidation (the IB phase) with cyclophosphamide, cytarabine, and mercaptopurine. In patients with B-ALL, 5-year EFS was 92.3% for those with negative MRD at the end of both the IA phase (day 33) and the IB phase (day 78), which was better than the 5-year EFS for those with positive MRD at one or both time points but at a level of <10⁻³ on day 78 (77.6%) and for those with positive MRD at a level of ≥10⁻³ on day 78 (50.1%).[111] Interestingly, the MRD level on day 33 in patients with T-ALL was not relevant if MRD was negative on day 78, suggesting the importance of the IB phase in T-ALL.[112] Similarly, in ETP ALL, which is often associated with poor early response to 4-drug induction, IB-phase consolidation is effective at reducing MRD,[113] and outcomes were comparable among patients with ETP, near-ETP, and non-ETP ALL in the Children's Oncology Group AALL0434 study.[114]

Methotrexate is crucial for controlling systemic leukemia and also CNS and testicular disease. Methotrexate is administered as a high dose (2-5 g/m²) plus leucovorin rescue, together with 6-mercaptopurine,

or as escalating intermediate doses of methotrexate (100-300 mg/m²) without leucovorin rescue followed by asparaginase (the Capizzi regimen). In randomized studies, high-dose methotrexate was superior to the Capizzi methotrexate regimen in patients with high-risk B-ALL (Table 1).[2] Interestingly, in patients with T-ALL, Capizzi methotrexate was associated with better outcomes than high-dose methotrexate (Table 1).[4] However, approximately 90% of the patients received cranial irradiation, and those in the high-dose methotrexate arm underwent irradiation five months later than those in the Capizzi regimen arm. As cranial irradiation can control both CNS and systemic relapses, this difference in timing of irradiation might have contributed to the different outcomes.

In a randomized trial of nelarabine in patients with intermediate- or high-risk T-ALL, the 5-year DFS and CNS relapse (isolated and combined) rates were significantly better in patients who received nelarabine than in those who did not (88.2% *vs.* 82.1% and 1.3% *vs.* 6.9%, respectively).[115]

Consolidation therapy is followed by reinduction (delayed intensification) therapy, which consists of medication similar to that used during the IA and IB phases and is a critical component of ALL therapy in both standard-risk and high-risk patients. Reducing the duration and chemotherapy doses of delayed intensification led to an increased incidence of relapse in standard-risk patients, especially those who did not have *ETV6-RUNX1*-positive ALL or were aged ≥7 years at diagnosis.[116]

Maintenance therapy

Maintenance therapy typically lasts ≥1 year and consists of daily mercaptopurine and weekly methotrexate with or without vincristine and steroid pulses. One study found that completing maintenance therapy at one year after diagnosis resulted in a high relapse rate (38.8±2.8% at 12 years after diagnosis), although this approach cured more than half of the children with ALL, and some genetic subgroups, such as *TCF3-PBX1* and *ETV6-RUNX1*, were associated with excellent DFS.[117]

There is interpatient variability in mercaptopurine tolerance. Inherited heterozygous or homozygous deficiency of thiopurine methyltransferase (*TPMT*) leads to higher levels of active thiopurine metabolites and excess hematologic toxicities, which are more common in patients of European descent.[88] For patients with East Asian or Native American ancestry, germline variants of *NUDT15*, which encodes a nucleoside diphosphatase, reduce degradation of active thiopurine nucleotide metabolites and were strongly associated with mercaptopurine intolerance.[88] Therefore, thiopurine dosing adjustments based on *TPMT* and *NUDT15* genotypes are recommended.[118]

Adherence of <95% to planned daily mercaptopurine doses is associated with a 2.7-fold increase in incidence of relapse compared with that seen when adherence is ≥95%.[119] Confirming adherence by directly asking patients or by measuring their erythrocyte thioguanine nucleotide levels is important, especially for patients with persistently high WBC counts or absolute neutrophil counts, although self-reporting can overestimate the true intake in non-compliant patients. Patients were previously instructed to take mercaptopurine in the evening and without food/dairy products, but these restrictions did not affect outcomes or erythrocyte thioguanine

nucleotide levels as long as daily doses were administered at the same time of day.[120]

Central nervous system-directed therapy

Because of the high risk of late neurocognitive sequelae, endocrinopathy, and secondary cancers, cranial irradiation has been largely replaced by intrathecal chemotherapy, in addition to systemic chemotherapy that has CNS effects (e.g., dexamethasone, high-dose methotrexate, and asparaginase). In an international meta-analysis, cranial irradiation decreased the incidence of isolated CNS relapse in patients with overt CNS involvement at diagnosis (CNS 3) but the cumulative incidences of any event and the OS were similar to those in patients who did not receive cranial irradiation.[121]

The St. Jude Total XVI study used intensified intrathecal therapy during induction therapy and obtained a remarkable reduction in 5-year cumulative isolated and combined CNS relapses to 1.3% and 1.5%, respectively, without cranial irradiation (Table 1).[9] In addition to CNS 3 at diagnosis, CNS 2 status (<5 WBC/µL and blasts) at diagnosis is associated with worse outcomes and greater risk of CNS relapse, and augmented intrathecal chemotherapy is required.[122] Traumatic lumbar puncture at diagnosis can introduce circulating ALL blasts into the cerebrospinal fluid (CSF) and is also associated with worse outcomes. Delaying the first intrathecal therapy until circulating blasts had disappeared improved the control of CNS disease.[123]

Acute lymphoblastic leukemia blasts are typically detected in CSF by morphologic evaluation of cytospin samples. Flow cytometric analysis of CSF improved ALL blast detection, and positive results were associated with a higher incidence of any relapse,[124] although another study failed to show such an association.[125]

Molecularly targeted agents

With the increased understanding of genetic alterations in ALL, approaches targeting the driving genetic mutation and/or the associated signaling pathway are emerging (Table 2). Such an approach is attractive as it can augment or replace conventional chemotherapy with fewer off-target effects. In pediatric Ph-positive ALL, adding an ABL1 tyrosine kinase inhibitor, imatinib mesylate (340 mg/m^2/day), to intensive post-induction chemotherapy resulted in outcomes similar to those in patients who received HCT.[126] Newer generations of tyrosine kinase inhibitors are available, and a randomized study showed that pediatric patients who received chemotherapy with 80 mg/m^2/day of dasatinib, a dual ABL/SRC inhibitor with more potent activity against BCR-ABL1 and better CNS penetration than imatinib, had better EFS, OS, and CNS disease control when compared to patients who received imatinib (300 mg/m^2/day).[127] Ponatinib has potent activity in both wild-type and mutant *BCR-ABL1* ALL, including cells harboring the gatekeeper ABL1 T315I mutation. Combination chemotherapy with ponatinib and hyperfractionated cyclophosphamide, vincristine, doxorubicin, and dexamethasone (hyper-CVAD) alternating with high-dose methotrexate and cytarabine resulted in excellent 2-year EFS in adults with newly diagnosed Ph-positive ALL.[128] Because of the potential adverse effects, such as thrombosis and pancreatitis, the safety of ponatinib in combination with pediatric regimens should be evaluated.

For patients with Ph-like ALL and *ABL*-class gene fusions (*ABL1*, *ABL2*, *CSF1R*, *LYN*, *PDGFRA*, or *PDGFRB*), ABL1 inhibitors can be combined with chemotherapy.[129,130] For those patients with alterations that activate the JAK-STAT signaling pathway, such as rearrangements or a mutation of CRLF2 (*IGH-CRLF2*, *P2RY8-CRLF2*, or *CRLF2* F232C), rearrangements of *JAK2*, *EPOR*, or *TYK2*, or mutations/deletions of *IL7R*, *SH2B3*, *JAK1*, *JAK3*, *TYK2*, or *IL2RB*, clinical trials of a JAK inhibitor, ruxolitinib, are ongoing.

Venetoclax inhibits the anti-apoptotic regulator BCL-2. Deregulated cell death pathways contribute to treatment failure in ALL.[131] Preclinical studies have identified activities of venetoclax against high-risk leukemias such as ETP ALL, *KMT2A*-rearranged ALL, *TCF3-HLF*-positive ALL, and hypodiploid ALL (Table 2).[132,133] Proteasome and mTOR inhibitors have shown efficacy in relapsed ALL.[134,135] DOT1L, bromodomain, menin, and histone deacetylate inhibitors have shown promise in preclinical studies as therapies targeting unique molecular characteristics of *KMT2A*-rearranged ALL.[136]

Immunotherapy

Immunotherapy can be given as antibody-based therapy (e.g., blinatumomab or inotuzumab ozogamicin) or T-cell-based therapy (chimeric antigen receptor T [CAR T] cells, e.g., tisagenlecleucel), which have improved the response rate and outcomes in patients with relapsed/refractory B-ALL (Figure 4).[137] Antibodies (e.g., daratumumab directed against CD38) and CAR T cells (e.g., targeting CD1a, CD5, and CD7) against T-ALL are also under investigation.

Blinatumomab has two different single-chain Fv fragments: one binds the CD3 antigen and activates T-cell cytotoxicity, and the other binds the B-cell antigen CD19, which is expressed on most B-ALL cells.[138-140] In a randomized study of adults with refractory/relapsed B-ALL, patients who received blinatumomab had a better complete remission rate and survival than those who received the standard-of-care chemotherapy,[138] and blinatumomab was effective in eradicating MRD.[139] Patients aged 1-30 years with intermediate- or high-risk relapsed B-ALL were randomized to receive either two blocks of intensive chemotherapy or two 4-week blocks of blinatumomab after receiving re-induction chemotherapy.[140] The blinatumomab arm had better 2-year DFS, OS, and MRD clearance and lower incidences of febrile neutropenia, infection, and sepsis when compared with the chemotherapy arm. Cytokine release syndrome and neurotoxicity are adverse effects of blinatumomab, and their incidence and severity can be reduced by decreasing the disease burden before treatment.

Inotuzumab ozogamicin is a humanized anti-CD22 monoclonal antibody conjugated to calicheamicin.[141-143] A randomized study in adults with refractory/relapsed B-ALL showed that patients who received inotuzumab had a better remission rate and survival than did patients who received standard chemotherapy.[141] In a pediatric inotuzumab compassionate-use program, complete remission was seen in 67% of 51 children with relapsed/refractory ALL.[142] Inotuzumab is associated with sinusoidal obstruction syndrome, especially after HCT.[141-143] Fractionated use of low-dose inotuzumab and a longer interval between inotuzumab treatment and HCT can reduce the incidence of this syndrome.

Chimeric antigen receptor T cells express a synthetic
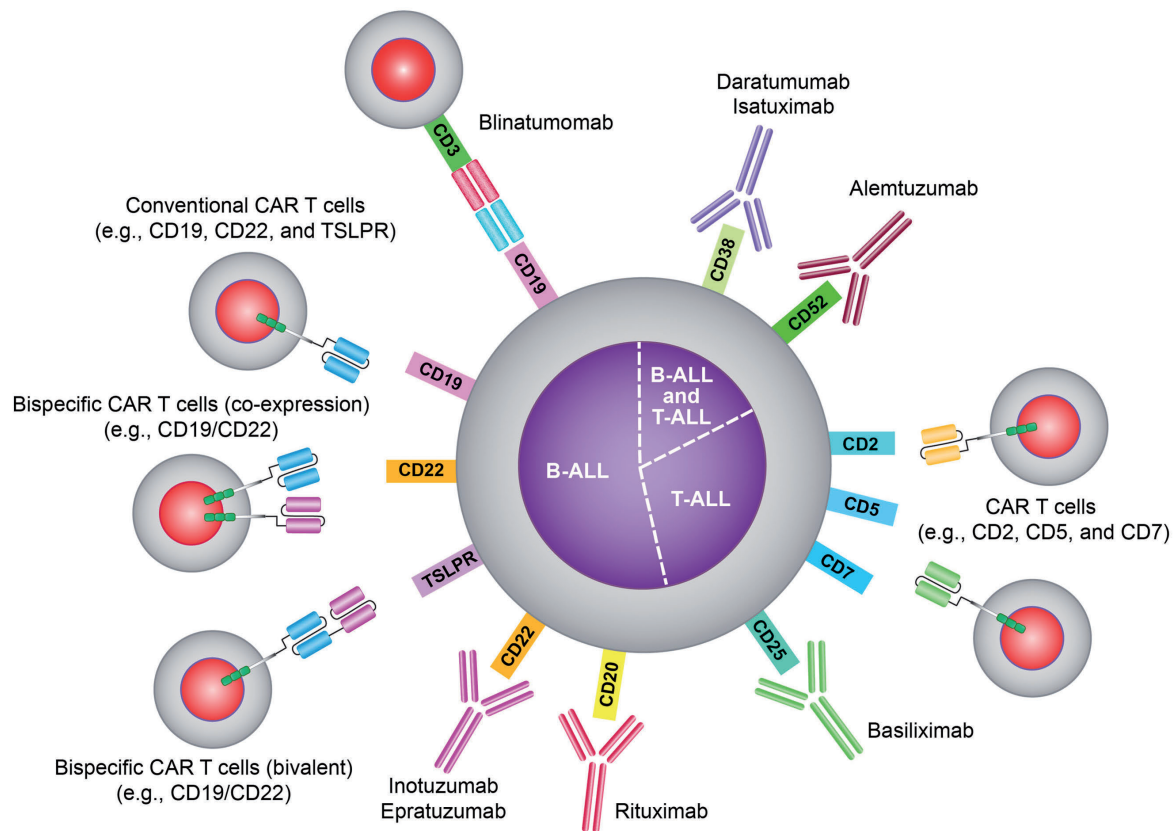
Figure 4. Immunotherapy in acute lymphoblastic leukemia. CAR T cells: chimeric antigen receptor T cells; ALL: acute lymphoblastic leukemia; TSLPR: thymic stromal lymphopoietin receptor.

receptor consisting of a single-chain variant fragment (scFv) domain directed against a B-lineage–associated antigen (e.g., CD19 and CD22) and intracellular signaling domains such as 4-1BB or CD28 with CD3ζ.[144] A study of CD19 CAR T cells in children and young adults with relapsed/refractory B-ALL showed a complete remission rate of 81% with 12-month EFS and OS of 50% and 76%, respectively.[144] CAR T cells can migrate to extramedullary sites such as the CNS and testes; therefore, they can be considered not only for patients with isolated bone marrow relapses but also for those with isolated or combined extramedullary relapses.[145] The persistence of CAR T cells and B-cell aplasia are important factors in long-term remission unless there is loss of the target antigen.[145,146] Therefore, CAR T cells have been developed that can target other antigens (e.g., CD22 or the thymic stromal lymphopoietin receptor) or simultaneously target dual antigens (e.g., CD19/CD22).[146] As with blinatumomab, cytokine release syndrome and neurotoxicity are major adverse effects. Tocilizumab (an anti-IL-6 receptor antibody) and/or steroid have been used to ameliorate these effects, and early intervention in patients who are developing signs of cytokine release syndrome is effective without compromising the anti-leukemia potency of CAR T cells.[147] Although CAR T cells can be curative by themselves, some consider them as a bridging therapy to subsequent HCT.[148]

To monitor MRD and antigen escape, the leukemia population should be characterized by multiparametric flow cytometry without using the targeted antigen prior to immunotherapy.[146] Alternatively, PCR or next-generation sequencing methods can be used.

Future perspectives

Comprehensive sequencing and integrative genome-wide analyses have profoundly refined the taxonomy of ALL, resulting in the identification of new entities with prognostic and therapeutic significance. There are distinct gene expression patterns in ALL caused by a wide range of genetic alterations that converge on specific pathways. Identifying these pathways is crucial for therapeutic targeting and demands the incorporation of gene expression approaches into the clinical diagnostic work-up of ALL. Mutation-agnostic approaches, such as drug sensitivity testing of panels of chemotherapeutic agents *ex vivo* and functional genomic screens, also offer the promise of identifying new therapeutic vulnerabilities and efficacious combinations.[149] Such intervention would lead to new therapeutic strategies incorporating individualized mutation-directed targeted therapy, immunotherapy, and reduced-intensity conventional chemotherapy or a chemotherapy-free regimen, which would ultimately improve patient survival and reduce adverse effects.

References

1. Moricke A, Zimmermann M, Valsecchi MG, et al. Dexamethasone versus prednisone in induction treatment of pediatric ALL: results of the randomized trial AIEOP-BFM ALL 2000. Blood. 2016;127(17):2101-2112.

2. Larsen EC, Devidas M, Chen S, et al. Dexamethasone and high-dose methotrexate improve outcome for children and young adults with high-risk B-acute lymphoblastic leukemia: a report from Children's Oncology Group Study AALL0232. J Clin Oncol. 2016;34(20):2380-2388.

3. Maloney KW, Devidas M, Wang C, et al. Outcome in children with standard-risk B-cell acute lymphoblastic leukemia: results of Children's Oncology Group Trial AALL0331. J Clin Oncol. 2020;38(6):602-612.

4. Winter SS, Dunsmore KP, Devidas M, et al. Improved survival for children and young adults with T-lineage acute lymphoblastic leukemia: results from the Children's Oncology Group AALL0434 Methotrexate Randomization. J Clin Oncol. 2018;36(29):2926-2934.

5. Place AE, Stevenson KE, Vrooman LM, et al. Intravenous pegylated asparaginase versus intramuscular native Escherichia coli L-asparaginase in newly diagnosed childhood acute lymphoblastic leukaemia (DFCI 05-001): a randomised, open-label phase 3 trial. Lancet Oncol. 2015;16(16):1677-1690.

6. Pieters R, de Groot-Kruseman H, Van der Velden V, et al. Successful therapy reduction and intensification for childhood acute lymphoblastic leukemia based on minimal residual disease monitoring: Study ALL10 from the Dutch Childhood Oncology Group. J Clin Oncol. 2016;34(22):2591-2601.

7. Vora A, Goulden N, Mitchell C, et al. Augmented post-remission therapy for a minimal residual disease-defined high-risk subgroup of children and young people with clinical standard-risk and intermediate-risk acute lymphoblastic leukaemia (UKALL 2003): a randomised controlled trial. Lancet Oncol. 2014;15(8):809-818.

8. Toft N, Birgens H, Abrahamsson J, et al. Results of NOPHO ALL2008 treatment for patients aged 1-45 years with acute lymphoblastic leukemia. Leukemia. 2018;32(3):606-615.

9. Jeha S, Pei D, Choi J, et al. Improved CNS control of childhood acute lymphoblastic leukemia without cranial irradiation: St Jude Total Therapy Study 16. J Clin Oncol. 2019;37(35):3377-3391.

10. Holmfeldt L, Wei L, Diaz-Flores E, et al. The genomic landscape of hypodiploid acute lymphoblastic leukemia. Nat Genet. 2013;45(3):242-252.

11. Moriyama T, Metzger ML, Wu G, et al. Germline genetic variation in ETV6 and risk of childhood acute lymphoblastic leukaemia: a systematic genetic study. Lancet Oncol. 2015;16(16):1659-1666.

12. Shah S, Schrader KA, Waanders E, et al. A recurrent germline PAX5 mutation confers susceptibility to pre-B cell acute lymphoblastic leukemia. Nat Genet. 2013;45(10):1226-1231.

13. Noetzli L, Lo RW, Lee-Sherick AB, et al. Germline mutations in ETV6 are associated with thrombocytopenia, red cell macrocytosis and predisposition to lymphoblastic leukemia. Nat Genet. 2015;47(5):535-538.

14. Mullighan CG, Goorha S, Radtke I, et al. Genome-wide analysis of genetic alterations in acute lymphoblastic leukaemia. Nature. 2007;446(7137):758-764.

15. Gu Z, Churchman ML, Roberts KG, et al. PAX5-driven subtypes of B-progenitor acute lymphoblastic leukemia. Nat Genet. 2019;51(2):296-307.

16. Churchman ML, Qian M, Te Kronnie G, et al. Germline genetic IKZF1 variation and predisposition to childhood acute lymphoblastic leukemia. Cancer Cell. 2018;33(5):937-948.

17. Kuehn HS, Boisson B, Cunningham-Rundles C, et al. Loss of B cells in patients with heterozygous mutations in IKAROS. N Engl J Med. 2016;374(11):1032-1043.

18. Mullighan CG, Miller CB, Radtke I, et al. BCR-ABL1 lymphoblastic leukaemia is characterized by the deletion of Ikaros. Nature. 2008;453(7191):110-114.

19. Mullighan CG, Su X, Zhang J, et al. Deletion of IKZF1 and prognosis in acute lymphoblastic leukemia. N Engl J Med. 2009;360(5):470-480.

20. Zhang J, McCastlain K, Yoshihara H, et al. Deregulation of DUX4 and ERG in acute lymphoblastic leukemia. Nat Genet. 2016;48(12):1481-1489.

21. Brown AL, Arts P, Carmichael CL, et al. RUNX1-mutated families show phenotype heterogeneity and a somatic mutation profile unique to germline predisposed AML. Blood Adv. 2020;4(6):1131-1144.

22. Feurstein S, Godley LA. Germline ETV6 mutations and predisposition to hematological malignancies. Int J Hematol. 2017;106(2):189-195.

23. Gocho Y, Yang JJ. Genetic defects in hematopoietic transcription factors and predisposition to acute lymphoblastic leukemia. Blood. 2019;134(10):793-797.

24. Papaemmanuil E, Hosking FJ, Vijayakrishnan J, et al. Loci on 7p12.2, 10q21.2 and 14q11.2 are associated with risk of childhood acute lymphoblastic leukemia. Nat Genet. 2009;41(9):1006-1010.

25. Trevino LR, Yang W, French D, et al. Germline genomic variants associated with childhood acute lymphoblastic leukemia. Nat Genet. 2009;41(9):1001-1005.

26. Perez-Andreu V, Roberts KG, Harvey RC, et al. Inherited GATA3 variants are associated with Ph-like childhood acute lymphoblastic leukemia and risk of relapse. Nat Genet. 2013;45(12):1494-1498.

27. Qian M, Xu H, Perez-Andreu V, et al. Novel susceptibility variants at the ERG locus for childhood acute lymphoblastic leukemia in Hispanics. Blood. 2019;133(7):724-729.

28. Qian M, Zhao X, Devidas M, et al. Genome-wide association study of susceptibility loci for T-cell acute lymphoblastic leukemia in children. J Natl Cancer Inst. 2019;111(12):1350-1357.

29. de Smith AJ, Lavoie G, Walsh KM, et al. Predisposing germline mutations in high hyperdiploid acute lymphoblastic leukemia in children. Genes Chromosomes Cancer. 2019;58(10):723-730.

30. Pouliot GP, Degar J, Hinze L, et al. Fanconi-BRCA pathway mutations in childhood T-cell acute lymphoblastic leukemia. PLoS One. 2019;14(11):e0221288.

31. Winer P, Muskens IS, Walsh KM, et al. Germline variants in predisposition genes in children with Down syndrome and acute lymphoblastic leukemia. Blood Adv. 2020;4(4):672-675.

32. Greaves M. Pre-natal origins of childhood leukemia. Rev Clin Exp Hematol. 2003;7(3):233-245.

33. Greaves MF, Maia AT, Wiemels JL, Ford AM. Leukemia in twins: lessons in natural history. Blood. 2003;102(7):2321-2333.

34. Ma Y, Dobbins SE, Sherborne AL, et al. Developmental timing of mutations revealed by whole-genome sequencing of twins with acute lymphoblastic leukemia. Proc Natl Acad Sci U S A. 2013;110(18):7429-7433.

35. Bueno C, Tejedor JR, Bashford-Rogers R, et al. Natural history and cell of origin of TC F3-ZN F384 and PTPN11 mutations in monozygotic twins with concordant BCP-ALL. Blood. 2019;134(11):900-905.

36. Roberts KG, Mullighan CG. The biology of B-progenitor acute lymphoblastic leukemia. Cold Spring Harb Perspect Med. 2020;10(7):a034835.

37. Paulsson K, Lilljebjorn H, Biloglav A, et al. The genomic landscape of high hyperdiploid childhood acute lymphoblastic leukemia. Nat Genet. 2015;47(6):672-676.

38. Carroll AJ, Shago M, Mikhail FM, et al. Masked hypodiploidy: hypodiploid acute lymphoblastic leukemia (ALL) mimicking hyperdiploid ALL in children: a report from the Children's Oncology Group. Cancer Genet. 2019;238(62-68).

39. Moorman AV, Robinson H, Schwab C, et al. Risk-directed treatment intensification significantly reduces the risk of relapse among children and adolescents with acute lymphoblastic leukemia and intrachromosomal amplification of chromosome 21: a comparison of the MRC ALL97/99 and UKALL2003 trials. J Clin Oncol. 2013;31(27):3389-3396.

40. Hunger SP, Galili N, Carroll AJ, Crist WM, Link MP, Cleary ML. The t(1;19)(q23;p13) results in consistent fusion of E2A and PBX1 coding sequences in acute lymphoblastic leukemias. Blood. 1991;77(4):687-693.

41. Crist WM, Carroll AJ, Shuster JJ, et al. Poor prognosis of children with pre-B acute lymphoblastic leukemia is associated with the t(1;19)(q23;p13): a Pediatric Oncology Group study. Blood. 1990;76(1):117-122.

42. Slayton WB, Schultz KR, Kairalla JA, et al. Dasatinib plus intensive chemotherapy in children, adolescents, and young adults with

Philadelphia chromosome-positive acute lymphoblastic leukemia: results of Children's Oncology Group Trial AALL0622. J Clin Oncol. 2018;36(22)2306-2314.

43. Lilljebjorn H, Henningsson R, Hyrenius-Wittsten A, et al. Identification of ETV6-RUNX1-like and DUX4-rearranged subtypes in paediatric B-cell precursor acute lymphoblastic leukaemia. Nat Commun. 2016;7:11790.

44. Zaliova M, Kotrova M, Bresolin S, et al. ETV6/RUNX1-like acute lymphoblastic leukemia: a novel B-cell precursor leukemia subtype associated with the CD27/CD44 immunophenotype. Genes Chromosomes Cancer. 2017;56(8):608-616.

45. Yasuda T, Tsuzuki S, Kawazu M, et al. Recurrent DUX4 fusions in B cell acute lymphoblastic leukemia of adolescents and young adults. Nat Genet. 2016;48(5):569-574.

46. Zaliova M, Stuchly J, Winkowska L, et al. Genomic landscape of pediatric B-other acute lymphoblastic leukemia in a consecutive European cohort. Haematologica. 2019;104(7):1396-1406.

47. Li JF, Dai YT, Lilljebjorn H, et al. Transcriptional landscape of B cell precursor acute lymphoblastic leukemia based on an international study of 1,223 cases. Proc Natl Acad Sci U S A. 2018;115(50):e11711-e11720.

48. Alexander TB, Gu Z, Iacobucci I, et al. The genetic basis and cell of origin of mixed phenotype acute leukaemia. Nature. 2018;562(7727):373-379.

49. Griffith M, Griffith OL, Krysiak K, et al. Comprehensive genomic analysis reveals FLT3 activation and a therapeutic strategy for a patient with relapsed adult B-lymphoblastic leukemia. Exp Hematol. 2016;44(7):603-613.

50. Oberley MJ, Gaynon PS, Bhojwani D, et al. Myeloid lineage switch following chimeric antigen receptor T-cell therapy in a patient with TCF3-ZNF384 fusion-positive B-lymphoblastic leukemia. Pediatr Blood Cancer. 2018;65(9):e27265.

51. Gu Z, Churchman M, Roberts K, et al. Genomic analyses identify recurrent MEF2D fusions in acute lymphoblastic leukaemia. Nat Comm. 2016;7(13331).

52. Suzuki K, Okuno Y, Kawashima N, et al. MEF2D-BCL9 fusion gene is associated with high-risk acute B-cell precursor lymphoblastic leukemia in adolescents. J Clin Oncol. 2016;34(28):3451-3459.

53. Ohki K, Kiyokawa N, Saito Y, et al. Clinical and molecular characteristics of MEF2D fusion-positive B-cell precursor acute lymphoblastic leukemia in childhood, including a novel translocation resulting in MEF2D-HNRNPH1 gene fusion. Haematologica. 2019;104(1):128-137.

54. Schwab C, Nebral K, Chilton L, et al. Intragenic amplification of PAX5: a novel subgroup in B-cell precursor acute lymphoblastic leukemia? Blood Adv. 2017;1(19): 1473-1477.

55. Passet M, Boissel N, Sigaux F, et al. PAX5 P80R mutation identifies a novel subtype of B-cell precursor acute lymphoblastic leukemia with favorable outcome. Blood. 2019;133(3):280-284.

56. Churchman ML, Low J, Qu C, et al. Efficacy of retinoids in IKZF1-mutated BCR-ABL1 acute lymphoblastic leukemia. Cancer Cell. 2015;28(3):343-356.

57. Chiaretti S, Vitale A, Cazzaniga G, et al. Clinico-biological features of 5202 patients with acute lymphoblastic leukemia enrolled in the Italian AIEOP and GIMEMA protocols and stratified in age cohorts. Haematologica. 2013;98(11):1702-1710.

58. Stanulla M, Dagdan E, Zaliova M, et al. IKZF1(plus) Defines a new minimal residual disease-dependent very-poor prognostic profile in pediatric B-cell precursor acute lymphoblastic leukemia. J Clin Oncol. 2018;36(12):1240-1249.

59. Den Boer ML, van Slegtenhorst M, De Menezes RX, et al. A subtype of childhood acute lymphoblastic leukaemia with poor treatment outcome: a genome-wide classification study. Lancet Oncol. 2009;10(2):125-134.

60. Ferrando AA, Neuberg DS, Staunton J, et al. Gene expression signatures define novel oncogenic pathways in T cell acute lymphoblastic leukemia. Cancer Cell. 2002;1(1):75-87.

61. Gianni F, Belver L, Ferrando A. The genetics and mechanisms of T-cell acute lymphoblastic leukemia. Cold Spring Harb Perspect Med. 2020 March 2. [Epub ahead of print]

62. Liu Y, Easton J, Shao Y, et al. The genomic landscape of pediatric and young adult T-lineage acute lymphoblastic leukemia. Nat Genet. 2017;49(8):1211-1218.

63. Mansour MR, Abraham BJ, Anders L, et al. Oncogene regulation. An oncogenic super-enhancer formed through somatic mutation of a noncoding intergenic element. Science. 2014;346(6215):1373-1377.

64. Abraham BJ, Hnisz D, Weintraub AS, et al. Small genomic insertions form enhancers that misregulate oncogenes. Nat Commun. 2017;8:14385.

65. Van Vlierberghe P, Ambesi-Impiombato A, Perez-Garcia A, et al. ETV6 mutations in early immature human T cell leukemias. J Exp Med. 2011;208(13):2571-2579.

66. Della Gatta G, Palomero T, Perez-Garcia A, et al. Reverse engineering of TLX oncogenic transcriptional networks identifies RUNX1 as tumor suppressor in T-ALL. Nat Med. 2012;18(3):436-440.

67. Zhang J, Ding L, Holmfeldt L, et al. The genetic basis of early T-cell precursor acute lymphoblastic leukaemia. Nature. 2012;481(7380):157-163.

68. Yui MA, Rothenberg EV. Developmental gene networks: a triathlon on the course to T cell identity. Nat Rev Immunol. 2014;14(8):529-545.

69. Weng AP, Ferrando AA, Lee W, et al. Activating mutations of NOTCH1 in human T cell acute lymphoblastic leukemia. Science. 2004;306(5694):269-271.

70. Palomero T, Lim WK, Odom DT, et al. NOTCH1 directly regulates c-MYC and activates a feed-forward-loop transcriptional network promoting leukemic cell growth. Proc Natl Acad Sci U S A. 2006;103(48): 18261-18266.

71. Herranz D, Ambesi-Impiombato A, Palomero T, et al. A NOTCH1-driven MYC enhancer promotes T cell development, transformation and acute lymphoblastic leukemia. Nat Med. 2014;20(10):1130-1137.

72. Hebert J, Cayuela JM, Berkeley J, Sigaux F. Candidate tumor-suppressor genes MTS1 (p16INK4A) and MTS2 (p15INK4B) display frequent homozygous deletions in primary cells from T- but not from B-cell lineage acute lymphoblastic leukemias. Blood. 1994;84(12):4038-4044.

73. Palomero T, Sulis ML, Cortina M, et al. Mutational loss of PTEN induces resistance to NOTCH1 inhibition in T-cell leukemia. Nat Med. 2007;13(10):1203-1210.

74. Zenatti PP, Ribeiro D, Li W, et al. Oncogenic IL7R gain-of-function mutations in childhood T-cell acute lymphoblastic leukemia. Nat Genet. 2011;43(10):932-939.

75. Kontro M, Kuusanmaki H, Eldfors S, et al. Novel activating STAT5B mutations as putative drivers of T-cell acute lymphoblastic leukemia. Leukemia. 2014;28(8):1738-1742.

76. Graux C, Stevens-Kroef M, Lafage M, et al. Heterogeneous patterns of amplification of the NUP214-ABL1 fusion gene in T-cell acute lymphoblastic leukemia. Leukemia. 2009;23(1):125-133.

77. Anderson K, Lutz C, van Delft FW, et al. Genetic variegation of clonal architecture and propagating cells in leukaemia. Nature. 2011;469(7330):356-361.

78. De Bie J, Demeyer S, Alberti-Servera L, et al. Single-cell sequencing reveals the origin and the order of mutation acquisition in T-cell acute lymphoblastic leukemia. Leukemia. 2018;32(6):1358-1369.

79. Ma X, Edmonson M, Yergeau D, et al. Rise and fall of subclones from diagnosis to relapse in pediatric B-acute lymphoblastic leukaemia. Nat Commun. 2015;6: 6604.

80. Mullighan CG, Zhang J, Kasper LH, et al. CREBBP mutations in relapsed acute lymphoblastic leukaemia. Nature. 2011;471 (7337):235-239.

81. Li B, Brady SW, Ma X, et al. Therapy-induced mutations drive the genomic landscape of relapsed acute lymphoblastic leukemia. Blood. 2020;135(1):41-55.

82. Mar BG, Bullinger LB, McLean KM, et al. Mutations in epigenetic regulators including SETD2 are gained during relapse in paediatric acute lymphoblastic leukaemia. Nat Commun. 2014;5:3469.

83. Waanders E, Gu Z, Dobson SM, et al. Mutational landscape and patterns of clonal evolution in relapsed pediatric acute lymphoblastic leukemia. Blood Cancer Disc. 2020;1(1):96-111.

84. Dobson SM, Garcia-Prat L, Vanner RJ, et al. Relapse-fated latent diagnosis subclones in acute B lineage leukemia are drug tolerant and possess distinct metabolic programs. Cancer Disc. 2020;10(4):568-587.

85. Li B, Li H, Bai Y, et al. Negative feedback-defective PRPS1 mutants drive thiopurine resistance in relapsed childhood ALL. Nat Med. 2015;21(6):563-571.

86. Meyer JA, Wang J, Hogan LE, et al. Relapse-specific mutations in NT5C2 in childhood acute lymphoblastic leukemia. Nat Genet. 2013;45(3):290-294.

87. Yang JJ, Cheng C, Devidas M, et al. Ancestry and pharmacogenomics of relapse in acute lymphoblastic leukemia. Nat Genet. 2011;43(3):237-241.

88. Yang JJ, Landier W, Yang W, et al. Inherited NUDT15 variant is a genetic determinant of mercaptopurine intolerance in children with acute lymphoblastic leukemia. J Clin Oncol. 2015;33(11):1235-1242.

89. Karol SE, Larsen E, Cheng C, et al. Genetics of ancestry-specific risk for relapse in acute lymphoblastic leukemia. Leukemia. 2017;31(6):1325-1332.

90. Arber DA, Orazi A, Hasserjian R, et al. The 2016 revision to the World Health Organization classification of myeloid neoplasms and acute leukemia. Blood. 2016;127(20):2391-2405.

91. Hrusak O, de Haas V, Stancikova J, et al. International cooperative study identifies treatment strategy in childhood ambiguous

lineage leukemia. Blood. 2018;132(3):264-276.

92. Fischer U, Forster M, Rinaldi A, et al. Genomics and drug profiling of fatal TCF3-HLF-positive acute lymphoblastic leukemia identifies recurrent mutation patterns and therapeutic options. Nat Genet. 2015;47(9):1020-1029.

93. Pui CH, Pei D, Raimondi SC, et al. Clinical impact of minimal residual disease in children with different subtypes of acute lymphoblastic leukemia treated with Response-Adapted therapy. Leukemia. 2017;31(2):333-339.

94. O'Connor D, Enshaei A, Bartram J, et al. Genotype-specific minimal residual disease interpretation improves stratification in pediatric acute lymphoblastic leukemia. J Clin Oncol. 2018;36(1):34-43.

95. Wood B, Wu D, Crossley B, et al. Measurable residual disease detection by high-throughput sequencing improves risk stratification for pediatric B-ALL. Blood. 2018;131(12):1350-1359.

96. Mulrooney DA, Hyun G, Ness KK, et al. The changing burden of long-term health outcomes in survivors of childhood acute lymphoblastic leukaemia: a retrospective analysis of the St Jude Lifetime Cohort Study. Lancet Haematol. 2019;6(6):e306-e316.

97. Inaba H, Pui CH. Glucocorticoid use in acute lymphoblastic leukaemia. Lancet Oncol. 2010;11(11):1096-1106.

98. Wolf J, Tang L, Flynn PM, et al. Levofloxacin prophylaxis during induction therapy for pediatric acute lymphoblastic leukemia. Clin Infect Dis. 2017;65(11):1790-1798.

99. Alexander S, Fisher BT, Gaur AH, et al. Effect of levofloxacin prophylaxis on bacteremia in children with acute leukemia or undergoing hematopoietic stem cell transplantation: a randomized clinical trial. JAMA. 2018;320(10):995-1004.

100. Mattano LA Jr, Devidas M, Nachman JB, et al. Effect of alternate-week versus continuous dexamethasone scheduling on the risk of osteonecrosis in paediatric patients with acute lymphoblastic leukaemia: results from the CCG-1961 randomised cohort trial. Lancet Oncol. 2012;13(9):906-915.

101. Warris LT, van den Heuvel-Eibrink MM, Aarsen FK, et al. Hydrocortisone as an intervention for dexamethasone-induced adverse effects in pediatric patients with acute lymphoblastic leukemia: results of a double-blind, randomized controlled trial. J Clin Oncol. 2016;34(19):2287-2293.

102. Diouf B, Crews KR, Lew G, et al. Association of an inherited genetic variant with vincristine-related peripheral neuropathy in children with acute lymphoblastic leukemia. JAMA. 2015;313(8):815-823.

103. Kloos RQH, Pieters R, Jumelet FMV, de Groot-Kruseman HA, van den Bos C, van der Sluis IM. Individualized asparaginase dosing in childhood acute lymphoblastic leukemia. J Clin Oncol. 2020;38(7):715-724.

104. Albertsen BK, Grell K, Abrahamsson J, et al. Intermittent versus continuous PEG-asparaginase to reduce asparaginase-associated toxicities: a NOPHO ALL2008 randomized study. J Clin Oncol. 2019;37(19):1638-1646.

105. Liu Y, Smith CA, Panetta JC, et al. Antibodies predict pegaspargase allergic reactions and failure of rechallenge. J Clin Oncol. 2019;37(23):2051-2061.

106. Maury S, Chevret S, Thomas X, et al. Rituximab in B-lineage adult acute lymphoblastic leukemia. N Engl J Med.

2016;375(11):1044-1053.

107. Gupta S, Wang C, Raetz EA, et al. Impact of asparaginase discontinuation on outcome in childhood acute lymphoblastic leukemia: a report from the Children's Oncology Group. J Clin Oncol. 2020;38(17):1897-1905.

108. Salzer WL, Asselin B, Supko JG, et al. Erwinia asparaginase achieves therapeutic activity after pegaspargase allergy: a report from the Children's Oncology Group. Blood. 2013;122(4):507-514.

109. Cooper SL, Young DJ, Bowen CJ, Arwood NM, Poggi SG, Brown PA. Universal premedication and therapeutic drug monitoring for asparaginase-based therapy prevents infusion-associated acute adverse events and drug substitutions. Pediatr Blood Cancer. 2019;66(8):e27797.

110. Swanson HD, Panetta JC, Barker PJ, et al. Predicting success of desensitization after pegaspargase allergy. Blood. 2020;135(1):71-75.

111. Conter V, Bartram CR, Valsecchi MG, et al. Molecular response to treatment redefines all prognostic factors in children and adolescents with B-cell precursor acute lymphoblastic leukemia: results in 3184 patients of the AIEOP-BFM ALL 2000 study. Blood. 2010;115(16):3206-3214.

112. Schrappe M, Valsecchi MG, Bartram CR, et al. Late MRD response determines relapse risk overall and in subsets of childhood T-cell ALL: results of the AIEOP-BFM-ALL 2000 study. Blood. 2011;118(8):2077-2084.

113. Conter V, Valsecchi MG, Buldini B, et al. Early T-cell precursor acute lymphoblastic leukaemia in children treated in AIEOP centres with AIEOP-BFM protocols: a retrospective analysis. Lancet Haematol. 2016;3(2):e80-86.

114. Raetz EA, Teachey DT. T-cell acute lymphoblastic leukemia. Hematology Am Soc Hematol Educ Program. 2016;2016(1):580-588.

115. Dunsmore KP, Winter SS, Devidas M, et al. Children's Oncology Group AALL0434: A phase III randomized clinical trial testing nelarabine in newly diagnosed T-cell acute lymphoblastic leukemia. J Clin Oncol. 2020 Aug 19 [Epub ahead of print]

116. Schrappe M, Bleckmann K, Zimmermann M, et al. Reduced-intensity delayed intensification in standard-risk pediatric acute lymphoblastic leukemia defined by undetectable minimal residual disease: results of an international randomized trial (AIEOP-BFM ALL 2000). J Clin Oncol. 2018;36(3):244-253.

117. Kato M, Ishimaru S, Seki M, et al. Long-term outcome of 6-month maintenance chemotherapy for acute lymphoblastic leukemia in children. Leukemia. 2017;31(3):580-584.

118. Relling MV, Schwab M, Whirl-Carrillo M, et al. Clinical Pharmacogenetics Implementation Consortium Guideline for Thiopurine Dosing Based on TPMT and NUDT15 Genotypes: 2018 update. Clin Pharmacol Ther. 2019;105(5):1095-1105.

119. Bhatia S, Landier W, Hageman L, et al. Systemic exposure to thiopurines and risk of relapse in children with acute lymphoblastic leukemia: a Children's Oncology Group Study. JAMA Oncol. 2015;1(3):287-295.

120. Landier W, Hageman L, Chen Y, et al. Mercaptopurine ingestion habits, red cell thioguanine nucleotide levels, and relapse risk in children with acute lymphoblastic leukemia: a report from the Children's Oncology Group Study AALL03N1. J Clin Oncol. 2017;35(15):1730-1736.

121. Vora A, Andreano A, Pui CH, et al. Influence of cranial radiotherapy on outcome in children with acute lymphoblastic leukemia treated with contemporary therapy. J Clin Oncol. 2016;34(9):919-926.

122. Winick N, Devidas M, Chen S, et al. Impact of initial CSF findings on outcome among patients with National Cancer Institute standard- and high-risk B-cell acute lymphoblastic leukemia: a report from the Children's Oncology Group. J Clin Oncol. 2017;35(22):2527-2534.

123. Liu HC, Yeh TC, Hou JY, et al. Triple intrathecal therapy alone with omission of cranial radiation in children with acute lymphoblastic leukemia. J Clin Oncol. 2014;32(17):1825-1829.

124. Thastrup M, Marquart HV, Levinsen M, et al. Flow cytometric detection of leukemic blasts in cerebrospinal fluid predicts risk of relapse in childhood acute lymphoblastic leukemia: a Nordic Society of Pediatric Hematology and Oncology study. Leukemia. 2020;34(2):336-346.

125. Gabelli M, Disaro S, Scarparo P, et al. Cerebrospinal fluid analysis by 8-color flow cytometry in children with acute lymphoblastic leukemia. Leuk Lymphoma. 2019;60(11):2825-2828.

126. Schultz KR, Carroll A, Heerema NA, et al. Long-term follow-up of imatinib in pediatric Philadelphia chromosome-positive acute lymphoblastic leukemia: Children's Oncology Group study AALL0031. Leukemia. 2014;28(7):1467-1471.

127. Shen S, Chen X, Cai J, et al. Effect of dasatinib versus imatinib in the treatment of pediatric Philadelphia chromosome-positive acute lymphoblastic leukemia: a randomized clinical trial. JAMA Oncol. 2020;6(3):358-366.

128. Jabbour E, Kantarjian H, Ravandi F, et al. Combination of hyper-CVAD with ponatinib as first-line therapy for patients with Philadelphia chromosome-positive acute lymphoblastic leukaemia: a single-centre, phase 2 study. Lancet Oncol. 2015;16(15):1547-1555.

129. Roberts KG, Li Y, Payne-Turner D, et al. Targetable kinase-activating lesions in Ph-like acute lymphoblastic leukemia. N Engl J Med. 2014;371(11):1005-1015.

130. Tanasi I, Ba I, Sirvent N, et al. Efficacy of tyrosine kinase inhibitors in Ph-like acute lymphoblastic leukemia harboring ABL-class rearrangements. Blood. 2019;134(16):1351-1355.

131. Seyfried F, Demir S, Horl RL, et al. Prediction of venetoclax activity in precursor B-ALL by functional assessment of apoptosis signaling. Cell Death Dis. 2019;10(8):571.

132. Khaw SL, Suryani S, Evans K, et al. Venetoclax responses of pediatric ALL xenografts reveal sensitivity of MLL-rearranged leukemia. Blood. 2016;128(10):1382-1395.

133. Diaz-Flores E, Comeaux EQ, Kim KL, et al. Bcl-2 is a therapeutic target for hypodiploid B-lineage acute lymphoblastic leukemia. Cancer Res. 2019;79(9):2339-2351.

134. Messinger YH, Gaynon PS, Sposto R, et al. Bortezomib with chemotherapy is highly active in advanced B-precursor acute lymphoblastic leukemia: Therapeutic Advances in Childhood Leukemia & Lymphoma (TACL) Study. Blood. 2012;120(2):285-290.

135. Place AE, Pikman Y, Stevenson KE, et al. Phase I trial of the mTOR inhibitor everolimus in combination with multi-agent chemotherapy in relapsed childhood acute lymphoblastic leukemia. Pediatr Blood

Cancer. 2018;65(7):e27062.

136. Brown P, Pieters R, Biondi A. How I treat infant leukemia. Blood. 2019;133(3):205-214.

137. Inaba H, Pui CH. Immunotherapy in pediatric acute lymphoblastic leukemia. Cancer Metastasis Rev. 2019;38(4):595-610.

138. Kantarjian H, Stein A, Gokbuget N, et al. Blinatumomab versus chemotherapy for advanced acute lymphoblastic leukemia. N Engl J Med. 2017;376(9):836-847.

139. Gokbuget N, Dombret H, Bonifacio M, et al. Blinatumomab for minimal residual disease in adults with B-cell precursor acute lymphoblastic leukemia. Blood. 2018;131(14): 1522-1531.

140. Brown PA, Ji L, Xu X, et al. A randomized phase 3 trial of blinatumomab versus chemotherapy as post-reinduction therapy in high and intermediate risk (HR/IR) first relapse of B-acute lymphoblastic leukemia (B-ALL) in children and adolescents/young adults (AYAs) demonstrates superior efficacy and tolerability of blinatumomab: a report from Children's Oncology Group Study AALL1331. Blood. 2019;134(Suppl 2):LBA-1.

141. Kantarjian HM, DeAngelo DJ, Stelljes M, et al. Inotuzumab ozogamicin versus standard therapy for acute lymphoblastic leukemia. N Engl J Med. 2016;375(8):740-753.

142. Bhojwani D, Sposto R, Shah NN, et al. Inotuzumab ozogamicin in pediatric patients with relapsed/refractory acute lymphoblastic leukemia. Leukemia. 2019;33 (4):884-892.

143. Jabbour E, Ravandi F, Kebriaei P, et al. Salvage chemoimmunotherapy with inotuzumab ozogamicin combined with mini-hyper-CVD for patients with relapsed or refractory Philadelphia chromosome-negative acute lymphoblastic leukemia: a phase 2 clinical trial. JAMA Oncol. 2018;4(2):230-234.

144. Maude SL, Laetsch TW, Buechner J, et al. Tisagenlecleucel in children and young adults with B-cell lymphoblastic leukemia. N Engl J Med. 2018;378(5):439-448.

145. Maude SL, Frey N, Shaw PA, et al. Chimeric antigen receptor T cells for sustained remissions in leukemia. N Engl J Med. 2014;371(16):1507-1517.

146. Shah NN, Fry TJ. Mechanisms of resistance to CAR T cell therapy. Nat Rev Clin Oncol. 2019;16(6):372-385.

147. Gardner RA, Ceppi F, Rivers J, et al. Preemptive mitigation of CD19 CAR T-cell cytokine release syndrome without attenuation of antileukemic efficacy. Blood. 2019;134(24):2149-2158.

148. Zhang X, Lu XA, Yang J, et al. Efficacy and safety of anti-CD19 CAR T-cell therapy in 110 patients with B-cell acute lymphoblastic leukemia with high-risk features. Blood Adv. 2020;4(10):2325-2338.

149. Frismantas V, Dobay MP, Rinaldi A, et al. Ex vivo drug response profiling detects recurrent sensitivity patterns in drug-resistant acute lymphoblastic leukemia. Blood. 2017;129(11):e26-e37.

New insights into the basic biology of acute graft-*versus*-host-disease

Alicia Li,[1] Ciril Abraham,[1] Ying Wang[1,2] and Yi Zhang[1,2]

[1]Fels Institute for Cancer Research & Molecular Biology and [2]Department of Microbiology and Immunology, Lewis Katz School of Medicine, Temple University, Philadelphia, PA, USA

ABSTRACT

Although allogeneic hematopoietic stem cell transplantation is an important therapy for many hematologic and non-hematologic diseases, acute graft-*versus*-host disease (aGvHD) is a major obstacle to its success. The pathogenesis of aGvHD is divided into three distinct phases which occur largely as the result of interactions between infused donor T cells and numerous cell types of both hematopoietic and non-hematopoietic origin. In light of the disease's immensely complex biology, epigenetics has emerged as a framework with which to examine aGvHD. This review focuses on new findings that clarify the roles that specific epigenetic regulators play in T-cell-mediated aGvHD development and discusses how their modulation could disrupt that process with beneficial effects. DNA methyltransferases, histone methyltransferases and histone deacetylases are the most closely studied regulators across aGvHD priming, induction and effector phases and have been manipulated using drugs and other methods in both murine models and clinical trials, with varying degrees of success. Antigen-presenting cells, effector T cells and memory T cells, among others, are targeted and affected by these regulators in different ways. Finally, our review highlights new directions for study and potential novel targets for modulation to abrogate aGvHD.

Introduction

The success of allogeneic hematopoietic stem cell transplantation (allo-HSCT) is significantly hampered by acute graft-*versus*-host disease (aGvHD), which is caused by donor T cells that recognize and react to histocompatibility differences between the donor and host. It occurs in sequential priming, induction and effector phases (Figure 1).[1] During priming, preparative irradiation and chemotherapeutic regimens for allo-HSCT can damage the patient's tissues, leading to release of damage-associated molecular patterns (DAMP) and pathogen-associated molecular patterns (PAMP), as well as activation of host antigen-presenting cells (APC) such as dendritic cells.[1-6] Activated APC, including hematopoietic and non-hematopoietic cells, upregulate antigen-presenting molecules and costimulatory molecules to prime transplanted donor T cells.[1-7] During induction, T-cell receptors on donor T cells react to alloantigens presented by host APC and undergo robust proliferation and differentiation into effector T cells that produce pro-inflammatory cytokines such as tumor necrosis factor (TNF)-α, interferon (IFN)-γ and interleukin (IL)-17.[1] Upon persistent exposure to host alloantigens, most of these effector cells (~90%) undergo apoptotic contraction, but a proportion survive and become memory T cells.[8-10] The final effector phase is characterized by infiltration of alloreactive effector cells into aGvHD target organs.[1] Tissues already damaged by preparative treatments produce chemokines, recruiting T cells to their vicinity.[1,11] The effector T cells recognize and react to host alloantigens, mediating host tissue injury. The damaged host tissues recruit more alloreactive T cells and other types of inflammatory cells (e.g., monocytes/macrophages and granulocytes), leading to feed-forward amplification and continuation of aGvHD (Figure 1).[1,2,4] Chronic GvHD may arise following or independently of aGvHD, but due to the conditions' differing pathogeneses and clinical manifestations, chronic GvHD will not be discussed in this review.

Because aGvHD is T-cell-mediated, significant progress has been made in understanding how alloreactive T cells are induced and sustained. APC may be primed

Figure 1. Role of epigenetic regulators in the development of acute graft-*versus*-host-disease. Acute graft-versus-host disease (aGvHD) develops through three sequential phases: priming, induction and effector. In some cases, following prophylactic treatment and conditioning, the integrity of the intestinal epithelium becomes compromised and leads to the release of damage-associated molecular patterns (DAMP) and pathogen-associated molecular patterns (PAMP). These molecules result in the activation of hematopoietic and non-hematopoietic antigen-presenting cells (APC). Subsequent APC interactions lead to the activation, differentiation and proliferation of T cells. The different subsets of T cells play numerous roles in the pathogenesis of aGvHD. Th1, Th2, Th17, and the cytotoxic T cells interact with target organs to promote tissue damage. In the intestines, intestinal stem cells are notably damaged, impairing tissue regeneration capabilities, contributing to the feed-forward cascade of aGvHD. Epigenetic regulators play a role in each of the three phases allowing for the possibility of therapeutic interventions. HDAC: histone deacetylase; IL: interleukin; DLL: delta-like; IFN: interferon; TNF: tumor necrosis factor; DNMT: DNA methyltransferases

to produce special cytokines (e.g., IL-12, IL-23) and Notch ligands (e.g., Delta-like 1 and 4; DLL1 and DLL4) which instruct antigen-activated T cells to differentiate into distinct lineages of GvHD-mediating effector T cells.[5,12-15] Other groups have reviewed these topics elegantly, so we focus on a related area of investigation: understanding how extracellular stimuli are converted to gene programs that promote or abrogate alloreactive T-cell development and responses, and leveraging them to reduce aGvHD.

Epigenetic modifications are one such mechanism. Epigenetics refers to heritable molecular determinants of phenotype that are independent of DNA sequence. Major contributors include DNA methylation on cytosine nucleotides, histone modification and chromatin structure. Proteins governing these modifications have loosely been termed epigenetic regulators.[16] This review will discuss advances in our understanding of epigenetic regulation, either by direct effects or *via* interactions with other molecules, of alloreactive T-cell responses and these responses' roles in aGvHD; we identify the roles that specific regulators play and interventions targeting these reg-

ulators for aGvHD prevention and treatment (Table 1). We also acknowledge the contributions of non-hematopoietic cells to the development of aGvHD, whether *via* their own function or their impact on T cells.

Epigenetic effects on and sensitization of antigen-presenting cells

To allow for proper engraftment, allo-HSCT patients may undergo conditioning regimens before donor T cells are infused. Consequently, DAMP from injured cells, PAMP from gut bacteria and pro-inflammatory cytokines are released, priming APC.[1] In the setting of murine allo-HSCT, non-hematopoietic APC, alongside professional hematopoietic APC, are also known to prime alloreactive T cells.[2,6,17] Upon activation following tissue damage, APC upregulate major histocompatibility complex class II and costimulatory molecules (e.g., CD40, CD80, CD86) and secrete cytokines (e.g., IL-4, IL-12, IL-23, DLL1, DLL4),

Table 1. Preclinical studies of acute graft-*versus*-host disease investigating epigenetic mechanisms.

Enzyme	Cells	Key findings
EZH2	CD8+/CD4+ T cells	*Ezh2* KO impairs proliferation, differentiation and expansion; it reduces aGvHD but preserves GvL.[28] Ezh2 inhibition with DZNep inhibits ongoing GvHD but preserves the GvL effect.[30]
	CD8+/CD4+ T cells	Administration of the EZH2 inhibitor GSK126, which specifically reduces H3K27me3 without affecting the protein, failed to prevent aGvHD in mice. In contrast, targeting T-cell EZH2 protein by inhibiting HSP90 reduced aGvHD in mice undergoing allo-HSCT.[33]
	CD8+ T cells	EZH2 controls CD8+ T memory precursor formation and antitumor activity.[32]
DNMT	CD8+/CD4+ T cells	Inhibition impairs activation, expansion, and secretion of cytokines.[43]
	Treg	Inhibition by Aza increased Treg frequency through hypomethylation of *Foxp3*.[42, 43, 67]
HDAC (Pan)	CD8+/CD4+ T cells	Pan-inhibition using SAHA results in reduced proliferative and cytotoxic activity of anti-CD3 activated T cells.[34]
HDAC6	CD8+ T cells	Inhibition of HDAC6 impairs CD8+ T-cell proliferation and function in a GvHD-like model.[38]
HDAC11	CD8+/CD4+ T cells	KO of *Hdac11* increased T-cell proliferation rates and effector function resulting in more rapid and potent aGvHD.[36]
SIRT3	CD8+/CD4+ T cells	Loss of *Sirt3* results in decreased aGvHD severity due to decreased activation and production of ROS while maintaining GvT.[40]
HDAC (Pan)	APC	Pan-inhibition of HDAC with SAHA reduced aGvHD, resulting in a drastic decrease in pro-inflammatory cytokine expression and induced high level expression of IDO to suppress alloreactive T cells.[20, 23]
HDAC (Pan)	IEC	Butyrate treatment reduced GvHD severity, improved IEC junction integrity and reduced IEC apoptosis. In addition, the decrease in H4 acetylation, butyrate transporter and receptor levels due to allo-HSCT inflammation were reversed.[90]

EZH2: enhancer of zeste homolog 2; KO: knockout; aGvHD: acute graft-*versus*-host-disease; GvL:graft-*versus*-leukemia; H3K27me3: histone 3 lysine 27 trimethylation; HSP90: heat shock protein 90; allo-HSCT: allogeneic hematopoietic stem cell transplantation; DNMT: DNA methyltransferases; Treg: regulatory T cell; Aza: 5-azacytidine; HDAC: histone deacetylase; SAHA: suberoylanilide hydroxamic acid; ROS: reactive oxygen species; GvT: graft-*versus*-tumor; IDO: indoleanime-2,3-deoxygenase; APC: antigen-presenting cell; IEC: intestinal epithelial cell; H4: histone 4

shaping T-cell responses.[5,12-15] Immunosuppressive molecules such as IL-10, indoleamine-2,3-dioxygenase (IDO) and programmed death ligand 1 (PD-L1) may be upregulated to repress alloreactive T-cell responses, shifting them to become tolerogenic.[18-21] Epigenetic regulators convert these signals into the aforementioned markers and molecules.

Histone deacetylases' multiple functions in the sensitization of hematopoietic antigen-presenting cells

Two classes of enzyme regulate histone acetylation status: histone acetyltransferases (HAT) and histone deacetylases (HDAC). HAT acetylate histone lysine substrates and open compacted chromatin, allowing transcription factors to access DNA.[22] HDAC decrease histone lysine tail acetylation, repressing gene transcription.[16] Epigenetic studies of hematopoietic APC sensitization have primarily focused on the impact of HDAC (Figure 1).

One of the first studies anchoring epigenetics to aGvHD, helmed by Reddy and colleagues, brought to light the role of histone acetylation in aGvHD.[23] HDAC are important for APC production of pro-inflammatory cytokines and immunosuppressive molecules.[20,23] Preclinical studies have shown that *in vivo* administration of the pan-HDAC inhibitor suberoylanilide hydroxamic acid (SAHA) reduced aGvHD.[23] SAHA treatment did not impair T-cell responses to host antigens, but significantly decreased the production of inflammatory cytokines, TNF-α, IL-1 and IFN-γ, by APC. Subsequent studies confirmed that treatment with SAHA resulted in a marked decrease in pro-inflammatory cytokines (e.g., TNF-α, IL-

12, IL-6) in APC, which are important in promoting alloreactive T-cell responses.[20] SAHA inhibited IL-6 production in dendritic cells stimulated by variable toll-like receptor (TLR) agonists (e.g., TLR2, TLR3, TLR4 and TLR9). In lipopolysaccharide-stimulated dendritic cells, SAHA treatment induced high-level expression of IDO to suppress alloreactive T-cell responses.[20]

Villagra *et al.* highlighted the importance of HDAC11 in repressing the negative regulation that murine APC exerted on T-cell responses.[18] Using chromatin immunoprecipitation, researchers determined that upon overexpression of HDAC11 in APC, there was decreased acetylation of histone 4 (H4) at the distal *Il10* promoter. This was associated with decreased IL-10 transcription upon lipopolysaccharide stimulation. In contrast, HDAC11 knockdown using shRNA had the opposite effect, resulting in the induction of IL-10 expression. Accordingly, silencing HDAC11 expression in APC impaired antigen-specific T-cell responses, whereas overexpression of HDAC11 in APC caused tolerant CD4+ T cells to transition to an immunogenic phenotype.[18]

HDAC6 is a positive regulator of tolerogenic APC. Normally, HDAC6 forms a complex with signal transducer and activator of transcription (STAT) 3 that is recruited to the *Il10* promoter. Silencing HDAC6 resulted in decreased STAT3 phosphorylation and reduced IL-10 production.[19] The opposing effects of HDAC11 and HDAC6 in regulating IL-10, a cytokine that can tip the balance between reactivity and tolerance in dendritic cells,[18,19] underline the importance of understanding how individual HDAC regulate APC function. More specific HDAC

inhibitors, rather than pan-HDAC inhibitors, may be appropriate targets for further study.

Sensitization of non-hematopoietic cells

Emerging evidence indicates the importance of non-hematopoietic cells in aGvHD.[17] Koyama *et al.* demonstrated that antigen presentation from non-hematopoietic cells could induce lethal aGvHD independently of T-cell interactions with hematopoietic APC.[2] Microbiota in the gastrointestinal tract can secrete IL-12 to induce major histocompatibility complex class II upregulation on intestinal epithelial cells (IEC), initiating lethal aGvHD.[6] In addition, fibroblastic stromal cells in the lymph nodes have been shown to drive aGvHD through the presentation of Delta-like Notch ligands, DLL1 and DLL4 specifically.[5] Inhibition of the Notch ligands and receptors conferred protection against GvHD in murine models.[5] However, we have a limited understanding of the epigenetic effects these non-hematopoietic cells have on aGvHD. In the light of these striking findings, this represents an important avenue for future investigation.

Epigenetic control of alloreactive T cells

Upon encountering allogeneic host APC, infused donor T cells are activated and undergo robust proliferation and differentiation into effector T cells (Figure 1), which include IFN-γ-producing CD4+ Th1 cells, IL-4-producing CD4+ Th2 cells, IL-17-producing CD4+ Th17 cells and cytotoxic CD8+ T cells.[1] Effector T cells mediate tissue injury during aGvHD. Alloantigen-sensitized donor T cells can also become memory T cells that mediate persistent host tissue injury. Over the past two decades, much research has been undertaken to understand the molecular mechanisms that control the generation and maintenance of alloreactive effector and memory T cells during the induction phase of aGvHD.

Epigenetic programming of effector T-cell responses
EZH2

Enhancer of zeste homolog 2 (EZH2) is a histone methyltransferase that catalyzes histone 3 lysine 27 trimethylation (H3K27me3), which primarily silences genes,[24] and is a core component of the polycomb repressive complex-2 (PRC2).[24] Evidence suggests that EZH2 is involved in Th1 and Th2 polarization[25] as well as the proliferation and differentiation of hematopoietic stem cells.[26] EZH2 is also involved in cancer development and progression,[24] which has stimulated efforts to develop methods of inhibiting the enzyme.

EZH2 plays an essential role in T-cell immune responses. Studies by our group[27-30] and others[31] have demonstrated the functional relevance of EZH2 in regulating antigen-driven T-cell responses. Using experimental murine models, we discovered EZH2's role in regulating allogeneic T-cell proliferation, differentiation and function.[27,28] Conditional loss of *Ezh2* in donor T cells inhibited aGvHD in mice. Although EZH2-deficient T cells could be activated and underwent initial proliferation, their ability to undergo continual proliferation and expansion became defective during the later stage of aGvHD induction.[28] Unexpectedly, as a gene silencer, EZH2 was required to promote the expression of transcription factors T-bet and STAT4, which are critical for effector differentiation.[27]

Subsequent studies revealed that EZH2 regulation of transcription factor expression and function depends on the differentiation stage of antigen-driven T cells.[32] *Ezh2* knockout in T cells impaired their differentiation into IFN-γ-producing effector cells.[28] However, *Ezh2* ablation, EZH2 protein inhibition and EZH2 protein destabilization all did not affect graft-*versus*-leukemia activity, leading to improved overall survival in recipients.[28,30,33] Thus, targeting EZH2 may represent an effective therapeutic strategy for aGvHD prevention and treatment.

HDAC1, HDAC6 and HDAC11

HDAC are important for regulating the proliferative and cytotoxic capabilities of activated T cells. Pharmacological inhibition of HDAC by SAHA has been shown to suppress T-cell-receptor-mediated T-cell proliferation through the induction of apoptosis.[34] *Hdac1* knockout in a murine allergic asthma model showed a significant increase in airway inflammation and Th2 cytokine production.[35] Upon *Hdac1* deletion, *in vitro* studies noted an enhanced induction of Th1 and Th2 cells.[35] Thus, HDAC1 plays a negative regulatory role for the functions of Th1 and Th2 subsets.

In T cells, HDAC11 may suppress the graft-*versus*-host reaction. *Hdac11* knockout resulted in increased T-cell proliferation and release of pro-inflammatory cytokines associated with upregulation of eomesodermin (EOMES) and T-bet which are important in effector differentiation.[36] Indeed, decreased expression of HDAC11 exacerbated aGvHD in mice.[36]

HDAC6 can deacetylate non-histone proteins such as heat shock protein 90 (HSP90).[37] Acetylation disrupts HSP90's chaperone function and inhibits LCK phosphorylation.[38] In a GvHD-like model involving OT-I T-cell transplants to K14-mnOVA mice, control mice developed mucosal and skin lesions, while inhibition of HDAC6 using a specific inhibitor, ACY-1215, prevented similar lesions from forming for 14 days after transplantation. This protective effect was accompanied by dramatically decreased production of CD8+ effector T cells that secreted high levels of IL-2 and IFN-γ.[38] Further studies of these HDAC should be conducted in GvHD models to definitively validate their roles in driving or mitigating aGvHD.

SIRT3

SIRT3 is a mitochondrial HDAC that regulates metabolic enzyme acetylation.[39] SIRT3 is expressed in metabolically stressed cells such as alloreactive T cells.[40] Loss of SIRT3 in donor T cells led to decreased GvHD severity in mice. The protective effect associated with *Sirt3* deletion was associated with a reduction in reactive oxygen species and decreased activation and expression of chemokine receptor CXCR3.[40]

DNMT

Because DNA methyltransferases (DNMT) – DNMT1, DNMT3A, DNMT3B and DNMT3L – can enact global transcription suppression, they have been widely studied in the context of immunity. DNMT1 is the principal enzyme that maintains methylation across DNA replication.[41] DNMT3A and DNMT3B contribute to methylation maintenance and are also responsible for *de novo* DNA methylation.[41] DNMT inhibitors such as 5-azacytidine (Aza) have been shown to impair T-cell activation, expansion and cytokine release early in culture *via* downregula-

tion of cell cycle- and cytokine-related genes.[42] Sánchez-Abarca *et al.* treated mice undergoing allo-HSCT with Aza and found that early treatment prevented aGvHD development without increasing regulatory T cells (Treg); researchers speculated that this was likely due to Aza inhibition of T-cell expansion, which had been demonstrated *in vitro*.[42] In a humanized murine allo-HSCT, xenogeneic GvHD model, Aza treatment was also noted to decrease the frequency of IFN-γ-secreting CD4^{+} human T cells and granzyme B- and perforin 1-secreting CD8^{+} human T cells *in vivo*.[43] Using *Dnmt3a* conditional knockout mice, a recent study by Youngblood *et al.* revealed the importance of DNMT3A in the regulation of T-cell exhaustion.[44] Moving forward, similar genetic approaches will be useful in understanding the precise mechanisms of the effect of DNMT inhibition on aGvHD.

Epigenetic programming of alloreactive memory T cells

A hallmark of aGvHD is cytopathic injury mediated by persistent alloreactive effector T cells, which can occur within weeks and persist for years after transplantation.[1,7-9,29] Data from our[8,9,29] studies suggest that memory T cells that develop during aGvHD sustain alloreactive effector cells.[8,9,29] These alloantigen-sensitized memory T cells differ from naturally-occurring T cells because the ability of memory T cells to mediate aGvHD is limited by their T-cell receptor repertoires.[45] Memory T cells are generated during the primary immune response from proliferating T cells upon APC activation.[46] After re-encountering antigens, they undergo rapid and robust proliferation and elaboration of effector function. They have stem cell-like self-renewal properties, are distinguishable from both naïve and effector T cells and are resistant to existing immunosuppressive agents.[47,48] In fact, whether or not their resilience contributes to the low response rates to current aGvHD therapies (~40%) is the subject of ongoing debate.[1, 7-9]

EZH2

EZH2 is required for the development of memory precursors early after antigenic priming, for the maturation of memory T cells and for the recall response of mature memory T cells.[32] EZH2 deficiency in activated CD8^{+} T cells caused significant skewing toward central memory precursors and drastically increased the relative proportion of terminally differentiated effector cells that were unable to contribute to further expansion.[32] EZH2 repressed the expression of Blimp-1, ID2 and EOMES, which promote effector differentiation, and promoted and sustained expression of ID3, a gatekeeper critical for memory formation and survival.[32] Given EZH2's crucial roles in the regulation of alloreactive T cells, EZH2-mediated memory formation may be responsible for the generation and maintenance of alloreactive memory T cells during aGvHD.

Other regulators

Histone methyltransferase SUV39H1 may play a role in repressing memory genes. Upon infection with *Listeria monocytogenes*, SUV39H1-defective CD8^{+} T cells demonstrated enhanced "long-term memory reprogramming," allowing them to persist in mice.[49] The Mixed-Lineage Leukemia gene encodes histone lysine methyltransferase 2A and may be a regulator of memory Th2 cells.[50] Protein arginine methyltransferase 5 (PRMT5) has also been implicated as a supporter of memory T-cell reactivation; its inhibition suppressed memory Th1 responses in experimental autoimmune encephalitis.[51] We anticipate continued studies of these epigenetic regulators that consider their relevance to aGvHD.

Epigenetic regulation of regulatory T cells

Treg with CD4^{+}CD25^{+}FOXP3^{+} phenotype can suppress immune responses *via* cytokine- and contact-dependent mechanisms.[1,52] Stable Forkhead box P3 (FOXP3) expression has been considered a critical determinant of Treg identity and activity, but some suggest this characterization may be incomplete, pointing to the importance of independent epigenetic alterations.[53] Natural Treg (nTreg) and induced Tregs (iTreg) are the most closely-studied Treg subsets in aGvHD; nTreg develop within the thymus while iTreg arise from activated CD4^{+} T cells in the periphery.[54] Because they can repress T-cell proliferation and survival, Treg have been established as an important cell population in reducing aGvHD.[55,56] Indeed, infusion of nTreg into allo-HSCT mice abrogated aGvHD lethality,[57] and iTreg have been shown to suppress aGvHD in allogeneic models.[58,59] While nTreg use has achieved preliminarily promising results in clinical trials,[56] the potential of iTreg is less clear. Each has disadvantages; there are few nTreg in the peripheral blood and their use requires *ex vivo* expansion.[60] On the other hand, iTreg, with unstable FOXP3 expression, are often unable to maintain a suppressive phenotype.[61-63]

DNMT

Researchers have attempted to stabilize FOXP3 expression by maintaining demethylation of the *Foxp3* locus.[64,65] As DNMT are involved in maintaining methylation, they are thought to contribute to Foxp3 suppression. Indeed, without demethylation of a CpG island in the *Foxp3* locus, cells' FOXP3 expression and suppressive ability are limited.[66] The use of DNMT inhibitors to sustain Treg stability and abrogate aGvHD has achieved some success.

Choi *et al.* showed that treatment with the DNMT inhibitors decitabine and Aza induced Treg from CD4^{+}CD25^{-} cells.[67] Transplantation of decitabine- and Aza-treated cells into mice undergoing allo-HSCT reduced clinical aGvHD and improved survival.[67] Directly treating mice with Aza after allo-HSCT resulted in similar effects. Interestingly, these suppressive effects of iTreg were found to be maintained even in *Foxp3* knockout cells, suggesting that their anti-GvHD activity may be downstream or independent of FOXP3 expression.[67] In a humanized murine allo-HSCT, xenogeneic GvHD model, *in vivo* Aza treatment was associated with longer survival and lower xenogeneic GvHD scores.[43] Researchers suggested that Aza treatment induced Il2 promoter hypomethylation, leading to increased IL-2 expression and augmented Treg proliferation.[43]

EZH2

EZH2 is known to co-localize with FOXP3[68] and has also been implicated in the maintenance of Treg identity after activation.[69] Tumes *et al.* noted that iTreg differentiation is impaired without EZH2.[31] Ablation of *Ezh2* led to autoimmunity associated with a faulty FOXP3-depen-

dent gene expression program in activated Treg.[69] *Ezh2* deletion in *in vivo* murine Treg reprogrammed them to express an effector phenotype that could potentially be unfavorable for aGvHD.[70] *In vitro* pharmacological EZH2 inhibition also impaired iTreg differentiation, resulting in a significantly decreased frequency of iTreg.[70] Human iTreg treated with the same inhibitor were unable to maintain suppressive activity.[70] However, since inhibition of EZH2 potently suppressed persistence and expansion of effector T cells, the impact of pharmacological inhibition of EZH2 on Treg is likely context-dependent.

HDAC

Akimova *et al.* established that human Treg express a unique combination of HDAC compared to effector T cells, and that treatment with several different HDAC inhibitors augmented the suppressive function of Treg *in vitro*.[71] Specific HDAC have been implicated in modulating Treg function, including HDAC3 (for both nTreg and iTreg),[72] HDAC9 and HDAC6. Inhibition of HDAC9 had a positive effect on FOXP3 expression and nTreg generation.[73] Deletion of *Hdac6* or *Sirt1* resulted in similar increases in FOXP3 expression and augmented nTreg function.[74] Interestingly, combined pharmacological inhibition of HDAC6 and SIRT1 had a synergistic effect on increasing nTreg function *in vivo* in mice. It is likely that the two enzymes share mechanisms in their effect *via* the deacetylation of FOXP3.[74] However, because these studies were not conducted in the context of GvHD, their results should be taken as an indication for GvHD study in the future.

In the gut, butyrate and other short-chain fatty acids (SCFA) produced by commensal bacteria may also assist with the induction and maintenance of Treg in the periphery.[75,76] Possessing more Lachnospiraceae- and Ruminococcaceae-family bacteria, which belong to the class *Clostridia*, was correlated with greater H3 acetylation, a greater Treg/Th17 cell ratio and greater protection against aGvHD.[77] Members of the *Clostridia* class produce SCFA that comprise colonocytes' primary energy source.[78] The SCFA butyrate has notable HDAC inhibitory activity.[79] Butyrate delivery *via* drinking water increased peripheral Treg in mice treated with broad-spectrum antibiotics.[75] Notably, this increase did not occur in mice deficient in the conserved non-coding sequence (CNS) 1 enhancer, which is part of the *Foxp3* locus. Treg isolated from these mice exhibited improved suppressor function *in vitro* compared to antibiotic-treated mice that did not receive butyrate. Treating CD4+ T cells with butyrate during non-specific activation *in vitro* was also able to induce Treg, so researchers examined the effect of the treatment on *Foxp3* locus deacetylation. Butyrate-treated naïve CD4+FOXP3- T cells that were non-specifically activated for 3 days showed significant increases in *Foxp3* promoter and CNS 1, 2 and 3 acetylation at H3K27.[75]

Furusawa *et al.* noted that feeding mice with butyrylated high-amylose maize starches significantly increased differentiation of colonic Treg; these Treg were able to suppress chronic intestinal inflammation brought on by adoptive transfer of CD4+CD45RBhi cells into *Rag1−/−* mice.[76] Through chromatin immunoprecipitation analysis, researchers verified that butyrate treatment increased global acetylation levels, but also acetylation at histone H3 at (i) the *Foxp3* promotor region and CNS3 prior to FOXP3 induction and (ii) CNS1 over the course of Treg differentiation.[76] Though not directly related to aGvHD, these are important findings pertaining to gut inflammation that should provide direction for further study.

Other regulators

Endothelial cell dysfunction, specifically the loss of endothelial cell-derived thrombomodulin, has been associated with steroid-refractory aGvHD.[80] Ranjan *et al.* showed that thrombomodulin is essential for the generation of protease-activated protein C; incubation of human T cells with activated protein C prior to their transplantation into humanized mice increased Treg frequency and improved xenogeneic GvHD compared to non-incubated human T cells.[80] This activity was speculated to take place *via* an epigenetic pathway that has yet to be investigated.

Epigenetic programs that influence tissue injury and regeneration during acute graft-*versus*-host disease

The effector phase is characterized by migration and infiltration of alloreactive effector cells into aGvHD target organs and cytotoxic attack (Figure 1). Areas surrounding tissue commonly affected by aGvHD produce chemokines (e.g., CXCL9 and CXCL10) that recruit effector T cells.[1,11] The cells recognize major histocompatibility complex and/or minor histocompatibility antigen mismatches and attack tissue *via* a cytotoxic response mediated by cell-surface factors and cytokines. Alloreactive effector T cells attack tissue through mechanisms that include Fas-Fas ligand interactions, perforin- and granzyme-mediated killing and TNF-α induction of cell death.[1]

Concurrently, tissue regeneration from both cytotoxic damage and potentially pre-allo-HSCT conditioning commences. Intestinal stem cells (ISC) are crucial for the regeneration of the intestinal epithelium after injury. However, ISC are also a target of effector T cells during aGvHD, causing the intestinal epithelium to be trapped in a cycle of repeated damage. Interestingly, IL-22 plays a central role in protecting the intestinal epithelium and ISC.[81,82] During aGvHD, IL-23-responsive intestinal lymphoid cells produce and secrete IL-22. However, intestinal lymphoid cells are also targeted and eliminated during disease progression, leading to IL-22 deficiency and further ISC damage.[81] Regeneration can be boosted through Wnt pathway stimulation using the Wnt agonist R-Spondin1.[83] Treatment with R-Spondin1 before allo-HSCT expanded ISC and treatment after transplant enhanced surviving ISC proliferation, allowing for fortification of the intestinal lumen and aGvHD inhibition.[83]

Little is known about epigenetic regulation of the Wnt pathway-dependent and IL-22-mediated regeneration processes in the context of GvHD. Recent studies have suggested that BMI1, a polycomb repressive complex-1 (PRC1) component important for hematopoietic stem cell renewal, is expressed in the ISC and progenitor compartments.[84] PRC1 is known to enact its function in gene silencing *via* recognition of H3K27me3.[85] *Bmi1* knockout resulted in reduced ISC proliferation and significant increases in cell cycle regulators p16INK4a and p19ARF84.[84]

BMI1 contributes to ISC self-renewal, which is co-regulated by the Wnt pathway and Notch. The interaction between BMI1 and the Wnt pathway in regulating stem cell self-renewal has been validated in a separate study.[86]

Yeste *et al.* noted that STAT3 regulates *Il22* promoter accessibility.[87] When STAT3-deficient CD4^{+} T cells were activated in the presence of IL-21, which normally induces *Il22* transcription, IL-22 production was significantly decreased. STAT3-deficient cells also showed decreases in H3 and H4 acetylation, decreases in H3K4me3 and increases in H3K9me3 and H3K27me3 at the *Il22* promoter. This could involve a number of epigenetic regulators, including histone methyltransferases (e.g., G9A, SUV39H1, EZH2) and enzymes that modify histone acetylation.[87]

Recent studies have also implicated the microbiome in aGvHD development and exacerbation. The inflammatory conditions associated with aGvHD, as well as pre-transplant preparatory regimens, can harm commensal bacteria populations and compromise the normal functioning of gastrointestinal cells, which in turn result in more severe aGvHD.[88-90] For instance, aGvHD inflammation was associated with a loss of SCFA-producing bacteria in the *Clostridiales* order in both humans and mice.[89] Mathewson *et al.* showed that the levels of the HDAC inhibitor butyrate in IEC were significantly decreased after exposure to allo-HSCT inflammation; this led to decreased histone H4 acetylation and decreased expression of the butyrate transporter and receptor, SLC5A8 and GPR43, respectively, in IEC.[90] Increasing intragastric butyrate levels restored H4 acetylation, decreased GvHD severity and improved IEC junction integrity.[90] Butyrate treatment was also associated with significantly less IEC apoptosis; among other effects, treatment led to lower expression of pro-apoptotic proteins, higher expression of the anti-apoptotic protein BCL-2 and higher expression of junctional proteins occludin and JAM.[90] The promoter regions of *Bcl220* (encoding BCL-2) and *Fllr* (encoding JAM) were noted to be directly associated with H4 acetylation.[90] Though the study did not discuss these changes' impact on recipient physiology, it is plausible that increased IEC junction integrity and decreased apoptosis prevented immune cell infiltration and PAMP/DAMP from escaping the gut, reducing the severity of the aGvHD.

Deeper examination of this aspect of aGvHD biology and its associated pathways is crucial because it represents a less commonly pursued paradigm in aGvHD treatment: fostering recovery of damaged tissues (Figure 1).[91]

Pharmacological modulation of acute graft-*versus*-host disease by targeting epigenetic pathways

Development of epigenetic therapy is a particularly active area of cancer research because of such therapies' potential to selectively target chromatin-modifying enzyme-mediated disease mechanisms.[16] Epigenetic therapy may produce fewer adverse effects than conventional cytotoxic chemotherapies and may influence response to immunotherapy in various cancers. This logic applies to the search for drugs which modify epigenetic mechanisms controlling alloreactive T-cell responses to reduce aGvHD while preserving graft-*versus*-leukemia activity (Table 2).

HDAC inhibitors

In two clinical trials, patients receiving related and unrelated donor HSCT were treated with the pan-HDAC inhibitor vorinostat (SAHA) after myeloablative conditioning to determine the drug's efficacy at preventing aGvHD. Clinical trials showed a cumulative incidence of grade II-IV aGvHD of 22% by day 100.[92,93] Correlative tests on vorinostat-treated patients' blood samples showed a significant reduction in IL-6.[93] Overall, treatment with vorinostat was deemed a safe and efficacious strategy for preventing GvHD. Treatment with the pan-HDAC inhibitor panobinostat, in conjunction with corticosteroids, was also recently investigated for the mitigation of ongoing GvHD.[94] Treatment had an approximately 40% response rate, and these responses were noted across grades II and III GvHD in different organ systems. The results are inconclusive because the trial lacked sufficient power, but are nevertheless promising.[94]

DNMT inhibitors

Clinically, Aza and decitabine have been used in the context of allo-HSCT for the express purpose of reducing the disease burden before transplantation and as maintenance

Table 2. Selected clinical trials of epigenetic inhibitors in acute graft-*versus*-host disease.

Drug	Main Conclusion
Vorinostat (SAHA)	HDAC inhibition with vorinostat in combination with standard prophylaxis resulted in reduced incidence of severe aGvHD. Phase I/II trial.[92]
	HDAC inhibition with vorinostat was safe and efficacious in unrelated donor allo-HSCT patients receiving myeloablative conditioning and methotrexate. Results showed a low cumulative incidence of severe aGvHD. Phase II trial.[93]
Panobinostat	HDAC inhibition with panobinostat in addition to glucocorticoids as primary therapy for aGvHD was deemed safe. However, the study did not have sufficient power to address efficacy. Phase I/II trial.[94]
5-Azacytidine	DMNT inhibition by Aza after donor lymphocyte infusion as salvage therapy was well tolerated and no patients developed grade III-IV aGvHD. Phase I trial.[95]
	DMNT inhibition by Aza after allogenic stem cell transplantation increased circulating Treg in patients. Phase I/II trials.[96]

SAHA: suberoylanilide hydroxamic acid; HDAC: histone deacetylase; aGVHD: acute graft-*versus*-host-disease; allo-HSCT: allogeneic hematopoietic stem cell transplantation; Aza: 5-azacitidine; DNMT: DNA methyltransferase; Treg: regulatory T cell

and salvage therapy.[99] In studies using Aza or decitabine treatment in the setting of blood cancers or myelodysplastic syndromes to reduce disease burden before transplantation, there were no significant findings with regard to aGvHD.[98,99] DNMT inhibitor treatment after allo-HSCT has typically been a component of salvage or maintenance therapy and has had some success in mitigating aGvHD. Ghobadi *et al.* treated patients with Aza after donor lymphocyte infusion; no patients developed severe aGvHD (III-IV) and there was no aGvHD-caused mortality.[95] Similarly, Schroeder *et al.* provided Aza treatment alongside donor lymphocyte infusion upon patients' relapse and saw a 3.2-fold increase in Treg and a 1.9-fold increase in Treg frequency after four cycles of Aza treatment in patients who relapsed early after allo-HSCT.[96] Goodyear *et al.* found that although the incidence of aGvHD was lower in treatment groups than in control groups, Treg increases in post-transplant acute myeloid leukemia patients were only observed within the first 3 months of treatment.[97] These results suggest that early treatment may be required for a beneficial effect on aGvHD.

Because of its comparative success, it may be fruitful for future clinical trials to expand on the post-transplant, early HDAC inhibitor treatment paradigm. Of note, DNMT inhibitors were not typically used for aGvHD prevention, so patients often received other treatments (e.g., methotrexate) which were not standardized across studies.

EZH2 inhibitors

In vivo administration of GSK126 failed to reduce aGvHD and did not affect the development of alloreactive effector T cells in preclinical studies.[33] This is in contrast to observations that EZH2 deficiency led to aGvHD blockade in various murine allo-HSCT models.[28] The mechanism of action of EZH2 in mediating aGvHD induction is therefore likely independent of its canonical target H3K27me3.[33] Notably, EZH2 protein depletion by DZNep led to arrest of ongoing GvHD in experimental mice,[30] indicating that targeting EZH2 may lead to new strategies to treat ongoing GvHD.

An interaction between HSP90 and EZH2 has also been shown to be vital for the stability and function of EZH2.[33] A lack of HSP90 marks EZH2 for ubiquitination *via* the proteasome. Treatment of activated T cells with the HSP90 inhibitor AUY922 significantly decreased EZH2 protein levels while leaving histone methylation intact. HSP90 inhibitor treatment significantly decreased alloreactive T-cell responses and aGvHD in mice, affirming EZH2's involvement in aGvHD pathogenesis and the non-canonical hypothesis.[33]

The Food and Drug Administration has approved the EZH2 inhibitor tazemetostat specifically for the treatment of epithelioid sarcoma. We anticipate that this inhibitor may be used to target alloreactive memory T cells to reduce aGvHD in the future.

Future directions

As the epigenetics of aGvHD biology is a young area of study, there is much room for further investigation, both in elucidating mechanisms surrounding the action of known enzymes and in exploring the roles of new regulators documented here and beyond. Nevertheless, enormous progress has been made through the identification of critical enzymes and mechanisms. Next steps will be to further map how their pathways intersect amid the multitude of cell types and interactions that comprise aGvHD. Some epigenetic regulators (e.g., EZH2 and HDAC6) have points of commonality in their mechanisms of action (*via* HSP90).[19,33,37] Advances will illuminate these locations of confluence such that more effective, integrated therapies may be developed. Additionally, a single regulator (e.g., HDAC11) may have beneficial or detrimental effects at different stages of cell development; understanding these situations will be vital for treatment. Also bringing promise for epigenetic intervention are those aspects of aGvHD pathogenesis that are T-cell-independent, such as microbiome injury.

Different tissues, hematopoietic and non-hematopoietic, have distinct roles in mediating aGvHD immunopathology. Further investigation of the epigenetics surrounding the role of non-hematopoietic APC would likely be beneficial for the field. In addition, tissue-intrinsic mechanisms that contribute to inhibition of aGvHD have been somewhat overlooked. These include those controlling tissue regeneration,[81-83] and those modulating tissue-resident APC, which are critical for local aGvHD induction.[100] Furthermore, aGvHD blocks peripheral tolerance of host-reactive T cells by elimination of lymph node fibroblastic reticular cells that induce T-cell tolerance in the gut.[101] Thus, future studies should also investigate the epigenetic mechanisms that regulate tissue regeneration and regulation of the graft-*versus*-host reaction, as suggested by Reddy and colleagues.[91]

References

1. Zeiser R, Blazar BR. Acute graft-versus-host disease - biologic process, prevention, and therapy. N Engl J Med. 2017;377(22):2167-2179.
2. Koyama M, Kuns RD, Olver SD, et al. Recipient nonhematopoietic antigen-presenting cells are sufficient to induce lethal acute graft-versus-host disease. Nat Med. 2011;18(1):135-142.
3. Shlomchik WD, Couzens MS, Tang CB, et al. Prevention of graft versus host disease by inactivation of host antigen-presenting cells.

Science. 1999;285(5426):412-415.
4. Zhang Y, Louboutin JP, Zhu J, Rivera AJ, Emerson SG. Preterminal host dendritic cells in irradiated mice prime CD8+ T cell-mediated acute graft-versus-host disease. J Clin Invest. 2002;109(10):1335-1344.
5. Chung J, Ebens CL, Perkey E, et al. Fibroblastic niches prime T cell alloimmunity through Delta-like Notch ligands. J Clin Invest. 2017;127(4):1574-1588.
6. Koyama M, Mukhopadhyay P, Schuster IS, et al. MHC class II antigen presentation by the intestinal epithelium initiates graft-versus-host disease and is influenced by the microbiota. Immunity. 2019;51(5):885-

898.e7.
7. Wu CJ, Ritz J. Induction of tumor immunity following allogeneic stem cell transplantation. Adv Immunol. 2006;90:133-173.
8. Zhang Y, Joe G, Hexner E, Zhu J, Emerson SG. Host-reactive CD8+ memory stem cells in graft-versus-host disease. Nat Med. 2005;11(12):1299-1305.
9. Zhang Y, Joe G, Hexner E, Zhu J, Emerson SG. Alloreactive memory T cells are responsible for the persistence of graft-versus-host disease. J Immunol. 2005;174(5):3051-3058.
10. Kaech SM, Wherry EJ, Ahmed R. Effector and memory T-cell differentiation: implications for vaccine development. Nat Rev

Immunol. 2002;2(4):251-262.

11. Reshef R, Luger SM, Hexner EO, et al. Blockade of lymphocyte chemotaxis in visceral graft-versus-host disease. N Engl J Med. 2012;367(2):135-145.

12. Palucka K, Banchereau J. Dendritic-cell-based therapeutic cancer vaccines. Immunity. 2013;39(1):38-48.

13. Sandy AR, Chung J, Toubai T, et al. T cell-specific notch inhibition blocks graft-versus-host disease by inducing a hyporesponsive program in alloreactive CD4+ and CD8+ T cells. J Immunol. 2013;190(11):5818-5828.

14. Amsen D, Antov A, Flavell RA. The different faces of Notch in T-helper-cell differentiation. Nat Rev Immunol. 2009;9(2):116-124.

15. Tran IT, Sandy AR, Carulli AJ, et al. Blockade of individual Notch ligands and receptors controls graft-versus-host disease. J Clin Invest. 2013;123(4):1590-1604.

16. Baylin SB, Jones PA. Epigenetic Determinants of Cancer. Cold Spring Harb Perspect Biol. 2016;8(9):a019505.

17. Jones SC, Murphy GF, Friedman TM, Korngold R. Importance of minor histocompatibility antigen expression by non-hematopoietic tissues in a CD4+ T cell-mediated graft-versus-host disease model. J Clin Invest. 2003;112(12):1880-1886.

18. Villagra A, Cheng F, Wang HW, et al. The histone deacetylase HDAC11 regulates the expression of interleukin 10 and immune tolerance. Nat Immunol. 2009;10(1):92-100.

19. Cheng F, Lienlaf M, Wang HW, et al. A novel role for histone deacetylase 6 in the regulation of the tolerogenic STAT3/IL-10 pathway in APCs. J Immunol. 2014;193(6):2850-2862.

20. Reddy P, Sun Y, Toubai T, et al. Histone deacetylase inhibition modulates indoleamine 2,3-dioxygenase-dependent DC functions and regulates experimental graft-versus-host disease in mice. J Clin Invest. 2008;118(7):2562-2573.

21. Ni X, Song Q, Cassady K, et al. PD-L1 interacts with CD80 to regulate graft-versus-leukemia activity of donor CD8+ T cells. J Clin Invest. 2017;127(5):1960-1977.

22. Lee DY, Hayes JJ, Pruss D, Wolffe AP. A positive role for histone acetylation in transcription factor access to nucleosomal DNA. Cell. 1993;72(1):73-84.

23. Reddy P, Maeda Y, Hotary K, et al. Histone deacetylase inhibitor suberoylanilide hydroxamic acid reduces acute graft-versus-host disease and preserves graft-versus-leukemia effect. Proc Natl Acad Sci U S A. 2004;101(11):3921-3926.

24. Margueron R, Reinberg D. The Polycomb complex PRC2 and its mark in life. Nature. 2011;469(7330):343-349.

25. Jacob E, Hod-Dvorai R, Ben-Mordechai OL, Boyko Y, Avni O. Dual function of polycomb group proteins in differentiated murine T helper (CD4+) cells. J Mol Signal. 2011;6:5.

26. Kamminga LM, Bystrykh LV, de Boer A, et al. The Polycomb group gene Ezh2 prevents hematopoietic stem cell exhaustion. Blood. 2006;107(5):2170-2179.

27. Tong Q, He S, Xie F, et al. Ezh2 Regulates transcriptional and posttranslational expression of T-bet and promotes Th1 cell responses mediating aplastic anemia in mice. J Immunol. 2014;192(11):5012-5022.

28. He S, Xie F, Liu Y, et al. The histone methyltransferase Ezh2 is a crucial epigenetic regulator of allogeneic T cell responses mediating graft-versus-host disease. Blood. 2013;122(25):4119-4128.

29. Kato K, Cui S, Kuick R, et al. Identification of stem cell transcriptional programs normally expressed in embryonic and neural stem cells in alloreactive CD8+ T cells mediating graft-versus-host disease. Biol Blood Marrow Transplant. 2010;16(6):751-771.

30. He S, Wang J, Kato K, et al. Inhibition of histone methylation arrests ongoing graft-versus-host disease in mice by selectively inducing apoptosis of alloreactive effector T cells. Blood. 2012;119(5):1274-1282.

31. Tumes DJ, Onodera A, Suzuki A, et al. The polycomb protein Ezh2 regulates differentiation and plasticity of CD4(+) T helper type 1 and type 2 cells. Immunity. 2013;39(5):819-832.

32. He S, Liu Y, Meng L, et al. Ezh2 phosphorylation state determines its capacity to maintain CD8(+) T memory precursors for antitumor immunity. Nat Commun. 2017;8(1):2125.

33. Huang Q, He S, Tian Y, et al. Hsp90 inhibition destabilizes Ezh2 protein in alloreactive T cells and reduces graft-versus-host disease in mice. Blood. 2017;129(20):2737-2748.

34. Li N, Zhao D, Kirschbaum M, et al. HDAC inhibitor reduces cytokine storm and facilitates induction of chimerism that reverses lupus in anti-CD3 conditioning regimen. Proc Natl Acad Sci U S A. 2008;105(12):4796-4801.

35. Grausenburger R, Bilic I, Boucheron N, et al. Conditional deletion of histone deacetylase 1 in T cells leads to enhanced airway inflammation and increased Th2 cytokine production. J Immunol. 2010;185(6):3489-3497.

36. Woods DM, Woan KV, Cheng F, et al. T cells lacking HDAC11 have increased effector functions and mediate enhanced alloreactivity in a murine model. Blood. 2017;130(2):146-155.

37. de Zoeten EF, Wang L, Butler K, et al. Histone deacetylase 6 and heat shock protein 90 control the functions of Foxp3(+) T-regulatory cells. Mol Cell Biol. 2011;31(10):2066-2078.

38. Tsuji G, Okiyama N, Villarroel VA, Katz SI. Histone deacetylase 6 inhibition impairs effector CD8 T-cell functions during skin inflammation. J Allergy Clin Immunol. 2015;135(5):1228-1239.

39. Hirschey MD, Shimazu T, Goetzman E, et al. SIRT3 regulates mitochondrial fatty-acid oxidation by reversible enzyme deacetylation. Nature. 2010;464(7285):121-125.

40. Toubai T, Tamaki H, Peltier DC, et al. Mitochondrial deacetylase SIRT3 plays an important role in donor T cell responses after experimental allogeneic hematopoietic Transplantation. J Immunol. 2018;201(11):3443-3455.

41. Bestor TH. The DNA methyltransferases of mammals. Hum Mol Genet. 2000;9(16):2395-2402.

42. Sanchez-Abarca LI, Gutierrez-Cosio S, Santamaria C, et al. Immunomodulatory effect of 5-azacytidine (5-azaC): potential role in the transplantation setting. Blood. 2010;115(1):107-121.

43. Ehx G, Fransolet G, de Leval L, et al. Azacytidine prevents experimental xenogeneic graft-versus-host disease without abrogating graft-versus-leukemia effects. Oncoimmunology. 2017;6(5):e1314425.

44. Youngblood B, Hale JS, Kissick HT, et al. Effector CD8 T cells dedifferentiate into long-lived memory cells. Nature. 2017;552(7685):404-409.

45. Anderson BE, McNiff J, Yan J, et al. Memory CD4+ T cells do not induce graft-versus-host disease. J Clin Invest. 2003;112(1):101-108.

46. Masopust D, Kaech SM, Wherry EJ, Ahmed R. The role of programming in memory T-cell development. Curr Opin Immunol. 2004;16(2):217-225.

47. Wu Z, Bensinger SJ, Zhang J, et al. Homeostatic proliferation is a barrier to transplantation tolerance. Nat Med. 2004;10(1):87-92.

48. Maltzman JS, Turka LA. T-cell costimulatory blockade in organ transplantation. Cold Spring Harbor Perspect Med. 2013;3(12):a015537.

49. Pace L, Goudot C, Zueva E, et al. The epigenetic control of stemness in CD8(+) T cell fate commitment. Science. 2018;359(6372):177-186.

50. Yamashita M, Hirahara K, Shinnakasu R, et al. Crucial role of MLL for the maintenance of memory T helper type 2 cell responses. Immunity. 2006;24(5):611-622.

51. Webb LM, Amici SA, Jablonski KA, et al. PRMT5-selective inhibitors suppress inflammatory T cell responses and experimental autoimmune encephalomyelitis. J Immunol. 2017;198(4):1439-1451.

52. Negrin RS. Graft-versus-host disease versus graft-versus-leukemia. Hematology. 2015;2015(1):225-230.

53. Ohkura N, Hamaguchi M, Morikawa H, et al. T cell receptor stimulation-induced epigenetic changes and Foxp3 expression are independent and complementary events required for Treg cell development. Immunity. 2012;37(5):785-799.

54. Workman CJ, Szymczak-Workman AL, Collison LW, Pillai MR, Vignali DA. The development and function of regulatory T cells. Cell Mol Life Sci. 2009;66(16):2603-2622.

55. Cohen JL, Trenado A, Vasey D, Klatzmann D, Salomon BL. CD4(+)CD25(+) immunoregulatory T cells: new therapeutics for graft-versus-host disease. J Exp Med. 2002;196(3):401-406.

56. Di Ianni M, Falzetti F, Carotti A, et al. Tregs prevent GVHD and promote immune reconstitution in HLA-haploidentical transplantation. Blood. 2011;117(14):3921-3928.

57. Taylor PA, Lees CJ, Blazar BR. The infusion of ex vivo activated and expanded CD4(+)CD25(+) immune regulatory cells inhibits graft-versus-host disease lethality. Blood. 2002;99(10):3493-3499.

58. Hippen KL, Merkel SC, Schirm DK, et al. Generation and large-scale expansion of human inducible regulatory T cells that suppress graft-versus-host disease. Am J Transplant. 2011;11(6):1148-1157.

59. Li J, Heinrichs J, Haarberg K, et al. HY-Specific induced regulatory T cells display high specificity and efficacy in the prevention of acute graft-versus-host disease. J Immunol. 2015;195(2):717-725.

60. Tang Q, Henriksen KJ, Bi M, et al. In vitro-expanded antigen-specific regulatory T cells suppress autoimmune diabetes. J Exp Med. 2004;199(11):1455-1465.

61. Zhou X, Bailey-Bucktrout SL, Jeker LT, et al. Instability of the transcription factor Foxp3 leads to the generation of pathogenic memory T cells in vivo. Nat Immunol. 2009;10(9):1000-1007.

62. Koenecke C, Czeloth N, Bubke A, et al. Alloantigen-specific de novo-induced Foxp3+ Treg revert in vivo and do not protect from experimental GVHD. Eur J Immunol. 2009;39(11):3091-3096.

63. Beres A, Komorowski R, Mihara M, Drobyski WR. Instability of Foxp3 expres-

sion limits the ability of induced regulatory T cells to mitigate graft versus host disease. Clin Cancer Res. 2011;17(12):3969-3983.

64. Polansky JK, Kretschmer K, Freyer J, et al. DNA methylation controls Foxp3 gene expression. Eur J Immunol. 2008;38(6):1654-1663.

65. Zheng Y, Josefowicz S, Chaudhry A, Peng XP, Forbush K, Rudensky AY. Role of conserved non-coding DNA elements in the Foxp3 gene in regulatory T-cell fate. Nature. 2010;463(7282):808-812.

66. Floess S, Freyer J, Siewert C, et al. Epigenetic control of the foxp3 locus in regulatory T cells. PLoS Biol. 2007;5(2):e38.

67. Choi J, Ritchey J, Prior JL, et al. In vivo administration of hypomethylating agents mitigate graft-versus-host disease without sacrificing graft-versus-leukemia. Blood. 2010;116(1):129-139.

68. Arvey A, van der Veeken J, Samstein RM, Feng Y, Stamatoyannopoulos JA, Rudensky AY. Inflammation-induced repression of chromatin bound by the transcription factor Foxp3 in regulatory T cells. Nat Immunol. 2014;15(6):580-587.

69. DuPage M, Chopra G, Quiros J, et al. The chromatin-modifying enzyme Ezh2 is critical for the maintenance of regulatory T cell identity after activation. Immunity. 2015;42(2):227-238.

70. Goswami S, Apostolou I, Zhang J, et al. Modulation of EZH2 expression in T cells improves efficacy of anti-CTLA-4 therapy. J Clin Invest. 2018;128(9):3813-3818.

71. Akimova T, Ge G, Golovina T, et al. Histone/protein deacetylase inhibitors increase suppressive functions of human FOXP3+ Tregs. Clin Immunol. 2010;136(3):348-363.

72. Wang L, Liu Y, Han R, et al. FOXP3+ regulatory T cell development and function require histone/protein deacetylase 3. J Clin Invest. 2015;125(3):1111-1123.

73. Tao R, de Zoeten EF, Ozkaynak E, et al. Deacetylase inhibition promotes the generation and function of regulatory T cells. Nat Med. 2007;13(11):1299-1307.

74. Beier UH, Wang L, Han R, Akimova T, Liu Y, Hancock WW. Histone deacetylases 6 and 9 and sirtuin-1 control Foxp3+ regulatory T cell function through shared and isoform-specific mechanisms. Sci Signal. 2012;5(229):ra45.

75. Arpaia N, Campbell C, Fan X, et al. Metabolites produced by commensal bacteria promote peripheral regulatory T-cell generation. Nature. 2013;504(7480):451-455.

76. Furusawa Y, Obata Y, Fukuda S, et al. Commensal microbe-derived butyrate induces the differentiation of colonic regulatory T cells. Nature. 2013;504(7480):446-

450.

77. Han L, Jin H, Zhou L, et al. Intestinal Microbiota at engraftment influence acute graft-versus-host disease via the Treg/Th17 balance in allo-HSCT recipients. Front Immunol. 2018;9:669.

78. Lopetuso LR, Scaldaferri F, Petito V, Gasbarrini A. Commensal Clostridia: leading players in the maintenance of gut homeostasis. Gut Pathog. 2013;5(1):23.

79. Waldecker M, Kautenburger T, Daumann H, Busch C, Schrenk D. Inhibition of histone-deacetylase activity by short-chain fatty acids and some polyphenol metabolites formed in the colon. J Nutr Biochem. 2008;19(9):587-593.

80. Ranjan S, Goihl A, Kohli S, et al. Activated protein C protects from GvHD via PAR2/PAR3 signalling in regulatory T-cells. Nat Commun. 2017;8(1):311.

81. Hanash AM, Dudakov JA, Hua G, et al. Interleukin-22 protects intestinal stem cells from immune-mediated tissue damage and regulates sensitivity to graft versus host disease. Immunity. 2012;37(2):339-350.

82. Lindemans CA, Calafiore M, Mertelsmann AM, et al. Interleukin-22 promotes intestinal-stem-cell-mediated epithelial regeneration. Nature. 2015;528(7583):560-564.

83. Takashima S, Kadowaki M, Aoyama K, et al. The Wnt agonist R-spondin1 regulates systemic graft-versus-host disease by protecting intestinal stem cells. J Exp Med. 2011;208(2):285-294.

84. Lopez-Arribillaga E, Rodilla V, Pellegrinet L, et al. Bmi1 regulates murine intestinal stem cell proliferation and self-renewal downstream of Notch. Development. 2015;142(1):41-50.

85. Sangiorgi E, Capecchi MR. Bmi1 is expressed in vivo in intestinal stem cells. Nat Genet. 2008;40(7):915-920.

86. Cho JH, Dimri M, Dimri GP. A positive feedback loop regulates the expression of polycomb group protein BMI1 via WNT signaling pathway. J Biol Chem. 2013;288(5):3406-3418.

87. Yeste A, Mascanfroni ID, Nadeau M, et al. IL-21 induces IL-22 production in CD4+ T cells. Nat Commun. 2014;5:3753.

88. Lee SE, Lim JY, Ryu DB, et al. Alteration of the intestinal microbiota by broad-spectrum antibiotic use correlates with the occurrence of intestinal graft-versus-host disease. Biol Blood Marrow Transplant. 2019;25(10):1933-1943.

89. Jenq RR, Ubeda C, Taur Y, et al. Regulation of intestinal inflammation by microbiota following allogeneic bone marrow transplantation. J Exp Med. 2012;209(5):903-911.

90. Mathewson ND, Jenq R, Mathew AV, et al. Gut microbiome-derived metabolites

modulate intestinal epithelial cell damage and mitigate graft-versus-host disease. Nat Immunol. 2016;17(5):505-513.

91. Wu SR, Reddy P. Tissue tolerance: a distinct concept to control acute GVHD severity. Blood. 2017;129(13):1747-1752.

92. Choi SW, Braun T, Chang L, et al. Vorinostat plus tacrolimus and mycophenolate to prevent graft-versus-host disease after related-donor reduced-intensity conditioning allogeneic haemopoietic stem-cell transplantation: a phase 1/2 trial. Lancet Oncol. 2014;15(1):87-95.

93. Choi SW, Braun T, Henig I, et al. Vorinostat plus tacrolimus/methotrexate to prevent GVHD after myeloablative conditioning, unrelated donor HCT. Blood. 2017;130(15):1760-1767.

94. Perez L, Fernandez H, Horna P, et al. Phase I trial of histone deacetylase inhibitor panobinostat in addition to glucocorticoids for primary therapy of acute graft-versus-host disease. Bone Marrow Transplant. 2018;53(11):1434-1444.

95. Ghobadi A, Fiala MA, Abboud CN, et al. A phase I study of azacitidine after donor lymphocyte infusion for relapsed acute myeloid leukemia post allogeneic stem cell transplantation. Blood. 2013;122(21):3320-3320.

96. Schroeder T, Frobel J, Cadeddu RP, et al. Salvage therapy with azacitidine increases regulatory T cells in peripheral blood of patients with AML or MDS and early relapse after allogeneic blood stem cell transplantation. Leukemia. 2013;27(9):1910-1913.

97. Goodyear OC, Dennis M, Jilani NY, et al. Azacitidine augments expansion of regulatory T cells after allogeneic stem cell transplantation in patients with acute myeloid leukemia (AML). Blood. 2012;119(14):3361-3369.

98. Lübbert M, Bertz H, Ruter B, et al. Non-intensive treatment with low-dose 5-aza-2'-deoxycytidine (DAC) prior to allogeneic blood SCT of older MDS/AML patients. Bone Marrow Transplant. 2009;44(9):585-588.

99. Field T, Perkins J, Huang Y, et al. 5-Azacitidine for myelodysplasia before allogeneic hematopoietic cell transplantation. Bone Marrow Transplant. 2010;45(2):255-260.

100. Zhang Y, Shlomchik WD, Joe G, et al. APCs in the liver and spleen recruit activated allogeneic CD8+ T cells to elicit hepatic graft-versus-host disease. J Immunol. 2002;169(12):7111-7118.

101. Dertschnig S, Evans P, Santos ESP, et al. Graft-versus-host disease reduces lymph node display of tissue-restricted self-antigens and promotes autoimmunity. J Clin Invest. 2020;130(4):1896-1911.

Ferrata Storti Foundation

Translational and clinical advances in acute graft-*versus*-host disease

Mahasweta Gooptu and John Koreth

Dana-Farber Cancer Institute, Boston, MA, USA

ABSTRACT

Acute graft-*versus*-host disease (aGvHD) is induced by immunocompetent alloreactive T lymphocytes in the donor graft responding to polymorphic and non-polymorphic host antigens and causing inflammation in primarily the skin, gastrointestinal tract and liver. aGvHD remains an important toxicity of allogeneic transplantation, and the search for better prophylactic and therapeutic strategies is critical to improve transplant outcomes. In this review, we discuss the significant translational and clinical advances in the field which have evolved based on a better understanding of transplant immunology. Prophylactic advances have been primarily focused on the depletion of T lymphocytes and modulation of T-cell activation, proliferation, effector and regulatory functions. Therapeutic strategies beyond corticosteroids have focused on inhibiting key cytokine pathways, lymphocyte trafficking, and immunologic tolerance. We also briefly discuss important future trends in the field, the role of the intestinal microbiome and dysbiosis, as well as prognostic biomarkers for aGvHD which may improve stratification-based application of preventive and therapeutic strategies.

Introduction

Allogeneic hematopoietic stem cell transplantation (HSCT) remains one of the most important curative modalities for marrow failure and various advanced/aggressive hematologic malignancies. Acute graft-*versus*-host disease (aGvHD) remains an important HSCT toxicity with significant associated morbidity and mortality. aGvHD clinical manifestations typically involve skin (rash), upper (nausea, anorexia) or lower (diarrhea, abdominal pain) gastrointestinal (GI) tract, or liver dysfunction (elevated bilirubin, transaminases).[1] Its pathology is typically induced by immunocompetent effector T lymphocytes responding to donor/recipient polymorphic and non-polymorphic antigens on host tissues, with activation, inflammation and eventual cytolytic activity.

Despite advances in HSCT, such as high resolution HLA genotyping and the routine use of calcineurin-inhibitor (CNI)-based prophylaxis, aGvHD incidence remains in the 30-35% range with HLA-matched donors. While aGvHD outcomes have improved (largely due to advances in supportive care, e.g., infectious disease interventions), patients with severe and steroid-refractory (SR) aGvHD still have impaired survival, estimated to be in the 5-30% range.

aGvHD control is a cornerstone of successful transplantation. Effective interventions should not cause excessive toxicity, impair the curative graft-*versus*-leukemia (GvL) effect of allotransplantation, or contribute to graft failure. In this review, we summarize aGvHD pathogenesis and discuss novel advances in the prevention and treatment of aGvHD that have evolved as our understanding of pathogenesis has grown. In addition, we highlight areas of burgeoning interest in the field: microbiota dysbiosis, and the development of aGvHD biomarkers.

Biology of acute graft-*versus*-host disease

In an early model of aGvHD, Antin and Ferrara described a three-step process comprising: (i) host tissue injury due to the conditioning regimen, with the production of inflammatory cytokines; (ii) stimulation and proliferation of effector T lymphocytes (Teff); and, finally, (iii) recruitment and activation of additional mononuclear effectors and amplification of a 'cytokine storm'.[2] This basic model has stood the test of time, although it has been refined thanks to a deeper and more sophisticated understand-

ing of transplant biology, briefly outlined below.

In the initial host tissue injury phase, exogenous and endogenous antigens classified as sterile damage-associated molecular patterns (DAMP; e.g., uric acid, ATP, heparan sulfate, HMGB-1 or IL-33) and pathogen-associated molecular patterns (PAMP; e.g., bacterial lipopolysaccharides) interact with antigen-presenting cells (APC) in the innate and adaptive immune systems, with activation of cytokine cascades (IL-1, IL-6, TNF-α, etc.) that set the stage for T-cell priming and expansion.[1]

The second phase involves Teff trafficking (mediated by L-selectin, CCR7, etc.) to lymphoid organs and host tissues. CD8+ and CD4+ Teff cells homing to the gut express high levels of integrin β7 (α4β7) which bind corresponding host tissue ligands. At their destination, Teff activation *via* APC-mediated host tissue:TCR interaction is initiated. This step, modulated by anti- *versus* co-stimulatory pathways and cytokine cascades, finally leads to the third phase, self-potentiating Teff cell proliferation and activation causing tissue damage *via* direct cellular cytotoxicity and indirectly *via* release of soluble mediators (TNF-α, IFN-γ, IL-1 and nitric oxide).[3] The canonical NOTCH pathway is involved in regulating GvHD pathogenesis[4] and using humanized monoclonal antibodies, it was shown that Notch-deprived T cells (with predominant roles for NOTCH1 and Dll-4) produce less inflammatory cytokines but proliferate normally, with a preferential increase in regulatory T cells (Tregs), without compromising GvL.[5] Selective NOTCH blockade offers potential for clinical translation.

Such immune activation is opposed by anti-inflammatory Tregs, a T-cell subset important in immunologic tolerance, in part *via* release of anti-inflammatory cytokines such as IL-10 and TGF-β.[6] Additionally, the balance of effector T-helper (Th) type 1 (IL-2, INF-γ) and type 2 (IL-4, IL-10) cytokine responses may govern the ultimate outcomes of inflammation since type 2 cytokines can inhibit potent proinflammatory type 1cytokines, and a Th1 to Th2 shift could be beneficial in aGvHD.[7] A distinct subset of CD4+ cells (characterized by production of *IL-17A* and *F*, IL-21 and IL-22) called Th17 cells has also been identified, which in murine models migrate to GvHD target organs causing severe pulmonary and GI lesions and GvHD lethality,[8] and may play a critical role in GvHD pathogenesis[9] antagonistic to Tregs. Invariant natural killer T (iNKT) cells (discussed below) are another cellular subset with putative immunoregulatory functions, in part *via* an increase in Treg numbers and IL-4 secretion, that may be important in GvHD pathophysiology.

Here we discuss novel advances in the prevention and therapy of aGvHD built on the understanding of these concepts.

Acute graft-*versus*-host disease prevention

Established determinants of acute graft-*versus*-host disease

The well-established impact of conditioning regimen intensity, donor-recipient HLA-mismatch and graft source (bone marrow [BM], peripheral blood stem cell [PBSC]) on aGvHD outcomes is briefly discussed below.

Conditioning regimen intensity - the impact of conditioning intensity on aGvHD is primarily due to tissue damage-induced DAMP/PAMP release (see above). In general, myeloablative conditioning (MAC) (particularly total body irra-

diation [TBI])-containing regimens are associated with higher aGvHD rates, an effect more pronounced with PBSC grafts.[10] Non-myeloablative (NMA) and reduced-intensity conditioning (RIC) transplants have been associated with lower aGvHD rates[11,12] than MAC, and even the newer reduced-toxicity regimens (e.g., ablative busulfan/fludarabine) as per a large randomized controlled trial (RCT).[13] There has, therefore, been a shift towards minimizing TBI except when absolutely necessary (e.g., acute lymphoblastic leukemia).

Novel therapeutic targeting of DAMP/PAMP:immune cell interactions are being investigated. For example, ATP (a DAMP) interacts with APC to activate inflammatory STAT1 signaling. Interruption of this pathway reduced GvHD in murine models[14] although translation into clinical practice is still awaited.

Donor-recipient human leukocyte antigen (HLA)-mismatch - HLA-mismatch is an aGvHD risk factor. Large registry studies document increased aGvHD rates (including severe aGvHD grades III-IV) and impaired survival for 1-2 locus HLA-mismatch *versus* 8 of 8 HLA-matched MAC and RIC HSCT.[15,16] With the advent of post-transplant cyclophosphamide (PTCy)-based regimens, the effect of HLA-mismatch may be less deleterious. PTCy was initially introduced in haploidentical (haplo) HSCT, but in a trial of matched and single-antigen mismatched unrelated donors (MUD, MMUD) it was found superior to standard CNI-based prophylaxis (discussed below).[17] The role of PTCy in single-antigen MMUD HSCT is being further explored, with one study showing better rates of acute and chronic GvHD, non-relapse mortality (NRM), and relapse with PTCy compared to anti-thymocyte globulin (ATG).[18] Many centers are adopting a PTCy-based platform for MUD/MMUD HSCT.

Graft source - while unmanipulated donor BM grafts were initially used in transplantation, there is now a secular trend towards use of PBSC grafts, due to logistical reasons and donor preference. In a large meta-analysis comparing the two graft sources, there was no difference in overall aGvHD rates, although severe grade III-IV aGvHD and chronic severe GvHD was lower with BM. However, relapse in that analysis appeared higher with BM grafts leading to impaired disease-free survival (DFS) and overall survival (OS) in late stage disease.[19] In a phase III RCT of MUD PBSC *versus* BM HSCT, OS was similar (albeit with relatively short follow-up) with no differences in aGvHD or relapse, but chronic GvHD rates were lower with BM.[20] Hence BM is arguably the better graft source, although the effect on relapse needs longer term follow-up. Cord blood transplants have resulted in similar rates of aGvHD as conventional sources although with lower rates of cGvHD.[21] It should be mentioned that many GvHD prophylaxis regimens have been tested in association with specific stem cell sources making the interpretation of these data difficult.

Innovations in acute graft-*versus*-host disease prophylaxis

Since the cardinal events in aGvHD etiopathogenesis involve T-cell trafficking, interaction with host antigens and activation to cause tissue injury, the cornerstone of aGvHD prevention remains depletion or modulation of donor T

lymphocytes.

Since the 1990s, standard of care (SOC) aGvHD prophylaxis has incorporated a CNI (e.g., tacrolimus [Tac], cyclosporine [CyA]) plus another agent (e.g., methotrexate [MTX]), mycophenolate mofetil [MMF], sirolimus [Siro]).[22,23] CNI inhibit alloreactive T-cell proliferation and activation. However, even with CNI-based platforms, rates of grade II-IV aGvHD are 30-40%, with 10-15% severe grade III-IV aGvHD. Furthermore, CNI are associated with various toxicities (e.g., renal dysfunction, thrombotic microangiopathy [TMA]) which can add to transplant-related mortality (TRM). Hence novel prophylactic therapies with improved efficacy and less toxicity are of great interest in transplantation. Recent advances in aGvHD prevention, some of which are challenging the established CNI-based platform, are discussed below.

In vivo T-cell depletion/modulation

Anti-thymocyte globulin - ATG is the polyclonal purified IgG fraction of sera from horses or rabbits immunized with human thymocytes or T-cell lines. *In vivo* T-cell depletion (TCD) with ATG has been extensively evaluated to reduce the incidence of acute and chronic GvHD with HLA-matched as well as cord blood and haploHSCT.

In the CNI-era, four RCT evaluated CNI/MTX prophylaxis ± ATG.[24] In the first, using horse ATG, a reduction in aGvHD was offset by higher rates of infection with no difference in NRM or OS; however, there was a reduction in severe chronic GvHD.[25,26] In the second, using rabbit ATG,[27,28] and the third, mainly using PBSC grafts, there was no effect on aGvHD, with a reduction in cGvHD.[29] These studies concluded that reduction in severe cGvHD with no deleterious effect on OS is a true ATG effect; however, aGvHD was not reduced. More recently, an RCT evaluated Tac/MTX ± anti T-lymphocyte globulin (ATLG) in MAC MUD HSCT, with a significant reduction in grade II-IV aGvHD and moderate/severe cGvHD. However, NRM and OS was impaired in the ATLG arm.[30] A higher dose of ATLG in the trial may have contributed to increased infections and mortality.

In pioneering studies by Storek *et al.*, persistence of therapeutic ATG levels on days +7 and +28 were found to reduce acute and chronic GvHD.[31] There is also evidence that excessive persistence or dosing of ATG may have immunosuppressive toxicity with increased NRM and relapse. Individualized ATG dosing, based on absolute lymphocyte count beyond recipient weight, could be a way forward to control GvHD without impairing NRM and relapse.[32]

Post-transplant cyclophosphamide - the use of PTCy-based GvHD prophylaxis has been a major advance allowing the widespread use of haploHSCT with increasing importance also in HLA-matched and mismatched HSCT.

Haplo-hematopoietic stem cell transplantation was initially associated with increased graft rejection and GvHD due to strong bidirectional donor *versus* recipient alloreactive responses. HaploHSCT regimens utilized highly immunosuppressive conditioning with high transplant-associated toxicity. The innovative use of PTCy dosed at 50 mg/kg on days +3 and +4 following NMA haploHSCT resulted in a grade II-IV aGvHD rate of 34%, with a low grade III-IV aGvHD rate of 6% and a trend towards reduction in severe cGvHD. Relapse rates were around 50%.[33] Numerous subsequent studies replicated these results, and PTCy is now the most widely used haploHSCT regimen.

It is worth noting that overall aGvHD rates with PTCy, at 30-80%, are not necessarily lower than SOC, but severe aGvHD and cGvHD rates are lower.

PTCy was initially thought to act *via* depletion of alloreactive T cells by elimination of proliferating cells and intrathymic clonal deletion of alloreactive T-cell precursors.[34] More recent data suggest important roles for Treg preservation and Teff exhaustion as additional mechanisms of effect.[34]

PTCy has also been evaluated in alternative donor HSCT. In a phase II RCT of MUD/MMUD PBSC HSCT, three GvHD prophylaxis regimens were compared with SOC Tac/MTX: PTCy/Tac/MMF, Tac/MTX/bortezomib, and Tac/MTX/maraviroc. The primary 1-year GvHD free, relapse-free survival (GRFS) endpoint was improved in the PTCy-based arm.[17] Interestingly, grade II-IV aGvHD was similar; however, impressive gains were seen for severe grade III-IV aGvHD. Chronic GvHD requiring immunosuppression also fared much better with PTCy.

Recently, a small European RCT compared PTCy/Tac/MMF to CyA/MMF in HLA-matched RIC PBSC HSCT. Grade II-IV aGvHD was lower with PTCy (P=0.014) while severe grade III-IV aGvHD was 6% *versus* 12%, respectively.[35] Importantly, CyA/MMF is considered inferior to Tac/MTX, and hence PTCy-based prophylaxis is being definitively evaluated in a large multi-center phase III RCT (BMT CTN 1703) of MUD PBSC RIC HSCT comparing PTCy/Tac/MMF with Tac/MTX.

Sirolimus - Siro is an mTOR inhibitor that synergizes with CNI in reducing Teff proliferation and activity. Siro inhibits CD8+ cells[36] while promoting Treg proliferation *in vitro*,[37] an attractive immunologic profile for GvHD prevention. Importantly, unlike CNI, it does not cause nephrotoxicity. Siro/MTX prophylaxis has been investigated in a large RCT of MAC HSCT, documenting similar grade II-IV but lower grade III-IV aGvHD compared to Tac/MTX.[38] In RIC transplants, a phase II RCT showed that combined Siro/Tac/MTX had less grade II-IV aGvHD but no survival benefit.[39] A recent phase III RCT of NMA HSCT concluded that adding Siro to CyA/MMF was superior to CyA/MMF.[40] Given that the combination of Tac and MMF is inferior to Tac/MTX in a phase II RCT in preventing grade II-IV aGvHD,[41] and CyA has also been shown to be inferior to Tac in the past for GvHD prophylaxis, it is unclear how these data impact centers that primarily use Tac/MTX-based regimens. Although less nephrotoxic, Siro has also been associated with higher rates of veno-occlusive disease (VOD), particularly with ablative busulfan and cyclophosphamide,[42] and is avoided in patients at a higher risk for VOD. It has also been associated with increased rates of TMA, particularly in combination with CNI.[43] Discontinuation of CNI typically resolves TMA in this setting.

Finally, the combination of Siro/PTCy as a CNI-free, less nephrotoxic regimen with acceptable rates of engraftment and aGvHD has been evaluated.[44] This is currently reserved for scenarios precluding CNI use (e.g., sickle cell HSCT, with renal dysfunction). Given the Treg-sparing effect of Siro,[45] novel combinations (e.g., with OX40L blockade) are being explored as GvHD prophylaxis platforms.[46]

Ex vivo T-cell depletion

A deeper understanding of transplant biology and the availability of sophisticated clinical-grade cell separation technology underpins advances in graft manipulation

involving both pan-T-cell and selective T-cell subset depletion for the clinic, reviewed below.

Pan-T-cell depletion - ex vivo TCD of the donor graft has been utilized as a method to prevent GvHD, considering competing risks of relapse and NRM. Methods have included monoclonal antibodies with or without complement,[47-50] immunotoxins,[51] and counter flow elutriation.[52]

Ex vivo TCD was evaluated in a multi-center RCT of TCD grafts *versus* CNI-based prophylaxis.[53] TCD was associated with lower rates of grade III-IV but not grade II-IV aGvHD, with no change in DFS. Graft failure and increased disease relapse (20% *vs.* 7%) was a concern, with increased relapse also noted in a seminal registry analysis.[54] Other studies also suggested increased rates of graft failure with TCD grafts, ameliorated by ATG or thiotepa conditioning to prevent host immune-mediated graft rejection.

T-cell depletion based on immunomagnetic CD34^{+} graft selection (to eliminate contaminating immune cells) was evaluated in a single-arm phase II multicenter trial and showed low rates of cGvHD and relapse.[55] This was compared to CNI-based prophylaxis in a retrospective analysis, where outcomes were similar, with lower rates of cGvHD in the CD34 arm.[56] *Ex vivo* TCD remains the primary mode of transplantation in certain centers, although infectious complications, particularly viral infections, can be problematic. To better define optimal GvHD prophylaxis, results from an ongoing RCT of *ex vivo* TCD *versus* PTCy with MMF only *versus* standard CNI-based regimen are eagerly awaited (*clinicaltrials.gov identifier: NCT02345850*).

Beyond pan-T-cell depletion, subset-selective T-cell depletion and modulation strategies to ameliorate GvHD without compromising GvL effect by using antibodies with narrow specificities has become an area of great interest.[50] Depletion of CD5^{+} T cells[51] and CD8^{+} T cells were tried in the 1990s, but abandoned primarily due to higher rates of relapse. Other novel strategies are discussed below.

α/β T-cell depletion - the majority of T lymphocytes express α/β T-cell receptors (TCR), while γ/δ TCR are expressed by 2-10% of circulating T cells. γ/δ T cells have important innate immune functions including rapid release of cytokines, and killing of tumor and virally infected cells without inducing GvHD.[57] They may have an important role in GvL effect and the preservation of NRM. Selective depletion of α/β T cells would preserve NK cells as well as γ/δ T cells. In a prospective study of 80 pediatric patients with acute leukemia, α/β TCD was studied with encouraging GRFS of 70%.[58] Ongoing studies are further evaluating this approach in adult and pediatric populations, including a CNI-free GvHD prophylaxis strategy for acute leukemia patients undergoing 1-2 locus MMUD MAC HSCT (*clinicaltrials.gov identifier: NCT03717480*).

CD45RA (naïve) T-cell depletion - conceptually, it is naïve T cells in the donor allograft that are primarily alloreactive. In a study in healthy individuals, the bulk of allo-HLA reactivity was derived from subsets enriched for naïve T cells.[59] Hence, removal of CD45RA^{+} naïve T cells from the donor graft could help prevent aGvHD alloreactivity. The CD45RA^{-} target fraction contains effector and central memory T cells that show preserved reactivity to common viral and fungal pathogens.[60] In a two-step immunomagnetic bead procedure for naïve TCD, Bleakley *et al.*[61] reported on a first-in-human single-arm trial (n=35) for patients with acute leukemia transplanted with HLA-matched related donors. Although 34 of 35 patients engrafted with lower rates of cGvHD, rates of aGvHD remained relatively high

(66%), suggesting a lack of efficacy with this approach alone.[62] A combinatorial approach using α/β TCD combined with CD45RA naïve cell depletion was not much better, with aGvHD rates in the 58% range.[63] Hence, for the moment, this approach remains only investigational.

CD6 depletion - CD6 is a co-stimulatory receptor, predominantly expressed on T cells that bind to activated leukocyte cell adhesion molecule (ALCAM), a ligand expressed on APC and various host tissues and plays an integral role in modulating T-cell activation, proliferation, differentiation and trafficking. CD6 depletion using a monoclonal antibody (mAb) (anti-T12, CD6) that recognized mature T cells but not other cellular elements (e.g., B, natural-killer [NK] cells, and myeloid precursors) was clinically evaluated in a single arm trial with 112 patients with a grade II-IV aGvHD rate of 18%.[48] More recently, itolizumab a humanized anti-CD6 mAb, was evaluated in human xenograft models, suggesting that itolizumab can modulate pathogenic Teff activity.[64] Itolizumab has been provided fast track status by the US Food and Drug Administration (FDA) for this indication and is undergoing evaluation in a phase I/II study for first-line treatment (with steroids) of severe aGvHD (*clinicaltrials.gov identifier: NCT03763318*).

Graft engineering: Treg/Tcon add back strategies - in haploHSCT, in the early 1990s, CD34^{+} cell selection was used by the Perugia group to generate T-cell depleted peripheral blood progenitor cell grafts. Although GvHD rates were low, there was poor immune reconstitution (IR) and high rates of infection.[65] The Perugia group then pioneered the use of a 'megadose' of CD34^{+} cells to facilitate engraftment and improve IR based on the increased tolerability effect of such a dose of CD34^{+} cells.[66] Subsequently, further TCD by negative selection of CD3/CD19^{+} cells was used. Most recently, CD34^{+} selection followed by graduated add back of Tregs and conventional T cells (Tcons) (in a 2:1 ratio) have been adopted, with promising early results for enhanced IR and GvL, but aGvHD remains a concern.[67] Further iterations of this approach may yield enhanced clinical benefit, despite their complexity and cost.

Regulatory T-cell enhancement

Tregs - Tregs are CD4^{+}CD25^{+}Foxp3^{+} cells which play an important role in immunologic homeostasis and the control of aberrant or overactive immune effectors. Tregs can be derived 'naturally' from the thymus (nTregs) or converted from CD4^{+}CD25^{-} cells (inducible or iTregs).[6] iTregs require IL-2 and TGF-β to fully develop their suppressive function. Blazar *et al.* showed that *ex vivo* activation and expansion of Treg is feasible, with efficacy in murine GvHD models.[68] Other approaches have utilized fucosylation[69] and TL1A/TNFRSF25 stimulation[70] for *ex vivo* Tregs. In clinical transplantation, they have confirmed the feasibility and safety of *ex vivo* Treg expansion and adoptive transfer, with preliminary clinical efficacy for aGvHD prevention in both cord[71] and haploHSCT.[67] However, concerns about stability of expanded Tregs has been a barrier to translation into the clinic.

Invariant natural killer T cells - invariant NK T (iNKT) cells are a rare T-lymphocyte subset which co-express both T- and NK-cell markers and are considered a bridge between innate and adaptive immunity. Their semi-invariant TCR recognizes glycolipid antigens presented by the major histocompatibility complex (MHC) class I-like molecule Cd1d. Despite their rarity, they have strong immunomodulatory functions through the secretion of IL-4 and IL-10,

as well as providing active immunologic surveillance against cancer.[72] Murine models suggested that iNKT cells have a protective effect against GvHD without impairing the GvL effect. This occurs in part *via* a switch of donor T cells to a Th2 cytokine profile and/or IL-4 dependent Treg expansion.[73,74] Observational studies suggest lower acute and chronic GvHD with improved iNKT cell reconstitution. Clinical translation has involved RIC HSCT utilizing total lymphoid irradiation plus ATG (TLI-ATG) conditioning (offering iNKT expansion in murine models) with promising outcomes,[75] as well as more direct *ex vivo* expansion and adoptive iNKT transfer peri-transplant, where clinical data are eagerly anticipated. KRN7000 (synthetic derivative of α-galactosylceramide and a CD1d ligand) when embedded in a lipid bilayer constitutes RGI-2001or REGiMMUNE which can expand FoxP3^{+} Tregs *via* iNKT cells in mice to reduce aGvHD lethality.[76] Recently a phase IIa trial of a combination of Siro and RGI-2001 showed lower incidence of overall and severe aGvHD in responders compared to non-responders.[77] Although promising, iNKT targeted approaches have not been widely adopted for the moment and more mature data are awaited.

Cytokine targeting

Tocilizumab - interleukin-6 (IL-6) is a key inflammatory cytokine in the early pathogenesis of aGvHD in murine models.[78] A logical next step was to investigate the role of IL-6 blocking agents in preventing aGvHD. Tocilizumab is a humanized mAb against the IL-6 receptor (IL-6R). Based on promising phase II data,[79] a placebo-controlled phase III study from Australia was reported, which, however, showed no significant difference in grades II-IV or III-IV aGvHD.[80] This is a salient reminder that, given the complex pathophysiology of aGvHD, with crosstalk between myriad cytokines and immune effector cells, it is possible that targeting multiple cytokine pathways will be required for efficacy.

Targeting T-cell co-stimulatory pathways

As mentioned previously, following initial engagement of an APC with the TCR, a number of secondary co-stimulatory signals come into play which are necessary to complete alloreactive T-cell activation, proliferation and eventual development of aGvHD. CD28 is a co-stimulatory receptor while CTLA-4 is a co-inhibitory receptor on the T cell, both of which bind to B7-1/CD80 and B7-2/CD86 ligands on APC. CTLA-4-Ig (abatacept) is the soluble extracellular portion of CTLA-4 complexed with immunoglobulin heavy chain which blocks CD28/CTLA-4 (CD28>CTLA-4) co-stimulation with an eventual T-cell inhibitory signal. Blazar *et al.* showed in murine models that blockade of the CD28/CTLA-4 and CD80/CD86 interaction reduced aGvHD lethality.[81] Following a promising feasibility study, Kean *et al.* then tested abatacept added to SOC *versus* SOC in a phase II RCT with 8/8 and 7/8 HLA-matched donors. There was significant reduction in grades III-IV aGvHD in the abatacept arm with improved OS[82] leading to FDA breakthrough designation for this drug. To avoid the undesirable effect of concomitantly blocking inhibitory pathways, more selective approaches to CD28 blockade are being investigated. FR104, an antagonistic CD28-specific pegylated-Fab' has shown promise with and without Siro in non-human primate models, with the caveat that a worrying inhibitory effect was seen on

the INF-γ axis with deaths secondary to sepsis.[83] The modulation of co-stimulatory/inhibitory pathways is one of the important new frontiers in aGvHD prevention.

These prophylactic strategies, along with the level of evidence supporting them, are summarized in Table 1.

Advances in acute graft-*versus*-host disease therapy

Systemic steroids, while not FDA-approved for this indication, remain a cornerstone of the initial treatment of moderate-severe aGvHD. In a seminal study, Blazar *et al.* showed that first-line therapy of aGvHD with corticosteroids (60 mg daily followed by an 8-week taper) resulted in response rates of 50% and 1-year survival of 53%.[84] Higher doses of steroids did not result in better outcomes. In a study comparing 10 mg/kg to 2 mg/kg of methylprednisone, both resulted in transplant mortality of 30% at one year with no improvement in aGvHD responses at higher doses.[85] SR-aGvHD treatment remains a difficult problem, with 6-month survival in the 50% range, and long-term survival of only 5-30%.[86] Stratification systems such as the Minnesota risk score that take into account patterns of aGvHD by target organ involvement can further refine the prediction of transplant-related mortality, and are being considered in clinical trial risk stratification.[84] Finally, even when aGvHD is controlled, patients often succumb to infections exacerbated by additional immunosuppressive therapies. Novel therapies are, therefore, a critical unmet need. Here we outline some of the more promising approaches currently available or in early translation to the clinic.

Cytokine pathways

JAK-STAT pathway - the Janus Kinases (JAK) are intracellular tyrosine kinases investigated as GvHD therapeutic targets given their important role in cytokine signaling and effects on immune effector cells. In murine models, the role of IFNγ on T-lymphocyte trafficking to GvHD target organs (particularly the GI tract) *via* CXCR upregulation was studied. Inhibition of interferon (IFN)γR signaling *via* JAK1/JAK2 inhibitors resulted in decreased CXCR3 expression and altered Teff trafficking to target organs, reducing GvHD.[87] Ruxolitinib (Rux) is a potent oral JAK-1/JAK-2 inhibitor. In a proof of concept study, Rux reduced Teff proliferation and activity, increased Tregs and decreased cytokine production, with excellent responses in six SR-aGvHD patients.[88]

A retrospective survey of off-label Rux in SR aGvHD documented overall response rate (ORR) of 81.5% (complete responses [CR] 46%). Cytopenias and cytomegalovirus (CMV) reactivation were seen.[89] A phase II single-arm multicenter study of Rux (REACH-1) in 71 patients documented ORR at 28 days of 54.9% (complete remission/CR, 26.8%), irrespective of aGvHD grade and steroid refractoriness.[90] In addition to cytopenias and CMV reactivation, serious bacterial infections were reported. The phase III RCT of Rux *versus* investigator's choice for SR aGvHD has now been reported (REACH-2). Rux was superior in terms of ORR; however, there was no difference in cumulative incidence of 18-month NRM.[91] Infections and cytopenias remain limiting toxicities. The FDA has approved Rux for SR aGvHD.

In contrast, failure of the selective JAK1 inhibitor itaci-

Table 1. Prophylactic strategies for acute graft-*versus*-host-disease.

Prophylaxis strategy	Intervention	Level of evidence	Comments
***In vivo* T-cell depletion/modulation**	Calcineurin inhibitors (tacrolimus, cyclosporine)	Phase III RCT	Tac *vs.* CyA, less aGvHD with Tac but no survival advantage.
	ATG	Phase III RCT	Either no reduction in aGvHD or reduction in aGvHD with significant increase in NRM.
	PTCy	Phase II/III RCT	Lower rates of severe aGvHD but not grades II-IV aGvHD compared to CNI.
	Sirolimus (mTOR inhibitor)	Phase II/III RCT	Lower rates of grades III-IV aGvHD in MAC and grades II-IV aGvHD in RIC HSCT but no survival advantage.
***Ex vivo* T-cell depletion**	Pan T-cell depletion	Phase II/III RCT	Lower rates of grades III-IV aGvHD but no survival advantage. Graft failure sometimes an issue.
	α/β T-cell depletion	Phase II single arm	Promising GRFS of 70% in pediatric acute leukemia. Adult studies ongoing.
	CD45RA (naïve) T-cell depletion	First-in-human phase I/II	High aGvHD rates of 66% and hence investigational only for the moment.
	CD6 depletion Itolizumab	Phase II single arm Ongoing phase I/II	aGvHD rates of 18%; monoclonal antibody (itolizumab) with FDA fast-track status now being tested.
	Treg:Tcon add back strategies	First-in-human phase I/II	Operationally complex and for the moment difficult to generalize.
Regulatory T-cell enhancement	Tregs	Phase I	Preliminary safety results encouraging; concerns about stability of *ex vivo* Treg expansion.
	iNKT cells	Phase I/II	TLI-ATG regimen *via* iNKT cells with reported GvHD in only 2 of 37 recipients. REGIMMUNE/sirolimus combination promising.
Cytokine targeting	Tociluzumab	Phase III RCT	Tocilizumab *vs.* placebo; no improvement in aGvHD of any grade.
Targeting T-cell co-stimulatory pathways	CD28/CTLA-4 targeting (abatacept)	Phase II RCT	CTLA-4 Ig (abatacept)+SOC compared to SOC in 8/8 and 7/8 HLA-matched HSCT with lower rates of grades III-IV aGvHD outcomes and OS leading to FDA breakthrough designation.

aGvD: acute graft-*versus*-host disease; HSCT: hematopoietic stem cell transplantation; PTCy: post-transplant cyclophosphamide; ATG: anti-thymocyte globulin; RCT: randomized controlled trial; iNKT: invariant natural killer T cells; OS: overall survival; SOC: standard of care; FDA: US Food and Drug Administration; NRM: non-relapse mortality; aGvHD: acute graft-*versus*-host disease; GRFS: GvHD free, relapse-free survival; CNI: calcineurin inhibitor.

tinib when added to steroids (*vs.* steroids alone) for upfront therapy of aGvHD in the closed GRAVITAS 301 trial (*clinicaltrials.gov NCT03139604*) is notable. JAK-1 inhibition is capable of selectively suppressing Th1 and Th17 Teff cell subsets, with preserved activation of anti-inflammatory Treg cells dependent on the JAK2/JAK3 pathway; however, the drug failed clinical efficacy, highlighting limitations in clinical trial design, optimal therapeutic target identification, or both. Data on the efficacy of selective JAK2 inhibitors in aGvHD are eagerly awaited, but it is possible that combination JAK1/2 blockade may be required for appropriate suppression of activation in Teff cells.

Although a number of cytokine-directed therapies previously failed in the therapy of aGvHD (denileukin diftitox, tocilizumab, anti TNF-α), the efficacy of Rux is a milestone in the field, and a testament to the critical role of a 'cytokine storm' in aGvHD.

Alpha-1-antitrypsin - alpha-1-antitrypsin (AAT) is a serine protease inhibitor produced by the liver which has myriad functions including inhibition of proinflammatory plasma cytokines and induction of anti-inflammatory IL10, and *in vivo* induction of Treg. In preclinical aGvHD models, AAT reduced inflammatory cytokines, altered the ratio of Teff and Tregs and reduced levels of DAMP.[92] In a phase I/II open label single center study in SR aGvHD patients (n=12), responses were seen in 8 of 12 patients with no significant toxicity.[93] In a larger phase II multicenter study (n=40), ORR at D28 was 65% (CR 35%).[94] Upfront AAT is being evaluated in a Blood and Marrow Transplant Clinical

Trials Network (BMT-CTN) phase III RCT evaluating corticosteroids ± AAT (*clinicaltrials.gov NCT04167514*) as a promising non-toxic agent for high-risk aGvHD.

Targeting lymphocyte trafficking

Vedolizumab - lymphocyte trafficking to GvHD target organs is a key event leading to aGvHD. In the lower GI tract, Peyer's patches (PP) and gut-associated lymphoid tissue (GALT) are the targets for alloreactive CD8+ T cells. Gut-tropic CD8+ cells express high levels of integrin β7 (α4β7) that binds its ligand mucosal addressin cell adhesion molecule 1 (MAdCAM 1) in the PP and GALT. Vedolizumab, a humanized mAb, targets α4β7 integrins and prevents Teff trafficking to the gut. A small proof of concept study (n=6) demonstrated responses in all patients with SR lower GI GvHD. In an international, retrospective review to evaluate the off-label use of vedolizumab (n=29), ORR was 64% and OS at 6 months was 54%.[95] CMV reactivation and *Clostridium difficile* colitis were noted. Natalizumab, a selective α4 subunit adhesion molecule inhibitor was studied in a phase II study with a response rate of approximately 30%.[96] Vedolizumab is being studied in larger prophylactic (*clinicaltrials.gov NCT03657160*) and therapeutic (*clinicaltrials.gov NCT02993783*) trials for aGvHD.

Targeting immunologic tolerance

Extracorporeal photochemotherapy - extracorporeal photochemotherapy (ECP) has been used for cGvHD for decades, and more recently for aGvHD with some suc-

cess. Although the mechanism by which ECP improves GvHD is a matter of debate, its immunomodulatory effects include Treg upregulation, a change from Th1 to Th2 cytokine profile, as well as modulation of APC.[97] Importantly ECP may not result in additional immuno-suppression in GvHD patients. In a RCT evaluating ECP in cGvHD therapy, there was no increased risk of infec-tion in the ECP arm,[98] which, if also true in the aGvHD setting, would be a major benefit. Initially evaluated in pediatric cohorts, ECP resulted in a response rate of 67% in a small study of adult aGvHD.[99] In another small ECP study (n=23), CR was achieved in 70%, 42% and 0% of patients with grades II, III and IV aGvHD respectively. With regards to end-organ based efficacy, complete responses were seen in 66%, 27% and 40% of patients with skin, liver and gut involvement, respectively.[100] However, the data are limited to small non-randomized studies and effi-cacy needs to be confirmed.

Finally, another novel therapeutic intervention for aGvHD, fecal microbiota transplantation (FMT), is further discussed in the section on microbiome and the role of dys-biosis.

These therapeutic strategies, along with the level of evi-dence supporting them, are summarized in Table 2.

Future trends

Finally, we highlight the emerging role of early prognostic biomarkers as well as the potentially critical role of the intestinal microbiome in influencing aGvHD and transplant outcomes.

Novel biomarkers in acute graft-*versus*-host disease

Identifying predictive biomarkers for aGvHD develop-ment and/or prognosis has been an important question in the field. Hypothesis-driven markers based on the patho-physiology of aGvHD include acute phase reactants (e.g., IL-6, C-reactive protein [CRP]), Th1 cytokines (e.g., IL-12, IL-18), anti-inflammatory cytokines (e.g., IL-10, TGF-β), other circulating markers (e.g., IL-8, HGF, cytokeratin-18, CD30), and lymphocyte trafficking molecules (e.g., CXCL10, CCL8) have been evaluated with limited success. In contrast, unbiased marker discovery typically involved proteomic screening of GvHD and non-GvHD samples. In a discovery study from Ann Arbor, IL-2Rα, TNFR1, HGF and IL-8 identified early after aGvHD onset demonstrated impressive accuracy confirmed in a larger validation set.[101] Another panel comprising IL-2Rα, TNFR1 and elafin has also been validated.[102]

The Mount Sinai Acute GvHD International Consortium (MAGIC) was established to identify potential biomarkers to risk stratify GvHD. Investigators tested previously iden-tified biomarkers, namely suppressor of tumorigenicity-2 (ST2) and regenerating islet-derived protein 3-α (REG3α), in SR aGvHD and found that marker elevation 7 days after aGvHD was a better predictor of NRM than the Minnesota clinical risk score.[103] Another approach has evaluated mark-ers of endothelial toxicity documenting follistatin and endoglin as being associated with higher rates of grade III-IV aGvHD and NRM.[104]

The appropriate clinical application of these biomarker panels is a complex issue, with the underlying principle that test results should change therapy and, ideally, outcome. Risk-adapted approaches have proposed using these panels

in two different ways: (i) early post-transplant prior to diag-nosis of aGvHD, with allocation of high-risk patients to novel GvHD trials; and (ii) after the diagnosis of aGvHD, to stratify patients at high NRM risk and risk-adapt therapy accordingly.

Future clinical trials that use biomarkers to risk stratify aGvHD patients for eligibility or therapy will be important to prospectively evaluate their utility as a first step to their broader use in clinical practice.

The microbiome in acute graft-*versus*-host disease

The many micro-organisms which constitute the human gut are collectively called the intestinal microbiota while their genetic make-up has often been referred to as the 'microbiome'.[105] Diversity is a hallmark of the healthy gut microbiome. There is a growing appreciation of the role of the microbiome in various health and disease states. In HSCT, the loss of microbiota diversity (dysbiosis) has been associated with the risk of aGvHD.[105]

This association between aGvHD and gut dysbiosis relates to immunologic and metabolic imbalances in the gut wrought by HSCT, with loss of diversity of the microbiome. Under normal circumstances, diverse gut commensals result in healthy tissue immune cells, including recruitment of Treg cells, secretion of TGF-β and IL-10, as well as TH17 cells secreting IL-17 and IL-22.[106] Another protective immune response modulated by gut bacteria relates to their produc-tion of short chain fatty acids (SCFA), a nutritional source for intestinal epithelial cells. Disruption of the intestinal micro-biome triggered by conditioning chemoradiotherapy and antibiotic use during transplantation results in overgrowth of bacteria (e.g., enterococci, *Proteus spp.*), and reduction in firmicutes (e.g., *Blautia spp.*), which generally are producers of SCFA, is considered an inciting stimulus for GvHD.[107]

Further studies are needed to develop actionable targets in this arena. It is a complex endeavor given the variations in gut microbiome over different geographical areas, across transplant strategies, and inpatient and outpatient settings. It is heartening that a recent study from four international centers showed that the patterns of loss of microbiome diversity during HSCT was similar across countries, and that lower diversity at time of neutrophil engraftment was associated with higher mortality.[108] A large biorepository of stool samples along with blood and other samples is being built as the correlative arm of the large BMT CTN RCT 1703 (Mi-immune) study in which the biology of the micro-biome and correlations with transplant outcomes will be interrogated.

Fecal microbiota transplant as an effort to repopulate the gut with normal gut flora has been proposed as a means to control aGvHD, based on data limited to pilot studies[109] and limited case series.[110] Infection with extended spectrum β-lactamase (ESBL) producing *Escherichia coli* bacteria has been reported in at least two transplant patients post allogeneic transplantation who underwent FMT, one of whom died.[111] Hence the safety and efficacy of FMT in aGvHD remains an open question.

Conclusion

To summarize, aGvHD remains an important problem in HSCT. However, where effective treatment options had previously been very limited, there are now multiple excit-ing translational advances.

Table 2. Therapeutic strategies for acute graft-*versus*-host disease.

Prophylaxis strategy	Intervention	Level of evidence	Comments
Non-specific immunosuppression	Corticosteroids	Phase II/III RCT	RCT comparing different steroid doses, no RCT comparing steroids *vs.* placebo.
Cytokine targeting	JAK-2 inhibition: ruxolitinib	Phase III RCT	Ruxolitinib *vs.* investigator's choice in SR-aGvHD: superior ORR but no difference in 18-month NRM.
	JAK-1 inhibition: itacitinib	Phase III RCT	Itacitinib *vs.* itacitinib+steroids in upfront therapy: negative trial.
	Alpha-1 anti-trypsin (AAT)	Phase II, ongoing Phase III RCT	ORR of 65% in SR-aGvHD in Phase II, ongoing phase III RCT of AAT+steroids *vs.* steroids alone for high-risk aGvHD.
Targeting lymphocyte trafficking	Vedolizumab	Proof-of-concept, retrospective review, ongoing Phase II randomized study	ORR of 64% in retrospective studies, CMV reactivation, *C Diff.* colitis seen
	Natalizumab	Phase II single-arm	ORR of approx. 30%
Targeting immunologic tolerance	Extra-corporeal photochemotherapy	Phase II single-arm	ORR varies from 40-70% in small non-randomized studies.
	NOTCH inhibition	Investigational	No reported clinical studies at this time
Targeting dysbiosis	Fecal microbiota transplant	Pilot studies, case series	Concern for fatal bloodstream infection hence still investigational

aGvD: acute graft-*versus*-host disease; AAT: alpha-1-antitrypsin; aGvHD: acute graft-*versus*-host disease; ATG: anti-thymocyte globulin; *C Diff.: Clostridium difficile* colitis; CMV: cytomegalovirus; HSCT: hematopoietic stem cell transplantation; NRM: non-relapse mortality; ORR: overall response rate; RCT: randomized controlled trial; SR: steroid-refractory.

In the arena of prevention, PTCy-based GvHD prophylaxis has been a significant advance and some selective methods of T-cell depletion and modulation of co-stimulatory pathways appear promising. In the therapeutic arena, cytokine targeting with Rux is an exciting novel therapy for SR-aGvHD, while immunomodulatory strategies (e.g., ECP, AAT) offer therapeutic potential without immunosuppressive toxicity, and strategies targeting lymphocyte trafficking and inhibition of key canonical pathways (e.g., Notch) offer future potential. For the more long-term future, the importance of the gut microbiome in aGvHD is becoming increasingly apparent, and offers an opportunity for future therapeutic targeting (e.g., probiotics, metabolic modifications).

A long-term rational approach to aGvHD care would involve precision prognostics pre- and peri-transplantation (e.g., plasma biomarkers, microbiota dysbiosis, etc.) to select patients for innovative GvHD preventive strategies, as well as the early identification of high-risk patients at aGvHD onset, for novel treatment trials, ideally avoiding additional immunologic dysfunction or impairing GvL.

References

1. Zeiser R, Blazar BR. Acute graft-versus-host disease - biologic process, prevention, and therapy. N Engl J Med. 2017;377(22):2167-2179.
2. Antin JH, Ferrara JL. Cytokine dysregulation and acute graft-versus-host disease. Blood. 1992;80(12):2964-2968.
3. Ferrara JLM, Levine JE, Reddy P, Holler E. Graft-versus-host disease. Lancet. 2009;373(9674):1550-1561.
4. Zhang Y, Sandy AR, Wang J, et al. Notch signaling is a critical regulator of allogeneic CD4+ T-cell responses mediating graft-versus-host disease. Blood. 2011;117(1):299-308.
5. Tran IT, Sandy AR, Carulli AJ, et al. Blockade of individual Notch ligands and receptors controls graft-versus-host disease. J Clin Invest. 2013;123(4):1590-1604.
6. Sakaguchi S, Yamaguchi T, Nomura T, Ono M. Regulatory T cells and immune tolerance. Cell. 2008;133(5):775-787.
7. Krenger W, Ferrara JLM. Graft-versus-host disease and the Th1/Th2 paradigm. Immunol Res. 1996;15(1):50-73.
8. Carlson MJ, West ML, Coghill JM, Panoskaltsis-Mortari A, Blazar BR, Serody JS. In vitro-differentiated TH17 cells mediate lethal acute graft-versus-host disease with severe cutaneous and pulmonary pathologic manifestations. Blood. 2009;113(6):1365-1374.
9. Yu Y, Wang D, Liu C, et al. Prevention of GVHD while sparing GVL effect by targeting Th1 and Th17 transcription factor T-bet and RORγt in mice. Blood. 2011;118(18):5011-5020.
10. Jagasia M, Arora M, Flowers MED, et al. Risk factors for acute GVHD and survival after hematopoietic cell transplantation. Blood. 2012;119(1):296-307.
11. Couriel DR, Saliba RM, Giralt S, et al. Acute and chronic graft-versus-host disease after ablative and nonmyeloablative conditioning for allogeneic hematopoietic transplantation. Biol Blood Marrow Transplant. 2004;10(3):178-185.
12. Sorror ML, Maris MB, Storer B, et al. Comparing morbidity and mortality of HLA-matched unrelated donor hematopoietic cell transplantation after nonmyeloablative and myeloablative conditioning: influence of pretransplantation comorbidities. Blood. 2004;104(4):961-968.
13. Scott BL, Pasquini MC, Logan BR, et al. Myeloablative versus reduced-intensity hematopoietic cell transplantation for acute myeloid leukemia and myelodysplastic syndromes. J Clin Oncol. 2017;35(11):1154-1161.
14. Wilhelm K, Ganesan J, Müller T, et al. Graft-versus-host disease is enhanced by extracellular ATP activating P2X7R. Nat Med. 2010;16(12):1434-1438.
15. Lee SJ, Klein J, Haagenson M, et al. High-resolution donor-recipient HLA matching con-

tributes to the success of unrelated donor marrow transplantation. Blood. 2007;110 (13):4576-4583.

16. Verneris MR, Lee SJ, Ahn KW, et al. HLA mismatch is associated with worse outcomes after unrelated donor reduced-intensity conditioning hematopoietic cell transplantation: an analysis from the Center for International Blood and Marrow Transplant Research. Biol Blood Marrow Transplant. 2015;21(10):1783-1789.

17. Bolaños-Meade J, Reshef R, Fraser R, et al. Three prophylaxis regimens (tacrolimus, mycophenolate mofetil, and cyclophosphamide; tacrolimus, methotrexate, and bortezomib; or tacrolimus, methotrexate, and maraviroc) versus tacrolimus and methotrexate for prevention of graft-versus-host disease with haemopoietic cell transplantation with reduced-intensity conditioning: a randomised phase 2 trial with a non-randomised contemporaneous control group (BMT CTN 1203). Lancet Haematol. 2019;6(3):e132-e143.

18. Nykolyszyn C, Granata A, Pagliardini T, et al. Posttransplantation cyclophosphamide vs. antithymocyte globulin as GVHD prophylaxis for mismatched unrelated hematopoietic stem cell transplantation. Bone Marrow Transplant. 2020;55(2):349-355.

19. Stem Cell Trialists' Collaborative Group. Allogeneic peripheral blood stem-cell compared with bone marrow transplantation in the management of hematologic malignancies: an individual patient data meta-analysis of nine randomized trials. J Clin Oncol. 2005;23(22):5074-5087.

20. Anasetti C, Logan BR, Lee SJ, et al. Peripheral-blood stem cells versus bone marrow from unrelated donors. N Engl J Med. 2012;367(16):1487-1496.

21. Chen Y-B, Wang T, Hemmer MT, et al. GVHD after umbilical cord blood transplantation for acute leukemia: an analysis of risk factors and effect on outcomes. Bone Marrow Transplant 2017;52(3):400-408.

22. Nash RA, Antin JH, Karanes C, et al. Phase 3 study comparing methotrexate and tacrolimus with methotrexate and cyclosporine for prophylaxis of acute graft-versus-host disease after marrow transplantation from unrelated donors. Blood. 2000;96(6):2062-2068.

23. Ratanatharathorn V, Nash RA, Przepiorka D, et al. Phase III study comparing methotrexate and tacrolimus (prograf, FK506) with methotrexate and cyclosporine for graft-versus-host disease prophylaxis after HLA-identical sibling bone marrow transplantation. Blood. 1998;92(7):2303-2314.

24. Bacigalupo A. ATG in allogeneic stem cell transplantation: standard of care in 2017? Point. Blood Adv. 2017;1(9):569-572.

25. Bacigalupo A, Lamparelli T, Bruzzi P, et al. Antithymocyte globulin for graft-versus-host disease prophylaxis in transplants from unrelated donors: 2 randomized studies from Gruppo Italiano Trapianti Midollo Osseo (GITMO). Blood. 2001;98(10):2942-2947.

26. Bacigalupo A, Lamparelli T, Barisione G, et al. Thymoglobulin prevents chronic graft-versus-host disease, chronic lung dysfunction, and late transplant-related mortality: long-term follow-up of a randomized trial in patients undergoing unrelated donor transplantation. Biol Blood Marrow Transplant. 2006;12(5):560-565.

27. Finke J, Bethge WA, Schmoor C, et al. Standard graft-versus-host disease prophylaxis with or without anti-T-cell globulin in haematopoietic cell transplantation from matched unrelated donors: a randomised, open-label, multicentre phase 3 trial. Lancet Oncol. 2009;10(9):855-864.

28. Socié G, Schmoor C, Bethge WA, et al. Chronic graft-versus-host disease: long-term results from a randomized trial on graft-versus-host disease prophylaxis with or without anti–T-cell globulin ATG-Fresenius. Blood. 2011;117(23):6375-6382.

29. Kröger N, Solano C, Wolschke C, et al. Antilymphocyte globulin for prevention of chronic graft-versus-host disease. N Engl J Med. 2016;374(1):43-53.

30. Soiffer RJ, Kim HT, McGuirk J, et al. Prospective, randomized, double-blind, phase III clinical trial of anti–T-lymphocyte globulin to assess impact on chronic graft-versus-host disease–free survival in patients undergoing HLA-matched unrelated myeloablative hematopoietic cell transplantation. J Clin Oncol. 2017;35(36):4003-4011.

31. Podgorny PJ, Ugarte-Torres A, Liu Y, Williamson TS, Russell JA, Storek J. High rabbit-antihuman thymocyte globulin levels are associated with low likelihood of graft-vs-host disease and high likelihood of posttransplant lymphoproliferative disorder. Biol Blood Marrow Transplant. 2010;16(7):915-926.

32. Admiraal R, Nierkens S, de Witte MA, et al. Association between anti-thymocyte globulin exposure and survival outcomes in adult unrelated haemopoietic cell transplantation: a multicentre, retrospective, pharmacodynamic cohort analysis. Lancet Haematol. 2017;4(e):e183-e191.

33. Luznik L, O'Donnell PV, Symons HJ, et al. HLA-haploidentical bone marrow transplantation for hematologic malignancies using nonmyeloablative conditioning and high-dose, posttransplantation cyclophosphamide. Biol Blood Marrow Transplant. 2008;14(6):641-650.

34. Wachsmuth LP, Patterson MT, Eckhaus MA, Venzon DJ, Gress RE, Kanakry CG. Posttransplantation cyclophosphamide prevents graft-versus-host disease by inducing alloreactive T cell dysfunction and suppression. J Clin Invest. 2019;129(6):2357-2373.

35. De Jong CN, Meijer E, Bakunina K, et al. Post-transplantation cyclophosphamide after allogeneic hematopoietic stem cell transplantation: results of the prospective randomized HOVON-96 trial in recipients of matched related and unrelated donors. Blood. 2019;134(Suppl 1):1.

36. Slavik JM, Lim DG, Burakoff SJ, Hafler DA. Uncoupling p70(s6) kinase activation and proliferation: rapamycin-resistant proliferation of human CD8(+) T lymphocytes. J Immunol. 2001;166(5):3201-3209.

37. Battaglia M, Stabilini A, Roncarolo M-G. Rapamycin selectively expands CD4+CD25+FoxP3+ regulatory T cells. Blood. 2005;105(12):4743-4748.

38. Cutler C, Logan B, Nakamura R, et al. Tacrolimus/sirolimus vs tacrolimus/methotrexate as GVHD prophylaxis after matched, related donor allogeneic HCT. Blood. 2014;124(8):1372-1377.

39. Armand P, Kim HT, Sainvil M-M, et al. The addition of sirolimus to the graft-versus-host disease prophylaxis regimen in reduced intensity allogeneic stem cell transplantation for lymphoma: a multicentre randomized trial. Br J Haematol. 2016;173(1):96-104.

40. Sandmaier BM, Kornblit B, Storer BE, et al. Addition of sirolimus to standard cyclosporine plus mycophenolate mofetil-based graft-versus-host disease prophylaxis for patients after unrelated non-myeloablative haemopoietic stem cell transplantation: a multicentre, randomised, phase 3 trial. Lancet Haematol. 2019;6(8):e409-e418.

41. Perkins J, Field T, Kim J, et al. A randomized phase II trial comparing tacrolimus and mycophenolate mofetil to tacrolimus and methotrexate for acute graft-versus-host disease prophylaxis. Biol Blood Marrow Transplant. 2010;16(7):937-947.

42. Cutler C, Stevenson K, Kim HT, et al. Sirolimus is associated with veno-occlusive disease of the liver after myeloablative allogeneic stem cell transplantation. Blood. 2008;112(12):4425-4431.

43. Cutler C, Henry NL, Magee C, et al. Sirolimus and thrombotic microangiopathy after allogeneic hematopoietic stem cell transplantation. Biol Blood Marrow Transplant. 2005;11(7):551-557.

44. Solomon SR, Sanacore M, Zhang X, et al. Calcineurin inhibitor-free graft-versus-host disease prophylaxis with post-transplantation cyclophosphamide and brief-course sirolimus following reduced-intensity peripheral blood stem cell transplantation. Biol Blood Marrow Transplant. 2014;20 (11):1828-1834.

45. Gooptu M, Kim HT, Howard A, et al. Effect of sirolimus on immune reconstitution following myeloablative allogeneic stem cell transplantation: an ancillary analysis of a randomized controlled trial comparing tacrolimus/sirolimus and tacrolimus/methotrexate (Blood and Marrow Transplant Clinical Trials Network/BMT CTN 0402). Biol Blood Marrow Transplant. 2019;25(11):2143-2151.

46. Tkachev V, Furlan SN, Watkins B, et al. Combined OX40L and mTOR blockade controls effector T cell activation while preserving Treg reconstitution after transplant. Sci Transl Med. 2017;9(408):eaan3085.

47. Reinherz EL, Geha R, Rappeport JM, et al. Reconstitution after transplantation with T-lymphocyte-depleted HLA haplotype-mismatched bone marrow for severe combined immunodeficiency. Proc Natl Acad Sci U S A. 1982;79(19):6047-6051.

48. Soiffer RJ, Murray C, Mauch P, et al. Prevention of graft-versus-host disease by selective depletion of CD6-positive T lymphocytes from donor bone marrow. J Clin Oncol. 1992;10(7):1191-1200.

49. Drobyski WR, Ash RC, Casper JT, et al. Effect of T-cell depletion as graft-versus-host disease prophylaxis on engraftment, relapse, and disease-free survival in unrelated marrow transplantation for chronic myelogenous leukemia. Blood. 1994;83(7):1980-1987.

50. Champlin RE, Passweg JR, Zhang MJ, et al. T-cell depletion of bone marrow transplants for leukemia from donors other than HLA-identical siblings: advantage of T-cell antibodies with narrow specificities. Blood. 2000;95(12):3996-4003.

51. Antin JH, Bierer BE, Smith BR, et al. Selective depletion of bone marrow T lymphocytes with anti-CD5 monoclonal antibodies: effective prophylaxis for graft-versus-host disease in patients with hematologic malignancies. Blood. 1991;78(8):2139-2149.

52. Wagner JE, Donnenberg AD, Noga SJ, et al. Lymphocyte depletion of donor bone marrow by counterflow centrifugal elutriation: results of a phase I clinical trial. Blood. 1988;72(4):1168-1176.

53. Wagner JE, Thompson JS, Carter SL, Kernan NA, Unrelated donor marrow transplantation trial. Effect of graft-versus-host disease

prophylaxis on 3-year disease-free survival in recipients of unrelated donor bone marrow (T-cell Depletion Trial): a multi-centre, randomised phase II-III trial. Lancet. 2005;366(9487):733-741.

54. Horowitz MM, Gale RP, Sondel PM, et al. Graft-versus-leukemia reactions after bone marrow transplantation. Blood. 1990;75(3): 555-562.

55. Devine SM, Carter S, Soiffer RJ, et al. Low risk of chronic graft versus host disease and relapse associated with T-cell depleted peripheral blood stem cell transplantation for acute myeloid leukemia in first remission: results of the Blood and Marrow Transplant Clinical Trials Network (BMT CTN) Protocol 0303. Biol Blood Marrow Transplant. 2011;17(9):1343-1351.

56. Pasquini MC, Devine S, Mendizabal A, et al. Comparative outcomes of donor graft CD34+ selection and immune suppressive therapy as graft-versus-host disease prophylaxis for patients with acute myeloid leukemia in complete remission undergoing HLA-matched sibling allogeneic hematopoietic cell transplantation. J Clin Oncol. 2012;30(26):3194-3201.

57. Daniele N, Scerpa MC, Caniglia M, et al. Transplantation in the onco-hematology field: focus on the manipulation of αβ and γδ T cells. Pathol Res Pract. 2012;208(2):67-73.

58. Locatelli F, Merli P, Pagliara D, et al. Outcome of children with acute leukemia given HLA-haploidentical HSCT after αβ T-cell and B-cell depletion. Blood. 2017;130(5):677-685.

59. Distler E, Bloetz A, Albrecht J, et al. Alloreactive and leukemia-reactive T cells are preferentially derived from naïve precursors in healthy donors: implications for immunotherapy with memory T cells. Haematologica. 2011;96(7):1024-1032.

60. Teschner D, Distler E, Wehler D, et al. Depletion of naive T cells using clinical grade magnetic CD45RA beads: a new approach for GVHD prophylaxis. Bone Marrow Transplant. 2014;49(1):138-144.

61. Bleakley M, Heimfeld S, Jones LA, et al. Engineering human peripheral blood stem cell grafts that are depleted of naïve T cells and retain functional pathogen-specific memory T cells. Biol Blood Marrow Transplant. 2014;20(5):705-716.

62. Bleakley M, Heimfeld S, Loeb KR, et al. Outcomes of acute leukemia patients transplanted with naive T cell-depleted stem cell grafts. J Clin Invest. 2015;125(7):2677-2689.

63. Poon LM, Linn YC, Tan PL, et al. HLA-haploidentical hematopoietic cell transplantation after TCR-Aβ and CD45RA+ depletion following reduced intensity conditioning in adults and children with hematological malignancies - two-year follow-up of multicenter study in Singapore. Blood. 2019;134(Suppl 1):abstract 2039.

64. Ng CT, Ampudia J, Soiffer RJ, Ritz J, Connelly S. Itolizumab as a potential therapeutic for the prevention and treatment of graft vs host disease. Blood. 2019;134(Suppl 1):5603.

65. Aversa F, Pierini A, Ruggeri L, Martelli MF, Velardi A. The evolution of T cell depleted haploidentical transplantation. Front Immunol. 2019;10:2769.

66. Rachamim N, Gan J, Segall H, et al. Tolerance induction by "megadose" hematopoietic transplants: donor-type human CD34 stem cells induce potent specific reduction of host anti-donor cytotoxic T lymphocyte precursors in mixed lymphocyte culture. Transplantation. 1998;65(10):

1386-1393.

67. Di Ianni M, Falzetti F, Carotti A, et al. Tregs prevent GVHD and promote immune reconstitution in HLA-haploidentical transplantation. Blood. 2011;117(14):3921-3928.

68. Taylor PA, Lees CJ, Blazar BR. The infusion of ex vivo activated and expanded CD4(+)CD25(+) immune regulatory cells inhibits graft-versus-host disease lethality. Blood. 2002;99(10):3493-3499.

69. Parmar S, Liu X, Najjar A, et al. Ex vivo fucosylation of third-party human regulatory T cells enhances anti–graft-versus-host disease potency in vivo. Blood. 2015;125(9):1502-1506.

70. Copsel SN, Barreras H, Lightbourn CO, et al. IL-2/IL-2R, TL1A/TNFRSF25 or their combined stimulation results in distinct CD4+FoxP3+ regulatory T cell phenotype and suppressive function. Biol Blood Marrow Transplant. 2020;26(3):S169.

71. Brunstein CG, Miller JS, Cao Q, et al. Infusion of ex vivo expanded T regulatory cells in adults transplanted with umbilical cord blood: safety profile and detection kinetics. Blood. 2011;117(3):1061-1070.

72. Mavers M, Maas-Bauer K, Negrin RS. Invariant natural killer T cells as suppressors of graft-versus-host disease in allogeneic hematopoietic stem cell transplantation. Front Immunol. 2017;8:900.

73. Pillai AB, George TI, Dutt S, Teo P, Strober S. Host NKT cells can prevent graft-versus-host disease and permit graft antitumor activity after bone marrow transplantation. J Immunol. 2007;178(10):6242-6251.

74. Pillai AB, George TI, Dutt S, Strober S. Host natural killer T cells induce an interleukin-4-dependent expansion of donor CD4+CD25+Foxp3+ T regulatory cells that protects against graft-versus-host disease. Blood. 2009;113(18):4458-4467.

75. Lowsky R, Takahashi T, Liu YP, et al. Protective conditioning for acute graft-versus-host disease. N Engl J Med. 2005;353(13):1321-1331.

76. Duramad O, Laysang A, Li J, Nguyen N, Ishii Y, Namikawa R. A liposomal formulation of KRN7000 (RGI-2001) potently reduces GvHD lethality through the expansion of CD4+Foxp3+ regulatory T cells in murine models. Blood. 2008;112(11):3500.

77. Chen Y-B, Efebera YA, Johnston L, et al. Increased Foxp3+Helios+ regulatory T cells and decreased acute graft-versus-host disease after allogeneic bone marrow transplantation in patients receiving sirolimus and RGI-2001, an activator of invariant natural killer T cells. Biol Blood Marrow Transplant. 2017;23(4):625-634.

78. Tawara I, Koyama M, Liu C, et al. Interleukin-6 modulates graft-versus-host responses after experimental allogeneic bone marrow transplantation. Clin Cancer Res. 2011;17(1):77-88.

79. Drobyski WR, Szabo A, Zhu F, et al. Tocilizumab, tacrolimus and methotrexate for the prevention of acute graft-versus-host disease: low incidence of lower gastrointestinal tract disease. Haematologica. 2018;103(4):717-727.

80. Kennedy GA, Tey S-K, Curley C, et al. Results of a phase III double-blind study of the addition of tocilizumab vs. placebo to cyclosporin/methotrexate GvHD prophylaxis after HLA-matched allogeneic stem cell transplantation. Blood. 2019;134(Suppl 1):368.

81. Blazar BR, Taylor PA, Linsley PS, Vallera DA. In vivo blockade of CD28/CTLA4: B7/BB1 interaction with CTLA4-Ig reduces lethal

murine graft-versus-host disease across the major histocompatibility complex barrier in mice. Blood. 1994;83(12): 3815-3825.

82. Watkins B, Qayed M, Bratrude B, et al. T cell costimulation blockade with abatacept nearly eliminates early severe acute graft versus host disease after HLA-mismatched (7/8 HLA matched) unrelated donor transplant, with a favorable impact on disease-free and overall survival. Blood. 2017;130(Suppl 1):212.

83. Watkins BK, Tkachev V, Furlan SN, et al. CD28 blockade controls T cell activation to prevent graft-versus-host disease in primates. J Clin Invest. 2018;128(9):3991-4007.

84. MacMillan ML, Weisdorf DJ, Wagner JE, et al. Response of 443 patients to steroids as primary therapy for acute graft-versus-host disease: comparison of grading systems. Biol Blood Marrow Transplant. 2002;8(7):387-394.

85. Van Lint MT, Uderzo C, Locasciulli A, et al. Early treatment of acute graft-versus-host disease with high- or low-dose 6-methylprednisolone: a multicenter randomized trial from the Italian Group for Bone Marrow Transplantation. Blood. 1998;92(7):2288-2293.

86. Jagasia M, Zeiser R, Arbushites M, Delaite P, Gadbaw B, von Bubnoff N. Ruxolitinib for the treatment of patients with steroid-refractory GVHD: an introduction to the REACH trials. Immunotherapy. 2018;10(5):391-402.

87. Choi J, Ziga ED, Ritchey J, et al. IFNγR signaling mediates alloreactive T-cell trafficking and GVHD. Blood. 2012;120(19):4093-4103.

88. Spoerl S, Mathew NR, Bscheider M, et al. Activity of therapeutic JAK 1/2 blockade in graft-versus-host disease. Blood. 2014;123 (24):3832-3842.

89. Zeiser R, Burchert A, Lengerke C, et al. Ruxolitinib in corticosteroid-refractory graft-versus-host disease after allogeneic stem cell transplantation: a multicenter survey. Leukemia. 2015;29(10):2062-2068.

90. Jagasia M, Ali H, Schroeder MA, et al. Ruxolitinib in combination with corticosteroids for the treatment of steroid-refractory acute graft-vs-host disease: results from the phase 2 REACH1 trial. Biol Blood Marrow Transplant. 2019;25(3):S52.

91. Zeiser R, von Bubnoff N, Butler J, et al. Ruxolitinib for glucocorticoid-refractory acute graft-versus-host disease. N Engl J Med. 2020;382(19):1800-1810.

92. Tawara I, Sun Y, Lewis EC, et al. Alpha-1-antitrypsin monotherapy reduces graft-versus-host disease after experimental allogeneic bone marrow transplantation. Proc Natl Acad Sci U S A. 2012;109(2):564-569.

93. Marcondes AM, Hockenbery D, Lesnikova M, et al. Response of steroid-refractory acute GVHD to α1-antitrypsin. Biol Blood Marrow Transplant. 2016;22(9):1596-1601.

94. Magenau JM, Goldstein SC, Peltier D, et al. α1-antitrypsin infusion for treatment of steroid-resistant acute graft-versus-host disease. Blood. 2018;131(12):1372-1379.

95. Fløisand Y, Lazarevic VL, Maertens J, et al. Safety and effectiveness of vedolizumab in patients with steroid-refractory gastrointestinal acute graft-versus-host disease: a retrospective record review. Biol Blood Marrow Transplant. 2019;25(4):720-727.

96. Kekre N, Kim HT, Ho VT, et al. Phase II trial of natalizumab (Tysabri®) with corticosteroids as initial treatment of gastrointestinal acute graft versus host disease. Biol Blood Marrow Transplant. 2018;24(3):S81.

97. Klassen J. The role of photopheresis in the

treatment of graft-versus-host disease. Curr Oncol. 2010;17(2):55-58.

98. Flowers MED, Apperley JF, van Besien K, et al. A multicenter prospective phase 2 randomized study of extracorporeal photopheresis for treatment of chronic graft-versus-host disease. Blood. 2008;112(7):2667-2674.

99. Greinix HT, Volc-Platzer B, Rabitsch W, et al. Successful use of extracorporeal photochemotherapy in the treatment of severe acute and chronic graft-versus-host disease. Blood. 1998;92(9):3098-3104.

100. Perfetti P, Carlier P, Strada P, et al. Extracorporeal photopheresis for the treatment of steroid refractory acute GVHD. Bone Marrow Transplant. 2008;42(9):609-617.

101. Paczesny S, Krijanovski OI, Braun TM, et al. A biomarker panel for acute graft-versus-host disease. Blood. 2009;113(2):273-278.

102. Paczesny S, Braun T, Lugt MV, et al. A three biomarker panel at days 7 and 14 can predict development of grade II-IV acute graft-versus-host disease. Biol Blood Marrow Transplant. 2011;17(2):S167.

103. Major-Monfried H, Renteria AS, Pawarode A, et al. MAGIC biomarkers predict long-term outcomes for steroid-resistant acute GVHD. Blood. 2018;131(25):2846-2855.

104. Newell LF, Defor TE, Cutler CS, et al. Follistatin and endoglin: potential biomarkers of endothelial damage and non-relapse mortality after myeloablative allogeneic hematopoietic cell transplantation in Blood and Marrow Transplant Clinical Trials Network (BMT CTN) 0402. Biol Blood Marrow Transplant. 2017;23(3):S73-S74.

105. Staffas A, Burgos da Silva M, van den Brink MRM. The intestinal microbiota in allogeneic hematopoietic cell transplant and graft-versus-host disease. Blood. 2017;129(8):927-933.

106. Ivanov II, Atarashi K, Manel N, et al. Induction of intestinal Th17 cells by segmented filamentous bacteria. Cell. 2009;139 (3):485-498.

107. Jenq RR, Taur Y, Devlin SM, et al. Intestinal blautia is associated with reduced death from graft-versus-host disease. Biol Blood Marrow Transplant. 2015;21(8):1373-1383.

108. Peled JU, Gomes ALC, Devlin SM, et al. Microbiota as predictor of mortality in allogeneic hematopoietic-cell transplantation. N Engl J Med. 2020;382(9):822-834.

109. van Lier YF, Davids M, Haverkate NJE, et al. Fecal microbiota transplantation can cure steroid-refractory intestinal graft-versus-host disease. Biol Blood Marrow Transplant. 2019;25(3):S241.

110. Qi X, Li X, Zhao Y, et al. Treating steroid refractory intestinal acute graft-vs.-host disease with fecal microbiota transplantation: a pilot study. Front Immunol. 2018;9:2195.

111. DeFilipp Z, Bloom PP, Torres Soto M, et al. Drug-resistant E. coli bacteremia transmitted by fecal microbiota transplant. N Engl J Med. 2019;381(21):2043-2050.

Prospective isolation of radiation induced erythroid stress progenitors reveals unique transcriptomic and epigenetic signatures enabling increased erythroid output

Sofie Singbrant,[1] Alexander Mattebo,[1] Mikael Sigvardsson,[2] Tobias Strid[2] and Johan Flygare[1]

[1]Division of Molecular Medicine and Gene Therapy, Lund Stem Cell Center, Lund University and [2]Division of Molecular Hematology, Lund Stem Cell Center, Lund University, Lund, Sweden

Ferrata Storti Foundation

ABSTRACT

Massive expansion of erythroid progenitor cells is essential for surviving anemic stress. Research towards understanding this critical process, referred to as stress-erythropoiesis, has been hampered due to the lack of specific marker-combinations enabling analysis of the distinct stress-progenitor cells capable of providing radioprotection and enhanced red blood cell production. Here we present a method for the precise identification and *in vivo* validation of progenitor cells contributing to both steady-state and stress-erythropoiesis, enabling for the first time in-depth molecular characterization of these cells. Differential expression of surface markers CD150, CD9 and Sca1 defines a hierarchy of splenic stress-progenitors during irradiation-induced stress recovery in mice, and provides high-purity isolation of the functional stress erythroid burst-forming-units (stress-BFU-E) with a 100-fold improved enrichment compared to the state-of-the-art. By transplanting purified stress-progenitors expressing the fluorescent protein Kusabira Orange, we determined their kinetics *in vivo* and demonstrated that CD150$^+$CD9$^+$Sca1$^-$ stress-BFU-E provide a massive but transient radioprotective erythroid wave, followed by multi-lineage reconstitution from CD150$^+$CD9$^+$Sca1$^+$ multi-potent stem/progenitor cells. Whole genome transcriptional analysis revealed that stress-BFU-E express gene signatures more associated with erythropoiesis and proliferation compared to steady-state BFU-E, and are bone morphogenetic protein 4-responsive. Evaluation of chromatin accessibility through ATAC sequencing reveals enhanced and differential accessibility to binding sites of the chromatin-looping transcription factor CTCF in stress-BFU-E compared to steady-state BFU-E. Our findings offer a molecular insight into the unique capacity of stress-BFU-E to rapidly form erythroid cells in response to anemia and constitute an important step towards identifying novel erythropoiesis stimulating agents.

Introduction

Steady-state erythropoiesis is regulated mainly by changes in erythropoietin (EPO) levels that fine-tune survival and proliferation of erythroid colony-forming-units (CFU-E) and downstream precursor cells. In contrast, acute anemia induces a broader physiological response referred to as stress-erythropoiesis, which involves stimulation also of earlier progenitors to further increase the out-put of erythrocytes. This process is less characterized and mainly occurs in the murine spleen[1] after seeding of progenitors from the bone marrow (BM).[2,3] Stress-erythropoiesis is differentially regulated, including increased responsiveness to additional factors like hypoxia, corticosteroids and bone morphogenetic protein 4 (BMP4).[1,4-7] Importantly, stress-erythroid progenitors have the capacity to generate larger numbers of red blood cells than steady-state progenitors, and precise identification and enhanced understanding of their regulation are important steps towards discovering potential new erythroid-enhancing drugs for anemia treatment.

While fluorescence-activated cell sorting (FACS)-based methods for fractionation of distinct erythroid progenitor cells in murine and human during steady-state[8-11] has enabled in-depth characterization of mechanisms regulating steady-state erythropoiesis,[11-15] the cells and mechanisms regulating stress-erythropoiesis remain poorly defined. To enable studies of stress-erythropoiesis we set out to identify novel marker-combinations separating and enriching for the early stress-progenitors mediating radioprotection and recovery from severe anemia. We previously demonstrated that fetal erythroid burst-forming-units (BFU-E) can be isolated as lineage-cKit$^+$CD71/CD24a^{low}Sca1$^-$CD34$^-$ with high purity from murine fetal liver, where erythropoiesis in many ways resemble stress-erythropoiesis.[16] Attempts by other groups to isolate adult stress-erythroid progenitors from spleens of anemic mice and *in vitro* cultures have shown stress-BFU-E to be lineage-cKit$^+$CD71/Ter119^{low}, and further enriched in the Sca1$^+$CD34$^-$CD133$^-$ fraction. However, very few of these cells possess BFU-E potential (0.1-0.2%). Furthermore, in the active debate on lineage potential of stem- and progenitor cells, genuine megakaryocytic/erythroid potential is often overlooked since mature erythrocytes and platelets are difficult to trace *in vivo* after transplantation. Hence, the identity of pure stress-BFU-E remains largely elusive.

Using a novel combination of surface markers together with the tracing marker Kusabira Orange which is expressed in all cells, we have developed a method for high purity fractionation of a hierarchy of multi-potent progenitors, stress-BFU-E, and stress-CFU-E within the lineage-cKit$^+$CD71/CD24a^{low} cells in spleen during irradiation-induced stress-erythropoiesis as well as in steady-state BM, and for the first time determined their kinetics and full differentiation potential *in vivo*. The formation of stress-BFU-E was highly dependent on functional BMP-signaling, and stress-BFU-E displayed enhanced expression of BMP-responsive genes, as well as gene signatures associated with erythropoiesis and proliferation compared to their steady-state counterpart. In addition, discrepancies in the epigenetic landscape were selectively enriched for putative binding sites for the chromatin-looping transcription factor CTCF. In conclusion, our findings provide high-purity isolation of both steady-state BFU-E and the stress-BFU-E mediating recovery from severe anemia, and offer molecular insight to and functional determination of the unique capacity of stress-BFU-E to rapidly form erythroid cells in response to anemia.

Methods

Mice and transplantations

All procedures involving mice were approved by the Animal Ethics Committee of Malmö/Lund, Sweden. Anemia was induced by lethally irradiating 8-12 week-old recipient mice (C57Bl/6; Ly5.2) with a split dose of 2x500 cGy, followed by transplantation of 2x10^6 unfractionated BM cells to rescue and trigger stress-erythropoiesis. Donor mice (B6SJL; Ly5.1) were either Kusabira Orange (KuO) positive or negative. Recipients were sacrificed on day 8 for analysis of stress recovery in the spleen.

For *in vivo* tracing, 500 multipotent progenitors (sMPP), 5,000 sBFU-E or 5,000 sCFU-E, all KuO$^+$, were FACS-sorted from day 8 stressed spleens and transplanted into lethally irradiated secondary recipients together with 105 unfractionated wild-type

BM cells as support. Secondary recipients were bled at 1, 2 and 4 weeks, and sacrificed at 2 or 4 weeks post transplantation for analysis of lineage potential and kinetics in peripheral blood (PB), BM and spleen.

Flow cytometry

A complete description of all antibodies used is listed in the *Online Supplementary Materials and Methods*.

Hematopoietic progenitor assays

All colony assays were incubated at 37°C incubators in 5% CO2 with either 21% or 1-4% O$_2$ as indicated, and scored on day 4 (CFU-E) or 7-8 (BFU-E and mixed colonies).

RNA sequencing

Splenic stress- and BM steady-state progenitors were FACS-sorted in triplicates. Strand specific RNA-sequencing libraries were constructed using SMARTer Stranded Total RNA-Seq Kit v2 (Takara Bio) followed by sequencing on a HiSeq3000 (Illumina).

Assay for Transposase Accessible Chromatin sequencing

3,000 splenic stress- and BM steady-state BFU-E were FACS-sorted in triplicates for the assay of Transposase Accessible Chromatin (ATAC) library preparation and sequencing as described previously.[18] Libraries were subject to single-end sequencing on a NextSeq500 (Illumina).

Statistical analysis

For all statistical analysis, apart from RNA- and ATAC-sequencing for which the specifications are stated in the *Online Supplemental Materials and Methods*, statistical significance was calculated using ANOVA accounting for multiple comparisons, followed by Tukey's multiple comparisons test. One-way ANOVA was used for single time point analysis and Two-way ANOVA was used when measuring potential over time (Figure 2). *$P \leq 0.05$, **$P \leq 0.01$, ***$P \leq 0.001$, ****$P \leq 0.0001$.

A detailed description of all methods used is available online in the *Online Supplementary Materials and Methods*.

Results

CD150, CD9 and Sca1 identify a hierarchy of splenic stress-progenitors during irradiation-induced stress recovery

To identify the stress-progenitors involved in irradiation-induced anemia and stress recovery, we subjected mice to lethal irradiation followed by BM transplantation and analyzed recipient spleens on day 8 (Figure 1A) when the greatest expansion of stress-progenitors occurs.[3] Using this model, stress-progenitors were previously identified as Lin$^-$cKit$^+$CD71/Ter119^{low}, although at low frequencies (0.2%).[3] To further enrich for stress-erythroid progenitors we included CD150, known to mark megakaryocytic/erythroid progenitors during steady-state hematopoiesis.[9] All BFU-E potential in the cKit$^+$CD71^{low}/Ter119^{low} population resided in the CD150$^+$ fraction (Figure 1B-C). Extramedullary expansion of early erythroid progenitors during stress-erythropoiesis is reminiscent of fetal liver erythropoiesis. We therefore analyzed previously published mRNA expression data (GSE26086)[16] from E14.5 to E15.5 fetal liver erythroid progenitors to identify possible additional markers for further sub-division of adult stress-erythroid progenitors (*Online Supplementary Figure S1A*).
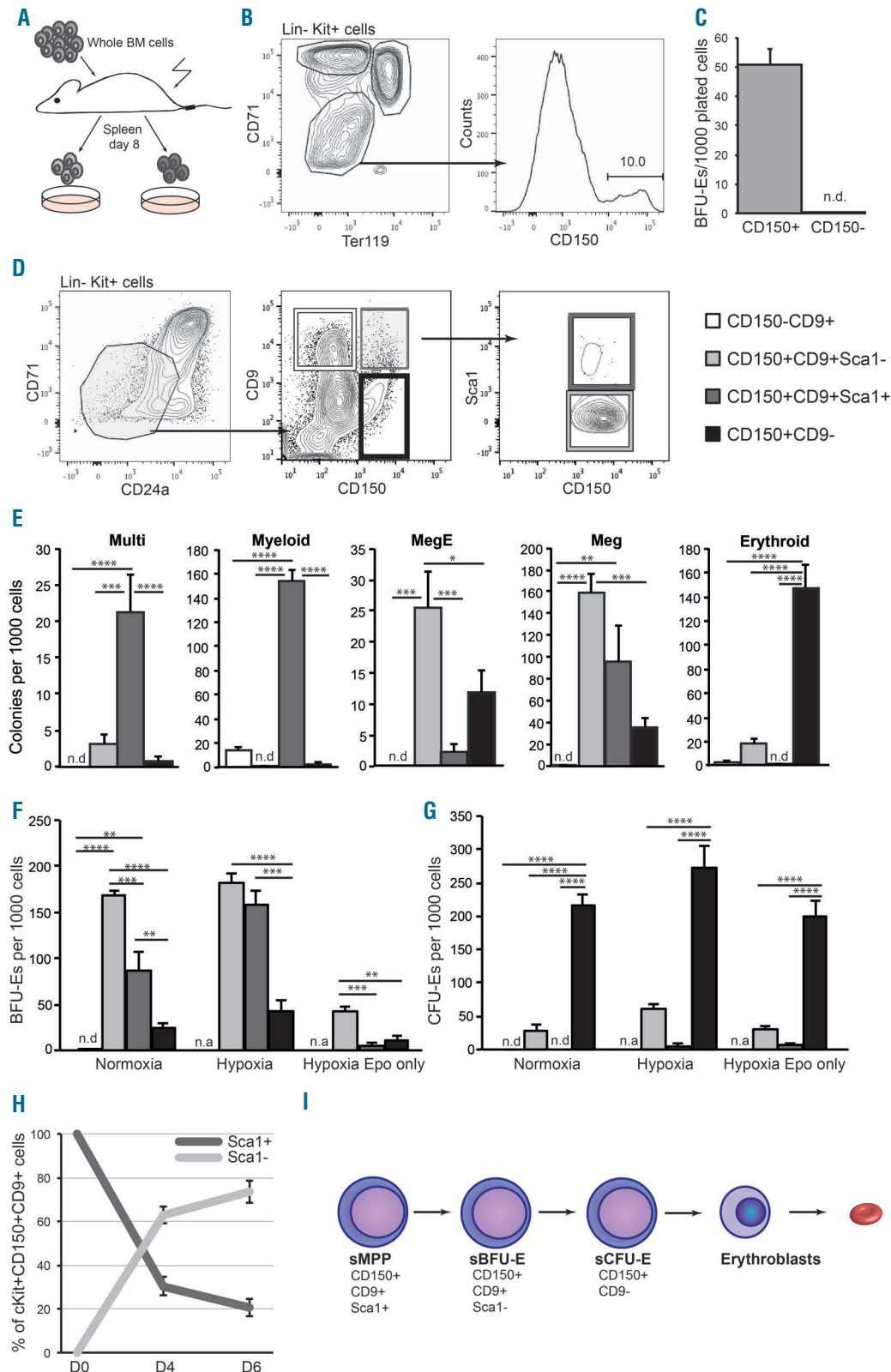
Figure 1. CD150, CD9 and Sca1 identify a hierarchy of splenic stress-progenitors during irradiation-induced stress recovery. (A) Stress-erythropoiesis was induced using lethal irradiation followed by transplantation of unfractionated bone marrow (BM), and splenic stress-progenitors were assessed on day 8 using colony assays. (B) Gating strategy and (C) BFU-E potential of FACS-sorted stress-progenitors from spleen day 8 based on CD150 expression (n=5). (D) Gating strategy for further fractionation of stress-progenitors within lineage-Kit+ cells using CD150 and CD9 and Sca1. (D-G) Colony forming capacity of splenic day 8 stress-progenitors, FACS-sorted based on (D) CD150/CD9 (normoxia, n=4), and (E-G) CD150/CD9/Sca1 (n=7 for normoxia, n=4 for hypoxia) within the Lin-cKit+CD71lowCD24low fraction. The cells were incubated in normoxia (21% O2) or hypoxia (1% O2) as indicated, and scored on day 4 (CFU-E) or day 7-8 (mixed and BFU-E). (H) FACS sorted CD150+CD9+Sca1+ progenitors were cultured *in vitro* and analyzed at indicated time points for the formation of CD150+CD9+Sca1- cells (n=4). I) Expression pattern of novel surface markers within the Lin-cKit+CD71lowCD24low fraction separating multi-potent stem/progenitor cells (sMPPs), stress-BFU-Es (sBFU-Es) and stress-CFU-E (sCFU-Es), defining a stress-progenitor hierarchy in spleen during irradiation-induced stress recovery, where Sca1 and subsequently CD9 are downregulated with increased differentiation. Data displayed as average ± standard error of the mean (SEM), n.d: not detectable, n.a: not applicable, *P≤0.05, **P≤0.01, ***P≤0.001, ****P≤0.0001.

As previously reported by us in fetal liver,[16] exclusion of mature erythroid precursor cells in spleen was facilitated by inclusion of CD24a as a negative selection marker (*Online Supplementary Figure S1B*). Of the surface markers tested (CD9, CD11a, CD34, CD48, CD63, and CD79b), only CD9 could further fractionate the BFU-E-containing CD150^{+} population in stressed spleen (*Online Supplementary Figure S1C*). CD133 was used in a recent study together with CD34 to fractionate stress-progenitor potential of cultured Sca1^{+}cKit^{+}CD71/Ter119^{low} cells.[17] However, neither CD34 nor CD133 could further fractionate CD150^{+} stress-progenitors (*Online Supplementary Figure S1C* and *Online Supplementary Figure S2A*, respectively). To further discriminate putative multi-potent stress-progenitors from lineage restricted stress-BFU-E we also included Sca1, which in steady-state BM separates Sca1^{+} hematopoietic stem cells (HSC) and Sca1^{-} myelo-erythroid progenitors.[9] Analysis of Lin[-]cKit^{+}CD71^{low}/CD24a^{low} splenic stress-progenitors fractionated based on

CD150/CD9/Sca1 expression (Figure 1D), clearly demonstrated that the majority of multi-lineage, megakaryocytic and BFU-E colony forming potential resided in the CD150^{+}CD9^{+} population (Figure 1E-F). Stress-progenitors negative for CD9 gave rise to more mature erythroid colonies (Figure 1E, G), which was also true for CD133^{+} cells (*Online Supplementary Figure S2B*), whereas CD150^{-} cells mainly gave rise to myeloid colonies (Figure 1E). Only Sca1 expressing CD150^{+}CD9^{+} cKit^{+} CD71^{low}/CD24a^{low} stress-progenitors (about 10%) gave rise to mixed and myeloid colonies (Figure 1E), while megakaryocytic/erythroid potential was retained in Sca1^{-} stress-progenitors (Figure 1E-F). Stress-BFU-E are reported to form BFU-E colonies with Epo alone,[1] but require hypoxia and additional cytokines for maximum expansion.[3] Colony assays demonstrated that BFU-E-forming potential resided almost exclusively in the CD150^{+}CD9^{+} population (Figure 1F). Importantly, as many as 21.4±2.2% of CD150^{+}CD9^{+} cells gave rise to BFU-E
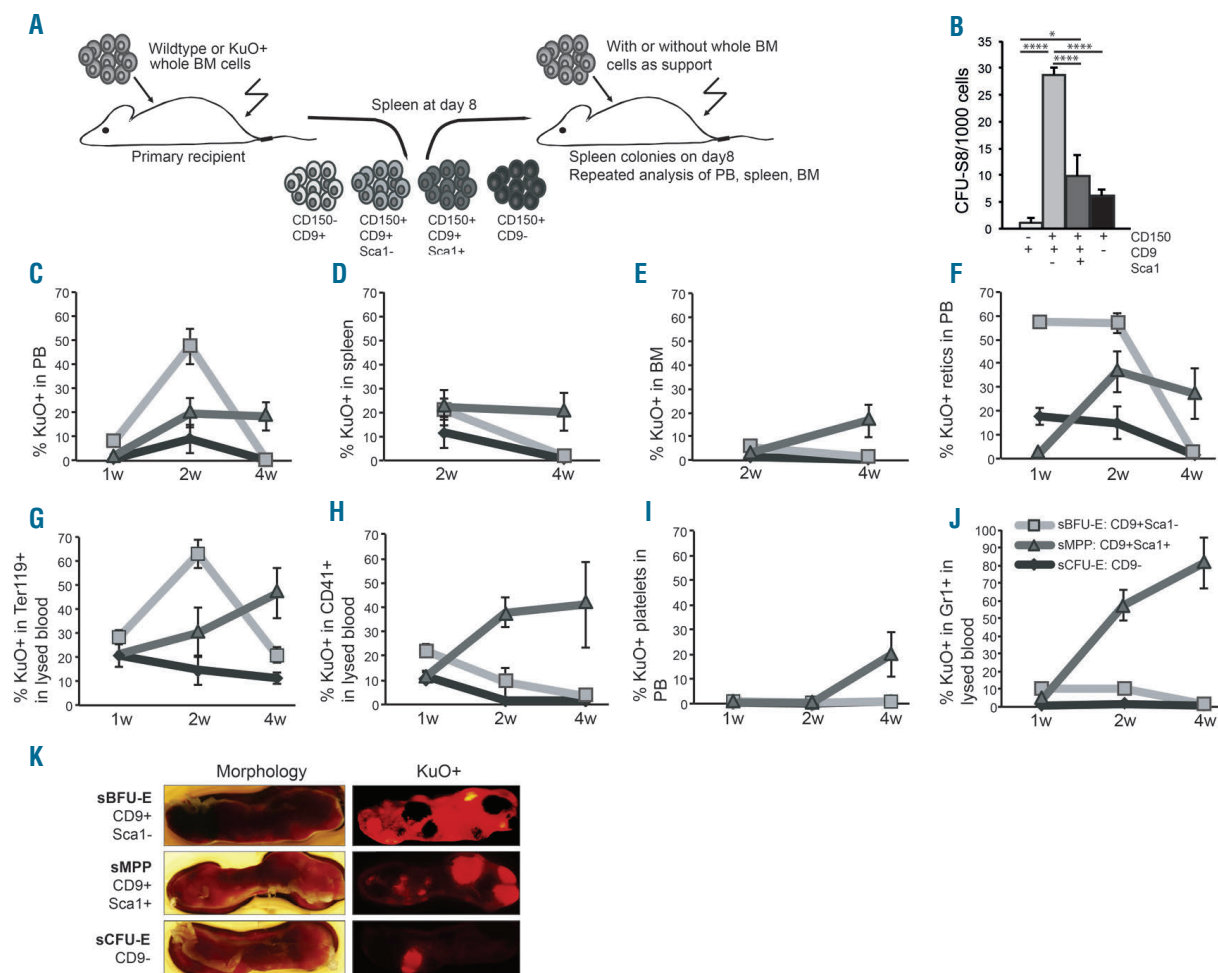
Figure 2. Stress-BFU-E provide a transient wave of primarily erythroid cells, followed by multi-lineage reconstitution from stress-MPP. (A) Stress-erythropoiesis was induced using lethal irradiation followed by transplantation of unfractionated bone marrow (BM) from (B) wild-type or (C-K) transgenic Kusabira Orange (KuO) mice. Splenic stress-progenitor populations were FACS-sorted on day 8, transplanted into lethally irradiated secondary recipients (B) without support to evaluate spleen colony formation (CFU-S8) (n=3-7; 600 cells per recipient without support) or (C-K) together with 105 unfractionated wild-type BM support cells to monitor their repopulation capacity *in vivo* over time in (C) peripheral blood (PB), (D) spleen and (E) BM, as determined by KuO fluorescence and FACS (n=6 at 1-2 weeks and n=3 at 4 weeks; 500 sMPP or 5,000 of each stress-erythroid progenitor per recipient, all with 105 wild-type support BM cells). (F-J) Contribution of sorted KuO+ progenitors in PB to (F) reticulocytes (whole PB), (G) Ter119^{+} erythroid cells, (H) CD41^{+} cells, (I) platelets (whole PB), and (J) Gr1+ myeloid cells in PB, as determined by FACS (after lysis of red blood cells if not stated otherwise). (K) Representative picture of whole spleens 2 weeks after transplantation assessing KuO contribution using epifluorescence microscopy and green filtered laser excitation. Data displayed as average ± standard error of the mean (SEM), *P≤0.05, **P≤0.01, ***P≤0.001, ****P≤0.0001.

colonies, providing over 100-fold improved purity compared to the state-of-the-art (0.1-0.2%). Although both Sca1^{−} and Sca1^{+} cells formed BFU-E colonies when stem cell factor (SCF) was present, only Sca1- cells formed BFU-E in erythropoietin (Epo) alone (Figure 1F). Furthermore, Sca1^{−} progenitors generally gave rise to larger colonies

than Sca1^{+} progenitors (*data not shown*). A notable 27.4±3.2% of CD150^{+}CD9^{−} cells gave rise to CFU-E, which were mainly independent of hypoxia and SCF (Figure 1G). Although the number of colonies was not affected, hypoxia resulted in increased proliferation and larger colonies (*data not shown*). FACS-sorted
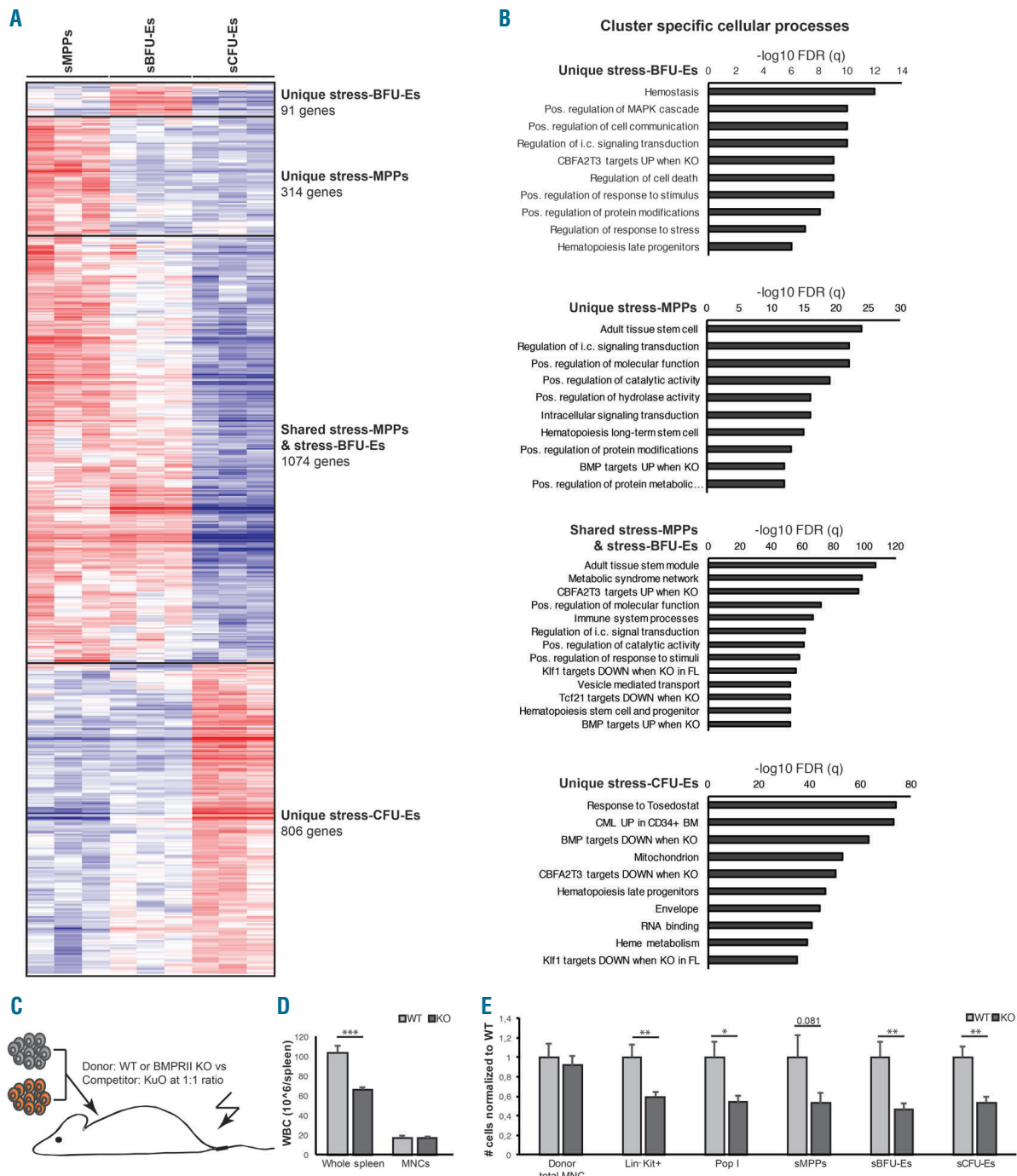
Figure 3. Stress-BFU-E and stress-CFU-E display opposing expression patterns of BMP- and CBFA2T3-responsive genes. (A) Unsupervised clustering of RPKM normalized data on genes with a significantly different expression between any of the samples (FDR<0.05, log₂ fold change>0.58) from RNA-sequencing of FACS sorted stress-progenitor populations as indicated (n=3, for further details see the Methods section). (B) Cellular processes for each of the clusters generated in (A), as analyzed by GSEA. For a complete gene lists for each cluster see the *Online Supplementary Table S1*. (C) Experimental outline of competitive transplantation of wild-type or BMP receptor II (BMPRII) deficient bone marrow against KuO[+] wild-type bone marrow. The stress recovery was analyzed in spleens of recipients on day 8 after transplantation (n=7 per group). (D) White blood cell count (WBC) per spleen before and after enrichment of mononuclear cells (MNC). (E) Detailed analysis of donor-derived (KuO-) MNC and stress-populations within MNC spleen cells as indicated. Data displayed as average ± standard error of the mean (SEM) of total number of cells/spleen (D) and normalized to wild-type (E), *P≤0.05, **P≤0.01.

CD150⁺CD9⁺Sca1⁺ progenitors gave rise to CD150⁺CD9⁺Sca1⁻ in culture (Figure 1H), indicating that more restricted Sca1- progenitors arise from multi-potent Sca1+ progenitors. Taken together, differential expression of cell surface markers CD150, CD9 and Sca1 defines a hierarchy of splenic Lin⁻cKit⁺CD71/CD24a^{low} stress-progenitors during irradiation-induced stress recovery in mice (Figure 1I). The stress-BFU-E, forming BFU-E colonies *in vitro* (CD150⁺CD9⁺Sca1⁻, hereafter referred to as stress-BFU-E or sBFU-E), can be separated from multi-potent stress-progenitors (CD150⁺CD9⁺Sca1⁺, hereafter referred to as stress-MPP or sMPP) and stress-CFU-E (CD150⁺CD9⁻, hereafter referred to as stress-CFU-E or sCFU-E) by Sca1 and CD9 expression respectively.

Stress-BFU-E provide a transient wave of primarily erythroid cells, followed by multi-lineage reconstitution from stress-MPP

To determine the kinetics and full *in vivo* potential of the identified stress-progenitors, we used a transgenic mouse that constitutively expresses the fluorescent protein Kusabira Orange (KuO) in all cells, including erythrocytes and platelets.[20] Lethally irradiated recipients were transplanted with BM from KuO mice, and KuO⁺ splenic stress-progenitors isolated on day 8 were subsequently transplanted into secondary recipients, either without support cells to score spleen colony-forming-units day 8 (CFU-S8),[21] or together with 10⁵ unfractionated wild-type BM support cells to monitor their *in vivo* repopulation capacity over time (Figure 2A). sBFU-E demonstrated the highest CFU-S8 potential (Figure 2B), indicative of robust short-term radio-protective capacity. Analysis of overall repopulation potential of sorted KuO⁺ progenitors demonstrated

Table 1. Top 20 up-regulated genes in stress-BFU-E compared to steady-state.

Gene symbol	log2 fold change	-log10 FDR
Ctse	2,254	19,109
Myh10	1,542	7,858
Aldh1a1	1,529	5,762
Pop1	1,178	2,814
Tfrc	1,171	4,072
Psat1	1,133	3,136
Timm10b	1,123	2,505
Vkorc1	1,119	2,652
Sipa1	1,117	5,900
Tmem70	1,082	2,401
Usp14	1,063	6,477
Emilin2	1,062	3,012
Josd1	1,039	3,305
Psmb2	1,036	2,079
Suclg1	1,035	5,608
Trip13	1,014	2,078
Arap2	1,005	2,132
Tmem201	1,001	2,320
Mob1b	0,992	2,190
Atl2	0,984	3,323

The most highly up-regulated genes in sBFU-E compared to steady-state BFU-E were Ctse/Cathepsin E: an erythrocyte membrane aspartic proteinase previously described as a down-stream target of Foxo3 in erythroid regulation,[38] Myh10: a non-muscle myosin involved in cell division of erythroblasts and other cells,[39] Aldh1a1: a critical enzyme involved in metabolism of reactive oxygen species and retinoic acid shown to mark adult definitive erythroid fate in mouse and human blood development, and the transferrin receptor Tfrc/CD71.

Figure 4. CD150 and CD9 mark BFU-E potential during steady-state erythropoiesis, providing improved identification of myelo-erythroid progenitors in the bone marrow. Gating strategy and colony forming potential (CFU-E; light grey, BFU-E; dark grey) of FACS sorted (A-D) steady-state bone marrow progenitors based on (A-B) classical fractionation using CD150 and CD1059, and (C-D) the new markers CD150/CD9/Sca1. All cells were incubated in 4% O₂, and scored on day 4 (CFU-E) or day 7-8 (BFU-E). Data displayed as average ± standard error of the mean (SEM), n.d: not detectable. *P≤0.05, **P≤0.01.

that sBFU-E and sCFU-E provide a transient wave of reconstitution in PB and spleen, with limited contribution to BM hematopoiesis. In contrast, sMPP increased their output over time, and was the only population that efficiently populated the BM and still contributed to hematopoiesis at four weeks (Figure 2C-E).

At two weeks 47.4±7.6% of PB cells were KuO[+] in mice transplanted with sBFU-E, compared to 9.0±5.9%

($P \le 0.0001$) for sCFU-E (Figure 2C). Analysis of the differentiation potential of transplanted stress-progenitors revealed that sBFU-E gave rise to 57.4±1.9% of reticulocytes compared to 17.5±3.5% ($P \le 0.0001$) for sCFU-E, while reticulocytes from sMPP were barely detected (Figure 2F; PB 1 week). Furthermore, the initial overall formation of reticulocytes was 2-fold higher in mice transplanted with sBFU-E compared to sCFU-E (*Online*

Figure 5. Compared to steady-state BFU-E, stress-BFU-E have enhanced expression of genes associated with BMP signaling, erythropoiesis and proliferation, and have enhanced and differential accessibility to CTCF binding sites. (A) RNA-sequencing was conducted on BFU-E FACS-sorted from steady-state bone marrow and day 8 stress spleens respectively (n=3). Significant differential expression was determined as -log$_{10}$ FDR>2 and log$_2$ fold change>0.58, for a full list of differentially expressed genes see the *Online Supplementary Table S2*. (B-C) Cellular processes for genes that were (B) up- and (C) down-regulated in stress-BFU-E compared to steady-state respectively, as analyzed by GSEA. (D) Fishbone heatmap outlining specific and shared ATAC-seq peaks in steady-state and stress BFU-E respectively. Each row represents one peak, and the color represents the intensity of chromatin accessibility. Peak files for heatmap were created in HOMER44 and grouped based on K-means clustering (3-clusters, 100-runs) performed in Cluster3, revealing clusters of peaks enriched in stress- (orange) and steady-state BFU-E (blue) respectively. (E-F) Motif analysis was performed on stress (E) and steady-state (F) enriched regions from peak lists extracted from panel D using findMotifsGenome.pl in HOMER. (G) Distribution of identified top motifs was investigated +/- 500 bp from corresponding peak centers. (H) Annotation of the CTCF motif within stress-(orange) and steady-state (blue) BFU-E enriched peaks respectively.

Supplementary Figure 3A), albeit from low levels, with virtually no contribution to reticulocytes from sMPP during the first week (*Online Supplementary Figure 3B*). sBFU-E also dominated the overall contribution to erythroid cells during the first two weeks of recovery (Figure 2G, $P \leq 0.0001$ and $P \leq 0.01$, respectively.). All cell populations gave rise to CD41$^+$ cells short after transplantation (Figure 2H), whereas only sMPP produced platelets, which displayed slower kinetics compared to the formation of erythroid cells (Figure 2I; $P \leq 0.0001$). In agreement with the colony formation ability *in vitro*, myeloid (Figure 2J) as well as lymphoid lineages (*Online Supplemental Figure S3C-D*) were mainly derived from sMPP.

The KuO$^+$ blood lineage distribution and repopulation kinetics in spleen after transplantation was largely reflected by that observed in PB (*Online Supplemental Figure S4*), while the BM had a considerably slower repopulation pattern (*Online Supplemental Figure S5*).

Morphological analysis of spleens at 2 weeks post transplantation revealed a strikingly different distribution of repopulating cells (Figure 2K). Progeny from sBFU-E was evenly distributed throughout the spleen with occasional KuO$^-$ clones possibly arising from the support BM. In contrast, sMPP gave rise to a limited number of large clones, consistent with spleen colonies formed by more primitive stem/progenitor cells (CFU-S12).[23] Taken together, *in vivo* tracing demonstrated clear separation of functionally distinct populations within cKit$^+$CD71^{low}/CD24a^{low} cells using the additional markers CD150, CD9 and Sca1, where sBFU-E mediated recovery from irradiation-induced acute anemia by providing a transient wave of erythroid cells in the PB and spleen, followed by multi-lineage reconstitution in the PB, spleen and BM from sMPP.

Stress-BFU-E and stress-CFU-E display opposing expression patterns of BMP- and CBFA2T3-responsive genes

To identify gene expression patterns associated with the distinct features of the radio-protective sBFU-E, RNA-sequencing was performed on FACS sorted stress-progenitor populations from day 8 spleens. Unsupervised clustering of genes with significant differential expression between any of the investigated populations revealed that relatively few genes were uniquely expressed by sBFU-E, about half of the genes differing between progenitor populations were shared between sMPP and sBFU-E (Figure 3A, gene lists for each cluster in the *Online Supplemental Table S1*), while the sCFU-E were clearly distinct from the other two populations. Gene set enrichment analysis (GSEA)[24] revealed that genes that were uniquely up-regulated in sMPP were associated with adult tissue stem cells and long-term hematopoietic stem cells (Figure 3B), while genes up-regulated in sBFU-E were associated with MAPK signaling, response to stress and stimulus, and more mature hematopoietic progenitors (Figure 3B). Interestingly, both sMPP and sBFU-E expressed BMP- as well as CBFA2T3 target genes known to be up-regulated in response to Bmp or Cbfa2t3 inactivation respectively (Figure 3B). sCFU-E on the other hand, uniquely expressed genes correlating with late progenitors, heme metabolism, and BMP- and CBFA2T3-responsive genes reported to be down-regulated in response to Bmp or Cbfa2t3 inactivation (Figure 3B).

The differential expression of BMP-responsive genes in sCFU-E and more primitive stress-progenitors is well in line with previous findings showing that effective generation of erythroid stress-progenitors is BMP-dependent. To explore

Table 2. Top 20 down-regulated genes in stress-BFU-E compared to steady-state.

Gene symbol	log2 fold change	-log10 FDR
Fl3a1	-2,754	29,923
Snord15a	-2,519	23,305
Tifab	-2,413	16,746
Csf1r	-2,358	16,322
Cybb	-2,344	13,756
Unc93b1	-2,321	25,436
Lgals1	-2,265	14,959
Cf10	-2,250	14,576
Snord15b	-2,197	43,032
Rasa4	-2,127	13,580
Cd209a	-2,124	10,439
Klf4	-2,115	10,450
Lrp1	-2,024	9,143
Pik3r5	-1,939	8,927
Itsn1	-1,907	21,849
Ccr2	-1,860	7,775
Ly6c2|	-1,859	7,727
Trim47	-1,847	8,101
Nhsl2	-1,796	7,029
Irf8	-1,783	7,515

The genes most down-regulated in sBFU-E compared to steady-state included the coagulation factor *F13a1/FxIIIa* expressed by monocytes and megakaryocytes, *Tifab*; a del(5q) MDS gene known to regulate hematopoiesis and mediate immune signaling through the Toll-like receptor–TRAF6 pathways,[41] the Kit paralog *Csf1r*; essential for the survival of monocytes and macrophages,[42] and *Cybb/gp91-phox*; a heme-binding membrane glycoprotein that is a phagocyte respiratory burst oxidase component induced by inflammation.[43]

the functional importance of BMP-signaling for the generation of stress-progenitor populations, BM cells deficient in BMP receptor II from conditional knock out mice (BmprIIfl/fl Vav-Cre) or wild-type littermate controls (BmprIIfl/fl Cre-negative) were competitively transplanted at a 1:1 ratio with KuO$^+$ wild-type BM, and analyzed for stress recovery contribution in the spleen on day 8 (Figure 3C). Mice transplanted with BMPRII deficient BM had smaller spleens and a 36% reduction in cells/spleen (Figure 3D), despite the fact that 50% of the transplanted BM cells were wild-type. This difference was no longer apparent after lymphoprep-enrichment of mononuclear cells, indicating that spleens of mice transplanted with 100% wild-type cells contained more erythroid cells (Figure 3D). Accordingly, BMPRII-deficient BM displayed a substantially decreased potential to form stress-progenitors from the stage of lineage negative cKit$^+$ progenitors (59.6±5,0% of wild-type), with the most prominent reduction observed in the number of sBFU-E (46.4±6.7% of wild-type) (Figure 3E, see Figure 1C for gating). Hence, in agreement with previous studies, our prospectively isolated stress-progenitor populations are dependent on BMP signaling for a full stress-response.
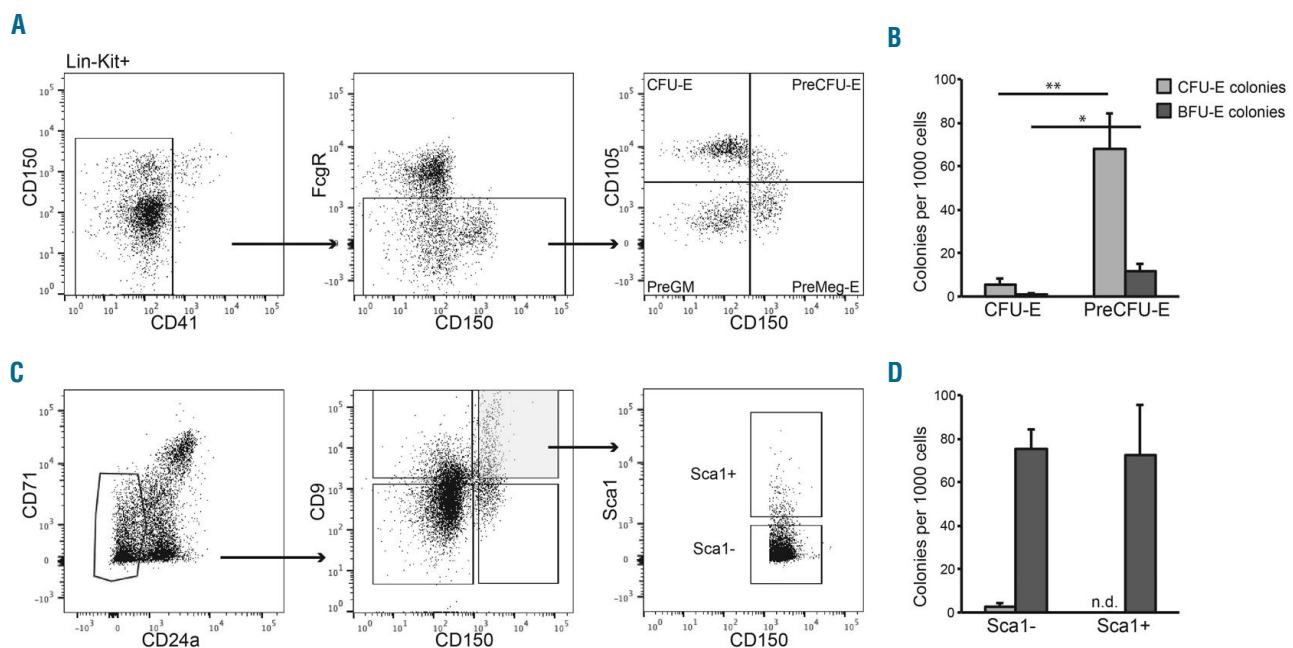
CD150 and CD9 mark BFU-E potential during steady-state erythropoiesis, providing improved identification of myelo-erythroid progenitors in the BM

Mapping transcriptional profiles of the splenic stress-progenitor populations (see Figure 3) to transcriptional pro-

files of steady-state progenitors from BM as recently defined by single-cell transcriptomics and fate assays,[15] demonstrated that splenic stress-progenitors map closely with their steady-state BM counterparts (*Online Supplementary Figure S6*). The most widely used protocol for delineating myelo-erythroid progenitors in steady-state BM nicely demonstrates that BFU-E potential resides in the Lin⁻cKit⁺CD150⁺CD105⁺ "Pre-CFU-E" fraction,[9] also confirmed in our hands (Figure 4A-B). However, since the "Pre-CFU-E" population contains relatively few BFU-E progenitors (Figure 4B and Pronk *et al.*),[9] a specific cell population possessing the BFU-E potential remains poorly defined. We therefore asked if CD9 could be used to also enrich for steady-state BFU-E. Progenitor populations were FACS-sorted from steady-state BM using the same marker-combinations as in stressed spleen (CD150⁺CD9⁺Sca1⁻), and plated for erythroid colony formation. The FACS profile of steady-state BM was very similar to that of stressed spleen (Figure 1C and Figure 4C), and both Sca1⁻ and Sca1⁺ CD150⁺CD9⁺ BM cells efficiently gave rise to BFU-E colonies (BFU-E/CFU-E colony formed from CD150⁺CD9⁺Sca1⁻: 30.0, frequency: 7.5±0.9%, Figure 4C-D), representing a 45-fold improved BFU-E/CFU-E ratio compared to previously used marker combination. In contrast, CD150⁺CD9⁺ cells were hardly present in spleens from steady-state mice, and of these only a few comprised BFU-E-forming potential (BFU-E/CFU-E colony formed from CD150⁺CD9⁺Sca1⁻: 10.8, frequency: 1.0±0.4%; *Online Supplementary Figure S7*). Furthermore, steady-state BM progenitors gave rise to highly proliferative BFU-E colonies, whereas steady-state spleen progenitors resulted in much smaller BFU-E colonies (*data not shown*). In conclusion, CD150 and CD9 expression mark BFU-E potential, both during steady-state in the BM and in the spleen during acute anemia.

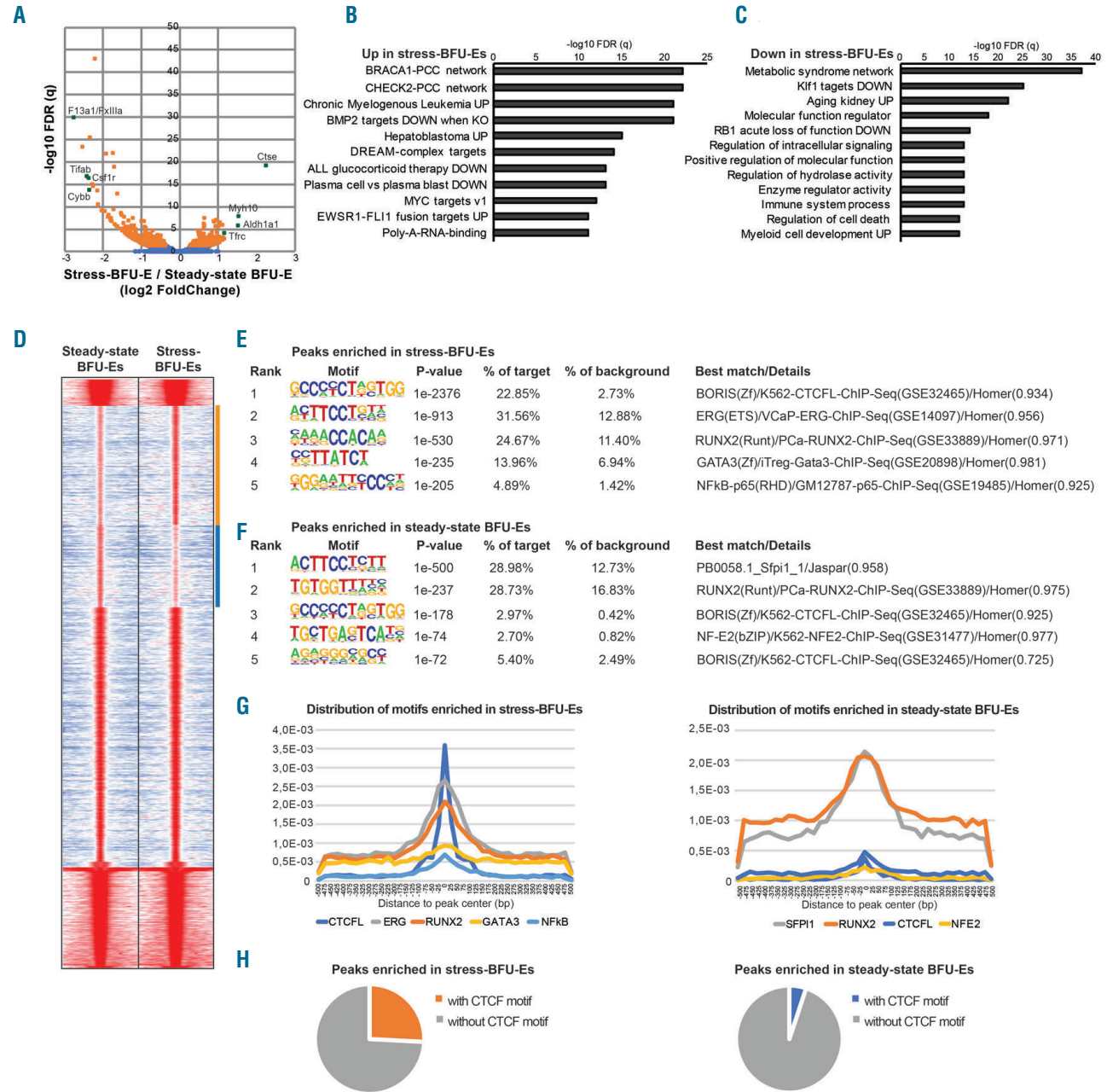### Compared to steady-state BFU-E, stress-BFU-E have enhanced expression of genes associated with BMP signaling, erythropoiesis and proliferation

To investigate prospective mechanisms giving stress-BFU-E their unique capacity to rapidly produce large numbers of erythroid cells in response to anemia, BFU-E (CD150⁺CD9⁺Sca1⁻) were sorted from steady-state BM and day 8 stressed spleens and analysed for transcriptional differences using RNA-seq. Analysis demonstrated a large overlap between stress- and steady-state BFU-E, with only 277 genes being differentially expressed (Figure 5A, full list of differentially expressed genes in the *Online Supplemental Table S2*). Gene set enrichment analysis demonstrated that sBFU-E expressed higher levels of genes associated with BMP and glucocorticoid signaling, proliferation, maturation block, and erythropoiesis (Figure 5B and *Online Supplementary Figure S8*) with several erythropoiesis-related genes among the most highly up-regulated genes in stress- compared to steady-state BFU-E (Table 1). Steady-state BFU-E on the other hand retained gene signatures associated with myeloid cell development and immune response (Figure 5C), which was also reflected by the genes most down-regulated in stress- compared to steady-state BFU-E (Table 2).

Strong prevalence for the binding motif of chromatin-looping transcription factor CTCF under ATAC-seq peaks enriched in stress-BFU-E

To define potential differences in active regulatory DNA elements across the genome, we performed the assay for transposase-accessible chromatin sequencing (ATAC-seq) analysis[18] on the same stress- and steady-state BFU-E populations as used for transcriptional profiling. ATAC-seq peaks (open chromatin regions) were detected using ENCODE ATAC-seq pipeline (*https://github.com/kundaje-lab/atac_dnase_pipelines*). K-means clustering demonstrated a relatively large overlap in chromatin availability between the two populations, with some of the peaks being enriched in stress- (orange) or steady-state (blue) BFU-E (Figure 5D and *Online Supplementary Figure S9*). The absolute majority of peaks with differential accessibility were located at distal elements (>1,000 bp away from the transcription start site) with only 5% situated around the promoter regions in both stress- and steady-state BFU-E, indicating that transcriptional differences between stress- and steady-state BFU-E are likely to be regulated by distal chromatin interactions.

To identify DNA-binding factors with differential chromatin availability in stress-erythropoiesis we performed motif analysis using peak files extracted from the heatmap clusters. This detected the transcriptional regulator CTCF (CCCTC-binding factor, CTCFL; testis-specific paralog) as the most significantly enriched DNA-binding factor in stress-BFU-E peaks followed by ERG (Figure 5E), whereas steady-state BFU-E peaks most significantly enriched for SFBPI1 and RUNX2 (Figure 5F). Notably, only for CTCF was the motif distributed closely around the peak center (Figure 5G). CTCF is known to regulate the formation of chromatin loops by binding together strands of DNA, and also constitutes a primary part of insulators by blocking the interaction between enhancers and promoters (reviewed by Phillips *et al.*).[29] Interestingly, CTCF has been shown to mark active promoters and boundaries of repressive chromatin domains in primary human erythroid cells,[30] and LDB1-CTCF enhancer looping has recently been shown to underlie activation of a substantial fraction of erythroid genes.[31] Furthermore, CTCF has been shown to regulate growth and erythroid differentiation of human myeloid leukemia cells (K562 cell line).[32] Although both steady-state and stress-BFU-E enriched for the CTCF motif, the frequency was considerably higher in sBFU-E, where 24,3% of the enriched peaks marked a CTCF motif, compared to 8,5% in steady-state BFU-E (Figure 5H). In conclusion, while the transcriptional and chromatin landscape of stress- and steady-state BFU-E display a high degree of similarity, distinctions in gene expression patterns and in the epigenetic landscape might underlie the unique capacity of sBFU-E to rapidly make large numbers of erythroid cells in response to anemia.

Discussion

The identity of stress-erythroid progenitors has remained largely elusive, and their precise identification is important to understand the mechanisms governing recovery from anemia. Previous studies have identified stress-progenitors to be cKit⁺CD71ˡᵒʷ/Ter119ˡᵒʷ,[14] and after culture the BFU-E potential is found in the CD34⁻CD133⁻ fraction of the Sca1⁺cKit⁺CD71ˡᵒʷ/Ter119ˡᵒʷ population. However, only a small fraction of these cells (0.12-0.2%) gave rise to BFU-E colonies. Here we demonstrate that the differential expression of the surface markers CD150, CD9 and Sca1 provide fractionation and definition of a

hierarchy of functionally diverse splenic stress-progenitors during irradiation-induced recovery, providing 100-fold improved enrichment of stress-BFU-E compared to the current state-of-the-art.

Analysis of megakaryocytic-erythroid differentiation kinetics has been hampered by the lack of markers expressed by mature erythrocytes and platelets. By transplanting sorted stress-progenitor populations from transgenic mice expressing Kusabira Orange in all cells including erythrocytes and platelets,[20] we determined their kinetics and full differentiation potential *in vivo*. Although sBFU-E gave rise to megakaryocytic colonies *in vitro* and CD41^{+} cells *in vivo*, only sMPP produced platelets *in vivo*, demonstrating the importance of *in vivo* experiments and the ability to trace all mature cell types for defining progenitor potential. In agreement with previous studies,[33] this shows that CD41 is not specific for the megakaryocytic lineage.

We further demonstrate that splenic sBFU-E provide a massive but transient erythroid wave, followed by multilineage reconstitution from sMPP. Harandi *et al.*[14] previously suggested that cKit^{+}CD71^{-}Ter119^{-} cells were erythroid restricted.[14] However, using the same starting population of cells and *in vivo* reconstitution we now demonstrate that these cells contain both multi-potent progenitors (CD150^{+}CD9^{+}Sca1^{+}) and more erythroid restricted BFU-E (CD150^{+}CD9^{+}Sca1^{-}) and CFU-E (CD150^{+}CD9^{-}). The same group also proposes that stress-BFU-E are Sca1^{+}, whereas we show that Sca1^{+} stress-progenitors are multi-potent with the capacity to give rise to more restricted Sca- sBFU-E. Sca1 is known to mark multi-potent HSC, and that Sca1 as a single surface marker can differentiate between multilineage and BFU-E potential is well in line with cellular hierarchy mapping in steady-state hematopoiesis.[34] Interestingly, CD9 has recently been reported to be expressed in murine HSC with MegE differentiation bias.[34] While Pronk *et al.*[9] have identified that CD150 marks "PreCFU-E" colony-forming potential in the BM during steady-state, we for the first time describe a FACS method for identifying progenitors with BFU-E potential, which resides in the cKit^{+}CD71^{low}/CD24a^{low}CD150^{+}CD9^{+} population. This demonstrates that these markers can be used to enrich for both steady-state BFU-E and stress-BFU-E.

BMP-regulation of stress-erythropoiesis has previously been described by Paulson and colleagues, whereas we have shown that steady-state erythropoiesis remains unaffected by disruption of canonical BMP-signaling. Investigation of the functional importance of BMP-signaling in our system revealed that transplantation of BMP-deficient BM resulted in an impaired stress-response with substantially smaller spleens and decreased potential to form stress-progenitors, despite 50% of the transplanted BM cells being wild-type. In addition, genes upregulated in sBFU-E compared to their steady-state counterpart were associated with gene sets activated downstream of the BMP signaling pathway.[33] Within the stress-erythroid progenitor populations, sCFU-E expressed the same set of BMP-responsive

genes to a higher degree than sBFU-E and sMPP. Taken together, these results model stress-erythroid progenitors in general and sCFU-E in particular as BMP-responsive cells. sCFU-E also displayed the highest expression of a set of genes that is down-regulated in response to inactivation of Cbfa2t3,[26] a transcriptional co-repressor that promotes degradation of hypoxia regulating protein Hif1a,[35] regulates Gata1-target genes critical for erythroid differentiation,[36] and maintains an erythroid-specific genetic program in progenitors primed for rapid activation when terminal erythroid differentiation is induced.[37] Stress-erythropoiesis is severely impaired in mice lacking Cbfa2t3.[26] Collectively, this makes Cbfa2t3 an interesting target to study further in stress-erythropoiesis regulation.

Analysis of active regulatory DNA elements across the genome using ATAC-seq revealed that sBFU-E displayed a stronger prevalence for the binding motif of chromatin-looping transcription factor CTCF compared to steady-state BFU-E which are less efficient in producing erythrocytes. CTCF has previously been implicated in marking active promoters in primary human erythroid cells,[30] and LDB1-CTCF enhancer looping underlies activation of a substantial fraction of erythroid genes.[31] In accordance, ectopic expression of CTCF in K562 cells promotes erythroid differentiation whereas CTCF knock-down significantly inhibits differentiation into the erythroid lineage.[32] Taken together, chromatin accessibility of CTCF is the most striking epigenetic difference between stress- and steady-state BFU-E, suggesting a role for CTCF-dependent mechanisms in stress-BFU-Es.

In conclusion, combining novel surface markers with the KuO tracing mouse, we have for the first time defined a cellular hierarchy of stress-progenitors, separating sMPP from sBFU-E and more mature sCFU-E based on their kinetics and differentiation potential *in vivo*. We further demonstrate that sBFU-E express gene signatures more associated with erythropoiesis and proliferation compared to steady-state BFU-E, and have enhanced and differential accessibility to CTCF binding sites. Our findings open up the field for further mechanistic and functional studies of how stress-erythropoiesis is regulated, and how sBFU-E contribute during recovery of erythroid disorders. Since the mechanisms regulating stress-erythropoiesis may be targeted for treatment of anemia, this is an important step towards identifying and studying novel erythropoiesis stimulating agents.

References

1. Lenox LE, Perry JM, Paulson RF. BMP4 and Madh5 regulate the erythroid response to acute anemia. Blood. 2005;105(7):2741-2748.

2. Peslak SA, Wenger J, Bemis JC, et al. EPO-mediated expansion of late-stage erythroid progenitors in the bone marrow initiates recovery from sublethal radiation stress. Blood. 2012;120(12):2501-2511.

3. Harandi OF, Hedge S, Wu DC, McKeone D, Paulson RF. Murine erythroid short-term

radioprotection requires a BMP4-dependent, self-renewing population of stress erythroid progenitors. J Clin Invest. 2010; 120(12):4507-4519.

4. Perry JM, Harandi OF, Paulson RF. BMP4, SCF, and hypoxia cooperatively regulate the expansion of murine stress erythroid pro-

genitors. Blood. 2007;109(10):4494-4502.

5. Singbrant S, Karlsson G, Ehinger M, et al. Canonical BMP signaling is dispensable for hematopoietic stem cell function in both adult and fetal liver hematopoiesis, but essential to preserve colon architecture. Blood. 2010;115(23):4689-4698.

6. Singbrant S, Moody JL, Blank U, et al. Smad5 is dispensable for adult murine hematopoiesis. Blood. 2006;108(12):3707-3712.

7. Paulson RF, Shi L, Wu DC. Stress erythropoiesis: new signals and new stress progenitor cells. Curr Opin Hematol. 2011;18(3):139-145.

8. Zhang J, Socolovsky M, Gross AW, Lodish HF. Role of Ras signaling in erythroid differentiation of mouse fetal liver cells: functional analysis by a flow cytometry-based novel culture system. Blood. 2003;102(12):3938-3946.

9. Pronk CJ, Rossi DJ, Mansson R, et al. Elucidation of the phenotypic, functional, and molecular topography of a myeloerythroid progenitor cell hierarchy. Cell Stem Cell. 2007;1(4):428-442.

10. Hu J, Liu J, Xue F, et al. Isolation and functional characterization of human erythroblasts at distinct stages: implications for understanding of normal and disordered erythropoiesis in vivo. Blood. 2013;121(16):3246-3253.

11. Li J, Hale J, Bhagia P, et al. Isolation and transcriptome analyses of human erythroid progenitors: BFU-E and CFU-E. Blood. 2014;124(24):3636-3645.

12. Kingsley PD, Greenfest-Allen E, Frame JM, et al. Ontogeny of erythroid gene expression. Blood. 2013;121(6):e5-e13.

13. Pishesha N, Thiru P, Shi J, Eng JC, Sankaran VG, Lodish HF. Transcriptional divergence and conservation of human and mouse erythropoiesis. Proc Natl Acad Sci U S A. 2014;111(11):4103-4108.

14. An X, Schulz VP, Li J, et al. Global transcriptome analyses of human and murine terminal erythroid differentiation. Blood. 2014;123(22):3466-3477.

15. Tusi BK, Wolock SL, Weinreb C, et al. Population snapshots predict early haematopoietic and erythroid hierarchies. Nature. 2018;555(7694):54-60.

16. Flygare J, Rayon Estrada V, Shin C, Gupta S, Lodish HF. HIF1alpha synergizes with glucocorticoids to promote BFU-E progenitor self-renewal. Blood. 2011;117(12):3435-3444.

17. Xiang J, Wu DC, Chen Y, Paulson RF. In vitro culture of stress erythroid progenitors identifies distinct progenitor populations and analogous human progenitors. Blood. 2015;125(11):1803-1812.

18. Buenrostro JD, Giresi PG, Zaba LC, Chang HY, Greenleaf WJ. Transposition of native chromatin for fast and sensitive epigenomic profiling of open chromatin, DNA-binding proteins and nucleosome position. Nat Methods. 2013;10(12):1213-1218.

19. Porayette P, Paulson RF. BMP4/Smad5 dependent stress erythropoiesis is required for the expansion of erythroid progenitors during fetal development. Dev Biol. 2008;317(1):24-35.

20. Hamanaka S, Ooehara J, Morita Y, et al. Generation of transgenic mouse line expressing Kusabira Orange throughout body, including erythrocytes, by random segregation of provirus method. Biochem Biophys Res Commun. 2013;435(4):586-591.

21. Till J, McCulloch E. A direct measurement of the radiation sensitivity of normal mouse bone marrow cells. Radiat Res. 1961;14(2):213-222.

22. Na Nakorn T, Traver D, Weissman IL, Akashi K. Myeloerythroid-restricted progenitors are sufficient to confer radioprotection and provide the majority of day 8 CFU-S. J Clin Invest. 2002;109(12):1579-1585.

23. Siminovitch L, McCulloch EA, Till JE. The distribution of colony-Forming cells among spleen colonies. J Cell Physiol. 1963;62(3):327-336.

24. Subramanian A, Tamayo P, Mootha VK, et al. Gene set enrichment analysis: a knowledge-based approach for interpreting genome-wide expression profiles. Proc Natl Acad Sci U S A. 2005;102(43):15545-15550.

25. Lee KY, Jeong JW, Wang J, et al. Bmp2 is critical for the murine uterine decidual response. Mol Cell Biol. 2007;27(15):5468-5478.

26. Chyla BJ, Moreno-Miralles I, Steapleton MA, et al. Deletion of Mtg16, a target of t(16;21), alters hematopoietic progenitor cell proliferation and lineage allocation. Mol Cell Biol. 2008;28(20):6234-6247.

27. Lenox LE, Shi L, Hegde S, Paulson RF. Extramedullary erythropoiesis in the adult liver requires BMP-4/Smad5-dependent signaling. Exp Hematol. 2009;37(5):549-558.

28. Perry JM, Harandi OF, Porayette P, Hegde S, Kannan AK, Paulson RF. Maintenance of the BMP4-dependent stress erythropoiesis pathway in the murine spleen requires hedgehog signaling. Blood. 2009;113(4):911-918.

29. Phillips JE, Corces VG. CTCF: master weaver of the genome. Cell. 2009;137(7):1194-1211.

30. Steiner LA, Schulz V, Makismova Y, Lezon-Geyda K, Gallagher PG. CTCF and CohesinSA-1 mark active promoters and boundaries of repressive chromatin domains in primary human erythroid cells. PLoS One. 2016;11(5):e0155378.

31. Lee J, Krivega I, Dale RK, Dean A. The LDB1 Complex co-opts CTCF for erythroid lineage-specific long-range enhancer interactions. Cell Rep. 2017;19(12):2490-2502.

32. Torrano V, Chernukhin I, Docquier F, et al. CTCF regulates growth and erythroid differentiation of human myeloid leukemia cells. J Biol Chem. 2005;280(30):28152-28161.

33. Gekas C, Graf T. CD41 expression marks myeloid-biased adult hematopoietic stem cells and increases with age. Blood. 2013;121(22):4463-4472.

34. Guo G, Luc S, Marco E, et al. Mapping cellular hierarchy by single-cell analysis of the cell surface repertoire. Cell Stem Cell. 2013;13(4):492-505.

35. Kumar P, Gullberg U, Olsson I, Ajore R. Myeloid translocation gene-16 co-repressor promotes degradation of hypoxia-inducible factor 1. PLoS One. 2015;10(5):e0123725.

36. Fujiwara T, Alqadi YW, Okitsu Y, et al. Role of transcriptional corepressor ETO2 in erythroid cells. Exp Hematol. 2013;41(3):303-315.

37. Stadhouders R, Cico A, Stephen T, et al. Control of developmentally primed erythroid genes by combinatorial co-repressor actions. Nat Commun. 2015;6:8893.

38. Bakker WJ, van Dijk TB, Parren-van Amelsvoort M, et al. Differential regulation of Foxo3a target genes in erythropoiesis. Mol Cell Biol. 2007;27(10):3839-3854.

39. Roy A, Lordier L, Mazzi S, et al. Activity of nonmuscle myosin II isoforms determines localization at the cleavage furrow of megakaryocytes. Blood. 2016;128(26):3137-3145.

40. Mirabelli P, Di Noto R, Lo Pardo C, et al. Extended flow cytometry characterization of normal bone marrow progenitor cells by simultaneous detection of aldehyde dehydrogenase and early hematopoietic antigens: implication for erythroid differentiation studies. BMC Physiol. 2008;8:13.

41. Varney ME, Niederkorn M, Konno H, et al. Loss of Tifab, a del(5q) MDS gene, alters hematopoiesis through derepression of Toll-like receptor-TRAF6 signaling. J Exp Med. 2015;212(11):1967-1985.

42. Chitu V, Stanley ER. Colony-stimulating factor-1 in immunity and inflammation. Curr Opin Immunol. 2006;18(1):39-48.

43. Belambri SA, Rolas L, Raad H, Hurtado-Nedelec M, Dang PM, El-Benna J. NADPH oxidase activation in neutrophils: role of the phosphorylation of its subunits. Eur J Clin Invest. 2018;48 Suppl 2:e12951.

44. Heinz S, Benner C, Spann N, et al. Simple combinations of lineage-determining transcription factors prime cis-regulatory elements required for macrophage and B cell identities. Mol Cell. 2010;38(4):576-589.

Ferrata Storti Foundation

Leukemia cells remodel marrow adipocytes *via* TRPV4-dependent lipolysis

Shaoxin Yang,[1*] Wei Lu,[1*] Chong Zhao,[2] Yuanmei Zhai,[3] Yanyu Wei,[1] Jiali Liu,[2] Yehua Yu,[1] Zhiqiang Li[4] and Jun Shi[1]

[1]Department of Hematology, Shanghai Ninth People's Hospital, Shanghai JiaoTong University School of Medicine; [2]Department of Hematology, Shanghai Jiao Tong University Affiliated Sixth People's Hospital; [3]Department of Hematology, Tongren Hospital, Shanghai Jiao Tong University School of Medicine and [4]Department of Blood Transfusion, Shanghai Jiao Tong University Affiliated Sixth People's Hospital, Shanghai, China.

*SY and WL contributed equally as co-first authors.

ABSTRACT

Remodeling of adipocyte morphology and function plays a critical role in prostate cancer development. We previously reported that leukemia cells secrete growth differentiation factor 15 (GDF15), which remodels the residual bone marrow (BM) adipocytes into small adipocytes and is associated with a poor prognosis in patients with acute myeloid leukemia. However, little is known about how GDF15 drives BM adipocyte remodeling. In this study, we examined the role of the transient receptor potential vanilloid (TRPV) channels in the remodeling of BM adipocytes exposed to GDF15. We found that TRPV4 negatively regulated GDF15-induced remodeling of BM adipocytes. Furthermore, transforming growth factor-β type II receptor was identified as the main receptor for GDF15 on BM adipocytes. PI3K inhibitor treatment reduced GDF15-induced pAKT, identifying PI3K/AKT as the downstream stress response pathway. Subsequently, GDF15 reduced the expression of the transcription factor Forkhead box C1 (FOXC1) in BM adipocytes subjected to RNA-sequencing screening and western blot analysis. Moreover, it was also confirmed that FOXC1 combined with the TRPV4 promoter by chromatin immunoprecipitation with quantitative polymerase chain reaction experiments, which suggests that FOXC1 mediates GDF15 regulation of TRPV4. In addition, an acute myeloid leukemia mouse model exhibited smaller BM adipocytes, whereas the TRPV4 activator 4α-phorbol 12,13-didecanoate partly rescued this process and increased survival. In conclusion, TRPV4 plays a critical role in BM adipocyte remodeling induced by leukemia cells, suggesting that targeting TRPV4 may constitute a novel strategy for acute myeloid leukemia therapy.

Correspondence:

JUN SHI
junshi@sjtu.edu.cn

ZHIQIANG LI
kcb039@126.com

Introduction

The development of acute myeloid leukemia (AML) is closely related to the bone marrow (BM) microenvironment.[1,2] As a critical component of the BM microenvironment, BM adipocytes provide energy for both the infinite proliferation of leukemia cells and the normal growth of hematopoietic stem cells.[3,4] Leukemia cells proliferate to an overwhelming number in a limited marrow cavity, likely because these cells are more efficient in capturing energy for growth. Accordingly, BM adipocytes are remodeled in response to leukemia cells, generating a pro-tumoral microenvironment.[5,6] However, the mechanism whereby leukemia cell growth induces BM adipocyte remodeling is still unclear.

Induced BM adipocyte remodeling involves several specific processes, including lipolysis, dedifferentiation and lipid accumulation. Consequently, the remodeled adipocytes show morphological and functional changes.[7] Breast cancer cells reportedly secrete soluble factor Wnt3a which reduces the number and size of adipocytes surrounding the malignant cells and thus contributes to disease devel-

opment.[8] As the breast cancer progresses, adipocytes de-differentiate to fibroblast-like cells.[8] In mouse models of bone metastasis following prostate cancer, Herroon *et al.* showed that remodeled BM adipocytes support tumor growth by fatty acid-binding protein 4 (FABP4) transportation of fatty acids.[9] These studies identified a functional role of remodeled adipocytes in supporting solid tumor metabolism. Thus, the adipocytes remodeled by cancer cells are also known as cancer-associated adipocytes.[10] In the context of leukemia, there is a growing consensus that reduction in BM adipocyte number, once believed to be merely due to mechanical squeezing by the rapid proliferation of leukemia cells in the limited BM cavity, is also actively regulated by leukemia cells.[5,11] Indeed, we previously reported that growth differentiation factor 15 (GDF15) derived from leukemia cells regulates BM adipocyte remodeling by enhancing lipolysis.[12] However, how extracellular GDF15 induces lipolysis within BM adipocytes remains elusive.

It has been reported that GDF15 enhances intracellular Ca^{2+} by increasing calcium voltage-gated channel subunit alpha1 C (Cav1.3) expression in rat cerebellar granule neurons, which induces the expression of genes essential for synaptic plasticity.[13] As an important cellular signal for lipid metabolism, intracellular Ca^{2+} is involved in lipid synthesis and lipolysis in adipocytes.[14,15] When the calcium channels in the adipocytes are activated or upregulated, accumulation of lipids is enhanced through increased $[Ca^{2+}]_i$.[16,17] Conversely, when calcium channels are inhibited or downregulated, decreased calcium influx may accelerate fat breakdown.[18,19] Thus, we hypothesized that calcium channels are involved in GDF15-induced BM adipocyte remodeling.

In this study, we examined a possible role of transient receptor potential vanilloid 4 (TRPV4) calcium channels in GDF15-driven remodeling of BM adipocytes. We unravel a novel function of transforming growth factor-β type II receptor (TGFβRII) that, in responding to GDF15 in BM adipocytes, activates the phosphatidylinositol 3-kinase (PI3K)/AKT transduction pathway, which in turn reduces the transcript factor Forkhead box C1 (FOXC1) level and subsequently downregulates TRPV4. We also provide evidence that inhibition of BM adipocyte remodeling increases survival in the AML mouse model, implying a novel therapeutic target for AML.

Methods

Patients' samples

BM aspirates were collected from 16 patients diagnosed as having lymphoma without BM invasion, using procedures approved by the Ethics Committee of Shanghai Jiao Tong University Affiliated Hospital. Mesenchymal stem cells were derived from the BM of lymphoma patients without BM invasion, because marrow mesenchymal stem cells in this type of patients can be considered normal. The adipogenic induction of mesenchymal stem cells is described in the *Online Supplementary Methods*.

Chromatin immunoprecipitation-quantitative polymerase chain reaction

Adipocytes were collected from different groups and crosslinked with 1% formaldehyde for 10 min at 37°C. Cross-linking was blocked, then the cells were washed and lysed in sodium dodecylsulfate lysis buffer (50 mM HEPE NaOH 7.5, 500 mM NaCl, 1 mM EDTA, 0.1% Na-deoxycholate, 1% Triton X100). The lysates were sonicated to shear DNA to a length between 200 and 500 base pairs with 10-second pulses using sonication. The antibody against FOXC1 (5 μL, Abcam5079, USA) was then added to the supernatant, incubated overnight at 4°C with rotation and incubated with 100 μL Salmon Sperm DNA/Protein A agarose beads for 2 h at 4°C. The immunoprecipitated complex was then washed and eluted. The histone DNA crosslinks were reversed and DNA was purified for real-time polymerase chain reaction (PCR). Quantitative real-time PCR (RT-qPCR) was performed on bound and input DNA with the following primers for TRPV4: forward: 5-CTTTGCACTGGGGAGCA-GAGT-3, reverse: 5-ATTAACCG TGGGCTTCAGGCA-3.

Cell cultures and reagents

The cell cultures and reagents, as well as the co-culture assays are described in detail in the *Online Supplementary Methods*.

Animal experiments

All animal experiments were performed according to procedures approved by the Ethics Committee of Shanghai Jiao Tong University Affiliated Hospital. Five-week old C57BL/6 mice were fed with 60% high-fat diet (Research Diets, Inc. New Brunswick, NJ, USA) for 3 months to create an obese mouse model. Mice injected with FBL-3 cells (5×10^5) and mice injected with both FBL-3 cells (5×10^5) and 4α-phorbol 12,13-didecanoate (4αPDD) (200 μg/Kg according to the instructions for reagents) were used as experimental groups. The untreated obese mice were used as a control group. The volume of all solutions injected was 200 μL. Mice were sacrificed and femora were removed after 3 weeks of treatment. Femora were fixed for 24 h with 4% paraformaldehyde and were decalcified for 2 days. BM sections from the mice were dewaxed by conventional methods and incubated with anti-perilipin1 monoclonal antibody (1:50, CST, USA) at 4°C overnight.

Other experimental details

Full descriptions of free fatty acid detection, lentiviral knock-down, RNA sequencing, western blot analysis and enzyme-linked immunosorbent assays, RT-qPCR (primers shown in Table 1), the cell counting and apoptosis assays, oil red O staining, immunofluorescence studies, and adipocyte measurements are provided in the *Online Supplementary Methods*.

Statistical analysis

All statistical tests were performed with GraphPad Primer5. The data are presented as the mean ± standard deviation. A Student *t*-test was used for comparisons between two groups. A *P* value of less than 0.05 was considered statistically significant.

Results

Downregulated TRPV4 contributes to increased bone marrow adipocyte lipolysis

As an important channel for calcium ions, TRPV plays a critical role in the energy balance of adipocytes. RT-qPCR analysis showed that *TRPV4* mRNA in BM adipocytes had the highest expression among TRPV family members (Figure 1A). Moreover, western blot analysis showed that BM adipocytes expressed TRPV4 protein highly (Figure 1B). To investigate whether TRPV4 plays an important role in BM adipocytes, we used TRPV4 inhibitor (RN1734) and agonist (4αPDD) to verify the
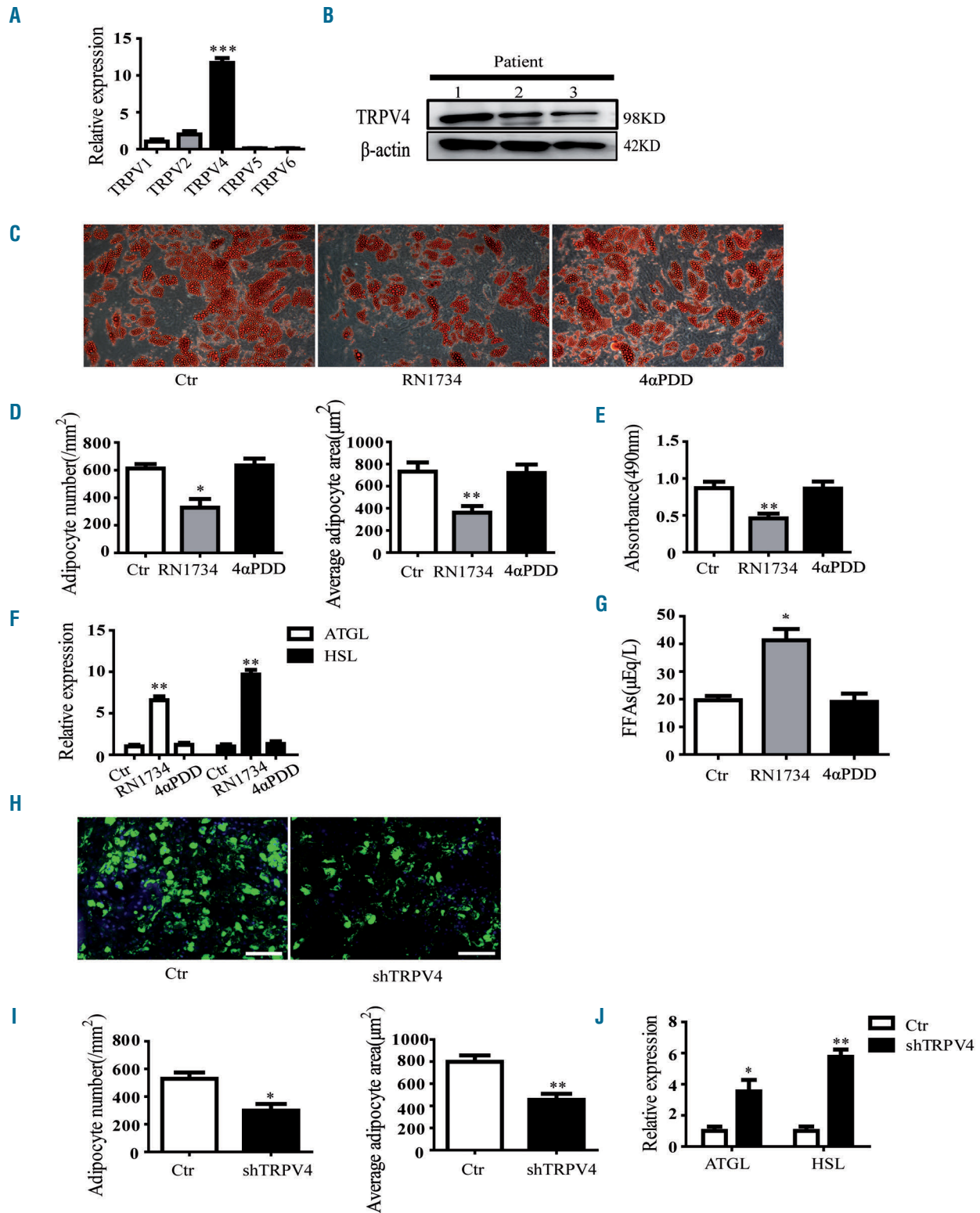
Figure 1. Downregulated TRPV4 contributes to increased bone marrow adipocyte lipolysis. (A) Reverse transcriptase quantitative polymerase chain reaction (RT-qPCR) verification of the expression of transient receptor potential vanilloid (*TRPV*) channel genes in bone marrow (BM) adipocytes. (B) Western blot analysis of TRPV4 protein in BM adipocytes from three patients. (C) BM adipocytes treated with dimethylsulfoxide (Ctr), RN1734 (5 μM) or 4α-phorbol 12,13-didecanoate (4αPDD, 0.25 μg/mL) for 4 days. Adipocytes were stained by oil red O (ORO). All images were at a magnification of 200×. (D) The number and average area of BM adipocytes from the indicated groups were measured using Image-Pro-Plus 5.1. (E) The content of lipid droplets in BM adipocytes from the indicated groups was detected by optical density values after ORO staining. (F) RT-qPCR was used to analyze adipose triglyceride lipase (*ATGL*) and hormone-sensitive triglyceride lipase (*HSL*) mRNA in BM adipocytes from the indicated groups. (G) The content of free fatty acids (FFA) in the supernatant of BM adipocytes treated with dimethylsulfoxide (Ctr), RN1734 or 4αPDD was detected using the colorimetric method. (H) BM adipocytes were infected with TRPV4-targeted shRNA (shTRPV4) lentivirus for 6 days. Adipocytes were stained with Alexa Fluor 493/503-conjugated BODIPY. 4′,6-diamidino-2-phenylindole (DAPI) stained blue and lipid droplets showed green fluorescence. The scale bar represents 50 μm. (I) The number and area of BM adipocytes infected with shTRPV4 lentivirus, quantitatively analyzed by Image-Pro-Plus 5.1. (J) The mRNA level of *HSL* and *ATGL* in BM adipocytes infected with shTRPV4 lentivirus on the fourth day, detected by RT-qPCR. β-actin protein was used as an internal control for the western blot analysis. Three independent experiments were performed. ***$P<0.001$, **$P<0.01$, *$P<0.05$.

function of TRPV4 in BM adipocytes, respectively. 4αPDD is the first synthetic TRPV4 agonist and is a non-protein kinase C activated phorbol ester.[20] *Online Supplementary Figure S1A* shows the half maximal inhibitory concentration (IC_{50}) of the effects of RN1734 on BM adipocytes. Considering excessive Ca^{2+} influx could cause some toxicity to adipocytes,[21] we aimed to find a concentration that has minimum cellular toxicity and promotes the Ca^{2+} influx needed for our experiments. As *Online Supplementary Figure S1B* shows, 4αPDD at a concentration of 0.25 μg/mL resulted in an acceptable level of toxicity of adipocytes, while allowing Ca^{2+} influx to reach the level required for the experiment. Oil red O staining and quantitative analysis showed that RN1734 reduced the number and area of BM adipocytes, whereas 4αPDD did not induce a similar change (Figure 1C, D), suggesting that the inhibition of TRPV4 contributes to reducing BM adipocyte number and size. Furthermore, optical density value measurements showed that lipid droplets in BM adipocytes treated with RN1734 decreased significantly (Figure 1E).

In order to determine whether the phenomenon is related to lipolysis, we determined the rate-limiting enzymes (adipose triglyceride lipase, ATGL and hormone sensitive lipase, HSL) of lipolysis.[22] ATGL catalyzes the first step of lipolysis and converts triglyceride to diacylglycerol and free fatty acids.[23] HSL is a hydrolase of glycerides and cholesterol esters.[24] Along with TRPV4 channel inhibition, BM adipocytes subsequently exhibited increased expression of *ATGL* and *HSL*, which resulted in increased free fatty acids in the supernatant (Figure 1F, G). Furthermore, it was found that RN1734 could significantly inhibit Ca^{2+} influx in BM adipocytes, while 4αPDD promoted Ca^{2+} influx in BM adipocytes (*Online Supplementary Figure S1C*). However, 4αPDD activates calcium channels in BM adipocytes by promoting Ca^{2+}

influx, while the expression of TRPV4 could not increase (*Online Supplementary Figure S2A*).

To further confirm that TRPV4 regulates lipolysis of BM adipocytes, we used shTRPV4 lentivirus to knock down TRPV4 (*Online Supplementary Figure S2B, C*). As shown in Figure 1H, I and *Online Supplementary Figure S2D*, quantitative analysis showed that the number (control *vs*. shTRPV4, 528.1±46.4/mm², *vs*. 298.9±48.3/mm², *P*<0.05) and area (control *vs*. shTRPV4, 798.7±57.5 μm² *vs*. 454.7±54.0 μm², *P*<0.01) of BM adipocytes decreased in TRPV4 knockdown samples. *ATGL* and *HSL* mRNA levels were also increased in TRPV4 knockdown adipocytes (Figure 1J). These data indicate a critical role for TRPV4 in the regulation of lipolysis in BM adipocytes.

TRPV4 mediates GDF15-induced bone marrow adipocyte remodeling

Increased lipolysis can result in a decrease in the number and area of BM adipocytes. Therefore, lipolysis is also a form of adipocyte remodeling. Our previous studies found that GDF15 secreted by leukemia cells promoted BM adipocyte lipolysis, decreasing the number and area of BM adipocytes.[5,12] As shown by western blot analysis, TRPV4 expression was inhibited in BM adipocytes when co-cultured with leukemia cell lines (THP-1, K562, HL-60), whereas anti-GDF15 neutralizing antibodies partly reversed the effect (Figure 2A). Given the above results, we added recombinant human GDF15 (rhGDF15) to BM adipocytes to clarify this effect. It was shown that the inhibitory effect on TRPV4 was enhanced with the increase of rhGDF15 concentration and treatment duration (Figure 2B, C). Moreover, rhGDF15 could significantly inhibit *TRPV4* mRNA expression and increase pHSL protein expression on the fourth day (Figure 2C and *Online Supplementary Figure S2E*). However, the pHSL protein and the release of free fatty acids did not increase sig-

Table 1. Sequences of the primers used to detect gene expression by reverse transcriptase quantitative polymerase chain reaction.

Species	Name	Forward	Reverse
human	GAPDH	CGGAGTCAACGGATTTGGTCGTAT	AGCCTTCTCCATGGTGGTGAAGAC
human	TRPV1	CAGGCTCTATGATCGCAGGAG	TTTGAACTCGTTGTCTGTGAGG
human	TRPV4	CGTCCAAACCTGCGAATGAAGTTC	CCTCCATCTCTTGTTGTCACTG
human	TRPV5	GGTTTTCTACCTAAGGCAGAAGG	CTCGAAGCAGTGGAGACTCT
human	TRPV6	ACTGACCTCGACTCTCTATGAC	GTGGTGATGATAAGTTCCAGCAG
human	ALK4	GCCATGGGAAGTTGTAATGG	GTCCAGGTGCCATTATTCAG
human	ACVR2	GCCACCCTATTACAACATCCTG	GGTCCTGGGTCTTGAGTTG
human	TGFβRI	GAAGAGGACCCTTCATTAG	TGCCTCACGGAACCACGAACG
human	TGFβRII	CAACAACATCAACCACAACA	TTATAGACCTCAGCAAAGCG
human	GFRAL	ATGGATTCAAAGGGATGTG	TGATAGAAGAACCGTATGGC
human	ATGL	GCGTGTCAGACGGCGAGAATG	GCAGCTCGTGGATGTTGGTGG
human	HSL	CACTACAAACGCAACGAGAC	CCAGAGACGATAGCACTTCC
human	FOXC1	TAAGCCCATGAATCAGCCG	GCCGCACAGTCCCATCTCT
human	Cav1.3	CTTCCTCTTCATCATCATCTTC	TCATACATCACCGCATTCC
human	Cav3.1	CCACGTGGTCCTTGTCATCA	GGGTCAGGAAGATGCGTTCA
human	Cav3.2	TCGAGGAGGACTTCCACAAG	TGCATCCAGGAATGGTGAG
human	Cav3.3	AGGATGAGCTATGACCAGCG	CAGAGAGCAGGGACTCATGC

GAPDH: glyceraldehyde 3-phosphate dehydrogenase; TRPV: transient receptor potential vanilloid; ALK4: activin A receptor type 1B; ACVR2: activin receptor type 2; TGFβRII: transforming growth factor-β type II receptor; TGFβRI: transforming growth factor-β type I receptor; GFRAL: GDNF family receptor α-like; ATGL: adipose triglyceride lipase; HSL: hormone-sensitive triglyceride lipase; FOXC1: Forkhead box C1; Cav1.3: calcium voltage-gated channel subunit alpha1 C; Cav3.1: calcium voltage-gated channel subunit alpha1 G; Cav3.2: calcium voltage-gated channel subunit alpha1 H; Cav3.1: calcium voltage-gated channel subunit alpha1 I.
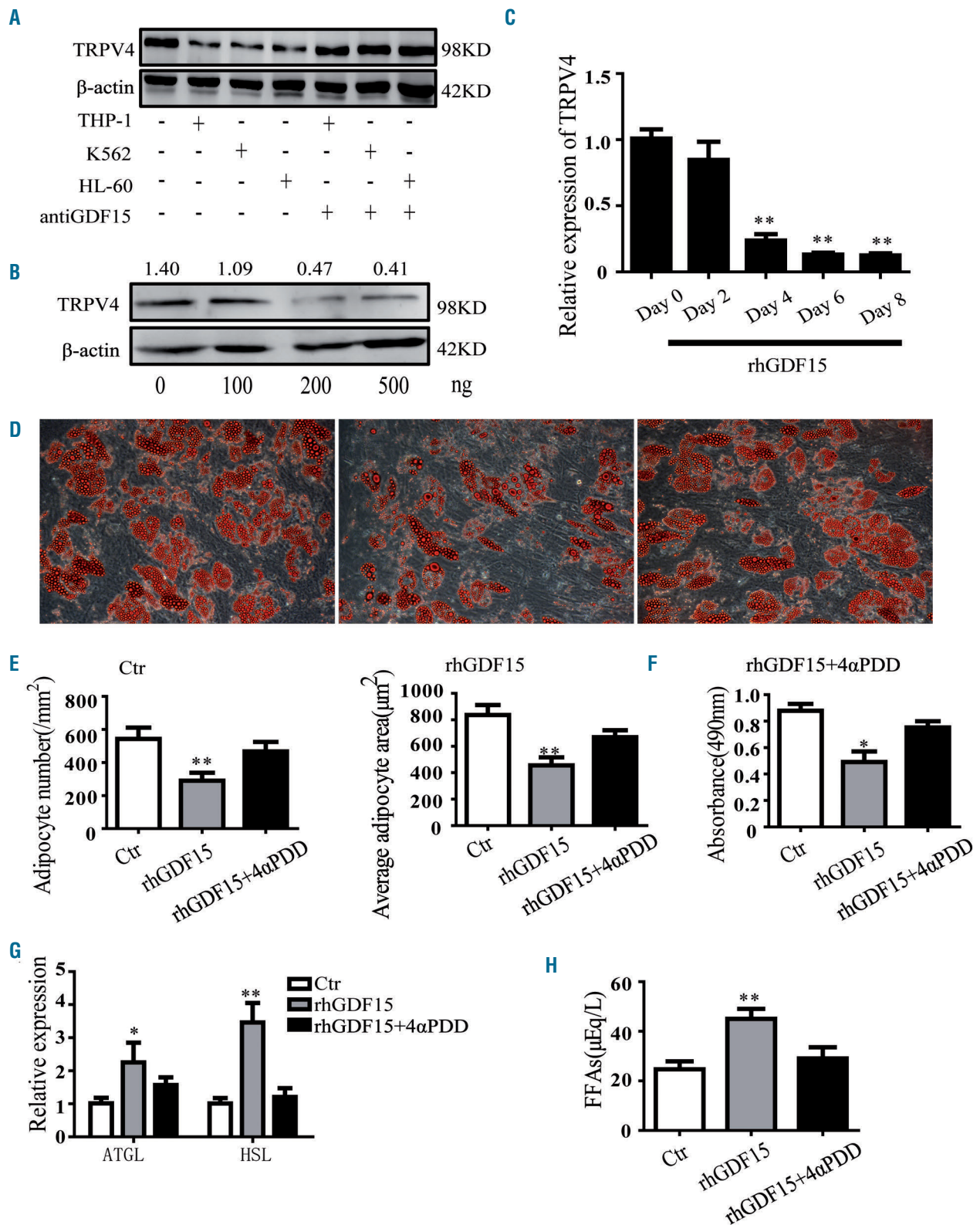
Figure 2. TRPV4 mediates GDF15-induced bone marrow adipocyte remodeling. (A) Bone marrow (BM) adipocytes were co-cultured with leukemia cell lines (THP-1, K562, HL-60) or leukemia cells and anti-GDF15 neutralizing antibody (200 ng/mL) for 4 days. The protein of TRPV4 was detected using western blot analysis. (B) The effect of different concentrations (100 ng, 200 ng, 500 ng) of recombinant human GDF15 (rhGDF15) on the expression of TRPV4 protein for 4 days was analyzed by western blot. (C) Reverse transcriptase quantitative polymerase chain reaction (RT-qPCR) was performed to analyze the expression of *TRPV4* mRNA after the addition of 200 ng rhGDF15 in BM adipocytes for 2, 4, 6, 8 days. (D) BM adipocytes were treated with dimethylsulfoxide (Ctr), rhGDF15 (200 ng/mL) or rhGDF15 (200 ng/mL) and 4α-phorbol 12,13-didecanoate (4αPDD, 0.25 μg/mL) for 6 days. Adipocytes were stained by oil red O. All images were at a magnification of 200×. (E) The number and average area of adipocytes from the indicated groups were measured using Image-Pro-Plus 5.1. (F) The content of lipid droplets in the indicated groups was detected by optical density values. (G) RT-qPCR was used to analyze *HSL* and *ATGL* mRNA in adipocytes from the indicated groups on the fourth day. (H) The content of free fatty acids in the supernatant of BM adipocytes from each group was detected using a colorimetric method. β-actin protein was used as an internal control for the western blot analysis. Three independent experiments were performed. **$P<0.01$, *$P<0.05$.

nificantly after BM adipocytes were treated with rhGDF15 for 1 h (*Online Supplementary Figure S2F, G*), suggesting that the role of GDF15 in promoting lipolysis may be different from the rapid action of β-adrenaline.[25] Oil red O staining and quantitative analysis showed that the number and area of adipocytes did not change significantly on the fourth day, but decreased significantly from the sixth day (*Online Supplementary Figure S2H, I*). These results indicate that TRPV4 regulates the remodeling of BM adipocytes.

To further explore the potential role of TRPV4 in GDF15-induced BM adipocyte remodeling, oil red O staining and quantitative analysis was conducted and showed that the number and area of BM adipocytes were decreased in BM adipocytes treated with rhGDF15, whereas 4αPDD partly reversed the effect of rhGDF15 (Figure 2D, E). Optical density value measurements of lipid droplets showed similar results (Figure 2F). Accordingly, rhGDF15 could induce increased expression of lipolysis genes (*ATGL* and *HSL*) and increased release of free fatty acids from BM adipocytes, but activation of TRPV4 by 4αPDD partly reversed the effect of rhGDF15 (Figure 2G, H). Furthermore, rhGDF15 can inhibit Ca^{2+} influx in BM adipocytes (*Online Supplementary Figure S3A*). These findings strongly suggest that TRPV4 contributes to GDF15-induced remodeling of BM adipocytes. Although GDF15 has been reported to act on Cav1.3, Cav3.1, Cav3.2, Cav3.3,[13,26] the expression of these channels in BM adipocytes is much lower than that of TRPV4 (*Online Supplementary Figure S3B*). Moreover, when BM adipocytes were co-cultured with leukemia cell lines (THP-1, K562, HL-60), the expression of *TRPV4* changed significantly (*Online Supplementary Figure S3C*). These results further suggest that TRPV4 may play an important role in GDF15-induced remodeling of BM adipocytes.

GDF15 activates the downstream genes PI3K and pAKT in bone marrow adipocyte remodeling

Extracellular GDF15 must bind to a receptor on the membrane surface to cause intracellular changes in BM adipocytes. We screened all of the reported GDF15 receptors by RT-qPCR and found that BM adipocytes mainly express TGFβRI and TGFβRII (Figure 3A). In order to determine whether GDF15 acts through binding to TGFβRI or TGFβRII on BM adipocytes, we conducted inhibitor experiments *in vitro*.[27,28] Western blot results showed that rhGDF15 could downregulate TRPV4 expression in BM adipocytes treated with RepSox (a TGFβRI inhibitor) rather than ITD1 (a TGFβRII inhibitor) (Figure 3B). Moreover, we found that rhGDF15 could reduce the number and area of BM adipocytes treated with RepSox as compared to those treated with ITD1 (Figure 3C, D). In accordance with data from RT-qPCR experiments, the levels of expression of lipolysis genes (*ATGL* and *HSL*) were significantly elevated in BM adipocytes treated with RepSox compared with the levels in BM adipocytes treated with ITD1 (*Online Supplementary Figure S3D*). These results suggest that TGFβRII is the major receptor that mediates GDF15 action on BM adipocytes.

To further verify the function of TGFβRII on BM adipocytes, we knocked down TGFβRII expression by shTGFβRII lentivirus (*Online Supplementary Figure S4A, B*). As shown in Figure 3E and F, when TGFβRII was knocked down in BM adipocytes, rhGDF15 did not significantly

reduce the number and area of BM adipocytes. Accordingly, rhGDF15 did not significantly reduce the TRPV4 protein (Figure 3G). These results further confirmed that GDF15 regulates BM adipocyte remodeling by binding to TGFβRII.

As an important signaling downstream pathway of the TGFβ family, GDF15 could not cause significant changes in Smad2 and Smad4 proteins in BM adipocytes (Figure 3H and *Online Supplementary Figure S4C*). Notably, when PI3K was blocked by PI3K-IN-1 (a PI3K inhibitor), rhGDF15 could not regulate AKT phosphorylation (Figure 3I), suggesting that GDF15 is involved in the remodeling of BM adipocytes by activating the PI3K/AKT pathway.

The PI3K/AKT pathway inhibits the TRPV4 promoter FOXC1

PI3K/AKT acts as a signaling pathway downstream of GDF15, which may affect the transcription or translation of TRPV4. We compared the expression of different transcription factors with or without rhGDF15 treatment by RNA-sequencing analysis. The results showed that the expression of several transcription factors decreased, including FOXC1, Spalt-like gene-2 (SALL2), and MYC associated factor X (MAX) (Figure 4A). Based on the criteria of a fold-change >2.0 and *P*-value <0.05, FOXC1 was identified as a transcription factor that was significantly changed in BM adipocytes after rhGDF15 treatment (Figure 4B). To investigate whether FOXC1 is responsible for GDF15 regulating TRPV4, we knocked down FOXC1 in BM adipocytes (*Online Supplementary Figure S4D, E*). The results showed that the expression of TRPV4 at both the mRNA and protein levels was inhibited in FOXC1 knockdown adipocytes (Figure 4C, D), suggesting that GDF15 reduced the expression of TRPV4 by negatively regulating the transcription factor FOXC1.

To further demonstrate the link between FOXC1 and TRPV4, we used a FOXC1 antibody to pull DNA fragments containing FOXC1 and used RT-qPCR to detect the *TRPV4* gene in the fragment. The results showed that the control group had the sequence of the *TRPV4* gene and the amount of *TRPV4* gene was correspondingly decreased after knocking down FOXC1 (Figure 4E). These data suggest that FOXC1 combines directly with TRPV4. As shown in Figure 4F, rhGDF15 downregulated the expression of FOXC1 and TRPV4 protein, but PI3K-IN-1 can block this process. Taken together, these results again demonstrate that GDF15 regulates TRPV4 channels through the PI3K/AKT pathway.

TRPV4 plays an important role in bone marrow adipocyte remodeling in acute myeloid leukemia mice

To better understand the role of TRPV4 in leukemia cell-induced BM adipocyte remodeling, we investigated the changes in number and size of BM adipocytes with 4αPDD in mice with leukemia. FBL-3 is a mouse-derived AML cell line, which can spontaneously induce leukemia. We first confirmed that FBL-3 cells secrete GDF15 (*Online Supplementary Figure S5A*). *In vitro*, FBL-3 cells co-cultured with BM adipocytes inhibited the expression of TRPV4 protein (*Online Supplementary Figure S5B*). *Online Supplementary Figure S5C, D* shows that FBL-3 cells reduced the number and area of BM adipocytes, while 4αPDD could partly reverse this effect. Correspondingly, FBL-3 cells significantly promoted the expression of *ATGL* and *HSL* mRNA in BM adipocytes, but 4αPDD
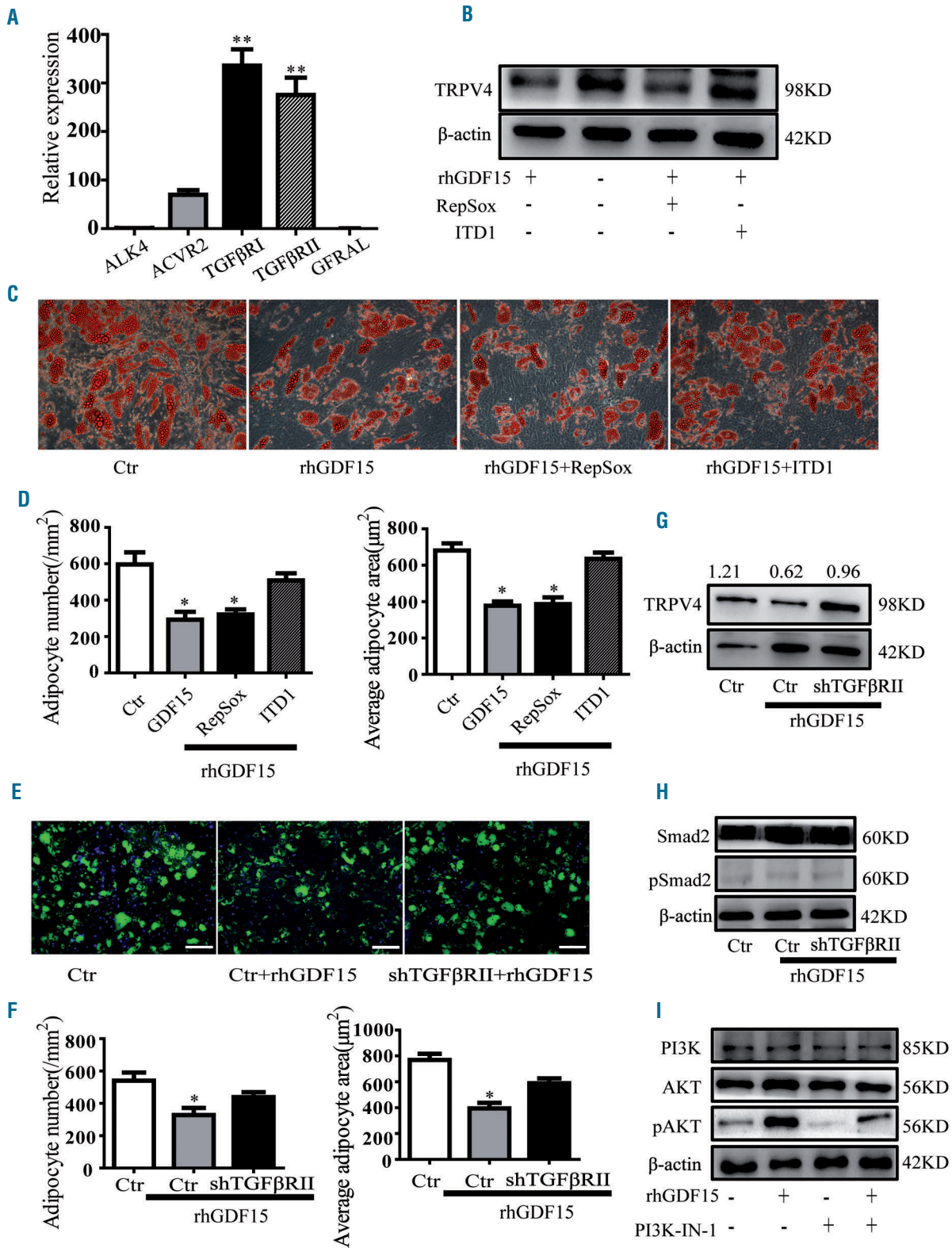
Figure 3. GDF15 activates the downstream genes PI3K and pAKT in bone marrow adipocyte remodeling. (A) Reverse transcriptase quantitative polymerase chain reaction (RT-qPCR) analysis of GDF15-related receptors in bone marrow (BM) adipocytes. (B) Western blot analysis of the expression of TRPV4 protein in BM adipocytes induced by recombinant human GDF15 (rhGDF15) after treatment with TGFβRI inhibitor (RepSox) or TGFβRII inhibitor (ITD1) for 4 days. (C) Oil red O staining analysis of BM adipocytes induced by rhGDF15 after treatment with RepSox and ITD1 for 6 days. All images were at a magnification of 200×. (D) The number and average area of BM adipocytes from the indicated groups were measured using Image-Pro-Plus 5.1. (E, F) BM adipocytes were infected with TGFβRII-targeted shRNA (shTGFβRII) lentivirus for 48 and then cultured with rhGDF15 for 6 days. Adipocytes were stained with Alexa Fluor 493/503-conjugated BODIPY. 4′,6-diamidino-2-phenylindole (DAPI) stained blue and lipid droplets showed green fluorescence. The number and average area of adipocytes from the indicated groups were measured using Image-Pro-Plus 5.1. The scale bar represents 50 μm. (G, H) BM adipocytes were infected with shTGFβRII lentivirus for 48 h and then cultured with rhGDF15 for 4 days. The levels of TRPV4, Smad2 and pSmad2 proteins were detected using western blot analysis. (I) BM adipocytes were treated with or without rhGDF15 and PI3K inhibitor (PI3K-IN-1, 2 μM) for 4 days. The levels of PI3K, AKT and pAKT proteins were detected using western blot analysis. β-actin protein was used as an internal control for the western blot analysis. Three independent experiments were performed. **$P<0.01$, *$P<0.05$.

could partly prevent this process (*Online Supplementary Figure S5E*). Additionally, 4αPDD had no significant effect on the proliferation and apoptosis of FBL-3 cells, as determined by a CCK8 assay (*Online Supplementary Figure S5F*)

and flow cytometry analysis (*Online Supplementary Figure S5G*). Thus, these results suggest that this dose of 4αPDD affects adipocytes, rather than directly affecting FBL-3 cells in the co-culture system.
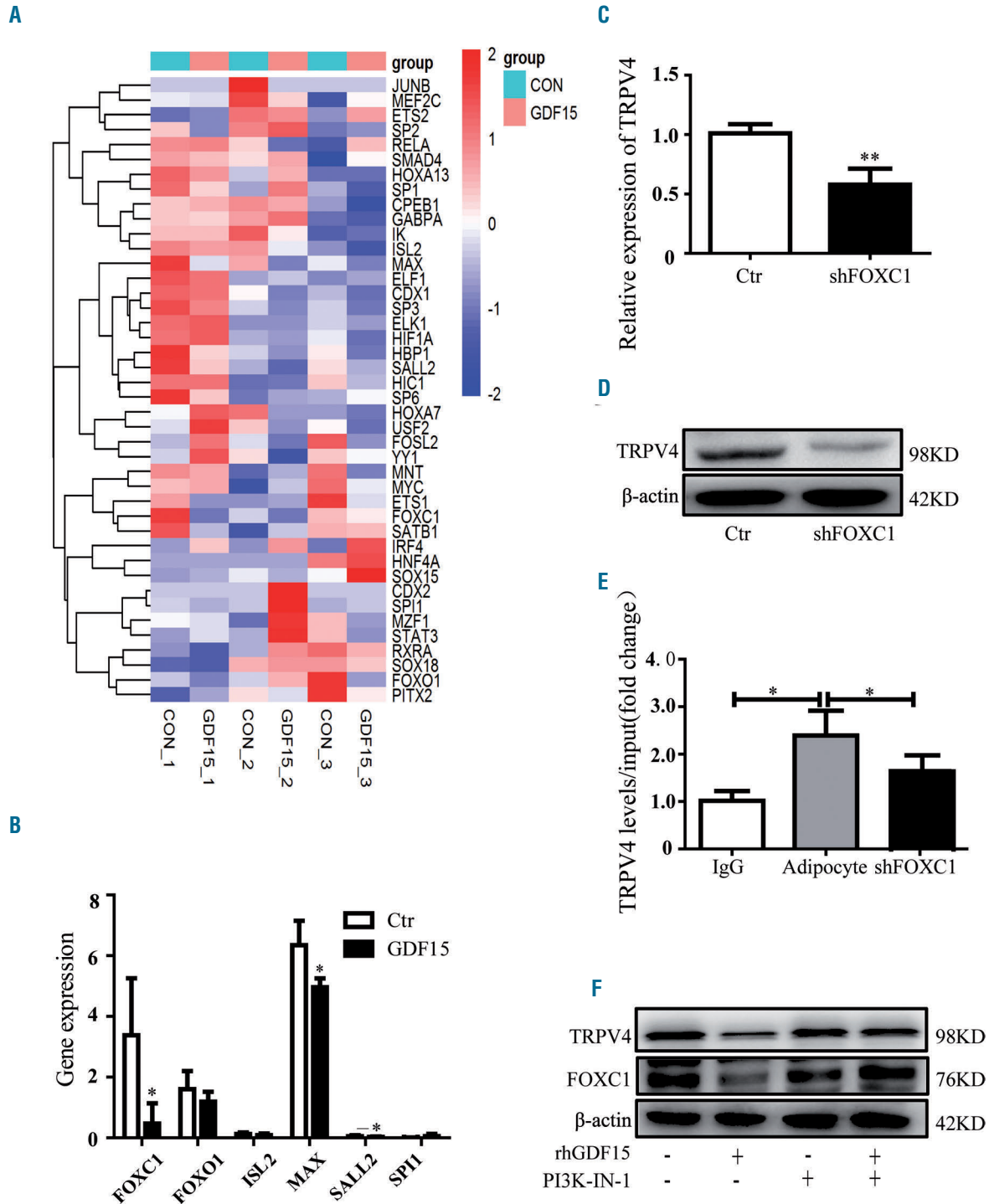
Figure 4. The PI3K/AKT pathway inhibits the TRPV4 promoter FOXC1. (A) Analysis of TRPV4 upstream transcription factor expression of bone marrow (BM) adipocytes treated with or without recombinant human GDF15 (rhGDF15) for 2 days by RNA sequencing). (B) Different expression of TRPV4-related transcription factor genes following rhGDF15 treatment for 2 days. (C) Reverse transcriptase quantitative polymerase chain reaction (RT-qPCR) was used to analyze *TRPV4* mRNA level after treatment with FOXC1-targeted shRNA (shFOXC1) lentivirus for 48 h. (D) Western blot was used to analyze the expression of TRPV4 protein after treatment with shFOXC1 lentivirus for 48 h. (E) Chromatin immunoprecipitation-qPCR analysis of TRPV4 gene level in adipocytes with or without FOXC1 knockdown. (F) BM adipocytes were treated with or without rhGDF15 and PI3K inhibitor (PI3K-IN-1, 2 μM) for 4 days. The levels of FOXC1 and TRPV4 proteins were determined using western blot analysis. β-actin protein was used as an internal control for the western blot analysis. Three independent experiments were performed. **$P<0.01$, *$P<0.05$.

Considering that there were few adipocytes in the BM of C57BL/6 mice, we raised the mice with a high-fat diet to increase the number of adipocytes in the BM. BM adipocytes in obese mice are round or elliptical in shape

(Figure 5A). Immunohistochemical staining of perilipin1 protein in the BM adipocytes showed that the BM adipocytes stained yellow (Figure 5A). According to the pathogenic characteristics of FBL-3 cells,[29] BM samples
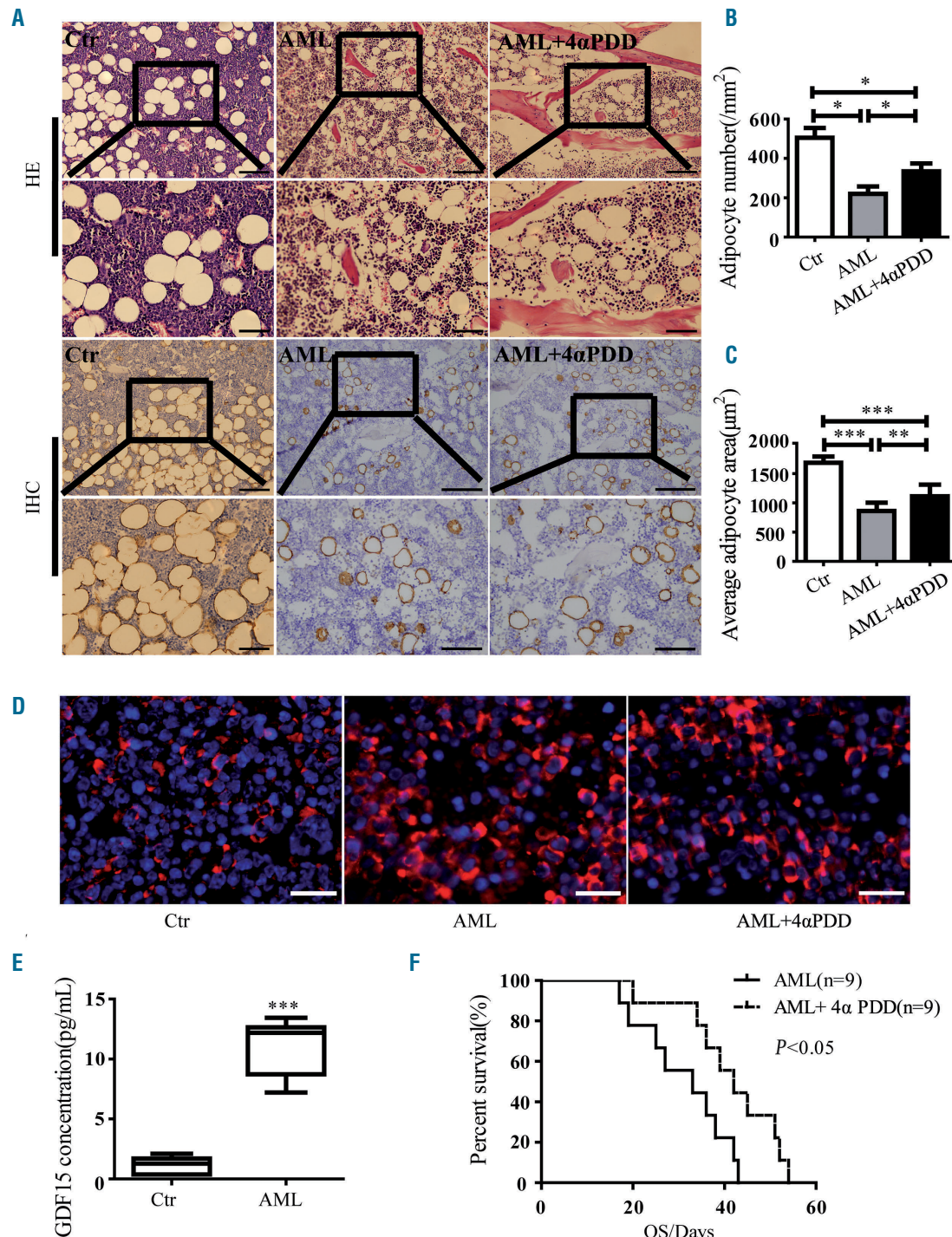
Figure 5. TRPV4 plays an important role in bone adipocyte remodeling in acute myeloid leukemia mice. (A) Hematoxylin & eosin staining and immunohistochemical staining with perilipin1 antibody in bone marrow (BM) sections from the controls (Ctr, n=5) and experimental mice, (mice with acute myeloid leukemia [AML], n=5; AML mice treated with 4α-phorbol 12,13-didecanoate [4αPDD], n=5). Ten fields were analyzed for each mouse at 400× magnification. Three independent experiments were performed. Scale bars represent 50 μm and 100 μm, respectively. (B, C) Adipocyte number and area in the controls, AML mice and AML mice treated with 4αPDD, quantitatively analyzed by Image-Pro-Plus 5.1. (D) Immunofluorescence was used to analyze the expression of CD117 in BM sections of the controls, AML mice and AML mice treated with 4αPDD. 4′,6-diamidino-2-phenylindole (DAPI) stained blue and CD117 showed red fluorescence. Scale bars represent 100 μm. (E) The GDF15 content of the BM supernatant in the controls and AML mice was analyzed by enzyme-linked immunosorbent assay. (F) Kaplan-Meier curves showing the overall survival rate of AML mice (n=9) and AML mice treated with 4αPDD (n=9). Three independent experiments were performed. ***$P<0.001$, **$P<0.01$, *$P<0.05$.

were taken 21 days after tail vein injection of FBL-3 cells. The shape of BM adipocytes did not change significantly, but the number and area decreased (Figure 5A). Further quantitative analysis showed that the number of BM adipocytes in AML mice (219±37.7/mm²) was lower than that in the controls (505±49.7/mm²) and AML mice treated with 4αPDD (334.4±39.6/mm²), but the number of BM adipocytes in AML mice treated with 4αPDD was still lower than that in the controls (the *t*-test for any two groups: *P*<0.05) (Figure 5B). Similarly, the BM adipocyte area in mice with leukemia was 860.0±142.5 μm², which was smaller than that in the controls (1686.4±106.7 μm², *P*<0.001). Meanwhile, the area of BM adipocytes in AML mice treated with 4αPDD was 1111.8±201.5 μm², which was larger than that of the BM adipocytes in AML mice (*P*<0.01), and did not return to normal (*P*<0.001) (Figure 5C).

We further found that there were more CD117 (a progenitor cell expression marker, red fluorescence)-positive cells in AML mice than in the AML mice treated with 4αPDD (Figure 5D). This may be due to the fact that GDF15 secreted by AML cells promotes lipolysis and is beneficial to the proliferation of leukemia cells, while 4αPDD partly prevents lipolysis. In fact, the content of GDF15 in the BM supernatant was higher in AML mice than in the controls (Figure 5E), suggesting that GDF15 secreted by leukemia cells can promote lipolysis of BM adipocytes. Furthermore, we observed that treatment with 4αPDD significantly extended overall survival of AML mice (Figure 5F). In brief, these results suggest that targeting TRPV4 in BM adipocytes can delay the progression of leukemia in mice.

Discussion

We have demonstrated a possible mechanism whereby TRPV4 mediates BM adipocyte responses to extracellular GDF15. Our data show that AML cells drive this remodeling process, at least in part, through TRPV4-dependent lipolysis in the adipocytes. Our previous reports linked increased levels of small adipocytes in BM to poor prognosis in AML patients, and revealed that GDF15 derived from leukemia cells remodels mature BM adipocytes into small adipocytes.[5,12] Here, we found that GDF15 binds to its receptor TGFβRII on BM adipocytes, which in turn activates downstream target genes, including *PI3K* and *AKT*. Subsequently, TRPV4 is inhibited *via* downregulation of its transcription factor FOXC1. These results suggest that GDF15 regulates TRPV4 through the above pathway, thereby promoting BM adipocyte remodeling (*Online Supplementary Figure S6*). This finding is consistent with several reports that TRPV4 acts as a volume receptor rather than an osmotic receptor.[30-32]

There has been a report that TRPV4 is located on the cell membrane and acts as a calcium channel.[33] Therefore, TRPV4 can regulate energy metabolism of peripheral white adipocytes by facilitating Ca²⁺ influx, which in turn stimulates the ERK1/2-dependent pathway.[34] GDF15 inhibits the expression of TRPV4 in BM adipocytes, resulting in a decrease of Ca²⁺ influx (*Online Supplementary Figure S3A*) and an increase in pHSL protein (*Online Supplementary Figure S2E*) after BM adipocytes were treated with rhGDF15 for 4 days. It has been reported that reduced Ca²⁺ influx causes an increase in the expression of

pHSL, leading to lipolysis of adipocytes.[17] Notably, the TRPV4 channel is a tetrameric complex formed by the same or similar monomeric subunits.[35] Interestingly, cytosolic N- and C-terminal domains are involved in channel gating and mediating intracellular signaling,[35,36] indicating that it is impossible for TRPV4 to interact directly with exogenous chemical factors. Hence, it would be interesting to examine how TRPV4 communicates with extracellular GDF15.

Given our findings that extracellular GDF15 inhibited the expression of TRPV4 in BM adipocytes, we speculated that GDF15 acts on BM adipocytes through TGFβ receptors. As a member of the TGFβ superfamily, GDF15 is known to interact with receptors of TGFβ members, such as TGFβRI, TGFβRII, ALK4 and ACVR2.[37-39] In addition, GDF15 has unique cognate receptors, such as GFRAL, which is mainly expressed in the central nervous system and, at low levels, in testicular tissue.[39] Our data show that BM adipocytes express TGFβ receptors, but not the known unique GDF15 receptors. Moreover, TGFβRII was shown to be associated with GDF15 activity on BM adipocytes (Figure 3B-G). These experiments inform the first step of GDF15 acting on the adipocytes.

Our study further revealed that PI3K/AKT activation plays an essential role in driving GDF15 regulation of target genes in BM adipocytes. In fact, GDF15 induced the activation of Smad, a component of the classic anti-apoptosis pathway of cardiomyocytes which promotes the progression of lung cancer.[40,41] However, we did not focus on the Smad pathway in this study because the activated Smad protein type is known to be determined by the TGFβRI present in the ligand-bound signal complex.[42] In fact, GDF15 did not affect the Smad signaling pathway in BM adipocytes, which is consistent with our results (Figure 3H and *Online Supplementary Figure S4C*). Taken together, our data, when interpreted in the context of previous reports, suggest that the PI3K/AKT pathway may be important for GDF15-induced remodeling of BM adipocytes.

Interestingly, we observed that PI3K/AKT activation downregulated the TRPV4-associated transcription factor FOXC1. FOXC1 is also a transcription factor of ITGA7 and FGFR4 in colorectal cancer, CXCR4 in endothelial cells, and FGF19 in ciliary body-derived cells.[43-45] Moreover, the transcriptional function of FOXC1 has not been described previously for some pivotal adipogenic genes (*FABP4*, *CEBPA* and *PPARG*) and lipolytic genes (*ATGL* and *HSL*). Based on the knockdown of *FOXC1* gene, the lipolytic gene in BM adipocytes increases (*Online Supplementary Figure S4F*), which confirmed that FOXC1 is important for regulating the metabolism of BM.

In addition, TRPV4 can be activated or inhibited by physical and chemical factors. When it comes to the matter of the size of cells, TRPV4 acts as a volume receptor rather than an osmotic receptor,[30] suggesting that TRPV4 is involved in the regulation of cell volume. Previous studies have suggested that TRPV4 is an important inflammatory factor because TRPV4 levels are increased in inflamed tissues and activation of TRPV4 causes inflammation.[46] This protein is also closely related to inflammation of white adipose tissue.[33,47] However, the decreased expression of TRPV4 in leukemia-associated BM adipocytes implies that TRPV4 is not a major pro-inflammatory factor of leukemia-associated BM adipocytes. We conclude that downregulated TRPV4 preferentially pro-

motes lipolysis in BM adipocytes, contributing to their remodeling into small adipocytes in the pathogenesis of AML.

Moreover, we also found that treatment with the TRPV4 agonist 4αPDD rescued BM adipocyte remodeling, which was correlated with increased survival in AML-bearing mice, supporting a crucial role of TRPV4 in the growth and progression of AML. Although there are unstained positive white circles in the BM of AML mice (Figure 5A), we suspect that these circles may represent an increase in blood vessels or sinuses in the BM of these animals. Leukemia cells can promote angiogenesis, which in turn contributes to the proliferation of leukemia cells.[48] Of course, it cannot be excluded that a few adipocytes were not stained positively. Many studies have also reported the effect of circulating factors in obese animals on leukemia.[49,50] However, in our study, both experimental groups and control groups were obese mice, and their basic background was the same. This should, therefore, have allowed us to control for the impact of the circulating factors, which sould not have been responsible for observed differences in mouse survival and other variables. Future studies *in vivo* are needed to validate the specific modulatory role of GDF15 on TRPV4.

In conclusion, leukemia cells activate a transcriptional network that includes GDF15-related-PI3K/AKT activation and subsequent TRPV4 downregulation, which promotes BM adipocyte remodeling. The morphological adaptation of BM adipocytes and the modulation of lipolysis may represent a novel strategy for the treatment of hematologic malignancies, especially in elderly patients, whose aging and increased adiposity of the BM microenvironment reduce the efficacy of cytotoxic chemotherapy.

References

1. Asada N. Regulation of malignant hematopoiesis by bone marrow microenvironment. Front Oncol. 2018;8:119.
2. Schepers K, Campbell TB, Passegue E. Normal and leukemic stem cell niches: insights and therapeutic opportunities. Cell Stem Cell. 2015;16(3):254-267.
3. Tabe Y, Yamamoto S, Saitoh K, et al. Bone marrow adipocytes facilitate fatty acid oxidation activating AMPK and a transcriptional network supporting survival of acute monocytic leukemia cells. Cancer Res. 2017;77(6):1453-1464.
4. Lee MKS, Al-Sharea A, Dragoljevic D, Murphy AJ. Hand of FATe: lipid metabolism in hematopoietic stem cells. Curr Opin Lipidol. 2018;29(3):240-245.
5. Lu W, Weng W, Zhu Q, et al. Small bone marrow adipocytes predict poor prognosis in acute myeloid leukemia. Haematologica. 2018;103(1):e21-e24.
6. Shafat MS, Oellerich T, Mohr S, et al. Leukemic blasts program bone marrow adipocytes to generate a protumoral microenvironment. Blood. 2017;129(10):1320-1332.
7. Choe SS, Huh JY, Hwang IJ, Kim JI, Kim JB. Adipose tissue remodeling: its role in energy metabolism and metabolic disorders. Front Endocrinol (Lausanne). 2016;7:30.
8. Bochet L, Lehuede C, Dauvillier S, et al. Adipocyte-derived fibroblasts promote tumor progression and contribute to the desmoplastic reaction in breast cancer. Cancer Res. 2013;73(18):5657-5668.
9. Herroon MK, Rajagurubandara E, Hardaway AL, et al. Bone marrow adipocytes promote tumor growth in bone via FABP4-dependent mechanisms. Oncotarget. 2013;4 (11):2108-2123.
10. Dirat B, Bochet L, Dabek M, et al. Cancer-associated adipocytes exhibit an activated phenotype and contribute to breast cancer invasion. Cancer Res. 2011;71(7):2455-2465.
11. Fraczak E, Olbromski M, Piotrowska A, et al. Bone marrow adipocytes in haematological malignancies. Acta Histochem. 2018;120(1):22-27.
12. Lu W, Wan Y, Li ZQ, et al. Growth differentiation factor 15 contributes to marrow adipocyte remodeling in response to the growth of leukemic cells. J Exp Clin Cancer Res. 2018;37(1):66.
13. Lu JM, Wang CY, Hu CL, Fang YJ, Mei YA. GDF-15 enhances intracellular Ca2+ by increasing Cav1.3 expression in rat cerebellar granule neurons. Biochem J. 2016;473 (13):1895-1904.
14. Zemel M, Thompson W, Milstead A, Morris K, Campbell P. Calcium and dairy acceleration of weight and fat loss during energy restriction in obese adults. Obes Res. 2004;12(4):582-590.
15. Shi H, Dirienzo D, Zemel MB. Effects of dietary calcium on adipocyte lipid metabolism and body weight regulation in energy restricted aP2-agouti transgenic mice. FASEB J. 2001;15(2):291-293.
16. Hashimoto R, Katoh Y, Miyamoto Y, et al. High extracellular Ca2+ enhances the adipocyte accumulation of bone marrow stromal cells through a decrease in cAMP. Cell Calcium. 2017;67:74-80.
17. Xue B, Greenberg AG, Kraemer FB, Zemel MB. Mechanism of intracellular calcium ([Ca2+]i) inhibition of lipolysis in human adipocytes. FASEB J. 2001;15(13):2527-2529.
18. Kim JH,Mynatt RL, Moore JW, Woychik RP, Moustaid N, Zemel MB. The effects of calcium channel blockade on agouti-induced obesity. FASEB J. 1996;10(14):1646-1652.
19. He YH, Zhang HQ, Teng JH, Huang LN, Li Y, Sun CH. Involvement of calcium-sensing receptor in inhibition of lipolysis through intracellular cAMP and calcium pathways in human adipocytes. Biochem Biophys Res Commun. 2011;404(1):393-399.
20. Alexander R, Kerby A, Aubdool AA, et al. 4alpha-phorbol 12,13-didecanoate activates cultured mouse dorsal root ganglia neurons independently of TRPV4. Br J Pharmacol. 2013;168(3):761-772.
21. Sergeev IN, Li S, Ho CT, Rawson NE, Dushenkov S. Polymethoxyflavones activate Ca2+-dependent apoptotic targets in adipocytes. J Agric Food Chem. 2009;57(13):5771-5776.
22. Camell CD, Sander J, Spadaro O, et al. Inflammasome-driven catecholamine catabolism in macrophages blunts lipolysis during ageing. Nature. 2017;550(7674):119-123.
23. Li JY, Gong L, Liu SZ, et al. Adipose HuR protects against diet-induced obesity and insulin resistance. Nat Commun. 2019;10(1):2375.
24. Wang F, Ren XF, Chen Z, et al. The N-terminal His-tag affects the triglyceride lipase activity of hormone-sensitive lipase in testis. J Cell Biochem. 2019;120(8):13706-13716.
25. Eguchi J, Wang X, Yu ST, et al. Transcriptional control of adipose lipid handling by IRF4. Cell Metab. 2011,13(3):249-259.
26. Liu DD, Lu JM, Zhao QR, Hu CL, Mei YA. Growth differentiation factor-15 promotes glutamate release in medial prefrontal cortex of mice through upregulation of T-type calcium channels. Sci Rep. 2016;6:28653.
27. Xu MY, Pang QQ, Xu SQ, et al. Hypoxia-inducible factor-1α activates transforming growth factor-β1/Smad signaling and increases collagen deposition in dermal fibroblasts. Oncotarget. 2017;9(3):3188-3197.
28. Bansal V, De D, An J, et al. Chemical induced conversion of mouse fibroblasts and human adipose-derived stem cells into skeletal muscle-like cells. Biomaterials. 2019;193:30-46.
29. Herberman RB, Holden HT, Ting CC, Lavrin DL, Kirchner H. Cell-mediated immunity to leukemia virus- and tumor-associated antigens in mice. Cancer Res. 1976;36:615-621.
30. Toft-Bertelsen TL, Krizaj D, MacAulay N. When size matters: transient receptor potential vanilloid 4 channel as a volume-sensor rather than an osmo-sensor. J Physiol. 2017;595(11):3287-3302.
31. Rübenhagen R, Rönsch H, Jung H, Krämer R, Morbach S. Osmosensor and osmoregulator properties of the betaine carrier BetP from Corynebacterium glutamicum in proteoliposomes. J Biol Chem. 2000;275(2):735-741.
32. Heide T, Stuart MC, Poolman B. On the osmotic signal and osmosensing mechanism of an ABC transport system for glycine betaine. EMBO J. 2001;20(24):7022-7032.
33. Ramsey IS, Delling M, Clapham DE. An introduction to TRP channels. Annu Rev

Physiol. 2006;68:619-647.

34. Ye L, Kleiner S, Wu J, et al. TRPV4 is a regulator of adipose oxidative metabolism, inflammation, and energy homeostasis. Cell. 2012;51(1):96-110.

35. Venkatachalam K, Montell C. TRP channels. Annu Rev Biochem. 2007;76:387-417.

36. Taberner FJ, Fernández-Ballester G, Fernández-Carvajal A, Ferrer-Montiel A. TRP channels interaction with lipids and its implications in disease. Biochim Biophys Acta. 2015;1848(9):1818-1827.

37. Artz A, Butz S, Vestweber D. GDF-15 inhibits integrin activation and mouse neutrophil recruitment through the ALK-5/TGF-betaRII heterodimer. Blood. 2016;128(4):529-541.

38. Mullican SE, Lin-Schmidt X, Chin CN, et al. GFRAL is the receptor for GDF15 and the ligand promotes weight loss in mice and nonhuman primates. Nat Med. 2017;23(10):1150-1157.

39. Yang L, Chang CC, Sun Z, et al. GFRAL is the receptor for GDF15 and is required for the anti-obesity effects of the ligand. Nat Med. 2017;23(10):1158-1166.

40. Heger J, Schiegnitz E, von Waldthausen D, Anwar MM, Piper HM, Euler G. Growth differentiation factor 15 acts anti-apoptotic and pro-hypertrophic in adult cardiomyocytes. J Cell Physiol. 2010;224(1):120-126.

41. Lu Y, Ma J, Li Y, et al. CDP138 silencing inhibits TGF-beta/Smad signaling to impair radioresistance and metastasis via GDF15 in lung cancer. Cell Death Dis. 2017;8(9):e3036.

42. Olsen OE, Skjaervik A, Stordal BF, Sundan A, Holien T. TGF-beta contamination of purified recombinant GDF15. PLoS One. 2017;12(11)e0187349.

43. Liu J, Zhang Z, Li X, et al. Forkhead box C1 promotes colorectal cancer metastasis through transactivating ITGA7 and FGFR4 expression. Oncogene. 2018;37(41):5477-5491.

44. Hayashi H, Kume T. Forkhead transcription factors regulate expression of the chemokine receptor CXCR4 in endothelial cells and CXCL12-induced cell migration. Biochem Biophys Res Commun. 2008;367(3):584-589.

45. Tamimi Y, Skarie JM, Footz T, Berry FB, Link BA, Walter MA. FGF19 is a target for FOXC1 regulation in ciliary body-derived cells. Hum Mol Genet. 2006;15(21):3229-3240.

46. Ryskamp DA, Iuso A, Krizaj D. TRPV4 links inflammatory signaling and neuroglial swelling. Channels (Austin). 2015;9(2):70-72.

47. Sanchez JC, Rivera RA, Munoz LV. TRPV4 channels in human white adipocytes: electrophysiological characterization and regulation by insulin. J Cell Physiol. 2016;231(4):954-963.

48. Hussong JW, Rodgers GM, Shami PJ. Evidence of increased angiogenesis in patients with acute myeloid leukemia. Blood. 2000;95(1):309-313.

49. Lu Z, Xie J, Wu G, et al. Fasting selectively blocks development of acute lymphoblastic leukemia via leptin-receptor upregulation. Nat Med. 2017;23(1):79-90.

50. Yan F, Shen N, Pang JX, et al. Fatty acid-binding protein FABP4 mechanistically links obesity with aggressive AML by enhancing aberrant DNA methylation in AML cells. Leukemia. 2017;31(6):1434-1442.

Ferrata Storti Foundation

Targeting CD205 with the antibody drug conjugate MEN1309/OBT076 is an active new therapeutic strategy in lymphoma models

Eugenio Gaudio,[1*] Chiara Tarantelli,[1*] Filippo Spriano,[1] Francesca Guidetti,[1] Giulio Sartori,[1] Roberta Bordone,[2] Alberto J. Arribas,[1] Luciano Cascione,[1,3] Mario Bigioni,[4] Giuseppe Merlino,[4] Alessio Fiascarelli,[4] Alessandro Bressan,[4] Afua Adjeiwaa Mensah,[1] Gaetanina Golino,[1] Renzo Lucchini,[5] Elena Bernasconi,[1] Davide Rossi,[1,2] Emanuele Zucca,[2] Georg Stussi,[2] Anastasios Stathis,[2] Robert S. Boyd,[6] Rachel L. Dusek,[6] Arnima Bisht,[7] Nickolas Attanasio,[7] Christian Rohlff,[7] Andrea Pellacani,[8] Monica Binaschi[4] and Francesco Bertoni[1,2]

[1]Università della Svizzera italiana, Istituto Oncologico di Ricerca, Bellinzona, Switzerland; [2]Oncology Institute of Southern Switzerland, Bellinzona, Switzerland; [3]Swiss Institute of Bioinformatics (SIB), Lausanne, Switzerland; [4]Menarini Ricerche S.p.A., Pomezia, Italy; [5]Laboratorio di Diagnostica Molecolare, Dipartimento di Medicina di Laboratorio EOLAB, Bellinzona, Switzerland; [6]Oxford BioTherapeutics Ltd., Abingdon, UK; [7]Oxford BioTherapeutics Inc., San Jose, CA, USA and [8]Menarini Ricerche S.p.A - Menarini Group, Florence, Italy

*EG and CT contributed equally as co-first authors.

ABSTRACT

Antibody drug conjugates represent an important class of anti-cancer drugs in both solid tumors and hematologic cancers. Here, we report preclinical data on the anti-tumor activity of the first-in-class antibody drug conjugate MEN1309/OBT076 targeting CD205. The study included preclinical *in vitro* activity screening on a large panel of cell lines, both as single agent and in combination, and validation experiments on *in vivo* models. CD205 was first shown frequently expressed in lymphomas, leukemias and multiple myeloma by immunohistochemistry on tissue microarrays. Anti-tumor activity of MEN1309/OBT076 as single agent was then shown across 42 B-cell lymphoma cell lines with a median IC_{50} of 200 pM and induction of apoptosis in 25 of 42 (59.5%) of the cases. The activity appeared highly correlated with its target expression. After *in vivo* validation as the single agent, the antibody drug conjugate synergized with the BCL2 inhibitor venetoclax and the anti-CD20 monoclonal antibody rituximab. The first-in-class antibody drug targeting CD205, MEN1309/OBT076, demonstrated strong pre-clinical anti-tumor activity in lymphoma, warranting further investigations as a single agent and in combination.

Introduction

Antibody drug conjugates (ADC) represent a class of anti-cancer agents that can have an important impact on the clinical outcome of cancer patients, as exemplified by brentuximab vedotin for Hodgkin lymphoma patients or ado-trastuzumab-emtansine (T-DM1) for breast cancer patients.[1] In lymphomas, different surface proteins (CD19, CD37, CD79B, CD25) have provided targets for active ADC.[1] CD205, encoded by the LY75 gene (Lymphocyte antigen 75, DEC-205), is a surface multi-lectin receptor with a cytoplasmatic domain containing protein motifs crucial for endocytosis and internalization upon ligation. Although its biologic role has not been fully defined, it is known to act as a surface receptor for apoptotic and necrotic cells,[2,3] leading to antigen uptake and processing. CD205 is expressed in hematopoietic cells, mainly by antigen presenting cells (APC), but also in other tissues, including solid tumors.[4-8] CD205 presents a rapid internalization rate and a favorable profile in terms of differential expression between neoplastic and healthy tissues, and is a potential new target for ADC.[7] MEN1309/OBT076 is a novel humanized IgG1 anti-

body directed against CD205, with no direct anti-tumor effect, conjugated through a cleavable N-succinimidyl-4-(2-pyridyldithio) butanoate linker to the potent maytansinoid microtubule disruptor DM4.[7] The ADC has shown potent *in vivo* anti-tumor activity with durable responses and complete tumor regressions in many models derived from triple negative breast cancer, pancreatic and bladder cancer cell lines and primary cells.[7] MEN1309/OBT076 is now under early clinical investigation for patients with solid tumors and lymphoma (CD205-Shuttle study; *clinicaltrials.gov identifier: NCT03403725*).[9] Here, we present the first preclinical data sustaining CD205 as a novel therapeutic target for lymphomas.

Methods

Cell lines

A total of 42 lymphoma cell lines derived from germinal center B-cell type (GCB, n=17) or activated B-cell-like (n=7) diffuse large B-cell lymphoma (DLBCL), mantle cell lymphoma (MCL, n=10), marginal zone lymphoma (MZL, n=6), and chronic lymphocytic leukemia (CLL, n=2) were used and cultured as previously described.[10] Cell line identity was validated by STR DNA fingerprinting using the Promega GenePrint 10 System kit (B9510) (*Online Supplementary Table S1*). *BCL2, MYC* and *TP53* status were defined as previously described.[11]

Compounds

MEN1309/OBT076, MBH1309 and IgG-DM4 for proliferation assay and MEN1309-PE for FACS analysis were provided by Menarini. Idelalisib, bortezomib, lenalidomide, venetoclax were purchased from Selleckchem (Houston, TX, USA) and rituximab from Roche (Basel, Switzerland).

Proliferation and apoptosis assays

Anti-proliferative activity of MEN1309/OBT076 or IgG-DM4 was assessed as before[12] and are described in the *Online Supplementary Appendix*. Methods for apoptosis detection are defined in the *Online Supplementary Appendix*. Peripheral blood mononuclear cells (PBMC) from healthy donors were isolated by using the Ficoll-Paque PLUS (Ge Heathcare Lifesciences) reagent according to its guidelines. CD19+ B-cell lymphocytes were isolated from PBMC using the CD19 MicroBeads (MACS Miltenyi Biotec). *In vitro* combinations were assessed as previously described.[10,12] Based on the Chou-Talalay Combination Index,[13] the effect of the combinations was defined as beneficial if synergistic (<0.9) or additive (0-9-1.1).

Western blotting analysis

Protein extraction, separation and immunoblotting were performed as previously described.[10] The following antibodies were used: anti-β-Tubulin (cst-2146, Cell Signaling Technology), anti-PARP1 (sc-8007, Santa Cruz Biotechnology), anti-BCL2 (sc-492), anti-MCL1 (cst-5453), anti-β BCLXL (sc-8392), and anti-CD20 (ab9475, Abcam).

Immunohistochemistry

Immunohistochemical staining was performed as described in the *Online Supplementary Appendix*.

CD205 surface expression by cytofluorimetry

CD205 expression was determined by flow cytofluorimetry (FACS) on fresh cells, as described in the *Online Supplementary Appendix*.

Real-time-polymerase chain reaction

Total RNA was extracted from cells by using TRIZOL. cDNA was prepared by using the Super script double strand cDNA synthesis kit (Thermo Fisher Scientific, Waltham, MA, USA). The expression levels of both CD205 and the reported intergenically spliced forms were analyzed as described in the *Online Supplementary Appendix*. RNA expression levels obtained with the HumanHT-12 v4 Expression BeadChip (Illumina, San Diego, CA, USA) were retrieved from our previous publication (GSE94669).[10]

Data mining

Associations in two-way tables were tested for statistical significance using either the χ^2 test or Fisher exact test (two-tailed), as appropriate. Binomial exact 95% confidence intervals (95%CI) were calculated for median percentages. Differences in IC_{50} values among subtypes were calculated using the Wilcoxon rank-sum test. Baseline gene expression levels of CD205 and of CD302 were extracted from the GSE9466910 dataset obtained using the HumanHT-12 v4 Expression BeadChip (Illumina, San Diego, CA, USA). The degree of correlation among genes was calculated by standard Pearson correlation coefficients. *P*<0.05 was considered statistically significant. Statistical analyses were conducted using Stata/SE 12.1 for Mac (Stata Corporation, College Station, TX, USA).

Animal studies

Mice maintenance and animal experiments were performed under the institutional guidelines established for the Animal Facility and with study protocols approved by the local Cantonal Veterinary Authority (license TI-22-2015). Methods are described in the *Online Supplementary Appendix*.

Results

Cluster of differentiation 205 (CD205) is expressed in most diffuse large B-cell lymphoma

Expression of CD205 was assessed using immunohistochemistry (IHC) on formalin-fixed paraffin embedded sections of clinical specimens of hematologic cancers derived from lymphomas (n=370), acute myeloid leukemia (n=26), and multiple myeloma (n=14) (Table 1). The antigen CD205 was expressed in the vast majority of the cases, and in entities comprising larger number of samples (DLBCL, MALT lymphomas) expression was detected in 73% and 88% of the cases with moderate-intense expression in 20-50% of the samples. Similar distribution was seen among T-cell lymphomas. CD205 exhibited both membranous and cytoplasmic localization in the lymphoma cells; expression varied within individual cases (*Online Supplementary Figure S1*).

MEN1309/OBT076 has *in vitro* anti-tumor activity in diffuse large B-cell lymphoma

Based on the expression data, we exposed 42 B-cell lymphoma cell lines derived from DLBCL, MCL, MZL, and CLL, to the anti-CD205 ADC MEN1309/OBT076 (*Online Supplementary Table S2*). The compound demonstrated a strong anti-tumor activity with a median IC_{50} of 200 pM (95%CI: 15 pM-20 nM). The control ADC, human IgG conjugated to the DM4 toxin, was 100 times less active (20 nM; 95%CI: 13-70 nM) (Table 2). The anti-tumor activity of MEN1309/OBT076 was mostly cytotoxic: apoptosis induction was observed in 25 of 42 (59.5%) cell lines at a concentration of 1 nM. Cell cycle analysis further
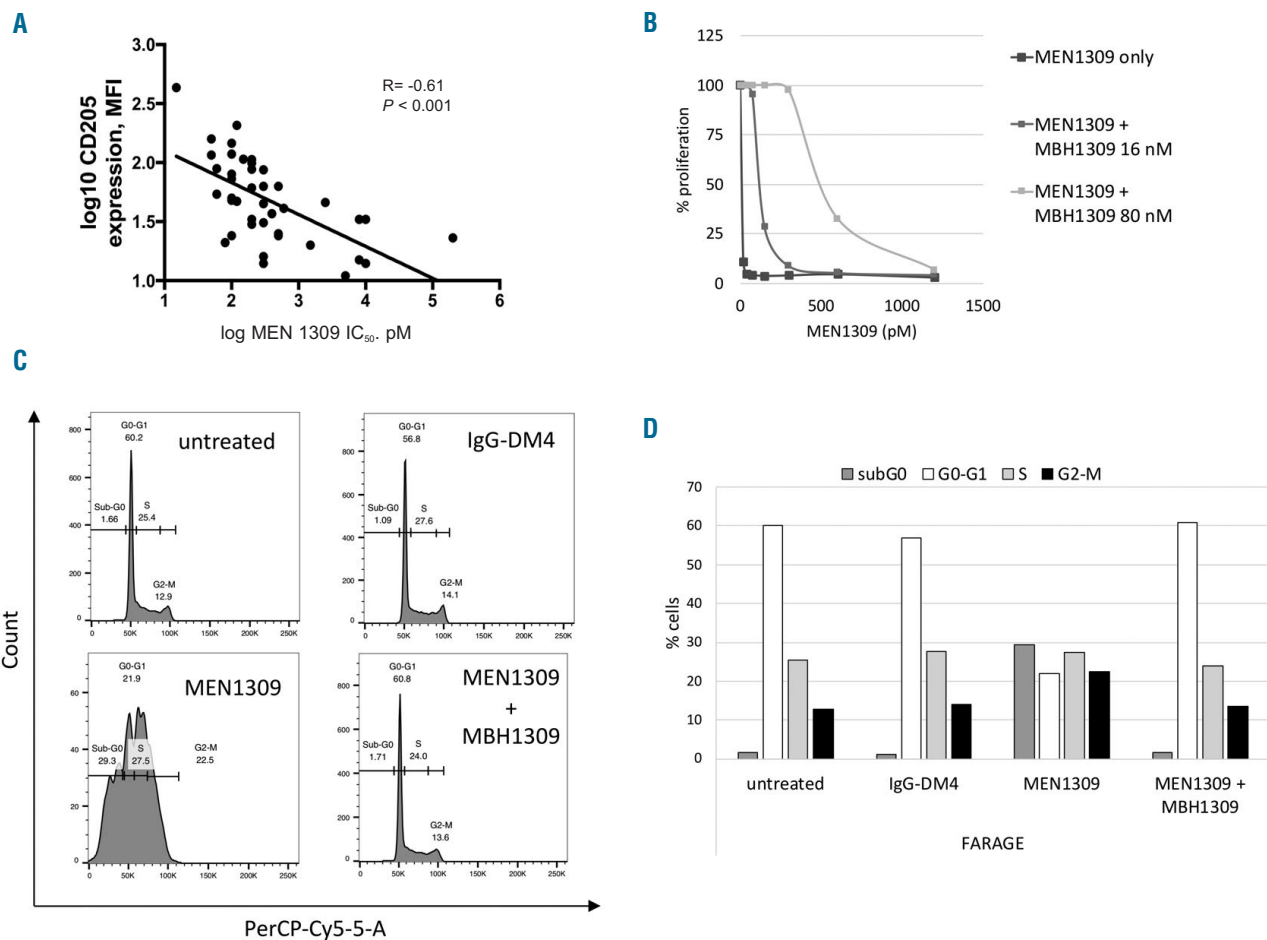
Figure 1. The antitumor of MEN1309/OBT076 is correlated to the expression of its target. (A) Correlation in all B-cell lymphoma. y-axis: Log10 MFI values of CD205 as measured by flow cytometry. x-axis: Log10 IC_{50} values of MEN1309/OBT076 (pM). (B) FARAGE cell lines were treated with MEN1309/OBT076 (0-1.2pM and two different concentrations of MBH1309: 16 and 80nM). (C) Representative histogram of cell cycle distribution in FARAGE cells treated with 100pM of IgG-DM4, MEN1309/OBT076 alone and in combination with MBH1309 (72 hours). (D) Cell cycle distribution after exposure with IgG-DM4, MEN1309/OBT076 or combination with MBH1309. Graph plots show mean±standard deviation for values from two biological replicates. MFI: mean fluorescence intensity.

confirmed the cytotoxic activity of MEN1309/OBT076. Four cell lines (Farage, OCI-LY-1, SU-DHL-4 and SU-DHL-10) were treated with MEN1309/OBT076 (low concentration and high concentration, reflecting IC_{50} values for each cell line), and with IgG-DM4 and the unconjugated anti-CD205 antibody for 72 hours. In all the cases, MEN1309/OBT076 induced a strong sub-G0 arrest in the cell lines, while the effect of the two control antibodies (IgG-DM4 and naked antibody MBH-1309) was minimal (*Online Supplementary Figure S2*). No differences in anti-tumor activity were seen according to DLBCL cell of origin, lymphoma histotype, the presence of *MYC* translocation or *BCL2* translocation or *TP53* inactivation (*Online Supplementary Table S2*). The ADC MEN1309/OBT076 did not exert any apoptotic effects against PBMC from two healthy donors who had CD205 expression on their $CD19^{+}$ B cells similar to one the most sensitive DLBCL cell lines (171 and 111 *vs.* 106 of the OCI-LY-10) (*Online Supplementary Figure S3*).

MEN1309/OBT076 anti-tumor activity was highly correlated with CD205 expression in diffuse large B-cell lymphoma cell lines

We then evaluated whether the activity of

MEN1309/OBT076 was affected by the expression levels of its target. Sensitivity to the ADC was correlated with the cell surface CD205 expression measured by flow cytometry in 41 lymphoma cell lines (*Online Supplementary Table S3*), as shown by the negative correlation between IC_{50} values and the mean fluorescence intensity values (*P*<0.0001) (Figure 1A).

Focusing on 23 DLBCL cells, we also assessed the correlation between sensitivity and RNA expression of the *LY75* gene, coding for CD205, as measured by gene expression profiling or real-time polymerase chain reaction (RT-PCR) (*Online Supplementary Table S3*). The expression levels obtained with the two modalities were positively correlated between them (*P*<0.001) and with cell membrane protein expression (*P*<0.001) (*Online Supplementary Figure S4*). Similar to protein expression, also RNA levels were negatively correlated with IC_{50} values (*P*<0.001) (*Online Supplementary Figure S5*).

The *LY75* gene, coding for CD205, is known to give rise to intergenically spliced transcripts with its centromeric neighboring gene *CD302*.[5] MEN1309/OBT076 activity significantly correlated with the expression of two CD205-CD302 intergenically spliced transcripts, measured by RT-PCR, indicating that this phenomenon does

Table 1. Prevalence of CD205 expression in hematologic cancers as demonstrated by immunohistochemistry (IHC) on tumor microarrays.

	N. of samples	CD205 expression (IHC)	
		≥ 1+ (%)	2-3+ (%)
Lymphoma			
B-cell neoplasms			
B cell lymphoma (undefined)	302	71	37
Diffuse large B-cell lymphoma	82	73	28
Burkitt's lymphoma	7	29	0
Follicular lymphoma	16	81	23
Lymphoplasmacytic lymphoma	13	31	23
Mantle cell lymphoma	7	71	29
Mucosa-associated lymphatic tissue lymphoma	40	88	50
Small lymphocytic lymphoma	3	0	0
T-cell rich B-cell lymphoma	3	33	33
Hodgkin lymphoma			
Hodgkin lymphoma (undefined)	5	80	20
Lymphocyte depleted Hodgkin lymphoma	2	50	50
Lymphocyte predominant Hodgkin lymphoma	7	57	14
Mixed cellularity	15	100	7
Nodular sclerosis	5	100	60
T-cell and NK-cell neoplasms			
T-cell lymphoma (undefined)	68	59	28
Anaplastic large cell lymphoma	8	88	50
Angioimmunoblastic T-cell lymphoma	7	86	43
Peripheral T-cell lymphoma	3	100	0
Leukemia			
Acute myeloid leukemia	26	62	58
Myeloma			
Multiple myeloma	14	100	79

N: number; NK: natural killer.

not reduce the anti-tumor activity of the compound (R=-0.78 and R= -0.72, P<0.001) (*Online Supplementary Table S3*), as well CD302 itself (R=0.67, P=0.001).

Finally, to further assess the specificity of MEN1309/OBT076, we treated cells with the ADC with or without the addition of MBH-1309, the naked anti-CD205 antibody. The latter molecule had no anti-tumor activity by itself (*Online Supplementary Figure S6*), but it decreased the activity of MEN1309/OBT076 in a dose dependent manner, as shown both in terms of IC$_{50}$ and of cell cycle analysis (Figure 1B-D).

MEN1309/OBT076 demonstrates *in vivo* anti-tumor activity in DLBCL

To confirm the observed *in vitro* MEN1309/OBT076 anti-lymphoma activity, we performed an *in vivo* xenograft experiment with the OCI-LY-10 model of DLBCL. Cohorts of mice were treated with vehicle control, IgG-DM4 (5 mg/kg, once every 3 weeks), or MEN1309/OBT076 (1.25, 2.5 or 5 mg/kg once every 3 weeks) (Figure 2A). Low activity was observed with MEN1309/OBT076 1.25 mg/kg (day [D] 7, P=0.012) and with IgG-DM4 (D21, P=0.049; D28, P=0.046). MEN1309/OBT076 at 2.5 mg/kg delayed tumor growth *versus* control (D21, P=0.039). MEN1309/OBT076 at 5 mg/kg eradicated tumors in all mice with a single dose, highlighted by highly significant differences in tumor vol-

ume *versus* control mice (D7, D21, D28; P<0.01). Tumor eradication led to an increase in the survival of the mice. While all other groups reached endpoint by D35, the MEN1309/OBT076 5 mg/kg group skipped the second planned treatment at D21 because there was no sign of tumors, and mice remained cured up to two months later (Kaplan-Meier, survival analysis, P<0.0001) (Figure 2B). One mouse belonging to the 5 mg/kg group showed tumor re-growth (D28 and D35), and a second MEN1309/OBT076 injection (D43) conferred tumor remission for the second time (D50 and D57).

MEN1309/OBT076 is synergistic with other targeted agents

MEN1309/OBT076 was then combined with targeted agents in four ABC-DLBCL cell lines (TMD8, HBL1, OCI-LY-10 and U2932) (Table 3). The most effective combinations were with the anti-CD20 monoclonal antibody rituximab (synergistic in all four), and with the BCL2 inhibitor venetoclax (synergistic in three, additive in one). Both combinations determined increased cell counts as shown by increased percentage of cells in sub-G0 phase during a cell cycle experiment (*Online Supplementary Figure S7*). Immunoblotting analyses of two ABC-DLBCL cell lines (TMD8 and OCI-LY-10) after exposure to MEN1309/OBT076 provided hints on the mechanism underlining the synergism (Figure 3). Protein levels of anti-

apoptotic proteins were affected by exposure to MEN1309/OBT076, which induced a downregulation of MCL1 protein and upregulation of BCL2 and BCX-L. The ADC also determined an upregulation of CD20 protein levels. All the changes were maintained when MEN1309/OBT076 was given in combination with the BCL2 inhibitor or the anti-CD20 monoclonal antibody,

and not seen after these two drugs were given as single agents. PARP1 cleavage confirmed apoptosis induction.

The combinations with the PI3K-δ inhibitor idelalisib was additive in two cell lines and of no benefit in the other two, while the immunomodulatory agent lenalidomide was additive in one cell line and of no benefit in the remaining three.
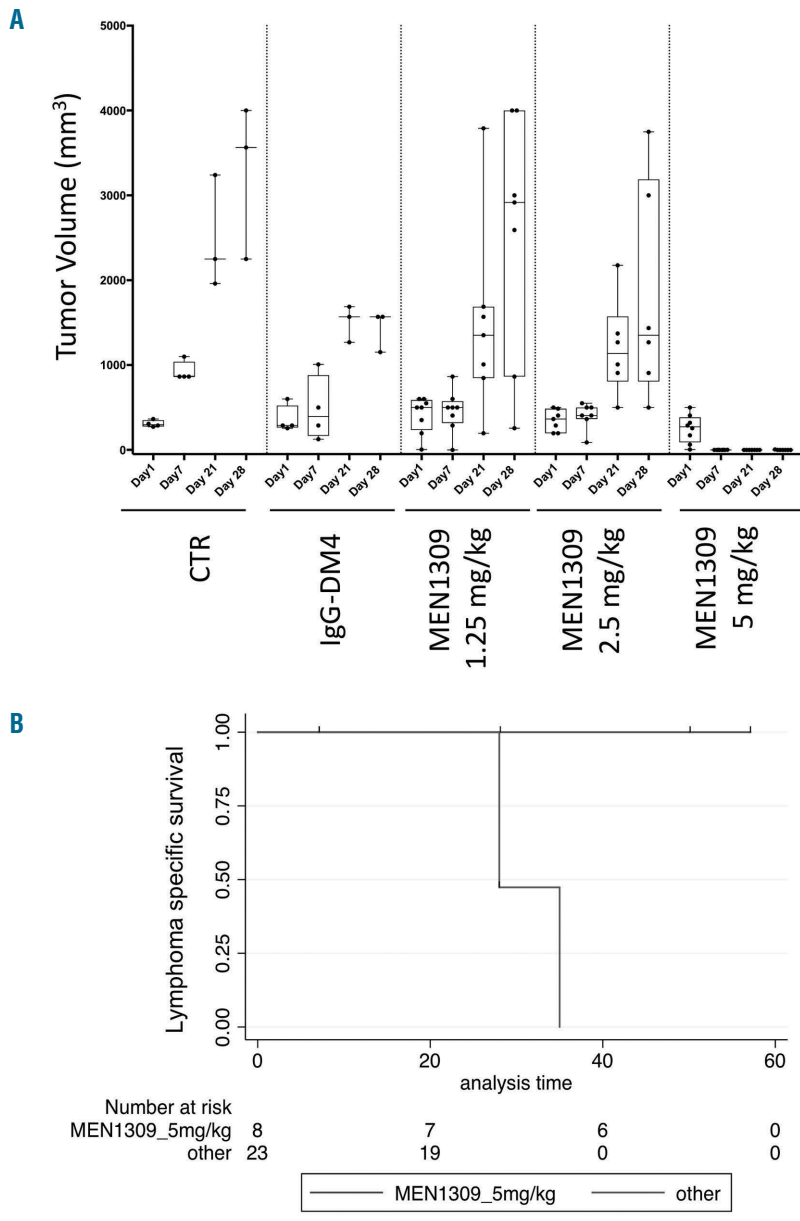
Figure 2. MEN1309/OBT076 as single agent has *in vivo* antitumor activity in the activated B-cell like diffuse large B-cell lymphoma OCI-LY10 xenograft model. Treatment with MEN1309/OBT076 and IgG-DM4 started when tumors became visible (100mm^3). (A) Control (CTR) group, n=4; IgG-DM4 group, n=4; MEN1309/OBT076 1.25 mg/kg, n=8; MEN1309/OBT076 2.5 mg/kg, n=7; MEN1309/OBT076 5 mg/kg, n=8. In each box-plot, the line in the middle of the box represents the median and the box extends from the 25th to the 75th percentile (IQ: interquartile range). Each dot represent a mouse. x-axis: days of treatment. y-axis: tumor volume expressed in mm^3. (B) Kaplan-Meier LSS (lymphoma specific survival). MEN1309/OBT076 (5 mg/kg) *versus* all other groups together. *P*<0.0001.

Table 2. Anti-tumor activity of MEN1309/OBT076 and IgG-DM4 in B-cell lymphoma cell lines.

		MEN1309/OBT076		IgG-DM4	
	N. of cell lines	**Median IC$_{50}$**	**95%CI**	**Median IC$_{50}$**	**95%CI**
GCB-DLBCL	15	200 pM	118 pM-4163 pM	30 nM	20-38 nM
ABC-DLBCL	8	300 pM	200 pM-3612 pM	30 nM	20-40 nM
MCL	10	100 pM	86-1883 pM	15 nM	15-54 nM
MZL	6	110 pM	55-465 pM	17.5 nM	15-38.5 nM
CLL	2	310 pM	n.d.	34 nM	n.d.

GCB-DLBCL: germinal center B-cell type diffuse large B-cell lymphoma; ABC-DLBCL: activated B-cell like diffuse large B-cell lymphoma; MCL: mantle cell lymphoma; MZL: marginal zone lymphoma; CLL: chronic lymphocytic leukemia; n.d.: not determined; N: number; CI: confidence interval.

Combined MEN1309/OBT076 and rituximab showed higher *in vivo* anti-tumor activity than the single agents

The *in vitro* synergism with rituximab was validated *in vivo* using an ABC-DLBCL lymphoma model, OCI-LY-10 (Figure 4). Mice were divided in four groups of ten animals each and were treated with MEN1309/OBT076 (2.5 mg/kg IV, D1 and D12), or rituximab (3 mg/kg IV on D1; 5 mg/kg IV on D12), or MEN1309/OBT076 plus rituximab (same schedule as single agents), or with vehicle only (IV).

Single agents and combinations were more active ($P<0.05$) than controls (MEN1309/OBT076, rituximab, MEN1309/OBT076 plus rituximab, starting at D10). The combination of MEN1309/OBT076 with rituximab gave significant differences at D17 ($P<0.05$) *versus* both single agent arms and tumor eradication. At the used doses, MEN1309/OBT076 presented higher anti-lymphoma activity compared to rituximab, although this was not statistically significant ($P=0.06$, D17).

Discussion

Here we have shown CD205 expression in hematologic cancers, including lymphomas. Results show that targeting this antigen with a first-in-class anti-CD205 ADC, MEN1309/OBT076, had both *in vitro* and *in vivo* anti-tumor activity in lymphomas. The novel ADC had an anti-tumor activity that was highly correlated with expression of its target CD205 and reached synergism when combined with other targeted agents.

Immunohistochemistry analysis of histological sections of lymphomas, myeloma and leukemia clinical specimens showed that a large percentage of cases (>70%) express CD205. This is in agreement with recently reported data in series of 100 DLBCL and 33 follicular lymphomas in which CD205 positivity was detected in 60% and 79% of the cases, respectively.[8] CD205 has also been detected at high expression level in solid tumors (gastric, pancreatic, bladder, breast and colon).[7]

CD205 is a type I transmembrane glycoprotein and a C-type lectin receptor, which undergoes endocytosis[7] and, thus, can be exploited as a novel target for ADC. The fully humanized ADC MEN1309/OBT076 binds to CD205 with high affinity and is rapidly internalized in the cells, delivering the microtubule disruptor DM4 as payload.[7] Based on expression pattern in lymphoma clinical specimens, we assessed the anti-tumor activity of MEN1309/OBT076 in lymphoma cell lines. The ADC presented a very strong anti-tumor activity with subnanomolar IC_{50} values. Of clinical relevance, at least in cell lines, sensitivity to MEN1309/OBT076 was not affected by DLBCL cell of origin, *MYC/BCL2* or *TP53* status. The *in vitro* results were confirmed in a xenograft model using an ABC DLBCL cell line. A single dose of MEN1309/OBT076 at 5 mg/kg led to a complete remission that lasted for at least two months. A second dose was able to obtain a second remission in the only tumor that presented a regrowth. These data are similar to recent observations in solid tumor models exposed to MEN1309/OBT076.[7] The strong *in vitro* and *in vivo* data, and the notion that its target
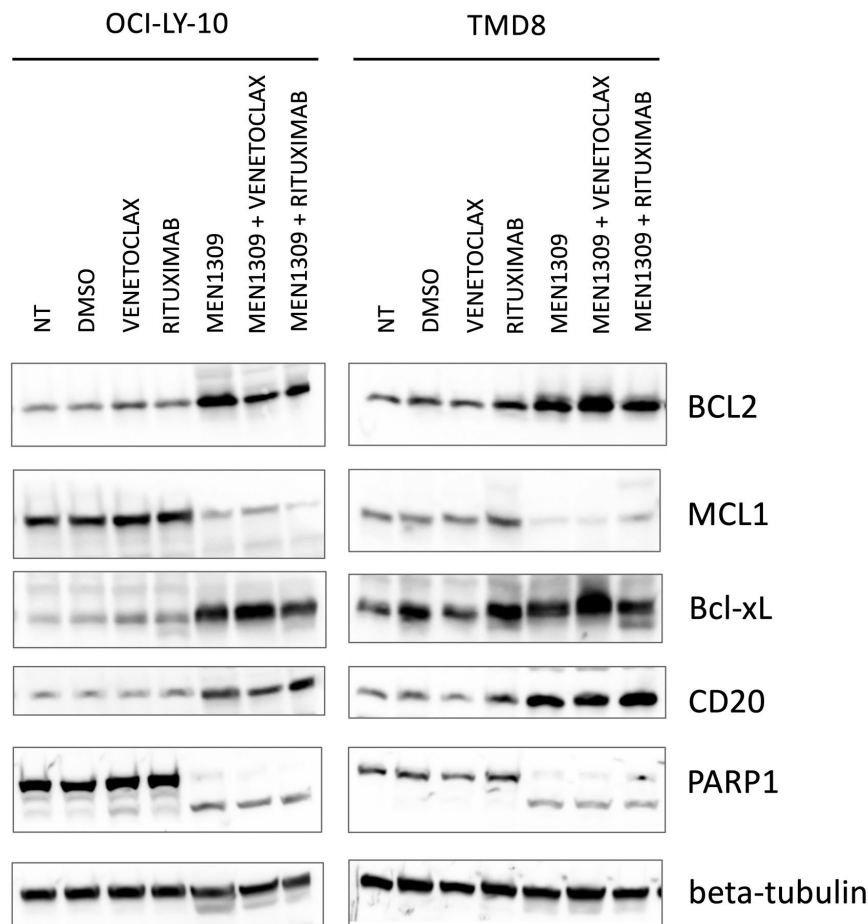
Figure 3. MEN1309/OBT076 combined with the BCL2 inhibitor venetoclax and the anti-CD20 monoclonal antibody rituximab exerts cytotoxicity downregulating MCL1, cleaving PARP and upregulating CD20 protein. Two cell lines were exposed to MEN1309/OBT076 (1nM), venetoclax (100 nM), rituximab (20 μg/mL) or the combination of the agents for 72 hours. β-tubulin was used as a loading control. Figure is representative of two independent experiments.
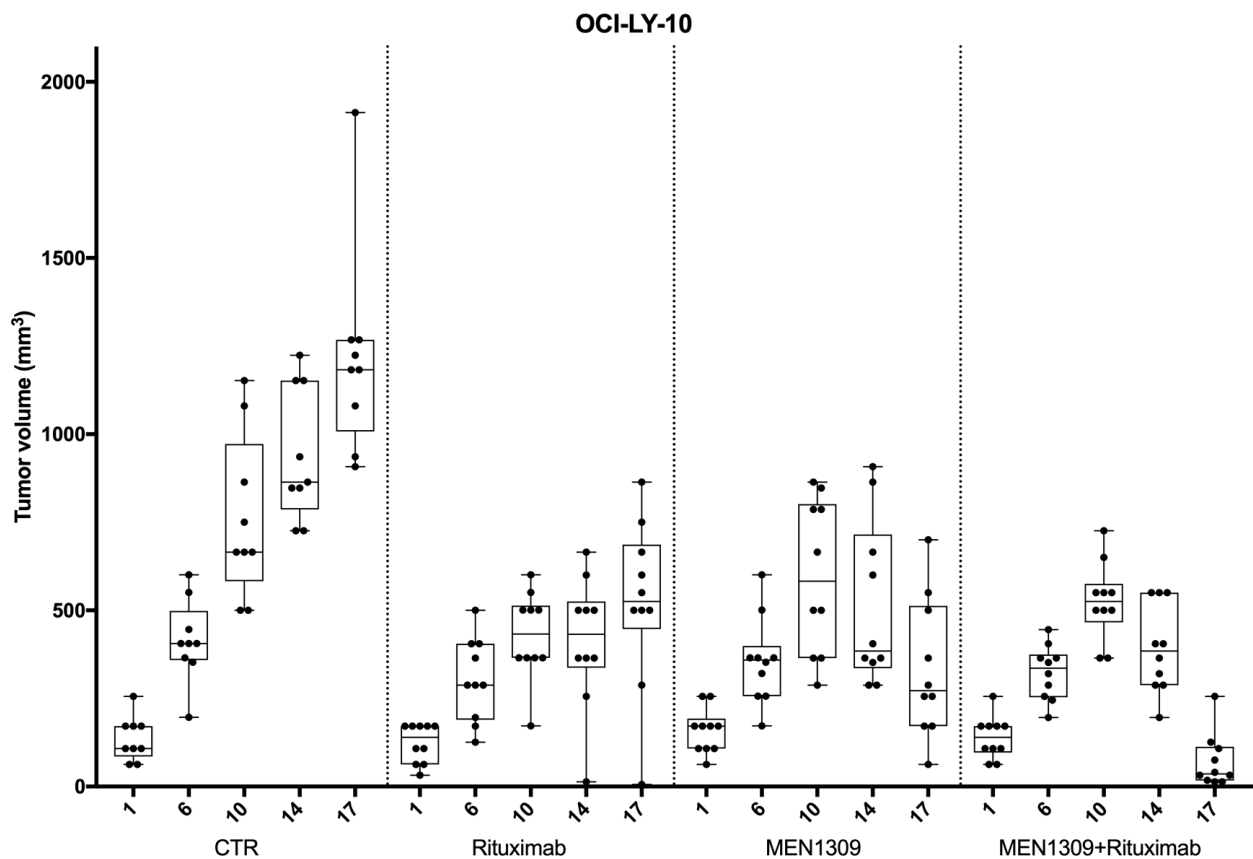
Figure 4. Combined MEN1309/OBT076 and rituximab shown higher *in vivo* anti-tumor activity than the single agents in the activated B-cell like diffuse large B-cell lymphoma OCI-LY10 xenograft model. Treatment with MEN1309/OBT076 (2.5 mg/kg), rituximab (5 mg/kg), their combination or vehicle started when tumors became visible (>100 mm³). In each box-plot, the line in the middle of the box represents the median and the box extends from the 25th to the 75th percentile. CTR: control; IQ: interquartile range. y-axis: tumor volume in mm³; x-axis: days of treatment.

is not shared by other antibody or cell[1,14-16] based therapies, make MEN1309/OBT076 a very interesting novel compound for lymphoma patients.

We did not observe toxicity in our *in vivo* models, in agreement with reports from *in vivo* studies of solid tumor models,[7] but MBH1309/OBT076 does not significantly cross-react to the mouse CD205.[7] Toxicity studies performed on cynomolgus monkeys, whose CD205 cross-reacts to MBH1309/OBT076, have shown moderate toxicity with neutropenia as main adverse event.[7] There is no difference in CD205 expression pattern between humans and cynomolgus monkeys across 33 different normal tissues, with a membranous/cytoplasmic staining of mononuclear cells in several tissues, including lymph nodes and spleen.[7] Here, we exposed human PBMC from two healthy donors to the MEN1309; no cytotoxicity was observed despite the fact that the B cells expressed CD205 levels similar to those observed in a sensitive DLBCL cell line. One reason could be that circulating B cells are not proliferating and are thus less sensitive to the payload. This would agree with the suggested explanation of the low toxicity observed in CD205 positive normal tissues in cynomolgus monkeys.[7]

The anti-tumor activity of MEN1309/OBT076 appeared to be mediated by the ADC binding to its target as shown by the very high correlation between IC$_{50}$ values and target expression, and by competition experiments with a

Table 3. *In vitro* assessment of MEN1309/OBT076 combinations with targeted agents.

Cell line	Drug 2	Median combination index	95% CI
HBL1	Idelalisib	0.96^	0.78-1
OCI-LY-10	Idelalisib	2.51	1.91-2.76
TMD8	Idelalisib	1.14	1.02-1.32
U2932	Idelalisib	0.91^	0.7-1.4
HBL1	Lenalidomide	1.31	0.92-2.34
OCI-LY-10	Lenalidomide	1.46	1.19-1.58
TMD8	Lenalidomide	0.94^	0.64-1.44
U2932	Lenalidomide	1.47	0.97-2.08
HBL1	Rituximab	0.57*	0.51-0.67
OCI-LY-10	Rituximab	0.8*	0.42-2.37
TMD8	Rituximab	0.27*	0.22-0.33
U2932	Rituximab	0.47*	0.39-0.8
HBL1	Venetoclax	0.51*	0.32-0.7
OCI-LY-10	Venetoclax	0.86*	0.68-0.53
TMD8	Venetoclax	1.04^	0.75-1.52
U2932	Venetoclax	0.49*	0.32-0.83

Cell lines were exposed to increasing concentrations of MEN1309/OBT076 and/or of the other compound (drug 2) for 72 hours. Based on the Chou-Talalay Combination Index, the effect of the combinations was defined as beneficial if synergistic (<0.9) or additive (0-9-1.1). CI: confidence interval.

naked antibody recognizing the same epitope targeted by MEN1309/OBT076. No direct anti-tumor effect is reported for the naked antibody MEN1309/OBT076.[7] It is noteworthy that the expression level of CD205 in cell lines measured at the level of mRNA, total protein or cell surface protein correlated with the sensitivity to MEN1309/OBT076. Furthermore, a clinical DLBCL specimen-derived CD205 signature also correlated with the *in vitro* response to the drug. In contrast, the expression of two annotated CD205-CD302 intergenically spliced transcripts[5] did not affect the anti-tumor activity of MEN1309/OBT076.

Finally, MEN1309/OBT076 was beneficially combined with other targeted agents, especially the BCL2 inhibitor venetoclax and the anti-CD20 monoclonal antibody rituximab. The latter combination, that had shown the best *in vitro* results, was successfully validated *in vivo* using a xenograft model.[17] Interesting clinical data are also already available for combinations with other ADC.[18,19] The mechanisms leading to better anti-tumor activity can differ. The concomitant exposure of lymphoma cells to rituximab and to the anti-CD37 ADC IMGN529/Debio1562 leads to

improved anti-lymphoma activity due to an increased internalization of the latter.[20] The benefit of combining the anti-CD22 inotuzumab ozogamicin (CMC-544) with rituximab could be due to both an early upregulation of CD20 with increased direct cytotoxicity of the anti-CD20[21] or to the addition of the direct (inotuzumab ozogamicin), complement and/or cellular dependent (rituximab) mechanisms of actions of the compounds.[22] Here, we observed that exposure to MEN1309/OBT076 was followed by upregulation of the rituximab target CD20 and downregulation of the anti-apoptotic protein MCL1, known to counteract the activity of venetoclax in DLBCL cells,[23] two changes that could support the observed synergisms. Moreover, the addition of venetoclax also counteracts the BCL2 upregulation seen after the ADC.

In conclusion, the first-in-class ADC targeting CD205, MEN1309/OBT076, demonstrated strong pre-clinical anti-tumor activity in lymphoma. Our data sustain the ongoing clinical CD205-Shuttle study (*clinicaltrials.gov identifier: NCT03403725*) of MEN1309/OBT076 as single agent, and provide the rationale for further investigations also in combination therapy.

References

1. Moek KL, de Groot DJA, de Vries EGE, Fehrmann RSN. The antibody-drug conjugate target landscape across a broad range of tumour types. Ann Oncol. 2017; 28(12):3083-3091.

2. Shrimpton RE, Butler M, Morel AS, Eren E, Hue SS, Ritter MA. CD205 (DEC-205): a recognition receptor for apoptotic and necrotic self. Mol Immunol. 2009; 46(6):1229-1239.

3. Cao L, Shi X, Chang H, Zhang Q, He Y. pH-Dependent recognition of apoptotic and necrotic cell by the human dendritic cell receptor DEC205. Proc Natl Acad Sci U S A. 2015;112(23):7237-7242.

4. Butler M, Morel AS, Jordan WJ, et al. Altered expression and endocytic function of CD205 in human dendritic cells, and detection of a CD205-DCL-1 fusion protein upon dendritic cell maturation. Immunology. 2007;120(3):362-371.

5. Kato M, Khan S, Gonzalez N, et al. Hodgkin's lymphoma cell lines express a fusion protein encoded by intergenically spliced mRNA for the multilectin receptor DEC-205 (CD205) and a novel C-type lectin receptor DCL-1. J Biol Chem. 2003; 278(36):34035-34041.

6. Uhlen M, Fagerberg L, Hallstrom BM, et al. Proteomics. Tissue-based map of the human proteome. Science. 2015; 347(6220):1260419.

7. Merlino G, Fiascarelli A, Bigioni M, et al. MEN1309/OBT076, a first-in-class antibody-drug conjugate targeting CD205 in solid tumors. Mol Cancer Ther. 2019;18(9):1533-1543.

8. Canzonieri V, Gattei V, Spina M, et al. CD205, a target antigen for a novel antibody drug conjugate (ADC): evaluation of antigen expression on non-Hodgkin lymphoma (NHL). J Clin Oncol. 2017;35(15 Suppl):e14039-e14039.

9. Garralda E, Tabernero J, Garcia VM, De Miguel MJ, Plummer ER, Jerusalem GHM. CD205-Shuttle study: a first-in-human trial of MEN1309/OBT076 an ADC targeting CD205 in solid tumor and NHL. J Clin Oncol. 2018;36(15):TPS2606.

10. Tarantelli C, Gaudio E, Arribas AJ, et al. PQR309 is a novel dual PI3K/mTOR inhibitor with preclinical antitumor activity in lymphomas as a single agent and in combination therapy. Clin Cancer Res. 2018;24(1):120-129.

11. Hicks SW, Tarantelli C, Wilhem A, et al. The novel CD19-targeting antibody-drug conjugate huB4-DGN462 shows improved anti-tumor activity compared to SAR3419 in CD19-positive lymphoma and leukemia models. Haematologica. 2019;104(8):1633-1639.

12. Boi M, Gaudio E, Bonetti P, et al. The BET bromodomain inhibitor OTX015 affects pathogenetic pathways in preclinical B-cell tumor models and synergizes with targeted drugs. Clin Cancer Res. 2015;21(7):1628-1638.

13. Chou TC. Preclinical versus clinical drug combination studies. Leuk Lymphoma. 2008;49(11):2059-2080.

14. Younes A, Ansell S, Fowler N, et al. The landscape of new drugs in lymphoma. Nat Rev Clin Oncol. 2017;14(6):335-346.

15. Pianko MJ, Moskowitz AJ, Lesokhin AM. Immunotherapy of lymphoma and myeloma: facts and hopes. Clin Cancer Res. 2018; 24(5):1002-1010.

16. Chow VA, Shadman M, Gopal AK. Translating anti-CD19 CAR T-cell therapy into clinical practice for relapsed/refractory diffuse large B-cell lymphoma. Blood. 2018; 132(8):777-781.

17. Karmali R, Kimby E, Ghielmini M, Flinn IW, Gordon LI, Zucca E. Rituximab: a benchmark in the development of chemotherapy-free treatment strategies for follicular lymphomas. Ann Oncol. 2018;29(2):332-340.

18. Advani RH, Lebovic D, Chen A, et al. Phase I study of the anti-CD22 antibody-drug conjugate pinatuzumab vedotin with/without rituximab in patients with relapsed/refractory B-cell non-Hodgkin lymphoma. Clin Cancer Res. 2017;23(5):1167-1176.

19. Fayad L, Offner F, Smith MR, et al. Safety and clinical activity of a combination therapy comprising two antibody-based targeting agents for the treatment of non-Hodgkin lymphoma: results of a phase I/II study evaluating the immunoconjugate inotuzumab ozogamicin with rituximab. J Clin Oncol. 2013;31(5):573-583.

20. Hicks SW, Lai KC, Gavrilescu LC, et al. The antitumor activity of IMGN529, a CD37-targeting antibody-drug conjugate, is potentiated by rituximab in non-Hodgkin lymphoma models. Neoplasia. 2017;19(9):661-671.

21. Takeshita A, Yamakage N, Shinjo K, et al. CMC-544 (inotuzumab ozogamicin), an anti-CD22 immuno-conjugate of calicheamicin, alters the levels of target molecules of malignant B-cells. Leukemia. 2009; 23(7):1329-1336.

22. Dijoseph JF, Dougher MM, Kalyandrug LB, et al. Antitumor efficacy of a combination of CMC-544 (inotuzumab ozogamicin), a CD22-targeted cytotoxic immunoconjugate of calicheamicin, and rituximab against non-Hodgkin's B-cell lymphoma. Clin Cancer Res. 2006;12(1):242-249.

23. Klanova M, Andera L, Brazina J, et al. Targeting of BCL2 family proteins with ABT-199 and homoharringtonine reveals BCL2- and MCL1-dependent subgroups of diffuse large B-cell lymphoma. Clin Cancer Res. 2016;22(5):1138-1149.

Ferrata Storti Foundation

Early progression of disease predicts shorter survival in patients with mucosa-associated lymphoid tissue lymphoma receiving systemic treatment

Annarita Conconi,[1] Catherine Thieblemont,[2] Luciano Cascione,[3] Valter Torri,[4] Barbara Kiesewetter,[5] Gloria Margiotta Casaluci,[6] Gianluca Gaidano,[6] Markus Raderer,[5] Franco Cavalli,[3] Armando Lopez Guillermo,[7] Peter W. Johnson[8] and Emanuele Zucca[3,9] on behalf of the International Extranodal Lymphoma Study Group (IELSG)

[1]Division of Hematology, Ospedale degli Infermi, Biella, Italy; [2]Hemato-Oncology Department, Saint Louis Hospital, Paris, France; [3]Institute of Oncology Research, Bellinzona, Switzerland; [4]Clinical Research Methodology Laboratory, IRCCS–Mario Negri Institute, Milan, Italy; [5]Division of Oncology, Department of Internal Medicine I, Medical University of Vienna, Vienna, Austria; [6]Division of Hematology, Department of Translational Medicine, University of Eastern Piedmont, Novara, Italy; [7]Department of Hematology, Hospital Clinic, Barcelona, Spain; [8]Cancer Research UK Centre Southampton General Hospital, Southampton, UK and [9]Division of Medical Oncology, Oncology Institute of Southern Switzerland, Bellinzona, Switzerland

Correspondence:

ANNARITA CONCONI
annarita.conconi@aslbi.piemonte.it

ABSTRACT

Early progression of disease, within 2 years of diagnosis, is linked with poor overall survival in follicular lymphoma but its prognostic role in extranodal marginal zone B-cell lymphoma is less clear. We sought to identify prognostic factors associated with early progression of disease and to determine whether early progression is associated with inferior overall survival. We analyzed the impact of early progression of disease using the dataset of the International Extranodal Lymphoma Study Group-19 (IELSG-19) clinical trial (training set of 401 patients randomly assigned to chlorambucil or rituximab or chlorambucil plus rituximab). Reproducibility was examined in a validation set of 287 patients who received systemic treatment. We excluded from the analysis patients in both sets who, within 24 months of starting treatment, died without progression or were lost to follow-up without prior progression. Overall survival was calculated from progression in patients with early disease progression and from 24 months after the start of treatment in those whose disease did not progress early (reference group). Early disease progression occurred in 69 of the 384 (18%) evaluable patients of the IELSG-19 study. Patients with a high-risk Mucosa-Associated Lymphoid Tissue - International Prognostic Index score were more likely to have early disease progression (*P*=0.006). The 10-year overall survival rate was 64% in the group with early disease progression and 85% in the reference group (hazard ratio = 2.42; 95% confidence interval: 1.35-4.34; log-rank *P*=0.002). This prognostic impact was confirmed in the validation set, in which early progression was observed in 64 out of 224 (29%) evaluable patients with 10-year overall survival rates of 48% in the group with early disease progression and 71% in the reference group (hazard ratio = 2.15; 95% confidence interval: 1.19-3.90; log-rank *P*=0.009). In patients with extranodal marginal zone B-cell lymphoma who received front-line systemic treatment, early disease progression is associated with poorer survival and may represent a useful endpoint in future prospective clinical trials.

Introduction

Marginal zone lymphomas (MZL) comprise three separate disease entities, which have individual epidemiological, molecular and clinical features. Extranodal marginal zone lymphoma (EMZL), also known as mucosa-associated lymphoid tissue (MALT) lymphoma, is the most common MZL subtype, accounting for approximately 50 to 70% of MZL and 5% to 8% of all B-cell lymphomas.[1-3] EMZL may involve virtually any tissue but most often affects organs that are normally devoid of lymphocytes, where it arises from lymphoid populations associated with chronic inflammatory processes of either infectious or autoimmune origin.[4] The clinical presentation is very heterogeneous and EMZL patients are managed with a variety of treatments. The natural course is usually indolent, particularly in patients with gastric lymphomas, and aggressive therapy is rarely required.[1,3,5] Outcomes may, however, differ depending on the organ involved.[2,6] We recently proposed a prognostic model, the MALT-lymphoma International Prognostic Index (MALT-IPI), which is based on age, disease stage and lactate dehydrogenase (LDH) concentration at diagnosis. MALT-IPI discriminated between patients with different progression-free survival (PFS) and overall survival (OS), and retained its prognostic utility in both gastric and non-gastric MALT lymphomas.[7] In this context, the identification of the minority of patients with shorter survival may become important, especially in the perspective of personalized medicine, and might form the basis for adapting therapeutic approaches.

In follicular lymphoma early progression of disease (POD), namely, within 24 months after diagnosis, has been reported to be associated with poor outcomes.[8] Currently, the clinical significance of early POD in EMZL is uncertain, and the impact of early POD on subsequent survival has not been properly explored yet.

The present study aimed to understand whether time to progression after first-line systemic therapy may be a factor affecting survival outcomes in EMZL. We analyzed data from the International Extranodal Lymphoma Study Group 19 (IELSG-19) clinical trial to determine whether early POD is predictive of inferior OS in this disease, and then validated our findings in an independent cohort.

Methods

Patients

Details regarding the IELSG-19 randomized phase III trial (ClinicalTrials.gov Identifier: NCT 00210353) have been published elsewhere.[6,9] All patients provided written informed consent and the study was approved by the institutional review board or ethics committee of each institution involved. This trial compared chlorambucil alone to rituximab alone and to the combination of rituximab and chlorambucil as front-line therapy in EMZL patients, with event-free survival as the primary endpoint.[6]

Early POD was defined as in the follicular lymphoma study by Casulo *et al.*[8] Patients enrolled in the IELSG-19 study were divided into two groups: a group formed of patients with early POD, that is, progression within 24 months from the start of first-line treatment, and a reference group, consisting of patients without early POD. An independent validation set, comprising only patients who received front-line systemic treatment (chemotherapy, immunotherapy or both), was derived from the validation cohort of the MALT-IPI study, which included patients from different sources (the databases of the IELSG-1 multicenter study and of a retrospective survey conducted at the Oncology Institute of Southern Switzerland, and at the Hematology Division of the University of Eastern Piedmont, in Novara Italy, and a cohort of patients diagnosed at the Medical University of Vienna, Austria) whose details have also been published elsewhere.[7]

Statistical methods

Primary analysis of OS from risk-defining events was performed in both the test and validation sets, commencing the observation for the group with early POD from the time progression occurred, and for the reference group from 24 months after the start of front-line therapy.

Statistical analysis was performed using the Stata/SE 11.0 software package (StataCorpLP, College Station, TX, USA). The median follow-up was computed as the median time to censoring or death using the reverse Kaplan-Meier method.[10] Survival probabilities were calculated using life tables and survival curves were estimated by the method of Kaplan-Meier; differences between groups of patients were evaluated using the log-rank test.[11] Binomial exact 95% confidence intervals (95% CI) were calculat-

Table 1. The characteristics of the patients in the validation and test sets.

	Test set (IELSG-19)	Validation set
Number of patients	401	287
Years of diagnosis	2003-2010	1983-2014
Median age at diagnosis (IQR)	61 years (51-69)	63 years (51-72)
Male/female ratio	197/204	115/172
Stage III-IV, n (%)	175 (44%)	140 (49%)
Performance status>1[a], n (%)	6 (1.5%)	14 (5%)
LDH >UNL[b], n (%)	42 (10.5%)	42 (16%)
β_2-microglobulin >UNL[c], n (%)	46 (16%)	73 (43%)
Primary gastric lymphoma, n (%)	171 (43%)	125 (44%)
IPI, high-intermediate/high risk[d], n (%)	77 (19%)	88 (31%)
MALT-IPI, high risk[e], n (%)	68 (17%)	69 (26%)
First-line treatment, n (%)		
Chemotherapy only	131 (33%)	158 (55%)
Rituximab and chemotherapy	132 (33%)	64 (22%)
Doxorubicin-containing regimen	0%	60 (21%)
Rituximab only	138 (34%)	28 (10%)
Other[f]	0%	37 (13%)
Median follow-up (IQR)	7.4 years (5.6-9.7)	5.7 years (2.3-9.2)
Progression-free survival		
5-year PFS rate (95% CI)	62.8% (57.6-67.6)	46.9% (39.8-53.6)
10-year PFS rate (95% CI)	50.8% (44.5-56.8)	29.7% (21.6-38.2)
Median (IQR)	NR (2.6-NR)	4.6 years (1.8-15.1)
Overall survival		
5-year OS rate (95% CI)	90.3% (86.9-92.9)	85.7% (80.1-89.9)
10-year OS rate (95% CI)	80.0% (74.3-84.7)	70.3% (61.3-77.6)
Median (IQR)	NR	17 years (8.18-NR)

IELSG-19: International Extranodal Lymphoma Study Group-19 study; IQR: interquartile range; LDH: serum lactate dehydrogenase; UNL: upper normal limit; IPI: International Prognostic Index; MALT-IPI: Mucosa-Associated Lymphoid Tissue lymphoma International Prognostic Index; PFS: progression-free survival, 95% CI: 95% confidence interval; OS: overall survival; NR: not reached. [a]Eastern Cooperative Oncology Group performance status reported in 282 cases in the validation set. [b]Reported in 264 cases in the validation set. [c]Assessed in only 289 patients in the test set and 168 in the validation set. [d]Defined in 281 patients in the validation set. [e]Defined in 267 patients in the validation set. [f]Other comprises: lenalidomide in combination with rituximab (15 patients), lenalidomide as a single agent (12 patients), interferon-α (4 patients), bortezomib (3 patients), thalidomide (2 patients), and ofatumomab (1 patient).

ed for proportions. The χ^2 test or Fisher exact test was used as appropriate for comparing proportions. Hazard ratios (HR) and their 95% confidence intervals (95% CI) were estimated using a Cox proportional hazard model. Multivariable analysis of clinical prognostic factors (including the international prognostic scores, IPI[12] and MALT-IPI[7]) for OS was performed by Cox regression[13] with backward stepwise selection. To identify factors associated with early POD, logistic regression was also performed with backwards stepwise selection. *P*-values <0.05 (two-sided test) were considered statistically significant.

Results

Test set

The analyzed population consisted of 401 patients enrolled in the IELSG-19 study, 131 treated with chlorambucil, 132 with chlorambucil and rituximab and 138 with rituximab; their main clinical features are summarized in Table 1. Estimated hazard curves showed that the peak risk of progression occurred within the first 24 months after diagnosis (Figure 1A). Among these 401 patients, 69 (17%) had early POD, relapsing within 24 months of starting treatment. Of the remaining 332 patients, 315 (79%) had no relapse or death during the first 24 months and form the reference group. Relapses were observed later in 64 (20%) patients in the reference group. Nine patients were lost to follow-up and eight patients died without POD within 24 months of starting treatment (Figure 2, left panel).

The median age of the 69 patients with early POD was 62 years (range: 31 to 81 years), 32 (46%) patients were male and 26 patients (38%) had a primary gastric localization (Table 2).

Early POD was most frequent in patients with Eastern Cooperative Oncology Group performance status >1 (*P*=0.042) and elevated serum LDH (*P*=0.002). Patients with early POD were more likely to have high-risk MALT-IPI scores (*P*=0.005) and high-risk IPI scores (*P*=0.013) than

the reference group. In contrast, elevated serum β_2-microglobulin level, advanced disease stage (III-IV *vs.* I-II), multiple extranodal sites of involvement, primary site of disease localization (gastric *vs.* extra-gastric), age at diagnosis (with either 60 or 70 years cut-off) were not associated with early POD. An unbalanced distribution of patients with early POD was evident across the treatment arms, with early POD occurring more frequently (34/132, 26%) in the single agent rituximab arm and less frequently in the combination treatment arm (13/125, 10%) when compared with the standard arm of single agent chlorambucil (22/127, 17%) (χ^2 test, *P*=0.006) (Table 2).

In a stepwise logistic regression (including the above-mentioned individual factors predicting early POD at univariate analysis: treatment arm, LDH concentration, performance status, high-risk IPI score, high-risk MALT-IPI score), only high-risk MALT-IPI score retained statistical significance (*P*=0.006; odds ratio: 2.39; 95% CI: 1.29-4.45).

The proportion of subjects with early POD was also higher among patients achieving partial remission after first-line therapy than among complete responders (*P*<0.0001) and, notably, transformation into aggressive histology was detected more frequently in patients with early POD than in the reference group (7/69 *vs*. 3/315; *P*<0.0001).

With a median follow-up time of 7.4 years, 18 of 69 patients with early POD died and the OS rates at 5 and 10 years after the risk-defining event were 80% (95% CI: 69-88%) and 64% (95% CI: 45-78%), respectively, in the early POD group *versus* 91% (95% CI: 87-94%) and 85% (95% CI: 79-90%), respectively, in the reference group (HR=2.42; 95% CI: 1.35-4.35; log-rank *P*=0.002) (Figure 3A).

Early POD maintained its predictive power with regards to OS (after a risk-defining event) together with a high-risk MALT-IPI score and age (as a continuous variable) in a stepwise Cox model after controlling for treatment arm, LDH concentration, performance status, disease stage, age, B-symptoms, multiple extranodal sites and high-risk IPI groups (Table 3).

Table 2. The distribution of patients' characteristics in the test and validation sets according to whether they had early progression of disease or not.

	Test set (IELSG-19)			Validation set		
	Early POD subset	Reference subset	*P*-value	Early POD subset	Reference subset	*P*-value
Number of patients	69	315		64	160	
Median age at diagnosis (IQR)	62 years (40-78)	60 years (28-80)	0.667	64 years (31-87)	60 years (23-92)	0.410
Male/female ratio	32/37	153/162	0.741	24/40	67/93	0.547
Stage III-IV, n (%)	36 (52%)	131 (42%)	0.108	41 (64%)	68 (43%)	0.004
Performance status >1, n (%)	3 (4%)	2 (1%)	0.042	5 (8%)	6 (4%)	0.300
Lactate dehydrogenase >UNL, n (%)	14 (20%)	25 (8%)	0.002	18 (31%)	16 (11%)	<0.001
β_2 microglobulin >UNL, n (%)	36 (16%)	8 (16%)	0.906	15 (41%)	39 (41%)	0.957
Primary gastric lymphoma, n (%)	26 (38%)	136 (43%)	0.403	27 (42%)	71 (44%)	0.766
IPI, high-intermediate/high risk, n (%)	20 (29%)	51 (16%)	0.013	30 (48%)	40 (26%)	0.001
MALT-IPI, high risk, n (%)	19 (28%)	43 (14%)	0.005	25 (43%)	28 (19%)	0.001
First-line treatment, n (%)						
Chemotherapy	22 (32%)	105 (33%)		42 (66%)	85 (53%)	
Immuno-chemotherapy	13 (19%)	112 (36%)		11 (17%)	42 (26%)	
Immunotherapy	34 (49%)	98 (31%)	0.006	11 (17%)	33 (21%)	0.210
Median follow-up (IQR)	6.0 years (5.2-9.4)	8.0 years (5.9-9.9)	0.024	7.0 years (3.5-10.2)	6.9 years (4.3-10.9)	0.569

IELSG-19: International Extranodal Lymphoma Study Group-19 study; POD: progression of disease; IQR: interquartile range; LDH: serum lactate dehydrogenase; UNL: upper normal limit; IPI: International Prognostic Index; MALT-IPI, Mucosa-Associated Lymphoid Tissue lymphoma International Prognostic Index. *P*-values refer to the comparison of proportions in early POD *versus* reference subsets by a χ^2 or Fisher exact test, as appropriate.

Validation set

Table 1 shows the main characteristics of the patients in the validation cohort, which comprised 287 MALT lymphoma patients who received front-line systemic treatment (chemotherapy, immunotherapy or both). The median age of this set of patients was 63 years (range: 23 to 92 years). Most of these patients were female (60%).

Estimated hazard curves showed a peak risk of progression at approximately 24 months after diagnosis (Figure 1B). After a median follow-up of 5.7 years, 64 patients (22%) had early POD. Fifty-four patients had a follow-up shorter than 2 years and nine died without prior disease progression within 2 years of starting treatment (Figure 2, right panel). Hence, the reference cohort comprised 160 patients, among whom relapses were later observed in 51 (33%). The early POD rates were similar in the groups of patients receiving different initial therapy (chemotherapy alone, rituximab alone or rituximab combined with different chemotherapeutic or immunomodulatory agents). Similar to the testing cohort, the early POD group was enriched in cases with transformation to aggressive histology (6 of 64 *vs.* 3 of 160 patients in the reference group, *P*=0.018) and early POD was most frequent in patients with elevated LDH (*P*<0.001), high-risk MALT-IPI scores

(*P*=0.001) and high-risk IPI scores (*P*=0.001) (Table 2). In addition, in the validation cohort, early POD was associated with advanced disease stage (*P*=0.004) (Table 2).

As in the IELSG-19 study cohort, the patients in the validation set who experienced early POD after systemic therapy had an increased risk of death (HR=2.15; 95% CI: 1.19-3.90; log-rank *P*=0.009). In the early-POD group, the 5-year OS rate was 70% (95% CI: 54-81%), and the 10-year OS rate was 48% (95% CI: 28-66%). In comparison, the 5-year OS rate in the reference group was 88% (95% CI: 80-93%), and the 10-year OS rate was 71% (95% CI: 58-81%) (Figure 3B).

Table 3. Multivariate analysis for overall survival in the test set (stepwise Cox model, 383 patients).

	HR	95% CI	*P*-value
Early POD	1.90	1.03-3.49	0.039
Age	1.13	1.08-1.18	<0.001
MALT-IPI high risk	2.71	1.43-5.13	0.002

HR: hazard ratio; 95% CI: 95% confidence interval; POD: progression of disease; MALT-IPI: Mucosa-Associated Lymphoid Tissue lymphoma International Prognostic Index.
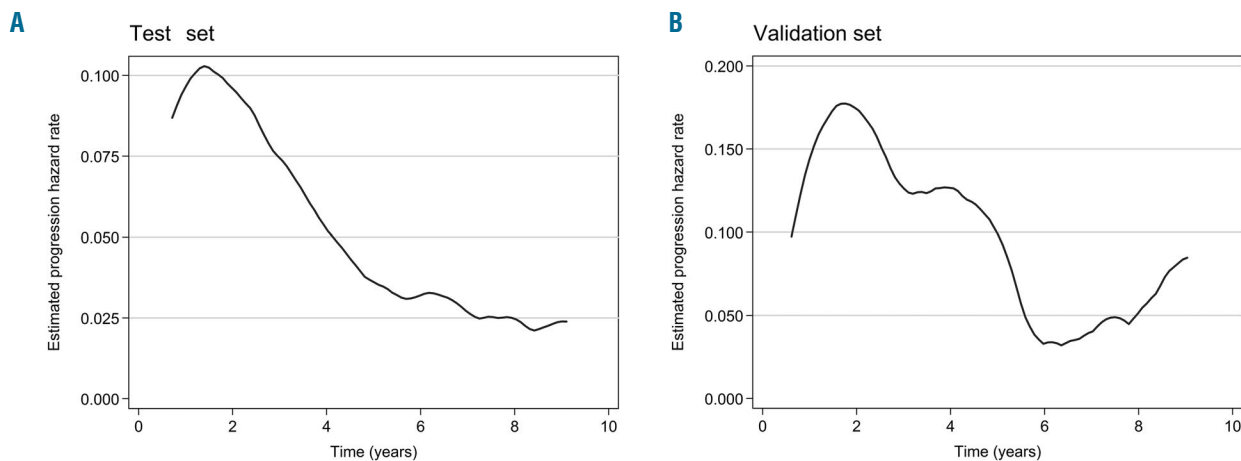
Figure 1. Risk of disease progression. (A, B) Estimated hazard of progression for patients in the test set, formed of a cohort of individuals from the International Extranodal Lymphoma Study Group-19 (IELSG-19) study (A) and for the patients included in the validation set (B).
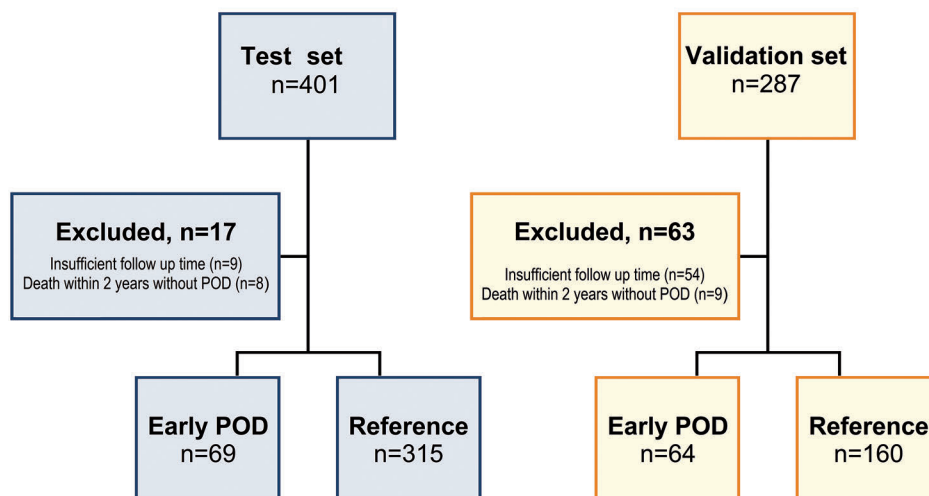
Figure 2. Patients' distribution. The selection and distribution of patients according to timing of disease progression in the test and validation sets. POD: progression of disease.

A Test set

B Validation set

Number at risk						
— No early POD	315	298	211	142	64	1
— Early POD	69	62	54	26	17	8

Number at risk						
— No early POD	160	121	84	55	36	25
— Early POD	64	44	31	20	9	6
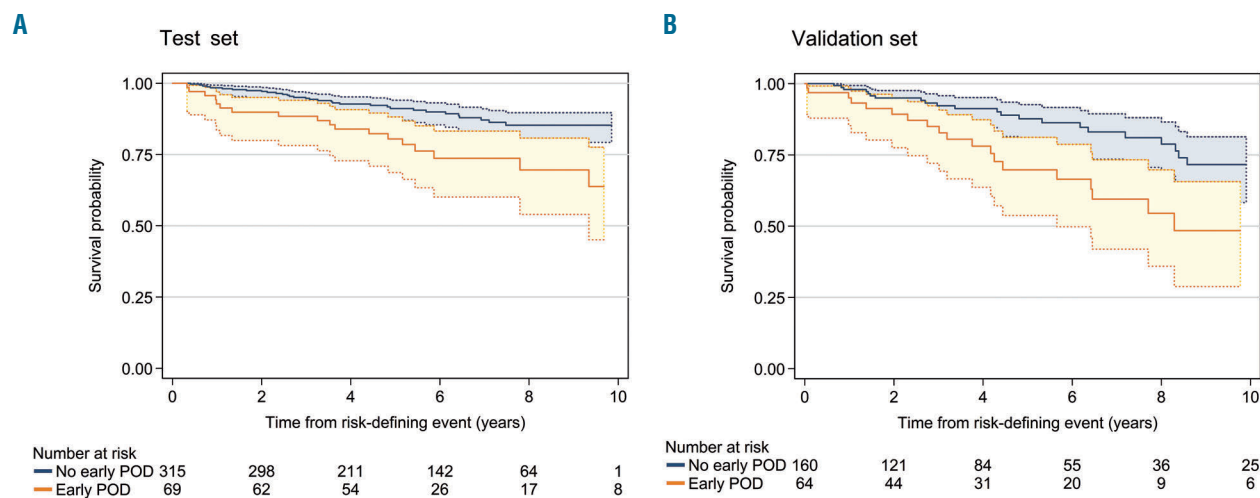
Figure 3. Overall survival. (A, B) Kaplan-Meier estimates of overall survival and their confidence intervals according to the occurrence of early progression of disease in patients enrolled in the International Extranodal Lymphoma Study Group-19 randomized clinical trial (A) and in the validation set of patients who received front-line systemic therapy (B). POD: progression of disease.

Discussion

The present study provides the first validated evidence that early POD, defined as lymphoma progression within 2 years after initial treatment, is a powerful tool to predict long-term survival in EMZL.

Early POD is a widely accepted survival predictor in follicular lymphoma,[8,14-18] with many studies showing that 20% of patients relapse within 2 years of treatment regardless of the addition of maintenance rituximab.[8] In a heterogeneous group of indolent non follicular B-cell lymphomas, a retrospective study from the Mayo Clinic and University of Iowa found that event-free survival at 12 months was associated with a better outcome.[19] However, in keeping with follicular lymphoma, the IELSG-19 study showed a PFS at 2 years of approximately 20%.[6] A large retrospective series from the University of Miami including only EMZL also showed similar PFS rates.[20] We therefore decided to maintain the 24-month time-span, already validated in follicular lymphoma, in our EMZL analysis. Our choice was further justified by the estimated hazard curves showing that the peak risk of progression occurred within 2 years.

A potential prognostic relevance of early POD was suggested by the abovementioned study from the University of Miami.[20] An observational study of non-follicular indolent lymphomas by the Italian Lymphoma Foundation (FIL) also found that early POD has a prognostic value in MZL.[21] However, none of these reports provided a thorough description of the clinical features of the EMZL patients with early POD and they did not include independent validation of their findings. Compared to these studies, the present study has additional strengths. It analyzed the impact of early POD in a cohort of patients prospectively collected in the largest controlled clinical trial performed so far in EMZL, with histological diagnosis confirmed by central pathology review and with uniformly defined follow-up investigations.

The external validation strengthens our findings. The

prognostic impact of early POD in EMZL was confirmed in an independent cohort, obtained by merging three heterogeneous series of EMZL cases.[7] which included patients treated with a variety of conventional chemotherapy regimens and immunomodulatory agents in combination with rituximab or not. We showed that our results might be applied to both gastric and extra-gastric primary lymphomas, and to patients receiving different initial therapies.

Histological transformation of MZL is a well-recognized risk factor, which affects the clinical course of the disease.[22-24] The significant proportion of cases with evidence of transformation to aggressive histologies among patients relapsing early after systemic treatment may contribute to the inferior outcome seen in this study. This observation emphasizes the need for repeated histological evaluations, in particular in the case of early relapse, since cases with transformed histology require more intensive therapy.

In conclusion, we provide novel evidence that, in patients with EMZL who received front-line systemic treatment, early POD is associated with poor survival and should be further investigated as a potentially useful endpoint in future prospective clinical trials.

References

1. Zucca E, Bertoni F. The spectrum of MALT lymphoma at different sites: biological and therapeutic relevance. Blood. 2016;127(17):2082-2092.

2. Olszewski AJ, Castillo JJ. Survival of patients with marginal zone lymphoma: analysis of the Surveillance, Epidemiology, and End Results database. Cancer. 2013;119(3):629-638.

3. Raderer M, Kiesewetter B, Ferreri AJ. Clinicopathologic characteristics and treatment of marginal zone lymphoma of mucosa-associated lymphoid tissue (MALT lymphoma). CA Cancer J Clin. 2016;66(2):153-171.

4. Isaacson PG, Chott A, Nakamura S, Muller-Hermelink HK, Harris NL, Swerdlow S. Extranodal marginal zone B-cell lymphoma of mucosa-associated lymphoid tissue (MALT lymphoma). In: Swerdlow S, Campo E, Harris NL, Jaffe ES, Pileri SA, Stein H, et al., eds. WHO Classification of Tumours of Haematopoietic and Lymphoid Tissues Lyon: IARC. 2008:214-217.

5. Thieblemont C. Clinical presentation and management of marginal zone lymphomas. Hematology Am Soc Hematol Educ Program. 2005:307-313.

6. Zucca E, Conconi A, Martinelli G, et al. Final results of the IELSG-19 randomized trial of mucosa-associated lymphoid tissue lymphoma: improved event-free and progression-free survival with rituximab plus chlorambucil versus either chlorambucil or rituximab monotherapy. J Clin Oncol. 2017;35(17):1905-1912.

7. Thieblemont C, Cascione L, Conconi A, et al. A MALT lymphoma prognostic index. Blood. 2017;130(12):1409-1417.

8. Casulo C, Byrtek M, Dawson KL, et al. Early relapse of follicular lymphoma after rituximab plus cyclophosphamide, doxorubicin, vincristine, and prednisone defines patients at high risk for death: an analysis from the National LymphoCare Study. J Clin Oncol. 2015;33(23):2516-2522.

9. Zucca E, Conconi A, Laszlo D, et al. Addition of rituximab to chlorambucil produces superior event-free survival in the treatment of patients with extranodal marginal-zone B-cell lymphoma: 5-year analysis of the IELSG-19 randomized study. J Clin Oncol. 2013;31(5):565-572.

10. Altman DG, De Stavola BL, Love SB, Stepniewska KA. Review of survival analyses published in cancer journals. Br J Cancer. 1995;72(2):511-518.

11. Bland JM, Altman DG. The logrank test. BMJ. 2004;328(7447):1073.

12. International Non-Hodgkin's Lymphoma Prognostic Factor Project. A predictive model for aggressive non-Hodgkin's lymphoma. N Engl J Med. 1993;329(14):987-994.

13. Cox DR. Regression models and life tables. J R Stat Soc. 1972;34:187-220.

14. Lockmer S, Ostenstad B, Hagberg H, et al. Chemotherapy-free initial treatment of advanced indolent lymphoma has durable effect with low toxicity: results from two Nordic Lymphoma Group trials with more than 10 years of follow-up. J Clin Oncol. 2018 Oct 4. [Epub ahead of print]

15. Jurinovic V, Kridel R, Staiger AM, et al. Clinicogenetic risk models predict early progression of follicular lymphoma after first-line immunochemotherapy. Blood. 2016;128(8):1112-1120.

16. Lansigan F, Barak I, Pitcher B, et al. The prognostic significance of PFS24 in follicular lymphoma following firstline immunotherapy: a combined analysis of 3 CALGB trials. Cancer Med. 2019;8(1):165-173.

17. Maurer MJ, Bachy E, Ghesquieres H, et al. Early event status informs subsequent outcome in newly diagnosed follicular lymphoma. Am J Hematol. 2016;91(11):1096-1101.

18. Seymour JF, Marcus R, Davies A, et al. Association of early disease progression and very poor survival in the GALLIUM study in follicular lymphoma: benefit of obinutuzumab in reducing the rate of early progression. Haematologica. 2019;104(6):1202-1208.

19. Tracy SI, Larson MC, Feldman AL, et al. The utility of prognostic indices, early events, and histological subtypes on predicting outcomes in non-follicular indolent B-cell lymphomas. Am J Hematol. 2019;94(6):658-666.

20. Alderuccio JP, Zhao W, Desai A, et al. Short survival and frequent transformation in extranodal marginal zone lymphoma with multiple mucosal sites presentation. Am J Hematol. 2019;94(5):585-596.

21. Luminari S, Marcheselli L, Defrancesco I, et al. Early progression as a predictor of survival in marginal zone lymphomas: an analysis from the prospective international NF10 study by Fondazione Italiana Linfomi. Blood. 2019;134(10):798-801.

22. Alderuccio JP, Zhao W, Desai A, et al. Risk factors for transformation to higher-grade lymphoma and its impact on survival in a large cohort of patients with marginal zone lymphoma from a single institution. J Clin Oncol. 2018 Oct 12. [Epub ahead of print]

23. Conconi A, Franceschetti S, Aprile von Hohenstaufen K, et al. Histologic transformation in marginal zone lymphomas. Ann Oncol. 2015;26(11):2329-2335.

24. Meyer AH, Stroux A, Lerch K, et al. Transformation and additional malignancies are leading risk factors for an adverse course of disease in marginal zone lymphoma. Ann Oncol. 2014;25(1):210-215.

Ferrata Storti Foundation

Prognostic impact of prevalent chronic lymphocytic leukemia stereotyped subsets: analysis within prospective clinical trials of the German CLL Study Group

Sonia Jaramillo,[1] Andreas Agathangelidis,[2] Christof Schneider,[1] Jasmin Bahlo,[3] Sandra Robrecht,[3] Eugen Tausch,[1] Johannes Bloehdorn,[1] Manuela Hoechstetter,[4] Kirsten Fischer,[3] Barbara Eichhorst,[3] Valentin Goede,[3] Michael Hallek,[3] Hartmut Döhner,[1] Richard Rosenquist,[5] Paolo Ghia,[6] Kostas Stamatopoulos[2,5] and Stephan Stilgenbauer[1]

[1]Department of Internal Medicine III, Ulm University, Ulm, Germany; [2]Institute of Applied Biosciences, Centre for Research and Technology, Thessaloniki, Greece; [3]Department I of Internal Medicine and Center of Integrated Oncology Cologne Bonn, University of Cologne, Cologne, Germany; [4]Department of Hematology, Oncology, Immunology, Palliative Care, Infectious Diseases and Tropical Medicine, München Klinik Schwabing, Munich, Germany; [5]Department of Molecular Medicine and Surgery, Karolinska Institutet, Stockholm, Sweden and [6]Università Vita-Salute San Raffaele and IRCCS Ospedale San Raffaele, Milan, Italy

ABSTRACT

Almost one-third of all patients with chronic lymphocytic leukemia (CLL) express stereotyped B-cell receptor immunoglobulins (BcR IG) and can be assigned to distinct subsets, each with a particular BcR IG. The largest stereotyped subsets are #1, #2, #4 and #8, associated with specific clinico-biological characteristics and outcomes in retrospective studies. We assessed the associations and prognostic value of these BcR IG in prospective multicenter clinical trials reflective of two different clinical situations: (i) early-stage patients ('watch and wait' arm of the CLL1 trial) (n=592); (ii) patients in need of treatment, enrolled in three phase III trials (CLL8, CLL10, CLL11), treated with different chemo-immunotherapies (n=1,861). Subset #1 was associated with del(11q), higher CLL International Prognostic Index (CLL-IPI) scores and similar clinical course to CLL with unmutated immunoglobulin heavy variable (IGHV) genes (U-CLL) in both early and advanced stage groups. IGHV-mutated (M-CLL) subset #2 cases had shorter time-to-first-treatment (TTFT) *versus* other M-CLL cases in the early-stage cohort (hazard ratio [HR]: 4.2, confidence interval [CI]: 2-8.6, *P*<0.001), and shorter time-to-next-treatment (TTNT) in the advanced-stage cohort (HR: 2, CI: 1.2-3.3, *P*=0.005). M-CLL subset #4 was associated with lower CLL-IPI scores and younger age at diagnosis; in both cohorts, these patients showed a trend towards better outcomes *versus* other M-CLL. U-CLL subset #8 was associated with trisomy 12. Overall, this study shows that major stereotyped subsets have distinctive characteristics. For the first time in prospective multicenter clinical trials, subset #2 appeared as an independent prognostic factor for earlier TTFT and TTNT and should be proposed for risk stratification of patients. (Trials registered at clinical trials.gov identifiers: *NCT00262782, NCT00281918, NCT2000769522, and NCT01010061*).

Introduction

Chronic lymphocytic leukemia (CLL) is a clinically and biologically heterogeneous disease.[1] Important prognostic markers include clinical stage (Rai and Binet), presence of deletions in the long arm of chromosome 11 (del(11q)) and in the short arm of chromosome 17(del(17p)), *TP53* gene mutations, complex karyotype (CK) as defined by ≥3 chromosomal abnormalities by conventional cytogenetics, markers of tumor load (e.g., thymidine kinase [TK], and 2-microglobulin [β2MG], and genetic parameters such as immunoglobulin heavy variable (IGHV) gene somatic

hypermutation (SHM) status, genomic aberrations, and gene mutations such as *SF3B1* and *NOTCH1* detected by next-generation sequencing (NGS).[1-4] Based on IGHV gene mutational status, CLL can be divided into mutated (M-CLL) and unmutated (U-CLL) with indolent and aggressive disease courses, respectively.[5,6]

The combinatorial and junctional diversity of the IGHV-IGHD-IGHJ recombination along with the SHM mechanism can lead to the potential synthesis of almost 10^{12} different IG. At odds with this diversity, the B-cell receptor (BcR) IG of about one-third of CLL display highly homologous variable heavy complementarity-determining region 3 (VH CDR3), which led to their being grouped into different subsets carrying (almost) identical alias stereotyped BcR IG.[7-12] Subset #1 represents approximately 5% of U-CLL and is characterized by the combination of a heavy chain IGHV1-5-7/IGHD6-19/IGHJ4 gene rearrangement with a light chain IGKV1-39/IGKJ1-2 gene rearrangement.[10] The IGHV gene bears little or no SHM and the VH CDR3 length is 13 amino acids (aa) long. Subset #1 is associated with a poor outcome in terms of patient survival and short time-to-first-treatment (TTFT) in comparison to U-CLL using the same IGHV genes.[13-15] Subset #2 represents 3% of all CLL and is defined by the IGHV3-21/IGLV3-21 combination with a short VH CDR3 of 9 aa.[10] Of note, subset #2 comprises both U-CLL and M-CLL cases and has been associated with an aggressive clinical course, irrespective of SHM status.[16-18] Subset #4 is the largest subset of M-CLL, carrying a BcR IG that consists of a heavy chain IGHV4-34/IGHD5-18/IGHJ6 gene rearrangement (20 aa long VH CDR3) and a light chain IGKV2-30/IGKJ1-2 rearrangement.[10] In previous studies, subset #4 was associated with indolent disease, enriched in young patients, and a long TTFT.[11,15,19] Finally, subset #8 is composed of cases with unmutated IGHV4-39/IGHD6-13/IGHJ5 gene rearrangements. Furthermore, in a case control study, a strong association with Richter syndrome and poor outcome was reported.[8,20]

Using the data of four prospective multicenter clinical trials of the German CLL study group (GCLLSG), the primary objective of the current study was to search for associations between the most common and best characterized CLL stereotyped subsets (#1, 2, 4 and 8) and disease characteristics as well as outcome, and also compare these findings against non-subset U-CLL and M-CLL. The secondary objective was to study the prognostic value of subset #2 irrespective of its IGHV mutational status.

Methods

Study population

To assess the prognostic value of the most prevalent CLL subsets, we evaluated patients recruited in four randomized phase III trials conducted by the GCLLSG. None of the patients had received any prior treatment and all had a diagnosis of CLL according to the International Workshop on Chronic Lymphocytic Leukemia criteria.[1] All trials were approved by the leading ethics committee. Written informed consent was obtained from all patients according to the Declaration of Helsinki. To provide data about the clinical course of newly diagnosed patients not requiring treatment, we evaluated an "early-stage CLL cohort" of 710 asymptomatic Binet stage A patients from the CLL1-trial (*clinical trials.gov identifier:* NCT00262782). The study compared a 'watch and wait' strategy to upfront fludarabine (F) monotherapy.[21] In

total, 639 (90.0%) patients were followed with the 'watch and wait' approach. Patients treated with F (71, 10.0%) were excluded from our analyses.

To evaluate the clinical course of patients needing treatment, we evaluated an "advanced-stage cohort" from three phase III trials enrolling patients with CLL requiring front-line treatment. The CLL8-trial (*clinical trials.gov identifier: NCT00281918*) included 817 fit patients and compared fludarabine and cyclophosphamide (FC) to FC plus rituximab (FCR).[22,23] The CLL10-study (*clinical trials.gov identifiers: NCT00262782 and NCT2000769522*) included 561 fit patients and compared FCR to bendamustine and rituximab.[24] Finally, the CLL11-study (*clinical trials.gov identifier: NCT01010061*) enrolled 781 unfit patients and compared chlorambucil with or without rituximab or obinutuzumab.[25]

To evaluate the first objective, we classified patients into six groups: subsets #1, #2, #4, #8, non-subset M-CLL, and U-CLL. To evaluate the second objective, we classified patients into three categories: (i) subset #2; (ii) IGHV3-21 rearrangement not meeting the subset #2 criteria ("IGHV3-21"); and (iii) all other cases ("IGHV"). Each group was sub-divided into mutated ("m") and unmutated ("u") cases, resulting in six subgroups.

Biological markers and clinical characteristics

Baseline clinical and laboratory characteristics evaluated for associations and potential prognostic relevance are listed in Tables 1 and 2. Detailed descriptions of the diagnostic methods have been published previously.[3,8,26-30]

Statistical analysis

Time-to-first-treatment was defined as the time between diagnosis and date of first treatment. For the advanced stage CLL cohort, time-to-next-treatment (TTNT), progression-free survival (PFS) and overall survival (OS) were calculated from randomization to the initiation of subsequent treatment, disease progression or death, and death, respectively. For the early stage cohort, PFS and OS were calculated from diagnosis. Subjects without an event were censored at the time of last assessment. Survival rates were estimated using the Kaplan-Meier method and compared using non-stratified log-rank tests. Hazard ratios and 95% confidence intervals were calculated using Cox proportional hazards regression model.[31] All variables that showed significant association with TTFT, TTNT, PFS or OS in univariate Cox regression analyses were included in multivariable analyses applying forward and backward stepwise selection procedures. Adjustments for multiple testing were not applied and all reported *P*-values have an exploratory character. We performed two analyses in both cohorts. In the first one, we compared subsets #1, 2, 4 and 8 individually to non-subset U-CLL and M-CLL, and in the second one, we evaluated the prognostic value of subset #2 in terms of mutational status and IGHV3-21 usage.

Results

Subset assignment and distribution overview

Of 639 patients from the CLL1 'watch and wait' cohort, immunogenetic data were available for 592 (92.6%); 402 (67.9%) patients carried mutated IGHV genes and 190 (32.1%) patients expressed unmutated IGHV genes. Eight cases (1.35%) were assigned to subset #1, 16 cases (2.7%) to subset #2, 8 cases (1.35%) to subset #4, and 2 cases (0.34%) to subset #8. With regard to the rest of the cases, 174 (29.4%) belonged to non-subset U-CLL and 384 (64.9%) to M-CLL. For the second analysis differentiating the impact of subset #2, we found 29 cases (4.9%)

Table 1. Baseline characteristics early stage chronic lymphocytic leukemia (CLL) according to subset assignment.

	Subset #1	Subset #2	Subset #4	Subset #8	u-IGHV	m-IGHV	All
Target analysis population, n (%)	8 (1.35%)	16 (2.7%)	8 (1.35%)	2 (0.337%)	174 (29.39%)	384 (64.86%)	592
Age at study entry (years) median (range)	64 (56-70)	62 (45-75)	58 (41-72)	61 (56-66)	60 (37-75)	60 (32-75)	60 (32-75)
Gender, n (%) male	6 (75.0)	6 (37.5)	4 (50.0)	1 (50.0)	114 (65.5)	233 (60.7)	364 (61.5)
ECOG performance status median (range)	0 (0-0)	0 (0-1)	0 (0-0)	0 (0-0)	0 (0-1)	0 (0-2)	0 (0-2)
CLL-IPI risk group, n (%)	8	15	8	2	160	371	564
Low	0 (0.0)	9 (60.0)	8 (100.0)	0 (0.0)	0 (0.0)	347 (93.5)	364 (64.5)
Intermediate	6 (75.0)	6 (40.0)	0 (0.0)	2 (100.0)	130 (81.3)	16 (4.3)	160 (28.4)
High	2 (25.0)	0 (0.0)	0 (0.0)	0 (0.0)	26 (16.3)	7 (1.9)	35 (6.2)
Very high	0 (0.0)	0 (0.0)	0 (0.0)	0 (0.0)	4 (2.5)	1 (0.3)	5 (0.9)
Leukocyte count (x 10⁹/L) median (range)	36.9 (19.2-128.7)	23.9 (4.7-94.4)	21.3 (4.7-94.4)	10.7 (8.9-12.4)	23.3 (4.6-184.0)	20.4 (6.3-184.2)	21.2 (4.6-184.2)
Serum thymidine kinase c(U/L) median (range)	13.0 (3.5-109.0)	8.9 (2.9-23.9)	3.8 (2.0-6.5)	8.6 (6.5-10.6)	7.3 (2.0-56.0)	5.1 (1.1-80.0)	5.7 (1.1-109.0)
Serum β2-microglobulin(MG/L) median (range)	2.3 (1.6-6.7)	2.8 (1.1-4.4)	1.5 (1.0-3.4)	1.8 (1.3-2.3)	2.0 (0.2-9.4)	1.7 (0.4-8.9)	1.8 (0.2-9.4)
Deletion 11Q by FISH, n (%)	3 (37.5)	1 (6.7)	0 (0.0)	0 (0.0)	32 (19.6)	5 (1.3)	39 (6.9)
Deletion 17P by FISH, n (%)	0 (0.0)	0 (0.0)	0 (0.0)	0 (0.0)	7 (4.3)	8 (2.1)	15 (2.7)
Trisomy 12 by FISH, n (%)	1 (12.5)	0 (0.0)	1 (12.5)	2 (100.0)	33 (20.0)	20 (5.3)	51 (9.1)
Deletion 13Q by FISH, n (%)	3 (37.5)	9 (60.0)	2 (25.0)	1 (50.0)	87 (52.4)	250 (67.2)	295 (52.4)
NOTCH1 MUTATED, n (%)	2 (25.0)	1 (6.7)	0 (0.0)	1 (50.0)	10 (6.6)	4 (1.1)	18 (3.4)
SF3B1 MUTATED, n (%)	2 (25.0)	8 (53.3)	0 (0.0)	0 (0.0)	17 (11.3)	11 (3.1)	38 (7.1)
Richter syndrome status, n (%)	0	0	0	0	4 (2.3)	5 (1.3)	9 (1.5)

n: number of cases; u: unmutated; m: mutated; IGHV: non-subset immunoglobulin heavy variable; ECOG: Eastern Cooperative Oncology Group; IPI: International Prognostic Index;FISH: fluorescence *in situ* hybridization.

expressing the IGHV3-21 gene. Among those, 16 cases (2.7%) belonged to subset #2, of which 6 cases (1%) were u-subset #2 and 10 cases (1.7%) were m-subset #2. The remaining 13 cases (2.2%) carried heterogeneous (non-subset) BcR IG (IGHV3-21). Of these, 3 (0.5%) were u-IGHV3-21 and 10 (1.7%) were m-IGHV3-21 (*Online Supplementary Table S1*).

For patients requiring front-line treatment from the CLL8, CLL10 and CLL11 trials or advanced stage cohort, immunogenetic data were available in 1,861 cases (86.2%), of which 39 (2.1%) were assigned to subset #1, 61 (3.3%) to subset #2, 11 (0.6%) to subset #4, and 16 (0.9%) to subset #8. The remaining 1,734 cases did not belong to these subsets; 1,088 (58.4%) were U-CLL and 646 (34.7%) cases were M-CLL. For the second analysis, we identified 126 cases (6.8%) expressing IGHV3-21 BcR IG. Of these, 61 (3.3%) were assigned to subset #2, 18 (1.0%) were u-subset #2, and 43 (2.3 %) m-subset #2, while 65 (3.5%) cases belonged to the group expressing heterogeneous IGHV3-21. Of these, 35 (1.9%) were u-IGHV3-21 and 30 (1.6%) were m-IGHV3-21 (*Online Supplementary Table S2*).

Association of subsets with clinical and biological characteristics

Clinical and biological characteristics in the early stage CLL cohort according to subset assignment and IGHV mutational status are listed in Table 1. Despite the size of the overall cohort, small case numbers in patient subgroups precluded valid statistical assessment, but a pattern similar to that observed in the advanced stage cohort (see below) was seen. Subset #1 showed a high frequency of del(11q) and *NOTCH1* mutations, subset #2 had a lower rate of male patients and a high frequency of *SF3B1* mutations, and subset #4 were younger at study entry. Both cases of subset #8 had trisomy 12 and intermediate risk according to CLL-IPI, and neither of them displayed a Richter transformation. In the second analysis, when we compared m-subset #2 with m-IGHV3-21 and m-IGHV, we found an imbalance of *SF3B1* mutations (*P*<0.001) and a higher presence of del(11q) (*P*=0.014).

The clinical and biological characteristics of the advanced stage cohort according to BcR IG stereotype and IGHV SHM status are listed in Table 2. Subset #1 together with subset #8 showed higher frequencies of NOTCH1 mutations and del(11q). Subset #2 demonstrated an enrichment for *SF3B1* mutations. As in the early stage cohort, subset #4 were younger at diagnosis. Finally, subset #8 showed a higher frequency of Richter transformation. In the second analysis, we observed a higher prevalence of del(13q) in u-subset #2 (88.9%) compared to the u-IGHV3-21 (46.9%) and u-IGHV patients (45.1%, *P*=0.001). A higher frequency of *SF3B1* mutations was also seen in subset #2 patients independently of the IGHV SHM status (u-subset #2, 41.7 % and m-subset #2, 46.7%, respectively). M-subset #2 showed a higher prevalence of del(11q) compared to m-IGHV3-21 and m-IGHV (32.5% *vs.* 13.3% *vs.* 5.5%, respectively).

Association between stereotyped subsets and clinical outcomes

After a median observation time of 97.8 (range, 2.5-166.9) months (ms) of the early stage cohort, there were 246, 362 and 106 events for TTFT, PFS, and OS, respec-

Table 2. Baseline characteristics of the advanced stage chronic lymphocytic leukemia (CLL) cases according to subset classification.

	Subset #1	Subset #2	Subset #4	Subset #8	u-IGHV	m-IGHV	All
Target analysis population, n (%)	39 (2.09%)	61 (3.28%)	11 (0.59%)	16 (0.86%)	1088 (58.46%)	646 (34.71%)	1,861
Age at study entry (years) median (range)	66 (43-84)	66 (48-88)	52 (42-74)	67 (35-84)	65 (30-90)	65 (36-89)	65 (30-90)
Gender, n (%) Male	24 (61.5)	36 (59.0)	6 (54.5)	8 (50.0)	775 (71.2)	437 (67.6)	1286 (69.1)
ECOG performance status median (range)	0.5 (0-2)	1 (0-2)	1 (0-1)	0.5 (0-2)	1 (0-3)	0 (0-3)	1 (0-3)
Binet stage, n (%)	39	61	11	16	1087	646	1860
A	6 (15.4)	7 (11.5)	1 (9.1)	2 (12.5)	180 (16.6)	112 (17.3)	308 (16.6)
B	20 (51.3)	33 (54.1)	6 (54.5)	11 (68.8)	568 (52.3)	243 (37.6)	881 (47.4)
C	13 (33.3)	21 (34.4)	4 (36.4)	3 (18.8)	339 (31.2)	291 (45.0)	671 (36.1)
CLL-IPI risk group, n (%)	38	57	11	16	1029	593	1744
Low	1 (2.6)	18 (31.6)	7 (63.6)	0 (0.0)	0 (0.0)	252 (42.5)	278 (15.9)
Intermediate	10 (26.3)	19 (33.3)	3 (27.3)	4 (25.0)	388 (37.7)	228 (38.4)	652 (37.4)
High	26 (68.4)	18 (31.6)	1 (9.1)	12 (75.0)	534 (51.9)	105 (17.7)	696 (39.9)
Very high	1 (2.6)	2 (3.5)	0 (0.0)	0 (0.0)	107 (10.4)	8 (1.3)	118 (6.8)
Leukocyte count (x 10^9/L)	104.7	72.3	73.5	56.4	85.3	65.9	79.1
median (range)	(13.7-375.0)	(3.1-492.0)	(19.2-144.1)	(12.9-118.0)	(0.2-867.0)	(3.1-741.9)	(0.2-867.0)
Serum thymidine kinase c(U/L)	26.6	20.2	10.2	55.9	19.2	11.3	16.5
median (range)	(0.5-330.6)	(0.0-163.0)	(4.1-36.3)	(0.5-165.3)	(0.0-848.0)	(0.0-970.0)	(0.0-970)
Serum β2-microglobulin (MG/L)	3.4	3.0	2.2	3.8	3.0	2.8	3.0
median (range)	(0.6-8.1)	(0.0-9.8)	(0.5-5.1)	(0.3-8.1)	(0.0-17.8)	(0.0-12.2)	(0.0-17.8)
Deletion 17P by FISH, n (%)	1 (2.6)	0 (0.0)	0 (0.0)	0 (0.0)	79 (7.5)	21 (3.4)	101 (5.6)
Deletion 11Q by FISH, n (%)	17 (43.6)	18 (31.0)	0 (0.0)	6 (37.5)	316 (29.8)	37 (6.0)	378 (21.0)
Trisomy 12 by FISH, n (%)	4 (10.3)	2 (3.4)	1 (9.1)	11 (68.8)	163 (15.4)	80 (13.0)	222 (12.3)
Deletion 13Q by FISH, n (%)	23 (59.0)	49 (84.5)	6 (54.5)	2 (12.5)	477 (45.1)	409 (66.3)	648 (36.0)
TP53 mutated, n (%)	1 (3.8)	2 (4.8)	0 (0.0)	0 (0.0)	103 (13.6)	30 (6.9)	136 (10.6)
NOTCH1 mutated, n (%)	4 (16.0)	2 (4.8)	0 (0.0)	5 (38.5)	154 (20.5)	20 (4.7)	185 (14.6)
SF3B1 mutated, n (%)	0 (0.0)	19 (45.2)	0 (0.0)	0 (0.0)	131 (17.4)	52 (12.1)	202 (15.9)
Richter syndrome status, n (%)	1 (2.6)	2 (3.3)	0	1 (6.3)	35 (3.2)	14 (2.2)	53 (2.8)

n: number of cases; u: unmutated; m: mutated; IGHV: non-subset immunoglobulin heavy variable; ECOG: Eastern Cooperative Oncology Group; IPI: International Prognostic Index; FISH: fluorescence *in situ* hybridization.

tively. TTFT was significantly longer in M-CLL as compared to U-CLL (*P*<0.001). Subset #4 had a longer TTFT compared to subsets #1, #2 and #8 (*P*=0.002), but similar to M-CLL (*P*=0.338) (Figure 1A). Therapy was needed only for 1 of 8 patients assigned to subset #4. Statistically, there was no difference in TTFT between subsets #1, 2 and 8, and U-CLL (*P*=0.204) (Figure 1A). Regarding PFS, a significant difference was observed between M-CLL and U-CLL (*P*<0.001). Subset #4 had a longer PFS than subsets #1, 2 and 8 (*P*=0.014) that was similar to M-CLL cases (*P*=0.249), with only two patients progressing. Subsets #1, 2, 8 and U-CLL had a similar PFS (*P*=0.198) (Figure 1B). Regarding OS, M-CLL had a significantly longer time to event compared to U-CLL (*P*<0.001). Subsets #1, 2, 4, and 8 showed no statistically significant differences in terms of OS; however, the OS curves followed a similar pattern to that observed for PFS and TTFT with subsets #1, 2, and 8, showing more events as compared to subset #4 where no incidents of death were observed (Figure 1C).

During a median observation time of 55.1 ms of the advanced stage cohort, there were 1,847, 1,258, 739 and 512 events for TTFT, PFS, TTNT, and OS, respectively. TTFT was longer for M-CLL as compared to U-CLL (*P*<0.001). Subset #4 had a similar TTFT to that of M-CLL that was longer as compared to subsets #1, 2 and 8

(*P*=0.009). Subsets #1, 2 and 8 had a similar TTFT as U-CLL (Figure 2A). Regarding PFS, M-CLL had a longer time to event compared to U-CLL (*P*<0.001). Subset #4 patients had a longer PFS compared to subsets #1, 2, and 8; however; this difference was not statistically significant. Subset #8 had a shorter PFS compared to subsets #1, 2 and U-CLL (*P*=0.042) (Figure 2C). Regarding TTNT, M-CLL had a longer time to event compared to U-CLL (*P*<0.001). No subset #4 patient needed subsequent therapy during the observation time and TTNT was longer as compared to subsets #1, 2, and 8 (*P*=0.027). Subset #4 also had a longer TTNT compared to M-CLL without reaching statistical significance (*P*=0.058) (Figure 2B). Regarding OS, we observed a significant difference between M-CLL and U-CLL (*P*<0.001). None of the subset #4 patients died before time of analysis; subset #4 patients had a longer OS than subsets #1, 2 and 8 (*P*=0.011) (Figure 2D).

Cases expressing IGHV3-21: subset #2 and others

In the cohort of early stage CLL patients, m-subset #2 had a significantly shorter TTFT compared to m-IGHV3-21 and m-IGHV patients (*P*<0.001). While m-subset #2 had an outcome similar to that of the u-IGHV group (*P*=0.794), m-IGHV3-21 was comparable to m-IGHV (Figure 3A). Similarly, PFS was shorter in m-subset #2

Figure 1. Outcomes of early stage chronic lymphocytic leukemia (CLL) cases according to subset classification. (A) Median time-to-first-treatment (TTFT) subset #1: 33.7 months, subset #2: 65.0 months, subset #4: not reached, subset #8: 26.3 months, U-CLL: 52.2 months, M-CLL: not reached. (B) Median progression-free survival (PFS) from diagnosis subset #1: 15.9 months, subset #2: 22.8 months, subset #4: not reached, subset #8: 25.7 months, U-CLL: 28.8 months, M-CLL: 92.6 months. (C) Median overall survival (OS) from diagnosis subset #1: 112.5 months, subset #2: not reached, subset #4: not reached, subset #8: 49.0 months, U-CLL: not reached, M-CLL: not reached; Cum: cumulative.

compared to m-IGHV3-21 and m-IGHV cases, but did not reach statistical significance (P=0.161). However, the u-subset #2 cases had a shorter time to event compared to u-IGHV3-21 and u-IGHV (P=0.006) (Figure 3B). Regarding OS, there was no significant difference between m-subset #2, m-IGHV3-21 and m-IGHV (P=0.221) (Figure 3C); however, small event numbers precluded robust comparisons despite the long observation time.

In the advanced stage cohort, m-subset #2 cases had a shorter TTFT compared to m-IGHV3-21 and m-IGHV (P=0.056), and showed similar behavior to that of the u-IGHV group (P=0.215). u-IGHV3-21 patients showed a shorter TTFT compared to u-subset #2 and u-IGHV cases (P=0.050) (Figure 4A). Similarly, m-subset #2 cases showed a shorter TTNT than m-IGHV3-21 and m-IGHV patients (P=0.001). Furthermore, m-subset #2 had a similar clinical course to u-IGHV cases in terms of TTFT (P=0.401) (Figure 4B). No difference was observed between u-IGHV3-21, u-subset #2 and u-IGHV (P=0.536). In the PFS analysis, m-subset #2 showed a significantly shorter PFS compared to m-IGHV3-21 and m-IGHV (P=0.020) (Figure 4C). No difference was observed between m-subset #2 and u-IGHV (P=0.065) (Figure 4C). Regarding OS, we observed no significant difference in terms of survival rate at 5 years between m-subset #2, m-IGHV3-21 and m-IGHV or u-subset #2, u-IGHV3-21 and u-IGHV (P=0.717, P=0.752, respectively) (Figure 4D).

Multivariate analyses

Due to the resemblance in all clinical outcomes, the sim-

ilarities between subsets (Figures 1 and 2) and the small size of the subset population, we grouped subsets #1, 2 and 8 together to be able to analyze their relevance as a group in the clinical outcomes of interest. Subset #4 was analyzed as part of M-CLL for the same reasons. We compared this group of subsets to M-CLL and U-CLL. In a supplementary analysis, we also compared subset #2 to subsets #1 and 8 as well as to M-CLL and U-CLL.

A Cox multivariate regression analysis was chosen to adjust for the variables that were significant in the univariate analysis.

For the early stage cohort, the variables included in the final model for TTFT are listed in Table 3. M-CLL and subset #4 had a longer TTFT compared to subsets #1, 2 and 8 (P<0.01). In the supplementary analysis, subset #2 alone showed the same differences (*Online Supplementary Table S3*). M-CLL and subset #4 had also a longer PFS and OS compared to the group of subsets (hazard ratio [HR]:0.44, confidence interval [CI]: 0.272-0.712, P=0.001 and HR:0.431, CI: 0.19-0.978, P<0.044, respectively). In a second multivariate analysis, we tested for the independent value of the m-subset #2 subgroup, including the variables listed in Table 4. This identified m-subset #2 as an independent adverse prognostic marker for shorter TTFT as compared to m-IGHV (P<0.001) (Table 4). For the PFS multivariate analysis, we observed no differences between m-subset #2 and m-IGHV or m-IGHV3-21 and m-IGHV (P=0.556).

In the advanced stage cohort, the TTNT final model found a significant difference between M-CLL and subsets

Figure 2. Outcomes of advanced stage chronic lymphocytic leukemia (CLL) cases according to subset classification. (A) Median time-to-first-treatment (TTFT) for the subset #1: 20.6 months, subset #2: 28.5 months, subset #4: 42.8 months, subset #8: 5.5 months, U-CLL: 17.8 months, M-CLL: 36.1 months. (B) Median time-to-next-treatment (TTNT) for the subset #1: 60.2 months, subset #2: 57.3 months, subset #4: not reached, subset #8: 43.7 months, U-CLL: 47.4 months, M-CLL: not reached. (C) Median progression-free survival (PFS) for subset #1: 41.7 months, subset #2: 33.3 months, subset #4: not reached, subset #8: 26.3 months, U-CLL: 26.5 months, M-CLL: 54.7 months. (D) Median overall survival (OS) for subset #1: 67.5 months, subset #2: not reached, subset #4: not reached, subset #8: 43.3 months, U-CLL: 78.9 months, M-CLL: not reached; Cum: cumulative.

#1, 2 and 8 (HR: 0.53, CI: 0.38-0.74, $P<0.001$). This same pattern was also seen when M-CLL was compared to subset #2 alone; however, this difference was not statistically significant ($P=0.052$) (*Online Supplementary Table S4*). U-CLL had a significantly shorter PFS compared to subsets #1, 2 and 8 ($P=0.028$) as opposed to M-CLL that showed a significantly longer PFS ($P=0.002$) (*Online Supplementary Table S5*). In the supplementary analysis, U-CLL also had a shorter PFS compared to subset #2 ($P<0.05$) (*Online Supplementary Table S6*). In the OS final model, we observed a significant difference between M-CLL and subsets #1, 2 and 8 ($P=0.002$). In the second analysis, we found a statistically significant difference between TTNT in m-subset #2 and m-IGHV ($P=0.005$) (*Online Supplementary Table S7*). With regards to PFS, no differences were found between m-subset #2 and m-IGHV ($P=0.122$).

Discussion

Our study evaluated the impact of BcR IG stereotype on four relevant clinical outcomes (TTFT, TTNT, PFS, and OS) with a sufficient follow-up period in four major CLL stereotyped subsets, i.e., subsets #1, 2, 4 and 8. Two different clinical scenarios were considered in the present analysis: early stage patients with CLL included in the 'watch and wait' arm of the CLL1 study, and advanced stage, treatment-naïve patients with CLL treated within three clinical trials of the GCLLSG. The analysis was performed in patients within prospective clinical trials, where the information regarding the most relevant clinical and genetic characteristics of subsets #1, 2, 4 and 8 could be analyzed in a controlled setting with mature follow-up.

Subset #1 had a similar prognosis to U-CLL in both early stage and advanced stage CLL patients. These findings were consistent with previous publications, where this subset has been associated with a poor prognosis in terms of survival and TTFT even when compared to CLL with the same IGHV genes but a heterogenous BcR IG.[14]

Subset #2 patients are known to have a shorter TTFT as well as OS regardless of IGHV mutational status.[15,33,34] In our study, we observed this same behavior in both early and advanced stage CLL. Furthermore, consistent with previous publications, we found that subset #2 cases had a higher rate of *SF3B1* mutations in both the *IGHV* mutat-

ed and unmutated state, which, however, does not seem to explain the unfavorable clinical prognosis.[29,32,33]

It has been reported that subset #2 has a higher progression rate to disease requiring treatment and also a shorter OS.[15,33,34] In our analysis, in both early and advanced stage CLL, m-subset #2 showed higher presence of del(11q) and unfavorable prognosis compared to other IGHV-mutated CLL cases. This difference was also observed in a multivariate analysis, where m-subset #2 patients had a worse outcome compared to m-IGHV with regards to TTFT in early stage CLL, and TTNT in advanced stage CLL

patients. Our data showed for the first time in clinical studies that subset #2 is an independent prognostic factor for earlier TTFT in early stage CLL. There was a significant difference in TTFT between mutated subsets #2 and m-IGHV in both the univariate and multivariate analysis. This finding was also based on multiple validation analyses that corroborated our results. Therefore, it is safe to say that the conclusion is valid despite the small sample. No significant differences were observed between m-subset #2, m-IGHV3-21 and m-IGHV in early or advanced stage CLL in terms of PFS or OS. This implies that patients
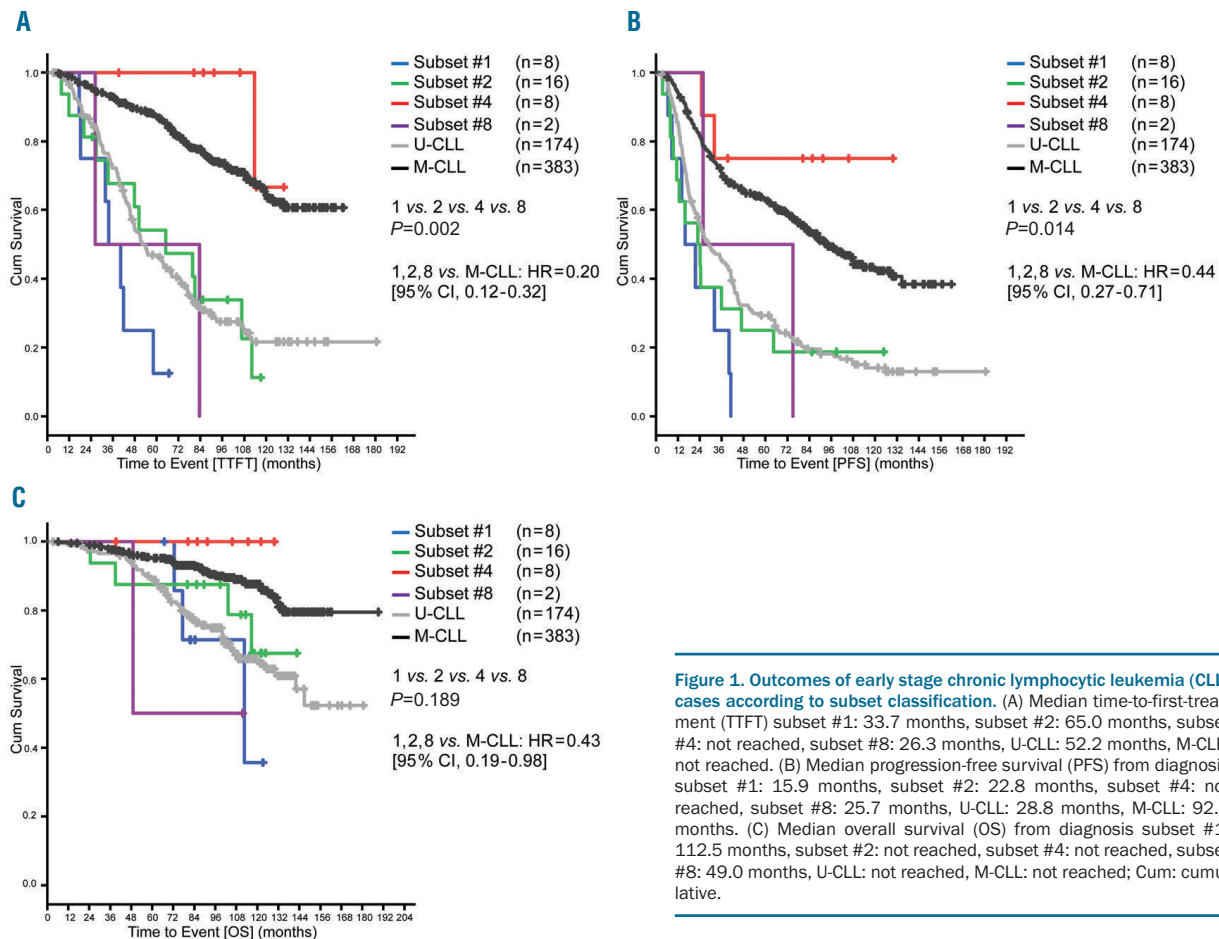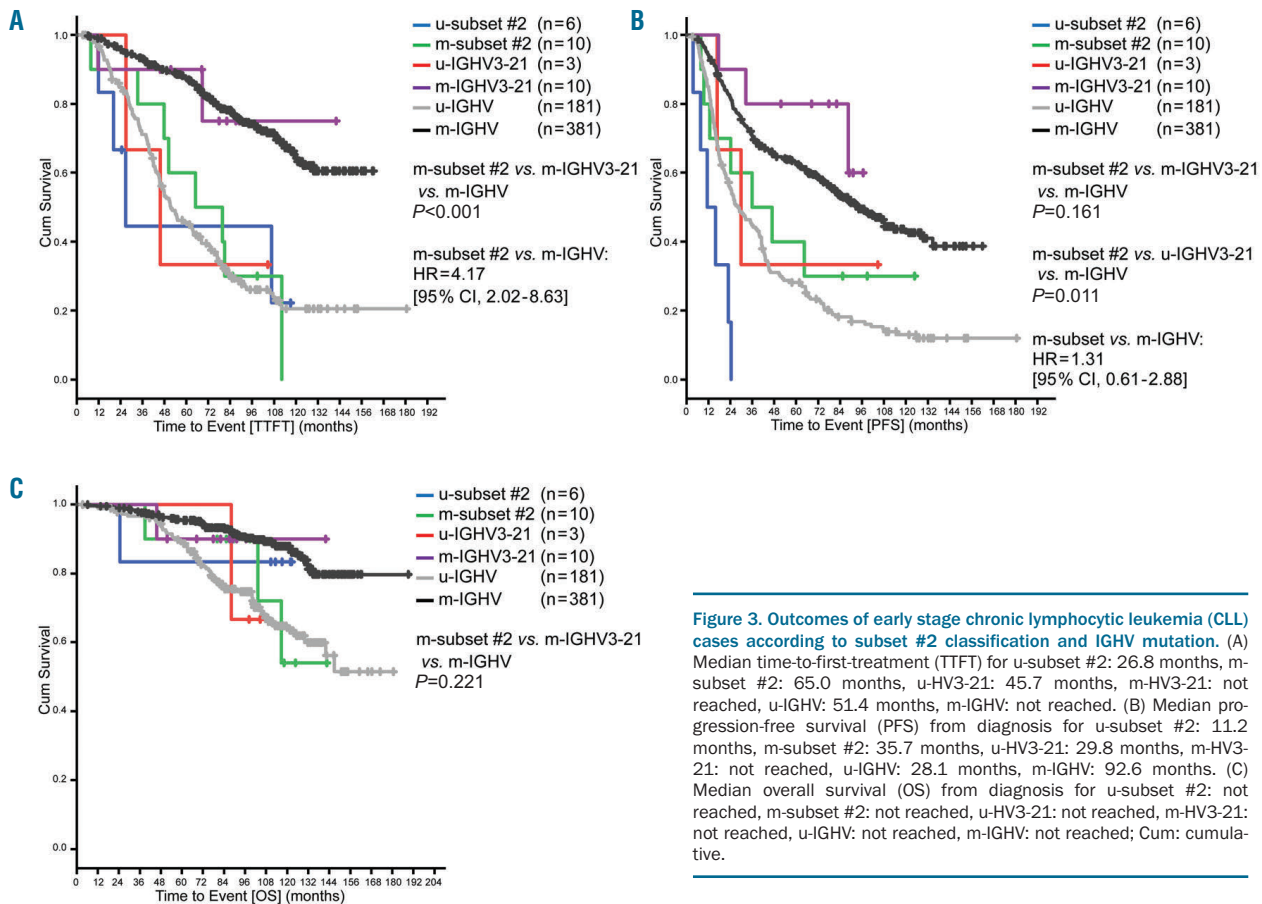

Figure 3. Outcomes of early stage chronic lymphocytic leukemia (CLL) cases according to subset #2 classification and IGHV mutation. (A) Median time-to-first-treatment (TTFT) for u-subset #2: 26.8 months, m-subset #2: 65.0 months, u-HV3-21: 45.7 months, m-HV3-21: not reached, u-IGHV: 51.4 months, m-IGHV: not reached. (B) Median progression-free survival (PFS) from diagnosis for u-subset #2: 11.2 months, m-subset #2: 35.7 months, u-HV3-21: 29.8 months, m-HV3-21: not reached, u-IGHV: 28.1 months, m-IGHV: 92.6 months. (C) Median overall survival (OS) from diagnosis for u-subset #2: not reached, m-subset #2: not reached, u-HV3-21: not reached, m-HV3-21: not reached, u-IGHV: not reached, m-IGHV: not reached; Cum: cumulative.

Table 3. Time-to-first-treatment (TTFT) Cox regression in early stage chronic lymphocytic leukemia (CLL) subsets # 1, 2 and 8.

Cox regression TTFT	Univariable comparison	Hazard ratio	95% confidence interval		P
			Lower	Upper	
Subset and IGHV analysis group					
U-CLL	*vs.* Subset #1,2,8	0.812	0.504	1.308	0.392
M-CLL and subset #4	*vs.* Subset #1,2,8	0.195	0.119	0.318	< 0.001
Deletion in 17p					
Yes	*vs.* no	2.332	1.287	4.224	0.005
Deletion in 11q					
Yes	*vs.* no	1.765	1.182	2.635	0.005
Leukocyte count (x 10^9/L)					
≥ 50	*vs.* < 50	3.197	2.251	4.541	< 0.001
Lymphocyte doubling time					
≤ 12 months	*vs.* > 12 months	2.178	1.632	2.907	< 0.001

TTFT: time to first treatment; U: unmutated; M: mutated; IGHV: immunoglobulin heavy variable; HR: hazard ratio.

belonging to subset #2 should have closer clinical follow-up, and, in particular, that patients of m-subset #2 should be considered as high risk despite their formal assignment to the M-CLL group. Correspondingly, this indicates that the BcR IG structure determined by subset assignment may be more important in determining disease biology

Table 4. Time-to-first-treatment (TTFT) Cox regression in early stage chronic lymphocytic leukemia (CLL) subset #2.

Cox regression TTFT	Univariable comparison	Hazard ratio	95% confidence interval		P
			Lower	Upper	
IGHV analysis group					
M-IGHV3-21	*vs.* m-IGHV	1.105	0.271	4.498	0.889
M-subset #2	*vs.* m-IGHV	4.172	2.017	8.628	< 0.001
U-IGHV	*vs.* m-IGHV	4.308	3.253	5.705	< 0.001
Deletion in 17p					
Yes	*vs.* no	2.305	1.273	4.172	0.006
Deletion in 11q					
Yes	*vs.* no	1.749	1.169	2.615	0.006
Leukocyte count (x10⁹/L)					
≥ 50	*vs.* < 50	3.209	2.260	4.556	< 0.001
Lymphocyte doubling time					
≤ 12 months	*vs.* > 12 months	2.181	1.633	2.912	< 0.001

TTFT: time to first treatment; U: unmutated; M: mutated; IGHV: immunoglobulin heavy variable; HR: hazard ratio.

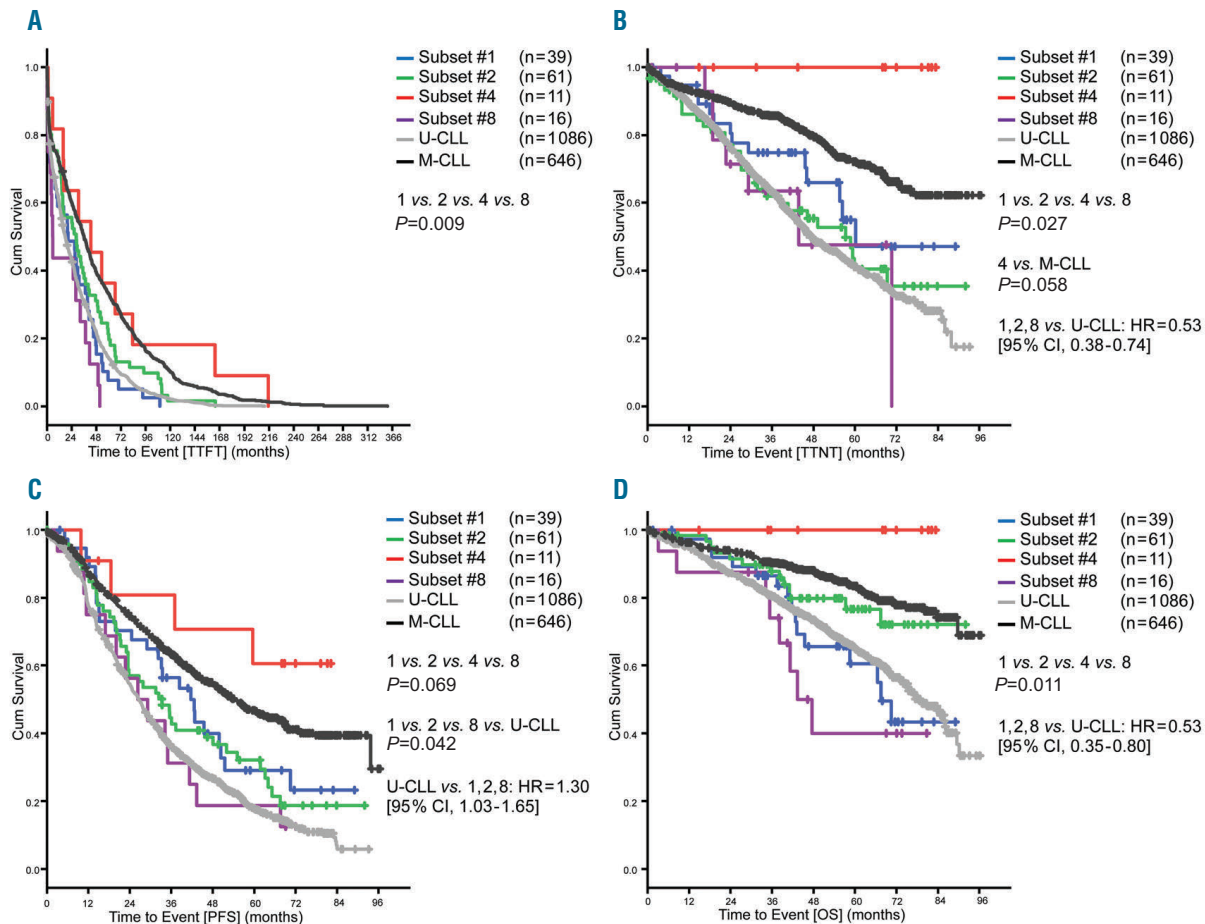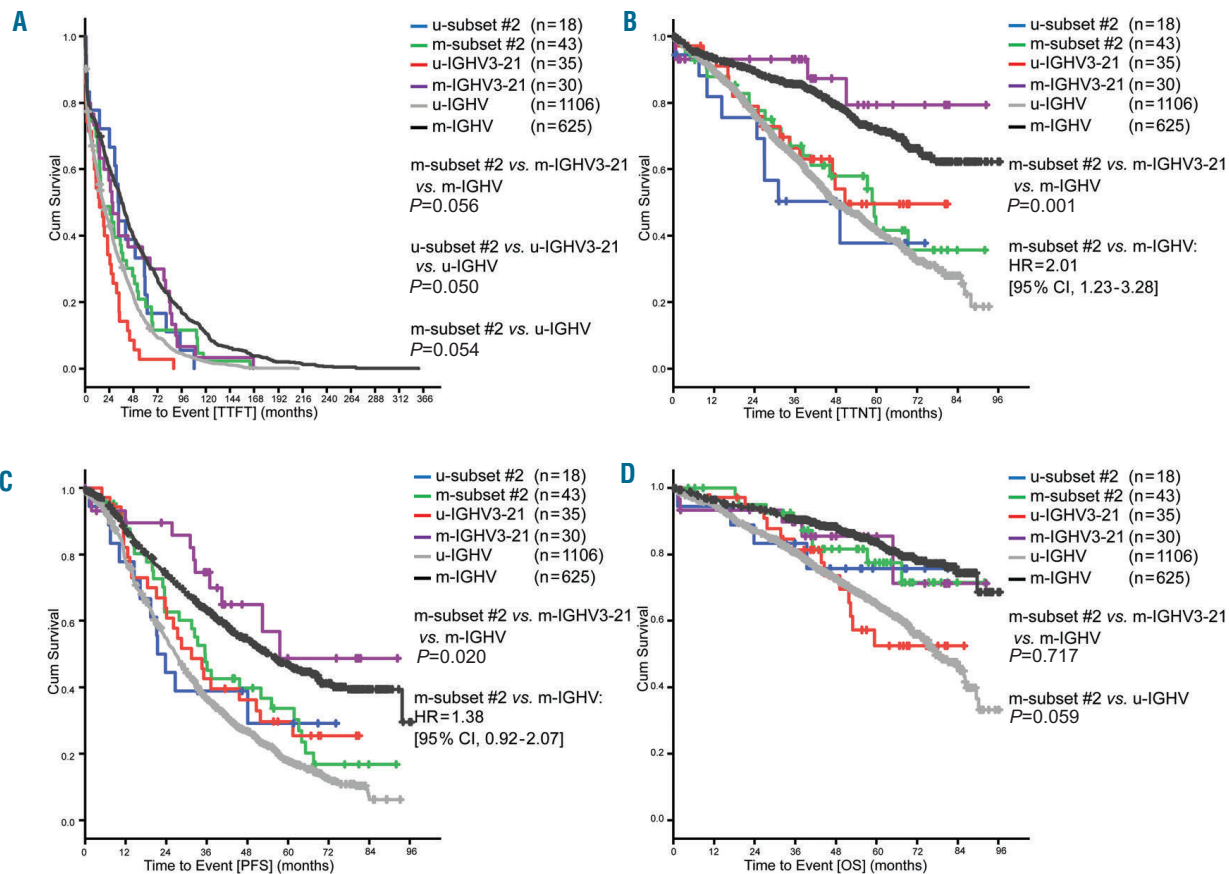**Figure 4. Outcomes of advanced stage chronic lymphocytic leukemia (CLL) cases according to subset #2 classification and IGHV mutation.** (A) Median time-to-first-treatment (TTFT) u-subset #2: 32.9 months, m-subset #2: 16.5 months, u-HV3-21: 14.2 months, m-HV3-21: 26.8 months, u-IGHV: 18.1 months, m-IGHV: 36.3 months. (B) Median time-to-next-treatment (TTNT) u-subset #2: 49.2 months, m-subset # 2: 58.7 months, u-HV3-21: 50.6 months, m-HV3-21: not reached, u-IGHV: 47.8 months, m-IGHV: not reached. (C) Median progression-free (PFS) survival u-subset #2: 21.4 months, m-subset #2: 35.5 months, u-HV3-21: 31.4 months, m-HV3-21: 57.6 months, u-IGHV: 26.7 months, m-IGHV: 54.7 months. (D) Median overall survival (OS) from diagnosis u-subset #2: not reached, m-subset #2: not reached, u-HV3-21: not reached, m-HV3-21: not reached, u-IGHV: 77.4 months, m-IGHV: not reached; Cum: cumulative.

and clinical behavior than IGHV mutational status alone, at least in certain cases.

Subset #4 is known to have an indolent clinical course and is most frequent among younger patients.[15,19] According to our findings, subset #4 had the most favorable prognosis regarding PFS and TTFT compared to the remaining subsets in the early stage CLL population. Furthermore, in the advanced stage CLL analysis, subset #4 showed a longer TTNT compared to mutated CLL and a longer PFS compared to all other subsets. It is striking that for all time-dependent endpoints in the early stage as well as the advanced stage cohort, the outcome of subset #4 patients appeared to be even better than M-CLL. This again points to the hypothesis that subset and therefore BcR IG structure may be more relevant in pathogenesis and prognosis than IGHV mutational status.

Subset #8 has been associated with increased risk of Richter transformation and trisomy 12.[35,36] In the advanced stage CLL, we observed a higher rate of trisomy 12 and a higher incidence of Richter transformation compared to the other subsets. Subset #8 showed a shorter PFS compared to subsets #1 and 2 in advanced stage CLL cases. However, due to the small size of this subgroup population, this could not be tested in a multivariable analysis.

The strength of the current study is also one of its weaknesses, as due to the long follow-up time there was no inclusion of novel agents such as ibrutinib, idelalisib and venetoclax in the treatment schedules. Data of patients treated within clinical studies of novel agents including long follow-up with relevant event numbers and categorized according to the subset classification are not yet available. First analyses indicate that the prognostic power of IGHV mutational status is lost with these agents,[37] and it would be interesting to see if the subset assignment remains a prognostic factor with these treatments. Furthermore, chemo-immunotherapy remains a possible standard of care for patients without high-risk markers and mutated IGHV.[38] According to our data, subset assignment by BCR stereotype is relevant for therapy assessment. Therefore, the patients mentioned above

should be treated taking into consideration the subset assignment. Future studies will evaluate the relevance of the subset classification regarding the response to novel therapies.

Taken together, we confirmed for the first time in prospective clinical trials that subset #2 is an independent prognostic marker for shorter TTFT, TTNT and PFS in CLL, regardless of the IGHV mutational status. Therefore, patients with CLL subset #2 should be closely monitored. Given this, CLL clinical guidelines should include subset #2 also when mutated as an independent marker for high risk in patients receiving chemo-immunotherapy. Furthermore, our study showed that assignment to stereotyped subsets may have a different impact depending on clinical stage in chemo-immunotherapy settings. Subsets #1, 2 and 8 had similar prognosis in most clinical outcomes to U-CLL. However, advanced stage CLL subsets #1, 2 and 8 had a longer PFS than U-CLL. Subset #4 was found to have a better clinical course compared to other subsets in both early and advanced stage CLL and was similar to M-CLL.

For the first time in prospective multicenter clinical trials, subset #2 appeared as an independent prognostic factor and subsets #1, 8 and 4 were found to have a distinctive clinical course and should be proposed for risk stratification of patients.

References

1. Hallek M, Cheson BD, Catovsky D, et al. iwCLL guidelines for diagnosis, indications for treatment, response assessment, and supportive management of CLL. Blood.2018;131(25):2745-2760.
2. Puiggros A, Blanco G, Espinet B. Genetic abnormalities in chronic lymphocytic leukemia: where we are and where we go. Biomed Res Int. 2014;2014:435983.
3. Stilgenbauer S, Schnaiter A, Paschka P, et al. Gene mutations and treatment outcome in chronic lymphocytic leukemia: results from the CLL8 trial. Blood. 2014;123(21):3247-3254.
4. Landau DA, Tausch E, Taylor-Weiner AN, et al. Mutations driving CLL and their evolution in progression and relapse. Nature. 2015;526(7574):525-530.
5. Damle RN, Wasil T, Fais F, et al. Ig V gene mutation status and CD38 expression as novel prognostic indicators in chronic lymphocytic leukemia. Blood. 1999;94(6):1840-1847.
6. Hamblin TJ, Davis Z, Gardiner A, et al. Unmutated Ig V(H) genes are associated with a more aggressive form of chronic lymphocytic leukemia. Blood. 1999;94(6):1848-1854.
7. Messmer BT, Albesiano E, Efremov DG, et al. Multiple distinct sets of stereotyped antigen receptors indicate a role for antigen in promoting chronic lymphocytic leukemia. J Exp Med. 2004;200(4):519-525.
8. Rossi D, Gaidano G. Biological and clinical significance of stereotyped B-cell receptors in chronic lymphocytic leukemia. Haematologica. 2010;95(12):1992-1995.
9. Murray F, Darzentas N, Hadzidimitriou A, et al. Stereotyped patterns of somatic hypermutation in subsets of patients with chronic lymphocytic leukemia: implications for the role of antigen selection in leukemogenesis. Blood. 2008;111(3):1524-1533.
10. Agathangelidis A, Darzentas N, Hadzidimitriou A, et al. Stereotyped B-cell receptors in one-third of chronic lymphocytic leukemia: a molecular classification with implications for targeted therapies. Blood. 2012;11(19):4467-4475.
11. Stamatopoulos K, Belessi C, Moreno C, et al. Over 20% of patients with chronic lymphocytic leukemia carry stereotyped receptors: Pathogenetic implications and clinical correlations. Blood. 2007;109(1):259-270.
12. Stamatopoulos K, Agathangelidis A, Rosenquist R, et al. Antigen receptor stereotypy in chronic lymphocytic leukemia. Leukemia. 2017;31(2):282-291.
13. Bomben R, Dal Bo M, Capello D, et al. Molecular and clinical features of chronic lymphocytic leukaemia with stereotyped B cell receptors: results from an Italian multicentre study. Br J Haematol. 2009; 144(4):492-506.
14. Del Giudice I, Chiaretti S, Santangelo S, et al. Stereotyped subset #1 chronic lymphocytic leukemia: a direct link between B-cell receptor structure, function, and patients' prognosis. Am J Hematol. 2014;89(1):74-82.
15. Baliakas P, Hadzidimitriou A, Sutton L-A, et al. Clinical effect of stereotyped B-cell receptor immunoglobulins in chronic lymphocytic leukaemia: a retrospective multicentre study. Lancet Haematol. 2014;1(2):e74-84.
16. Baliakas P, Agathangelidis A, Hadzidimitriou A, et al. Not all IGHV3-21 chronic lymphocytic leukemias are equal: prognostic considerations. Blood. 2015;125(5):856-859.

17. Bomben R, Dal Bo M, Capello D, et al. Comprehensive characterization of IGHV3-21-expressing B-cell chronic lymphocytic leukemia: an Italian multicenter study. Blood. 2007;109(7):2989-2998.

18. Jeromin S, Haferlach C, Dicker F, et al. Differences in prognosis of stereotyped IGHV3-21 chronic lymphocytic leukaemia according to additional molecular and cytogenetic aberrations. Leukemia. 2016; 30(11):2251-2253.

19. Xochelli A, Baliakas P, Kavakiotis I, et al. Chronic Lymphocytic Leukemia with Mutated IGHV4-34 Receptors: Shared and Distinct Immunogenetic Features and Clinical Outcomes. Clin Cancer Res. 2017; 23(17):5292-5301.

20. Gounari M, Ntoufa S, Apollonio B, et al. Excessive antigen reactivity may underlie the clinical aggressiveness of chronic lymphocytic leukemia stereotyped subset #8. Blood. 2015;125(23):3580-3587.

21. Hoechstetter MA, Busch R, Eichhorst B, et al. Early, risk-adapted treatment with fludarabine in Binet stage A chronic lymphocytic leukemia patients: results of the CLL1 trial of the German CLL study group. Leukemia. 2017;31(12):2833-2837.

22. Hallek M, Fischer K, Fingerle-Rowson G, et al. Addition of rituximab to fludarabine and cyclophosphamide in patients with chronic lymphocytic leukaemia: a randomised, open-label, phase 3 trial. Lancet. 2010;376(9747):1164-1174.

23. Fischer K, Bahlo J, Fink AM, et al. Long-term remissions after FCR chemoimmunotherapy in previously untreated patients with CLL: updated results of the CLL8 trial. Blood. 2016;127(2):208-215.

24. Eichhorst B, Fink A-M, Bahlo J, et al. First-line chemoimmunotherapy with bendamustine and rituximab versus fludarabine, cyclophosphamide, and rituximab in patients with advanced chronic lymphocytic leukaemia (CLL10): an international, open-label, randomised, phase 3, non-inferiority trial. Lancet Oncol. 2016;17(7):928-942.

25. Goede V, Fischer K, Busch R, et al. Obinutuzumab plus chlorambucil in patients with CLL and coexisting conditions. N Engl J Med. 2014;370(12):1101-1110.

26. Döhner H, Stilgenbauer S, Benner A, et al. Genomic aberrations and survival in chronic lymphocytic leukemia. N Engl J Med. 2000;343(26):1910-1916.

27. Kröber A, Seiler T, Benner A, et al. V(H) mutation status, CD38 expression level, genomic aberrations, and survival in chronic lymphocytic leukemia. Blood. 2002; 100(4):1410-1416.

28. Thunberg U, Johnson A, Roos G, et al. CD38 expression is a poor predictor for VH gene mutational status and prognosis in chronic lymphocytic leukemia. Blood. 2001; 97(6):1892-1894.

29. Strefford JC, Sutton L-A, Baliakas P, et al. Distinct patterns of novel gene mutations in poor-prognostic stereotyped subsets of chronic lymphocytic leukemia: the case of SF3B1 and subset #2. Leukemia. 2013; 27(11):2196-2199.

30. Hallek M, Wanders L, Ostwald M, et al. Serum beta(2)-microglobulin and serum thymidine kinase are independent predictors of progression-free survival in chronic lymphocytic leukemia and immunocytoma. Leuk Lymphoma. 1996;22(5-6):439-447.

31. Kaplan EL, Meier P. Nonparametric estimation from incomplete observations. J. Amer. Statist. Assn. 1958;53(282):457-481.

32. Tobin G, Thunberg U, Johnson A, et al. Somatically mutated Ig V(H)3-21 genes characterize a new subset of chronic lymphocytic leukemia. Blood. 2002;99(6):2262-2264.

33. Thorsélius M, Kröber A, Murray F, et al. Strikingly homologous immunoglobulin gene rearrangements and poor outcome in VH3-21-using chronic lymphocytic leukemia patients independent of geographic origin and mutational status. Blood. 2006;107(7):2889-2894.

34. Ghia EM, Jain S, Widhopf GF, et al. Use of IGHV3-21 in chronic lymphocytic leukemia is associated with high-risk disease and reflects antigen-driven, post-germinal center leukemogenic selection. Blood. 2008; 111(10):5101-5108.

35. Rossi D, Spina V, Bomben R, et al. Association between molecular lesions and specific B-cell receptor subsets in chronic lymphocytic leukemia. Blood. 2013;121(24): 4902-4905.

36. Rossi D, Spina V, Cerri M, et al. Stereotyped B-cell receptor is an independent risk factor of chronic lymphocytic leukemia transformation to Richter syndrome. Clin Cancer Res. 2009;15(13):4415-4422.

37. Kipps TJ, Fraser G, Coutre S, et al. Unmutated IGHV is not an adverse predictor of outcome to therapy with ibrutinib in patients with chronic lymphocytic leukemia/small lymphocytic lymphoma (CLL/SLL). Cancer Res 2017;77(13 Suppl):abstract CT158.

38. Wierda WG, Byrd JC, Abramson JS, et al. NCCN guidelines insights: chronic lymphocytic leukemia/small lymphocytic lymphoma, version 2.2019. J Natl Compr Canc Netw. 2019;17(1):12-20.

Migfilin supports hemostasis and thrombosis through regulating platelet αIIbβ3 outside-in signaling

Yangfan Zhou,[1,2] Mengjiao Hu,[1,2] Xiaoyan Chen,[1,2] Shuai Wang,[1,2] Jingke Li,[1,2] Lina Sa,[1,2] Li Li,[1,2] Jiaqi Huang,[3] Hongqiang Cheng[3] and Hu Hu[1,2,4]

[1]Department of Pathology and Pathophysiology and Bone Marrow Transplantation Center of the First Affiliated Hospital, Zhejiang University School of Medicine; [2]Institute of Hematology, Zhejiang University & Zhejiang Engineering Laboratory for Stem Cell and Immunotherapy; [3]Department of Pathology and Pathophysiology, and Department of Cardiology, Sir Run Run Shaw Hospital, Zhejiang University School of Medicine and [4]Key Laboratory of Disease Proteomics of Zhejiang Province, Hangzhou, China

ABSTRACT

Elucidating the regulation mechanism of integrin αIIbβ3 is key to understanding platelet biology and thrombotic diseases. Previous *in vitro* studies have implicated a role of migfilin in the support of platelet αIIbβ3 activation, however, contribution of migfilin to thrombosis and hemostasis *in vivo* and a detailed mechanism of migfilin in platelets are not known. In this study, through migfilin knock-out (*migfilin-/-*) mice, we report that migfilin is a pivotal positive regulator of hemostasis and thrombosis. *Migfilin-/-* mice show a nearly doubled tail-bleeding time and a prolonged occlusion time in FeCl₃-induced mesenteric arteriolar thrombosis. Migfilin deficiency impedes platelet thrombi formation on a collagen surface and impairs platelet aggregation and dense-granule secretion. Supported by characteristic functional readings and the phosphorylation status of distinctive signaling molecules in the bidirectional signaling processes of αIIbβ3, the functional defects of *migfilin-/-* platelets appear to be mechanistically associated with a compromised outside-in signaling, rather than inside-out signaling. A synthesized cell-permeable migfilin peptide harboring filamin A binding sequence rescued the defective function and phosphorylation of signaling molecules of *migfilin-/-* platelets. Finally, migfilin does not influence the binding of filamin A and β3 subunit of αIIbβ3 in resting platelets, but hampers the re-association of filamin A and β3 during the conduct of outside-in signaling, suggesting that migfilin functions through regulating the interaction dynamics of αIIbβ3 and filamin A in platelets. Our study enhances the current understanding of platelet integrin αIIbβ3-mediated outside-in signaling and proves that migfilin is an important regulator for platelet activation, hemostasis and thrombosis.

Introduction

Platelets are essential for thrombosis and hemostasis. At the sites of vascular injury, platelets instantly activate, adhere to the exposed subendothelial matrix and form a hemostatic or thrombotic plug. Idiosyncratically expressed by platelets, integrin αIIbβ3 is the central adhesion molecule that governs the process of thrombus formation. αIIbβ3 characteristically transmits signals bidirectionally across the plasma membrane, processes termed inside-out and outside-in signaling, respectively.[1] Inside-out signaling conveys the activation information from stimuli and culminates in the high affinity binding of αIIbβ3 to its ligands, which forms bridges to support platelet-vessel wall adhesion and platelet homotypic aggregation. Outside-in signaling, which is initiated by ligand binding and αIIbβ3 clustering, is essential for platelet spreading, clot retraction and thrombus consolidation.[2]

Platelet αIIbβ3 signaling is regulated by the binding of several molecules to the cytoplasmic domain of integrin β-subunits.[3] The cytoplasmic integrin-binding protein talin has been known as the central regulator for αIIbβ3.[4] There are also other

important integrin-binding proteins such as kindlins and filamin A, which can potentially profoundly influence the function of αIIbβ3.[5-7] Thus, kindlin-3 co-operates with talin and positively regulates the activation of integrin αIIbβ3,[3] whereas filamin A competitively blocks the talin-integrin interaction[5] and negatively regulates αIIbβ3.[3,8] Intriguingly, the interactions between integrin β3 and integrin-binding proteins are highly dynamic, even the same pair of interactive partners may serve distinctive roles in different phases of the platelet activation pathway. For example, talin-β3 binding is the essential step for αIIbβ3 activation for inside-out signaling, whilst the subsequent G13-regulated dissociation and re-association between talin and β3 are not only pivotal steps for outside-in signaling but are also the crucial events that differentiate thrombosis from hemostasis.[9] This example highlights the importance of clarifying the dynamic interaction between integrin and integrin-binding proteins during αIIbβ3 activation. However, the spatial temporal dynamics for most other integrin-binding proteins remain largely unknown.

Migfilin, also known as FBLIM1/FBLP-1,[10] is a putatively expressed protein consisting of an N-terminal filamin-binding domain, a central proline rich domain and three C-terminal LIM domains. Through participation in cytoskeleton reorganization, migfilin is involved in cellular functions such as adhesion, morphological change, and motility.[11] Migfilin has also been reported to promote cardiomyocyte differentiation.[12] There are multiple binding partners of migfilin, including mitogen inducible gene-2 (*MIG-2*), VASP, and transcriptional factor CSX/NKX2-5.[10] Particularly, migfilin is capable of strong interaction with filamin A, which raises the possibility that migfilin could competitively dissociate filamin A from integrin and thus promote talin-αIIbβ3 interaction.[13] Indeed, migfilin peptides are capable of inducing PAC-1 binding in human platelets.[14] However, these findings were obtained in *in vitro* conditions and neither the contribution of migfilin to thrombosis and hemostasis *in vivo* nor to integrin dynamics during platelet activation are clear.

With *migfilin*^{-/-} mice, the current study investigated the role of migfilin in platelet activation, hemostasis and thrombosis. The phenotype exhibited by *migfilin*^{-/-} mice indicated that migfilin is an important positive regulator for hemostasis and thrombosis. Mechanistically, migfilin promotes early outside-in signaling of platelet αIIbβ3, possibly through binding to filamin A and sequestering the αIIbβ3-inhibiting effect of filamin A.

Methods

Generation of migfilin deficient mice

Migfilin^{-/-} mice were bred as described,[15] ablation of migfilin was achieved by the deletion of exon 7. The loss of exon 7 of *migfilin* in *migfilin*^{-/-} platelets was confirmed by mRNA expression, using littermate wild-type (WT) mice platelets as a control. All experimental procedures were reviewed and approved by the Animal Care and Use Committee of the Zhejiang University School of Medicine. Total RNA of platelets and heart was extracted using Trizol (Thermo Fisher Scientific, MA, USA) according to the manufacturer's instructions. RNA was reversely transcribed to cDNA using the ReverTraAce qPCR RT kit (Toyobo, Osaka, Japan). PCR was performed using the primers P1: GCTGTTGAG-GCCATGAAGAG and P2: TCCTTCCCATGCACTCGATT.

Migfilin gene expression was quantified by real-time quantitative PCR based on SYBR Green, using -actin RNA as the loading control.[16] The sequence of the primers used were as follows: migfilin forward primer (mFBLIM1-qRCR-F): TAGCCGTGAGTGAG-GAAGTG, reverse primer (mFBLIM1-qRCR-R): CAGAGAGT-GAGGCATTGGTCT.

Migfilin peptides

As previously reported,[13] WT migfilin ([4]KPEKRVASSVFITLAP[19]C) and mutant (MT) peptides ([4]KPEKR-VA**DSA**FITLAP[19]C) with an additional C-terminal cysteine residue were synthesized by ChinaPeptides (Suzhou, China). WT-migfilin peptide harbors the filamin A binding sequence and the MT-migfilin peptide contains two point mutations (Ser[11] was replaced by Asp, and Val[13] was replaced by Ala, bold type in the sequence) with substantially reduced ability to bind filamin A (at least 12.5-times weaker than the WT peptide).[13] To render them cell permeable, a CR7 transport peptide was conjugated to the migfilin peptides through a disulfide bond.[17] The conjugated peptides were purified by high pressure liquid chromatography and conjugation confirmed by electrospray ionization mass spectrometry.

Tail bleeding assay

As previously described,[18] tails of anesthetized mice were cut 0.5 cm from the tip and immediately immersed in microtubes filled with 1.7 ml of saline at 37°C. The time for the bleeding to stop (no blood flow for 1 min) and the weight of blood loss were recorded. Tail bleeding assays were stopped at 900 seconds if the bleeding did not stop. The same procedure was used for the evaluation of migfilin peptides in hemostatic function after their intravenous injection.

Platelet preparation

Whole blood was collected from the inferior vena cava into 0.1 vol of ACD buffer (75 mM sodium citrate, 39 mM citric acid, and 135 mM dextrose, pH 6.5), and was diluted 1:2 with modified Tyrode's buffer (in mM: 20 HEPES, 137 NaCl, 13.8 NaHCO$_3$, 2.5 KCl, 0.36 NaH$_2$PO$_4$, 5.5 glucose, pH 7.4). Diluted whole blood was centrifuged at 180×g for 10 minutes (min) at room temperature, and platelet-rich-plasma was collected into a fresh tube. The platelet-rich-plasma was diluted in ACD buffer, and centrifuged at 700×g for 10 min. Platelet pellet was then re-suspended in modified Tyrode's buffer.

Detailed information of the reagents, platelet function measurements, Western blotting and statistical analysis is provided in the *Online Supplementary Materials and Methods*.

Results

Migfilin deficiency impairs hemostasis and thrombosis.

The truncation of exon 7 of *migfilin* in platelets was validated by PCR measurement of *migfilin* messenger RNA (Figure 1A). Multiple commercially available antibodies (Santa Cruz Biosciences sc-162823, sc-162822, sc-134724; ABclonal A15850; GeneTex GTX116584) were used to detect migfilin. These antibodies did not clearly reveal the expression of migfilin protein in murine platelets, although they did confirm the presence of migfilin in murine hearts as previously reported (Figure 1B). Real-time quantitative PCR experiments were performed as a surrogate method to quantify *migfilin* expression in murine platelets. The results not only confirmed the loss of *migfilin* mRNA in the platelets from KO mice, but also showed
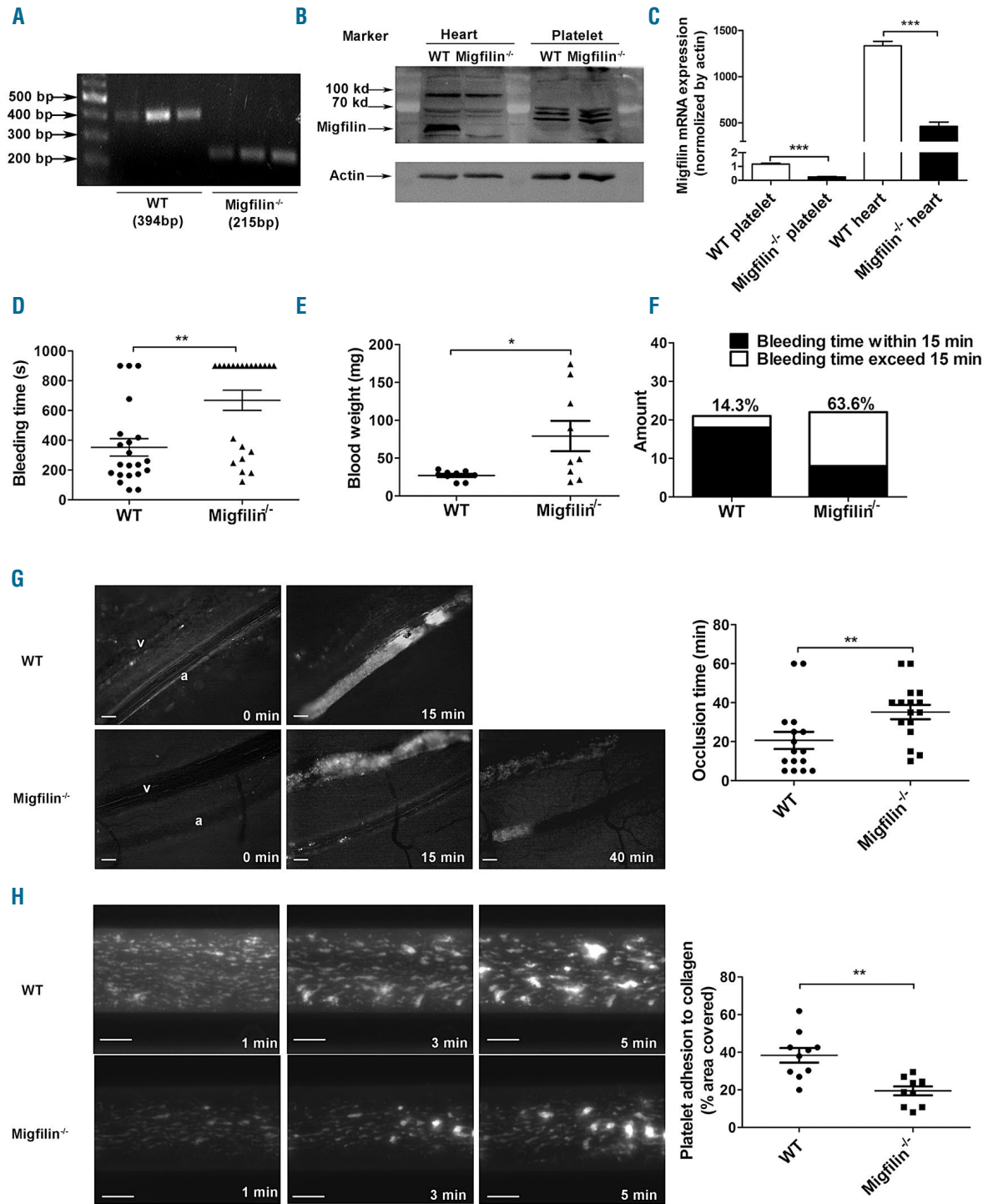
Figure 1. *Migfilin⁻ᐟ⁻* mice display impaired hemostatic and thrombotic functions. (A) *Migfilin* mRNA expression in wild-type (WT) platelets and exon 7 (179 bp) deleted *migfilin⁻ᐟ⁻* mice platelets. (B) Analysis of migfilin protein expression by Western blotting in heart tissues and platelets from WT and *migfilin⁻ᐟ⁻* mice. (C) Quantitative real-time PCR results analysing the expression of *migfilin* in platelets and heart tissues. Data are represented as a ratio relative to an internal control (β-actin) (mean ± standard error of the mean [SEM], n=3), ***P<0.001, Student *t* test. (D) Bleeding times for WT (●) and *migfilin⁻ᐟ⁻* mice (▲). Means are indicated by horizontal lines. **P<0.01, evaluated with 2-tailed Mann-Whitney U tests. (E) Weight of blood loss from WT (●) and *migfilin⁻ᐟ⁻* mice (▲) during bleeding time. Results are expressed as the mean ± SEM (n = 9). *P<0.05, evaluated with 2-tailed Mann-Whitney U tests. (F) Percentages of WT and *migfilin⁻ᐟ⁻* mouse bleeding times exceeded 15 minutes (min) (□) or were within 15 min (■). Results were obtained from 21 WT and 22 *migfilin⁻ᐟ⁻* mice. (G) Representative images of thrombi in FeCl₃-injured mesenteric arterioles at indicated post-injury time points in WT (upper row) and *migfilin⁻ᐟ⁻* mice (lower row). a, arteriole; v: venule. Scale bars, 100 μm (left panel). Occlusion times of FeCl₃-induced thrombosis in arterioles of WT (n=16) and *migfilin⁻ᐟ⁻* mice (n=16). Means are indicated by horizontal lines. **P<0.01, 2-tailed Mann-Whitney test (right panel). (H) Adhesion of platelets from WT and *migfilin⁻ᐟ⁻* mice on collagen. Mepacrine-labeled whole blood from WT and *migfilin⁻ᐟ⁻* mice was perfused over collagen-coated bioflux plates at a shear rate of 40 dynes/cm² for 5 min. Original magnification 10x. Scale bar, 100 μm (left panel). Area coverage of platelets from WT and *migfilin⁻ᐟ⁻* mice (n=10 for both groups) after 5 min perfusion over a collagen surface, **P<0.01, 2-tailed Mann-Whitney test (right panel).

that expression of *migfilin* mRNA is about 1,500-fold lower in platelets than that in heart of WT mice (normalized by *actin* mRNA) (Figure 1C). *Migfilin^-/-* mice were viable and fertile, and did not exhibit any evident bleeding tendency or thrombotic events over their lifespan. *Migfilin^-/-* mice did not differ significantly from their WT littermates in platelet counts, white cell counts, hematocrits, and hemoglobin concentrations (Table 1). Electron microscopy showed that *migfilin^-/-* platelets had normal discoid morphology (*Online Supplementary Figure S1A*). No significant differences in the surface expression of the platelet glycoproteins GPVI, CD41 (αIIb subunit) and CD42b (GPIb subunit) were found between WT and *migfilin^-/-* platelets (*Online Supplementary Figure S1C*).

Notably, *migfilin^-/-* mice exhibited tail-bleeding times twice as long as their WT littermates (Figure 1D), consistent with the comparison of the weight of blood loss between *migfilin^-/-* and WT mice (Figure 1E). Moreover, 63.6% of the *migfilin^-/-* mice had bleeding times exceeding 15 min, in comparison, only 14.3% of WT littermates had bleeding times over 15 min (Figure 1F). These data suggest that migfilin positively regulates hemostasis.

In a model of FeCl₃-induced mesenteric arteriole thrombosis, the time of forming stable occlusive thrombi in mesenteric arterioles were significantly longer in *migfilin^-/-* mice than in WT mice (35.19±3.656 min *vs.* 20.63±4.422 min, *P*<0.01; Figure 1G). To confirm that the observed hemostatic functional defects are due to migfilin deficiency, we synthesized cell-deliverable migfilin peptides as described in the previous study.[13] WT-migfilin-CCR7 peptide (range: 0.5-1.5 nM/kg) dose-dependently shortened the prolonged tail bleeding time in *migfilin^-/-* mice (*Online Supplementary Figure S2A*), whereas MT-migfilin-CCR7 peptide did not show any effect on the bleeding time. WT-migfilin-CCR7 peptide restored the prolonged bleeding time of *migfilin^-/-* mice to a comparable level of WT mice (*Online Supplementary Figure S2B-C*). WT-migfilin-CCR7, but not MT-migfilin-CCR7, also restored the occlusion time in Fecl₃-induced mesenteric arterial injury in *migfilin^-/-* mice (*Online Supplementary Figure S2D*).

Thrombus formation was also assessed using a microfluidic whole-blood perfusion assay. After a 5-minute perfusion at a shear rate of 1000 s⁻¹, thrombi formed on an immobilized collagen surface by *migfilin^-/-* platelets were significantly smaller (average of a 50% reduction) than those by WT platelets (Figure 1H). In the meanwhile, as shown in the *Online Supplementary Video S1*, thrombi formed by *migfilin^-/-* platelets displayed a severely compromised stability compared to WT platelets. In order to assess whether the observed phenotype of *migfilin^-/-* platelets is due to a reduced ability of adhesion during the initiation of thrombosis, a recombinant whole-blood system with a reduced concentration of platelets (10⁷/mL) was employed in the perfusion assay. Without the interference from massive platelet aggregation, *migfilin^-/-* and WT platelets had similar coverage area on the collagen surface (*Online Supplementary Figure S3*). These findings indicate that migfilin promotes thrombosis, possibly through influencing the extension and perpetuation of thrombi.

Migfilin^-/- platelets have a decreased capability of aggregation due to a hampered dense granule secretion

To further evaluate the function of migfilin in platelets, aggregation and dense granule secretion in response to

Table 1. Hematologic analysis.

	WT	*Migfilin^-/-*	P
RBC×10¹²/L	10.72±1.01	10.96±1.63	0.6974
WBC×10⁹/L	14.26±4.51	14.93±8.92	0.8345
Platelets×10⁹/L	676±271.26	562±268.03	0.3570
Hematocrit %	47.40±4.45	49.40± 7.27	0.4680
Hemoglobin g/dL	15.8±1.62	16.5±2.677	0.4883
MPV fL	5.2±0.33	5.3±0.18	0.4198

Data are ± standard error of the mean (SEM). No abnormalities or significant differences between wild-type (WT) and *migfilin^-/-* mice were found for hematologic parameters (n = 3-5; unpaired Student *t* test). RBC: red blood cells; WBC: white blood cells; MPV: mean platelet volume.

common platelet stimuli were measured. Compared to WT platelets, *migfilin^-/-* platelets displayed a prominently decreased aggregation rates in response to low dose collagen (0.4 µg/mL), and a mildly decreased aggregation rates in response to thrombin (0.018 U/mL) (Figure 2A). Platelet aggregation induced by ADP (10 µM; 20 µM), U46619 (0.3 M; 0.6 M) or higher concentrations of thrombin (0.025 U/mL) and collagen (0.8 µg/mL) was not affected by migfilin deficiency. Notably, *migfilin^-/-* platelets exhibited a markedly decreased ATP secretion in response to all stimuli including U46619, thrombin and collagen, even when the aggregation difference was no longer present (Figure 2A). Apyrase (0.25 U/mL) hydrolyzed secreted ADP and eliminated the aggregation difference between WT and *migfilin^-/-* platelets induced by low concentrations of thrombin or collagen (Figure 2B). Supplementation with a low concentration of ADP (1 µM), insufficient to induce aggregation on its own, reversed the inhibitory effect of migfilin deficiency on collagen- and thrombin-stimulated platelet aggregation (Figure 2B). In addition, thrombin- and collagen-induced secretion of serotonin from *migfilin^-/-* platelets was largely reduced compared to that of WT platelets, even though similar levels of serotonin were harbored inside resting *migfilin^-/-* and WT platelets (*Online Supplementary Figure S4*). These data suggest that an impaired dense granule secretion is the central functional defect exhibited by *migfilin^-/-* platelets.

WT-migfilin-CCR7 (5 µM), but not MT-migfilin-CCR7 (5 µM), rescued the impaired aggregation and ATP release of washed *migfilin^-/-* platelets in response to thrombin or collagen, and eliminated the difference between WT and *migfilin^-/-* platelets (Figure 3A-B). This result supports that the observed platelet phenotypes in the current study are *bona fide* migfilin effects.

Interestingly, an integrin αIIbβ3 inhibitor tirofiban (4 g/mL) eliminated the differences of aggregation and ATP secretion between *migfilin^-/-* and WT platelets in response to thrombin and collagen (*Online Supplementary Figure S6A-B*), suggesting that migfilin-regulated platelet function is αIIbβ3-dependent. However, neither the secretion of -granules nor the conformational change of αIIbβ3 on a single platelet, indicated by P-selectin expression and JON/A binding, respectively, was affected by migfilin deficiency or exogenously applying of migfilin peptide (*Online Supplementary Figure S7*). These findings therefore suggest that migfilin may not be involved in inside-out signaling of αIIbβ3, but rather participate in the process post ligand-αIIbβ3 engagement.

A

B
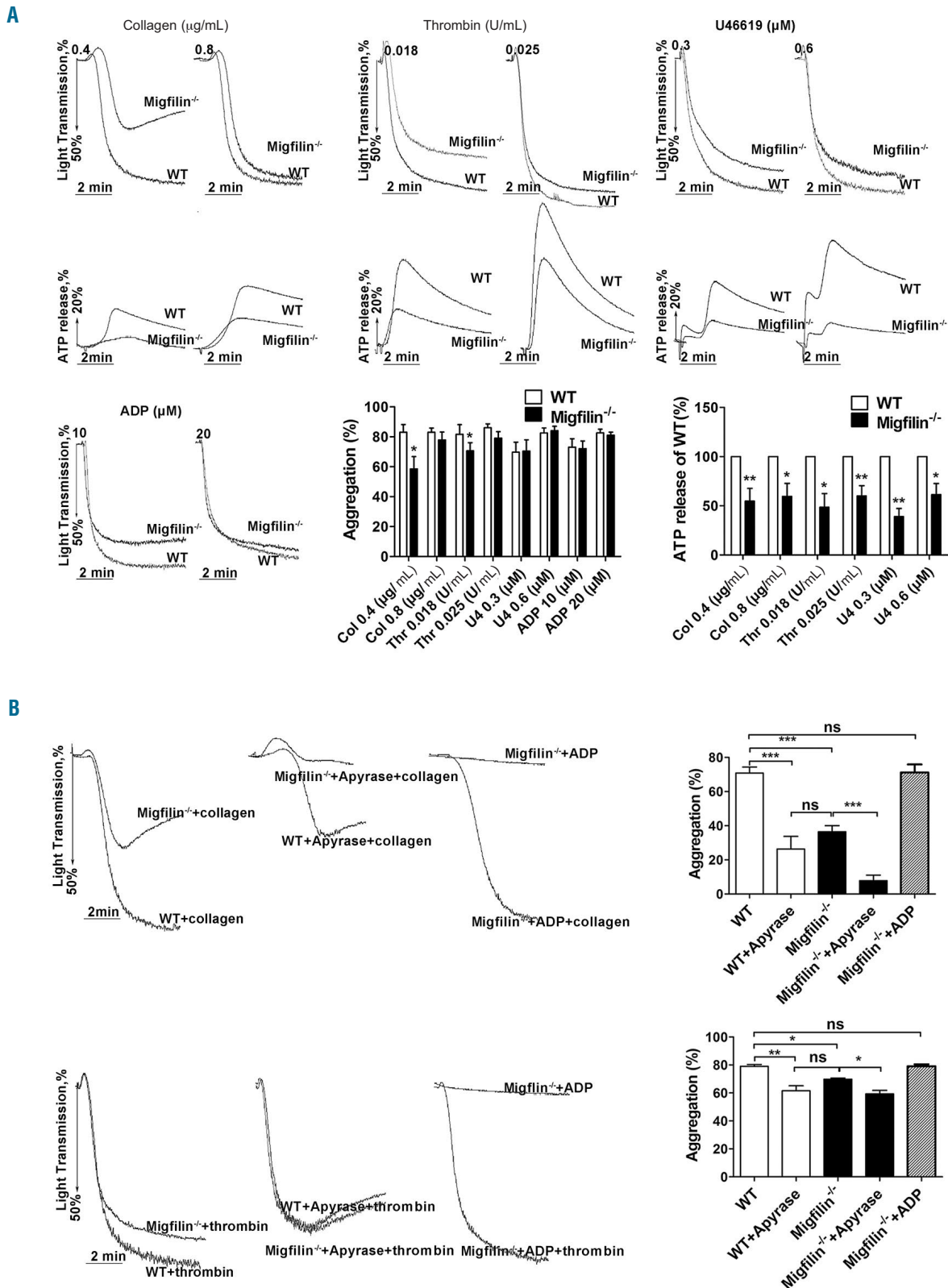
Figure 2. *Migfilin⁻ᐟ⁻* platelets display impaired aggregation responses due to defective dense granule secretion. (A) Platelets were stimulated with collagen, thrombin, U46619, and ADP (in the presence of fibrinogen). Aggregation and ATP release was assessed with a Chrono-log lumiaggregometer under stirring at 1,200 rpm. Traces are representative of at least three independent experiments. Results are expressed as mean ± standard error of the mean (SEM) from at least four independent experiments. Statistical significance was evaluated with paired Student *t* test. (*P<0.05, **P<0.01). (B) Aggregation of washed WT or *migfilin⁻ᐟ⁻* platelets stimulated with collagen (0.4 μg/mL) or thrombin (0.018 U/mL) in the presence of vehicle (left panel), or apyrase (0.25 U/mL) (middle panel), or a low concentration of ADP (1 μM) (right panel). Percentage of platelet aggregation from at least four independent experiments is depicted on the right, and the results are shown as mean ± SEM (*P<0.05, **P<0.01, ***P<0.001, ns: no significant difference, paired Student *t* test).

Migfilin positively regulates early αIIbβ3 outside-in signaling in platelets

Since the effects of migfilin in platelets are αIIbβ3-dependent, outside-in signaling mediated by αIIbβ3 was evaluated. First, early outside-in signaling was assessed by two functional assays, i.e., spreading of platelets on immobilized fibrinogen and Mn^{2+} (0.5mM)-caused platelet aggregation. Both spread areas on fibrinogen and the aggregation rates by manganese were largely reduced in *migfilin⁻/⁻* platelets (Figure 4A-B). WT-migfilin-CCR7, but not MT-migfilin-CCR7 peptide, fully rescued platelet spreading on fibrinogen and $Mn2^+$ induced platelet aggregation (Figure 4A-B). The late outside-in signaling was assessed by a clot retraction experiment.[21-23] Contrary to
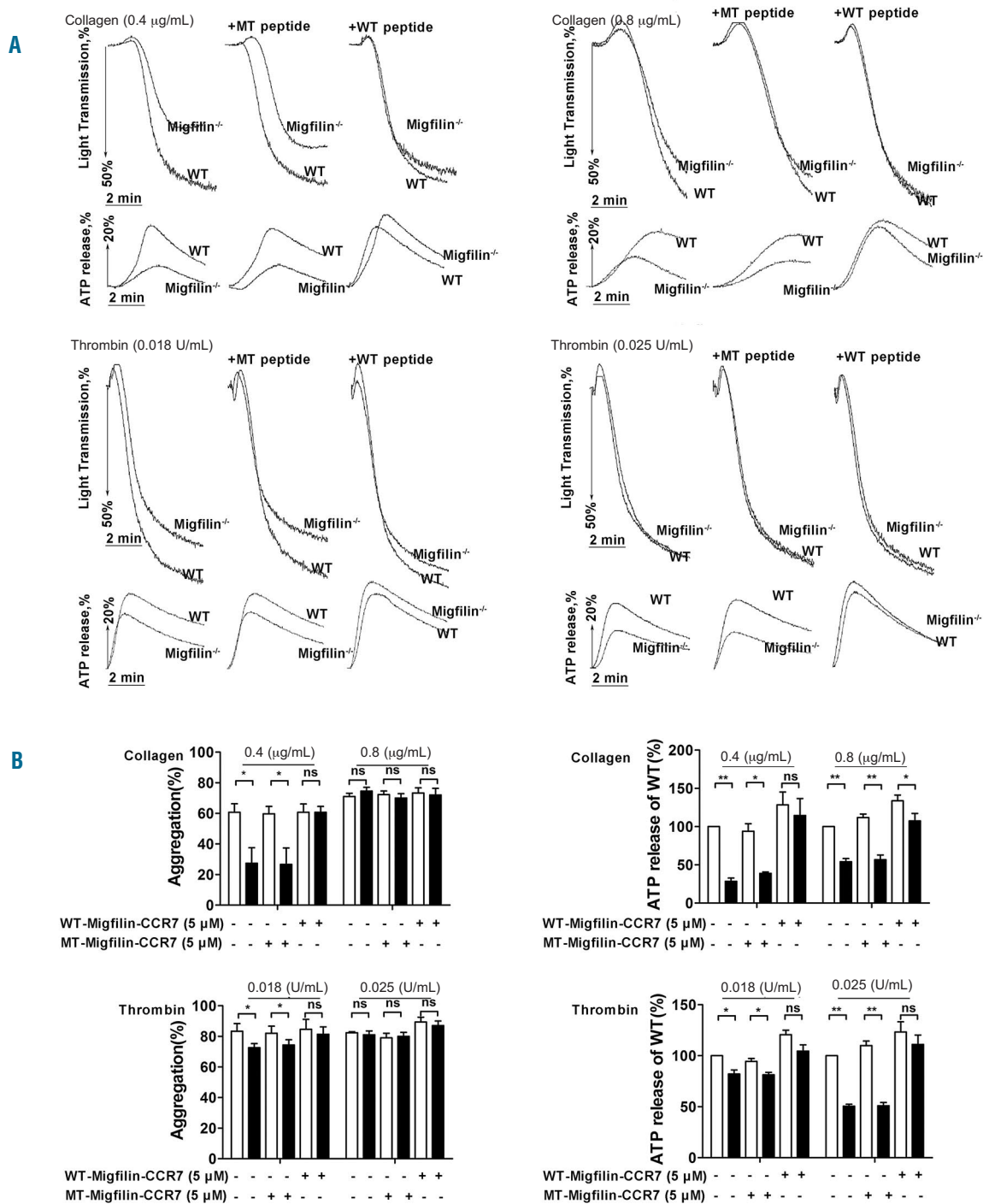
Figure 3. WT-migfilin-CCR7 (5 μM) rescued the impaired aggregation and ATP release of washed *migfilin⁻/⁻* platelet in response to thrombin or collagen. (A) Platelets were stimulated with collagen (0.4 μg/mL, 0.8 μg/mL), thrombin (0.018 U/mL, 0.025 U/mL) in the presence of WT-migfilin-CCR7 (5 μM) peptide or MT-migfilin-CCR7 (5 μM) peptide. Platelet aggregation and ATP release were assessed with a Chrono-log lumi-aggregometer under stirring at 1,200 rpm. Traces were representative of at least three independent experiments. (B) WT (□) and *migfilin⁻/⁻* (■) platelets treated with WT-migfilin-CCR7 and MT-migfilin-CCR7 respectively were stimulated by collagen and thrombin. Results are expressed as mean ± standard error of the mean (SEM) from at least three independent experiments. Statistical significance was evaluated with paired Student *t* test (*$P<0.05$, **$P<0.01$, ns: no significant difference).

A

B

C

D

E
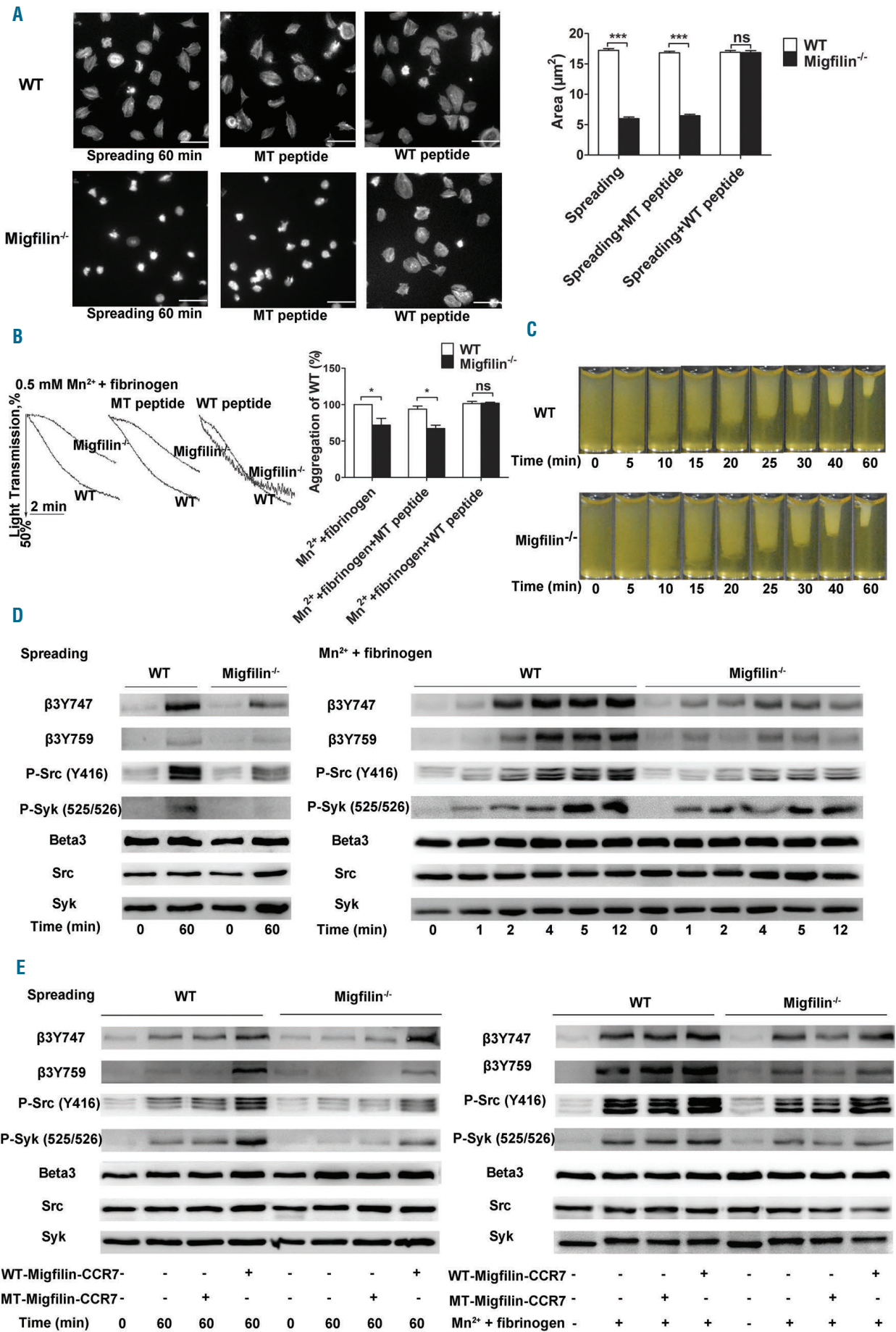
Figure 4 (*previous page*). Migfilin deficiency reduces outside-in signaling in platelets. (A) Spreading of WT and *migfilin⁻/⁻* platelets on immobilized fibrinogen in the presence or absence of migfilin peptides (5 μM). Images are representative of three independent experiments with similar results. Original magnification 100x. Scale bars, 10 μm (left panel). Quantification of the areas of spread (μm²) of WT and *migfilin⁻/⁻* platelets (mean ± standard error of the mean [SEM], ***$P<0.001$, ns: no significant difference, Student *t* test) (right panel). (B) Representative curves and quantification of Mn²⁺ (0.5 mM)-induced aggregation of washed WT and *migfilin⁻/⁻* platelets in the presence or absence of migfilin peptide. Platelets were stimulated in the cuvettes of a Chrono-log lumiaggregometer in the presence of fibrinogen (25 μg/mL) and under stirring at 1,200 rpm. Experiments were repeated at least four times and the results are shown as mean ± SEM (*$P<0.05$, ns: no significant difference, paired Student *t* test). (C) Platelets from WT or *migfilin⁻/⁻* mice were re-suspended with human platelet-poor plasma at a concentration of 4x10⁸/mL, and recombined plasma was stimulated to coagulate with thrombin (0.4 U/mL), then photographed at different time points. Experiments were repeated at least three times. (D) Measurement of early αIIbβ3 outside-in signaling in WT and *migfilin⁻/⁻* platelets spread on fibrinogen or stimulated with Mn²⁺ (0.5 mM) in the presence of fibrinogen (25 μg/mL) in suspension. At indicated time points, platelets were lysed and analyzed by Western blotting with antibodies recognizing phosphorylated β3 Tyr747, phosphorylated β3 Tyr759, phosphorylated SFK Ty⁴¹⁶, phosphorylated Syk Tyr525/526, Beta3, Src, and Syk. Experiments were repeated at least three times. (E) WT and *migfilin⁻/⁻* platelets were spread on fibrinogen for 60 minutes (min) or stimulated with Mn²⁺ (0.5 mM) in the presence of fibrinogen (25 μg/mL) for 10 min, in the presence or absence of migfilin peptides (5 μM). Platelets were lysed and analyzed by Western blotting with antibodies recognizing phosphorylated phosphorylated β3 Tyr747, phosphorylated β3 Tyr759, phosphorylated SFK Ty⁴¹⁶, phosphorylated Syk Tyr525/526, Beta3, Src and Syk. Experiments were repeated at least three times.

the spreading results, neither the rate of clot retraction nor the final volumes of clots differed between WT and *migfilin⁻/⁻* platelets (Figure 4C), indicating an intact late outside-in signaling upon migfilin deficiency.

Upon spread on immobilized fibrinogen or provoked by Mn2⁺ stimulation, the typical early outside-in signal molecules, including β3 cytoplasmic sites (Tyr⁷⁴⁷, Tyr⁷⁵⁹), Src-famliy kinase c-Src (Tyr⁴¹⁶) and Syk kinase (Tyr⁵²⁵/⁵²⁶), exhibited a significantly reduced phosphorylation in *migfilin⁻/⁻* platelets, compared to WT platelets (Figure 4D and *Online Supplemntary Figure S8A*). The phosphorylation defects of these signal molecules in *migfilin⁻/⁻* platelets were restored by exogenous WT-migfilin-CCR7 peptide (5 μM) (Figure 4E and *Online Supplemntary Figure S8B*). In contrast, late outside-in signaling events, such as phosphorylation of ERK and p38,²⁴ were not drastically changed (*Online Supplemntary Figure S9*). Together, these data suggest that migfilin contributes to the early but not late outside-in signaling of platelet αIIbβ3.

Migfilin promotes outside-in signaling through inhibiting filamin A-β3 interaction

Previous studies have established that migfilin promotes the activation of αIIbβ3 *via* binding to filamin and dissociate the latter from integrin β3 cytoplasmic tail. Limited by the expression level of migfilin in platelets, filamin A-β3 binding was used as a surrogate marker for a more detailed molecular mechanism of migfilin in the context of αIIbβ3 outside-in signaling. Shown in the Figure 5A, when platelets spread on immobilized fibrinogen were examined by confocal microscopy, both WT and *migfilin⁻/⁻* platelets exhibit a strong colocalization signal of β3 and filamin A at resting states. Upon the commencing of spreading, the co-localization signal of β3 and filamin A diminishes in WT platelets (nadir appears at 60 min) and gradually recovers. In contrast, the temporal changes of the colocalization signal is much less obvious in *migfilin⁻/⁻* platelets (Figure 5A-B). In addition, binding of filamin A to integrin β3 tails is clearly seen in resting WT platelets, Mn²⁺ stimulation induces a rapid and complete dissociation of filamin A and β3, followed by a later re-association of filamin A and β3. In resting *migfilin⁻/⁻* platelets, the initial association between filamin A and 3 is unchanged, however, upon Mn²⁺ stimulation, an obviously deterred dissociation of filamin A and β3 occurs (Figure 5C). Because filamin A also binds GPIbα,²⁵ platelet responses to von Willebrand factor (VWF) in the presence of ristocetin was measured. Neither spreading on immobilized VWF nor binding between filamin A and GPIbα upon ristocetin stimulation revealed difference between WT and *migfilin⁻/⁻*

platelets (*Online Supplemntary Figure S10*),²⁶ thus excluding the possibility that migfilin works through filamin A-GPIbα binding. Therefore, migfilin appears to modulate the interaction between filamin A and β3 and thus promote outside-in signaling of αIIbβ3 (Figure 6).

Discussion

The results presented here demonstrate that migfilin is an important regulator for the *in vivo* system of hemostasis and thrombosis. *In vitro*, migfilin deficiency impedes thrombus formation on collagen surface and impairs various platelet functions, including aggregation, dense-granule secretion, and spreading on immobilized fibrinogen. These defective functions of *migfilin⁻/⁻* platelets appear to be the results of a compromised outside-in signaling, rather than inside-out signaling. Furthermore, migfilin promotes the dissociation of filamin A from β3 subunit of αIIbβ3 in the milieu of early outside-in signaling.

Although a contribution to hemostasis by migfilin expressed on other vasculature components such as endothelium could not be absolutely excluded,¹⁴ observations from whole-blood perfusion and behavior of washed *migfilin⁻/⁻* platelets *in vitro* suggest that the hemostatic phenotype of *migfilin⁻/⁻* mice is most likely attributed to a compromised platelet function. Interestingly, a down-regulated dense-granule secretion underpins the functional phenotype of migfilin deficient platelets. In agreement with the firmly established role of secreted ADP from dense granule as the central promoter for the extension of thrombus, ADP hydrolase apyrase eliminates the aggregation difference between WT and *migfilin⁻/⁻* platelets, whereas exogenously supplemented ADP fully rescues the aggregation defect of *migfilin⁻/⁻* platelets. Moreover, migfilin deficiency largely hampers the stability of the platelet thrombi formed under high shear stress, consistent with the critical role of ADP in the perpetuation of thrombi.²⁷,²⁸ Multiple lines of evidences thus support that migfilin regulates the secretion of platelet dense granules. It is worth mentioning that this is the first time such a specific role of migfilin has been experimentally unveiled in platelets, owing largely to the availability of the KO model.

Previous studies found that a relatively high concentration of cell permeable migfilin peptides (50 μM) promotes PAC-1 binding and induces significant aggregation (10 μM peptide) in washed human platelets,¹³,¹⁴ thus suggesting that migfilin actively participates in the inside-out signal-

A

Time (min)   0   30   60   90   120
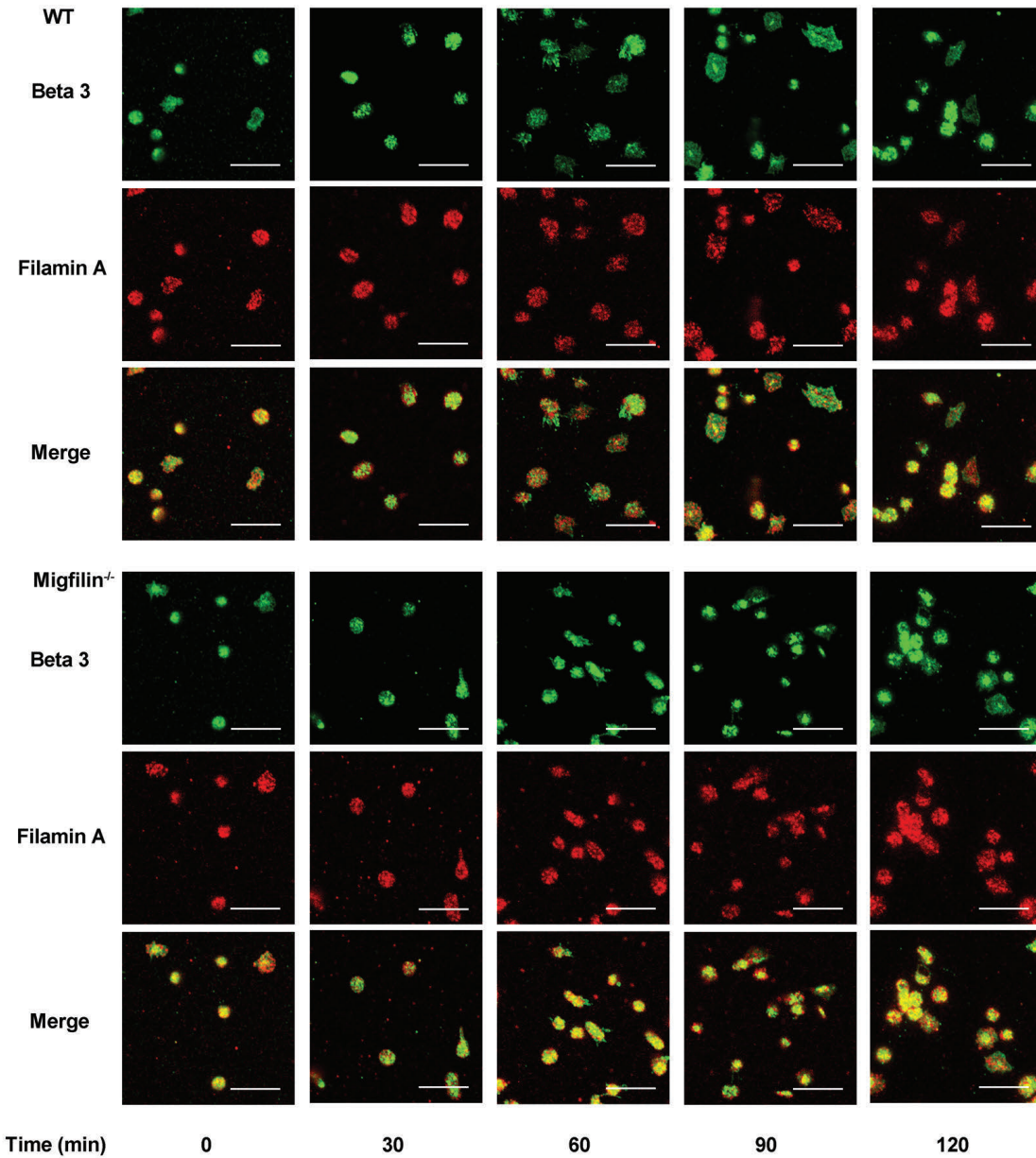
B
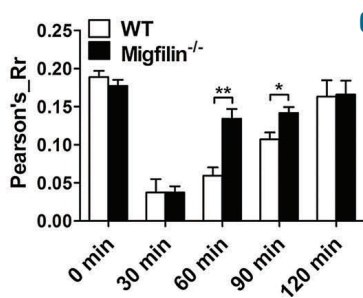
C
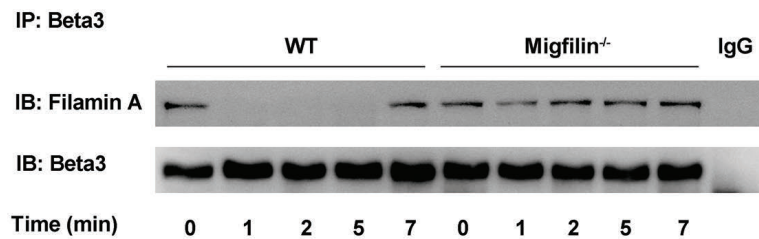
Figure 5. Migfilin promotes outside-in signaling through regulating filamin A-β3 interaction. (A) Representative confocal microscopic images of colocalization of Beta 3 (β3) and filamin A in WT and *migfilin⁻/⁻* platelets spread on fibrinogen at the indicated time points. Experiments were repeated independently at least three times with similar results. Scale bars, 10 μm. (B) Colocalization of filamin A and β3 was quantified by Pearson Correlation Coefficient calculation using NIH Image J software. Results are expressed as mean ± standard error of the mean (SEM) from at least three independent experiments. Statistical significance was evaluated with the Student *t* test (*$P<0.05$, **$P<0.01$). (C) Washed WT platelets were stimulated with Mn^{2+} (0.5 mM) in the presence of fibrinogen (25 μg/mL) in suspension and lysed at indicated time points. Platelet lysates were immunoprecipitated with antibody against β3 and then immunoblotted with antibodies against filamin A and β3, respectively. Representative result from at least three independent experiments.
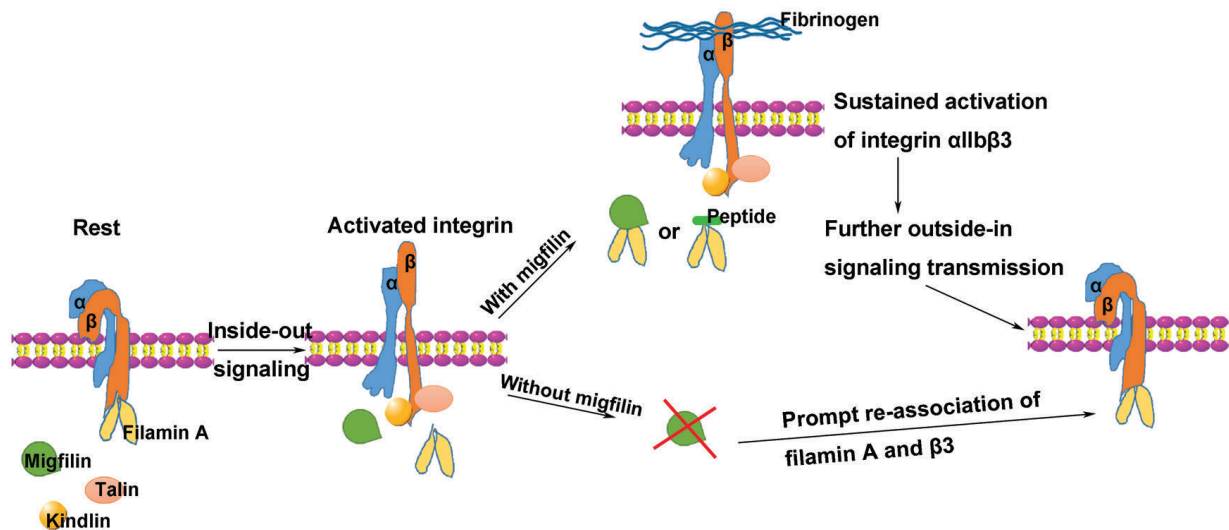
Figure 6. A model for the role of the migfilin in regulating filamin A-β3 interaction during platelet activation. In resting platelets, filamin A binding to the β3 tail prevents interactions among talin, kindlin, and integrin. When a platelet is activated, inside-out signals, through displacement of filamin A and enabling subsequent talin and kindlin binding to β3, culminate in the high affinity conformational change of αIIbβ3. Upon binding of activated αIIbβ3 to fibrinogen, migfilin (or WT-migfilin-CCR7 peptide) prevents the reassociation of filamin A to β3 and supports a sustained outside-in signaling. Without migfilin, filamin A binds back to β3 prematurely and inhibits further transmission of integrin outside-in signals.

ing associated with αIIbβ3. However, supported by the functional measurements and phosphorylation events representative of inside-out and outside-in signaling, our current study demonstrates that the involvement of migfilin is restricted to outside-in signaling of αIIbβ3. In particular, using migfilin peptide synthesized in the same way as described in the previous study,[13] the current study demonstrate that platelet aggregation is only induced by the peptide at a concentration above 10 μM. At a lower concentration (5 μM), the migfilin peptide does not induce platelet aggregation (*Online Supplementary Figure S5*), yet this concentration of migfilin peptide fully rescues the impaired function and αIIbβ3 outside-in signaling in *migfilin⁻/⁻* platelets. These results not only support that the observed platelet phenotypes in the current study are *bona fide* migfilin-dependent, but also reveal that platelets are sensitive to the amount of intracellular migfilin. Hence, combining the observations obtained in *migfilin⁻/⁻* platelets and those using migfilin peptides, it is possible to envisage that the natural amount of migfilin participates in outside-in signaling, while excessive migfilin might influence inside-out signaling. This may also justify the extremely low expression of migfilin in platelets. Intriguingly, the use of migfilin peptide could be further translated into a rescued hemostatic and thrombotic function *in vivo* in *migfilin⁻/⁻* mice.

Migfilin⁻/⁻ platelets exhibit a reduced phosphorylation level of the molecules corresponding to early outside-in signaling such as β3, Src, and Syk, as well as a hampered ability to spread on immobilized fibrinogen. On the contrary, the late outside-in signaling events, such as phosphorylation of ERK, and p38,[24] were not drastically changed, nor did migfilin-deficiency critically influence clot retraction. Corroborating these findings, migfilin peptides harboring the filamin A binding sequence rescue the phosphorylation events and sequential functions associated with early but not late outside-in signaling. Our results may have suggested that filamin A constitute the

major functional partner of migfilin in platelets. Yet the inability to visualize migfilin protein in platelets has presented itself as a large hurdle to further dissection of the mechanism of migfilin. Particularly, one question persists: how can migfilin have such an important role when the protein is present in such a low amount? Indeed, based on the published literature,[13] stoichiometry of migfilin binding to filamin A (IgFLNa21 domain) is either 1:1 or 1:2. However, since migfilin-filamin A interaction is much stronger than filamin A-integrin interaction,[29,14] the amount of migfilin required to trigger integrin activation is conceivably much lower than the proposed stoichiometry of migfilin-filamin A binding. Alternatively, migfilin may be enriched spatially to the integrin adhesion sites during activation,[30,31] which eliminates the needs of high expression in the cytoplasm. Moreover, migfilin interacts with multiple important proteins such as kindlin, Src and VASP,[30-33] the confluence of synergistic effects executed by these important platelet regulators may result in an amplified platelet activation.[7,34,35] We acknowledge that the mechanism of migfilin in platelet is only partially unveiled by the current study. A further elaboration of the migfilin interaction network in platelets is warranted.

A previous study has elegantly unveiled the important role of filamin A-αIIbβ3 interaction in pro-platelet formation and explained the pathogenesis of macrothrombocytopenia in filaminopathies (conditions connected to heterozygous filamin A mutations).[36] Intriguingly, although the current study has shown that migfilin regulates filamin A-αIIbβ3 interaction in platelets, deletion of migfilin seems to neither influence the platelet count nor the platelet morphology. It may be explained by the fact that loss of migfilin essentially enhances the interaction between filamin A and αIIbβ3, which contrasts the phenotype caused by filamin A mutations, whose ability to interact with αIIbβ3 is reduced. The heterogenous phenotypes of platelets and megakaryocytes associated with filamin A mutations indicate that com-

pared to migfilin, changes of filamin A has far more extensive impact on megakaryocytes and platelets.[6,37]

In conclusion, migfilin is an important positive regulator for hemostasis and thrombosis. Through regulating the binding dynamics of filamin A and αIIbβ3 (Figure 6), migfilin promotes early outside-in signaling of αIIbβ3 and supports platelet dense granule secretion. Further studies of migfilin will possibly lead to the discovery of new regulators important for platelet function and effective management of thrombosis.

References

1. Shattil SJ, Newman PJ. Integrins: dynamic scaffolds for adhesion and signaling in platelets. Blood. 2004;104(6):1606-1615.
2. Li Z, Delaney MK, O'Brien KA, Du X. Signaling during platelet adhesion and activation. Arterioscler Thromb Vasc Biol. 2010;30(12):2341-2349.
3. Metcalf DG, Moore DT, Wu Y, et al. NMR analysis of the alphaIIb beta3 cytoplasmic interaction suggests a mechanism for integrin regulation. Proc Natl Acad Sci U S A. 2010;107(52):22481-22486.
4. Tadokoro S, Shattil SJ, Eto K, et al. Talin binding to integrin beta tails: a final common step in integrin activation. Science. 2003;302(5642):103-106.
5. Kiema T, Lad Y, Jiang P, et al. The molecular basis of filamin binding to integrins and competition with talin. Mol Cell. 2006;21(3):337-347.
6. Berrou E, Adam F, Lebret M, et al. Gain-of-function mutation in filamin A potentiates platelet integrin alphaIIbbeta3 activation. Arterioscler Thromb Vasc Biol. 2017;37(6):1087-1097.
7. Moser M, Nieswandt B, Ussar S, et al. Kindlin-3 is essential for integrin activation and platelet aggregation. Nat Med. 2008;14(3):325-330.
8. Bouvard D, Pouwels J, De Franceschi N, et al. Integrin inactivators: balancing cellular functions in vitro and in vivo. Nat Rev Mol Cell Biol. 2013;14(7):430-442.
9. Shen B, Zhao X, O'Brien KA, et al. A directional switch of integrin signalling and a new anti-thrombotic strategy. Nature. 2013;503(7474):131-135.
10. Wu C. Migfilin and its binding partners: from cell biology to human diseases. J Cell Sci. 2005;118(Pt 4):659-664.
11. Tu Y, Wu S, Shi X, et al. Migfilin and Mig-2 link focal adhesions to filamin and the actin cytoskeleton and function in cell shape modulation. Cell. 2003;113(1):37-47.
12. Akazawa H, Kudoh S, Mochizuki N, et al. A novel LIM protein Cal promotes cardiac differentiation by association with CSX/NKX2-5. J Cell Biol. 2004;164(3):395-405.
13. Ithychanda SS, Das M, Ma YQ, et al. Migfilin, a molecular switch in regulation of integrin activation. J Biol Chem. 2009;284(7):4713-4722.
14. Das M, Ithychanda SS, Qin J, et al. Migfilin and filamin as regulators of integrin activation in endothelial cells and neutrophils. PLoS One. 2011;6(10):e26355.
15. Xiao G, Cheng H, Cao H, et al. Critical role of filamin-binding LIM protein 1 (FBLP-1)/migfilin in regulation of bone remodeling. J Biol Chem. 2012;287(25):21450-21460.
16. Gong H, Ni J, Xu Z, et al. Shp2 in myocytes is essential for cardiovascular and neointima development. J Mol Cell Cardiol. 2019;137 (71-81).
17. Chen L, Wright LR, Chen CH, et al. Molecular transporters for peptides: delivery of a cardioprotective epsilonPKC agonist peptide into cells and intact ischemic heart using a transport system, R(7). Chem Biol. 2001;8(12):1123-1129.
18. Mehta AY, Mohammed BM, Martin EJ, et al. Allosterism-based simultaneous, dual anticoagulant and antiplatelet action: allosteric inhibitor targeting the glycoprotein Ibalpha-binding and heparin-binding site of thrombin. J Thromb Haemost. 2016;14(4):828-838.
19. Moik DV, Janbandhu VC, Fassler R. Loss of migfilin expression has no overt consequences on murine development and homeostasis. J Cell Sci. 2011;124(Pt 3):414-421.
20. Haubner BJ, Moik D, Schuetz T, et al. In vivo cardiac role of migfilin during experimental pressure overload. Cardiovasc Res. 2015;106(3):398-407.
21. Chari-Turaga R, Naik UP. Integrin alphaIIbbeta3: a novel effector of Galpha13. Cell Adh Migr. 2011;5(1):4-5.
22. Gong H, Shen B, Flevaris P, et al. G protein subunit Galpha13 binds to integrin alphaIIbbeta3 and mediates integrin "outside-in" signaling. Science. 2010;327(5963):340-343.
23. Flevaris P, Stojanovic A, Gong H, et al. A molecular switch that controls cell spreading and retraction. J Cell Biol. 2007;179(3):553-565.
24. Flevaris P, Li Z, Zhang G, et al. Two distinct roles of mitogen-activated protein kinases in platelets and a novel Rac1-MAPK-dependent integrin outside-in retractile signaling pathway. Blood. 2009;113(4):893-901.
25. Falet H. New insights into the versatile roles of platelet FlnA. Platelets. 2013; 24(1):1-5.
26. Yin H, Stojanovic A, Hay N, et al. The role of Akt in the signaling pathway of the glycoprotein Ib-IX induced platelet activation. Blood. 2008;111(2):658-665.
27. Ren Q, Ye S, Whiteheart SW. The platelet release reaction: just when you thought platelet secretion was simple. Curr Opin Hematol. 2008;15(5):537-541.
28. Reed GL, Fitzgerald ML, Polgar J. Molecular mechanisms of platelet exocytosis: insights into the "secrete" life of thrombocytes. Blood. 2000;96(10):3334-3342.
29. Lad Y, Jiang P, Ruskamo S, et al. Structural basis of the migfilin-filamin interaction and competition with integrin beta tails. J Biol Chem. 2008;283(50):35154-35163.
30. Liu Z, Lu D, Wang X, et al. Kindlin-2 phosphorylation by Src at Y193 enhances Src activity and is involved in Migfilin recruitment to the focal adhesions. FEBS Lett. 2015;589(15):2001-2010.
31. Brahme NN, Harburger DS, Kemp-O'Brien K, et al. Kindlin binds migfilin tandem LIM domains and regulates migfilin focal adhesion localization and recruitment dynamics. J Biol Chem. 2013;288(49):35604-35616.
32. Zhao J, Zhang Y, Ithychanda SS, et al. Migfilin interacts with Src and contributes to cell-matrix adhesion-mediated survival signaling. J Biol Chem. 2009;284(49):34308-34320.
33. Zhang Y, Tu Y, Gkretsi V, et al. Migfilin interacts with vasodilator-stimulated phosphoprotein (VASP) and regulates VASP localization to cell-matrix adhesions and migration. J Biol Chem. 2006;281(18):12397-12407.
34. Senis YA, Mazharian A, Mori J. Src family kinases: at the forefront of platelet activation. Blood. 2014;124(13):2013-2024.
35. Benz PM, Laban H, Zink J, et al. Vasodilator-Stimulated Phosphoprotein (VASP)-dependent and -independent pathways regulate thrombin-induced activation of Rap1b in platelets. Cell Commun Signal. 2016;14 (1):21.
36. Donada A, Balayn N, Sliwa D, et al. Disrupted filamin A/alphaIIbbeta3 interaction induces macrothrombocytopenia by increasing RhoA activity. Blood. 2019;133(16):1778-1788.
37. Berrou E, Adam F, Lebret M, et al. Heterogeneity of platelet functional alterations in patients with filamin A mutations. Arterioscler Thromb Vasc Biol. 2013; 33(1):e11-18.

Modifying ADAMTS13 to modulate binding of pathogenic autoantibodies of patients with acquired thrombotic thrombocytopenic purpura

Nuno A. G. Graça,[1,2] Bogac Ercig,[2,3,4] Leydi Carolina Velásquez Pereira,[5] Kadri Kangro,[5] Paul Kaijen,[2] Gerry A. F. Nicolaes,[3,4] Agnès Veyradier,[6,7] Paul Coppo,[7-9] Karen Vanhoorelbeke,[5] Andres Männik[1] and Jan Voorberg[2]

[1]Icosagen Cell Factory OÜ, Õssu, Kambja, Tartumaa, Estonia; [2]Department of Molecular and Cellular Hemostasis, Sanquin-Academic Medical Center Landsteiner Laboratory, Amsterdam, the Netherlands; [3]Pharmatarget, Maastricht, the Netherlands; [4]Department of Biochemistry, Cardiovascular Research Institute Maastricht (CARIM), Maastricht University, Maastricht, the Netherlands; [5]Laboratory for Thrombosis Research, IRF Life Sciences, KU, Leuven Campus Kulak Kortrijk, Kortrijk, Belgium; [6]Service d'Hématologie Biologique and EA3518–Institut Universitaire d'Hématologie, Groupe Hospitalier Saint Louis-Lariboisière, AP-HP, Université Paris Diderot, Paris, France; [7]Centre de Référence des Microangiopathies Thrombotiques, Hôpital Saint-Antoine, AP-HP, Paris, France; [8]Service d'Hématologie, Hôpital Saint-Antoine, AP-HP, Paris, France and [9]Sorbonne Université, UPMC Université Paris, Paris, France

ABSTRACT

Antibodies that develop in patients with immune thrombotic thrombocytopenic purpura commonly target the spacer epitope R568/F592/R660/Y661/Y665 (RFRYY) of ADAMTS13 (**a d**isintegrin **a**nd **m**etalloproteinase with a **t**hrombo**s**pondin type 1 motif, member **13**). In this study we present a detailed contribution of each residue in this epitope for autoantibody binding. Different panels of mutations were introduced to create a large collection of full-length ADAMTS13 variants comprising conservative (Y←→F), semi-conservative (Y/F→L), non-conservative (Y/F→N) or alanine (Y/F/R→A) substitutions. Previously reported gain-of-function (KYKFF) and truncated 'MDTCS' variants were also included. Sera from 18 patients were screened against all variants. Conservative mutations of the aromatic residues did not reduce the binding of autoantibodies. Moderate resistance was achieved by replacing R568 and R660 by lysines or alanines. Semi-conservative mutations of aromatic residues showed a moderate effectiveness in autoantibody resistance. Non-conservative asparagine or alanine mutations of aromatic residues were the most effective. In the mixtures of autoantibodies from the majority (89%) of patients screened, autoantibodies targeting the spacer RFRYY epitope were preponderant compared to other epitopes. Reductions in ADAMTS13 proteolytic activity were observed for all full-length mutant variants, in varying degrees. The greatest reductions in activity were observed in the most autoantibody-resistant variants (15-35% residual activity in a FRETS-VWF73 assay). Among these, a triple-alanine mutant – RARAA – showed activity in a von Willebrand factor multimer assay. This study shows that non-conservative and alanine modifications of residues within the exosite-3 spacer RFRYY epitope in full-length ADAMTS13 resist the binding of autoantibodies from patients with immune thrombotic thrombocytopenic purpura, while retaining residual proteolytic activity. Our study provides a framework for the design of autoantibody-resistant ADAMTS13 variants for further therapeutic development.

Introduction

Thrombotic thrombocytopenic purpura (TTP) is a life-threatening rare disorder triggered by a lack of activity of the von Willebrand factor (VWF)-cleaving protease ADAMTS13 (**a d**isintegrin **a**nd **m**etalloproteinase with a **t**hrombo**s**pondin type 1 motif, member **13**). A limited number of cases are congenital, however approximately 95% of cases are of an acquired, autoimmune nature – immune TTP – in which autoantibodies targeting ADAMTS13 cause loss of enzyme activity resulting in accumulation of highly pro-thrombotic ultra-large VWF multimers.[1] ADAMTS13 is a large, complex enzyme comprising 14 domains which, from the N- to C-terminal, are: metalloprotease (M), disintegrin (D), thrombospondin-type 1-repeat 1 (TSP1), cysteine-rich (C), spacer (S), seven thrombospondin-type 1-repeats 2-8 (TSP2-8), and two CUB domains (CUB1 and CUB2)[2] (Figure 1). The mechanisms for the loss of self-tolerance towards ADAMTS13 are not completely understood, but include specific HLA alleles, ethnicity and other genetic traits.[3] Additionally, onset has also been associated with infections,[4,5] drugs,[6]

and cases of envenomation.[7,8] Most autoantibodies of patients with immune TTP are encoded by the heavy chain variable region genes V_H1-69[9-12] and V_H1-3.[12] However, the immune response is polyclonal,[13] usually targeting the spacer domain,[14] and may target other domains as well.[15-17] Antibodies targeting the MDTCS domains physically block interactions between ADAMTS13 and VWF.[18] So far, isolated autoantibodies against C-terminal TSP2-8 and CUB1-2 domains have not shown a clear direct inhibitory action, at least in static assays.[10] Both types can increase the clearance of ADAMTS13, which is considered the major mechanism inducing loss of ADAMTS13 activity.[17,19,20]

Several epitope mapping studies revealed that in the exosite-3 of the spacer domain, an epitope comprising residues R568/F592/R660/Y661/Y665 (RFRYY) is commonly targeted in nearly 95% of patients with immune TTP (*Online Supplementary Table S1*).[10,15-17,21-24] Studies of spacer exosite-3 alanine scans have shown that alanine modifications lead to reductions in exosite-3 spacer autoantibody binding,[22,23] but also result in reductions of activity.[23,25] Another study revealed that highly conserva-
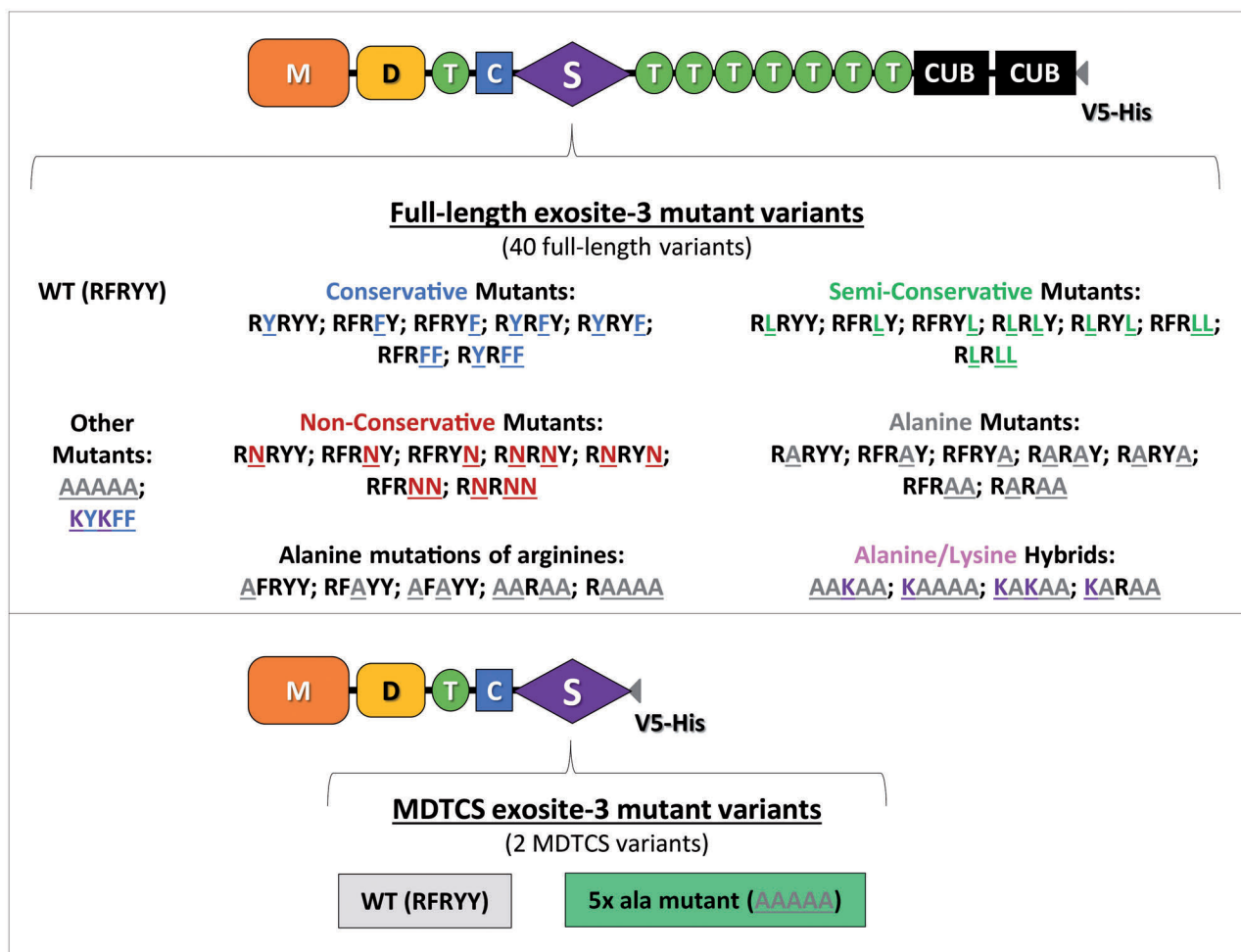
Figure 1. Overview of all ADAMTS13 spacer exosite-3 mutant variants created for this study. Full-length and MDTCS ADAMTS13 variants used in this study are shown. For ease and direct comparison with the original exosite-3 epitope (RFRYY), the mutations inserted are shown with the one-letter amino acid code in different colors and underlined. A total of 40 full-length variants were used, comprising conservative (Y↔F), semi-conservative (F/Y→L), non-conservative (F/Y→N), classic alanine (F/Y/R→A) and alanine/lysine hybrid mutations (F/Y→A + R→K). The residue substitutions were chosen based on the physicochemical characteristics of the amino acid side-chains (see *Online Supplementary Methods* for a more detailed description of the rationale for the different choices of amino acids). The classic gain-of-function (KYKFF) variant was also included in this study. In addition, two MDTCS variants were included (lower panel).

tive substitutions inserted in a full-length context confer resistance to autoantibodies while generating a gain-of-function (GoF) ADAMTS13 with more activity than the wild-type form.[26] These mutations were introduced cumulatively. At present, it is not clear how the degree of conservation of the amino-acid side-chains in the spacer exosite-3 RFRYY epitope affects both the autoantibody binding and the activity of ADAMTS13 variants.

In this study we present a refinement of the contribution of the residues in the exosite-3 RFRYY epitope to overall response of patients' autoantibodies. We included an extensive set of full-length spacer domain epitope variants with different degrees of residue conservation (Figure 1). The mutations inserted included single mutations and multiple progressively cumulative mutations, to scrutinize in more detail how they affect the binding of patients' autoantibodies. A total of 42 ADAMTS13 variants were screened for binding of autoantibodies from patients' samples. As expected, autoantibodies directed towards spacer domain exosite-3 constituted the most important subset of autoantibodies within the patients' response. We also demonstrated that within our panels of full-length ADAMTS13 variants, several displayed significantly reduced binding of autoantibodies while retaining residual proteolytic enzyme activity. Our study provides candidate molecules that could be used as a template for the design of novel therapeutic approaches that limit the binding of pathogenic autoantibodies to the spacer domain of ADAMTS13.

Methods

Patients

Patients' sera were obtained from the French Reference Center for Thrombotic Microangiopathies (CNR-MAT, Paris, France), from patients in the acute phase of onset of immune TTP, before treatment. All patients had ADAMTS13 activity <10% (FRETS-VWF73) and detectable autoantibodies against ADAMTS13 in varying titers (>15 IU/mL, Technozyme ADAMTS13-INH ELISA kit; Technoclone, Vienna, Austria). All patients included were described in previous studies[27,28] (Table 1). Informed consent was obtained from patients according to the Declaration of Helsinki. The study was approved by the Ethics Committee of Hôpital Pitié-Salpêtrière and Hôpital Saint-Antoine (Assistance Publique-Hôpitaux de Paris, France).

Assessment of reactivity of ADAMTS13 variants with patients' samples

The design, construction, production, and computational modeling of human ADAMTS13 variants, as well as

Table 1. Patients' clinical data.

Patient	Sex	Age	ADAMTS13 activity (FRETS-VWF73, %)	IgG anti-ADAMTS13 (IU/mL)	ADAMTS13 antigen (μg/mL)*	Treatment regimen in addition to PEX§	Detected anti-spacer idiotopes§	Cerebral involvement§
TTP-007	M	55	<5	100	0.05	+ steroids + rituximab + cyclophosphamide	Others	No
TTP-008	M	74	<5	120	0.05	+ steroids + rituximab	Others	Yes (confusion)
TTP-012	M	55	<5	260	<0.02	No treatment †	Others	No
TTP-017	F	48	<5	85	<0.02	+ steroids + rituximab	Others	Yes (headaches)
TTP-030	F	62	<5	59	0.35	PEX only	I-9 + II-1 + TTP73 idiotopes	Yes (aphasia)
TTP-041	F	68	<5	69	0.74	+ steroids + rituximab	II-1 + TTP73 idiotopes	Yes (seizure)
TTP-042	F	45	<5	69	0.16	+ steroids + rituximab	I-9 idiotope	Yes (transient focal defect)
TTP-049	F	35	<5	52	0.14	+ steroids	I-9 + TTP73 idiotopes	Yes (headaches, visual disorders)
TTP-052	F	24	<5	175	0.10	+ steroids + rituximab	I-9 + II-1 + TTP73 idiotopes	Yes (aphasia)
TTP-057	M	52	<5	87	0.11	+ steroids + rituximab + vincristine + splenectomy (anti-VWF antibodies)	Others	No
TTP-058	F	76	<5	>100	0.21	+ rituximab	Others	Yes (stroke)
TTP-075	M	27	<5	89	0.44	+ steroids	I-9 idiotope	Yes (headaches)
TTP-076	F	45	<5	65	0.09	+ steroids	I-9 + II-1 idiotopes	No
TTP-079	F	37	<5	180	<0.02	+ steroids	I-9 + TTP73 idiotopes	No
TTP-080	M	61	<10	210	<0.02	PEX only	I-9 idiotope	No
TTP-081	M	42	<5	100	0.03	+ steroids + rituximab	I-9 + II-1 + TTP73 idiotopes	Yes (stroke)
TTP-085	F	85	<5	>100	<0.02	+ steroids	Others	Yes (transient focal defect)
TTP-093	F	21	<5	160	0.02	+ rituximab	Others	Yes (headaches, transient focal defect)

PEX: plasma exchange; M: male; F: female; VWF: von Willebrand factor; *Data from Roose et al. 2018.[27] §Data from Schelpe et al. 2019.[28]

expression and purification of anti-ADAMTS13 monoclonal antibodies I-9 and II-1 are given in the *Online Supplementary Methods* (see *Online Supplementary Figures S1 and S2*, and *Online Supplementary Table S2*). Figure 1 provides an overview of the variants that were created and included in this study. Several panels of conservative (Y↔F), semi-conservative (Y/F→L), and non-conservative (Y/F→N) mutations and alanine (Y/F/R→A) substitutions, as well as a panel of alanine and lysine hybrids were employed in this study. For the non-conservative asparagine mutations no putative N-glycosylation sites were introduced. The rationale for the choice of each type of mutation is presented in the *Online Supplementary Methods*. For ease, from here on throughout the text the variants will be referred to by the final mutated epitope with the residue replacement underlined (e.g., RFRYY is the wild-type and RFR<u>LL</u> is a double leucine mutant carrying Y661L/Y665L mutations). Murine antibodies 3H9 (anti-metalloprotease), and biotinylated 19H4 (anti-TSP8) and 17G2 (anti-CUB1) have been previously described.[29,30] Anti-V5 conjugated with horseradish peroxidase was obtained from Invitrogen® (Catalog # R961-25).

To determine the binding of autoantibodies in patients' samples to the ADAMTS13 variants described, a sandwich enzyme-linked immunosorbent assay (ELISA) was developed in-house. Full details are provided in the *Online Supplementary Methods*. Briefly, antibody 3H9 was used to coat 96-well plates to capture ADAMTS13 from cell culture medium (coating done at 1 μg/mL). Each patient's sample was tested for binding of autoantibodies against the variants described above. The samples were assessed against 200 ng/well (1.05 nmol/well) of each ADAMTS13 full-length variant or against equal molar quantities of the MDTCS variants (78.75 ng/well), in duplicate. A pool of monoclonal antibodies against human-IgG1, IgG2, IgG3 and IgG4, each conjugated with horseradish peroxidase (Sanquin, the Netherlands) was used for detection. In each plate, a monoclonal antibody II-1 dilution curve against the full-length wild-type ADAMTS13 was fitted with a four-parameter fit model (GraphPad Prism 5.0). Serum reactivity (i.e., binding) against each ADAMTS13 variant was converted to II-1 equivalent units (ng/mL) through interpolation, and a ratio of the interpolated signals was expressed as a percentage of wild-type binding. A heat map with the average values obtained was used for data comparison (Figure 2). The median reactivity for each ADAMTS13 variant was calculated from its average reactivities against each patient's sample. An example of how the calculations were performed is given in *Online Supplementary Figure S3*.

Assessment of the activity of ADAMTS13 variants

All variants were assessed for activity through FRETS-VWF73 assays, as previously described,[31] using a Fluoroskan Ascent plate reader (Thermo Electron Corporation) with modifications. All FRETS assays were done using the supernatants of cell cultures, and a modified buffer was added to maintain the pH at 6.0[32] (composition: $CaCl_2$ 25 mM, Bis-Tris 20 mM, Tris-HCl 20 mM, HEPES 20 mM, Tween20 0.005%). The recombinant full-length wild-type ADAMTS13 was used as the calibrator for the assay (concentration range: 0.025-0.4 μg/mL). Supernatant from Chinese hamster ovary (CHO) cells not producing ADAMTS13 was included as a control. All variants were tested at the same molar concentration of 1.05

nM (0.2 μg/mL for full-length variants and 0.07875 μg/mL for MDTCS variants). An example of a calibration curve is shown in *Online Supplementary Figure S4*.

Selected variants were additionally tested for activity in a static VWF multimer assay as described in detail in the *Online Supplementary Methods*.

Results

The majority of autoantibodies in patients with immune thrombotic thrombocytopenic purpura target the spacer exosite-3 RFRYY epitope

All patients' samples were assessed for binding to each of the ADAMTS13 variants described with an in-house developed sandwich ELISA. Figure 2 shows the reactivity of all the different ADAMTS13 variants towards each patient's sample in a heat map format. To assess the potential presence of anti-TSP2-8 and CUB1-2 domain antibodies, we first compared the reactivity of the patients' samples with full-length wild-type ADAMTS13 and the MDTCS variants. Two patients (TTP-057 and 085) showed a loss of signal with wild-type MDTCS of more than 70%. All other patients showed either similar signals to the full-length wild-type enzyme or, in a limited number of cases, losses up to 48%. The MDTCS-<u>AAAAA</u> variant caused a major reduction in signal compared to wild-type MDTCS in all patients (with the exception of patient TTP-057). The same 5x ala mutations in a full-length context (<u>AAAAA</u>) caused large increases in signal for six patients compared to MDTCS 5x ala (6/18; 33%). These findings show that the autoantibodies targeting the spacer exosite-3 RFRYY epitope comprise the majority of the antibody mixture in most patients' autoantibody repertoire (16/18 cases, 89%). In rare cases, the repertoire was composed exclusively of autoantibodies targeting the TSP2-8 and/or CUB1-2 domains of ADAMTS13 (1/18 cases, 5%). However, in 12/18 cases (67%) the repertoire was composed almost exclusively of autoantibodies targeting the RFRYY epitope in the spacer domain.

Autoantibody resistance is obtained with non-conservative or alanine mutations

Next we assessed the efficacy of each type of mutation at inducing autoantibody resistance. We designed variants that retained R568 and R660 intact, as well as variants in which these residues were mutated. Within the variants in which R568 and R660 were kept intact, variants containing conservative mutations of aromatic residues were still recognized by autoantibodies present in the patients' sera (Figure 2). Semi-conservative mutations in the spacer domain epitope showed reduced binding to patients' antibodies with signals in the range of 30%-75% when compared to the wild-type form in 15 patients, and below 30% in one patient. The non-conservative asparagine mutations were the most successful of the aromatic residue mutations at escaping binding by patients' autoantibodies, presenting signals within the range of 0%-75% for 16 patients. RFR<u>NY</u> and RFRY<u>N</u> mutants were the least successful of this panel at escaping the autoantibody response, followed by RFR<u>NN</u>. The <u>RNRNN</u> mutant had the lowest median reactivity of all aromatic residue triple mutants (14%). Alanine mutations of aromatic residues (i.e., R<u>A</u>RYY, RFR<u>A</u>Y, RFRY<u>A</u>, R<u>A</u>R<u>A</u>Y, R<u>A</u>RY<u>A</u>, RFR<u>AA</u> and R<u>A</u>R<u>AA</u>) followed the same trend as the asparagine

Mutant Variants (exosite-3 residues)		TTP 007	TTP 008	TTP 012	TTP 017	TTP 030	TTP 041	TTP 042	TTP 049	TTP 052	TTP 057	TTP 058	TTP 075	TTP 076	TTP 079	TTP 080	TTP 081	TTP 085	TTP 093	Median Reactivity
Full-length vs MDTCS	WT full-length (R F R Y Y)	100%	100%	100%	100%	100%	100%	100%	100%	100%	100%	100%	100%	100%	100%	100%	100%	100%	100%	100%
	MDTCS WT (R F R Y Y)	81%	115%	70%	73%	104%	112%	106%	93%	88%	6%	84%	91%	90%	67%	52%	67%	27%	60%	83%
	MDTCS 5ala (A A A A A)	4%	6%	20%	8%	0%	0%	20%	7%	1%	0%	1%	0%	10%	11%	2%	1%	4%		3%
	Full-length Mutant A A A A A	10%	7%	77%	20%	0%	0%	19%	6%	4%	90%	2%	0%	0%	40%	49%	27%	101%	8%	9%
Conservative Mutant Variants	Mutant R Y R Y Y	89%	101%	102%	83%	101%	106%	105%	92%	104%	106%	92%	107%	84%	81%	88%	78%	105%	103%	101%
	Mutant R F R F Y	100%	114%	101%	86%	110%	118%	110%	108%	115%	111%	92%	105%	108%	105%	95%	164%	80%	109%	108%
	Mutant R F R Y F	98%	117%	118%	98%	128%	108%	107%	100%	112%	100%	95%	118%	104%	115%	94%	142%	91%	114%	108%
	Mutant R Y R F Y	87%	104%	107%	86%	110%	109%	109%	87%	108%	102%	77%	111%	79%	75%	87%	135%	99%	105%	103%
	Mutant R Y R Y F	89%	96%	121%	82%	101%	114%	111%	96%	116%	112%	93%	103%	62%	70%	92%	100%	121%	107%	100%
	Mutant R F R F F	87%	103%	100%	92%	121%	112%	103%	76%	109%	93%	84%	100%	110%	101%	86%	187%	83%	110%	101%
	Mutant R Y R F F	83%	102%	114%	93%	67%	105%	99%	86%	92%	106%	87%	102%	59%	64%	102%	85%	93%	89%	92%
Semi-Conservative Mutant Variants	Mutant R L R Y Y	89%	114%	110%	80%	105%	104%	98%	95%	101%	124%	90%	104%	62%	54%	75%	62%	79%	86%	93%
	Mutant R F R L Y	90%	108%	110%	91%	102%	105%	100%	102%	98%	119%	95%	111%	65%	74%	90%	82%	81%	94%	97%
	Mutant R F R Y L	96%	119%	119%	95%	120%	109%	101%	103%	113%	120%	101%	117%	100%	107%	96%	132%	81%	101%	105%
	Mutant R L R L Y	71%	92%	101%	58%	71%	70%	97%	83%	85%	119%	67%	85%	19%	39%	62%	53%	74%	76%	72%
	Mutant R L R Y L	81%	117%	104%	67%	98%	108%	105%	94%	101%	125%	75%	101%	53%	63%	80%	73%	85%	93%	93%
	Mutant R F R L L	78%	99%	102%	82%	94%	106%	100%	96%	106%	114%	87%	96%	53%	57%	90%	95%	102%	97%	96%
	Mutant R L R L L	61%	67%	78%	51%	72%	63%	98%	64%	73%	112%	47%	72%	14%	39%	55%	53%	64%	73%	64%
Non-Conservative Mutant Variants	Mutant R N R Y Y	60%	80%	110%	37%	61%	63%	91%	71%	73%	109%	61%	67%	14%	45%	77%	52%	81%	57%	65%
	Mutant R F R N Y	73%	82%	98%	56%	73%	81%	94%	78%	79%	87%	74%	79%	33%	51%	64%	53%	89%	68%	76%
	Mutant R F R Y N	92%	106%	128%	83%	96%	119%	99%	103%	118%	87%	98%	108%	84%	98%	89%	97%	102%	91%	98%
	Mutant R N R N Y	28%	33%	105%	19%	28%	11%	73%	36%	30%	85%	25%	27%	0%	55%	56%	43%	86%	27%	32%
	Mutant R N R Y N	32%	52%	113%	26%	49%	25%	74%	44%	47%	60%	39%	36%	2%	66%	64%	46%	98%	40%	47%
	Mutant R F R N N	57%	74%	97%	38%	54%	55%	88%	66%	69%	67%	65%	68%	15%	60%	55%	36%	95%	50%	62%
	Mutant R N R N N	11%	10%	88%	18%	8%	0%	47%	16%	9%	57%	6%	10%	1%	51%	51%	41%	98%	10%	14%
Alanine Aromatic and Arginine Residues Mutant Variants	Mutant R A R Y Y	56%	65%	60%	43%	51%	56%	84%	58%	58%	95%	56%	55%	4%	26%	38%	45%	54%	44%	55%
	Mutant R F R A Y	74%	98%	119%	67%	72%	87%	94%	87%	88%	99%	88%	90%	38%	56%	61%	60%	85%	79%	86%
	Mutant R F R Y A	87%	109%	115%	76%	87%	118%	99%	99%	105%	86%	105%	109%	72%	89%	71%	56%	101%	95%	97%
	Mutant R A R A Y	37%	52%	86%	29%	33%	27%	78%	47%	47%	99%	32%	48%	0%	51%	41%	33%	85%	44%	45%
	Mutant R A R Y A	49%	65%	77%	39%	46%	66%	82%	67%	69%	110%	57%	54%	6%	40%	48%	31%	82%	65%	61%
	Mutant R F R A A	54%	80%	87%	42%	51%	65%	92%	73%	84%	73%	75%	73%	20%	65%	48%	35%	99%	65%	69%
	Mutant A F R Y Y	70%	94%	85%	77%	66%	103%	90%	100%	103%	86%	92%	98%	91%	96%	82%	78%	112%	87%	91%
	Mutant R F A Y Y	57%	90%	83%	68%	76%	90%	86%	88%	101%	93%	85%	82%	83%	99%	83%	94%	113%	86%	86%
	Mutant A F A Y Y	32%	72%	65%	49%	54%	67%	62%	63%	78%	77%	69%	60%	63%	90%	62%	61%	105%	70%	64%
	Mutant R A R A A	26%	35%	72%	24%	10%	5%	57%	28%	25%	94%	17%	26%	3%	44%	47%	34%	83%	24%	27%
	Mutant A A R A A	7%	17%	91%	22%	10%	1%	28%	21%	12%	72%	9%	10%	0%	66%	47%	35%	136%	26%	21%
	Mutant R A A A A	10%	15%	85%	29%	27%	8%	31%	20%	14%	96%	14%	9%	2%	61%	40%	22%	155%	31%	24%
	Full-length Mutant A A A A A	10%	7%	77%	20%	0%	0%	19%	6%	4%	90%	2%	0%	0%	40%	49%	27%	101%	8%	9%
Alanine Lysine Hybrids	Mutant A A K A A	7%	14%	75%	21%	7%	0%	26%	19%	14%	63%	11%	9%	1%	60%	62%	31%	119%	19%	19%
	Mutant K A A A A	9%	13%	79%	23%	12%	0%	28%	27%	14%	98%	12%	9%	1%	65%	54%	34%	127%	25%	24%
	Mutant K A K A A	10%	23%	81%	20%	10%	1%	36%	27%	20%	73%	16%	18%	0%	72%	56%	35%	131%	30%	25%
	Mutant K A R A A	14%	34%	84%	22%	0%	6%	43%	33%	22%	82%	17%	25%	1%	71%	57%	38%	129%	41%	34%
GoF	Mutant K Y K F F	58%	84%	68%	60%	82%	84%	89%	73%	94%	76%	88%	85%	49%	52%	62%	56%	64%	73%	73%
	No Protein Supernatant	0%	0%	0%	0%	7%	0%	0%	1%	0%	0%	0%	0%	0%	0%	0%	0%	0%	0%	0%
	Dilution Factor for each patient (fold dilution)	80x	200x	60x	40x	30x	40x	40x	30x	400x	40x	60x	40x	40x	40x	40x	30x	200x	80x	-
	Autoantibodies titer (I.U./mL)	100	120	260	85	59	69	69	52	175	87	>100	89	65	180	210	100	>100	160	

| 0% | 5% | 10% | 15% | 20% | 25% | 30% | 35% | 40% | 45% | 50% | 55% | 60% | 65% | 70% | 75% | 80% | 85% | 90% | 95% | 100% |

Low reactivity — **High reactivity**

Ratio mutant variant reactivity / full-length WT reactivity (%)
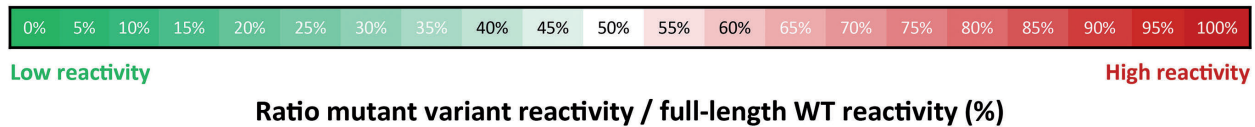
Figure 2. Heat map with reactivity of all the patients' samples tested against all ADAMTS13 spacer exosite-3 RFRYY mutant variants created for this study. Mutants (left) are organized by mutation type with residues mutated in color and underlined (blue: conservative mutations; green: semi-conservative mutations; red: non-conservative mutations; gray: alanine mutations; purple: arginine-to-lysine mutations), and by number of mutations introduced. The classic gain-of-function (GoF) variant is displayed separately for comparison. Patients' dilution factors and antibody titers are indicated in the rows below. The median reactivity of each mutant is displayed in the same heat-map fashion (right column). A color scale for reactivity is displayed below with green backgrounds indicating low reactivity, white backgrounds intermediate reactivity and red backgrounds high reactivity (n=2).

mutations, and were also effective at escaping binding of patients' antibodies, albeit to a lesser degree. The RARAA mutant had the second lowest median reactivity with patients' antibodies among this panel of alanine substitutions (27%). For both asparagine and alanine mutations, the more cumulative mutations were introduced, the higher was the effectiveness at escaping autoantibody binding.

Within the panels in which the R568 and R660 were also mutated, mutation of the arginines to alanines alone had a moderate effect on autoantibody resistance (median signal at 64% for mutant AFAYY) (Figure 2). The classic GoF molecule (KYKFF) also presented a moderate decrease in binding to patients' antibodies when compared to the wild-type form and to other mutations introduced. The median reactivity of the GoF variant was 73%, a mild improvement compared to a similar conservative mutant (RYRFF: median reactivity: 92%). As can be deduced from the RARAA mutant, addition of a further arginine mutation with alanine (AARAA and RAAAA mutants) promoted a further, but more limited, reduction of median reactivity (21% and 24%, respectively). Further mutating the remaining arginines to lysines (i.e., AAKAA, KAAAA, KAKAA mutants) produced little to no variation in median reactivity (19%-25%), with the KARAA mutant showing a small increase when compared to KAKAA. The 5x ala

full-length mutant (AAAAA) had the greatest decrease in median reactivity among all full-length variants (median signal: 9%). Our findings show that cumulative replacement of aromatic residues in the spacer RFRYY epitope of ADAMTS13 with asparagine or alanine provides superior resistance towards immune TTP patients' autoantibodies directed towards the spacer domain.

Autoantibody-resistant ADAMTS13 variants retain proteolytic activity

We subsequently assessed the impact of these mutations on the activity of ADAMTS13. All variants were tested in a FRETS-VWF73 assay at the same molar concentration and directly compared with the full-length wild-type ADAMTS13 (*Online Supplementary Figure S4*). The relative activities are shown in Figure 3. All full-length variants showed reduced activity in FRETS-VWF73 when compared to the full-length wild-type ADAMTS13. The degree of reduction varied depending on the mutations inserted. Conservative mutations retained the most activity on average. The RYRYY mutant had 39% activity while RFRFF had 76%. The triple conservative RYRFF mutant retained 56% of activity. Semi-conservative leucine mutants also retain overall high activity, with single and double mutations retaining between 35% and 76% activity. The RLRLL mutant had a larger loss of activ-
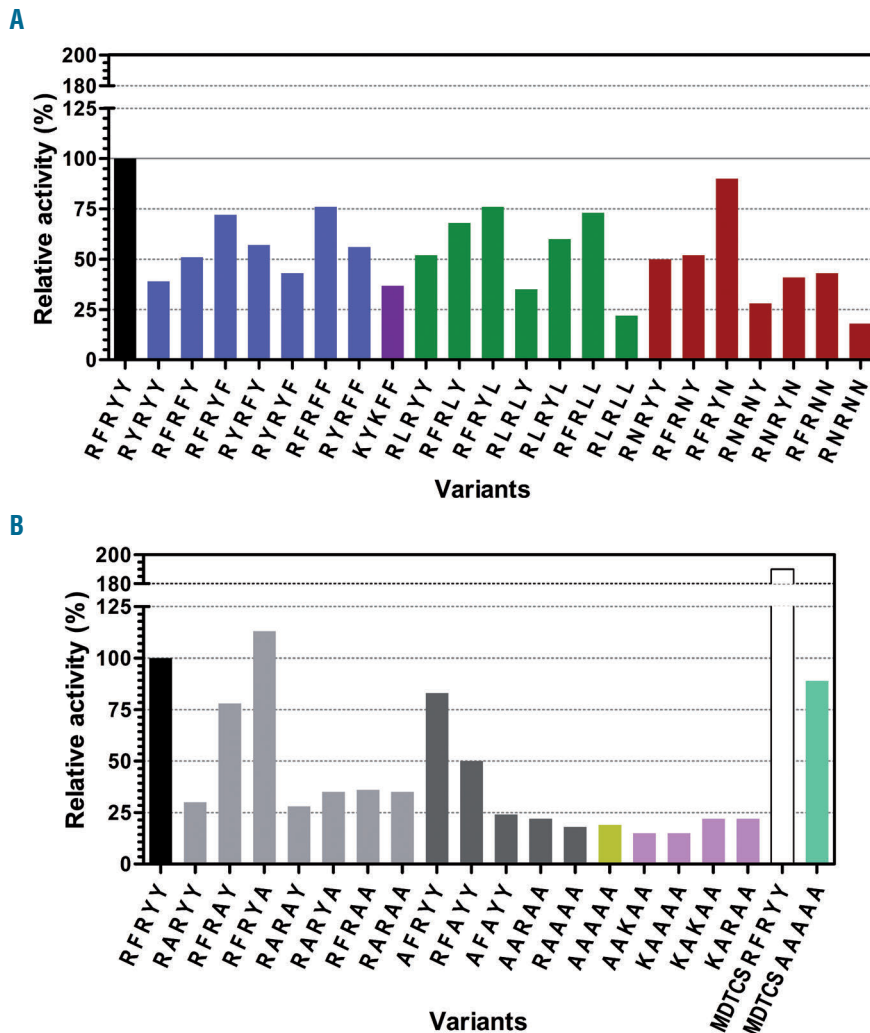
Figure 3. FRETS-VWF73 activity data of mutant ADAMTS13 variants. All mutant variants in this study were assessed for activity using a FRETS-VWF73 assay. Three independent assays were conducted, each one with its own calibration curve constructed using the recombinant full-length wild-type ADAMTS13 (an example of a calibration curve is shown in *Online Supplementary Figure S4*). In each assay, a limited number of variants could be introduced. All values are normalized to the full-length wild-type molecule (100% activity). (A) The relative activities of the variants are shown. The full-length wild-type ADAMTS13 is represented in black, the conservative variants in blue, the gain-of-function in purple, semi-conservative variants in green and non-conservative variants in red. (B) The relative activities of variants are shown. The full-length wild-type ADAMTS13 is represented in black, the aromatic-alanine variants in light gray, the arginine-alanine variants in dark gray, the full-length AAAAA in golden, the alanine/lysine hybrids in pink, the wild-type MDTCS in white and the MDTCS-AAAAA mutant in green.

ity, retaining only 22%. Single asparagine and alanine mutations of aromatic residues induced limited losses of activity. Cumulative double and triple asparagine or alanine mutations had more detrimental effects, with alanine mutations having less negative effects (RNRNN: 18%; RARAA: 35%). Mutation of the arginines by alanines had different impacts: R660A (RFAYY) had a higher reduction of activity (50% activity retained) compared to R568A (AFRYY) (83% activity retained). Mutation of both arginines (AFAYY) caused a large reduction of activity (24% that of the wild-type molecule). The classic GoF molecule (KYKFF) followed all trends observed for conservative mutations combined with arginine mutations and, surprisingly, also displayed reduced activity compared to the wild-type form (~37% activity retained). The full-length mutants AAAAA, AARAA, RAAAA, AAKAA, KAAAA, KAKAA, and KARAA all had similar activities (15-22%). The MDTCS variants displayed higher activities than each of their full-length counterparts (wild-type MDTCS with 190% and MDTCS-AAAAA with 89% *vs.* 100% and 19%, respectively). In general, an inverse correlation was observed: a higher resistance to autoantibody binding attained through spacer exosite-3 mutations resulted, in general, in a lower residual FRETS-VWF73 activity (Figure 4).

The activities of five variants were tested in the presence of patients' autoantibodies in a FRETS-VWF73 assay format (Figure 5). Samples from patients TTP-007, TTP-

008 (exclusively anti-spacer autoantibodies) and patient TTP-085 (anti-spacer and anti-C-terminal autoantibodies) were used to provide a proof-of-concept. While the wild-type and the classic GoF were clearly inhibited, all other selected variants retained the same levels of activity.

Subsequently, several mutants with different levels of FRETS-VWF73 activities were tested in a static VWF multimer assay (Figure 6). The wild-type molecule showed activity after 30 min, with high molecular weight VWF multimers being cleaved and satellite bands accumulating in the lower molecular weight regions. After 24 h, these differences were further pronounced. All of the mutants tested in this assay showed reduced activity compared to the wild-type molecule. The classic GoF (KYKFF) demonstrated the highest activity among all the mutants tested. Among the autoantibody-resistant mutants, RARAA had the highest activity, with a reduction of high molecular weight VWF multimers and accumulation of satellite bands. While the truncated wild-type MDTCS variant had equal activity to full-length wild-type ADAMTS13, the MDTCS-AAAAA variant had very low activity, comparable to that of its full-length counterpart, AAAAA.

Discussion

In the current study we assessed the relevance of the spacer RFRYY epitope residues for autoantibody binding,
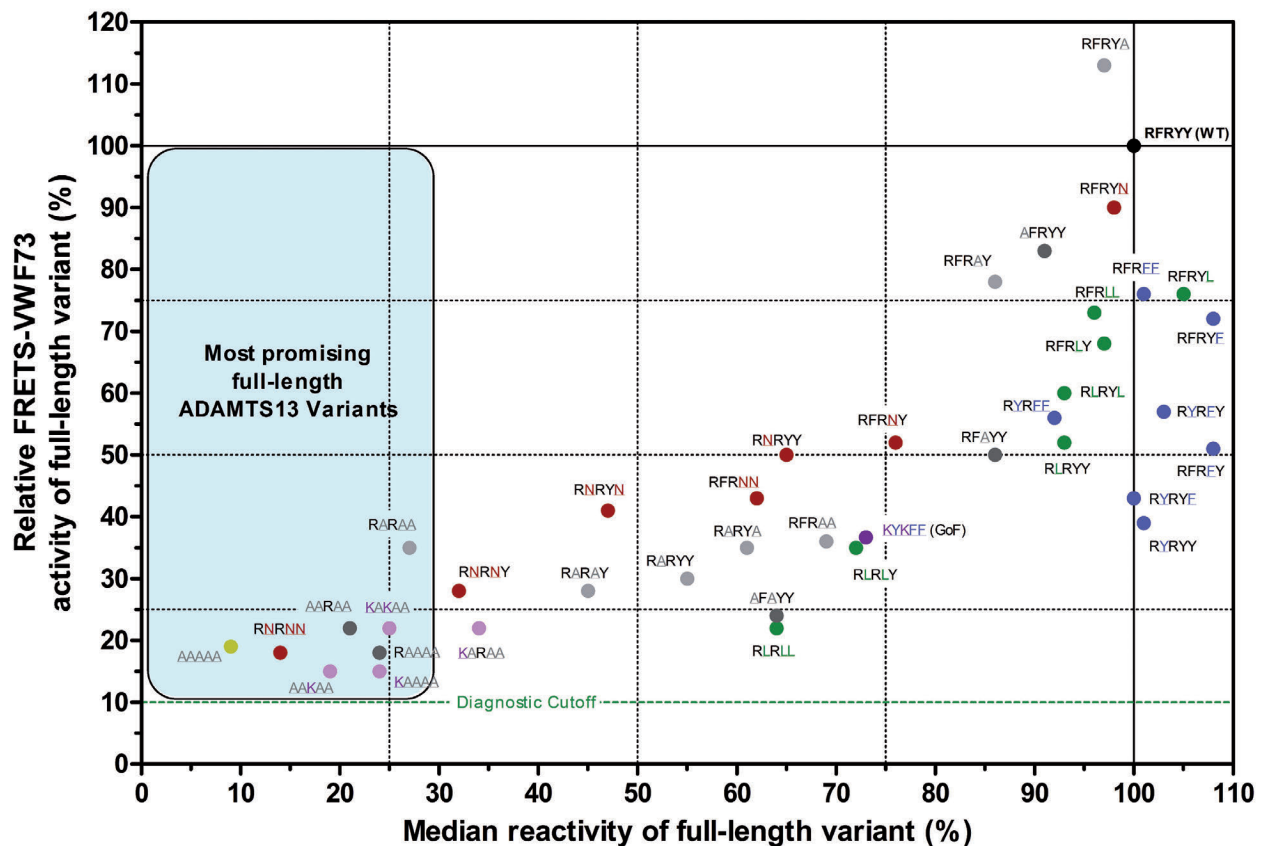
Figure 4. Inverse correlation observed between autoantibody reactivity and activity of ADAMTS13 variants. Only full-length ADAMTS13 variants are shown. The cyan-blue shading shows the area in which ADAMTS13 variants with reduced autoantibody binding are displayed. Blue dots represent conservative mutants; green dots represent semi-conservative mutants; red dots represent non-conservative mutants; gray dots represent alanine mutants (light-gray for only aromatic residues; dark-gray for arginine mutants); pink represents lysine/alanine hybrids.

and the types of mutations that confer highest resistance to binding of patients' anti-ADAMTS13 autoantibodies. In our study, the spacer RFRYY epitope made a major contribution to total autoantibody reactivity in 89% of the patients with immune TTP screened. Other studies reached similar conclusions.[17,18] In our study, 12/18 patients (67%), had autoantibody mixtures comprising almost exclusively anti-spacer RFRYY autoantibodies. We also had 6/18 patients (33%) who had C-terminal anti-TSP2-8 and/or anti-CUB1-2 domain autoantibodies, a prevalence slightly below the range reported in the literature (*Online Supplementary Table S1*). One patient (TTP-042) also had autoantibodies targeting other unknown areas in the N-terminal region (Figure 2).

We show that different types of mutations in ADAMTS13 spacer exosite-3 have different impacts on immune TTP patients' autoantibody binding. Our data indicate that the two arginines are less important for autoantibody binding than the three aromatic residues

present in this epitope (AFAYY had a median reactivity of 64%, while RARAA had only 27%). Conservative mutations of aromatic residues did not reduce reactivity towards patients' autoantibodies (RYRFF median reactivity: 92%). Replacing the arginines in this mutant by lysines (KYKFF, classic GoF mutant) led to a decrease in median reactivity (in agreement with the original study[26]), albeit quantitatively limited (73% binding). Thus, introduction of highly conservative mutations of aromatic residues is not sufficient to reduce the binding of autoantibodies targeting the RFRYY epitope. Semi-conservative mutations of aromatic residues with leucine had an intermediate, yet limited efficacy at autoantibody escape. Non-conservative asparagine or classic alanine mutations of the aromatic residues had the greatest success. Individual mutations had a low impact, and, by themselves, Y661 and Y665 appeared to be the least important residues for overall autoantibody binding. A more pivotal contribution was observed for F592, as shown when individually or cumu-
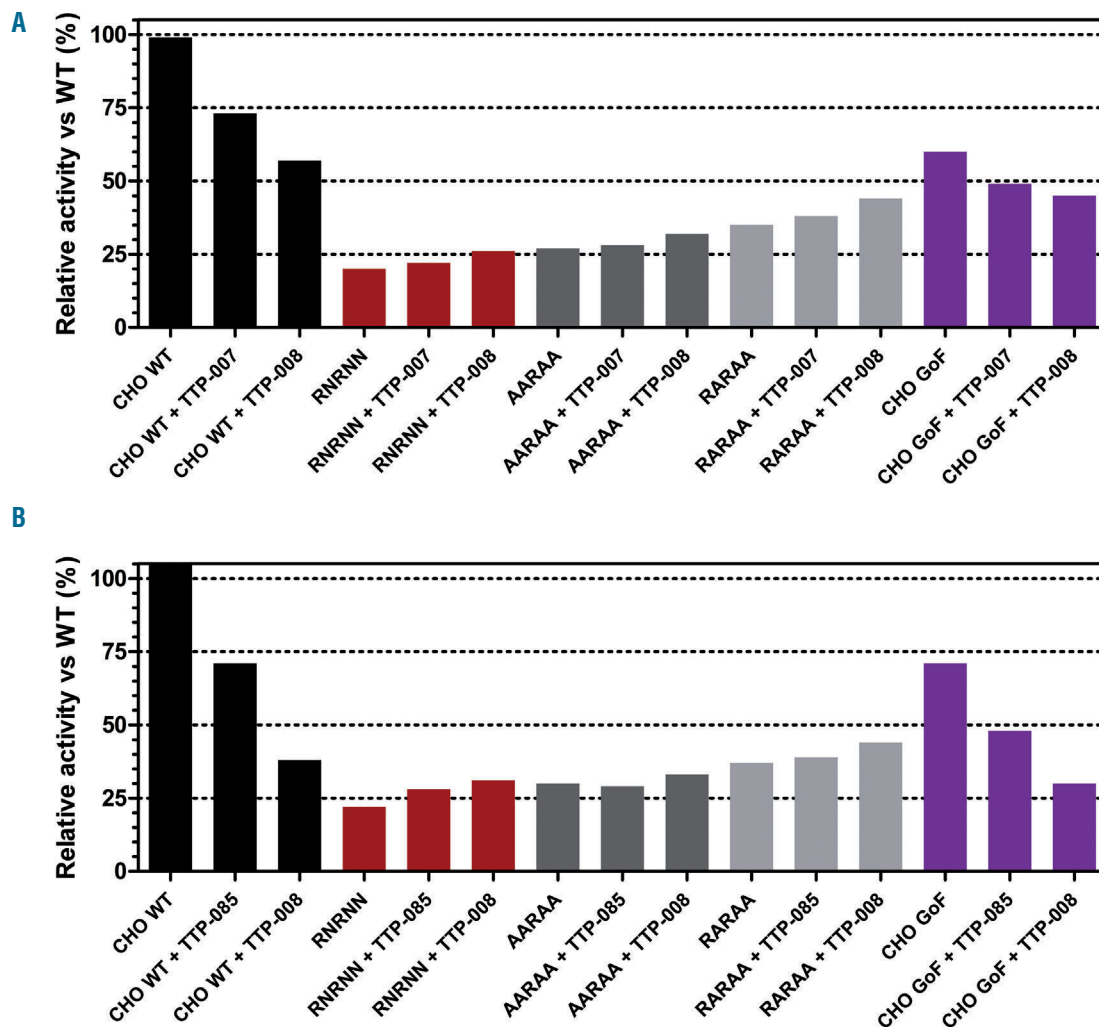
Figure 5. Patients' samples inhibit wild-type and gain-of-function (KYKFF) ADAMTS13 variants but not non-conservative or alanine ADAMTS13 variants. The activities of selected ADAMTS13 variants were tested in the presence of pathogenic patients' autoantibodies in FRETS-VWF73 assays. Three patients' samples, representative of the patients' autoantibody repertoire, were incubated directly with ADAMTS13 variants (each variant at 0.2 μg/mL). (A). samples from TTP-007 and TTP-008 (only anti-spacer autoantibodies) were diluted 40x. (B) Samples from TTP-008 (anti-spacer autoantibodies) and TTP-085 (anti-spacer and anti-C-terminal autoantibodies) were diluted 20x. As expected, both wild-type and gain-of-function variants were inhibited. Variants RNRNN, AARAA and RARAA displayed full-resistance and retained their baseline proteolytic activity levels. WT: wild-type; CHO: Chinese hamster ovary; GoF: gain-of-function.

latively mutated to either an asparagine or alanine. These mutations likely disrupt the hydrophobic cluster centered in F592 and formed together with Y661, Y665 and other neighboring residues.[33] The greatest impact was achieved with cumulative mutations of all three aromatic residues, alone or together with mutations of the arginines. The highest resistance to autoantibody binding was observed for the full-length 5x ala mutant (AAAAA), followed by the triple asparagine RNRNN mutant (Figure 2).

Protein surfaces enriched in tyrosine and arginine are usually involved in protein-protein interactions. Arginine salt-bridges are common players in these interactions.[34] Tyrosine itself is a highly promiscuous residue participating in many types of interactions.[35] This epitope contains two arginine residues, R568 and R660, which are likely involved in arginine-salt bridges for antibody binding (Figure 2), and also in intramolecular hydrogen bonds and cation-π interactions with Y661 and Y665 (*Online Supplementary Figure S5*). Paratopes of the antibodies are considered to have a core enriched in aromatic residues, particularly tyrosine.[36,37] The primary sequence of a large collection of anti-ADAMTS13 autoantibodies revealed that most autoantibodies targeting ADAMTS13 – encoded by heavy chain variable genes V_H1-69 and V_H1-3[11-13] – have a complementary determining region 3 (CDR3) consisting of multiple residues with either aromatic or negatively charged side chains.[11,12] Exchanging a tyrosine for a phenylalanine (and *vice versa*) within exosite-3 conserves
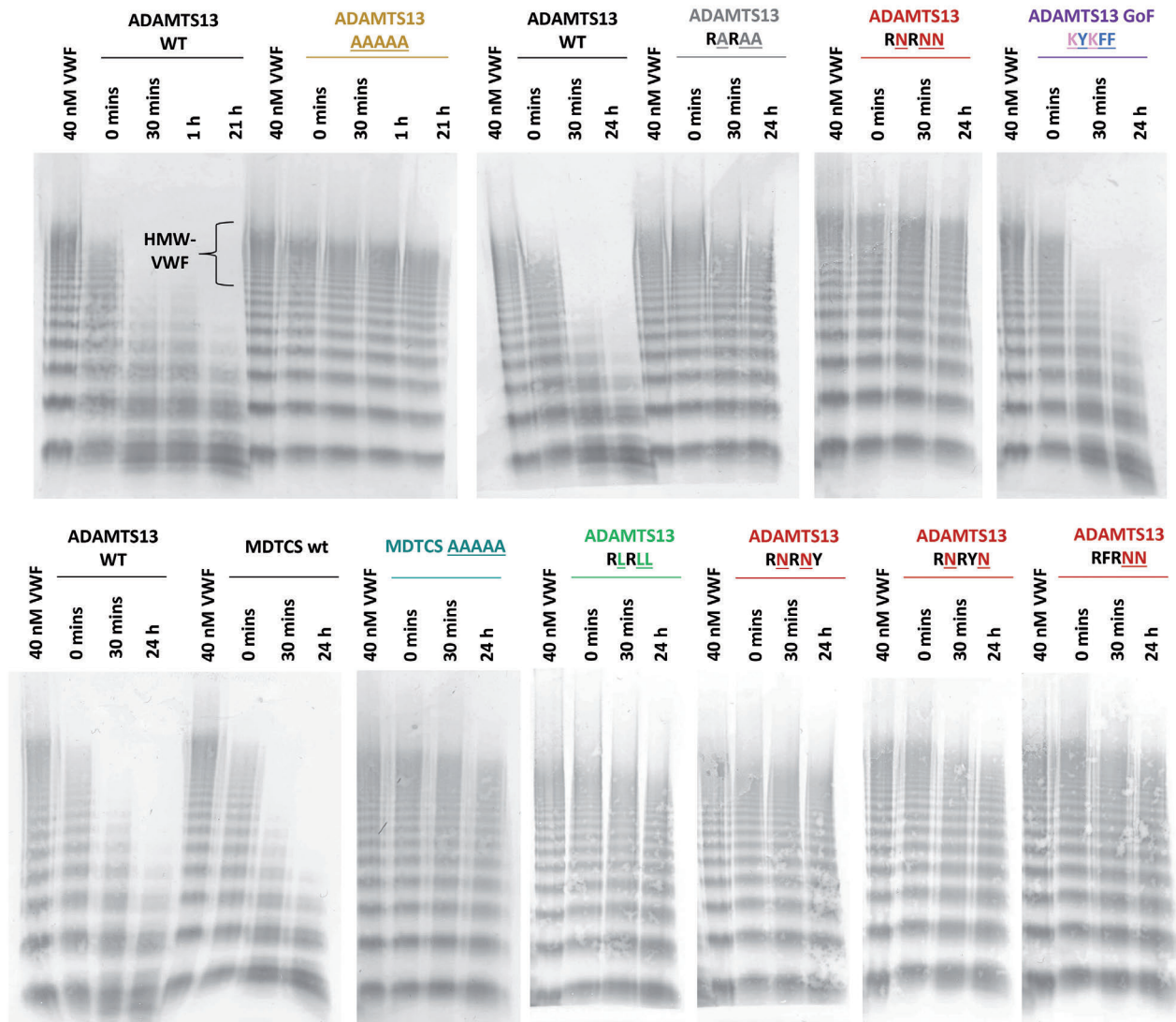
Figure 6. Autoantibody-resistant ADAMTS13 variants are capable of cleaving high-molecular weight multimers of von Willebrand factor. Selected variants with different levels of autoantibody reactivity/FRETS-VWF73 activity were tested for their proteolytic activity against recombinant multimeric von Willebrand factor (VWF) (1.9 nM ADAMTS13 for 40 nM VWF) in a static assay in which urea was used to denature VWF multimers. The full-length wild-type ADAMTS13 variant was used as a control for each individual reaction, with similar outcomes for all reactions. An example is shown in each panel for comparison. High-molecular weight VWF multimers are cleaved in a time-dependent manner, with accumulation of satellite bands in lower molecular weight regions. A lane containing 40 nM multimeric VWF without ADAMTS13 was included in the gels for comparison. All full-length variants displayed a reduction in proteolytic activity compared to the wild-type molecule. However, residual proteolytic activity was retained by several of them (including one of the most autoantibody-resistant variants, RARAA). The wild-type MDTCS and MDTCS-AAAAA were also tested, and while the wild-type MDTCS retained similar activity levels compared to the wild-type molecule, MDTCS-AAAAA displayed a reduction to the same level as its full-length counterpart, variant AAAAA.
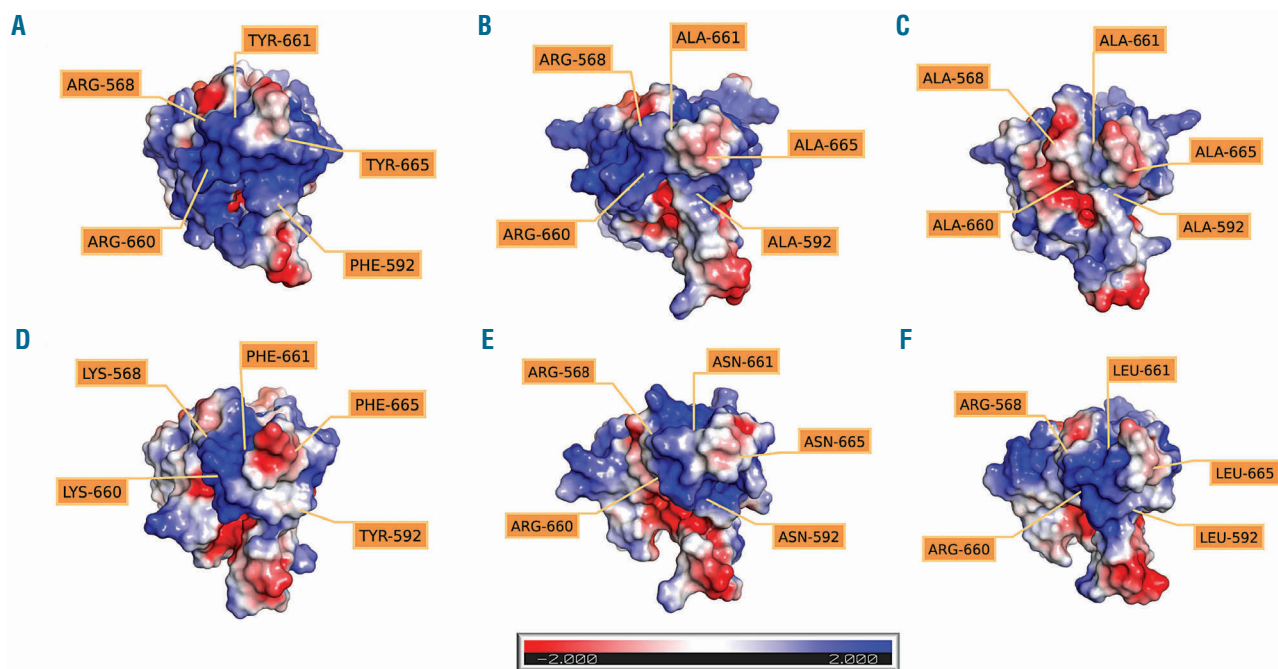
Figure 7. Models of three-dimensional structure and surface charge of ADAMTS13 spacer domain variants included in this study. (A-F) Three-dimensional structure model of the spacer domain of: (A) wild-type ADAMTS13 (RFRYY); (B) triple-alanine mutant variant (RARAA); (C). 5x alanine mutant variant (AAAAA); (D) gain-of-function variant (KYKFF); (E) triple-asparagine non-conservative mutant variant (RNRNN); and (F) semi-conservative variant (RLRLL). Negative charges are represented in red, neutral charges in white and positive charges in blue.

the aromatic ring and the capacity for establishing these intra- and other inter-molecular interactions. Replacement of arginines by lysines conserves the cationic charge in these positions. Our data clearly show that non-conservative arginine and alanine mutations in the ADAMTS13 spacer RFRYY epitope provide superior autoantibody resistance, likely because these mutations promote disruption of these intramolecular interactions and can potentially change the position of the loops of the epitope. We constructed three-dimensional models of selected epitope variants and these revealed reduction of total surface charge (Figure 7) and/or epitope surface size (*Online Supplementary Figure S6*).

The concept of ADAMTS13 variants that resist autoantibodies and remain active has been explored previously. However, the majority of previous studies designed with this intention were conducted with truncated ADAMTS13 variants,[23,38] with the exception of the GoF[26] and a few alanine variants.[22] We present here for the first time a comprehensive study in which, in the context of the full length ADAMTS13 molecule, the spacer domain was modified with different types of mutations. We also demonstrated quantitatively that several full-length ADAMTS13 mutants escape the majority of autoantibodies from most patients. Therefore, we sought to assess whether these variants conserved proteolytic activity. The activities of ADAMTS13 variants have been measured in several forms of *in vitro* and *in vivo* assays. Evidence strongly suggests that the C-terminal TSP2-8/CUB1-2 domains of ADAMTS13 are important for full *in vivo* proteolytic activity[39,40] because these domains allow ADAMTS13 to anchor itself onto the D4-CK domains of full-length VWF under shear flow conditions.[41,42] The static FRETS-VWF73 assay is commonly used to measure the activity of ADAMTS13 for the diagnosis of

TTP.[31] In minimal peptide assays, however, it appears that the C-terminal domains of ADAMTS13 and the spacer domain itself are less relevant for maintaining activity.[43] In FRETS-VWF73 the activity of the MDTCS fragment is higher than that of full-length ADAMTS13[32,44] due to the lack of the terminal TSP2-8 and CUB1-2 domains, eliminating their auto-inhibitory properties.[44] Our data are in agreement with these earlier findings: both the wild-type MDTCS and the MDTCS-AAAAA variant had higher activity in the FRETS-VWF73 assay compared to their full-length counterparts. In agreement with previous studies most alanine changes induced loss of activity.[22,23,25] Our data suggest that both aromatic residues and arginine residues have similar importance for activity. We observed a clear inverse correlation between resistance to autoantibodies and proteolytic activity of the variants (Figure 4). Selected mutants tested in our VWF multimer assay also had lower activity than the wild-type molecule, with the exception of wild-type MDTCS. This highlights the functional importance of the spacer exosite-3 in our VWF multimer assay. Among the selected full-length autoantibody-resistant mutants, the RARAA mutant demonstrated residual activity in conditions of sub-physiological ADAMTS13 concentrations (Figure 6). This variant was tested in FRETS-VWF73 together with patients' autoantibodies (Figure 5) exhibiting full resistance to the inhibitory action of polyclonal autoantibodies from patients.

Surprisingly, the GoF variant described previously showed less activity than that of wild-type ADAMTS13. The GoF variant was originally characterized in a COS-7 cell background[26] and in all subsequent *in vitro*[32,44,45] and *in vivo* studies[46,47] it was reported to be more active than wild-type ADAMTS13. We are the first group observing a loss of function of this molecule. The reasons for this are not clear.

It is possible that the differences observed may be due to post-translational modifications, such as different glycosylation patterns that may result from the CHO-based transient expression system that we used in our study.[48,49] To address this we also expressed the GoF variant in HEK293 cells, and under these conditions the GoF variant displayed increased activity, compared to the respective HEK293 wild-type ADAMTS13, in both FRETS-VWF73 and in the VWF multimer assay (*Online Supplementary Figure S7*). In the context of our ELISA, the GoF variant expressed in both CHO and HEK293 cells behaved in a similar way against the patients' samples (*Online Supplementary Figure S7*), and importantly our CHO-produced GoF variant was also inhibited by patients' autoantibodies (Figure 5), as anticipated by our ELISA results (Figure 2).

In conclusion, we have shown that less conservative mutations make it possible to obtain ADAMTS13 variants that resist the majority of patients' autoantibodies and retain residual levels of activity *in vitro*. Our data suggest a trade-off between the resistance towards patients' autoantibody binding and the loss of proteolytic activity in spacer exosite-3 ADAMTS13 variants. The study also reveals the importance of the side-chains of the RFRYY epitope in the spacer domain for autoantibody binding and ADAMTS13 activity, and it provides a basis for the development of novel therapeutic interventions that prevent the binding of pathogenic autoantibodies to the spacer domain of ADAMTS13.

References

1. Kremer Hovinga JA, Coppo P, Lämmle B, Moake JL, Miyata T, Vanhoorelbeke K. Thrombotic thrombocytopenic purpura. Nat Rev Dis Prim. 2017;3:17020.
2. Zheng X, Chung D, Takayama TK, Majerus EM, Sadler JE, Fujikawa K. Structure of von Willebrand factor-cleaving protease (ADAMTS13), a metalloprotease involved in thrombotic thrombocytopenic purpura. J Biol Chem. 2001;276(44):41059-41063.
3. Hrdinová J, D'Angelo S, Graça NAG, et al. Dissecting the pathophysiology of immune thrombotic thrombocytopenic purpura: interplay between genes and environmental triggers. Haematologica. 2018;103(7):1099-1109.
4. Booth KK, Terrell DR, Vesely SK, George JN. Systemic infections mimicking thrombotic thrombocytopenic purpura. Am J Hematol. 2011;86(9):743-751.
5. Koh YR, Hwang SH, Chang CL, Lee EY, Son HC, Kim HH. Thrombotic thrombocytopenic purpura triggered by influenza A virus subtype H1N1 infection. Transfus Apher Sci. 2012;46(1):25-28.
6. Medina PJ, Sipols JM, George JN. Drug-associated thrombotic thrombocytopenic purpura-hemolytic uremic syndrome. Curr Opin Hematol. 2001;8(5):286-293.
7. Ashley JR, Otero H, Aboulafia DM. Bee envenomation: a rare cause of thrombotic thrombocytopenic purpura. South Med J. 2003;96(6):588-591.
8. Valavi E, Ahmadzadeh A, Amoori P, Daneshgar A. High frequency of acquired ADAMTS13 deficiency after hemolysis in Hemiscorpius lepturus (scorpion) stung children. Indian J Pediatr. 2014;81(7):665-669.
9. Pos W, Luken BM, Sorvillo N, Hovinga JAK, Voorberg J. Humoral immune response to ADAMTS13 in acquired thrombotic thrombocytopenic purpura. J Thromb Haemost. 2011;9(7):1285-1291.
10. Ostertag EM, Kacir S, Thiboutot M, et al. ADAMTS13 autoantibodies cloned from patients with acquired thrombotic thrombocytopenic purpura: 1. Structural and functional characterization in vitro. Transfusion. 2016;56(7):1763-1774.

11. Pos W, Luken BM, Kremer Hovinga JA, et al. VH1-69 germline encoded antibodies directed towards ADAMTS13 in patients with acquired thrombotic thrombocytopenic purpura. J Thromb Haemost. 2009;7(3):421-428.
12. Schaller M, Vogel M, Kentouche K, Ammle B, Kremer Hovinga JA. The splenic autoimmune response to ADAMTS13 in thrombotic thrombocytopenic purpura contains recurrent antigen-binding CDR3 motifs. Blood. 2014;124(23):3469-3479.
13. Luken BM, Kaijen PHP, Turenhout EAM, et al. Multiple B-cell clones producing antibodies directed to the spacer and disintegrin/thrombospondin type-1 repeat 1 (TSP1) of ADAMTS13 in a patient with acquired thrombotic thrombocytopenic purpura. J Thromb Haemost. 2006;4(11):2355-2364.
14. Luken BM, Turenhout EAM, Hulstein JJJ, Van Mourik JA, Fijnheer R, Voorberg J. The spacer domain of ADAMTS13 contains a major binding site for antibodies in patients with thrombotic thrombocytopenic purpura. Thromb Haemost. 2005;93(2):267-274.
15. Klaus C, Plaimauer B, Studt JD, et al. Epitope mapping of ADAMTS13 autoantibodies in acquired thrombotic thrombocytopenic purpura. Blood. 2004;103(12):4514-4519.
16. Long Zheng X, Wu HM, Shang D, et al. Multiple domains of ADAMTS13 are targeted by autoantibodies against ADAMTS13 in patients with acquired idiopathic thrombotic thrombocytopenic purpura. Haematologica. 2010;95(9):1555-1562.
17. Thomas MR, de Groot R, Scully MA, Crawley JTB. Pathogenicity of anti-ADAMTS13 autoantibodies in acquired thrombotic thrombocytopenic purpura. EBioMedicine. 2015;2(8):942-952.
18. Casina VC, Hu W, Mao J-H, Lu R-N, Hanby HA, Pickens B, et al. High-resolution epitope mapping by HX MS reveals the pathogenic mechanism and a possible therapy for autoimmune TTP syndrome. Proc Natl Acad Sci U S A. 2015;112(31):9620-9625.
19. Scheiflinger F, Knöbl P, Trattner B, et al. Nonneutralizing IgM and IgG antibodies to von Willebrand factor-cleaving protease (ADAMTS-13) in a patient with thrombotic thrombocytopenic purpura. Blood. 2003;102(9):3241-3243.

20. Shelat SG, Smith P, Ai J, Zheng XL. Inhibitory autoantibodies against ADAMTS-13 in patients with thrombotic thrombocytopenic purpura bind ADAMTS-13 protease and may accelerate its clearance in vivo. J Thromb Haemost. 2006;4(8):1707-1717.
21. Yamaguchi Y, Moriki T, Igari A, et al. Epitope analysis of autoantibodies to ADAMTS13 in patients with acquired thrombotic thrombocytopenic purpura. Thromb Res. 2011;128(2):169-173.
22. Pos W, Crawley JTB, Fijnheer R, Voorberg J, Lane DA, Luken BM. An autoantibody epitope comprising residues R660, Y661, and Y665 in the ADAMTS13 spacer domain identifies a binding site for the A2 domain of VWF. Blood. 2010;115(8):1640-1649.
23. Pos W, Sorvillo N, Fijnheer R, et al. Residues arg568 and phe592 contribute to an antigenic surface for anti-ADAMTS13 antibodies in the spacer domain. Haematologica. 2011;96(11):1670-1677.
24. Luken BM, Turenhout EAM, Kaijen PHP, et al. Amino acid regions 572–579 and 657–666 of the spacer domain of ADAMTS13 provide a common antigenic core required for binding of antibodies in patients with acquired TTP. Thromb Haemost. 2006;96(3):295-301.
25. Jin S-Y, Skipwith CG, Zheng XL. Amino acid residues Arg659, Arg660, and Tyr661 in the spacer domain of ADAMTS13 are critical for cleavage of von Willebrand factor. Blood. 2010;115(11):2300-2310.
26. Jian C, Xiao J, Gong L, et al. Gain-of-function ADAMTS13 variants that are resistant to autoantibodies against ADAMTS13 in patients with acquired thrombotic thrombocytopenic purpura. Blood. 2012;119(16):3836-3843.
27. Roose E, Schelpe A-S, Joly BS, et al. An open conformation of ADAMTS-13 is a hallmark of acute acquired thrombotic thrombocytopenic purpura. J Thromb Haemost. 2018;16(2):378-388.
28. Schelpe A-S, Roose E, Joly BS, et al. Generation of anti-idiotypic antibodies to detect anti-spacer antibody idiotopes in acute thrombotic thrombocytopenic purpura patients. Haematologica. 2018;104(6):1268-1276.

29. Feys HB, Roodt J, Vandeputte N, et al. Thrombotic thrombocytopenic purpura directly linked with ADAMTS13 inhibition in the baboon (Papio ursinus). Blood. 2010;116(12):2005-2010.

30. Alwan F, Vendramin C, Vanhoorelbeke K, et al. Presenting ADAMTS13 antibody and antigen levels predict prognosis in immune-mediated thrombotic thrombocytopenic purpura. Blood. 2017;130(4):466-471.

31. Kokame K, Nobe Y, Kokubo Y, Okayama A, Miyata T. FRETS-VWF73, a first fluorogenic substrate for ADAMTS13 assay. Br J Haematol. 2005;129(1):93-100.

32. Muia J, Zhu J, Gupta G, et al. Allosteric activation of ADAMTS13 by von Willebrand factor. Proc Natl Acad Sci U S A. 2014;111 (52):18584-18589.

33. Akiyama M, Takeda S, Kokame K, Takagi J, Miyata T, Majerus PW. Crystal structures of the noncatalytic domains of ADAMTS13 reveal multiple discontinuous exosites for von Willebrand factor. Proc Natl Acad Sci U S A. 2009;106(46):19274-19279.

34. Bogan AA, Thorn KS. Anatomy of hot spots in protein interfaces. J Mol Biol. 1998;280 (1):1-9.

35. Ferreira De Freitas R, Schapira M. A systematic analysis of atomic protein-ligand interactions in the PDB. Medchemcomm. 2017;8(10):1970-1981.

36. Robin G, Sato Y, Desplancq D, Rochel N, Weiss E, Martineau P. Restricted diversity of

antigen binding residues of antibodies revealed by computational alanine scanning of 227 antibody-antigen complexes. J Mol Biol. 2014;426(22):3729-3743.

37. Peng H-P, Lee KH, Jian J-W, Yang A-S. Origins of specificity and affinity in antibody–protein interactions. Proc Natl Acad Sci U S A. 2014;111(26):E2656-E2665.

38. Zhou W, Dong L, Ginsburg D, Bouhdssira EE, Tsai HM. Enzymatically active ADAMTS13 variants are not inhibited by anti-ADAMTS13 autoantibodies: a novel therapeutic strategy? J Biol Chem. 2005;280 (48):39934-39941.

39. Banno F, Chauhan AK, Kokame K, et al. The distal carboxyl-terminal domains of ADAMTS13 are required for regulation of in vivo thrombus formation. Blood. 2009;113 (21):5323-5329.

40. Zhu J, Muia J, Gupta G, et al. Exploring the "minimal" structure of a functional ADAMTS13 by mutagenesis and small-angle X-ray scattering. Blood. 2019;133(17): 1909-1918.

41. Zhang P, Pan W, Rux AH, Sachais BS, Zheng XL. The cooperative activity between the carboxyl-terminal TSP1 repeats and the CUB domains of ADAMTS13 is crucial for recognition of von Willebrand factor under flow. Blood. 2007;110(6):1887-1894.

42. Crawley JTB, De Groot R, Xiang Y, Luken BM, Lane DA. Unraveling the scissile bond: how ADAMTS13 recognizes and cleaves

von Willebrand factor. Blood. 2011;118(12): 3212-3221.

43. Petri A, Kim HJ, Xu Y, et al. Crystal structure and substrate-induced activation of ADAMTS13. Nat Commun. 2019;10(1):1-16.

44. South K, Luken BM, Crawley JTB, et al. Conformational activation of ADAMTS13. Proc Natl Acad Sci U S A. 2014;111(52): 18578-18583.

45. South K, Freitas MO, Lane DA. Conformational quiescence of ADAMTS-13 prevents proteolytic promiscuity. J Thromb Haemost. 2016;14(10):2011-2022.

46. South K, Denorme F, Salles-Crawley II, De Meyer SF, Lane DA. Enhanced activity of an ADAMTS-13 variant (R568K/F592Y/ R660K/Y661F/Y665F) against platelet agglutination in vitro and in a murine model of acute ischemic stroke. J Thromb Haemost. 2018;16(11):2289-2299.

47. Liu-Chen S, Connolly B, Cheng L, Subramanian RR, Han Z. MRNA treatment produces sustained expression of enzymatically active human ADAMTS13 in mice. Sci Rep. 2018;8(1):7859.

48. Goh JB, Ng SK. Impact of host cell line choice on glycan profile. Crit Rev Biotechnol. 2018;38(6):851-867.

49. Werner RG, Kopp K, Schlueter M. Glycosylation of therapeutic proteins in different production systems. Acta Paediatr. 2007;96(455):17-22.

Novel aptamer to von Willebrand factor A1 domain (TAGX-0004) shows total inhibition of thrombus formation superior to ARC1779 and comparable to caplacizumab

Ferrata Storti Foundation

Kazuya Sakai,[1] Tatsuhiko Someya,[2] Kaori Harada,[2] Hideo Yagi,[1] Taei Matsui[3] and Masanori Matsumoto[1]

[1]Department of Blood Transfusion Medicine, Nara Medical University, Kashihara and [2]TAGCyx Biotechnologies Inc, Tokyo and [3]Clinical Laboratory Medicine, Fujita Health University School of Medical Sciences, Toyoake, Japan

ABSTRACT

Von Willebrand factor (VWF) is a blood glycoprotein that plays an important role in platelet thrombus formation through interaction between its A1 domain and platelet glycoprotein Ib. ARC1779, an aptamer to the VWF A1 domain, was evaluated in a clinical trial for acquired thrombotic thrombocytopenic purpura (aTTP). Subsequently, caplacizumab, an anti-VWF A1 domain nanobody, was approved for aTTP in Europe and the USA. We recently developed a novel DNA aptamer, TAGX-0004, to the VWF A1 domain; it contains an artificial base and demonstrates high affinity for VWF. To compare the effects of these three agents on VWF A1, their ability to inhibit ristocetin- or botrocetin-induced platelet aggregation under static conditions was analyzed, and the inhibition of thrombus formation under high shear stress was investigated in a microchip flow chamber system. In both assays, TAGX-0004 showed stronger inhibition than ARC1779, and had comparable inhibitory effects to caplacizumab. The binding sites of TAGX-0004 and ARC1779 were analyzed with surface plasmon resonance performed using alanine scanning mutagenesis of the VWF A1 domain. An electrophoretic mobility shift assay showed that R1395 and R1399 in the A1 domain bound to both aptamers. R1287, K1362, and R1392 contributed to ARC1779 binding, and F1366 was essential for TAGX-0004 binding. Surface plasmon resonance analysis of the binding sites of caplacizumab identified five amino acids in the VWF A1 domain (K1362, R1392, R1395, R1399, and K1406). These results suggest that TAGX-0004 possesses better pharmacological properties than caplacizumab *in vitro* and might be similarly promising for aTTP treatment.

Introduction

Von Willebrand factor (VWF) is a large multimeric plasma glycoprotein that plays an essential role in tethering circulating platelets to damaged endothelial cells.[1] Interaction between the VWF A1 domain and the platelet glycoprotein (GP) Ib receptor leads to rapid development of VWF-rich platelet thrombi, thus preventing further bleeding.[2] Although normal amounts of VWF are usually helpful in hemostasis reactions, several VWF-mediated diseases, such as acute coronary syndrome,[3,4] cerebral infarction,[5] and thrombotic thrombocytopenic purpura (TTP),[6] demonstrate remarkably elevated plasma levels of VWF. Inhibiting VWF activity by blocking its A1 domain has recently been demonstrated to be an attractive therapeutic target in these arterial thromboses.[7-10]

Caplacizumab (Ablynx), an anti-VWF A1 humanized nanobody,[11,12] was approved by the European Medicines Agency in 2018 and by the US Food and Drug Administration in 2019 for the treatment of acquired TTP (aTTP). The anti-VWF A1 aptamer ARC1779 (Archemix) was developed as an antithrombotic agent for use in patients with aTTP, and it showed sufficient inhibitory effects on VWF activity without any severe bleeding events in a randomized control trial.[13] However, ARC1779 has not yet been approved for the treatment of VWF-mediated

thrombosis. We recently generated a novel DNA aptamer, TAGX-0004, that contains the artificial hydrophobic base 7-(2-thienyl)imidazo[4,5-b]pyridine (Ds); this aptamer targets human VWF A1 with very high affinity (K_D = 61.3 pM) and specificity.[14]

In this study, we compared TAGX-0004, ARC1779, and caplacizumab in terms of their inhibitory effects on VWF activity, by performing conventional platelet aggregation assays, ristocetin- and botrocetin-induced platelet aggregation assays (RIPA and BIPA, respectively), and shear-stress–induced aggregation assays using the microchip flow chamber system (T-TAS®).[15] To assess the affinity and binding sites of the two aptamers, we performed biophysical interaction analysis and alanine scanning mutagenesis of the VWF A1 domain. In addition, we analyzed the binding sites of caplacizumab using surface plasmon resonance (SPR).

Methods

Details of the materials and methods are presented in the *Online Supplementary Materials and Methods* section.

Sources of nucleoside, oligonucleotides, nanobody, and protein

The artificial nucleoside phosphoramidite (dDs-CE Phosphoramidite) was synthesized as described previously.[16,17] The oligonucleotides TAGX-0004 and ARC1779 (without polyethylene glycol [PEG]) were synthesized by and purchased from GeneDesign, Inc. (Osaka, Japan). The oligonucleotide sequence of TAGX-0004 (as Rn-DsDs-51mh2)[14] and that of ARC1779[18] were reported previously. The anti-human VWF nanobody caplacizumab (as TAB-234) was purchased from Creative-Biolabs (New York, NY, USA). The recombinant human VWF A1 domain protein was purchased from U-Protein Express BV (Utrecht, the Netherlands), and was used for the measurement of the binding affinity to anti-human VWF A1 agents using SPR.

Alanine-scanning mutagenesis

Based on previous reports that described the interaction between VWF A1 and GPIb,[19] botrocetin,[20] or ARC1172,[21] we designed 16 alanine-substituted mutants of the human VWF A1 domain (R1287, K1312, R1334, R1336, K1348, K1362, F1366, K1371, E1376, R1392, R1395, R1399, K1406, K1423, R1426, and K1430). These mutant proteins were generated using a cell-free expression system (Taiyo Nippon Sanso Corporation, Tokyo, Japan).

Platelet aggregation test

A platelet aggregation test (PAT) was performed with PRP313M aggregometer (TAIYO Instruments INC, Osaka, Japan). Aggregation inducing substances and their final concentration were as follows; ristocetin (1.5 mg/mL), botrocetin (1.0 µg/mL), collagen (4 µg/mL), epinephrine (1.0×10^{-4} M) and adenosine diphosphate (ADP) (1.0×10^{-5} M).

Total thrombus formation analysis system

The total thrombus formation analysis system (T-TAS®) (Zacros, Fujimori Kogyo Co. Ltd., Tokyo, Japan) is a micro-chip flow-chamber device used to visually and quantitatively analyze thrombus formation in whole blood samples under various blood flow conditions.[15] Whole blood samples with each anti-VWF A1 agent were applied onto a collagen I coated micro-chip (PL chip). Subsequently, the thrombus formation in the capillaries and an increase in flow pressure were observed.

Electrophoresis mobility shift assay

The binding abilities of the two aptamers to the human VWF A1 domain and its alanine-substituted mutants were analyzed by electrophoresis mobility shift assay (EMSA). Each aptamer (final concentration of 100 nM) was mixed with VWF A1 (final concentration of 0-800 nM) in binding buffer and incubated at 37 °C for 30 minutes (min), then subjected to 8% native PAGE in 0.5× TBE buffer for 50 min at room temperature (200 V/cm). The aptamer-VWF A1 complexes were detected as a shift band, and the band patterns were detected by SYBR Gold. The dissociation rate (KD) was calculated by Scatchard plot analysis.

Surface plasmon resonance

Competition assays with the two aptamers were performed by surface plasmon resonance (SPR) analysis using Biacore T200 (GE Healthcare UK Ltd., Little Chalfont, UK), as described previously.[14]

We also performed SPR analysis to investigate the binding site of the VWF A1 domain to caplacizumab.

Structure models of the VWF A1 domain

Three-dimensional (3D) structure models of the VWF A1 domain were visualized with the PyMOL Molecular Graphics System (DeLano Scientific, San Carlos, CA, USA).

Ethical statement

This study was approved by the ethics committee of Nara Medical University. Written informed consent was obtained from the individual who donated plasma for the use in this study.

Results

Inhibitory effects on platelet aggregation

The inhibitory effects of TAGX-0004, ARC1779, and caplacizumab under static conditions were analyzed by PAT. Figure 1 shows representative results of the analyses of the three types of plasma. All three agents showed inhibition activities in both RIPA and BIPA. However, the inhibitory effects on platelet aggregation differed between the three agents. In RIPA, the 80% maximal inhibitory concentration (IC_{80}) of TAGX-0004 was 50 nM, whereas that of ARC1779 was 500 nM and that of caplacizumab was 50 nM; thus TAGX-0004 blocked VWF function *via* the A1 domain approximately 10 times more potently than ARC1779, and exhibited a similar potency as caplacizumab. In BIPA, the IC_{80} of TAGX-0004 was 50 nM, whereas that of ARC1779 was 500 nM and that of caplacizumab was 50 nM, respectively; thus TAGX-0004 blocked VWF function approximately 10 times more potently than ARC1779 showing a similar potency as caplacizumab. None of the three agents inhibited platelet aggregation induced by collagen, epinephrine, or ADP (*data not shown*).

Inhibitory effects on thrombus formation

To assess the inhibitory effect of the three agents on platelet thrombus formation, we performed T-TAS. In this study, complete inhibition was defined as an increase in flow pressure from baseline of no more than 10 kPa. TAGX-0004, ARC1779, and caplacizumab were analyzed three times each, and Figure 2 shows representative flow pressure curves. Both TAGX-0004 and caplacizumab prevented thrombus occlusion under the flow condition at 50 nM. In contrast, ARC1779 did not demonstrate complete inhibition, even at a concentration of 1,000 nM. These
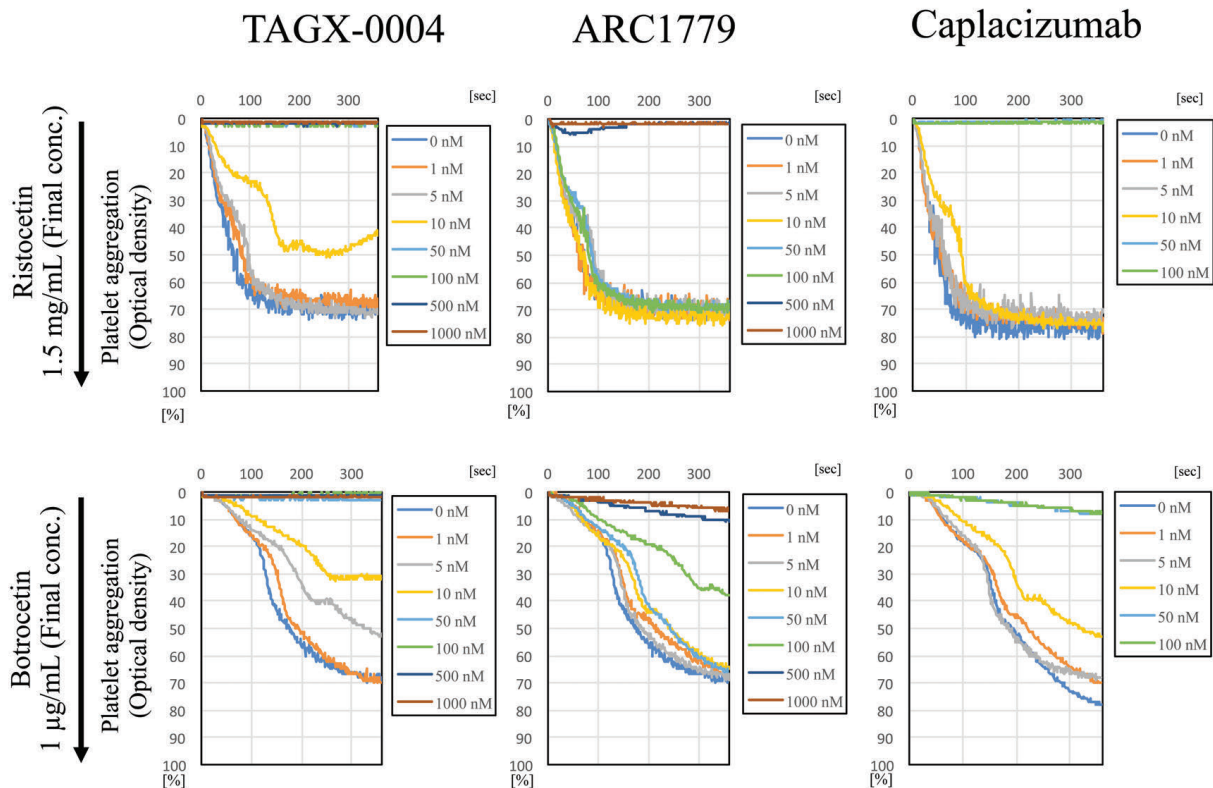
Figure 1. The inhibitory effects of TAGX-0004, ARC1779, and caplacizumab on platelet aggregation under static conditions. As shown in the upper left panel, TAGX-0004 completely inhibited ristocetin-induced platelet aggregation (RIPA) at a concentration of 50 nM. In contrast, the concentration required for ARC1779 was 500 nM, and that for caplacizumb was 50 nM. As shown in the lower left panel, TAGX-0004 inhibited botrocetin-induced platelet aggregation (BIPA) at a concentration of 50 nM. The concentration required for ARC1779 was 500 nM, and that for caplacizumab was 50 nM.

results indicate that TAGX-0004 inhibits platelet thrombus formation at least 20 times more potently than ARC1779 under high shear stress, and with a similar potency as caplacizumab.

Biophysical interaction analysis with EMSA

Biophysical interaction analysis with EMSA was performed four times for each aptamer. Figure 3 shows that the affinity of TAGX-0004 to VWF A1 domain (K_D=2.2± 0.9 nM [n=4]) was approximately 16-fold higher than that of ARC1779 (K_D =35.5±1.5 nM [n=4]).

Alanine scanning mutagenesis with EMSA

Figure 4 shows the results of EMSA using 16 alanine-mutated VWF A1 with TAGX-0004 (A) or ARC1779 (B). First, we analyzed nine mutants as shown in the left panels. Based on the results of this initial analysis, we then analyzed additional seven mutants as shown in the right panels. Of these, 10 VWF A1 mutants (K1312A, R1334A, R1336A, K1348A, K1371A, E1376A, K1406A, K1423A, R1426A, and K1430A) formed shifted bands representing complexes between an aptamer and VWF A1, as well as between wild-type (WT) VWF A1 and each aptamer. In the remaining six mutants, the intensity of the complexed bands was decreased, and the intensity of the unbound aptamer bands was increased. Of these mutants, R1395A and R1399A showed decreased intensity in both TAGX-0004 and ARC1779 band complexes.

While the binding affinity to ARC1779 was significantly decreased in R1287A, K1362A, and R1392A, the

binding affinity to TAGX-0004 was decreased in F1366A. These findings suggest that R1395 and R1399 are essential residues for binding to both aptamers, and that R1287, K1362, and R1392 probably contribute to binding to only ARC1779, while F1366 is required for binding to TAGX-0004. Our data indicate that both aptamers bind to the VWF A1 domain, even though the residues necessary for this binding are partially different, and these differences might affect their VWF inhibitory activity.

Competition assay with Biacore

To compare the binding sites of the aptamers to the VWF A1 domain, a competition assay was performed by SPR using Biacore. Biotinylated TAGX-0004 was immobilized on the sensor chip SA. Then, VWF A1 and a competitor aptamer (TAGX-0004 or ARC1779) as an analyte was injected onto the chip. The results of a self-competition assay using TAGX-0004 showed that the amount of VWF A1 binding to the chip decreased depending on the concentration of the competitor TAGX-0004 (*Online Supplementary Figure S1*). ARC1779 also dose-dependently decreased the response unit value. These results indicate that TAGX-0004 and ARC1779 bind to the overlapped region on the VWF A1 domain. Moreover, the competitive ability of ARC1779 against immobilized TAGX-0004 on the chip surface was lower than that of TAGX-0004 against TAGX-0004. These results were consistent with those of EMSA and indicated that the binding affinity of TAGX-0004 for VWF A1 was higher than that of ARC1779.

VWF A1 domain binding site of caplacizumab

We performed SPR analysis to investigate the VWF A1 domain binding site of caplacizumab. After immobilizing caplacizumab on the sensor chip CM5, 16 alanine-substituted mutants of VWF A1 were analyzed (Figure 5). The relative binding amount of WT was defined as 100%. The binding amount of each mutant was expressed as the relative ratio compared to that of WT. When a relative ratio of 80% was set as the cut-off, five mutants were judged as positive. These results indicate that these five residues (K1362, R1392, R1395, R1399, and K1406) are likely the binding sites of caplacizumab.

Comparison of VWF A1 domain binding sites of TAGX-0004, ARC1779, and caplacizumab

Figure 6 shows 3D structure models of the VWF A1 domain. The amino acid residues shown in red indicate the essential residues for binding to each aptamer or capla-cizumab. The residues shown in yellow are not involved in binding. Of the 16 alanine-substituted VWF A1 mutants, EMSA predicted that three amino acids (F1366, R1395, and R1399) are binding sites for TAGX-0004, as shown in red in Figure 6 on the left. The remaining 13 amino acid residues are shown in yellow. As for ARC1779, five amino acid residues (R1287, K1362, R1392, R1395, and R1399) play an important role in binding to VWF A1, as shown in red in Figure 6 in the middle. Of these, R1395 and R1399 are amino acids shared by both aptamers. Further, using Biacore we identified five amino acid residues in the VWF A1 domain (K1362, R1392, R1395, R1399, and K1406) that are binding sites to capla-cizumab, as shown in red in Figure 6 on the right. Of these, K1406 is unique to caplacizumab. The differences in VWF A1 domain binding sites suggest that these aptamers or nanobody might have unique effects on platelet aggregation and thrombosis formation.

TAGX-0004
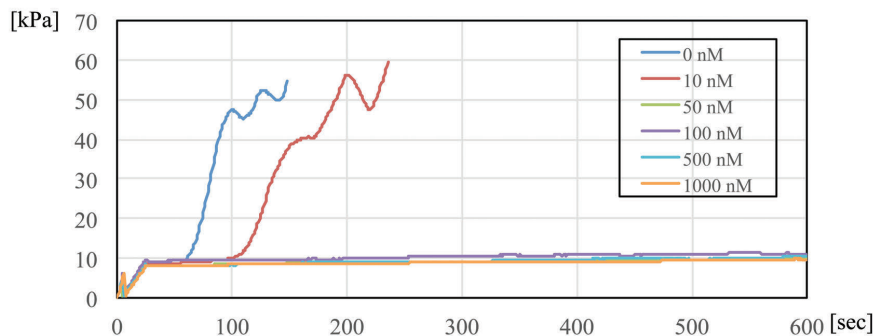
ARC1779
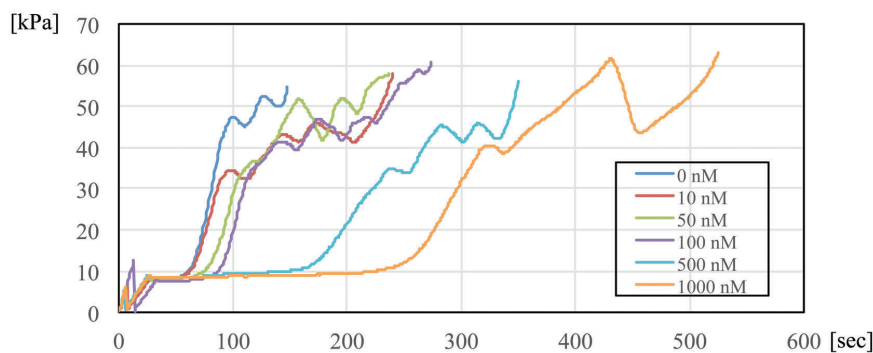
Caplacizumab
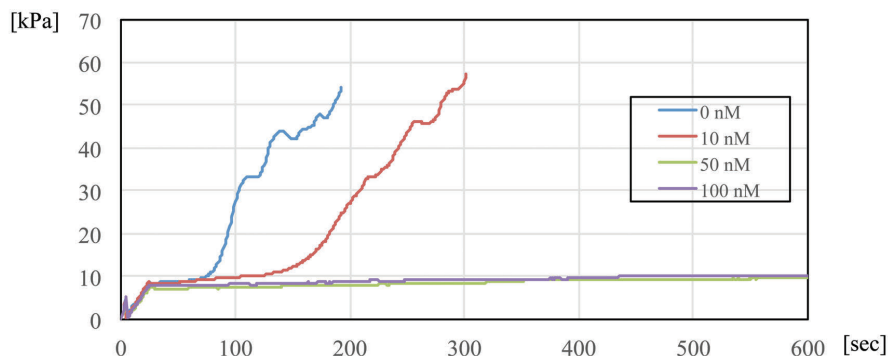
Figure 2. The inhibitory effects of TAGX-0004, ARC1779, and caplacizumab on platelet thrombus formation under high shear stress. Pressure curves at various concentrations of each agent are shown; curves end at the point of complete microcapillary occlusion. As shown in the upper panel, TAGX-0004 inhibited thrombus formation under high shear conditions at a final concentration of 50 nM. The middle panel shows that ARC1779 did not achieve complete inhibition even at a concentration of 1,000 nM. The lower panel shows that caplacizumab completely inhibited thrombus formation at a concentration of 50 nM.

Discussion

VWF plays a pivotal role in the initial phase of platelet thrombus formation under high shear stress through the interaction between its A1 domain and platelet GPIb.[1,2] The binding site of the VWF A1 domain is usually cryptic and prevents spontaneous binding to platelets. High shear stress of blood flow induces conformational changes in VWF and exposes the VWF A1 domain. Therefore, the association between VWF A1 and platelet GPIb usually occurs under high shear stress.[2]

Inhibition of VWF A1 domain binding to platelet GPIb can potentially prevent the development of platelet thrombus formation that causes cardiac infarction, cerebral infarction, and TTP. TTP results from the formation of platelet thrombi in the microvasculature due to a deficiency of ADAMTS13, a VWF-cleaving protease.[22,23] Therefore, preventing VWF A1 binding to platelet GPIb could be a promising therapeutic target for TTP. For this purpose, caplacizumab was evaluated for its anti-thrombotic effects in a phase II clinical trial (the TITAN study)[11] and a phase III clinical trial (the HERCULES study).[12] These studies reported a therapeutic effect of caplacizumab on aTTP, including faster recovery of platelet counts, fewer plasma exchange sessions, and shorter hospital stays. A bleeding event was reported as a common adverse event in patients treated with caplacizumab compared to patients without it.[12] In the TITAN and HERCULES study, 36 and 72 patients of aTTP were treated with caplacizumab and 19 (54%) and 46 (65%) patients had bleeding events, respectively. The most common adverse events were epistaxis and gingival bleeding, neither of which generally required treatment.

Nucleic acid aptamers are single-strand DNA or RNA molecules that can form 3D structures capable of specifically binding to proteins or other cellular targets. They are superior to existing antibody products in terms of their specificity, manufacturing cost, relatively small size, and non-immunogenicity. Pegaptanib (Macugen®, Pfizer) is the only aptamer approved by the Food and Drug Adminstration in 2004 for the treatment of wet age-related macular degeneration blocking vascular endothelial growth factor.[24] As of June 2019, no aptamer for the patients with coagulation or thrombotic disorder has been approved. However, some aptamers targeting coagulation factors, ARC 1779 against VWF A1, NU172 (ARCA Biopharma) against factor IIa, and REG1/REG2 (Regado Biosciences) against factor IXa, stepped into clinical trials.[13,25-27] ARC1779 was developed to target the VWF A1 domain and was evaluated in a phase II clinical trial in patients with aTTP.[13] Unfortunately, the recruitment of patients in this trial was terminated without completing the study due to sponsor-related financial issues, but seven patients with aTTP received combined therapy with intravenous ARC1779 injections and plasma exchange.[13] The trial showed no severe adverse events such as bleeding, even in patients with aTTP who had severe thrombocytopenia.[13] A study of healthy volunteers confirmed that this aptamer had an antithrombotic effect and did not cause severe bleeding events.[28]

TAGX-0004 is a novel DNA aptamer that targets the VWF A1 domain and contains Ds, an artificial nucleic acid. TAGX-0004 was obtained using modified SELEX (systemic evolution of ligands by exponential enrichment) methods incorporating the Ds base.[14] Since the Ds base has no complementary base in nature, Ds-containing DNA aptamers can have unique 3D structures. The high hydrophobicity of the Ds base may contribute to significantly high binding affinity to target proteins. In fact, the results of EMSA showed that the TAGX-0004 binding affinity for VWF (K_D=2.2±0.9 nM) is 16-fold higher than that of ARC1779 (K_D=35.5±1.5 nM) (Figure 3). However, the K_D values in this study might be underestimated in comparison with previous reports; the K_D value of TAGX-0004 was shown to be 61.3 pM by a SPR assay,[14] and the KD value of ARC1779 was 2 nM in a RI-labeled assay.[18] Previous results also indicated that the binding affinity of TAGX-0004 was much higher than that of ARC1779.

The binding affinity of aptamers to VWF A1 domain might affect the interaction between VWF and platelets. Although both TAGX-0004 and ARC1779 inhibited the platelet aggregations which were induced by ristocetin

A TAGX-0004

VWF A1 (nM)
0 6.25 12.5 25 50 100 200 400 800

Aptamer /VWF A1 ▷
Unbound Aptamer ▶

$K_D = 2.2 \pm 0.9$ nM

B ARC1779

0 6.25 12.5 25 50 100 200 400 800

$K_D = 35.5 \pm 1.5$ nM
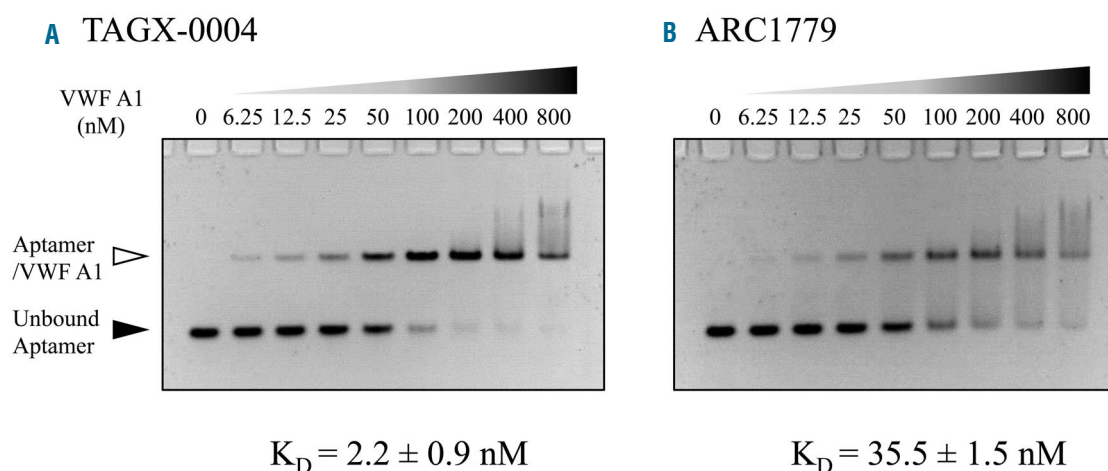
Figure 3. Biophysical interaction analysis of TAGX-0004 and ARC1779 with electrophoresis mobility shift assay (EMSA). The white arrowhead indicates the complex of wild-type (WT) recombinant von Willebrand factor (VWF) A1 with an aptamer (TAGX-0004 or ARC1779). The black arrowhead indicates unbound aptamer. Increasing the concentration of WT VWF A1 increased the density of complex bands and decreased that of unbound aptamer bands. These experiments were performed four times for each aptamer. The dissociation rates (KD) of TAGX-0004 and ARC1779 were 2.2±0.9 nM and 35.5±1.5 nM, respectively.

A TAGX-0004
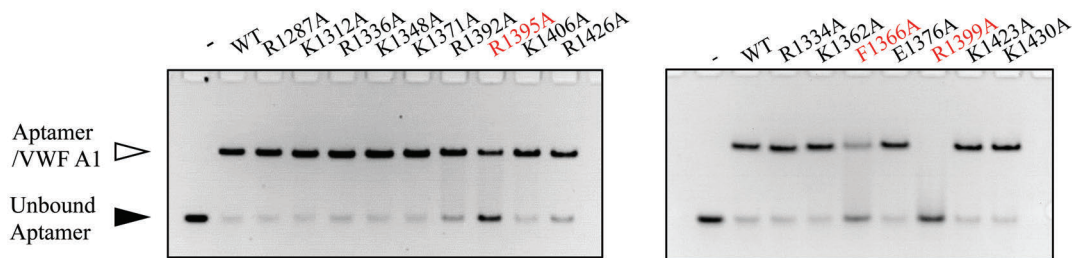
B ARC1779
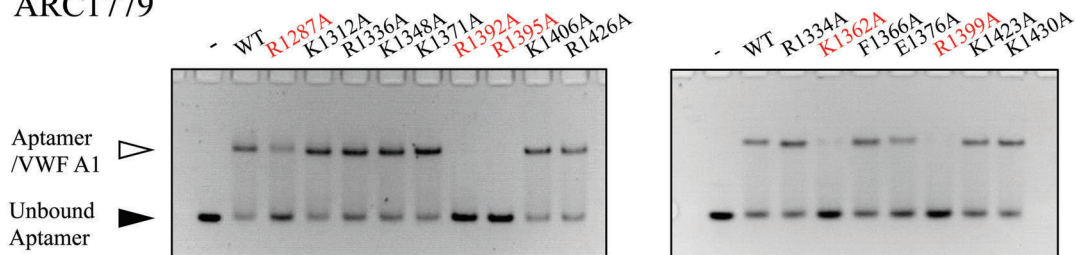
Figure 4. Electrophoresis mobility shift assay (EMSA) using alanine-scanning mutants for analyzing von Willebrand factor A1 binding to TAGX-0004 and ARC1779.
The white arrowhead indicates the complex of von Willebrand factor (VWF) A1 with an aptamer (TAGX-0004 or ARC1779). The black arrowhead indicates unbound aptamer. The leftmost lane in each gel (-) represents aptamer only, without a VWF A1 mutant. Using both aptamers, 10 VWF A1 mutants (K1312A, R1334A, R1336A, K1348A, K1371A, E1376A, K1406A, K1423A, R1426, and K1430A) formed complexes with aptamers, as did wild-type (WT) VWF A1. With TAGX-0004, as shown in the top panels, three mutants (F1366A, R1395A, and R1399A, indicated in red letters) demonstrated decreased densities of complex bands and increased densities of unbound bands, indicating that these amino acids were important for the binding of VWF A1 to TAGX-0004. With ARC1779, as shown in the lower panels, five mutants (R1287A, K1362A, R1392A, R1395A, and R1399A indicated in red letters) demonstrated decreased densities of complex bands and increased densities of unbound bands.

and botrocetin, the minimum concentration of TAGX-0004 necessary for inhibition is significantly lower than that of ARC1779 in both RIPA and BIPA (Figure 1). PAT analysis revealed that TAGX-0004 can block VWF function *via* the A1 domain at least 10 times more strongly than ARC1779. T-TAS also revealed that TAGX-0004 is superior to ARC1779 at inhibiting VWF function (Figure 2). In addition, compared with caplacizumab, TAGX-0004 showed equally effective inhibition against thrombosis formation under various blood flow conditions. Moreover, TAGX-0004 has a unique mini-hairpin DNA structure that offers benefits in pharmaceutical applications,[14] specifically by conferring resistance to degradation by nucleases. This structure should extend the half-life of this molecule *in vivo*.

As described above regarding the adverse effects of caplacizumab treatment, there are still concerns regarding bleeding caused by anti-VWF antagonists. Although anti-VWF agents have demonstrated superior safety profiles in this regard compared to anti-platelet agents, measures to quickly treat bleeding that occurs during aptamer treatment should be prepared. We speculate that if a neutralizing agent comprising a DNA sequence that is partially complementary to that of a specific aptamer is prepared, it may serve as an effective antidote as introduced in the literature.[29] In the case of TAGX-0004, such a partial DNA sequence may contain pyrrole-2-carbaldehyde (Pa), the complementary base pair to Ds.[16] In the past development of antithrombotic aptamer therapeutics, similar approaches of antidotes were taken to neutralize the

unwanted effect of an aptamer, even though such aptamers are still to be approved.[26] The specific antidote could contribute to control severe bleeding compared to caplacizumab.

Alanine mutagenesis analysis of the VWF A1 domain was performed in this study to determine the binding sites of TAGX-0004, ARC1779, and caplacizumab. The binding sites of ARC1779, but not TAGX-0004 or caplacizumab, were reported previously.[21] Our results show that the binding sites of these three agents only partially correspond to each other (Figure 6). Huang *et al.*[21] reported that 18 amino acid residues in the VWF A1 domain were binding sites for ARC1172, which has the same fundamental structure as ARC1779. That study did not identify R1399 as a binding site, even though in the present study it is a common binding site for all three agents. Chen *et al.* identified R1399 as one of the key amino acids for the effect of VWF to hemostasis and thrombosis.[30] Interestingly, a hydrophobic amino acid residue (F1366) is required to bind to TAGX-0004, which has two hydrophobic Ds bases. Matsunaga *et al.* previously reported that the number of Ds bases (0-2) strongly correlated with binding affinity to VWF A1[14] and we confirmed that Ds-free TAGX-0004 failed to inhibit thrombus formation on T-TAS (*data not shown*). These results indicate that the base of Ds interacts directly with the VWF A1 domain and therefore F1366 appears to be an essential and unique binding site of TAGX-0004 to the VWF-A1 domain with hydrophobic interaction (e.g., pi-stacking). Of note, alanine scanning of caplacizumab showed that like ARC1779 and TAGX-0004, both R1395 and R1399 are nec-

essary to bind the VWF A1 domain (Figure 6).

Due to the method limitations, the affinity between the VWF A1 domain and TAGX-0004 or ARC1779 was not analyzed by the SPR method. Since both oligonucleotides and the sensor chip are negatively charged, the K_D value was underestimated when we immobilized the VWF A1 protein on the sensor chip and applied TAGX-0004 or ARC1779 as an analyte. Therefore, we performed alanine scanning by EMSA for DNA aptamers. In addition, the binding site of caplacizumab to VWF A1 domain was not

analyzed with EMSA, which was used to assess TAGX-0004 and ARC1779, since this technique is not suitable for the analysis of proteins such as nanobodies and antibodies. Secondly, ARC1779 was originally PEGylated. However, we used ARC1779 without PEG in this study because we found no obvious differences between ARC1779 with and without PEG using RIPA, BIPA, T-TAS, and EMSA (*data not shown*).

In addition, caplacizumab was used in the clinical study and approved as a bivalent nanobody which has two
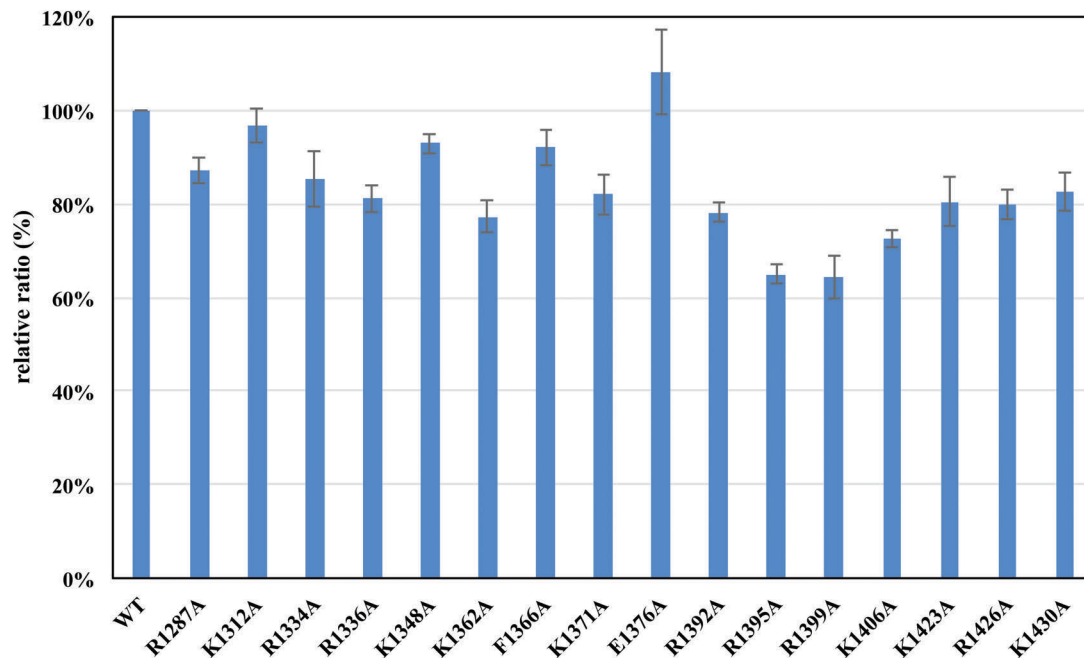
Figure 5. Analysis of caplacizumab binding sites to the von Willebrand factor A1 domain using alanine-scanning mutants with surface plasmon resonance. We performed surface plasmon resonance (SPR) analysis to investigate caplacizumab binding sites to the von Willebrand factor (VWF) A1 domain. After immobilizing caplacizumab on the sensor chip CM5, 16 alanine-substituted VWF A1 mutants were analyzed. The relative binding volume of wild-type (WT) VWF A1 was defined as 100%. The binding amount of each mutant was expressed as a ratio relative to WT. Five mutants were considered to bind to caplacizumab based on having a relative ratio above the cutoff of 80%. These results indicate that these five amino acids (K1362, R1392, R1395, R1399, and K1406) in the VWF A1 domain were important in caplacizumab binding.
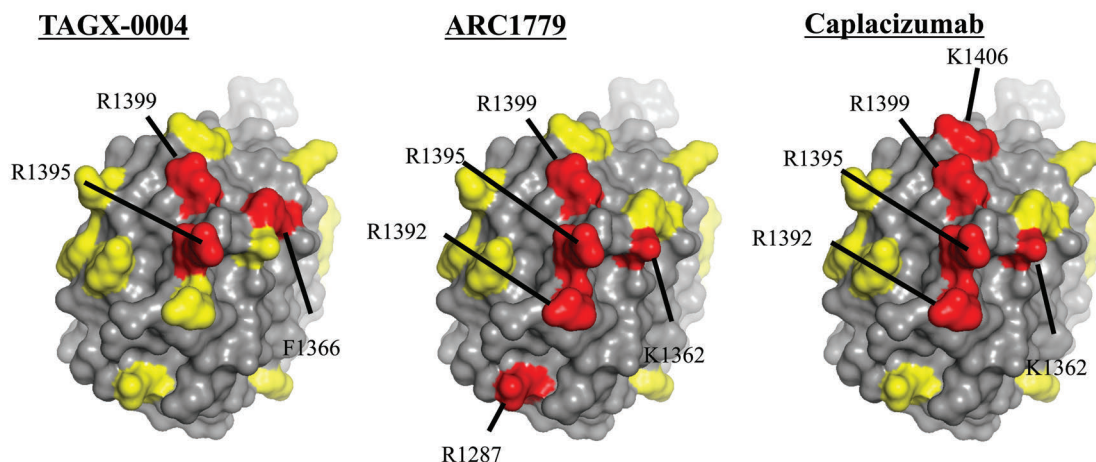
Figure 6. Von Willebrand factor A1 domain binding sites to TAGX-0004, ARC1779, and caplacizumab. Amino acids colored yellow did not contribute to von Willebrand factor (VWF) A1 binding to aptamers or caplacizumab. Amino acids colored in red were necessary for binding to aptamers or caplacizumab. Three amino acids (F1366, R1395, and R1399) in the VWF A1 domain were identified as TAGX-0004 binding sites. Five amino acids (R1287, K1362, R1392, R1395, and R1399) were important for binding to ARC1779. Finally, five amino acids (K1362, R1392, R1395, R1399, and K1406) were important for binding to caplacizumab.

binding sites to the target. On the other hand, two aptamers used in this study were formed as monovalent. It is known that the direct comparison of an affinity of monovalent entity with an avidity of bivalent entity is not straightforward. Nevertheless, it is intriguing that TAGX-0004 has shown a comparable inhibitory effect against caplacizumab in the studies we performed, and how the bivalent form of TAGX-0004, which is not available though, behaves in the same experiments.

Treatment with caplacizumab has demonstrated a rapid decrease of VWF ristocetin cofactor assay in patients with aTTP and the levels of VWF antigen and factor VIII were also transiently reduced with caplacizumab treatment compared with placebo due to an increased clearance of the caplacizumab-VWF complex.[11] Whether or not TAGX-0004 demonstrates an equivalent effect is still to be studied using an *in vivo* model. Nevertheless, judging from the binding ability of TAGX-0004 to plasma-derived human VWF confirmed with EMSA (*data not shown*), it is likely that the aptamer shows a similar effect as caplacizumab in aTTP patients.

In conclusion, we confirmed the potency of TAGX-0004 to prevent platelet thrombus formation *in vitro*. Epitope mapping of the binding sites of TAGX-0004 compared with ARC1779 and caplacizumab provided us with information on each molecule's efficacy and characteristics. Caplacizumab is now coming into use as a first-line therapy for aTTP. However, there are still challenges to be overcome with this agent, such as bleeding adverse events and high cost.[31] TAGX-0004 has the potential to overcome these problems and could be developed as a promising drug not only for aTTP, but also for various VWF-mediated thrombotic disorders such as acute coronary syndrome and cerebral infarction.

References

1. Sadler JE. Biochemistry and genetics of von Willebrand factor. Annu Rev Biochem. 1998;67:395-424.
2. Ruggeri ZM. Von Willebrand factor, platelets and endothelial cell interactions. J Thromb Haemost. 2003;1(7):1335-1342.
3. Montalescot G, Philippe F, Ankri A, et al. Early increase of von Willebrand factor predicts adverse outcome in unstable coronary artery disease: beneficial effects of enoxaparin. French Investigators of the ESSENCE Trial. Circulation. 1998;98(4):294-299.
4. Ray KK, Morrow DA, Gibson CM, Murphy S, Antman EM, Braunwald E. Predictors of the rise in vWF after ST elevation myocardial infarction: implications for treatment strategies and clinical outcome: An ENTIRE-TIMI 23 substudy. Eur Heart J. 2005;26(5):440-446.
5. Bath PM, Blann A, Smith N, Butterworth RJ. Von Willebrand factor, P-selectin and fibrinogen levels in patients with acute ischaemic and haemorrhagic stroke, and their relationship with stroke sub-type and functional outcome. Platelets. 1998;9(3-4):155-159.
6. Moake JL, Rudy CK, Troll JH, et al. Unusually large plasma factor VIII:von Willebrand factor multimers in chronic relapsing thrombotic thrombocytopenic purpura. N Engl J Med. 1982;307(23):1432-1435.
7. Gragnano F, Sperlongano S, Golia E, et al. The role of von Willebrand factor in vascular inflammation: from pathogenesis to targeted therapy. Mediators Inflamm. 2017;2017:5620314.
8. Siller-Matula JM, Krumphuber J, Jilma B. Pharmacokinetic, pharmacodynamic and clinical profile of novel antiplatelet drugs targeting vascular diseases. Br J Pharmacol. 2010;159(3):502-517.
9. Bae ON. Targeting von Willebrand factor as a novel anti-platelet therapy; application of ARC1779, an Anti-vWF aptamer, against thrombotic risk. Arch Pharm Res. 2012; 35(10):1693-1699.
10. Matsui T, Hori A, Hamako J, et al. Mutant botrocetin-2 inhibits von Willebrand factor-induced platelet agglutination. J Thromb Haemost. 2017;15(3):538-548.
11. Peyvandi F, Scully M, Kremer Hovinga JA, et al. Caplacizumab for acquired thrombotic thrombocytopenic purpura. N Engl J Med. 2016;374(6):511-522.
12. Scully M, Cataland SR, Peyvandi F, et al. Caplacizumab treatment for acquired thrombotic thrombocytopenic purpura. N Engl J Med. 2019;380(4):335-346.
13. Cataland SR, Peyvandi F, Mannucci PM, et al. Initial experience from a double-blind, placebo-controlled, clinical outcome study of ARC1779 in patients with thrombotic thrombocytopenic purpura. Am J Hematol. 2012;87(4):430-432.
14. Matsunaga KI, Kimoto M, Hirao I. High-affinity DNA aptamer generation targeting von Willebrand factor A1-domain by genetic alphabet expansion for systematic evolution of ligands by exponential enrichment using two types of libraries composed of five different bases. J Am Chem Soc. 2017;139(1):324-334.
15. Hosokawa K, Ohnishi T, Kondo T, et al. A novel automated microchip flow-chamber system to quantitatively evaluate thrombus formation and antithrombotic agents under blood flow conditions. J Thromb Haemost. 2011;9(10):2029-2037.
16. Hirao I, Kimoto M, Mitsui T, et al. An unnatural hydrophobic base pair system: site-specific incorporation of nucleotide analogs into DNA and RNA. Nat Methods. 2006;3(9):729-735.
17. Yamashige R, Kimoto M, Takezawa Y, et al. Highly specific unnatural base pair systems as a third base pair for PCR amplification. Nucleic Acids Res. 2012;40(6):2793-2806.
18. Diener JL, Daniel Lagasse HA, Duerschmied D, et al. Inhibition of von Willebrand factor-mediated platelet activation and thrombosis by the anti-von Willebrand factor A1-domain aptamer ARC1779. J Thromb Haemost. 2009; 7(7):1155-1162.
19. Huizinga EG, Tsuji S, Romijn RA, et al. Structures of glycoprotein Ibalpha and its complex with von Willebrand factor A1 domain. Science. 2002;297(5584):1176-1179.
20. Matsushita T, Meyer D, Sadler JE. Localization of von willebrand factor-binding sites for platelet glycoprotein Ib and botrocetin by charged-to-alanine scanning mutagenesis. J Biol Chem. 2000;275(15):11044-11049.
21. Huang RH, Fremont DH, Diener JL, Schaub RG, Sadler JE. A structural explanation for the antithrombotic activity of ARC1172, a DNA aptamer that binds von Willebrand factor domain A1. Structure. 2009;17(11):1476-1484.
22. Furlan M, Robles R, Galbusera M, et al. von Willebrand factor-cleaving protease in thrombotic thrombocytopenic purpura and the hemolytic-uremic syndrome. N Engl J Med. 1998;339(22):1578-1584.
23. Tsai HM, Lian EC. Antibodies to von Willebrand factor-cleaving protease in acute thrombotic thrombocytopenic purpura. N Engl J Med. 1998;339(22):1585-1594.
24. Gragoudas ES, Adamis AP, Cunningham ET, Jr., Feinsod M, Guyer DR, Group VISiONCT. Pegaptanib for neovascular age-related macular degeneration. N Engl J Med. 2004;351(27):2805-2816.
25. Gomez-Outes A, Suarez-Gea ML, Lecumberri R, Rocha E, Pozo-Hernandez C, Vargas-Castrillon E. New parenteral anticoagulants in development. Ther Adv Cardiovasc Dis. 2011;5(1):33-59.
26. Vavalle JP, Cohen MG. The REG1 anticoagulation system: a novel actively controlled factor IX inhibitor using RNA aptamer technology for treatment of acute coronary syndrome. Future Cardiol. 2012;8(3):371-382.
27. Ponce AT, Hong KL. A mini-review: clinical development and potential of aptamers for thrombotic events treatment and monitoring. Biomedicines. 2019;7(3):55.
28. Gilbert JC, DeFeo-Fraulini T, Hutabarat RM, et al. First-in-human evaluation of anti von Willebrand factor therapeutic aptamer ARC1779 in healthy volunteers. Circulation. 2007;116(23):2678-2686.
29. Nimjee SM, White RR, Becker RC, Sullenger BA. Aptamers as therapeutics. Annu Rev Pharmacol Toxicol. 2017; 6(57):61-79.
30. Chen Y, Roberts JR, Orje JN, et al. Identification of a VWFA1 mutation attenuating thrombus growth but not platelet adhesion. Blood. 2017;130(Suppl_1):547.
31. Mazepa MA, Masias C, Chaturvedi S. How targeted therapy disrupts the treatment paradigm for acquired TTP - the risks, benefits and unknowns. Blood. 2019;134(5):415-420.

Predictors of recovery following allogeneic CD34+-selected cell infusion without conditioning to correct poor graft function

Maria M. Cuadrado,[1] Richard M. Szydlo,[1,2] Mike Watts,[3] Nishil Patel,[4] Hanna Renshaw,[4] Jude Dorman,[5] Mark Lowdell,[6] Stuart Ings,[3] Chloe Anthias,[1] Alejandro Madrigal,[1] Stephen Mackinnon,[5] Panagiotis Kottaridis,[5] Ben Carpenter,[5] Rachael Hough,[5] Emma Morris,[5] Kirsty Thomson,[5] Karl S. Peggs[5,7] and Ronjon Chakraverty[5,7]

[1]Anthony Nolan Research Institute; [2]Department of Haematology, Imperial College London; [3]Wolfson Cellular Therapy Unit, University College Hospital London NHS Trust; [4]Department of Haematology, Royal Free London NHS Trust; [5]Department of Haematology, University College Hospital NHS Trust; [6]Centre for Cell, Gene & Tissue Therapeutics, Royal Free London NHS Trust and [7]Department of Hematology, Cancer Institute, University College London, London, UK

ABSTRACT

Poor graft function is a serious complication following allogeneic hematopoietic stem cell transplantation. Infusion of CD34+-selected stem cells without pre-conditioning has been used to correct poor graft function, but predictors of recovery are unclear. We report the outcome of 62 consecutive patients who had primary or secondary poor graft function who underwent a CD34+-selected stem cell infusion from the same donor without further conditioning. Forty-seven of 62 patients showed hematologic improvement and became permanently transfusion- and growth factor-independent. In multivariate analysis, parameters significantly associated with recovery were shared cytomegalovisur seronegative status of both the recipient and donor, the absence of active infection and matched recipient-donor sex. Recovery was similar in patients with mixed and full donor chimerism. Five-year overall survival rates were 74.4% (95% confidence interval [95% CI: 59-89]) in patients demonstrating complete recovery, 16.7% (95% CI: 3-46) in patients with partial recovery and 22.2% (CI 95% 5-47) in those who had no response. In patients with blood count recovery, those with poor graft function in one or two lineages had a better 5-year overall survival (93.8%, 95% CI: 82-99) than those with trilineage failure (53%, 95% CI: 34-88). New strategies including cytokine or agonist support, or a second transplant need to be investigated in patients whose blood counts do not recover.

Introduction

Graft failure is a severe complication of allogeneic hematopoietic stem cell transplantation (SCT), which is associated with reduced survival, especially in patients being treated for hematologic malignancies.[1,2] Graft failure caused by rejection is relatively uncommon with an incidence of 4-6%[3] and ensues as a result of an anti-donor response triggered by recipient T cells or NK cells or by pre-existing donor-specific antibodies (e.g., directed against human leukocyte antigens). Graft failure in the absence of rejection or tumor relapse is more common, with an incidence reported to be between 5-27%,[4] and is referred to as poor graft function. In practice, graft rejection and poor graft function can be distinguished by measuring chimerism: donor cells are undetectable in the former but persist in the latter.[5] Multiple risk factors are associated with poor graft function including issues related to the donor (low stem cell dose and ABO blood group incompatibility), the type of conditioning (reduced intensity or nonmyeloablative conditioning) or the patient (primary diseases such as aplastic anemia or myelofibrosis, viral infections, drugs or the presence of graft-*versus*-host disease [GvHD]).[1,3] Currently, there are no clear recommendations for the treatment of poor graft

function. Supportive care including growth factors and blood products are routinely administered but the latter can be associated with allo-immunization and transfusion-related iron overload. Other approaches, including the use of thrombopoietin-receptor agonists, are currently being investigated in early phase clinical trials. Second allogeneic SCT or infusions of unmanipulated peripheral blood stem cells are other options but are associated with a high risk of GvHD and non-relapse mortality.[6] Larocca *et al.*[7] reported on the use of CD34^{+}-selected stem cell infusions from the original donor without conditioning for correction of poor graft function based on the premise that the risk of GvHD would be low. Clinical outcomes were favorable when compared to those of historical cohorts of patients who were given either no treatment or unmanipulated bone marrow/peripheral blood stem cells without pre-conditioning. Several recent series of patients administered CD34^{+}-selected stem cell infusions have also shown promising results with an improvement of graft function reported in 72-81% of patients (*Online Supplementary Table S1*).[8-11] Although these studies were very important in establishing the principle of CD34^{+}-selected cells in the management of poor graft function, the small number of patients and heterogeneity, in terms of definitions of poor graft function or response, have made it difficult to predict which patients will benefit most from this treatment. Some studies excluded patients with GvHD, with active infection or use of myelosuppressive drugs, although in practice it is often difficult to determine the relative effect of such factors on the graft. Furthermore, all the studies to date have excluded patients with significant mixed chimerism, a group with increasing prevalence given the frequent use of reduced intensity conditioning and T-cell depletion. Thus, there is a need to identify predictors of response in clinically relevant populations of patients to ensure both suitable resource allocation and appropriate requests for repeat donor harvesting.

Here we report the outcome and analysis of predictors of recovery in 62 consecutive patients with poor graft function who were treated with donor CD34^{+}-selected infusion without conditioning. While the majority of patients had complete or partial recovery, cytomegalovirus (CMV) seropositivity, donor-recipient sex mismatching and active infection were all associated with inferior outcomes. Thus, our findings demonstrate the overall feasibility of the approach but also indicate that new strategies are still required in some groups of patients.

Methods

Definitions

Engraftment was defined as the first of 3 consecutive days when the absolute neutrophil count was ≥0.5x10^{9}/L and the absolute platelet count was ≥20x10^{9}/L with or without the administration of granulocyte colony-stimulating factor and without transfusion. Primary poor graft function was defined by: (i) failure to ever achieve count recovery in at least one lineage (neutrophils ≥0.5x10^{9}/L, platelets ≥20 x10^{9}/L and hemoglobin ≥8 g/dL in the absence of transfusion) after transplantation; (ii) a hypoplastic bone marrow; (iii) the absence of relapse; and (iv) the presence of donor cells as detected by peripheral blood chimerism studies. Secondary poor graft function was defined as for primary poor graft function with the exception that blood counts fell in at least one lineage after the initial achievement of engraftment. Recovery was categorized as complete or partial. Complete recovery was defined as a hematological improvement in all three cell lineages (hemoglobin ≥8 g/dL, platelets ≥30x10^{9}/L and neutrophils ≥1.5x10^{9}/L) without the need for transfusion or growth factor support. Partial recovery was defined as a hematologic improvement in one or two lineages. Acute GvHD after CD34^{+}-selected infusion was defined according to the criteria of Glucksberg *et al.*,[12] and chronic GvHD was defined as mild, moderate or severe, following the National Institutes of Health consensus criteria.[13] Active infection was identified using the surrogate of parenteral antimicrobial therapy at the time of CD34^{+}-selected infusion.

Patients

Between 1999-2018, 1996 allogeneic SCT were performed at University College Hospital and Royal Free Hospital in London, UK (Table 1). Seventy patients who received CD34^{+}-selected infusions were identified; eight patients were excluded from the analysis because of disease relapse. This research project was considered by the NHS Health Research Authority as a non-Research Ethics Committee study and was conducted in line with the harmonized UK-wide edition of the Governance Arrangements for Research Ethics Committees (GAfREC) 2018 and the UK Policy Framework for Health and Social Care Research (2017).

Chimerism analysis

Chimerism was analyzed by fluorescence *in situ* hybridization using the XX/XY dual color probe in whole blood or by lineage-specific chimerism using polymerase chain reaction analysis of informative minisatellite regions (short tandem repeat loci), as previously described,[14] within 60 days prior to CD34^{+}-selected infusion. This information was available for 87% of patients. Mixed chimerism of individual cell fractions was defined as the co-existence of donor and recipient DNA with the detection limit being 1-5% according to the individual short tandem repeat marker and the combination of homozygosity *versus* heterozygosity for each marker between donor and patient. Full donor chimerism was defined as the absence of detectable donor DNA in the relevant cell fraction using these sensitivity thresholds.

CD34^{+} stem cell selection

CD34^{+} cells were selected from peripheral blood stem cells that had been mobilized into the periphery by granulocyte colony-stimulating factor using the CliniMACS CD34 enrichment system (Miltenyi Biotec GmbH, Germany)[15] (*Online Supplementary Comment 1*). The CD34^{+}-selected cells were infused within 24 h of selection and without cryopreservation. In six patients with mixed chimerism, a fixed dose of T cells (median CD3^{+} dose of 1x10^{6}, range 1x10^{6} - 1x10^{8}) was administered at the time of the CD34^{+}-selected cell infusion.

Statistical analysis

Recovery was compared between categorical variables using the χ^2 test or Fisher exact test as appropriate, and between continuous variables using the Mann-Whitney U test. Variables for which significant differences were found in univariate analyses were entered into a logistic regression analysis with a forward stepping procedure to find the best model. Probabilities of overall survival were calculated using the Kaplan-Meier method and groups compared with the log-rank test. Probabilities of recovery were estimated using the cumulative incidence procedure, and groups compared using Gray's test. SPSS version 24.0 (IBM SPSS Statistics for Windows, version 24.0. IBM Corp, Armonk, NY, USA) and R version 3.4.2 [16] were used for all analyses.

Table 1. Allogeneic stem cell transplant characteristics.

Characteristics	N. of patients (%)
Number	62
Recipient age, median (range), years	49 (10-66)
Recipient sex	
Male	35 (57%)
Female	27 (43%)
Disease	
Lymphoproliferative disorder	30 (48%)
Acute myeloid leukemia	11 (18%)
Acute lymphoblastic leukemia	7 (11%)
Myelodysplastic syndrome	5 (8%)
Severe aplastic anemia	3 (5%)
Primary myelofibrosis	2 (3%)
Primary immunodeficiency	2 (3%)
Chronic myeloid leukemia	1 (2%)
Sickle cell disease	1 (2%)
EBMT Risk Score*	
Early disease stage	19 (31%)
Intermediate disease stage	28 (45%)
Late stage disease	9 (14%)
Not applicable (non-malignant disease)	6 (10%)
HCT-CI	
Low risk	45 (73%)
Intermediate risk	15 (24%)
High risk	2 (3%)
Donor type	
Related donor	28 (45%)
Matched unrelated donor	18 (29%)
Mismatched unrelated donor	16 (25%)
CMV status (R/D)	
Negative/negative	23 (37%)
Other	39 (63%)
ABO status (R/D)	
Major incompatibility	14 (23%)
Minor incompatibility	13 (21%)
No incompatibility	35 (57%)
Sex matching	
Matched	31 (50%)
Unmatched	31 (50%)
Acute GvHD	
Grades 0-I	42 (68%)
Grades II-IV	20 (32%)
Chronic GvHD	
None	37 (60%)
Mild	11 (18%)
Moderate	9 (15%)
Severe	3 (5%)
Non evaluable**	2 (3%)
CMV reactivation	
Yes	35 (56%)
No	27 (44%)
Conditioning regimen	
RIC (FMC)	40 (65%)
Other***	22 (35%)
Source of stem cells	
Bone marrow	8 (13%)
Peripheral blood	54 (87%)
Median CD34 dose (x10⁶/kg) (range)	5.0 (0.3-37.6)
T-cell depletion	
Yes	57 (92%)
No	5 (8%)

Poor graft function	
Primary	21 (34%)
Secondary	41 (66%)
Chimerism pre-CD34⁺- infusion	
Donor	21 (34%)
Mixed	32 (52%)
Missing values	9

EBMT: European Group for Blood and Marrow Transplantation; HCT-CI: Hematopoietic Cell Transplantation-specific Comorbidity Index; CMV: cytomegalovirus; R/D: recipient/donor; GvHD: graft-*versus*-host disease; RIC: reduced intensity conditioning; FMC: fludarabine, melphalan, alematuzumab. *EBMT Risk Score: early disease stage includes acute leukemia (AL) transplanted in first complete remission (CR), myelodysplastic syndrome (MDS) transplanted untreated or in first CR; intermediate disease stage includes AL in second CR, chronic myeloid leukemia (CML) in all other stages than first chronic phase or blast crisis, MDS in second CR or in partial remission (PR), lymphoma and multiple myeloma in second CR, in PR or stable disease; late disease stage includes AL in all other disease stages, CML in blast crisis, MDS in all other disease stages and lymphoma and multiple myeloma in all disease stages other than those defined as early or intermediate. Stage is not applicable for aplastic anemia, primary immunodeficiencies and sickle cell disease. **Patients died within 100 days after allogeneic stem cell transplantation. ***Conditioning regimen (other): Campath 1H/thiotepa/total body irradiation (TBI) (n=1); Campath 1H/cyclophosphamide/TBI (n=2); Campath 1H/fluradabine/ cyclophosphamide/TBI (n=1); cyclophosphamide/TBI (n=3); fluradabine/ cyclophosphamide/TBI (n=3); Campath 1H/BEAM (carmustine, etoposide, cytarabine, melphalan) (n=5); fluradabine/thiotepa (n=1); Campath 1H/ fluradabine/busulfan (n=2); Campath 1H/fluradabine/treosulfan (n=1); Campath 1H/ cyclophosphamide (n=1); antithymocyte globulin/fluradabine/busulfan (n=1); cyclophosphamide/ fluradabine/TBI (n=1).

Results

Primary and secondary poor graft function

The overall incidence of poor graft function treated with CD34⁺-selected infusion was 3.1% (62/1996) among the total population of patients transplanted. Twenty-one patients in this group (34%) had primary poor graft function and 41 had secondary poor graft function (66%). The median time from engraftment to the development of secondary poor graft function was 130 days (range, 5-2,694). Poor graft function was restricted to one or two hematopoietic cell lineages in 19 patients (31%), and occurred in all three lineages in 43 patients (69%), although patients with primary poor graft function were more likely to have trilineage cytopenia than those with secondary poor graft function (19 of 21 [91%] *versus* 24 of 41 [61%], respectively; $P=0.01$). In a multivariate analysis to determine factors associated with primary *versus* secondary poor graft function, a mismatched unrelated donor was associated with a higher probability of primary poor graft function ($P=0.03$), whereas CMV serostatus other than negative for both recipient and donor was associated with a higher risk of secondary poor graft function ($P=0.008$). No other significant associations for primary *versus* secondary poor graft function in the treated group were found for any of the following factors: donor-recipient sex matching, donor-recipient age, Hematopoietic Cell Transplantation-specific Comorbidity Index, European Group for Blood and Marrow Transplantation (EBMT) Risk Score, presence of GvHD, major ABO incompatibility or the original transplant CD34⁺ cell dose (*Online Supplementary Tables S2 and S3*).

Hematologic improvement following CD34⁺-selected infusion

The median interval from allogeneic SCT to CD34⁺-selected infusion was 15 months (range, 1-226); the medi-

an CD34+ cell dose/kg recipient weight was 3.2x10⁶/kg (range, 0.47-14.2) and the median CD3+ dose was 4.3x10³/kg (range, 0-13). At the time of CD34+-selected infusion, the median neutrophil count was 0.7x10⁹/L (range, 0.01-10), the median platelet count was 17x10⁹/L (range, 5-296) and the median hemoglobin concentration was 8.7 g/dL (range, 5.3 to 12.5). Of the 62 treated patients, 47 (76%) showed a hematologic improvement with complete (n=39) or partial recovery (n=8). Evidence of recovery was observed in 23 patients within 30 days; of these, 20 patients achieved complete recovery and three patients had partial recovery. Hematologic improvement after 30 days was observed in 23 patients; of these 18 patients achieved complete recovery and five patients had partial recovery. In patients showing hematologic improvement with complete or partial recovery, the median number of days required for the recovery of neutrophils was 29 days (range, 6-1,182), that for the recovery of platelets was 18 days (range, 5-600) and that for recovery of hemoglobin was 25 days (range, 6-511). The time range for recovery of neutrophils was especially prolonged and reflected the requirement for responding patients to be independent of any growth factor support. There were no differences in recovery times for patients showing complete *versus* partial recovery (Figure 1). The probability of complete or partial recovery was also analyzed according to the number of lineages affected and although there

were no differences in total rates of recovery, the proportion of patients achieving complete recovery was greater if poor graft function affected one or two lineages *versus* all three lineages (16/16 [100%] *versus* 23/31 [74%]; *P*=0.04). All patients who demonstrated complete or partial recovery after CD34+-selected infusion maintained their recovery throughout the follow-up period.

Factors associated with hematologic improvement

In univariate analyses to determine factors predictive of recovery, we found that shared donor-recipient CMV seronegative status, donor-recipient sex matching, absence of active infection at the time of CD34+-selected infusion and low EBMT Risk Score were associated with recovery (Table 2A, B). Patients sharing a CMV seronegative status with the donor achieved complete or partial recovery more frequently than any other recipient-donor serostatus combination (21/23 [91%] *versus* 26/39 [68%]; *P*=0.03). Sex matching between the donor and recipient was also associated with a better rate of recovery than mismatched combinations (28/31 [90%] *versus* 19/31 [61%]; *P*=0.008); female recipients of transplants from male donors had the worst rates of recovery (8/15 [53%] *versus* 39/47 [83%]; *P*=0.02). Patients without active infection during CD34+-selected infusion had higher rates of recovery than the patients with infection (33/36 [92%] *versus* 12/24 [50%]; *P*<0.001; data missing for 2 patients).
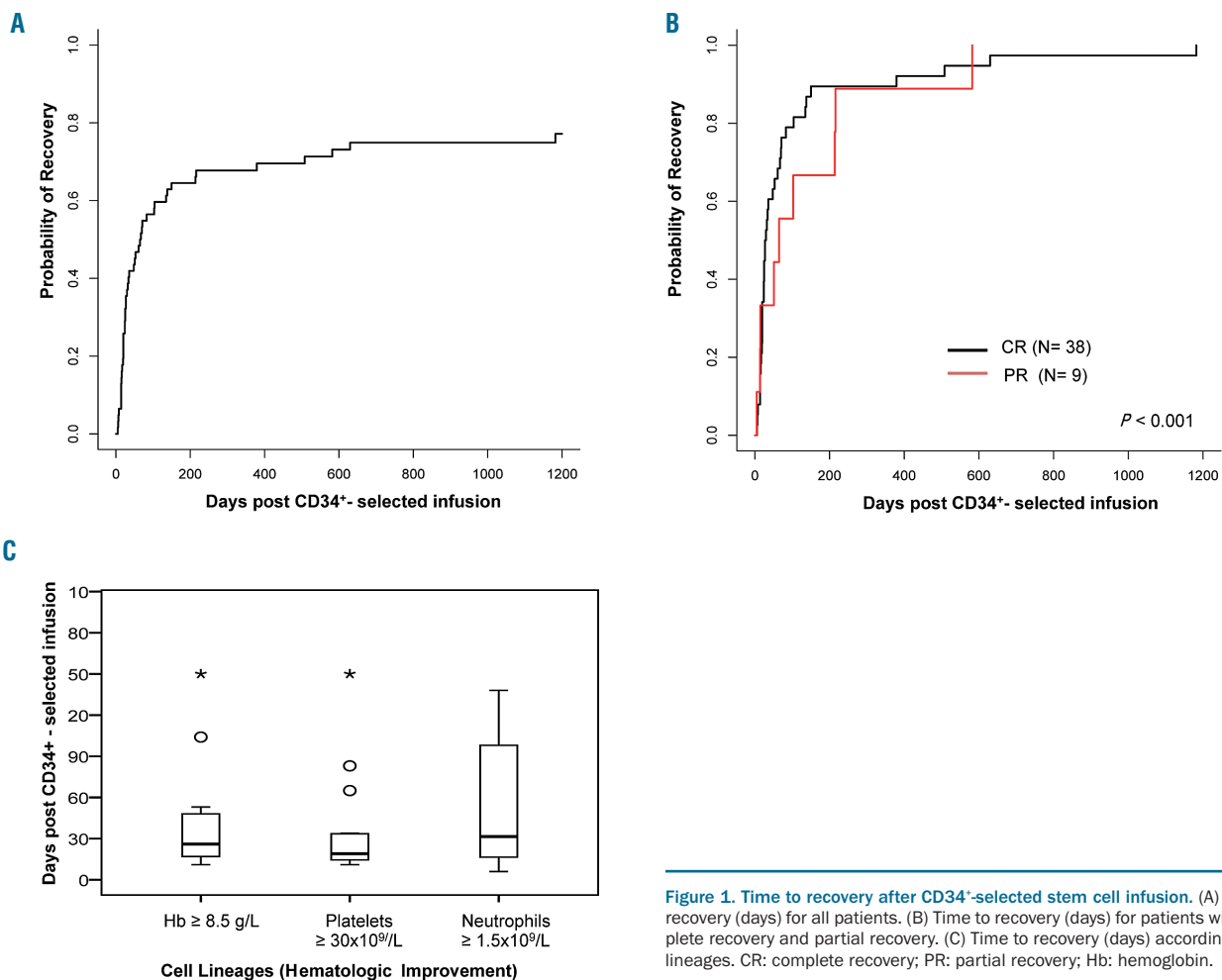
Figure 1. Time to recovery after CD34+-selected stem cell infusion. (A) Time to recovery (days) for all patients. (B) Time to recovery (days) for patients with complete recovery and partial recovery. (C) Time to recovery (days) according to cell lineages. CR: complete recovery; PR: partial recovery; Hb: hemoglobin.

Table 2A. Univariate analysis of pre-transplant variables as predictors of recovery after CD34+-selected infusion.

	N	Recovery, N (%)	P-value
HCT-CI			
Low risk	45	35 (78%)	
Intermediate risk	15	11 (73%)	0.6
High risk	2	1 (50%)	
R/D sex			
Unmatched	31	19 (61%)	0.008
Matched	31	28 (90%)	
Donor type			
Related donor	28	22 (79%)	
Matched unrelated donor	18	13 (72%)	
Mismatched unrelated donor	16	12 (75%)	0.9
ABO status			
No incompatibility	35	28 (80%)	
Major incompatibility	14	10 (71%)	0.7
Minor incompatibility	13	9 (69%)	
CMV status (R/D)			
Other	39	26 (67%)	
Negative/negative	23	21 (91%)	0.03
EBMT Risk Score*			
Early	19	15 (79%)	
Intermediate	28	25 (89%)	0.02
Advanced	9	4 (44%)	
Non-malignant	6	3 (50%)	

HCT-CI: Hematopoietic Cell Transplantation-specific Comorbidity Index; R/D: recipient/donor; CMV: cytomegalovirus; EBMT: European Group for Blood and Marrow Transplantation. *EBMT Risk Score: early disease stage includes acute leukemia (AL) transplanted in first complete remission (CR), myelodysplastic syndrome (MDS) transplanted untreated or in first CR; intermediate disease stage includes AL in second CR, chronic myeloid leukemia (CML) in all other stages than first chronic phase or blast crisis, MDS in second CR or in partial remission (PR), lymphoma and multiple myeloma in second CR, in PR or stable disease; late disease stage includes AL in all other disease stages, CML in blast crisis, MDS in all other disease stages and lymphoma and multiple myeloma in all disease stages other than those defined as early or intermediate. Stage is not applicable for aplastic anemia, primary immunodeficiencies and sickle cell disease.

Finally, patients with early or intermediate stage disease had better recovery rates than patients with advanced disease (15/19 [79%] and 25/28 [89%] *versus* 4/9 (44%), respectively; *P*=0.02). In multivariate analysis, only CMV serostatus, recipient-donor sex matching and infection remained statistically significant (Table 3). The type of poor graft function (primary or secondary), type of donor (related, matched or mismatched unrelated donor), ABO incompatibility, patient's age, previous or active acute or chronic GvHD, CD34+ and CD3+ cell dose of the top-up infusion, CMV reactivation, full *versus* mixed donor chimerism and the interval from the initial allogeneic SCT to CD34+-selected infusion had no impact on the achievement of complete or partial recovery (Table 2A, B). Chimerism status (available for 87% of patients in the 60 days prior to infusion) categorized into full donor or mixed chimerism also did not predict response. A subset of six patients with mixed chimerism received co-infusion of T cells at the time of CD34+-selected top-up. The co-transfer of donor T cells had no impact on recovery (5/6 [83%] who received co-infusion of T cells *versus* 16/22 [73%] who did not receive T cells showed complete or partial recovery; *P*=0.6).

Cytomegalovirus serostatus as a predictor of recovery

CMV monitoring by polymerase chain reaction was performed twice a week for the first 3 months and surveil-

Table 2B. Univariate analysis of post-transplant variables as predictors of recovery after CD34+-selected infusion.

	N	Recovery, N (%)	P-value
Acute GvHD after allo-SCT			
Grades 0-I	42	32 (76%)	
Grades II-IV	20	12 (75%)	0.9
Chronic GvHD after allo-SCT			
None	37	29 (78%)	
Mild	11	11 (64%)	
Moderate	9	8 (89%)	
Severe	3	3 (100%)	0.06
Not evaluable*	2	0	
Poor GF			
Primary	21	15 (71%)	
Secondary	41	32 (78%)	0.6
Poor GF			
3 lineages	43	31 (72%)	
1 or 2 lineages	19	16 (84%)	0.3
Time from engraftment to secondary poor GF (median)			
<130 days	18	14 (78%)	
≥130 days	23	18 (78%)	0.9
Time from secondary poor GF to CD34+-infusion (median)			
<88 days	21	15 (71%)	
≥88 days	20	17 (85%)	0.3
Time from allo-SCT to CD34+- infusion (median)			
<15 months	31	21 (68%)	
≥15 months	31	26 (84%)	0.1
CD34+- infusion dose (median)**			
<3.18	31	24 (77%)	
≥3.18	31	23 (74%)	0.8
CD3+- infusion dose (median)***			
<4.3	31	24 (77%)	
≥4.3	31	23 (74%)	0.8
Addition of T cells at the time of CD34+- infusion			
No addition and full donor chimerism	22	18 (82%)	
Addition and mixed donor chimerism	6	5 (83%)	0.7
No addition and mixed donor chimerism	25	16 (73%)	
Missing values	9		
Recipient age at CD34+- infusion (median)			
Age <50 years	31	22 (71%)	
Age ≥50 years	31	25 (81%)	0.4
Donor age at CD34+-infusion (median)			
Age <39 years	33	22 (67%)	
Age ≥39 years	29	25 (86%)	0.07
Active infection at the time of CD34+- infusion			
Yes	24	12 (50%)	
No	36	33 (92%)	<0.001
Missing values	2		
GvHD (acute/chronic) at the time of CD34+- infusion			
Yes	15	10 (67%)	
No	46	36 (78%)	0.4
Missing values	1		
Immunosuppression at the time of CD34+- infusion			
Yes	39	29 (74%)	
No	23	18 (78%)	0.7
Chimerism before CD34+- infusion			
Donor	21	17 (81%)	
Mixed	32	25 (78%)	0.8
Missing values	9		

GvHD: graft-*versus*-host disease; allo-SCT: allogeneic stem cell transplantation; GF: graft function. *Patients died within 100 days after allo-SCT. **Cell dose x 10^6/kg recipient weight. ***Cell dose x 10^3/kg recipient weight.

lance continued in a subset of patients at risk of late re-activation (e.g., patients with GvHD, prior multiple re-activations). Twenty-three recipients shared a CMV seronegative status with the donor and did not have CMV reactivation. Of the remaining 39 patients, 35 (92%) had CMV re-activation before the CD34+-selected infusion. No patients had CMV re-activation following infusion. The relationship between complete or partial recovery and CMV serostatus correlated with CMV re-activation, with 23/35 (66%) of patients who had CMV re-activation showing a response *versus* 24/27 (89%) of those who did not have CMV re-activation (*P*=0.04). However, other variables related to the severity of CMV infection including earlier re-activation, higher peak CMV viremia, longer duration of antiviral drug treatment, higher number of CMV re-activations, active CMV infection at the time of infusion and CMV disease did not correlate with worse recovery (*Online Supplementary Table S4*).

Table 3. Multivariate analysis for recovery after CD34+- selected infusion.

	N	OR (95% CI)	*P*-value
Active infection at the time of CD34+-selected infusion			
Yes	24	1.0	
No	36	38.9 (3.9-388.3)	0.002
Missing values	2		
R/D CMV status			
Other	37	1.0	
Negative/negative	23	16.8 (1.4-195.8)	0.02
Missing values	2		
R/D sex			
Unmatched	31	1.0	
Matched	29	24.4 (2.3-254.5)	0.008
Missing values	2		

R/D: recipient/donor; CMV: cytomegalovirus.

Graft-*versus*-host disease

Acute GvHD following CD34+- selected infusion occurred in a total of seven patients (11%) at a median of 15 days (range, 7-26 days; 3 patients had acute GvHD grade I-II and 4 patients had grade III-IV).

Chronic GvHD was seen in five patients (8%) who survived for more than 100 days following CD34+-selected infusion (1 patient had mild, 1 had moderate and 3 had severe chronic GvHD). Of the six patients who received co-transfer of donor T cells, two developed acute GvHD grade III-IV and two developed mild and severe chronic GvHD.

Survival

At a median follow up of 6.4 years (range, 2.8-9.9), 29 patients (11/15 non-responding [73%], 7/8 with partial recovery [87%] and 11/39 with complete recovery [28%]) had died. The causes of death included infection (38%), relapse (34%), GvHD (16%), secondary malignancies (3%) and others (9%). The median overall survival for all patients was 5.4 years (95% confidence interval [95% CI]: 1.3-9.4). One and 5-year overall survival rates were 70% (95% CI: 58-82) and 54% (95% CI: 41-68), respectively. In patients with complete recovery after CD34+-selected infusion, the overall survival rates at 1 and 5 years were 86.7% (95% CI: 76-98) and 74.4% (95% CI: 59-89), respectively, while those in patients with partial recovery were 62.5% (95% CI: 28-97) and 16.7% (95% CI: 3-46) respectively. Patients showing no response had poor outcomes with overall survival rates of 33.3% (95% CI: 9-58) and 22.2% (95% CI: 5-47) at 1 and 5 years respectively (Figure 2A). Of the 15 patients who did not recover, three (20%) remain alive: one patient had red cell aplasia and is currently on periodic red cell transfusions with iron chelation; a second patient underwent second allogeneic SCT; and the third patient with trilineage poor graft function is requiring ongoing transfusional support and growth factors. The remaining patients without response died, pri-
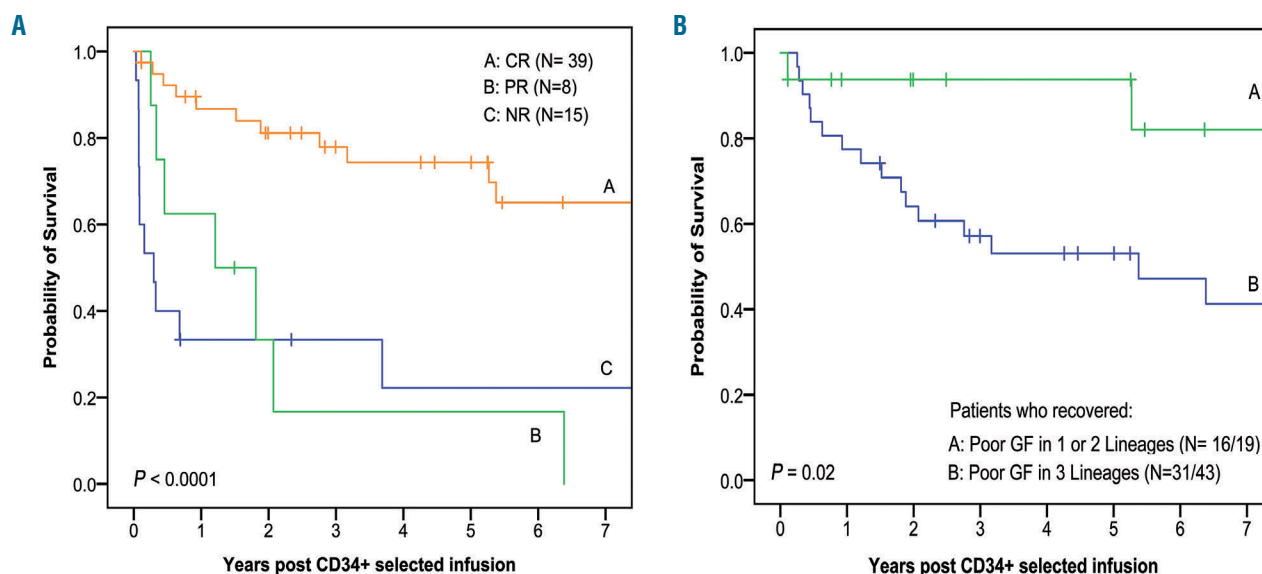
Figure 2. Kaplan-Meier estimate of overall survival after CD34+-selected stem cell infusion. (A) Survival curves according to type of recovery; complete, partial or no recovery. (B) Survival curves in patients who recovered after CD34+-selected infusion, according to whether they had poor graft function in one or two lineages or poor graft function in all three lineages. CR: complete recovery; PR: partial recovery; NR: no recovery.

marily as a result of infectious complications. Of the patients who showed blood count recovery, those who initially had poor graft function in one or two lineages had a superior 5-year overall survival rate of 93.8% (95% CI: 82-99) compared to those with trilineage poor graft function who had a 5-year overall survival rate of 53% (95% CI: 34-88) (Figure 2B). The rates or completeness of recovery together with their effect upon outcome were similar over time, as identified by comparing patient cohorts receiving CD34+-selected infusions in the early *versus* late time periods (2000-2009 *versus* 2010-2018) of the study (*data not shown*).

Discussion

Poor graft function occurs only in a minority of patients following allogeneic SCT but is associated with a high mortality. Management of such patients is resource-intensive with patients requiring multiple hospital visits or prolonged, inpatient admissions. Our study shows that the majority of patients with poor graft function who are given CD34+-selected infusion without conditioning will subsequently have a hematologic improvement; in more than six of ten patients, the recovery will be permanent and complete, avoiding the need for transfusion or growth factor support. The procedure is safe with low rates of acute and chronic GvHD, consistent with the low doses of T cells contained within the CD34+-selected graft. Our report does, however, highlight that there are subgroups of patients (those with recipient or donor CMV seropositivity, with active infection or with recipient-donor sex mismatching), who respond less favorably and for whom alternative strategies may be required.

Our study differs from other studies that employed CD34+-selected infusion only in patients with full donor chimerism. Reflecting the use of T-cell depletion in 91% of patients in our series, mixed chimerism was evident in 58% of recipients (affecting the T-cell lineage in all patients with or without involvement of B- and/or myeloid-lineages), with none of these patients having evidence of disease relapse. Our data confirm that the approach of CD34+-selected infusion is feasible in such patients with recovery rates similar to those of patients with full donor chimerism. Although a small subset of patients with mixed chimerism received a fixed dose of T cells at the time of CD34+-selected infusion, this had no effect upon outcome. To avoid the additional risk of GvHD, we do not routinely give additional T cells in this setting. We were unable to test whether the precise level of donor chimerism correlated with recovery because the analysis methods used to detect chimerism were only semi-quantitative at the time most patients were treated.

The main limitation of our analysis is the lack of a control group so that it is difficult to measure the effect of the CD34+-selected infusion *versus* the effect of other hematopoietic stem cell (HSC)-intrinsic or -extrinsic factors that lead to eventual recovery. The lack of a control group is particularly relevant to the observed kinetics of recovery with about one in two patients recovering more than 30 days following infusion (although most achieved complete or partial recovery within 3 months). We observed similar kinetics of recovery to those observed by other groups using CD34+-selected infusion without preconditioning.[7-11] We currently lack a clear framework in

human patients for understanding how niche function and availability found in patients with poor graft function influence the re-populating capacity of infused CD34+-selected cells. While we presume that there are too few endogenous HSC to outcompete the infused HSC in patients with poor graft function, the number of available niches in this clinical setting is unknown and likely to be influenced by multiple factors including prior therapies, host-pathogen interactions and immune dysregulation.

The larger number of patients in this series compared to the numbers in other reports afforded us the opportunity to explore predictors of response in more detail. We found that active infection (identified using the surrogate of antimicrobial therapy) at the time of CD34+-selected infusion was the strongest negative predictor of recovery. Of note, lack of recovery was not related to the level of neutropenia, a finding that is indicative that other factors independent of the overall severity of poor graft function may prevent a response (*data not shown*). Under conditions of replicative stress (e.g., allogeneic SCT) chronic inflammatory signals such as those mediated through Toll-like receptors or pro-inflammatory cytokines (e.g., tumor necrosis factor-α, interferon-γ or interleukin-1) impair HSC self-renewal through induction of apoptosis or by driving myeloid differentiation.[17] In humans, similar mechanisms have been invoked for bone marrow failure in the context of chronic infections. Thus, one possibility is that the pro-inflammatory conditions provoked by infection pose a significant barrier to establishing a functional HSC pool from infused CD34+-selected cells.

Although the infections in this cohort of patients were heterogeneous, CMV infection had the most noticeable impact on the response to CD34+-selected infusion. Both CMV seropositivity in the donor and/or recipient and a history of CMV re-activation predicted a worse recovery although the majority of patients in both groups achieved complete or partial recovery. We had reasoned that recovery would correlate inversely with surrogates of more severe infections (e.g., high peak CMV viremia or greater numbers of re-activations) but this was not the case; these data suggest that either the sample size of our cohort was not sufficiently powered to detect a relationship or that other mechanisms are involved. While the myelosuppressive effects of anti-CMV drugs are well described, CMV infection may also impair niche functions and HSC self-renewal by directly infecting bone marrow macrophages and stroma, or indirectly as a consequence of chronic inflammation.[18] Currently, it is difficult to conceive new strategies to overcome these issues other than accelerating restoration of anti-CMV immunity through adoptive transfer of CMV-specific or memory T cells, or the use of anti-CMV drugs that cause less myelosuppression (e.g., letermovir). It will be of interest, therefore, to evaluate how the introduction of CMV prophylaxis with letermovir affects the overall incidence of poor graft function and responses to CD34+-selected infusions. In our view, CMV-seropositive patients or those with CMV re-activation should not be excluded from consideration for CD34+-selected infusion; however, this approach should be considered as part of a broader plan to improve immune reconstitution and avoid excess use of drugs that are toxic to the bone marrow.

Sex matching between the donor and recipient also influenced recovery following CD34+-selected infusions, specifically when the transplant was from a male donor

into a female recipient. This finding was unexpected because female recipients of male grafts had either full donor chimerism or stable mixed chimerism prior to CD34^{+}-selected infusion (6/14 [30%] full donor and 8/14 [57%] stable mixed chimerism). This finding would be consistent with the concept of 'split tolerance' identified in animal models in which hematopoietic chimeras with mixed T-cell chimerism can nevertheless reject other donor tissues, including other hematopoietic cells.[19] It will therefore be important to track for evidence of anti-HY antibodies and HY-specific cytotoxic T lymphocytes either prior to or following infusion of male grafts into female recipients. Potential strategies that could be considered in future trials would be the use of nonmyeloablative conditioning prior to CD34^{+}-selected infusion, or the co-transfer of regulatory T cells;[20] in the latter case, the regulatory T cells may be particularly important in providing immune privileged sites for HSC within the bone marrow.[21]

The minority of patients showing no recovery or only partial recovery following CD34^{+}-selected infusion had worse overall survival, mostly explained by non-relapse deaths in the first 18 months following treatment (12/14 [86%] of patients with no or partial recovery died due to non-relapse causes, in the first 18 months). It will be crucial to implement alternative strategies in such patients including a second allogeneic SCT; in this case, use of the same donor can afford the opportunity to use less toxic regimens, even though these procedures still carry a high risk in patients who may have accumulated additional problems such as infection.

In conclusion, we confirm that CD34^{+}-selected donor infusion without conditioning is an important therapeutic option that should be considered in patients with poor graft function following allogeneic SCT. Our findings also indicate that this approach can be applied in patients with stable mixed chimerism, a group excluded from previous studies. The low risk of the procedure means that this strategy can be adopted even in patients with risk factors for lower rates of recovery (e.g., in patients with active infection, of whom 1 in 2 patients will still respond). However, the overall heterogeneity of response is indicative that multiple factors (both intrinsic and extrinsic) influence graft integrity and highlight the critical need for further investigation of mechanisms underlying poor graft function. The information gained could be used to define the role of emerging treatments such as thrombopoietin-receptor agonists,[22] which are the subject of ongoing trials. In the future, trials investigating combination therapies involving CD34^{+}-selected infusion and co-transfer of mesenchymal cells to improve niche function[23] or regulatory T cells to augment immune tolerance of transferred HSC should be conducted.

References

1. Olsson R, Remberger M, Schaffer M, et al. Graft failure in the modern era of allogeneic hematopoietic SCT. Bone Marrow Transplant. 2013;48(4):537-543.
2. Rondón G, Saliba RM, Khouri I, et al. Long-term follow-up of patients who experienced graft failure postallogeneic progenitor cell transplantation. Results of a single institution analysis. Biol Blood Marrow Transplant. 2008;14(8):859-866.
3. Cluzeau T, Lambert J, Raus N, et al. Risk factors and outcome of graft failure after HLA matched and mismatched unrelated donor hematopoietic stem cell transplantation: a study on behalf of SFGM-TC and SFHI. Bone Marrow Transplant. 2016;51(5):687-691.
4. Lee KH, Lee JH, Choi SJ, et al. Failure of trilineage blood cell reconstitution in patients undergoing allogeneic hematopoietic cell transplantation - frequency and outcomes. Bone Marrow Transplant. 2004;33(7):729-734.
5. Masouridi-Levrat S, Simonetta F, Chalandon Y. Immunological basis of bone marrow failure after allogeneic hematopoietic stem cell transplantation. Front Immunol. 2016;7:362.
6. Ferrà C, Sanz J, Morgades M, et al. Outcome of graft failure after allogeneic stem cell transplant : study of 89 patients. Leuk Lymphoma. 2015;56(3):656-662.
7. Larocca A, Piaggio G, Podestà M, et al. Boost of CD34+-selected peripheral blood cells without further conditioning in patients with poor graft function following allogeneic stem cell transplantation. Haematologica. 2006;91(7):935-940.
8. Askaa B, Fischer-Nielsen A, Vindeløv L, et al. Treatment of poor graft function after allogeneic hematopoietic cell transplantation with a booster of CD34-selected cells infused without conditioning. Bone Marrow Transplant. 2014;49(5):720-721.
9. Klyuchnikov E, El-Cheikh J, Sputtek A, et al. CD34+-selected stem cell boost without further conditioning for poor graft function after allogeneic stem cell transplantation in patients with hematological malignancies. Biol Blood Marrow Transplant. 2014;20(3):382-386.
10. Stasia A, Ghiso A, Galaverna F, et al. CD34 selected cells for the treatment of poor graft function after allogeneic stem cell transplantation. Biol Blood Marrow Transplant. 2014;20(9):1440-1443.
11. Ghobadi A, Fiala MA, Ramsingh G, et al. Fresh or cryopreserved CD34+-selected mobilized peripheral blood stem and progenitor cells for the treatment of poor graft function after allogeneic hematopoietic cell transplantation. Biol Blood Marrow Transplant. 2017;23(7):1072-1077.
12. Glucksberg H, Storb R, Fefer A, et al. Clinical manifestations of graft-verus-host disease in human recipients of marrow from HLA-matched sibling donors. Transplantation. 1974;18(4):295-304.
13. Jagasia MH, Greinix HT, Arora M, et al. National institutes of health consensus development project on criteria for clinical trials in chronic graft-versus-host disease: I. The 2014 diagnosis and staging working group report. Biol Blood Marrow Transplant. 2015;21(3):389-401.
14. Kottaridis P, Milligan D, Chopra R, et al. In vivo CAMPATH-1H prevents graft-versus-host disease following nonmyeloablative stem cell transplantation. Blood. 2000;96(7):2419-2425.
15. Ings SJ, Balsa C, Mackinnon S, et al. Peripheral blood stem cell yield in 400 normal donors mobilised with granulocyte colony-stimulating factor (G-CSF): impact of age, sex, donor weight and type of G-CSF used. Br J Haematol. 2006;134(5):517-525.
16. R Core Team (2014). R: A language and environment for statistical computing. R Foundation for statistical computing, Vienna, Austria. URL http://www.R-project.org/.
17. Pietras EM. Inflammation: a key regulator of hematopoietic stem cell fate in health and disease. Blood. 2017;130(15):1693-1698.
18. Reddehase MJ. Mutual interference between cytomegalovirus and reconstitution of protective immunity after hematopoietic cell transplantation. Front Immunol. 2016;7:294.
19. Al-Adra DP, Anderson CC. Mixed chimerism and split tolerance: mechanisms and clinical correlations. Chimerism. 2011;2(4):89-101.
20. Pilat N, Granofszky N, Wekerle T. Combining adoptive T reg transfer with bone marrow transplantation for transplantation tolerance. Curr Transplant Rep. 2017;4(4):253-261.
21. Fujisaki J, Wu J, Carlson AL, et al. In vivo imaging of T reg cells providing immune privilege to the haematopoietic stem-cell niche. Nature. 2011;474(7350):216-219.
22. Tang C, Chen F, Kong D, et al. Successful treatment of secondary poor graft function post allogeneic hematopoietic stem cell transplantation with eltrombopag. J Hematol Oncol. 2018;11(1):103.
23. Zhao K, Liu Q. The clinical application of mesenchymal stromal cells in hematopoietic stem cell transplantation. J Hematol Oncol. 2016;9(1):46.

NPAS4L is involved in avian hemangioblast specification

Vertebrate primitive hematopoietic and vascular development is regulated by a conserved set of transcription factors. Their common precursors, the hemangioblasts, express Stem cell leukemia/T-cell acute lymphoblastic leukemia 1 (*SCL/TAL1*)[1] and Lim only protein 2 (*LMO2*)[2] in all vertebrate groups examined. Hemangioblast specification from nascent mesoderm was reported to be less conserved, with Ets variant 2 (*ETV2*) and Neuronal PAS-domain containing protein 4-like (*NPAS4L*) identified as its master regulator in mammals[3] and zebrafish,[4] respectively. We show here that the ortholog of *NPAS4L*, but not of *ETV2*, is present in the avian genome. Chicken *NPAS4L* is expressed in hemangioblasts prior to *SCL/TAL1* and *LMO2*. CRISPR-on mediated ectopic expression of endogenous *NPAS4L* leads to ectopic *SCL/TAL1* and *LMO2*, as with ectopic expression of zebrafish *NPAS4L*. We propose that the ancestral amniote genome had both *NPAS4L* and *ETV2* genes. The *ETV2* gene was lost in the avian lineage without affecting direct transcriptional regulation of *SCL/TAL1* and *LMO2* by *NPAS4L*.[5,6] The *NPAS4L* gene was lost in the mammalian lineage, with its roles partially replaced by *ETV2*.

Vertebrate primitive hematopoietic and vascular systems are derived from the mesoderm germ layer.[7,8] Lineage specification events taking place between gastrulation and the onset of circulation are controlled by a set of evolutionarily-conserved transcription regulators.[8,9] In birds,[10-12] as in fish, amphibians and mammals,[13-17] common progenitors of blood and endothelial cells (the hemangioblasts) start to express transcription factors *SCL/TAL1* and *LMO2* at Hamburger and Hamilton stage 4$^+$ (HH4$^+$),[18] soon after their exit from posterior primitive streak where ventral mesoderm cells originate. This is followed by FGFR-mediated segregation of blood and endothelial lineages and functional differentiation of blood cells starting from HH7,[10] mediated by a conserved set of transcription factors including SCL/TAL1, LMO2, GATA-binding factor 2 (GATA2), LIM domain-binding protein 1 (LDB1) and transcription factor E2A (E2A).[19] After the onset of circulation from HH12/13, the hemangioblast markers *SCL/TAL1* and *LMO2* become restricted to the blood and endothelial lineages, respectively.
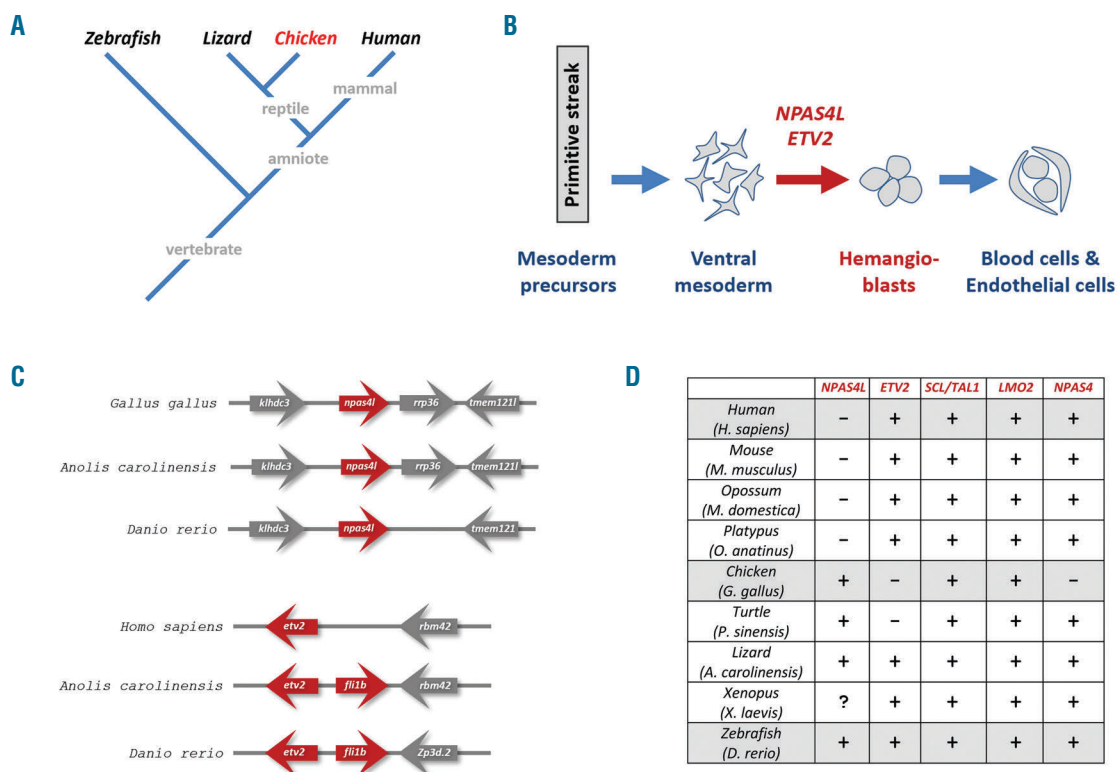
Figure 1. The chicken genome has *NPAS4L*, but not *ETV2* ortholog. (A) A simplified vertebrate phylogenetic tree. (B) Schematic view of blood and endothelial cell differentiation from mesoderm precursors in the streak. *NPAS4L* and *ETV2* are proposed to function during hemangioblast specification in the ventral mesoderm. (C) The chicken genome has the *NPAS4L* orthologous gene flanked by *KLHDC3* gene on one side and *RRP36* and *TMEM121L* genes on the other. Similar syntenic organization is seen in lizard A. carolinensis and zebrafish D. rerio. These genes are missing in mammalian genomes. The chicken genome does not have *ETV2* ortholog. The lizard genome has *ETV2* and *FLI1B* as in the zebrafish genome. Mammals have *ETV2*, but not *FLI1B*. (It is to be noted that vertebrate genomes have three copies of such tandemly duplicated ETS family genes; not shown). In addition to the *ETV2-FLI1B* couplet which is the least conserved, the other two couplets (*ETS1-FLI1* and *ETS2-ERG*) are well-conserved. (D) Summary of presence and absence of *NPAS4L, ETV2, SCL/TAL1, LMO2* and *NPAS4* genes in various vertebrate groups. The following protein sequences were used for comparison. For SCL/TAL1: NP_001274276.1 (human), NP_001274317.1 (mouse), XP_001374963.3 (opossum), DNA clone XX-200B24 (platypus), NP_990683.1 (chicken), XP_030427307.1 (desert turtle; sequence in Chinese soft-shell turtle is incomplete), XP_008114556.1 (lizard), NP_001081746.1 (Xenopus) and NP_998402.1 (zebrafish); for LMO2: AAH42426.1 (human), AAH57880.1 (mouse), XP_027693653.1 (opossum), XP_028917173.1 (platypus), AAL78036.1 (chicken), XP_030415938.1 (turtle), XP_003225211.1 (lizard), NP_001081112.1 (Xenopus) and AAH93136.1 (zebrafish); for ETV2: NP_055024.2 (human), NP_031985.2 (mouse), XP_007491908.1 (opossum), XP_028921116.1 (platypus), XP_008119144.1 (lizard), NP_001089600.1 (Xenopus) and NP_001032452.1 (zebrafish); for NPAS4L: EntrezID 101750093 (chicken), XP_008103134.1 (lizard), XP_008165306.1 (turtle) and NP_001316841.1 (zebrafish).

	NPAS4L	ETV2	SCL/TAL1	LMO2	NPAS4
Human (H. sapiens)	−	+	+	+	+
Mouse (M. musculus)	−	+	+	+	+
Opossum (M. domestica)	−	+	+	+	+
Platypus (O. anatinus)	−	+	+	+	+
Chicken (G. gallus)	+	−	+	+	−
Turtle (P. sinensis)	+	−	+	+	+
Lizard (A. carolinensis)	+	+	+	+	+
Xenopus (X. laevis)	?	+	+	+	+
Zebrafish (D. rerio)	+	+	+	+	+
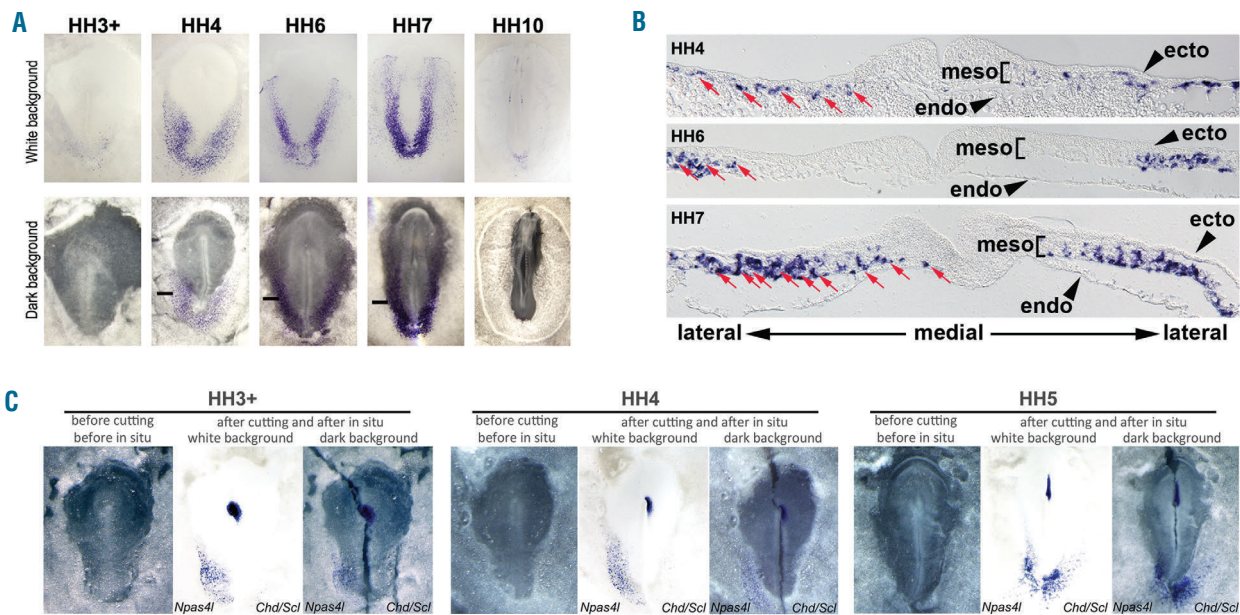
Figure 2. Chicken *NPAS4L* gene expression during hemangioblast specification. (A) Whole-mount *in situ* hybridization (WISH) of *NPAS4L* from HH3 to HH10. Fertilized hen's eggs were purchased from Takamoriryo in Aso (Kumamoto, Japan). (Top) White background for expression visualization; (bottom) dark background for stage visualization. Black lines indicate section levels shown in (B). (B) Section of embryos in (A). *NPAS4L*-expressing cells indicated by red arrows. Germ layers marked by black arrowheads (ectoderm and endoderm) and brackets (mesoderm). (C) Chicken *NPAS4L* is expressed starting from HH3⁺, earlier than *SCL/TAL1*. Embryos were fixed and processed to the pre-hybridization step (left panels) and were cut into left (stained for NPAS4L) and right (stained for *SCL/TAL1* and *Chordin* together) halves. Stained half embryos were then photographed together (middle panels: white background showing both halves; right panels: dark background showing both halves). *Chordin* expression was used to mark precise embryo stages. At HH3⁺ (top row) and HH4 (middle row), NPAS4L is expressed and SCL/TAL1 is not expressed. At HH5 (bottom row), both *NPAS4L* and *SCL/TAL1* are expressed.

Hemangioblast specification from their mesoderm precursors was reported to involve divergent transcriptional regulation, with *ETV2* in mammals[3,20] and *NPAS4L* in zebrafish[4] as the main driver. *ETV2* ortholog is present in the zebrafish genome, but its function was reported to be under the control of *NPAS4L*.[4,6] No *NPAS4L* ortholog has been identified in any mammalian species, suggesting that this gene is not involved in hemangioblast specification in mammals. Mammalian *NPAS4*, a homolog of *NPAS4L*, was able to rescue fish *cloche* (*npas4l*) mutant phenotypes.[4] Duplication of the *NPAS4* and *NPAS4L* genes, however, took place before the divergence of Actinopterygians (ray-finned fish, including the teleosts) and Sarcopterygians (lobe-finned fish, including the tetrapods) and *NPAS4* has not been associated so far with any aspect of vertebrate hematopoietic development, suggesting that these two genes have different biological functions involving separate molecular regulatory networks.

Since the mammals and birds are closely related both phylogenetically (Figure 1A) and ontogenetically (Figure 1B), we investigated whether avian *NPAS4* and *ETV2* genes are involved in early hematopoietic and vascular development. Molecular phylogenetic analysis indicated that an *NPAS4L* ortholog was present in the chicken (*G. gallus*) genome (in both galGal5 and galGal6 assemblies) (Figure 1C). Although this gene is annotated as *NPAS4* in the current assembly, syntenic analysis (Figure 1C) clearly indicated that it was the ortholog of *NPAS4L* in fish and other vertebrate groups (viewable through search term "npas4" in the NCBI genome data browser *https://www.ncbi.nlm.nih.gov/genome/gdv/?org=gallus-gallus* or the chicken FANTOM dataset browser *http://fantom.gsc.riken.jp/zenbu/gLyphs/#config=b1zZI1gUF Z6mHX6-4Gvxr*). Phylogenetic analyses also showed that the *NPAS4L* gene is present in all other bird species with

their genomes fully or partially assembled and in non-avian reptiles with their genomes assembled (*Anolis* lizard shown as an example in Figure 1C). In contrast, the *ETV2* ortholog is missing in the entire avian lineage, and also in crocodiles and turtles, suggesting a loss of this gene before avian evolution. The *ETV2* ortholog, however, was found in some of the reptilian lineages (e.g., lizards and snakes) (Figure 1C and D). Taken together, our phylogenetic analyses suggest that birds have the *NPAS4L*, but not the *ETV2*, gene in their genomes.

We next asked whether *NPAS4L* plays a role in early hemangioblast specification in chick as was shown in zebrafish. For this purpose, we generated an RNA whole-mount *in situ* hybridization (WISH) probe for chicken *NPAS4L* and performed WISH using embryos from stage HH3 (early gastrulation) to stage HH12 (onset of circulation). Expression of chicken *NPAS4L* was detected in territories marking nascent hemangioblasts in ventral mesoderm (Figure 2A) from stage HH3⁺, the earliest among all hemangioblast-specific genes (e.g., *SCL/TAL1* and *LMO2* expression starts from stage HH4⁺). This observation was confirmed by WISH using left-right bisected embryos, with the left half stained for *NPAS4L* and the right half stained for *SCL/TAL1* and *Chordin* (Figure 2C). Paraffin-sectioning of stained embryos (Figure 2B) showed that *NPAS4L*-positive cells are located in a subset of the mesoderm germ layer that will give rise to blood and endothelial cell lineages (red arrows; germ layers marked by arrowheads and brackets), as we had previously reported.[10,21] *NPAS4L* expression levels peaked at HH7 and declined soon afterwards (Figure 2A), suggesting that this gene is specifically and transiently involved in hemangioblast formation, but not in their differentiation.

We have previously generated the chicken promoterome database, spanning the entire 21-day period of embryonic development.[22] When we searched this data-

B

Chicken NPAS4L gene promoter (-500bp to +8bp)

TSS: underlined; red: sgRNA; blue: PAM

AGGGCTTCTCCAAGGAGAATAACA**AGCTTGGGGACACCGAGCAGA**_AGG_CCG
GAGAGGCTCAGTGCCCCATGCCAGCTCCCTGTTGGAGAGGAAACATTTGG
TGGGGAGAAGAAAGGGCCTTGCTGGGGAGGGGGGGGAGTTTTTGGCACCC
TCTCCAAGGGGCCCTGCACACACTGCAGGCTTCCCT**CCCATGGTAGGAAC**
TAGTGC_TGG_GCTGCTAGCTGTGGGCCAGGAGCCGGATGGACACATGCCTT
CCAGTGGGATCCCTGCTCCCTTCATCATCACCCCCTCCTGAGCCACCGAG
TTTGCTTTAAAGACCCCAGCTTTCCTTTTATTGCTTCCCCTCTCAGATTGC
AGCCGGCTGTGAGGGCTATTTTTAGCAGCCTGCTTTCTAAAAATAGCCCC
AAGATGTTTGGAGTTGCGTC_AGG_AGGGGTAC**CTCTCCTCCGCGCACCGAC**
T_TGG_CCCCTGCACCCCAGGAGGCTACAAAAGGAGGCCAGGAGCAGCGGGG
TCAGCAGG→

C

D

E

F

Figure 3. NPAS4L is involved in chicken hemangioblast specification. (A) Screenshot of *NPAS4L* locus in chicken promoterome database (see text for web link). *NPAS4L* transcription start site (TSS) is indicated by red label and black arrow. TSS activity levels at different developmental stages are shown at the bottom. The highest expression is seen at HH7. (B) Design of sgRNA for chicken *NPAS4L* CRISPRa. Mapped TSS is TCAGCAGG (underlined). Preceding 500 bp of promoter region is shown, with sgRNA sequences highlighted in red and PAM sequences in blue. (C) Schematic diagram of how embryos are electroporated and cultured. (D) *NPAS4L* CRISPRa constructs activate endogenous *NPAS4L* expression ectopically (oval). (Top) *NPAS4L* expression only; (bottom) *NPAS4L* expression together with anti-GFP staining marking the electroporated territories (brown). (E) *NPAS4L* CRISPRa constructs activate endogenous *LMO2* (left) and *SCL/TAL1* (middle) ectopically (oval). Zebrafish *NPAS4L* is also capable of activating hemangioblast markers (SCL/TAL1 shown in right panel, oval). (F) Hypothetic scenario of hemangioblast specification in the ancestral amniote and ancestral reptile. It is proposed that the zebrafish scenario (both *NPAS4L* and *ETV2* genes are present, with *NPAS4L* functioning upstream of *ETV2*) is the default one. Mammals have lost *NPAS4L* and birds have lost *ETV2*.

base (*http://fantom.gsc.riken.jp/zenbu/*), *NPAS4L* was shown (Figure 3A) to be only expressed in a narrow time window with its peak expression at HH7, consistent with the WISH data. To evaluate its molecular function, we used CRISPRa (CRISPR-mediated gene activation; also known as CRISPR-on)[23] to ectopically express this gene. CRISPRa utilizes a modified Cas9 protein (with dead nuclease activity and fused with ten copies of VP16 transactivation domain) to recruit transcriptional machinery to targeted promoters mediated by single guide RNA (sgRNA). We had previously confirmed the effectiveness of CRISPRa system in the avian model by taking advantage of the single-nucleotide level resolution in transcrip-

tion start site (TSS) mapping.[22] Four sgRNA sequences located within the 500-base pair region preceding the *NPAS4L* TSS were selected (Figure 3) (for interactive view of *NPAS4L* TSS, use the link *http://fantom.gsc.riken.jp/zenbu/gLyphs/#config=b1zZI1gUFZ6mHX6-4Gvxr;loc=galGal5::chr3:4300587..4304021+*) and cloned into expression construct pAC154-dual-dCas9VP160-sgExpression (Addgene #48240). Mesoderm precursors in the streak in HH2/3 embryos were targeted for electroporation (see Weng and Sheng[19] for electroporation protocol) with these four sgRNA expression constructs together with marker GFP expression construct (Figure 3C), and

electroporated embryos were assessed for ectopic expression of endogenous *NPAS4L* and of two hemangioblast markers *SCL/TAL1* and *LMO2*. *NPAS4L* CRISPRa constructs were able to ectopically activate endogenous *NPAS4L* (Figure 3D, oval areas) (11 of 12; 92%) in regions that are normally *NPAS4L*-negative (Figure 2A), as well as hemangioblast markers *SCL/TAL1* (9 of 25; 36%) and *LMO2* (6 of 21; 29%) (Figure 3E, oval areas in left two panels), albeit with reduced efficiency. Interestingly, similar inductive effect (5 of 13 for *LMO2* and 4 of 9 for *SCL/TAL1*) was observed when we used zebrafish *NPAS4L* expression construct[4] (cloned into the pCAGGS expression vector) (Figure 3E, oval area in right panel), supporting partial molecular conservation between the zebrafish and chicken *NPAS4L* genes.

In conclusion, we present evidence that during early chicken development, *NPAS4L*, instead of *ETV2*, is involved in hemangioblast formation. Data from our molecular phylogenetic analyses support the hypothesis that both the *NPAS4L* and *ETV2* genes were present in the common reptilian ancestor and likely also in the common amniote ancestor (Figure 3F). A conclusive confirmation of their epistatic relationship, however, requires additional evidence from gain-of-function of *ETV2* (e.g., using a reptilian *ETV2* ortholog) and loss-of-function of *NPAS4L* (e.g., through CRISPR-mediated transcription inhibition) studies. In birds and other reptilian lineages which lack the *ETV2* ortholog in their genome, it is possible that other ETS family genes have been co-opted to play hemangioblast-specific roles of *ETV2*. Because ETV2 and NPAS4L are transcription factors with different DNA binding specificities and co-factor requirements, it remains to be shown how *ETV2* took over molecular functions of *NPAS4L* during early mammalian evolution.

Wei Weng, Hiroki Nagai, Sofiane Hamidi and Guojun Sheng

International Research Center for Medical Sciences (IRCMS), Kumamoto University, Kumamoto, Japan

Correspondence:
GUOJUN SHENG -sheng@kumamoto-u.ac.jp

doi:10.3324/haematol.2019.239434

References

1. Porcher C, Chagraoui H, Kristiansen MS. SCL/TAL1: a multifaceted regulator from blood development to disease. Blood. 2017; 129(15):2051-2060.
2. Morishima T, Krahl AC, Nasri M, et al. LMO2 activation by deacetylation is indispensable for hematopoiesis and T-ALL leukemogenesis. Blood. 2019;134(14):1159-1175.
3. Kataoka H, Hayashi M, Nakagawa R, et al. Etv2/ER71 induces vascular mesoderm from Flk1+PDGFRalpha+ primitive mesoderm. Blood. 2011;118(26):6975-6986.
4. Reischauer S, Stone OA, Villasenor A, et al. Cloche is a bHLH-PAS transcription factor that drives haemato-vascular specification. Nature. 2016;535(7611):294-298.
5. Liao EC, Paw BH, Oates AC, Pratt SJ, Postlethwait JH, Zon LI. SCL/Tal-1 transcription factor acts downstream of cloche to specify hematopoietic and vascular progenitors in zebrafish. Genes Dev. 1998;12(5):621-626.
6. Marass M, Beisaw A, Gerri C, et al. Genome-wide strategies reveal target genes of Npas4l associated with vascular development in zebrafish. Development. 2019;146(11).
7. Nagai H, Shin M, Weng W, et al. Early hematopoietic and vascular development in the chick. Int J Dev Biol. 2018;62(1-2-3):137-144.
8. Zon LI. Developmental biology of hematopoiesis. Blood. 1995; 86(8):2876-2891.
9. Shivdasani RA, Orkin SH. The transcriptional control of hematopoiesis. Blood. 1996;87(10):4025-4039.
10. Nakazawa F, Nagai H, Shin M, Sheng G. Negative regulation of primitive hematopoiesis by the FGF signaling pathway. Blood. 2006; 108(10):3335-3343.
11. Shin M, Nagai H, Sheng G. Notch mediates Wnt and BMP signals in the early separation of smooth muscle progenitors and blood/endothelial common progenitors. Development. 2009; 136(4):595-603.
12. Minko K, Bollerot K, Drevon C, Hallais MF, Jaffredo T. From mesoderm to blood islands: patterns of key molecules during yolk sac erythropoiesis. Gene Expr Patterns. 2003;3(3):261-272.
13. Davidson AJ, Zon LI. The 'definitive' (and 'primitive') guide to zebrafish hematopoiesis. Oncogene. 2004;23(43):7233-7246.
14. Walmsley M, Cleaver D, Patient R. Fibroblast growth factor controls the timing of Scl, Lmo2, and Runx1 expression during embryonic blood development. Blood. 2008;111(3):1157-1166.
15. Orkin SH, Zon LI. Hematopoiesis: an evolving paradigm for stem cell biology. Cell. 2008;132(4):631-644.
16. Manaia A, Lemarchandel V, Klaine M, et al. Lmo2 and GATA-3 associated expression in intraembryonic hemogenic sites. Development. 2000;127(3):643-653.
17. Drake CJ, Fleming PA. Vasculogenesis in the day 6.5 to 9.5 mouse embryo. Blood. 2000;95(5):1671-1679.
18. Hamburger V, Hamilton HL. A series of normal stages in the development of the chick embryo. J Morphol. 1951;88(1):49-92.
19. Weng W, Sheng G. Five transcription factors and FGF pathway inhibition efficiently induce erythroid differentiation in the epiblast. Stem Cell Reports. 2014;2(3):262-270.
20. Liu F, Li D, Yu YY, et al. Induction of hematopoietic and endothelial cell program orchestrated by ETS transcription factor ER71/ETV2. EMBO Rep. 2015;16(5):654-669.
21. Weng W, Sukowati EW, Sheng G. On hemangioblasts in chicken. PLoS One. 2007;2(11):e1228.
22. Lizio M, Deviatiiarov R, Nagai H, et al. Systematic analysis of transcription start sites in avian development. PLoS Biol. 2017;15(9):e2002887.
23. Cheng AW, Wang H, Yang H, et al. Multiplexed activation of endogenous genes by CRISPR-on, an RNA-guided transcriptional activator system. Cell Res. 2013;23(10):1163-1171.

Real-time national survey of COVID-19 in hemoglobinopathy and rare inherited anemia patients

Faced with the rapidly evolving COVID-19 pandemic, in March 2020 the UK Government advocated strict self-isolation ('shielding') to protect extremely vulnerable patient groups deemed at high risk of severe SARS-CoV-2 infection.[1] These included children and adults with sickle cell anemia (HbSS). On the advice of the National Hemoglobinopathy Panel (NHP), a multidisciplinary expert advisory group, shielding guidance was extended to all sickle cell disease (SCD) sub-types. Patients with transfusion dependent (TDT) and non-transfusion dependent thalassemia (NTDT), Diamond-Blackfan anemia (DBA) and other rare inherited anemias were also advised to shield if considered at high risk based on agreed clinical criteria. These included severe iron overload, splenectomy, diabetes and cardiac disease.[2] Data provided by two participating centers with the largest thalassemia cohorts indicate up to 30% of patients meet these criteria.

In order to evaluate the impact of these measures and inform guidance on the clinical management of COVID-19 and public health policy, a real-time survey of confirmed and suspected cases of COVID-19 in hemoglobinopathy and rare inherited anemia patients was initiated on behalf of the NHP and National Health Service (NHS) England Clinical Reference Group for Hemoglobinopathies.

Data were submitted weekly by the 14 Hemoglobinopathy Coordinating Centers (HCC) in England, providing national coverage. HCC were encouraged to follow World Health Organization (WHO) case definitions which include both confirmed and clinically suspected COVID-19.[3] Anonymised data were collected using a standardised report template (see the *Online Supplementary Data*) and presented weekly to the NHP. Between April 8 and May 6, 2020, a total of 195 confirmed or suspected COVID-19 cases (male: 87; female: 108) were reported. The timeline of case accrual is shown in Figure 1A. The median age was 33 years (range: 6 weeks to 92 years). The distribution according to age and sex is shown in Figure 1B. PCR for SARS-CoV-2 RNA was positive in 99 of 157 (63%) cases tested (Figure 2A). Laboratory confirmation was not available for 34 (17.4%) cases, 31 of which were managed in the community for suspected COVID-19 before widespread testing became available.

SCD accounted for 166 (85.1%) of cases reported, with 129 (77.7%) severe (HbSS or HbSβ⁰-thalassemia) and 37 (22.3%) mild (HbSC, HbSβ⁺-thalassemia or HbSE) genotypes (Figures 2A-B). There were 149 adults and 17 children (defined as ≤18 years). Ninety-five (57%) were female. One hundred and twenty-eight (77.1%) SCD patients were admitted to hospital of whom 15 (11.7%), all adults, required non-invasive and/or mechanical ventilation (Figure 2B). The proportion of patients who required critical care was higher in mild genotypes, 8 of 29 (27.6%), than severe genotypes, 7 of 99 (7.1%) (Figure 2B). Sixty of 154 (39%) patients for whom data were available received transfusion (red cell exchange 46 [29%]; simple [top-up] transfusion 15 [10%]) during the COVID-19 episode. The proportion of transfused patients was similar for children and adults. Outcome was analyzed for cases with a completed COVID-19 course (n=142), excluding those with a continuing inpatient stay or missing data. Of patients with a completed course, 131 (92.2%) have recovered and 11 (8.4%) died. The median age of patients who died was higher (51 years, range: 19-68 years) than those who

Table 1. Association of patient variables with survival status in sickle cell disease patients with laboratory confirmed COVID-19 admitted to hospital and outcome according to RT-PCR status

	Alive	Dead	P
Patient sex			
Female	44 (92%)	4 (8%)	0.94
Male	25 (86%)	4 (14%)	
Patient age (years)			
<10	1 (100%)	0 (0%)	
10-19.9	8 (89%)	1 (11%)	
20-29.9	24 (92%)	2 (8%)	0.14
30-39.9	14 (93%)	1 (7%)	
40-49.9	5 (100%)	0 (0%)	
50-59.9	13 (93%)	1 (0%)	
>59.9	4 (57%)	3 (43%)	
Disease severity			
Mild	19 (86%)	3 (14%)	0.55
Severe	50 (91%)	5 (9%)	
PCR status			
Negative	47 (98%)	1 (2%)	0.081
Positive	69 (90%)	8 (10%)	

recovered (31 years, range: 6 weeks to 72 years, *P*=0.0042). No deaths occurred in children. Among adult patients admitted to hospital mortality was 9.2 % (10 of 109). One patient died outside hospital, in a community residential care facility. In six patients who died, comorbid conditions (stroke: 1, cardiopulmonary disease: 2; cancer: 1; chronic kidney disease (stage G5): 1; hypertension: 1) associated with increased risk of death in COVID-19 were present. Seven of 10 patients who required mechanical ventilation died. As of May 6, 2020, 19 patients were receiving inpatient treatment, including non-invasive ventilation in one case. Data were missing for five patients managed outside hospital.

The association of patient variables with survival status was analyzed in SCD patients (n=77) with a laboratory confirmed COVID-19 diagnosis who were admitted to hospital (Table 1). The overall mortality in the group was 10.4%. In contrast to the association of older age and male sex with risk of COVID-19 related death in other populations, no significant correlation was found with age, sex or SCD genotype. Mortality was higher in females and mild genotypes though the differences did not reach significance.

As of May 6, 2020, 206,715 cases of COVID-19 with 30,615 (14.8%) deaths had been reported in the UK. At first sight this suggests SCD patients are not more vulnerable to COVID-19. The age demographic profile of COVID-19 however differs markedly in the SCD and general population. In the ISARIC study[4] of 20,133 cases of confirmed COVID-19 admitted to hospitals in the UK between February 6 and April 19, 2020, the median age was 73 years compared with a median age of 31 years in our cohort. We therefore compared the age adjusted risk of COVID-19 related death in SCD with that of the general population combining contemporaneous data from our survey, the National Hemoglobinopathy Registry (NHR)[5] and OpenSAFELY study.[6] The latter (data cut May 6) quantified risk factors for COVID-19 related death in England by linking primary care electronic health records of 17 million patients with data from the COVID-19 National

A

B
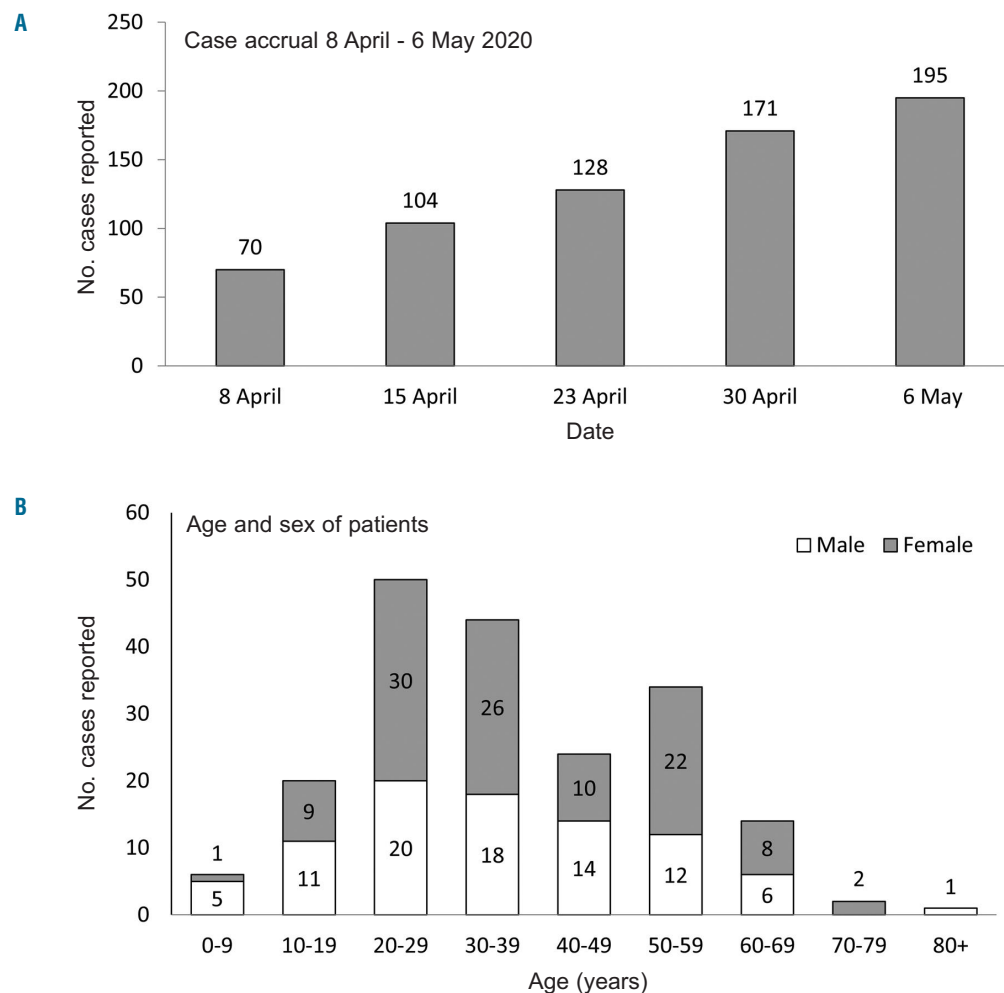
Figure 1. Number of confirmed and suspected COVID-19 cases reported over a 4-week period from April 8 to May 6, 2020 (A) subdivided according to age and sex (B).

Patient Reporting System. In this large cohort the COVID-19 related mortality rate in patients aged 18-49 years and 50-79 years was 194 of 8,764,368 (22.1 per million people) and 4,258 of 7,382,344 (576 per million people) respectively. Based on the number of patients registered on the NHR in the same age groups, equivalent figures for SCD are 4 of 5,242 (763 per million people) and 5 of 1,682 (2,972 per million people) respectively. Cases without a laboratory confirmed COVID-19 diagnosis were excluded from the analysis. Comparison of the proportions of deaths in SCD and the general population indicates that SCD patients in the age groups 18-49 years and 50-79 years have an increased risk of COVID-19 related death, odds ratio (OR) 34.5 (range: 12.8-92.8, $P<0.0001$) and OR 4.1 (range: 1.5-11.0, $P=0.0047$) respectively.

Patient characteristics and outcomes for thalassemia (n=26) are shown in Figure 2A and C. During the COVID-19 episode 8 (31%) thalassemia patients received transfusion. Two deaths were reported, in patients with hemoglobin H disease and TDT aged 92 and 53 years. Both had concurrent morbidities in the form of cancer and splenectomy, iron overload and diabetes respectively. Only three patients with rare inherited anemia (unstable hemoglobin Hb Köln: 2, hereditary elliptocytosis: 1) were reported (Figure 2A). All received transfusion for acute hemolysis

during the COVID-19 episode and subsequently recovered. No cases of COVID-19 were reported in DBA.

As part of the survey HCC were encouraged to notify adverse events impacted by, though not necessarily directly attributable to COVID-19. Two deaths were reported in SCD, in which delayed presentation may have contributed to the outcome. In one case there was confirmed gram-negative sepsis and in the other SARS-CoV-2 RNA was detected post-mortem.

Despite guidance to reduce the risk of SARS-CoV-2 infection in extremely vulnerable individuals by strict self-isolation (shielding) at home and government support with food and medicines, a significant number of hemoglobinopathy patients in the UK have developed COVID-19. It is likely that the reasons for this are complex. Identification of extremely vulnerable patients initially relied on national digital health data systems. In a survey conducted by one of the participating centers around 20% of patients reported they had not received the initial shielding guidance issued by the NHS. Socioeconomic factors such as low income and a need to preserve employment, poor housing, and lack of practical support limit the ability of some households to sustain effective shielding measures. Furthermore, nosocomial SARS-CoV-2 infection is a risk for patients who have to maintain contact with

A

Hemoglobinopathy and rare inherited anemia patients
14 HCC across England
8 April – 6 May 2020
N = 195

Phenotype

Sickle cell disease N = 166 (85.1%)	Thalassemia N = 26 (13.3%)	Rare inherited anemia N = 3 (1.5%)

HbSS N=125	HbSC N=30	Other N=11	TDT N=20	NTDT N=6	DBA N=0	Other N=3

COVID-19

Diagnosis

PCR positive N = 99 (50.8%) +	PCR negative N = 58 (29.7%) –	Not tested N = 34 (17.4%) *	Unknown N = 4 (2.1%) ?

Management

Admitted to hospital N = 143 (73.3%) 90+ 49– 2* 2?	Managed in community N = 52 (26.7%) 9+ 9– 31* 3?

Critical care
N = 16 (11.2%)

Non-invasive ventilation N = 7 (43.7%) ▲	Mechanical ventilation N = 4 (25.0%) ▼	Both types of ventilation N = 5 (31.3%) ▲▼

Outcome

Completed COVID-19 course N = 168 (86.2%)	Ongoing inpatient stay N = 21 (10.8%) 14+ 6– 1? ▲	Unknown N = 6 (3.1%)

Deaths N = 13 (7.7%)	Recovered N = 155 (92.3%) 73+ 50– 28* 4? ▲▲▲▲▲ ▼

HbSS N=7 +++++–* ▲▲▼▼▼	HbSC N=3 +++ ▲▼	HbSE N=1 + ▼	HbH N=1 +	TDT N=1 + ▼

B

Genotype/ Phenotype

Sickle cell disease
N = 166 (85.1%)

	Severe (HbSS, HbS/β⁰) N=129 (77.7%)	Mild (HbSC, HbSE, HbS/β⁺) N=37 (22.3%)

COVID-19 Diagnosis

PCR positive	N=60 (46.5%)	N=24 (64.9%)
PCR negative	N=50 (38.8%)	N=7 (18.9%)
Not tested	N=18 (14.0%)	N=5 (13.5%)
Unknown	N=1 (0.8%)	N=1 (2.7%)

Management

Managed in community	N=30 (23.3%)	N=8 (21.6%)
Admitted to hospital	N=99 (76.7%)	N=29 (78.4%)
Critical care	N=7 (7.1%)	N=8 (27.6%)
Non-invasive ventilation	N=3 (3.0%)	N=4 (13.8%)
Mechanical ventilation	N=2 (2.0%)	N=1 (3.4%)
Both types of ventilation	N=2 (2.0%)	N=3 (10.3%)

Outcome

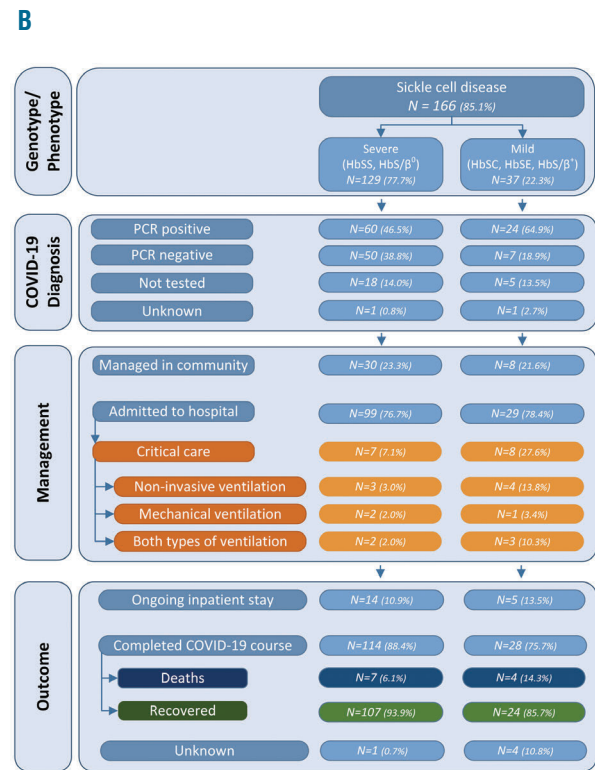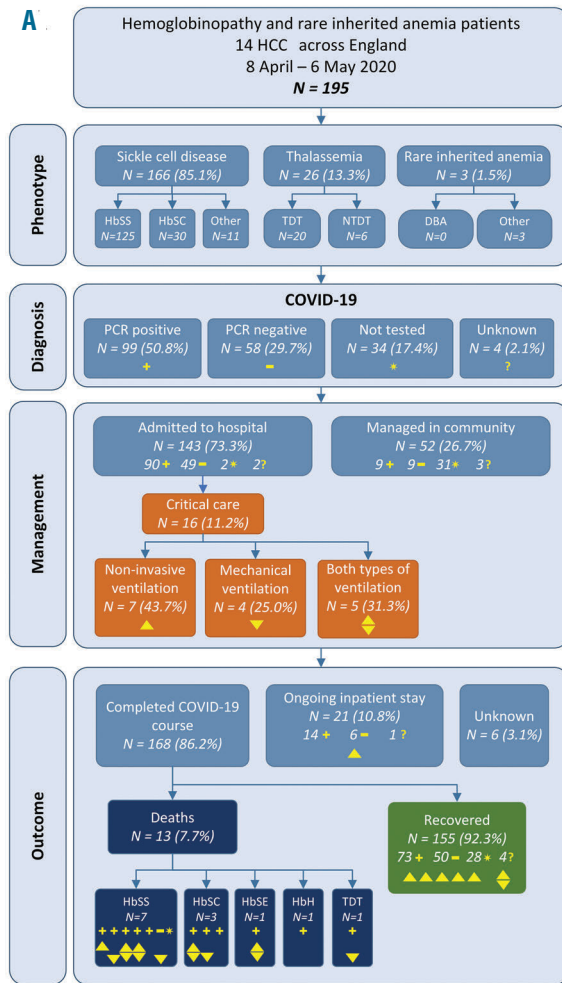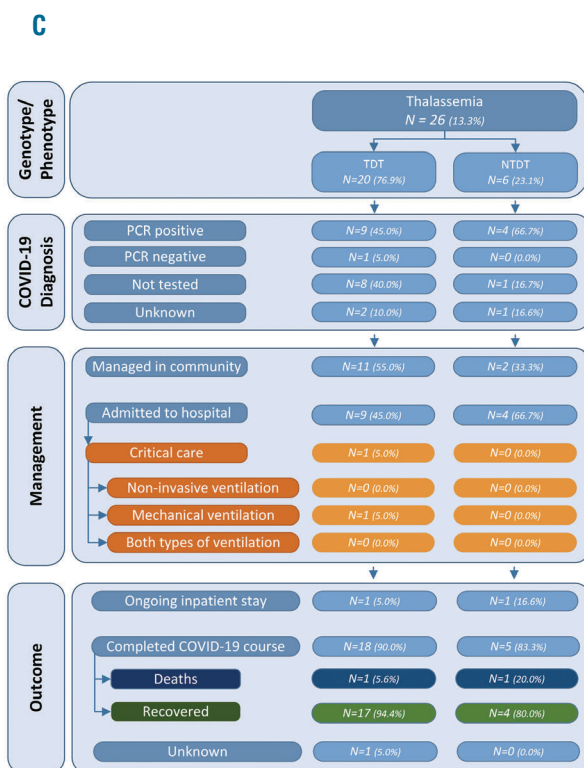| Ongoing inpatient stay	N=14 (10.9%)	N=5 (13.5%)
Completed COVID-19 course	N=114 (88.4%)	N=28 (75.7%)
Deaths	N=7 (6.1%)	N=4 (14.3%)
Recovered	N=107 (93.9%)	N=24 (85.7%)
Unknown	N=1 (0.7%)	N=4 (10.8%)

Figure 2. Schematic of the genotype/phenotype, COVID-19 diagnosis, management and outcome for patients with hemoglobinopathy or rare inherited anemia reported between April 8 and May 6, 2020. Total population (A), sickle cell disease (B) and thalassemia (C). TDT: transfusion dependent thalassemia; NTDT: non-transfusion dependent thalassemia; HbH: hemoglobin H disease. Symbols in yellow denote the PCR status and management of patients as follows: + PCR-positive; – PCR-negative; *: not tested; ?: status of testing unknown; triangle: non-invasive ventilation; inverted triangle: mechanical ventilation. For deaths, each column of symbols corresponds to an individual patient.

C

Genotype/ Phenotype

Thalassemia
N = 26 (13.3%)

	TDT N=20 (76.9%)	NTDT N=6 (23.1%)

COVID-19 Diagnosis

PCR positive	N=9 (45.0%)	N=4 (66.7%)
PCR negative	N=1 (5.0%)	N=0 (0.0%)
Not tested	N=8 (40.0%)	N=1 (16.7%)
Unknown	N=2 (10.0%)	N=1 (16.6%)

Management

Managed in community	N=11 (55.0%)	N=2 (33.3%)
Admitted to hospital	N=9 (45.0%)	N=4 (66.7%)
Critical care	N=1 (5.0%)	N=0 (0.0%)
Non-invasive ventilation	N=0 (0.0%)	N=0 (0.0%)
Mechanical ventilation	N=1 (5.0%)	N=0 (0.0%)
Both types of ventilation	N=0 (0.0%)	N=0 (0.0%)

Outcome

Ongoing inpatient stay	N=1 (5.0%)	N=1 (16.6%)
Completed COVID-19 course	N=18 (90.0%)	N=5 (83.3%)
Deaths	N=1 (5.6%)	N=1 (20.0%)
Recovered	N=17 (94.4%)	N=4 (80.0%)
Unknown	N=1 (5.0%)	N=0 (0.0%)

health care services for essential treatment. Our survey provides insight into the prevalence of COVID-19 in hemoglobinopathy and rare inherited anemia patients. It is estimated that there are 13,655 patients with SCD in England.[7] Based on the age distribution of patients on the NHR, cases reported represent 1.2% of the SCD patient population, comprising 1.8% of adults and 0.3% of children. The equivalent figures for thalassemia (with 1,564 patients on the NHR) are similar; overall 1.6%, adults 2.3% and children 0.4%. Nationally 35-40% of hemoglobinopathy patients fall into the pediatric age group. The low incidence of COVID-19 repor-ted in children with hemoglobinopathies is consistent with its characteristic course, which, with the exception of the hyperinflammatory syndrome described,[8] is generally mild in this age group. This implies shielding may not be necessary for children with sickle cell and thalassemia disorders, other than in defined risk categories such as after hematopoietic stem cell transplantation. This has important implications for schooling and social development.

Two recent reports from France and the USA have described patient characteristics and outcomes of confirmed COVID-19 in SCD.[9,10] In the USA registry hospitalization, intensive care unit (ICU) admission and case fatality rates were broadly similar to those seen in the UK. A higher rate of ICU admission (20.5%) and lower mortality (2.4%) was found among hospitalized patients in France.

Consistent with our findings both studies observed a disproportionate number of COVID-19 rela-ted deaths in mild SCD genotypes. Differing conclusions were drawn with respect to overall morbidity and mortality of COVID-19 in SCD. This highlights the importance of population-based risk estimates which neither study included. In this regard the preliminary results reported here suggest COVID-19 is associated with increased mortality in adults with SCD. Further studies are needed to refine the magnitude of risk and determine the extent to which it reflects an independent effect or association with other clinical, demographic or socioeconomic risk factors. Current evidence suggests patients with sickle-related chronic organ damage may be at increased risk irrespective of age and underpins a ratio-nale for individual risk assessment in shielding guidance. This has important implications for prevention as European countries proceed with a phased easing of lockdown measures in the population.

In thalassemia and rare anemias, only tentative conclusions can be drawn given the small number of cases reported. In the former, outcomes were in keeping with an initial report from Italy, which indicates the course of COVID-19 in thalassemia is generally favorable.[11] Both thalassemia cases associated with a fatal outcome in our survey had independent predictors of mortality.

HCC were instructed to notify both proven and clinically suspected cases of COVID-19, in contrast to the registry studies reported. In the early stages of the pandemic, laboratory capacity in the UK was limited and many patients with clinical features of COVID-19, particularly those with milder disease, were not tested. The limited sensitivity of RT-PCR testing for SARS-CoV-2 infection, with false negative rates up to 30%,[12] was a further consideration in our decision to include clinically suspected cases. In order to avoid ascertainment bias the use of WHO criteria for suspected cases was recommended. Nevertheless, this may have led to an overestimation of cases which, with the availability of testing for antibodies to SARS-CoV-2, it will be possible to evaluate retrospectively. Although all HCC were invited to participate not all returned complete data due to workforce constraints or competing priorities during the pandemic. HCC have been encouraged to retrospectively enter data. This will enable a complete analysis to be reported in due course, allowing estimates of incidence and morbidity to be refined.

Although not its primary purpose, our survey raises concern that an unintended consequence of shielding could be the delayed presentation of life-threatening complications in hemoglobinopathy and rare anemia patients. Observational studies to measure excess deaths in vulnerable patient groups during the COVID-19 pandemic are needed. In order to mitigate this risk the NHP in collaboration with NHS England and patient support groups issued guidance that while shielding patients should continue to access normal pathways for managing complications of their condition and notify their center of care immediately if they develop suspected COVID-19 symptoms to ensure presentations which overlap, inclu-ding bacterial infection and acute chest syndrome, are recognized and treated promptly.[2] Our national survey, undertaken in a real-world setting, expands on case series from single centers[13,14] and complements recently repor-ted registry data from France and the USA in contributing to an understanding of the direct and collateral impact of COVID-19 in SCD and other inherited anemias.

Paul Telfer,[1] Josu de la Fuente,[2,3] Mamta Sohal,[2]
Ralph Brown,[2] Perla Eleftheriou,[4] Noémi Roy,[5,6]
Frédéric B. Piel,[7] Subarna Chakravorty,[8] Kate Gardner,[9]
Mark Velangi,[10] Emma Drasar,[4,11] Farrukh Shah,[4,11]
John B. Porter,[4] Sara Trompeter,[4,12] Wale Atoyebi,[5]
Richard Szydlo,[13] Kofi A. Anie,[14] Kate Ryan,[15] Joseph Sharif,[15]
Josh Wright,[16] Emma Astwood,[17] C. Sarah Nicolle,[18]
Amy Webster,[18] David J. Roberts,[5,6,20] Sanne Lugthart,[21]
Banu Kaya,[1] Moji Awogbade,[8] David C. Rees,[8]
Rob Hollingsworth,[22] Baba Inusa,[9] Jo Howard[9] and
D. Mark Layton[2,3] for the Hemoglobinopathy Coordinating
Centers and National Hemoglobinopathy Panel, England

[1]Barts Health NHS Trust, London; [2]Imperial College Healthcare NHS Trust, London; [3]NIHR Imperial Biomedical Research Centre, London; [4]University College London Hospitals NHS Foundation Trust, London; [5]John Radcliffe Hospital, Oxford; [6]NIHR Biomedical Research Centre, Oxford; [7]School of Public Health, Faculty of Medicine, Imperial College London, London; [8]King's College Hospital NHS Foundation Trust, London; [9]Guy's and St Thomas' NHS Foundation Trust, London; [10]Birmingham Children's Hospital, Birmingham; [11]Whittington Health NHS Trust, London; [12]NHS Blood and Transplant, London; [13]Imperial College, London; [14]London North West University Healthcare NHS Trust, London; [15]Manchester University NHS Foundation Trust, Manchester; [16]Sheffield Teaching Hospital, Sheffield; [17]Sheffield Children's Hospital, Sheffield; [18]University Hospitals Coventry and Warwickshire NHS Trust, Coventry; [19]University Hospitals of Leicester, Leicester; [20]NHS Blood and Transplant, Oxford; [21]University Hospitals Bristol, Bristol, UK and [22]Medical Data Solutions and Services, Manchester, UK

Correspondence:
MARK LAYTON - m.layton@imperial.ac.uk

References

1. https://www.gov.uk/government/publications/guidance-on-shielding-and-protecting-extremely-vulnerable-persons-from-covid-19/guidance-on-shielding-and-protecting-extremely-vulnerable-persons-from-covid-19

2. https://b-s-h.org.uk/media/18244/hbp-hccs-response-to-covid-v9-200420.pdf

3. World Health Organization.(2020). Global surveillance for COVID-19 caused by human infection with COVID-19 virus: interim guidance, 20 March 2020.

4. Docherty AB, Harrison EM, Green CA, et al. Features of 20,133 UK patients in hospital with covid-19 using the ISARIC WHO Clinical Characterisation Protocol: prospective observational cohort study. BMJ. 2020;369:m1985.

5. http://nhr.mdsas.com

6. Williamson EJ, Walker AJ, Bhaskaran K, et al. Factors associated with COVID-19-related death using OpenSAFELY. Nature. 2020;584(7821):430-436.

7. Dormandy E, James J, Inusa B, Rees D. How many people have sickle cell disease in the UK? J Public Health (Oxf). 2018;40(3):e291-e295.

8. Riphagen S, Gomez X, Gonzalez-Martinez C, Wilkinson N, Theocharis P. Hyperinflammatory shock in children during COVID-19 pandemic. Lancet. 2020;395(10237):1607-1608.

9. Arlet JB, de Luna G, Khimoud D, et al. Prognosis of patients with sickle cell disease and COVID-19: a French experience. Lancet Haematol. 2020;7(9):e632-e634.

10. Panepinto JA, Brandow A, Mucalo L, et al. Coronavirus disease among persons with sickle cell disease, United States, March 20–May 21, 2020. Emerg Infect Dis. 2020;26(10).

11. Motta I, Migone De Amicis M, et al. SARS-CoV-2 infection in beta thalassemia: Preliminary data from the Italian experience. Am J Hematol. 2020;95(8):E198-E199.

12. Woloshin S, Patel N, Kesselheim AS. False negative tests for SARS-CoV-2 infection - challenges and implications. N Engl J Med. 2020; 383(6).e38.

13. McCloskey KA, Meenan J, Hall R, Tsitsikas DA. COVID-19 Infection and sickle cell disease: a UK centre experience. Br J Haematol. 2020;190(2):e57-e58.

14. Hussain FA, Njoku FU, Saraf SL, Molokie RE, Gordeuk VR, Han J. COVID-19 infection in patients with sickle cell disease. Br J Haematol. 2020;189(5):851-852.

Exome sequencing reveals heterogeneous clonal dynamics in donor cell myeloid neoplasms after stem cell transplantation

Allogeneic hematopoietic stem cell transplantation (allo-HSCT) is an established treatment option for myeloid neoplasms (MN). In rare cases, the development of *de novo* hematologic malignancies derived from cells of donor origin, named donor cell hematologic neoplasm (DCHN), can occur.[1,2] Although some mechanisms have been suggested, the etiological factors and mechanisms involved in DCHN onset remain elusive. Moreover, DCHN is an extremely unusual allo-HSCT complication. But it provides a useful *in vivo* model to understand the genomic processes driving the leukemic transformation of donor stem cells. This study collects the first large cohort in which whole exome sequencing (WES) was performed in several post-transplant bone marrow (BM) samples from DCHN patients and their donors.

A cohort of seven patients (Table 1 and *Online Supplementary Appendix*) recruited from three hospitals belonging to the Spanish Group of Hematopoietic Transplantation (GETH) and their donors were included. The study included 32 BM samples from different time points after allo-HSCT (*Online Supplementary Figure S1*) as well as one peripheral blood (PB) sample from each donor. The research protocol was approved by the Ethics Committee of Gregorio Marañón General University Hospital. The study WES workflow is summarized in Figure 1 and the *Online Supplementary Methods*.

The results of the analysis of the mutational profiles obtained from the sequential post-HSCT samples demonstrated high intra-tumor genetic heterogeneity and clonal dynamics for all seven donor cell myeloid neoplasm (DCMN) cases (Figure 2). Among the altered genes, 27 variants in 26 strong candidates with oncogenic potential were found. This analysis showed 19 variants in genes associated with RNA processing and metabolism (*LUC7L2, NOP14*), cell differentiation (*LAMA5,*

SKOR2, EML1), signal transduction (*SNX13, IRS1, TENM2*), including notch signaling pathway (*NOTCH4, DTX1*) and ERBB2 signaling pathway (*GRB7*), immunity regulator (*MEFV*), histone deacetylase (*GSE1*), DNA damage response (*PNKP*), post-translational modifications (*SENP7*), transcription factor (*TAF1L, ZKSCAN2, ZNF461*), and apoptotic process (*MEGF10*), as well as eight mutations in seven genes commonly found in adult acute myeloid leukemia (AML) or myelodysplastic syndromes (MDS) (*SETBP1, DNMT3A, TET2, RUNX1, CSF3R, EP300* and *IDH2*). All these mutations were confirmed by a customized targeted gene panel designed ad hoc to validate the variants selected in the WES which also included the most recurrent mutations in MN (*Online Supplementary Appendix*). By this approach, the gene panel analysis also allowed identification of mutations in *CSF3R, NPM1, TP53* and *ASXL1* genes (*Online Supplementary Table S1*).

Analysis of CNV revealed that the most common chromosomal alterations in DCMN were monosomy 7 (-7) or chromosome 7 abnormalities, which were detected in 6 out of 7 patients (Figure 2 and *Online Supplementary Figures S3-S9*).

Regarding the analysis performed on donor samples, copy number variation (CNV) analysis of stem cell apheresis from donor 1 revealed -7. Four years later, the recipient developed a donor cell myelodysplastic syndrome (DC-MDS), which showed -7 together with other molecular (*SETBP1, LUC7L2*) and cytogenetic alterations. This case highlights what has been described by other authors who suggested that *SETBP1* mutations occur at later stages of disease evolution, influencing the clinical course of the disease rather than its initiation; they are associated with a poor prognosis.

The other six donors presented variants in genes that have been involved in hematologic or solid tumors: *KLLN* (c.445T>A), *HOXD4* (c.242A>T), *MSR1* (c.877C>T), *HOXD12* (c.213T>C), *MOS* (c.426_432dupTGGCAAC), *SETBP1* (c.3962G>A), *MAD1L1* (c.851A>G).[3,4,5,6,7] Of note, variants present in

Table 1. Clinical features of donor cell myeloid neoplasm (DCMN) patients.

Patient	Age/Sex	Primary disease	Donor Age/Sex	Status pre-HSCT	Donor type	Stem cell source	Type of DCMN	Cytogenetics of DCMN	Time from allo-HSCT to DCMN (months)	Treatment	Outcome	Donor
1	56/M	MCL	72/M	2ªCR	MR	PB	MDS	45,XY,-7,del(12)(p12)	57	AZA + SCT	*Dead*	BM dysplasia
2	26/F	ALL	64/M	2ªCR	MMR*	BM	MDS	46,XY,del(5q),del(7q)	34	–	*Dead*	Healthy
3	39/M	CML-CP	49/M	NCR	MR	BM	MDS	45,XY,-7	249	AZA + SCT	Alive	Healthy
4	60/M	AML	55/F	1ªCR	MR	PB	AML	45,XX,t(3;16)(q21;q22),-7[16] 90-130,XXXX,t(3;16)(q21;q22), t(3;16)(q21;q22),-7,-7,+2-5 marc[2], 46,XX[2]	19	AZA + SCT	*Dead*	Healthy
5	55/M	MCL	59/M	1ªCR	MR	PB	AML	46,XY,del(7)(q31q36)// 47,XY,+1,der(1;7)(q10;p10)	67	AZA + SCT	*Dead*	Healthy
6	46/F	ALL	0/F	1ªCR	MU	CB	AML	46,XX	24	AZA + SCT	*Dead*	–
7	46/M	ALL	63/F	1ªCR	MMR*	BM	MDS	46,XX,t(10;11)(q24;p15)[13] 45,sl,-13,16,+mar[2] 46,sl,del(7)(q22)[5]	5	Hydroxyurea	*Dead*	Healthy

M: male; F: female; MCL: mantle cell lymphoma; ALL: lymphoblastic leukemia; AML: acute myeloid leukemia; CML-CP: chronic myelogenous leukemia *BCR-ABL1* positive-chronic phase; CR: complete remission; NCR: non-cytogenetic response; MDS: myelodysplastic syndrome; MR: matched related; MU: matched unrelated; MMR: mismatched related; PB: peripheral blood; CB: cord blood; CK: complex karyotype; AZA: azacitidine; HSCT: hematopoietic stem cell transplantation. *1-antigen HLA-mismatched. Patients were transplanted between 1994 to 2015. Donors were healthy at the time of DCMN diagnosis.
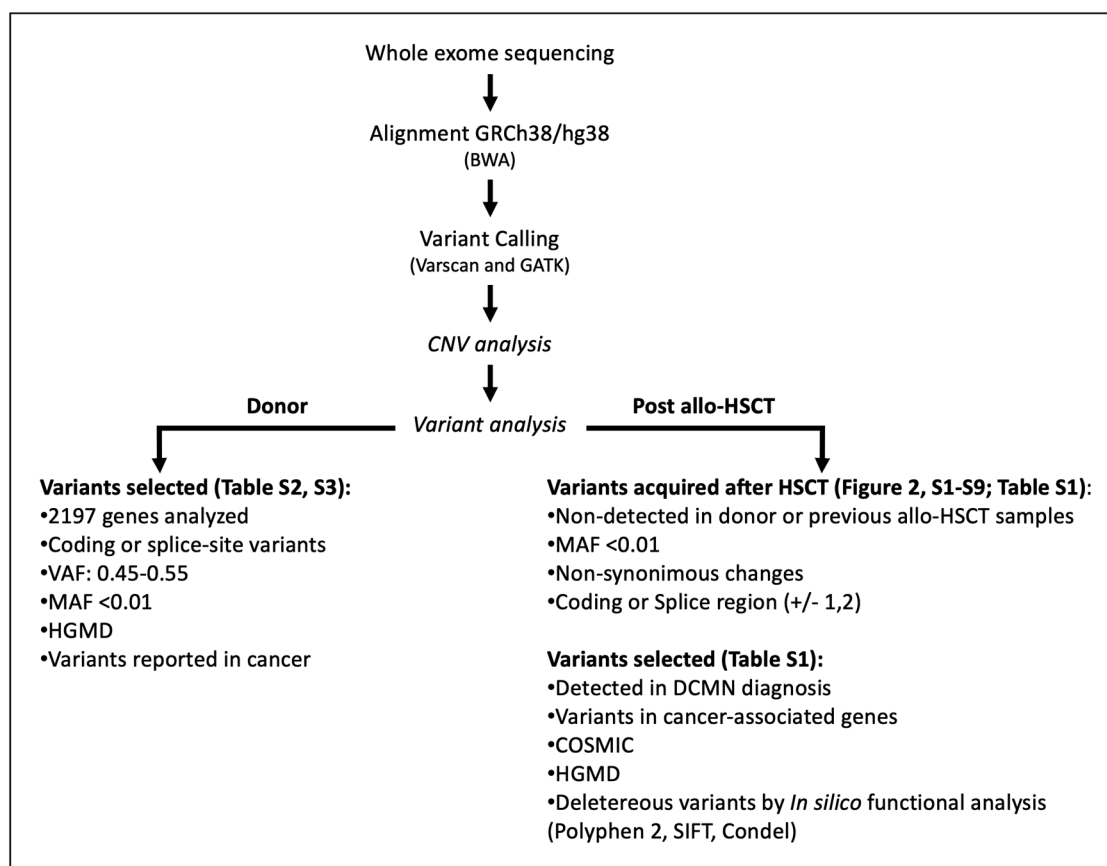
Figure 1. Flowchart of sequencing and filtering methods to identify and prioritize variants. Post-allogeneic hematopoietic stem cell transplantation (allo-HSCT) samples were matched against their donor peripheral blood (PB) and previous post allo-HSCT samples to identify the acquisition of mutations along post allo-HSCT period until donor cell myeloid neoplasm (DCMN) development. Those somatic variants detected in coding region and donor or acceptor splicing zone, missense, nonsense and frameshift variants with minor allele frequency (MAF) <0.01 were further studied. Copy number variation (CNV) analysis was performed in all samples. To perform the donor analysis a cancer-associated gene list was compiling, the list comprised of a total of 2197 genes and variants detected in coding or splice-site, with variant allele frequency (VAF) between 0.45-0.55, MAF <0.01 were further studied. BWA: Burrows-Wheeler Aligner; COSMIC: Catalogue Of Somatic Mutations In Cancer; HGMD: Human Gene Mutation Database). [1]See *Online Supplementary Tables S2* and *S3*. [2]See Figure 2, *Online Supplementary Table S1* and *Online Supplementary Figures S1-S9*.

donor stem cells were also detected in all the corresponding follow-up samples after allo-SCT. Based on the variant allele frequency (VAF), all variants seem to have germline origin except for those in *MOS* (donor 5) and that in *SETBP1* (donor 6), which appear be of somatic origin. Unfortunately, germline samples were not available to confirm this observation.

Interestingly, although acquired or inherited genetic alterations, which might be related to a predisposition to cancer, were observed in all donors, none of them had developed overt neoplasia at the moment of DCMN diagnosis in the recipients.

Considering the results in patients and donors described above, we propose a plausible model of leukemogenesis for each case, with progressive emergence of mutations in donor cells related to the development of AML or MDS after allo-HSCT (Figure 2). In cases 2, 4, 6 and 7, in which the median time to DCMN diagnosis was 21.5 months, the acquisition of mutations and the evolution of the leukemic clone occurs early after allo-HSCT, a period characterized by a marked immunosuppression state in the patients. Moreover, these four patients had received conditioning regimens based on chemotherapy combined with total body irradiation (TBI) and/or timoglobulin, which would also contribute to the development of MN.

The present study shows that MN evolve by an iterative process of genetic diversification derived from clonal selection and expansion that begin before the clinical onset, in accordance with the current multistep pathogenesis model of leukemogenesis.[8] After the initiating mutation, malignant clones evolve and accelerate disease progression through the acquisition of new mutations. Although no clear pattern of clonal mutation acquisition has been observed, initiating mutations appear to affect epigenetic regulators of transcription (*DNMT3A, TET2*) or genes involved in intracellular signal transduction (*SNX13, RHPN2, IRS4, CSF3R*).

Different factors can influence the development of a neoplasm in donor cells. Interestingly, cytogenetic abnormalities involving chromosome 7 were the most frequent in our DCMN cohort (6 of 7 patients). The frequency of -7 is particularly high among therapy or radiation-induced MDS or AML,[9] as well as *TP53* and epigenetic modifying gene somatic mutations,[10] as in 4 out of 7 patients. In the present cohort, 6 of 7 patients received an alkylating agent or antimetabolites within the conditioning regimen. Furthermore, four of them also received ionizing radiation therapy, and the time of leukemogenic transformation in these patients was shorter than in those who only received chemotherapy. Due to the high prevalence of chromosome 7 anomalies in this entity (a characteristic previously observed by others authors[2]), it seems that the residual
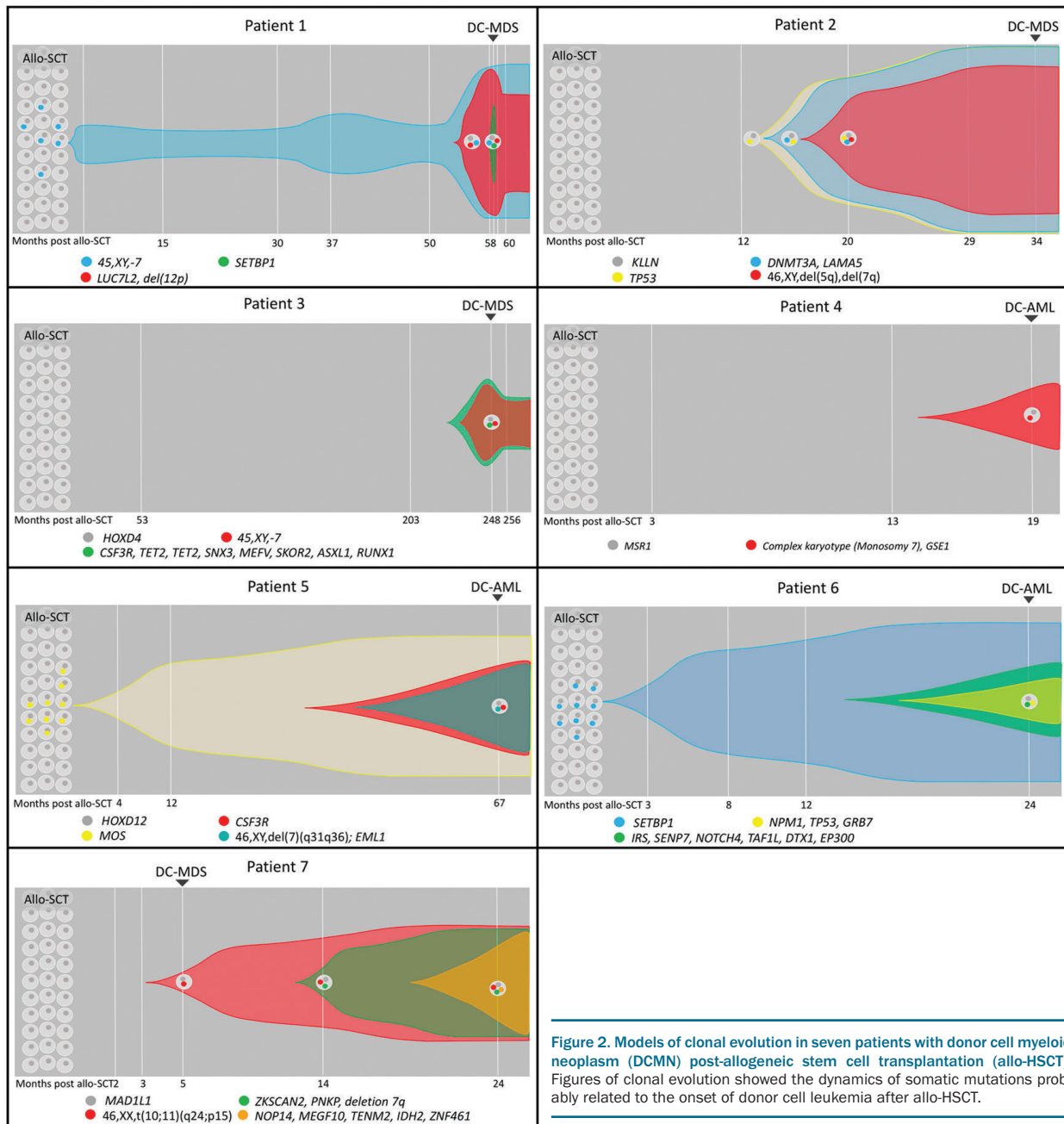
Figure 2. Models of clonal evolution in seven patients with donor cell myeloid neoplasm (DCMN) post-allogeneic stem cell transplantation (allo-HSCT). Figures of clonal evolution showed the dynamics of somatic mutations probably related to the onset of donor cell leukemia after allo-HSCT.

toxicity in the BM of prior chemotherapy and/or TBI plays an important role in pathophysiology of this disease. Of note, none of the donors had received chemotherapeutic or other toxic drugs.

Additionally, the post allo-HSCT period is characterized by a decreased immune surveillance caused by both conditioning regimens and by the immunosuppressive drugs administered to prevent graft-*versus*-host disease. Downregulation or inactivation of the immune system may facilitate malignant clonal progression. Consequently, the appearance or outgrowth of cells with potential to become cancerous is increased in this period.

Noteworthy, all seven donors in the present study had germline or acquired genetic alterations in genes which might be related to tumor development. Although some of the specific variants found in the donors have been described in low frequencies in particular human popula-

tions, all of them have also been previously described in families with a predisposition to cancer. Cancer-related genes usually show incomplete penetrance and variable expressivity, and need additional genomic events to lead to the development of a tumor.[11] In this regard, post-SCT conditions might contribute to the progression of the phenotype. The existence of an acquired premalignant state bearing the initiating lesions has been reported in some donors who have no other signs of disease. Moreover, somatic mutations in genes involved in leukemogenesis were found in 5%, 10% and 20% of 60-, 70-, and 90-year-old individuals, respectively.[12] Likewise, humans with clonal hematopoiesis have an increased risk of developing hematologic neoplasms compared with those without mutations.[13] However, the use of older donors with clonal hematopoiesis of indeterminate potential (CHIP), otherwise revealed as a safe approach, has recently been associ-

ated with an increased risk of developing DCMN.[14] Interestingly, CHIP-associated mutations were not found in any of the donors in our cohort, even though 5 of 7 were over 55 years old. This observation indicates that different mechanisms may be involved in the development of DCMN which would need further investigation.

Genetic predisposing factors are presumed to play an important role in the development of MN. Likewise, 16-21% of cancer survivors who developed t-MN have a germline mutation associated with inherited cancer susceptibility genes.[15] It could be that individuals with germline mutations in these genes are particularly susceptible to cytotoxic chemotherapy and/or radiation.

The growing use of next-generation sequencing (NGS) to study gene panels to define patient prognosis or identify targetable genomic alterations would allow detection of germline variants with clinical significance in tumor samples. Identification of germline mutations in the recipient could rule out the variant in family members. Relatives with the mutation would not be considered as donors and would eventually be referred for genetic counseling.

In most cases reported in the literature, the donor has no evidence of MN development.[2] Indeed, donors with such inherited molecular alterations do not necessarily develop leukemia, and they can live for many years without evidence of the disease, since other genetic or environmental factors, which are usually altered in transplanted patients, might play an important role in the development of malignant disease.

Presumably not just one mechanism from among those mentioned above is responsible for the leukemic transformation in donor cells. But a combination of various conditions would contribute to the development of DCMN after allo-HSCT. Such pre-leukemic stem cells from the donor might increase the likelihood that, later, co-operating mutations arise in cells that already contain the initiating mutations in a context of decreased immune surveillance. The relative contribution of each of the genetic and transplant-related factors to donor-derived leukemia is still not known. Novel approaches based on in-depth NGS to study consecutive samples from the post-transplant period in these patients appear promising to discover new genes involved in the development of MN and to decipher the ultimate mechanisms of leukemogenesis.

*Julia Suárez-González,[1,2] Juan Carlos Triviño,[3]
Guiomar Bautista,[4] José Antonio García-Marco,[4]
Ángela Figuera,[5] Antonio Balas,[6] José Luis Vicario,[6]
Francisco José Ortuño,[7] Raúl Teruel,[7] José María Álamo,[8]
Diego Carbonell,[2,9] Cristina Andrés-Zayas,[1,2]
Nieves Dorado,[2,9] Gabriela Rodríguez-Macías,[9] Mi Kwon,[2,9]
José Luis Díez-Martín,[2,9,10] Carolina Martínez-Laperche[2,9]*
and Ismael Buño[1,2,9,11]* on behalf of the Spanish Group for
Hematopoietic Transplantation (GETH)*

[1]Genomics Unit, Gregorio Marañón General University Hospital,
Gregorio Marañón Health Research Institute (IiSGM), Madrid;
[2]Gregorio Marañón Health Research Institute (IiSGM), Madrid;
[3]Sistemas Genómicos, Valencia; [4]Department of Hematology, Puerta de
Hierro General University Hospital, Madrid; [5]Department of
Hematology, La Princesa University Hospital, Madrid; [6]Department of
Histocompatibility, Madrid Blood Centre, Madrid; [7]Department of
Hematology and Medical Oncology Unit, IMIB-Arrixaca, Morales
Meseguer General University Hospital, Murcia; [8]Centro Inmunológico
de Alicante - CIALAB, Alicante; [9]Department of Hematology, Gregorio
Marañón General University Hospital, Madrid; [10]Department of
Medicine, School of Medicine, Complutense University of Madrid,
Madrid and [11]Department of Cell Biology, School of Medicine,
Complutense University of Madrid, Madrid, Spain

*CM-L and IB contributed equally as co-senior authors.

References

1. Fialkow PJ, Thomas ED, Bryant JI, Neiman PE. Leukaemic transformation of engrafted human marrow cells in vivo. Lancet. 1971; 1(7693):251-255.
2. Suárez-González J, Martínez-Laperche C, Kwon M, et al. Donor cell-derived hematologic neoplasms after hematopoietic stem cell transplantation: a systematic review. Biol Blood Marrow Transplant. 2018;24(7):1505-1513.
3. Nizialek EA, Peterson C, Mester JL, Downes-Kelly E, Eng C. Germline and somatic KLLN alterations in breast cancer dysregulate G2 arrest. Hum Mol Genet. 2013;22(12):2451-2461.
4. van Scherpenzeel Thim V, Remacle S, Picard J, et al. Mutation analysis of the HOX paralogous 4-13 genes in children with acute lymphoid malignancies: identification of a novel germline mutation of HOXD4 leading to a partial loss-of-function. Hum Mutat. 2005; 25(4):384-395.
5. Xu J, Zheng SL, Komiya A, et al. Germline mutations and sequence variants of the macrophage scavenger receptor 1 gene are associated with prostate cancer risk. Nat Genet. 2002;32(2):321-325.
6. Makishima H. Somatic SETBP1 mutations in myeloid neoplasms. Int J Hematol. 2017;105(6):732-742.
7. Tsukasaki K, Miller CW, Greenspun E, et al. Mutations in the mitotic check point gene, MAD1L1, in human cancers. Oncogene. 2001; 20(25):3301-3305.
8. Ding L, Ley TJ, Larson DE, et al. Clonal evolution in relapsed acute myeloid leukaemia revealed by whole-genome sequencing. Nature. 2012;481(7382):506-510.
9. McNerney ME, Godley LA, Le Beau MM. Therapy-related myeloid neoplasms: when genetics and environment collide. Nat Rev Cancer. 2017;17(9):513-527.
10. Nishiyama T, Ishikawa Y, Kawashima N, et al. Mutation analysis of therapy-related myeloid neoplasms. Cancer Genet. 2018;222-223:38-45.
11. Suárez-González J, Martínez-Laperche C, Martínez N, et al. Whole-exome sequencing reveals acquisition of mutations leading to the onset of donor cell leukemia after hematopoietic transplantation: a model of leukemogenesis. Leukemia. 2018;32(8):1822-1826.
12. Jaiswal S, Fontanillas P, Flannick J, et al. Age-related clonal hematopoiesis associated with adverse outcomes. N Engl J Med. 2014;371(26):2488-2498.
13. Genovese G, Kähler AK, Handsaker RE, et al. Clonal hematopoiesis and blood-cancer risk inferred from blood DNA sequence. N Engl J Med. 2014;371(26):2477-2487.
14. Frick M, Chan W, Arends CM, et al. Role of donor clonal hematopoiesis in allogeneic hematopoietic stem-cell transplantation. J Clin Oncol. 2019;37(5):375-385.
15. Churpek JE, Marquez R, Neistadt B, et al. Inherited mutations in cancer susceptibility genes are common among survivors of breast cancer who develop therapy-related leukemia. Cancer. 2016; 122(2):304-311.

Venetoclax as monotherapy and in combination with hypomethylating agents or low dose cytarabine in relapsed and treatment refractory acute myeloid leukemia: a systematic review and meta-analysis

Recent clinical data have shown a synergistic effect of venetoclax in combination with the hypomethylating agents (HMA) azacitidine and decitabine (complete remission [CR]/CR with incomplete cell count recovery [CRi]: 73%, median overall survival [OS] of 17.5 months) as well as low-dose cytarabine (LDAC; CR/CRi: 54%; median OS of 10.1 months) in the frontline setting in older patients with acute myeloid leukemia (AML) and those ineligible for intensive chemotherapy leading to approval of both combinations in the US.[1,2] However, data on relapsed/refractory (R/R)-AML are scarce and

heterogenous. Outcomes of patients with R/R-AML are dismal with a median OS of 3-7 months and there is no approved standard of care.[3] Multiple clinical trials combining either venetoclax alone, venetoclax + HMA or venetoclax + LDAC as the backbone of therapy with other novel agents in R/R-AML are ongoing. As many of these trials are not randomized, it is vital to understand the response rate to venetoclax alone and venetoclax + HMA/LDAC in R/R-AML to use it as a benchmark for comparison.

Therefore, we performed a systematic literature review and meta-analysis to objectively assess overall response rates (ORR), and rates of CR/CRi for R/R-AML patients treated with venetoclax or venetoclax + HMA/LDAC.

MEDLINE *via* PubMed, Ovid EMBASE, the COCHRANE registry of clinical trials (CENTRAL), Scopus and the Web of Science electronic databases were
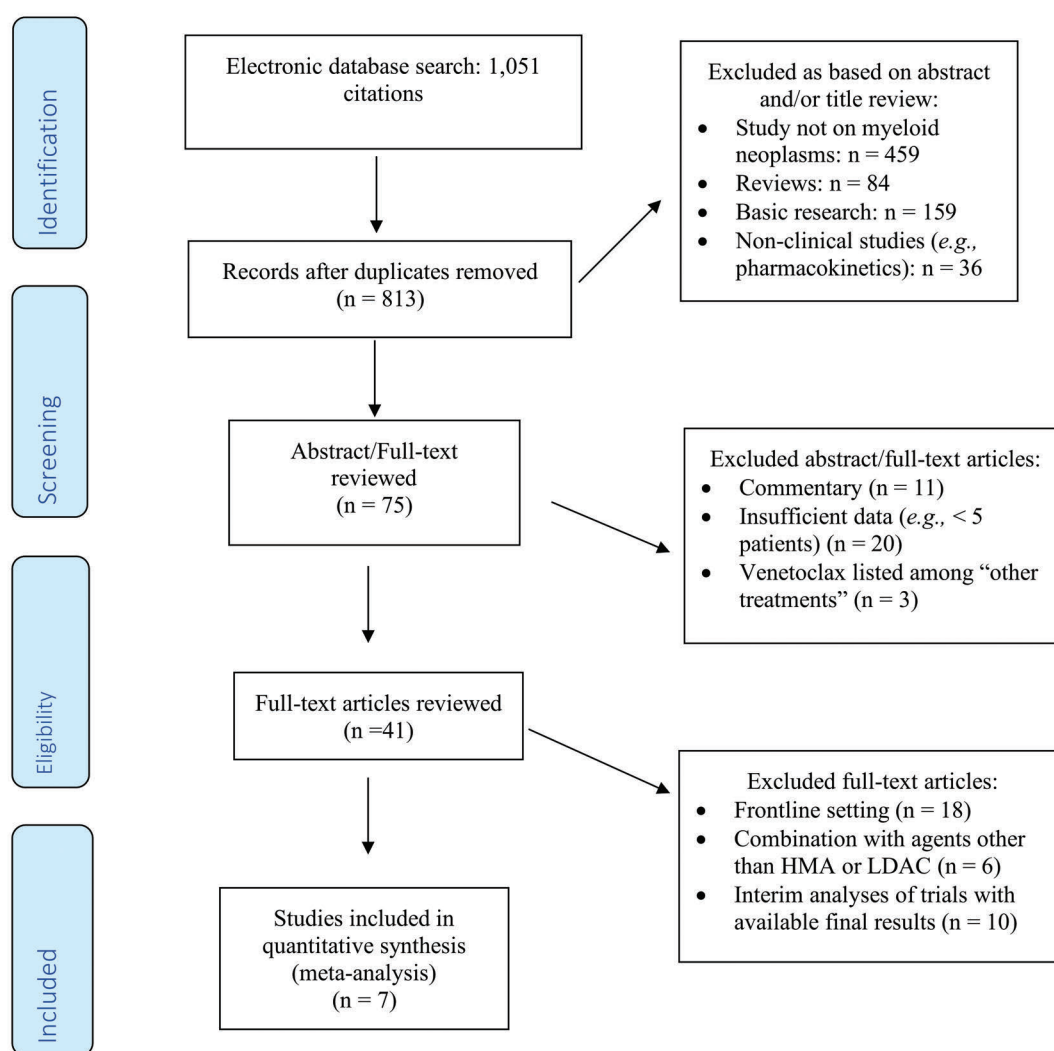
Figure 1. Flow chart showing study selection as per the MOOSE guidelines. Figure 1 illustrates the search strategy and stepwise process of the study selection used in this meta-analysis. MEDLINE *via* Ovid, Ovid EMBASE, Scopus, the COHRANE registry of clinical trials (CENTRAL), and the Web of Science electronic databases were searched with no language restriction from inception through August 2019, using the following combination of free-text terms linked by Boolean operators: "acute myeloid leukemia" OR "AML" OR "myelodysplastic syndrome" OR "MDS" AND "venetoclax". Two authors (MS and JPB) independently screened the titles and abstracts of all retrieved studies for eligibility and removed any duplicate records. In a second step, full texts of the potentially eligible studies were reviewed for the final eligibility. Reviews, basic science articles and articles with an insufficient patient number (<5 patients) were excluded. Furthermore, we excluded studies that i) lacked information on either overall response rate (ORR) or complete resposnse (CR) rate, ii) review articles, editorials, and correspondence letters that did not report independent data, iii) case series and studies reporting outcomes on fewer than five patients, iiii) studies that did were not conducted in acute myeloid leukemia (AML) or myelodysplastic syndromes (MDS) patients.

searched without language restriction from inception through August 2019, using the following combination of free-text terms linked by Boolean operators: "acute myeloid leukemia" OR "AML" OR "myelodysplastic syndrome" OR "MDS" AND "venetoclax". We performed a gray literature search through i) a manual search of bibliographies of all identified studies and ii) conference proceedings and abstracts of relevant annual meetings.

The study selection process is illustrated in Figure 1. The primary outcome was a combined rate of CR/CRi. Secondary outcome was ORR defined as CR + CRi + partial response (PR) + morphologic leukemia-free state (MLFS). Responses were reported by the individual publications using either the 2017 European Leukemia Network (ELN) AML response criteria[4,5] or International Working Group (IWG) criteria for AML.[6-9] Three studies

Table 1. Baseline characteristics of all relapsed/refractory acute myeloid leukemia patients treated with venetoclax among the included studies.

Author (Ref.)	Year	Treatment and treatment schedule	Number patients	Secondary AML (%)	Number prior HMA treatment (%)	ELN risk classification	Outcomes	Adverse effects
Konopoleva et al.[7]	2016	Venetoclax 800 mg/day (dose ramp up from 20 mg/day to target within 6 days; escalation to 1,200 mg/day permitted)	32	17 (54%)	24 (75%)	Not reported	ORR: 19% CR/CRi: 6%/13% Median OS: 4.7 months	All patients with any AE, 26 patients with grade 3/4
Huemer et al.[9]	2019	Venetoclax 800 mg/day (dose ramp up from 20 mg/day to target within 6 days)	7	7 (100%)	7 (100%)	Not reported	ORR: 29% CR/CRi: 29%/0% Median OS: 1.8 months (12.1 months in responders vs. 0.8 months in non-responders)	Not reported
Aldoss et al.[11]	2019	Venetoclax + AZA (9 patients) or DEC (81 patients); no dosing specified	90	22 (24%)	46 (51%)	Favorable: 8% Intermediate: 26% Adverse: 66%	ORR: 46% (AZA+VEN: 33%; DEC + VEN: 47%) CR/CRi: 26%/20% Median OS: 7.8 months (16.6 months in responders vs. 5.1 months in non-responders)	Not reported
DiNardo et al.[6]	2017	Venetoclax + AZA (8 patients), DEC (23 patients), LDAC (8 patients), or other (4 patients)	43	13 (31%)	33 (77%)	Favorable: 5% Intermediate: 49% Adverse: 47%	ORR: 21% (LDAC+VEN: 13%; AZA+VEN: 38%; DEC + VEN: 22%) CR/CRi: 5%/7% Median OS: 3.0 months (4.8 months in responders)	All patients with grade 3/4 AE 72% (infectious)
Ram et al.[10]	2019	Venetoclax 100-400 mg/day + AZA 37.5-75 mg/m² for 5-7 consecutive days or DEC 20 mg/m2 for 5 consecutive days	23	15 (66%)	23 (100%)	Favorable: 9% Intermediate: 48% Adverse: 43%	ORR: 43% CR/CRi: 21.5%/21.5% Median OS: 5.6 months (10.8 months in responders vs. 2.8 months in non-responders)	All patients with AE; no further information provided
Goldberg et al.[5]	2017	Venetoclax 400-800 mg (5-day ramp-up period during cycle 1) + AZA or DEC (8 patients) or LDAC (16 patients)	24	14 (58%)	16 (76%)	Favorable: 10% Intermediate: 28% Adverse: 62%	ORR: 29% (LDAC+ VEN: 23%; AZA+VEN: 50%; DEC + VEN: 0%) CR/CRi: 24% Median OS: not reported	Not reported
Shahswar et al.[12]	2017	Venetoclax 50-600 mg/day + AZA (5 patients) or DEC (1 patients) or LDAC (2 patients)	8	5 (63%)	7 (88%)	Not reported	ORR: 75% CR/CRi: 12.5%/37.5% Median OS: 6.6 months	Not reported

AE: adverse events; AML: acute myeloid leukemia AZA: azacitidine; CR: complete remission; CRi: complete remission with incomplete count recovery; DEC: decitabine; ELN: European Leukemia Network; HMA: hypomethylating agent; LDAC: low-dose cytarabine; ORR: overall response rate; OS: overall survival.

did not report which response criteria had been used.[10-12]

Quality assessments for individual studies using a modified Downs and Black checklist are provided in the *Online Supplementary Table S1*.[13]

Random-effects models were used to pool ORR, CR/CRi and CR rates. All effect sizes underwent logarithmic transformation prior to pooling using an inverse variance weighting approach. Heterogeneity of studies was determined using Cochran Q and I^2 indices and significant heterogeneity ($I^2 > 60\%$) was further explored with sensitivity analyses. Subgroup analyses were planned for venetoclax or venetoclax + HMA/LDAC. All analyses were performed with Comprehensive Meta-Analysis (CMA version 2.2, Biostat).

We identified 813 publications after removal of duplicates. Based on the title and the abstract review studies were excluded if they did not report results from AML or myelodysplastic syndromes (MDS) patients (n=459 studies), were reviews (n=84), basic research articles (n=159), or non-clinical studies (n=36). Of the remaining 75 articles, 34 were excluded because they were commentaries (n=11), had insufficient reporting of data (n=20) or listed venetoclax among "other treatments" (n=3). Articles reporting results of venetoclax in the frontline setting, in combination with agents other than HMA or LDAC, or publications of interim data were also

excluded. Of the seven studies included, five were retrospective studies,[5,6,8,11,12] one prospective cohort study,[10] and one phase I/II clinical trial.[7] Patients were treated with venetoclax monotherapy in two studies[7,8] and with venetoclax in combination with either HMA or LDAC in five studies (Table 1).[5,6,10-12]

There was a total of 224 patients of whom 219 patients had R/R-AML, three MDS patients, and two blastic plasmacytoid dendritic cell neoplasm (BPDCN) patients. The average median age was 68.9 years (range: 59-76). A total of 156 patients (69.6%) had previously received HMA and 48 patients (21.4%) had a prior allogeneic stem cell transplant. The average median duration of follow-up was 7.3 months (range: 1.8-15.8).

Among patients with a reported cytogenetic profile, 13 (7.3%) patients had a favorable, 61 patients (34.5%) had an intermediate and 102 patients (57.6%) had an unfavorable cytogenetic risk profile. Five studies (n=211 patients) reported data on molecular testing which showed rates of *IDH1/2, FLT3, NPM1,* and *TP53* mutations of up to 38%, 28%, 13%, and 23%, respectively (*Online Supplementary Table S2*).[6-8,10,11]

All seven studies reported the ORR (Figure 2A), composite CR/CRi rate (Figure 2B) and CR rate (Figure 2C). For all studies combined, the ORR was 31.1% (95% confidence interval [CI]: 21.8-42.2). The ORR was 20.7%
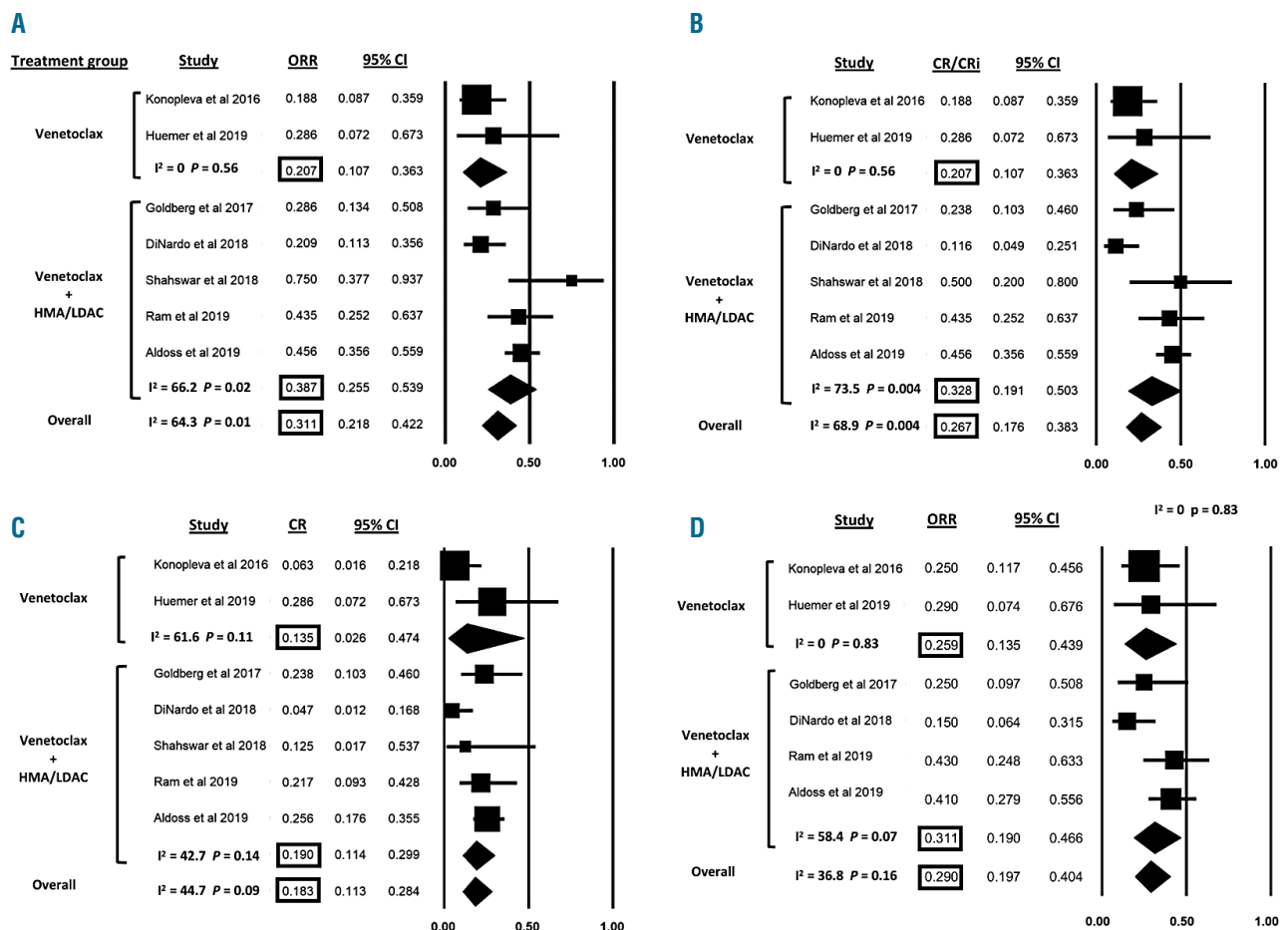
Figure 2. Response to venetoclax in relapsed/refractory acute myeloid leukemia (R/R-AML). Forest plots of odds ratios (squares, proportional to study weights used in meta-analysis, 95% confidence intervals) of response for venetoclax alone and in combination hypomethylating agents (HMA) or low-dose cytarabine (LDAC) with the summary measures (center line of diamond) and associated confidence intervals (lateral tips of diamond). Odds ratios for overall response rate (ORR), combined complete response (CR) and complete response with incomplete count recovery (CRi) rate and CR alone are shown in panel A, B and C respectively. Odds ratio for the ORR for patients, who received prior HMA therapy, is shown in panel D.

(95% CI: 10.7–36.3) for venetoclax monotherapy and 38.7% (95% CI: 25.5–53.9) for venetoclax + HMA/LDAC. There was significant heterogeneity among studies examining venetoclax + HMA/LDAC (Q=11.8; I^2=66.2%; P=0.02).

The CR/CRi rate was 26.7% (95% CI: 17.6–38.3), 20.7% (95% CI: 10.7–36.3) and 32.8% (95% CI: 19.1-50.3) for all studies combined, venetoclax monotherapy and venetoclax + HMA/LDAC, respectively. There was significant heterogeneity among studies examining venetoclax + HMA/LDAC (Q=15.1; I^2=73.5%; P=0.004).

The CR rate was 18.3% (95% CI: 11.3–28.4), 13.5% (95% CI: 2.6–47.4) and 19% (95% CI: 11.4–29.9) for all studies combined, venetoclax monotherapy and venetoclax + HMA/LDAC, respectively. There was significant heterogeneity for studies examining venetoclax alone (Q=2.6, I^2=61.6%, P=0.11).

Median OS reported in individual studies of all patients treated with venetoclax monotherapy and venetoclax + HMA/LDAC ranged between 1.8 to 7.8 months and 3.0 to 6.6 months, respectively. Among responding patients, the median OS in individual studies of all patients treated with venetoclax monotherapy and venetoclax + HMA/LDAC was 12.1 to 16.6 months and 4.8 to 12.1 months, respectively.[6-8,10-12]

In all studies combined, the ORR for patients with prior HMA exposure was 29% (95% CI: 19.7–40.4) (Figure 2D) and 25.9% (95% CI: 13.5–43.9) and 31.1% (95% CI: 19-46.6) for venetoclax monotherapy and venetoclax + HMA/LDAC, respectively. Data on the comparative efficacy of venetoclax + HMA *versus* venetoclax + LDAC were not available.

Separate analyses of response rates to various treatment combinations were available for only 3 of the 5 studies reporting venetoclax + HMA or LDAC.[5,6,11] The ORR ranged from 13-23%, 33-50%, and 0-47% for venetoclax in combination with LDAC, azacitidine, and decitabine, respectively.[5,6,11]

We have previously reported ORR and CR rates for HMA monotherapy in R/R-AML of 30% and 11%, respectively.[14] An ORR of 23% (18% CR) has been reported for LDAC monotherapy in R/R-AML.[15] In our meta-analysis, patients treated with venetoclax + HMA/LDAC demonstrated an ORR of 38.7% and a CR rate of 19% suggesting a greater efficacy of the combination treatment compared to HMA or LDAC monotherapy. Our results also suggest that prior exposure to HMA did not preclude a response to subsequent therapy with venetoclax-based therapies. Acknowledging the limitations of cross-study comparisons, our findings need to be verified in clinical trials directly comparing these treatment strategies.

Sensitivity analyses for ORR, CR/CRi and CR rate showed that exclusion of any one study did not change the overall effect size. The study by DiNardo *et al.* had the largest influence on the heterogeneity of the ORR, CR/CRi and CR rate.[6] Removal of this study increased the ORR by 5.4% (from 38.7% to 44.1%) in the subgroup analysis of studies examining venetoclax + HMA/LDAC and led to a loss of heterogeneity (Q=4.7, I^2= 36.6%, P=0.19).

Data on the mutational profile of patients were reported in five studies and the presence of *TET2-*, *IDH1/2-*, *ASXL1-*, and *RUNX1*-mutations were reported to be associated with higher response rates to treatment with venetoclax-based regimens.[6-8,10,11] However, reporting of predictive biomarkers was inconsistent among the studies.

Our study has several limitations. The significant heterogeneity between studies in terms of the number of patients included in each arm and the reporting of results precluded a comparison of the response rates for the various venetoclax combination strategies in a formal meta-analysis. While response rates seemed higher for the combination of HMA with venetoclax compared to LDAC with venetoclax, our study does not support any formal conclusion and highlights the lack of evidence. Second, there were insufficient data to assess adverse events in our meta-analysis. Third, we were unable to determine whether specific mutations could serve as biomarkers to predict response to venetoclax. Additionally, we could not differentiate between primary refractory, early and late relapses as well as first or advanced relapses and the impact of prior stem cell transplantation receipt or HMA treatment duration. Finally, we were unable to assess the effect of venetoclax-based treatment on OS.

In conclusion, this systematic review and meta-analysis of venetoclax treatment in R/R-AML included seven studies with a total of 224 patients and demonstrated an ORR of 38.7% and 20.7% for patients treated with venetoclax + HMA/LDAC and venetoclax monotherapy, respectively. Prior treatment with HMA did not preclude a response to subsequent venetoclax treatment. Additional studies testing venetoclax combination therapies in R/R-AML are ongoing and urgently needed.

Jan Philipp Bewersdorf,[1] Smith Giri,[2] Rong Wang,[3,4] Robert T. Williams,[5] Martin S. Tallman,[6] Amer M. Zeidan,[1,4] and Maximilian Stahl[6]

[1]*Department of Internal Medicine, Section of Hematology, Yale School of Medicine, New Haven, CT;* [2]*Division of Hematology and Oncology, University of Alabama at Birmingham School of Medicine, Birmingham, AL;* [3]*Cancer Outcomes, Public Policy, and Effectiveness Research (COPPER) Center, Yale University, New Haven, CT;* [4]*Department of Chronic Disease Epidemiology, School of Public Health, Yale University, New Haven, CT;* [5]*Rockefeller University, New York, NY and* [6]*Leukemia Service, Memorial Sloan Kettering Cancer Center, New York, NY, USA*

Correspondence: MAXIMILIAN STAHL - stahlm@mskcc.org

doi:10.3324/haematol.2019.242826

References

1. DiNardo CD, Pratz K, Pullarkat V, et al. Venetoclax combined with decitabine or azacitidine in treatment-naive, elderly patients with acute myeloid leukemia. Blood. 2019;133(1):7-17.

2. Wei AH, Strickland SA, Jr., Hou JZ, et al. Venetoclax combined with low-dose cytarabine for previously untreated patients with acute myeloid leukemia: results from a phase Ib/II study. J Clin Oncol. 2019;37(15):1277-1284.

3. Ganzel C, Sun Z, Cripe LD, et al. Very poor long-term survival in past and more recent studies for relapsed AML patients: The ECOG-ACRIN experience. Am J Hematol. 2018;93(8):1074-1081.

4. Dohner H, Estey E, Grimwade D, et al. Diagnosis and management of AML in adults: 2017 ELN recommendations from an international expert panel. Blood. 2017;129(4):424-447.

5. Goldberg AD, Horvat TZ, Hsu M, et al. Venetoclax combined with either a hypomethylating agent or low-dose cytarabine shows activity in relapsed and refractory myeloid malignancies. Blood. 2017; 130(Supplement 1):1353.

6. DiNardo CD, Rausch CR, Benton C, et al. Clinical experience with the BCL2-inhibitor venetoclax in combination therapy for relapsed and refractory acute myeloid leukemia and related myeloid malignancies. Am J Hematol. 2018;93(3):401-407.

7. Konopleva M, Pollyea DA, Potluri J, et al. Efficacy and biological correlates of response in a phase II Study of venetoclax monotherapy in patients with acute myelogenous leukemia. Cancer Discovery. 2016; 6(10):1106-1117.

8. Huemer F, Melchardt T, Jansko B, et al. Durable remissions with venetoclax monotherapy in secondary AML refractory to hypomethylating agents and high expression of BCL-2 and/or BIM. Eur J Haematol. 2019;102(5):437-441.

9. Cheson BD, Bennett JM, Kopecky KJ, et al. Revised recommendations of the International Working Group for diagnosis, standardization of responseCriteria, treatment outcomes, and reporting standards for therapeutic trials in acute myeloid leukemia. J Clin Oncol. 2003;21(24):4642-4649.

10. Ram R, Amit O, Zuckerman T, et al. Venetoclax in patients with acute myeloid leukemia refractory to hypomethylating agents-a multicenter historical prospective study. Ann Hematol. 2019; 98(8):1927-1932.

11. Aldoss I, Yang D, Pillai R, et al. Association of leukemia genetics with response to venetoclax and hypomethylating agents in relapsed/refractory acute myeloid leukemia. Am J Hematol. 2019; 94(10):E253-E255.

12. Shahswar R, Hamwi I, Lueck C, et al. Registry for the off-label use of venetoclax in patients with relapsed or refractory acute myeloid leukemia. HemaSphere. 2018;2(Supplement 2):794.

13. Downs SH, Black N. The feasibility of creating a checklist for the assessment of the methodological quality both of randomised and non-randomised studies of health care interventions. J Epidemiol Community Health. 1998;52(6):377-384.

14. Stahl M, DeVeaux M, Montesinos P, et al. Hypomethylating agents in relapsed and refractory AML: outcomes and their predictors in a large international patient cohort. Blood Adv. 2018;2(8):923-932.

15. Faderl S, Wetzler M, Rizzieri D, et al. Clofarabine plus cytarabine compared with cytarabine alone in older patients with relapsed or refractory acute myelogenous leukemia: results from the CLASSIC I Trial. J Clin Oncol. 2012;30(20):2492-2499.

Efficacy of anti-PD1 re-treatment in patients with Hodgkin lymphoma who relapsed after anti-PD1 discontinuation

Patients with relapsed/refractory Hodgkin lymphoma (R/R HL) experience high response rates upon anti-PD1 therapy. In these patients, there is limited data about the optimal duration of treatment and the risk of relapse after anti-PD1 discontinuation. We have previously reported the outcome of 11 patients with R/R HL who discontinued anti-PD1 therapy after achieving a complete response (CR) upon nivolumab.[1] These patients experienced a favorable outcome as only two of them had relapsed after a median follow-up of 21.2 months from discontinuation. Despite the low relapse rate observed in that study, physicians may be worried about the possibility to further rescue these heavily pre-treated patients in case of relapse after anti-PD1 discontinuation. Notably, it is still unknown whether these patients will remain sensitive to a second course of anti-PD1.

Here, we investigated the efficacy of anti-PD1 re-treatment in patients that were initially sensitive to anti-PD1 therapy but who relapsed after anti-PD1 discontinuation.

We retrospectively analyzed patients with R/R HL who experienced a partial (PR) or CR upon anti-PD1 monotherapy and discontinued the treatment either because of unacceptable toxicity or due to prolonged remission, based on the physician's decision. Patients who discontinued anti-PD1 therapy because of relapse/progression or underwent consolidation with allogenic stem cell transplantation (alloSCT) were not included. Patients meeting the eligibility criteria were identified through the French lymphoma network (LYSA).

We identified seven patients who met the inclusion criteria. Their characteristics are summarized in Table 1. At anti-PD1 initiation, most patients presented with advanced disease (five of them had Ann Arbor stage III/IV) and had been heavily pre-treated (median number of prior systemic lines =6, seven had received prior brentuximab vedotin, five prior autologous stem cell transplantation (SCT) and two prior allogenic SCT). Overall, anti-PD1 was discontinued after a median duration of 11.4 months (range: 0–26.7) and a median of 23 infusions (range: 1–51). Anti-PD1 was discontinued because of prolonged remission (n=5) or toxicity (n=2, patient 5 had experienced grade 4 acute liver graft-*versus*-host-disease [aGvHD] and patient 7 grade 3 laryngeal tightness). The disease status at anti-PD1 discontinuation was CR for six patients and PR for one patient. The median time to relapse after anti-PD1 discontinuation was 12.1 months (range: 5.3–26.7). All patients were re-treated with the same anti-PD1 antibody as initially administered (six with nivolumab and one with pembrolizumab).

All patients responded to anti-PD1 re-treatment (Figure 1). The best response was CR for four patients and PR for three patients. At the time of analysis (median follow-up of 19.2 months from anti-PD1 re-treatment), 4 of 7 patients have ongoing responses to anti-PD1 monotherapy, three of them beyond 12 months. Interestingly, three patients discontinued anti-PD1 treatment after achieving a second objective response upon anti-PD1 re-treatment (patients 3, 5 and 7). Patient 3 discontinued anti-PD1 treatment a second time due to hyper-eosinophilia and then relapsed 2

Table 1. Patients' characteristics at anti-PD1 initiation.

Patients' characteristics	N=7
Age, median, years (range)	47 (34-71)
Sex, male, number (%)	2 (28.6)
cHL subtype, number (%)	
Nodular sclerosis HL	6 (85.7)
Unclassifiable	1 (14.3)
Performance status (ECOG), No (%)	
0 – 1	5 (71.4)
≥ 2	2 (28.6)
Stage disease, number (%)	
I/II	2 (28.6)
III/IV	5 (71.4)
Prior lines of systemic therapy, median (range)	6 (4-11)
Prior radiation therapy, number (%)	4 (57.1)
Prior treatment with Brentuximab Vedotin, number (%)	7 (100)
Prior autologous HSCT, number (%)	5 (71.4)
Prior allogenic HSCT, number (%)	2 (28.6)
Anti-PD1, number (%)	
Nivolumab	6 (85.7)
Pembrolizumab	1 (14.3)
Number of anti-PD1 infusions during 1st course, median (range)	23 (1-51)
Duration of 1st course of anti-PD1 therapy (months), median (range)	11.4 (0-26.7)
Best Overall Response to 1st course of anti-PD1, number (%)	
CR	6 (85.7)
PR	1 (14.3)
Reason for anti-PD1 discontinuation, number (%)	
Prolonged response	5 (71.4)
Toxicity*	2 (28.6)
Disease status at anti-PD1 discontinuation, number (%)	
CR	6 (85.7)
PR	1 (14.3)
Time between discontinuation and relapse (months), median (range)	12.1 (5.3-26.7)
Follow-up from anti-PD1 re-treatment (months), median (range)	19.2 (4.8-39.9)
Best response to 2nd course of anti-PD1	
CR	4 (57.1)
PR	3 (42.9)

*One grade 4 acute liver graft-*versus*-host-disease, and one grade 3 laryngeal tightness. HL: Hodgkin lymphoma; cHL: chronic Hodgkin lymphoma; CR: complete response; PR: partial response.

months later. Patient 7 tolerated the second course of nivolumab well (notably, there was no recurrence of laryngeal tightness), achieved a PR and discontinued the treatment after 12 months. Unfortunately, he relapsed 5 months later. The patient then received a third course of nivolumab and achieved another PR which is still ongoing at 18 months.

Patient 5 had undergone alloSCT prior to anti-PD1 therapy. He discontinued nivolumab after a single infusion due to grade 4 liver GvHD. Nevertheless, he achieved a CR which lasted 9 months. At relapse, he
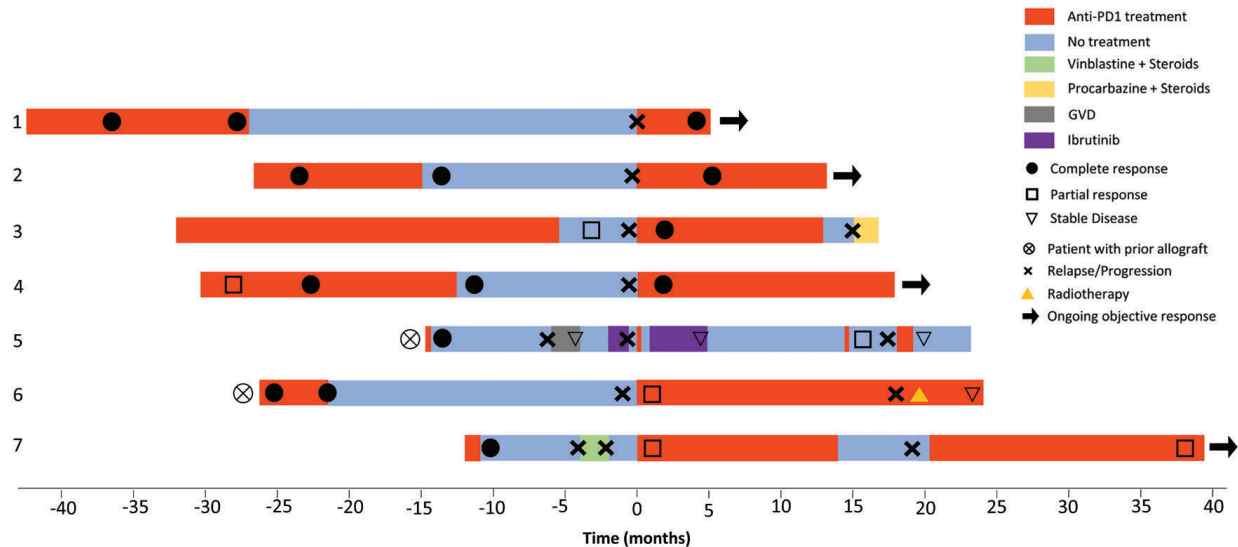
Figure 1. Efficacy of anti-PD1 re-treatment.

received a salvage therapy with GVD (gemcitabine, vinorelbine, and pegylated liposomal doxorubicin) followed by ibrutinib without efficacy. At progression, he received a reduced dose of nivolumab (total dose of 30 mg) which induced a GvHD flare. The patient further experienced two disease progressions which were treated with two additional infusions of low dose nivolumab (10 mg) which resulted again in GvHD flares. These sequential treatments induced transient lymphoma regression, with PR as the best response.

The GvHD flares observed in this patient are not unexpected. Indeed, prior studies have reported that anti-PD1 therapy potentially induces GvHD reactivation in patients that previously underwent alloSCT.[2,3] Anti-PD1 re-treatment did not induce other significant toxicities in the other patients.

There is only limited data regarding the efficacy of re-challenge with anti-PD1 antibodies in cancer patients. Only a few cases have been reported in patients with solid tumors, namely in non-small cell lung cancer[4] and melanoma.[5] However, most of these patients had failed initial anti-PD1 therapy and received chemotherapy prior to anti-PD1 re-treatment. This is in contrast to our study in which all patients were sensitive to initial anti-PD1 therapy and were responsive (CR or PR) at the time of discontinuation.

At the ISHL11 meeting, Ansell et al. reported in an abstract the efficacy of anti-PD1 re-treatment in five patients who achieved remission upon nivolumab but relapsed after treatment discontinuation.[4] All patients responded to nivolumab re-treatment (one CR and four PR).[6] Recently, Chen et al. reported an update of the KEYNOTE-087 study after 2 years of follow-up.[7] This study evaluated pembrolizumab in R/R HL. In a subset analysis, Chen et al. reported the outcome of 10 patients who received a second course of pembrolizumab after anti-PD1 discontinuation. Eight patients were evaluable and six of them (75%) experienced an objective response upon re-treatment with pembrolizumab (four CR and two PR). The study neither reported on the efficacy of the first course of anti-PD1, the reasons for anti-PD1 discontinuation nor the tumor status at anti-PD1

discontinuation in these patients. Nevertheless, the study shows that most patients responded to anti-PD1 re-treatment.

Our study, along with the studies recently published by Ansell et al.[6] and Chen et al.,[7] are the first to report on the efficacy of anti-PD1 re-treatment in anti-PD1 sensitive, R/R HL patients who relapsed/progressed after anti-PD1 discontinuation. These two studies show high response rates (75-100%) after anti-PD1 re-treatment suggesting that these patients usually remain "anti-PD1 sensitive" at relapse. These observations suggest that anti-PD1 is an effective salvage therapy for HL patients who relapse after anti-PD1 discontinuation. Larger studies are warranted to confirm these results.

Guillaume Manson,[1] Pauline Brice,[2] Charles Herbaux,[3] Kamal Bouabdallah,[4] Chloé Antier,[5] Florence Poizeau,[6,7] Laurent Dercle[8-10] and Roch Houot[1]

[1]Department of Hematology, University Hospital of Rennes, Rennes, France; [2]Department of Hematology, Saint-Louis Hospital, AP-HP, Paris, France; [3]Department of Hematology, University Hospital of Lille, Lille, France; [4]Department of Hematology, University Hospital of Bordeaux, Bordeaux, France; [5]Department of Hematology, Nantes University Hospital, Nantes, France; [6]Department of Dermatology, University hospital of Rennes, Rennes, France; [7]EA 7449 REPERES (Pharmacoepidemiology and Health Services Research), Rennes 1 University, Rennes, France; [8]Medical Imaging Department, Institut Gustave Roussy, Villejuif, France; [9]UMR1015, Institut Gustave Roussy, Villejuif, France and [10]Department of Radiology, Columbia University Medical Center, New York, NY, USA

Correspondence:
ROCH HOUOT - roch.houot@chu-rennes.fr

doi:10.3324/haematol.2019.242529

References

1. Manson G, Herbaux C, Brice P, et al. Prolonged remissions after anti-PD-1 discontinuation in patients with Hodgkin lymphoma. Blood. 2018;131(25):2856-2859.
2. Haverkos BM, Abbott D, Hamadani M, et al. PD-1 blockade for relapsed lymphoma post–allogeneic hematopoietic cell transplant: high response rate but frequent GVHD. Blood.

2017;130(2):221-228.

3. Herbaux C, Gauthier J, Brice P, et al. Efficacy and tolerability of nivolumab after allogeneic transplantation for relapsed Hodgkin lymphoma. Blood. 2017;129(18):2471-2478.

4. Fujita K, Uchida N, Kanai O, Okamura M, Nakatani K, Mio T. Retreatment with pembrolizumab in advanced non-small cell lung cancer patients previously treated with nivolumab: emerging reports of 12 cases. Cancer Chemother Pharmacol. 2018;81(6):1105-1109.

5. Nomura M, Otsuka A, Kondo T, et al. Efficacy and safety of retreatment with nivolumab in metastatic melanoma patients previously treated with nivolumab. Cancer Chemother Pharmacol. 2017;80(5):999-1004.

6. Ansell SM, Armand P, Timmerman JM, et al. Nivolumab re-treatment in patients with relapsed/refractory Hodgkin lymphoma. Presented at the 11th International Symposium on Hodgkin Lymphoma. Abstract #0116, 2018 Cologne, Germany.

7. Chen R, Zinzani PL, Lee HJ, et al. Pembrolizumab in relapsed or refractory Hodgkin lymphoma: two-year follow-up of KEYNOTE-087. Blood. 2019;134(14):114-1153.

A 70% cut-off for MYC protein expression in diffuse large B-cell lymphoma identifies a high-risk group of patients

We recently examined the reproducibility of MYC and BCL-2 immunohistochemical (IHC) scoring and the impact of high expression of MYC and BCL-2 (double expresser status, DE) on survival and progression in a large retrospective cohort of aggressive B-cell lymphoma patients treated with rituximab plus cyclophosphamide, doxorubicin, vincristine and prednisone (R-CHOP) or R-CHOP-like regimens.[1] We found that IHC scoring for MYC and BCL-2 was highly reproducible when cut-off values of ≥70% for MYC and ≥50% for BCL-2 were used. This threshold also predicted the presence of gene rearrangements identifying *MYC* translocations in 88% of cases. Patients with dual MYC expression of ≥70% and BCL-2 expression of ≥50% showed a significantly inferior clinical course and, therefore, represent candidates for novel treatment modalities.[1] We have now validated these findings in an independent cohort of 461 patients enrolled in prospective clinical trials of the German High-Grade Non-Hodgkin Lymphoma Study Group (DSHNHL).[2,3]

In these trials, patients underwent R-CHOP-14 if >60 years of age and R-CHOEP/R-MegaCHOEP if ≤60 years of age. In the MegaCHOEP trial reported by Schmitz *et al.*,[4] no significant differences in outcome between R-CHOEP-14 and R-MegaCHOEP had been observed, but to date, no randomized trial has been conducted to answer if R-CHOEP in younger patients is superior in comparison with R-CHOP. In a subgroup analysis for young low-risk patients from the MInT trial reported by Pfreundschuh *et al.*,[5] no difference in outcome was observed between R-CHOEP-21 and R-CHOP-21. In elderly patients, the Cunningham trial[6] revealed that the outcome of R-CHOP-14 is not better than that of R-CHOP-21. In the German cohort of 428 patients with MYC and BCL-2 IHC scoring available, 104 cases (24%) were MYC⁻/BCL-2⁻ (double negative, DN), 283 (66%) were MYC⁻/BCL-2⁺ (BCL2only), 8 (2%) were MYC⁺/BCL-2⁻ (MYConly), and 33 were MYC⁺/BCL-2⁺ using the above-mentioned cut-off values, meaning that 8% of DLBCL were assigned a DE status. Results from both MYC IHC scoring and MYC fluorescence *in situ* hybridization (FISH) were available from samples of 415 patients. In this analysis, 19 of 43 (44%) samples with high MYC expression (70/71-100%) harbored a MYC translocation (Table 1). The lower number of cases noted in our report with both high MYC expression and MYC breakage in comparison with the Ambrosio paper[1] are not easily explained. Most probably, this is due to a difference in the genetic constitution of the two different patient populations that were examined or to the analysis strategy: in the German cohort, the analysis was made on TMA while in the paper of Ambrosio *et al.*,[1] full sections were analyzed.[7] According to the results of molecular cell of origin (COO) analysis, we identified 50% of patients with an ABC subtype within the DE cohort using a MYC cut-off point of 70% and 68% using a cut-off point of 40%. The sample sizes, however, are too small to conclude that the groups differ from the proportion of the ABC subtype. It has to be stressed, however, that the DE status does not identify a homogeneous biological group of tumors and, especially, that the DE status in ABC-DLBCL arises through very different mechanisms.

In the German cohort, the DE subgroup had a significant inferior clinical course, while the DN subset had a

Table 1. Results from both MYC immunohistochemical (IHC) scoring and MYC fluorescence *in situ* hybridization.

| MYC IHC	MYC break		Total
	Negative	Positive	
0-40%*	257 (97%)	7 (3%)	264 (64%)
40%-70%*	96 (89%)	12 (11%)	108 (26%)
70%-100%*	24 (56%)	19 (44%)	43 (10%)
Total	377 (91%)	38 (9%)	415 (100%)

P<0.001. *Cut-off points were slightly different between clinical trials included in the analysis.

superior outcome and the MYC⁻/BCL-2⁺ subset had an intermediate prognosis. The differences were statistically significant for event-free survival (EFS), progression-free survival (PFS), and overall survival (OS) (EFS: DN *vs.* DE, *P*<0.001; DN *vs.* BCL2only *P*=0.004; BCL2only *vs.* DE *P*=0.032) (Figure 1A-C). These results could be confirmed in a multivariate analysis (Hazard ratios [HR] for DE *vs.* other: EFS: 2.1 95%CI:1.2-3.5, *P*=0.005; PFS: 2.5 95%CI:1.5-4.3, *P*=0.001; OS: 2.7 95%CI:1.5-4.8, *P*=0.001) adjusted for the factors of the International Prognostic Index (IPI) (age > 60 years, lactate dehydrogenase [LDH]>N, Eastern Cooperative Oncology Group [ECOG]>1, stage III/IV, extralymphatic involvement >1). In multivariate analyses adjusted for the International Prognostic Index (IPI) factors (age > 60 years, LDH>N, ECOG>1, stage III/IV and more than one site of extralymphatic involvement) both MYC (70/71-100% *vs.* other) and BCL2 (50/51-100% *vs.* other) expression were significant risk factors in EFS (MYC: HR1.9, 95%CI: 1.2-3.1, *P*=0.007 and BCL2: HR1.8, 95%CI: 1.2-2.7, *P*=0.006), PFS (MYC: HR2.1, 95%CI: 1.3-3.5, *P*=0.004 and BCL2: HR2.4, 95%CI: 1.5-3.8, *P*<0.001) and OS (MYC: HR2.3, 95%CI: 1.3-4.0, *P*=0.004 and BCL2: HR2.0, 95%CI: 1.2-3.3 and *P*=0.009). When cases were stratified according to MYC protein expression only, patients with MYC ≥70%, again, experienced inferior outcome in EFS (*P*=0.005), PFS (*P*=0.004), and OS (*P*=0.002) in comparison with patients with low MYC expression (≤40%) (Figure 1D-F), while no difference in prognosis was seen between patients whose tumors had MYC expression ≤40% and >40-70%. Within the DE group, the occurrence of a genetic double hit for *MYC* and *BCL-2* (n=8 of 32, 25%) failed to confer a significant prognostic difference in EFS (*P*=0.628), PFS (*P*=0.375), and OS (*P*=0.059) between patients with DH positive and DH negative tumors (Figure 2A-C). Within the non-DE group, we observed a genetic double hit for MYC and BCL-2 in only 11 of 354 (3%) patients with no relevant survival differences between patients with DH positive and DH negative tumors (Figure 2D-F). However, due to the low number of events, these results have to be interpreted with caution.

In essence, these results are in agreement with our previous findings indicating that high (≥70%) MYC expression identifies a subset of DLBCL with adverse clinical outcome independent of the presence of a double hit of *MYC* and *BCL-2*.

Increasing evidence suggests that the sole identification of the double hit (*MYC* and *BCL-2*) status may not be the optimal tool to identify patients in need of alternative therapies and in many studies, a proportion of DE patients nevertheless experience long-term survival. Two recent papers shed light on this seeming discrepancy.[8,9] In the first paper, the authors defined a clinically and biologically distinct subgroup of aggressive lymphomas with
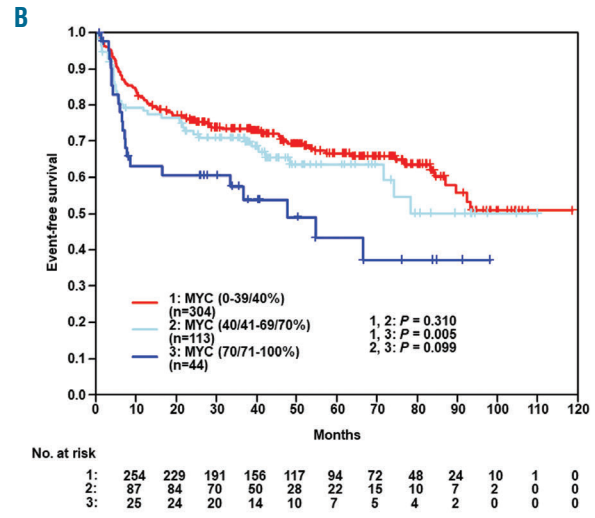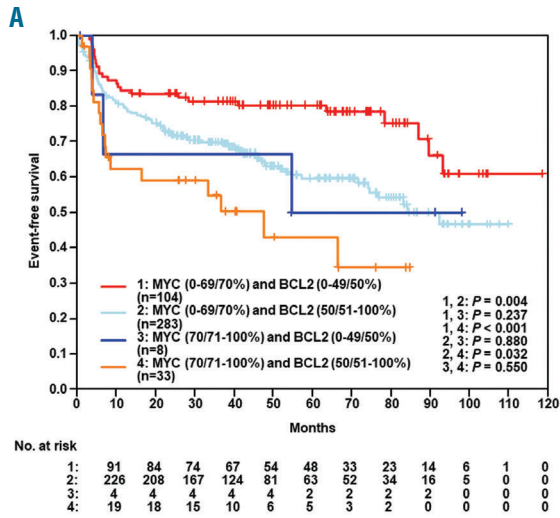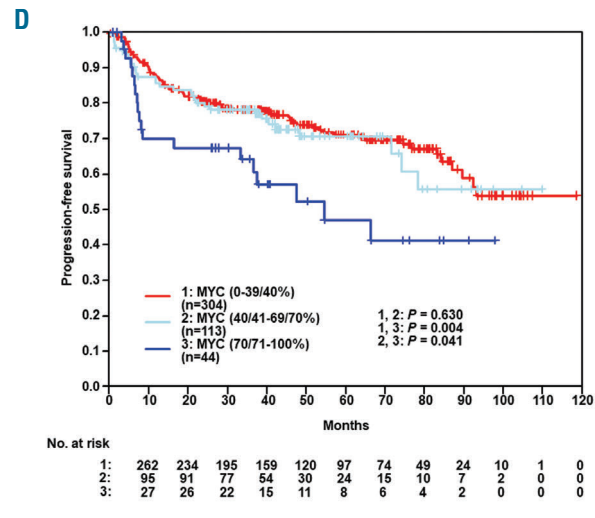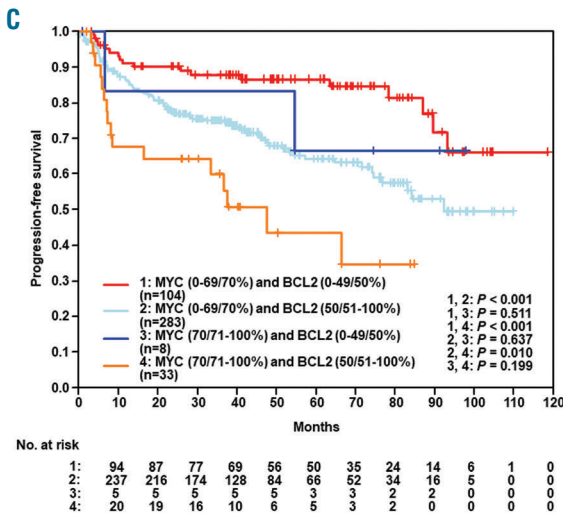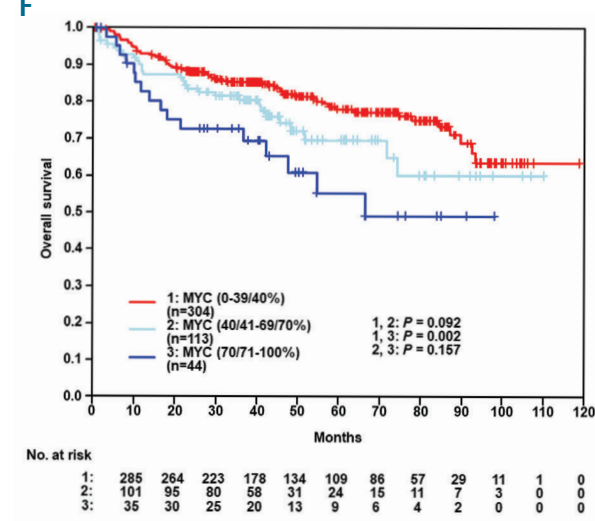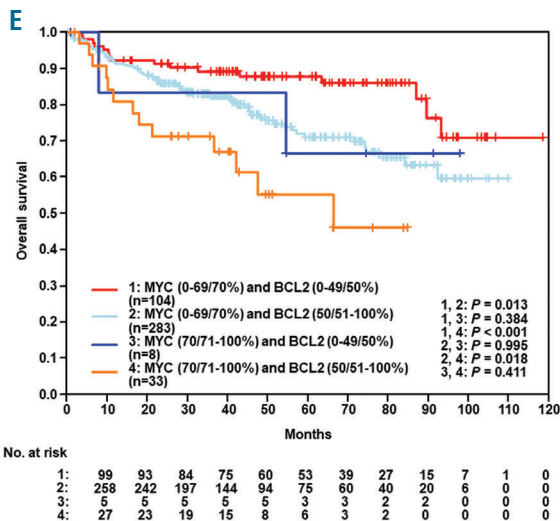
Figure 1. Event-free survival (EFS), progression-free survival (PFS) and overall survival (OS) of patients stratified according to Myc and BCL-2 expression. (A-C) The double expressor (DE) subgroup had a significant inferior clinical course, while the double negative (DN) subset had a superior outcome and the MYC-/BCL-2+ subset had an intermediate prognosis, with the differences being statistically significant for EFS, PFS and OS. (D-F) The cases were stratified according to MYC protein expression only, patients with MYC >70% experienced inferior outcome in EFS (P=0.005), PFS (P=0.004) and OS (P=0.002) in comparison to patients with low MYC expression (<40%). No difference in prognosis was seen between patients whose tumors had MYC expression <40% and 40-70%.

EFS
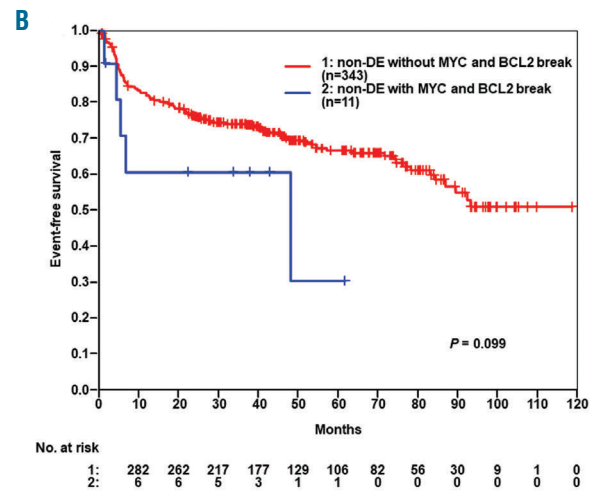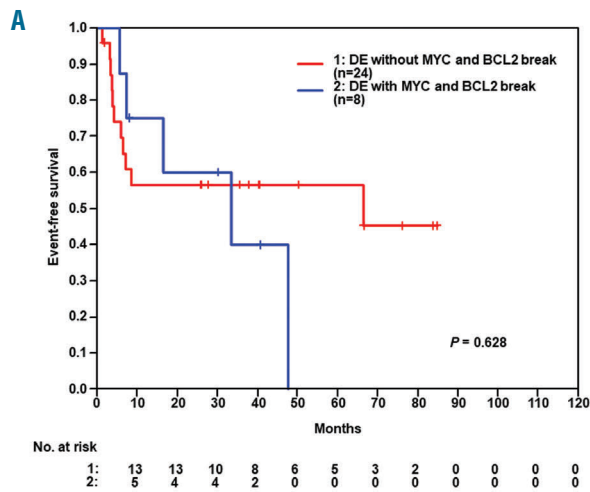
PFS
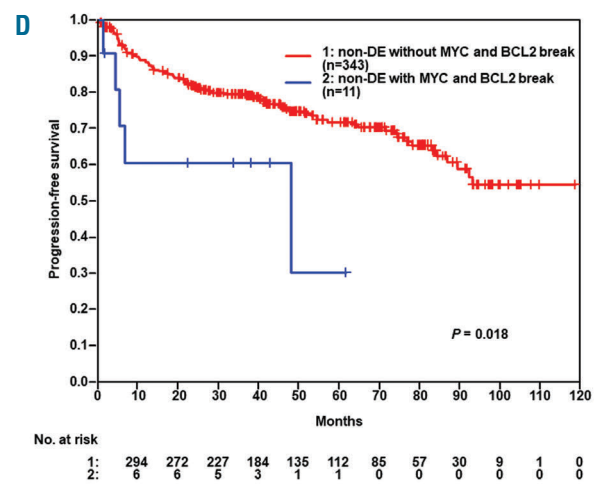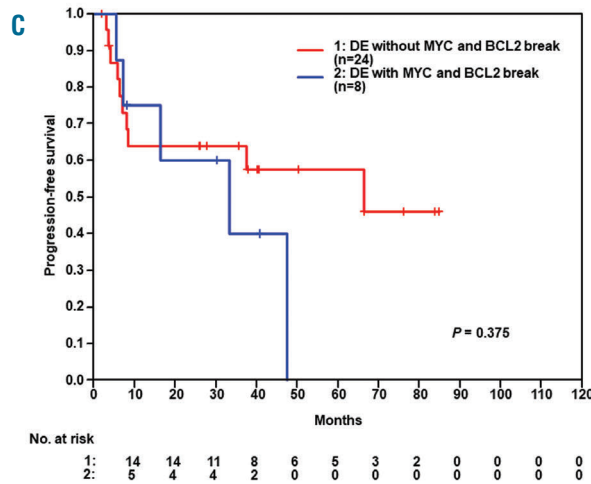
OS
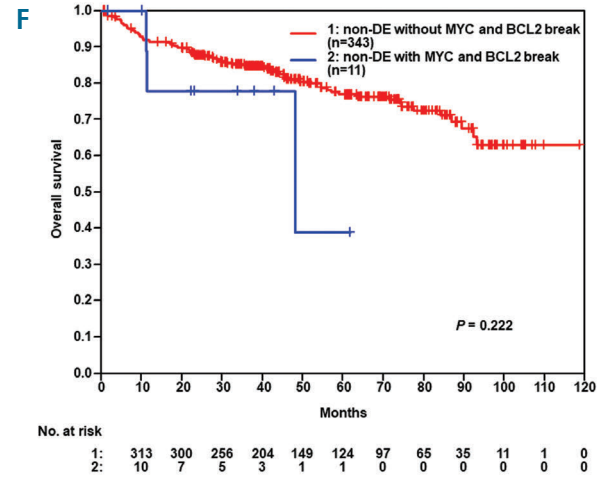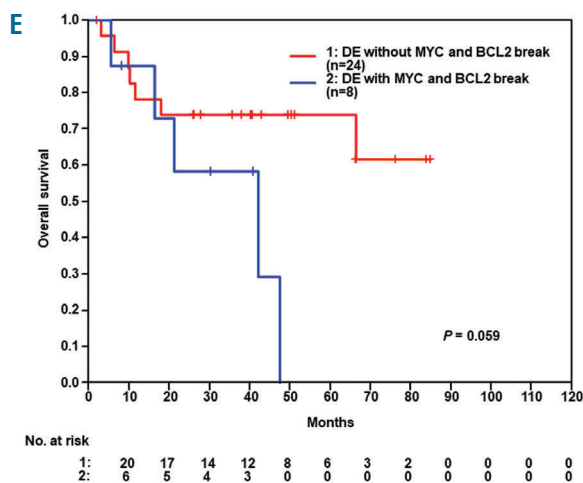
Figure 2. Comparison of double hit in double expressor and non-double expressor (DE). (A-C) Within the DE group, the occurrence of a genetic double hit for MYC and BCL-2 (n=8 of 32, 25%) failed to confer a significant prognostic difference in EFS (*P*=0.628), PFS (*P*=0.375) and OS (*P*=0.059) between patients with DH positive and DH negative tumors. (D-F) Within the non DE group, the occurrence of a genetic double hit for MYC and BCL-2 (n=11 of 354, 3%) failed to confer a significant prognostic difference in EFS (*P*=0.099) and OS (*P*=0.222) between patients with DH positive and DH negative tumors.

inferior prognosis among GCB-DLBCL. This tumor subgroup was characterized by a gene expression signature derived from HGBL-DH/TH lymphomas (DHIT signature).[8] Using this signature, however, only 50% of the cases stratified into the subgroup actually had dual rearrangements of *MYC* and *BCL-2* genes, and some DE cases were not assigned into the DHIT signature positive group. Gene set enrichment analysis demonstrated (over-) expression of MYC and E2F target genes, and of genes associated with oxidative phosphorylation and MTORC1 signaling in the DHIT-positive tumors, implying a pivotal role for MYC protein expression irrespective of the DH status. Unfortunately, the study did not document the precise percentage of MYC protein expression; it also did not correlate MYC protein expression to *MYC* gene rearrangements. The second paper identified 9% of DLBCL (83 of 928) as "molecular high grade (MHG)" B-cell lymphomas using gene expression analysis.[9] Most MHG (75 of 83) were GCB-like, and again, only half of them were *MYC* rearranged or double-hit lymphomas. The MHG subset treated with R-CHOP had a significantly poorer outcome than MHG negative DLBCL. Furthermore, *in vivo* experiments demonstrated that MYC-expressing lymphoma cells were obviously addicted to its oncogenic effect and, therefore, were critically relying on MYC expression regardless of *MYC* gene rearrangements.[10]

Although genomic testing has entered clinical practice, sophisticated tests like those reported are not yet widely available in all laboratories. Therefore, gene expression signatures identifying high-risk subgroups are currently difficult to apply in the clinic. Our findings describe a more readily available tool to identify patients at risk with a high MYC protein expression cut-off circumventing problems related to interobserver variability.[11] Our findings are corroborated in a recent paper by Pedersen *et al*.[12] who demonstrated that stratification by MYC expression has prognostic impact in *MYC* translocated DLBCL.[12]

In summary, we have confirmed that the prognosis of DLBCL is inversely correlated with MYC protein expression levels, and, by using diagnostic thresholds of high reproducibility, we were able to identify a subset of patients with adverse outcome in need of alternative therapeutic strategies.

Marita Ziepert,[1] Stefano Lazzi,[2] Raffaella Santi,[3] Federica Vergoni,[3] Massimo Granai,[2] Virginia Mancini,[2] Annette M. Staiger,[4,5] Heike Horn,[4,5] Markus Löffler,[6] Viola Pöschel,[7] Gerhald Held,[7] Gerald Wulf,[8] Lorenz H. Trümper,[9] Norbert Schmitz,[10] Andreas Rosenwald,[11] Elena Sabattini,[12] Kikkeri N. Naresh,[13] Harald Stein,[14] German Ott[4] and Lorenzo Leoncini[2]

[1]*University of Leipzig - Institute of Medical Informatics, Statistics and Epidemiology, Leipzig, Germany;* [2]*Department of Medical Biotechnology, Section of Pathology, University of Siena, Siena, Italy;* [3]*Department of Pathology, Careggi University Hospital, University of Firenze, Firenze, Italy;* [4]*Department of Clinical Pathology, Robert-Bosch-Krankenhaus, Stuttgart, Germany;* [5]*Dr. Margarete Fischer-Bosch-Institute of Clinical Pharmacology, Stuttgart, Germany and University of Tübingen, Germany;* [6]*Institute for Medical Informatics, Statistics and Epidemiology, University of Leipzig, Leipzig, Germany;* [7]*DSHNHL Studiensekretariat, Universitätsklinikum des Saarlandes, Homburg, Germany;* [8]*Department of Hematology and Oncology, Georg-August Universität, Göttingen, Germany;* [9]*G-CCC (Göttingen Comprehensive Cancer Center), University Medicine Göttingen, Göttingen, Germany;* [10]*Department of Medicine A, University Hospital Münster, Münster, Germany;* [11]*Institute of Pathology, Universität Würzburg and Comprehensive Cancer Center Mainfranken (CCCMF), Würzburg, Germany;* [12]*Institute of Hematology "L. and A. Seràgnoli", S. Orsola - Malpighi Hospital, Bologna, Italy;* [13]*Hammersmith Hospital and Imperial College, London, UK;* [14]*Pathodiagnostik Berlin, Berlin, Germany and* [15]*Department of Clinical Pathology, Robert-Bosch-Krankenhaus, Stuttgart, Germany*

Correspondence:
LORENZO LEONCINI - lorenzo.leoncini@dbm.unisi.it

References

1. Ambrosio MR, Lazzi S, Lo Bello G, et al. MYC protein expression scoring and its impact on the prognosis of aggressive B-cell lymphoma patients. Haematologica. 2019;104(1):e25-e28

2. Staiger AM, Altenbuchinger M, Ziepert, et al. A novel lymphoma-associated macrophage interaction signature (LAMIS) provides robust risk prognostication in diffuse large B-cell lymphoma clinical trial cohorts of the DSHNHL. Leukemia. 2019;34(2):543-552.

3. Mellert K, Martin M, Lennerz JK, et al. The impact of SOCS1 mutations in diffuse large B-cell lymphoma. Br J Haematol. 2019;187(5):627-637

4. Schmitz N, Nickelsen M, Ziepert M, et al. Conventional chemotherapy (CHOEP-14) with rituximab or high-dose chemotherapy (MegaCHOEP) with rituximab for young, high-risk patients with aggressive B-cell lymphoma: an open-label, randomised, phase 3 trial (DSHNHL 2002-1). Lancet Oncol. 2012;13(12):1250-1259

5. Pfreundschuh M, Trümper L, Osterborg A, et al. CHOP-like chemotherapy plus rituximab versus CHOP-like chemotherapy alone in young patients with good-prognosis diffuse large-B-cell lymphoma: a randomised controlled trial by the MabThera International Trial (MInT) Group. Lancet Oncol. 2006;7(5):379-391.

6. Cunningham D, Hawkes EA, Jack A, et al. Rituximab plus cyclophosphamide, doxorubicin, vincristine, and prednisolone in patients with newly diagnosed diffuse large B-cell non-Hodgkin lymphoma: a phase 3 comparison of dose intensification with 14-day versus 21-day cycles. Lancet. 2013;25;381(9880):1817-1826.

7. Hupp M, Williams S, Dunnette B, et al. Comparison of evaluation techniques, including digital image analysis, for MYC protein expression by immunohistochemical stain in aggressive B-cell lymphomas. Hum Pathol. 2019;83:124-132.

8. Ennishi D, Jiang A, Boyle M, et al. Double-hit gene expression signature defines a distinct subgroup of germinal center B-cell-like diffuse large B-cell lymphoma. J Clin Oncol. 2019;37(3):190-201.

9. Sha C, Barrans S, Cucco F, et al. Molecular high-grade B-cell lymphoma: defining a poor-risk group that requires different approaches to therapy. J Clin Oncol. 2019;37(3):202-212.

10. Li W, Gupta SK, Han W, et al. Targeting MYC activity in double-hit lymphoma with MYC and BCL2 and/or BCL6 rearrangements with epigenetic bromodomain inhibitors. J Hematol Oncol. 2019;12(1):73.

11. Mahmoud AZ, George TI, Czuchlewski DR, et al. Scoring of MYC protein expression in diffuse large B-cell lymphomas: concordance rate among hematopathologists. Mod Pathol. 2015;28(4):545-551.

12. Pedersen MØ, Gang AO, Clasen-Linde E, et al. Stratification by MYC expression has prognostic impact in MYC translocated B-cell lymphoma identifies a subgroup of patients with poor outcome. Eur J Haematol. 2019;102(5):395-406.

High rate of minimal residual disease responses in young and fit patients with IGHV mutated chronic lymphocytic leukemia treated with front-line fludarabine, cyclophosphamide, and intensified dose of ofatumumab (FCO2)

Since its first use at the MD Anderson Cancer Center, FCR (fludarabine, cyclophosphamide, rituximab) chemoimmunotherapy has been considered the gold standard for the front-line treatment of young and fit patients with chronic lymphocytic leukemia (CLL).[1-3] Superior outcomes with this regimen have been observed in IGHV mutated (M-IGHV) compared to IGHV unmutated (UM-IGHV) patients.[3-5] Responses with undetectable minimal residual disease (uMRD) have been associated with a significantly longer progression-free survival (PFS) and overall survival (OS). Ofatumumab, a fully human anti-CD20 monoclonal antibody, revealed *in vitro* higher complement-mediated activity compared to rituximab. The clinical efficacy of ofatumumab as a single agent or combined with chemotherapy has been demonstrated in relapsed/refractory (R/R) patients as well as in treatment naïve (TN) patients with CLL.[6-8] In a meta-analysis that included six randomized trials, an improvement in the PFS, with no differences in the OS, was seen in the group of patients who received an ofatumumab-based treatment compared to the group of patients who received different regimens or who were only observed.[9]

In a study by Wierda *et al.*,[10] 50% of fit patients with CLL who received the front-line FC regimen combined with ofatumumab (FCO), given at a flat dose of 1000 mg, achieved a complete response (CR). Based on the efficacy of this regimen, the Gruppo Italiano Malattie Ematologiche dell'Adulto (GIMEMA) carried out a prospective, multicenter study (the LLC 0911 study) to evaluate the efficacy and safety of a front-line FCO regimen that was intensified with an additional dose of 1,000 mg of ofatumumab (FCO2). The primary endpoint of this study was the rate of CR obtained with the FCO2 regimen.

Between November 2013 and November 2015, 78 fit and young patients with CLL requiring front-line therapy according to the 2008 International Workshop CLL (iwCLL) criteria[11] were enrolled in this study. Age ≤65 years, Cumulative Illness Rating Score (CIRS) score up to 6, creatinine clearance of at least 60 mL/min, Eastern Cooperative Oncology Group (ECOG) performance status 0-1, were required for inclusion in the study. A central screening included immunophenotype, fluorescence *in situ* hybridization, the assessment of the IGHV and *TP53* mutation status.

Treatment consisted of six cycles of intravenous fludarabine (25 mg/m² daily) and cyclophosphamide (250 mg/m² daily) given on the first three days of each 28-day cycle. Ofatumumab was administered intravenously on day 14 of cycle 1 at the dose of 300 mg and on day 21 at the dose of 1000 mg. During the subsequent five cycles (cycles 2-6), ofatumumab was given at the dose of 1,000 mg on days 1 and 14 of each course. An additional dose of 1,000 mg of ofatumumab was given on day 28 of cycle 6. To prevent infusion reactions with ofatumumab, a pre-medication consisting of paracetamol 1,000 mg, chlorphenamine 10-20 mg, prednisolone 100 mg, or equivalent, was administered. All patients received *Pneumocystis Carinii* prophylaxis with co-trimoxazole and, as primary prophylaxis of granulocytopenia, pegfilgrastim on day 5 of each FCO2 course.

Table 1. Intention-to-treat response to the FCO2 regimen.

	N (%)
All patients	78 (100)
ORR	72 (92.3)
CR	60 (77)
PB and BM Flow-uMRD-CR[1]	36 of 78 (46.1)
PB and BM PCR-uMRD-CR[2]	17 of 78 (21.8)
PR	12 (15.4)
Failures[3]	6 (7.7)

FCO2: front-line fludarabine, cyclophosphamide, and intensified dose of ofatumumab; N: number; ORR: overall response rate; CR: complete response; MRD: minimal residual disease; Flow-uMRD: undetectable minimal residual disease by flow-cytometry; PCR: polymerase chain reaction; PCR-uMRD: undetectable minimal residual disease by PCR. [1]Peripheral blood (PB) and bone marrow (BM) Flow-uMRD in 36 of 60 (60%) patients with CR. [2]PB and BM PCR-uMRD in 17 of 60 (28.3%) patients with CR. [3]Failures: no response in five patients (stable disease, n=4; progressive disease, n=1) and unknown in 1.

Response was assessed according to the iwCLL criteria.[11] In patients who achieved a CR, MRD was checked both in peripheral blood (PB) and bone marrow (BM) by a 6/4-color flow cytometry assay with a sensitivity of at least 10^{-4}.[12] MRD was further assessed by allele-specific oligonucleotide polymerase chain reaction (PCR) in the PB and BM of patients with no evidence of MRD by flow cytometry. According to the MRD levels, CR was sub-classified as follows: (i) MRD-positive CR in the presence of residual disease by flow cytometry in the PB and/or BM; (ii) CR with undetectable MRD by flow cytometry (Flow-uMRD-CR) in the absence of residual cytometric disease in both the PB and BM; (iii) CR with uMRD by flow cytometry and allele-specific oligonucleotide PCR (PCR-uMRD-CR) in the absence of MRD by flow cytometry and PCR in the PB and BM. In patients with a Flow-uMRD-CR or PCR-uMRD-CR, MRD was monitored during the follow-up every six months. The baseline clinical and biologic characteristics of patients and patient disposition are summarized in *Online Supplementary Table S1* and *Online Supplementary Figure S1*. Median follow-up of patients was 31 months; median age 55 years (range: 36-65 years). A *TP53* disruption, del17p and/or TP53 mutation, was detected in 11% of the cases, and 64% of patients were UM-IGHV.

Median number of administered cycles was six (range: 1-6). On an intention-to-treat (ITT) basis, 72 patients (92.3%) achieved a response with a CR in 60 (77%) (Table 1). The presence of *TP53* disruption was the only significant and independent variable with an impact on the achievement of CR (*P*=0.014) (*Online Supplementary Tables S2 and S3*). A Flow-uMRD-CR was achieved in 36 of 78 (46.1%) patients and a PCR-uMRD-CR in 17 of 78 (21.8%) (Table 1). In multivariate analysis (MVA), Binet stage was the only factor with statistical significance on the achievement of a Flow-uMRD-CR (*P*=0.042) while the IGHV mutational status was the only significant factor with an impact on the achievement of a PCR-uMRD-CR (*Online Supplementary Table S3*).

In the subset of patients without *TP53* aberrations, a CR was recorded in 84.4% of the cases, a Flow-uMRD-CR in 50% and a PCR-uMRD-CR in 23.4%. When the analysis was further restricted to the M-IGHV patients without *TP53* disruption, Flow-uMRD-CR and PCR-uMRD-CR rates were 68.2% and 45.4%, respectively, and significantly higher than those observed in UM-IGHV patients: 39% (*P*=0.036) and 12.2% (*P*=0.005), respectively (*Online Supplementary Table S4*). The IGHV
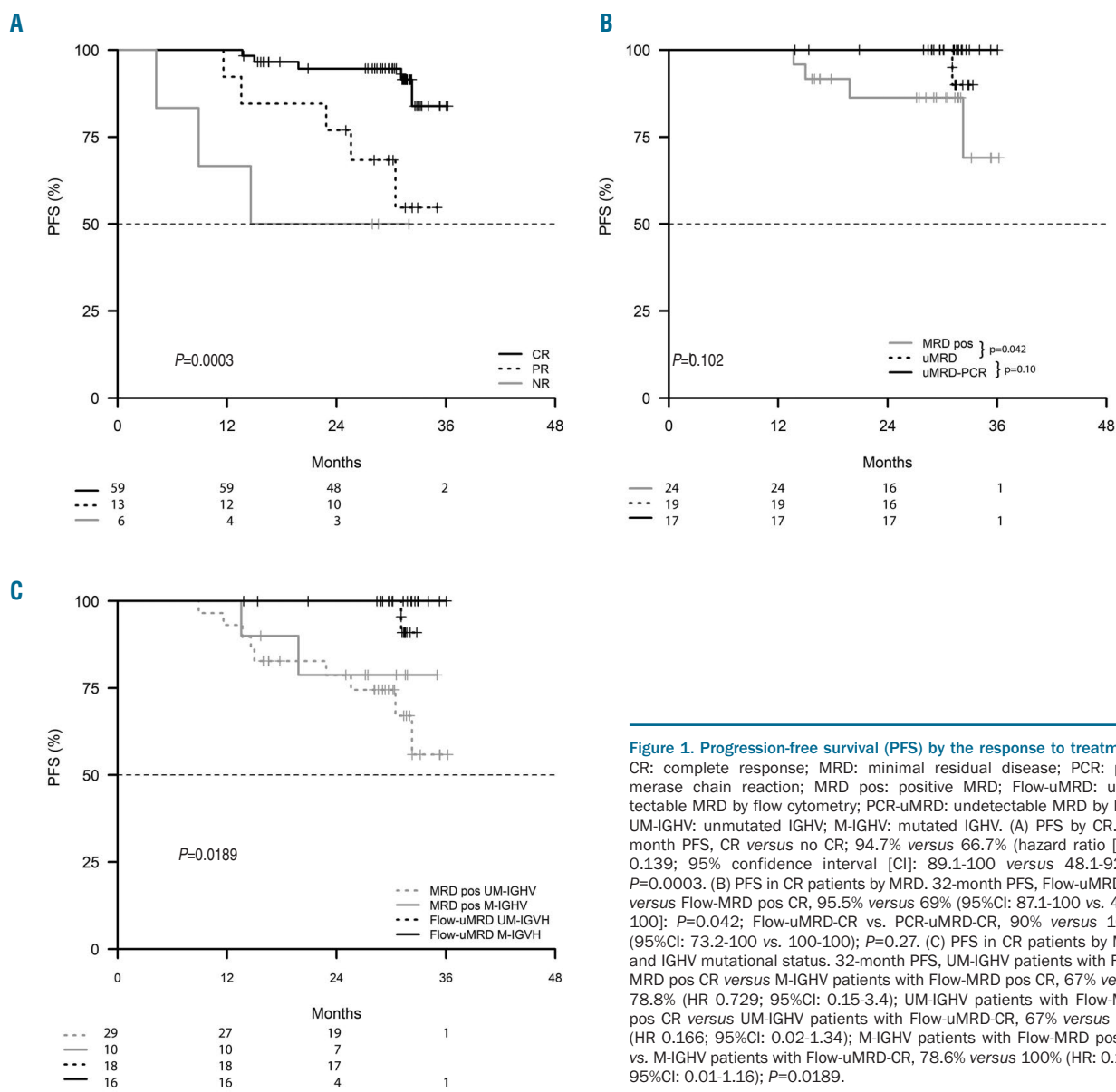
A

B

C

Figure 1. Progression-free survival (PFS) by the response to treatment. CR: complete response; MRD: minimal residual disease; PCR: polymerase chain reaction; MRD pos: positive MRD; Flow-uMRD: undetectable MRD by flow cytometry; PCR-uMRD: undetectable MRD by PCR; UM-IGHV: unmutated IGHV; M-IGHV: mutated IGHV. (A) PFS by CR. 24-month PFS, CR *versus* no CR; 94.7% *versus* 66.7% (hazard ratio [HR]: 0.139; 95% confidence interval [CI]: 89.1-100 *versus* 48.1-92.4); *P*=0.0003. (B) PFS in CR patients by MRD. 32-month PFS, Flow-uMRD-CR *versus* Flow-MRD pos CR, 95.5% *versus* 69% (95%CI: 87.1-100 *vs.* 43.1-100]: *P*=0.042; Flow-uMRD-CR vs. PCR-uMRD-CR, 90% *versus* 100% (95%CI: 73.2-100 *vs.* 100-100); *P*=0.27. (C) PFS in CR patients by MRD and IGHV mutational status. 32-month PFS, UM-IGHV patients with Flow-MRD pos CR *versus* M-IGHV patients with Flow-MRD pos CR, 67% *versus* 78.8% (HR 0.729; 95%CI: 0.15-3.4); UM-IGHV patients with Flow-MRD pos CR *versus* UM-IGHV patients with Flow-uMRD-CR, 67% *versus* 91% (HR 0.166; 95%CI: 0.02-1.34); M-IGHV patients with Flow-MRD pos CR *vs.* M-IGHV patients with Flow-uMRD-CR, 78.6% *versus* 100% (HR: 0.145; 95%CI: 0.01-1.16); *P*=0.0189.

mutational status was the only factor with a significant and independent impact on the achievement of both a Flow-uMRD-CR and a PCR-uMRD-CR in patients without *TP53* disruption (*Online Supplementary Table S3*).

The 36-month PFS was 76.4% (*Online Supplementary Figure S2A*). The only variable with a significant and independent impact on PFS was the presence of a *TP53* disruption (*Online Supplementary Tables 3* and *5*; *P*=0.002). After excluding patients with *TP53* disruption, none of the baseline factors revealed an impact on PFS (*Online Supplementary Table S6*). A significantly higher PFS was observed in patients who achieved a CR (*P*=0.0003). Moreover, a significantly higher PFS was seen in patients who achieved a CR with Flow-uMRD (*P*=0.042) (Figure 1A and B). All M-IGHV patients and 91% of UM-IGHV patients with a Flow-uMRD-CR were progression-free at 32 months (Figure 1C). All 17 patients (11 M-IGHV and 6 UM-IGHV) who achieved a PCR-uMRD-CR were projected as progression-free at 32 months. After a median time of 40 months (range: 28-56 months) from the initial response, residual disease was still absent in 11 of 13 patients at the last re-assessment of MRD by PCR. The

36-month OS was 94.7% (*Online Supplementary Figure S2B*). A significantly inferior survival probability was observed in patients with *TP53* disruption (*P*<0.001) and ≥5cm enlarged nodes (*P*=0.0015) (Figure 2). However, in MVA *TP53* disruption emerged as the only significant factor with an impact on OS (*Online Supplementary Tables S3* and *S7* and *Online Supplementary Figure S3A*). Patients who achieved a CR with Flow-uMRD showed a significantly superior survival than those with residual disease (*P*=0.055) (Figure 2). All CR patients with Flow-uMRD (19 patients) or PCR-uMRD (17 patients) were still alive at 32 months.

Adverse events recorded during treatment are listed in *Online Supplementary Table S8*. No unexpected toxicities were observed. Despite the prophylactic use of growth factors, grade ≥3 granulocytopenia leading to fludarabine and cyclophosphamide dose reduction was observed in 33 patients (42.3%). However, a severe infection was experienced by 21 (27%) patients. Taken together, the results of this study show that the FC regimen combined with a double dose of ofatumumab was associated with a high rate of CR and Flow-uMRD-CR in young and fit
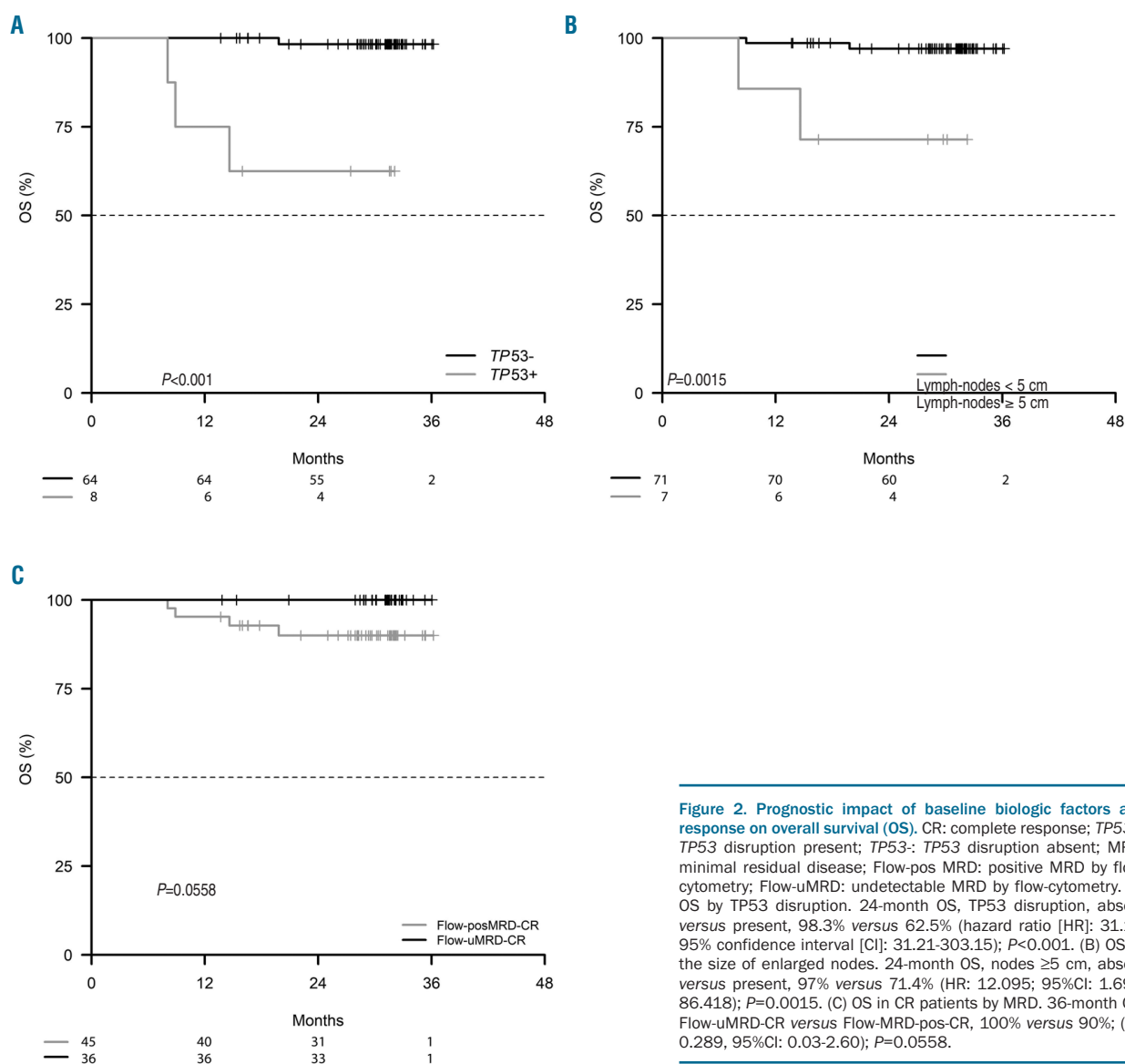
Figure 2. Prognostic impact of baseline biologic factors and response on overall survival (OS). CR: complete response; *TP53*+: *TP53* disruption present; *TP53*-: *TP53* disruption absent; MRD: minimal residual disease; Flow-pos MRD: positive MRD by flow-cytometry; Flow-uMRD: undetectable MRD by flow-cytometry. (A) OS by TP53 disruption. 24-month OS, TP53 disruption, absent *versus* present, 98.3% *versus* 62.5% (hazard ratio [HR]: 31.19; 95% confidence interval [CI]: 31.21-303.15); *P*<0.001. (B) OS by the size of enlarged nodes. 24-month OS, nodes ≥5 cm, absent *versus* present, 97% *versus* 71.4% (HR: 12.095; 95%CI: 1.693-86.418); *P*=0.0015. (C) OS in CR patients by MRD. 36-month OS, Flow-uMRD-CR *versus* Flow-MRD-pos-CR, 100% *versus* 90%; (HR 0.289, 95%CI: 0.03-2.60); *P*=0.0558.

patients with CLL. IGHV-M patients without *TP53* disruption had the highest benefit from the FCO2 chemoimmunotherapy; about two-thirds of them achieved a Flow-uMRD-CR and were progression-free at 32 months. These findings confirm the favorable outcomes of M-IGHV patients treated with the FCR regimen[3-5] and the survival benefit of patients who obtain an uMRD at response.[3-5,13] Direct cross-comparisons between the results of this study and those of other trials with the FCR regimen,[1-3] or with the FC schedule combined with obinutuzumab,[14] or a single dose of ofatumumab,[10] are methodologically incorrect. These studies differ on many points: the number and age of treated patients, inclusion criteria, selection of patients who had an MRD assessment, and supportive measures. In the absence of a randomized study, the FCR regimen remains the standard chemoimmunotherapy approach for fit and young patients with CLL and no deletion 17p. However, recent studies highlight the superiority of front-line chemo-free regimens over conventional chemoimmunotherapy. In the randomized ECOG E1912 study,[15] young and fit patients with CLL who received front-line treatment with ibrutinib and rituximab

showed a significantly higher PFS and OS than those treated with FCR. A superior PFS than that observed with FCR was seen in UM-IGHV patients, while it was less evident in M-IGHV patients. Given the favorable outcomes with front-line chemoimmunotherapy in young and fit patients, IGHV mutated and without *TP53* disruption, the role of novel agents in this subset of patients should be better defined.

Francesca R. Mauro,[1] Stefano Molica,[2] Stefano Soddu,[3] Fiorella Ilariucci,[4] Marta Coscia,[5] Francesco Zaja,[6] Emanuele Angelucci,[7] Francesca Re,[8] Anna Marina Liberati,[9] Alessandra Tedeschi,[10] Gianluigi Reda,[11] Daniela Pietrasanta,[12] Alessandro Gozzetti,[13] Roberta Battistini,[14] Giovanni Del Poeta,[15] Caterina Musolino,[16] Mauro Nanni,[1] Alfonso Piciocchi,[3] Marco Vignetti,[3] Antonino Neri,[11] Francesco Albano,[17] Antonio Cuneo,[18] Ilaria Del Giudice,[1] Irene Della Starza,[1] Maria Stefania De Propris,[1] Sara Raponi,[1] Anna R Guarini[1] and Robin Foà[1]

[1]Department of Hematology and Department of Translational and Precision Medicine, 'Sapienza' University, Rome; [2]Department of Hematology, Pugliese Ciaccio Hospital, Catanzaro; [3]Italian Group for Adult Hematologic Diseases (GIMEMA) Foundation, Rome;

[4]Department of Hematology, Arcispedale S. Maria Nuova, Reggio Emilia; [5]Division of Hematology, A.O.U. Città della Salute e della Scienza di Torino and Department of Molecular Biotechnology and Health Sciences, University of Torino, Torino; [6]SC Ematologia, Azienda Sanitaria Universitaria Integrata, Trieste; [7]Ematologia e Centro Trapianti, IRCCS Ospedale Policlinico San Martino, Genova; [8]Cattedra di Ematologia, CTMO University, Parma; [9]Department of Onco-Hematology, University of Perugia, Santa Maria Hospital, Terni; [10]Department of Hematology, Niguarda Ca Granda Hospital, Milan; [11]Department of Hematology, Foundation IRCCS Ca' Granda Ospedale Maggiore Policlinico of Milan, Milan; [12]Department of Hematology, SS. Antonio e Biagio e Cesare Arrigo Hospital, Alessandria; [13]Hematology, Department of Medical Science Surgery and Neurosciences, University of Siena, Siena; [14]Department of Hematology, S. Camillo Hospital, Rome; [15]Hematology, Department of Biomedicine and Prevention, University Tor Vergata, Rome; [16]Department of Hematology, University of Messina, Messina; [17]Emergency and Transplantation Department, Hematology Section, University of Bari, Bari and [18]Department of Hematology, S. Anna Hospital, Ferrara, Italy

Correspondence:
FRANCESCA R. MAURO - mauro@bce.uniroma1

doi:10.3324/haematol.2019.235705

References

1. Keating MJ, O'Brien S, Albitar M, et al. Early results of a chemoimmunotherapy regimen of fludarabine, cyclophosphamide, and rituximab as initial therapy for chronic lymphocytic leukemia. J Clin Oncol. 2005;23(18):4079-4088.
2. Hallek M, Fischer K, Fingerle-Rowson G, et al. Addition of rituximab to fludarabine and cyclophosphamide in patients with chronic lymphocytic leukemia: a randomized, open-label, phase 3 trial. Lancet. 2010;376(9747):1164-1174.
3. Fischer K, Bahlo J, Fink AM, et al. Long-term remissions after FCR chemoimmunotherapy in previously untreated patients with CLL: updated results of the CLL8 trial. Blood. 2016;127(2):208-215.
4. Thompson PA, Tam CS, O'Brien SM, et al. Fludarabine, cyclophosphamide, and rituximab treatment achieve long-term disease-free survival in IGHV-mutated chronic lymphocytic leukemia. Blood. 2016;27(3):303-309.
5. Rossi D, Terzi-di-Bergamo L, De Paoli L, et al. Molecular prediction of durable remission after first-line fludarabine-cyclophosphamide-rituximab in chronic lymphocytic leukemia. Blood. 2015; 126(16):1921-1924.
6. Wierda W, Kipps T, Mayer J, et al. Ofatumumab as single-agent CD20 immunotherapy in fludarabine-refractory chronic lymphocytic leukemia. J Clin Oncol. 2010;28(10):1749-1755.
7. Robak T, Warzocha K, Govind Babu K, et al. Ofatumumab plus fludarabine and cyclophosphamide in relapsed chronic lymphocytic leukemia: results from the COMPLEMENT 2 trial. Leuk Lymphoma. 2017;58(5):1084-1093.
8. Hillmen P, Robak T, Janssens A, et al. Chlorambucil plus ofatumumab versus chlorambucil alone in previously untreated patients with chronic lymphocytic leukaemia (COMPLEMENT 1): a randomised, multicentre, open-label phase 3 trial. Lancet. 2015;385(9980):1873-1883.
9. Wu Y, Wang Y, Gu Y, et al. Safety and efficacy of ofatumumab in chronic lymphocytic leukemia: a systematic review and meta-analysis. Hematology. 2017;22(10):578-584.
10. Wierda WG, Kipps TJ, Dürig J, et al. Chemoimmunotherapy with O-FC in previously untreated patients with chronic lymphocytic leukemia. Blood. 2016;117(24):6450-6458.
11. Hallek M, Cheson BD, Catovsky D, et al. Guidelines for the diagnosis and treatment of chronic lymphocytic leukemia: a report from the International Workshop on Chronic Lymphocytic Leukemia updating the National Cancer Institute-Working Group 1996 guidelines. Blood. 2008;111(12):5446-5456.
12. Rawstron AC, Böttcher S, Letestu R, et al. Improving efficiency and sensitivity: European Research Initiative in CLL (ERIC) update on the international harmonized approach for flow cytometric residual disease monitoring in CLL. Leukemia. 2013;27(1):142-149.
13. Kater AP, Seymour JF, Hillmen P, et al. Fixed duration of venetoclax-rituximab in relapsed/refractory chronic lymphocytic leukemia eradicates minimal residual disease and prolongs survival: post-treatment follow-up of the MURANO phase III study. J Clin Oncol. 2019;37(4):269-277.
14. Brown JR, O'Brien S, Kingsley CD, et al. Durable remissions with obinutuzumab-based chemoimmunotherapy: long-term follow-up of the phase 1b GALTON trial in CLL. Blood. 2019;133(9):990-992.
15. Shanafelt TD, Wang XV, Kay NE, Hanson CA, O'Brien S, Barrientos J, et al. Ibrutinib-rituximab or chemoimmunotherapy for chronic lymphocytic leukemia. N Engl J Med. 2019;381(5):432-443.

The role of ^{18}F-FDG-PET in detecting Richter transformation of chronic lymphocytic leukemia in patients receiving therapy with a B-cell receptor inhibitor

Chronic lymphocytic leukemia (CLL) is a low grade B-cell malignancy. Approximately 2-10% of CLL can undergo Richter transformation (RT) to an aggressive lymphoma, most commonly diffuse large B-cell lymphoma (DLBCL).[1-3] Management of RT is extremely challenging and the clinical outcome is dismal.[4] In CLL patients with suspected disease progression, distinguishing between progressive CLL and RT is critically important, as the management and prognosis are different.

While tissue biopsy is the gold standard for diagnosing progressive CLL *versus* RT, ^{18}F-fluorodeoxyglucose (FDG) positron emission tomography (PET) may play an important role in the diagnostic workup. In the chemoimmunotherapy (CIT) era, several studies showed that a maximum standardized uptake value (SUV$_{max}$) ≥5 had high sensitivity (88-91%) and varied specificity (47-80%) in detecting RT,[5-7] and a French study[8] reported high sen-

Table 1. Baseline characteristics at the time of B-cell receptor pathway inhibitors initiation.

	Total (N=92)	Without biopsy (N=38)	With biopsy (N=54)	P
Age at BCRi initiation				0.36
Median	68	70	67	
Range	(43-89)	(47-89)	(43-81)	
Sex				0.22
Female	23 (25.0%)	12 (31.6%)	11 (20.4%)	
Male	69 (75.0%)	26 (68.4%)	43 (79.6%)	
BCRi				0.80
Ibrutinib	90 (97.8%)	37 (97.4%)	53 (98.1%)	
Idelalisib	2 (2.2%)	1 (2.6%)	1 (1.9%)	
BCRi as first-line treatment				0.32
Yes	13 (14.1%)	7 (18.4%)	6 (11.1%)	
No	79 (85.9%)	31 (81.6%)	48 (88.9%)	
Rai category				0.27
Rai 0: Low risk	14 (15.4%)	5 (13.2%)	9 (17.0%)	
Rai 1 or 2: Intermediate risk	26 (28.6%)	8 (21.1%)	18 (34.0%)	
Rai 3 or 4: High risk	51 (56.0%)	25 (65.8%)	26 (49.1%)	
Missing	1	0	1	
IGHV mutation				0.56
Unmutated	60 (80.0%)	25 (83.3%)	35 (77.8%)	
Mutated	15 (20.0%)	5 (16.7%)	10 (22.2%)	
Missing	17	8	9	
CLL FISH category				0.13
Del(17p)	19 (27.5%)	8 (25.8%)	11 (28.9%)	
Del(11q)	16 (23.2%)	8 (25.8%)	8 (21.1%)	
Trisomy 12	10 (14.5%)	4 (12.9%)	6 (15.8%)	
Normal	12 (17.4%)	2 (6.5%)	10 (26.3%)	
Del(13q)	8 (11.6%)	6 (19.4%)	2 (5.3%)	
Other	4 (5.8%)	3 (9.7%)	1 (2.6%)	
Missing	23	7	16	
TP53 disruption (*TP53* mutation or FISH del(17p))				0.75
No	49 (70.0%)	23 (71.9%)	26 (68.4%)	
Yes	21 (30.0%)	9 (28.1%)	12 (31.6%)	
Missing	22	6	16	
CLL-IPI risk group				0.90
Intermediate (2-3)	12 (20.0%)	6 (22.2%)	6 (18.2%)	
High (4-6)	31 (51.7%)	14 (51.9%)	17 (51.5%)	
Very High (7-10)	17 (28.3%)	7 (25.9%)	10 (30.3%)	
Missing	32	11	21	

BCRi: B-cell receptor pathway inhibitor; *IGHV*: immunoglobulin heavy-chain variable region gene; CLL: chronic lymphocytic leukemia; FISH: fluorescence *in situ* hybridization; IPI: international prognostic index.
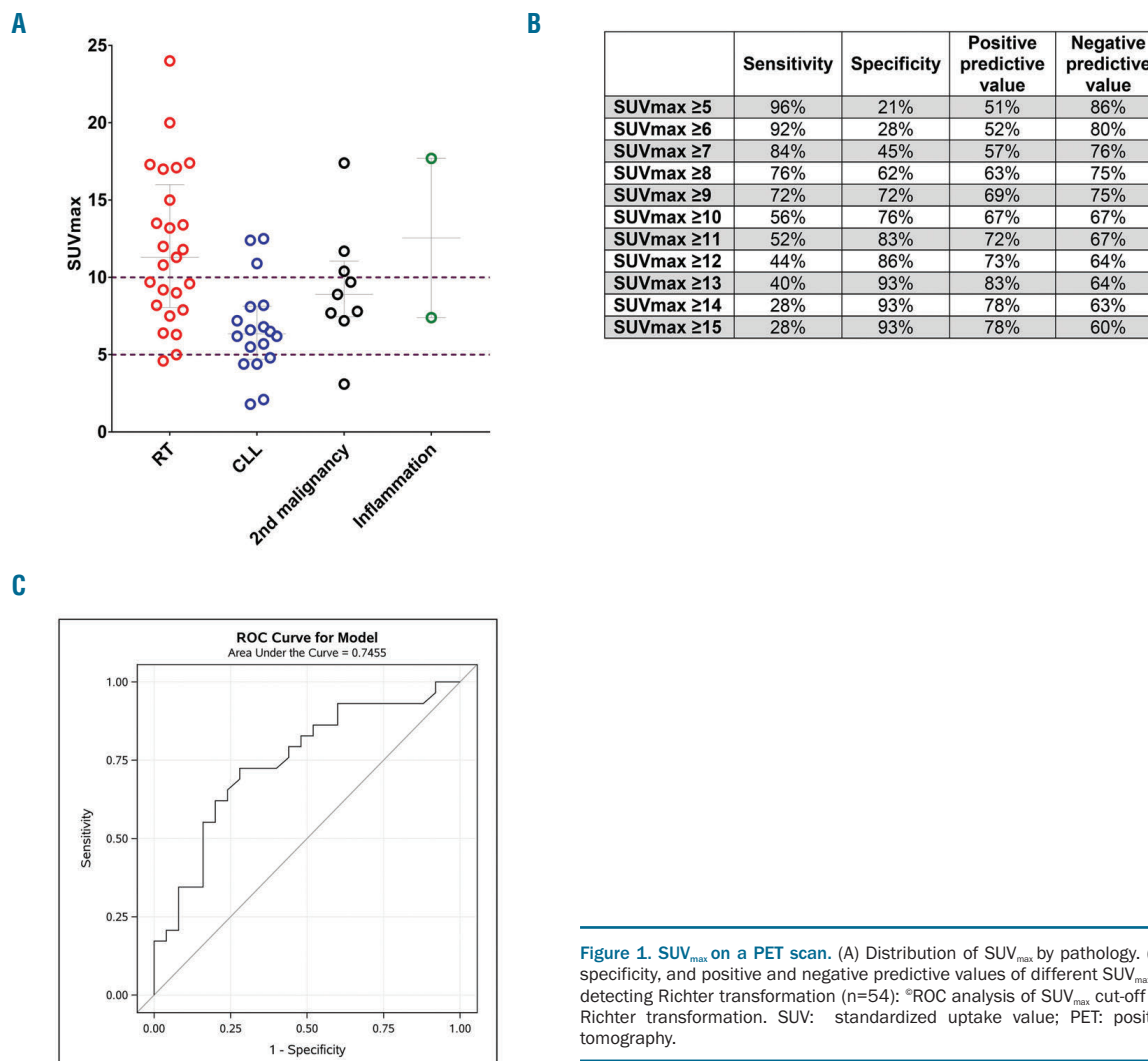
A

B

	Sensitivity	Specificity	Positive predictive value	Negative predictive value
SUVmax ≥5	96%	21%	51%	86%
SUVmax ≥6	92%	28%	52%	80%
SUVmax ≥7	84%	45%	57%	76%
SUVmax ≥8	76%	62%	63%	75%
SUVmax ≥9	72%	72%	69%	75%
SUVmax ≥10	56%	76%	67%	67%
SUVmax ≥11	52%	83%	72%	67%
SUVmax ≥12	44%	86%	73%	64%
SUVmax ≥13	40%	93%	83%	64%
SUVmax ≥14	28%	93%	78%	63%
SUVmax ≥15	28%	93%	78%	60%

C

Figure 1. SUV$_{max}$ on a PET scan. (A) Distribution of SUV$_{max}$ by pathology. (B) Sensitivity, specificity, and positive and negative predictive values of different SUV$_{max}$ thresholds in detecting Richter transformation (n=54): [a]ROC analysis of SUV$_{max}$ cut-off for identifying Richter transformation. SUV: standardized uptake value; PET: positron emission tomography.

sitivity (91%) and specificity (95%) using a cut-off of SUV$_{max}$ ≥10.

B-cell receptor pathway inhibitors (BCRi) such as Bruton tyrosine kinase (BTK) inhibitor ibrutinib and phosphatidylinositol 3-kinase (PI3K) inhibitor idelalisib have significantly improved the outcome of CLL. However, CLL patients who progress through BCRi often develop clinically aggressive disease.[9-12] Recently Mato et al.[12] reported that in CLL patients who progressed on a BCRi therapy and were screened for participation in a clinical trial of venetoclax, SUV$_{max}$ ≥10 on PET scan had a low sensitivity (71%) and specificity (50%) in detecting RT. However, this study included only eight patients with RT. Given the increasing use of BCRi in clinical practice and the importance of differentiating between RT and progressive CLL, we conducted a single-institution study to further evaluate the diagnostic role of PET scan in CLL patients receiving BCRi therapy with suspected disease progression.

CLL patients on a BCRi treatment who underwent a PET scan for evaluation of potential disease progression between November 2012 and March 2019 were identified from the Mayo Clinic CLL Database.[13] CLL patients with no clinical suspicion of disease progression who underwent a PET scan for restaging (i.e., evaluation of treatment response) were excluded. Patients with known

RT or a second malignancy who underwent a PET scan for initial staging or restaging were also excluded. PET images were centrally reviewed by a nuclear radiologist (MSB). Pathology slides in a subset of patients were independently reviewed by a hematopathologist (MS) for verification.

Between November 2012 and March 2019, 92 CLL patients, who were on a BCRi (ibrutinib [n=90] or idelalisib [n=2]) and underwent a PET scan to evaluate for potential disease progression, were identified (Table 1). The median age at BCRi initiation was 68 years (range: 43-89), and 69 (75%) were male. Sixty (80%) patients had unmutated immunoglobulin heavy-chain variable region (IGHV). The CLL fluorescence in situ hybridization (FISH) panel showed del(17p) in 19 (28%) and del(11q) in 16 (23%) patients. The median time from BCRi initiation to PET scan was 14 months (range: 0.3-62 months). The median SUV$_{max}$ was 7.0 (range: 1.1-27.3). The number of patients with a SUV$_{max}$ of <5 was 33 (36%), ≥5 but <10 was 34 (37%), and ≥10 was 25 (27%). After the PET scan, 38 patients did not undergo tissue biopsy; among those, 34 were treated as persistent CLL (median SUV$_{max}$ 3.6 [range: 1.1-10.3]), two were treated as presumed RT (SUV$_{max}$ 19.5 and 27.3, respectively), and two died before a biopsy could be performed (SUV$_{max}$ 7.8 and 13.5, respectively). There were no differences in baseline characteris-

Table 2. SUV$_{max}$ in patients with different pathology on biopsy (n=54).

Pathology	N	Median SUV$_{max}$ (range)	SUV$_{max}$ <5	SUV$_{max}$ ≥5 but <10	SUV$_{max}$ ≥10
Richter transformation	25	11.3 (4.6-24.0)	1	10	14
Progressive CLL	18	6.4 (1.8-12.5)	5	10	3
Second malignancy*	9	8.9 (3.1-17.4)	1	5	3
Inflammation†	2	12.6 (7.4-17.7)	0	1	1
Total	54	8.6 (1.8-24.0)	7	26	21

*Six with recurrent malignancy (two metastatic squamous cell carcinoma of the skin, one each with low grade B-cell lymphoma with plasmacytic differentiation, metastatic melanoma, metastatic Merkel cell carcinoma, and metastatic lung cancer) and three with new malignancy (one each with renal cell carcinoma, soft tissue sarcoma, and metastatic carcinoma of unknown primary origin). †One with reactive gastropathy, the other with acute and chronic granulomatous changes due to herpes simplex virus. SUV: standardized uptake value; CLL: chronic lymphocytic leukemia.

tics between patients who underwent a biopsy *versus* those who did not.

Fifty-four patients (median SUV$_{max}$ of 8.6 [range: 1.8-24.0]) underwent a tissue biopsy. The median time from PET scan to biopsy was 4 days (range: 0-40). The biopsy was targeted towards either the area of maximum SUV (n=29, median SUV$_{max}$ 7.8) or an alternative area that was easier to access (n=25; median SUV$_{max}$ 6.7, median SUV$_{max}$ difference=2.7 compared to the maximum SUV area). The biopsy sites included lymph node (n=34; 10 excisional and 24 core needle), soft tissue mass (n=9; two excisional and seven core needle), bone marrow (n=3), cerebrospinal fluid (n=1) and other organ (n=7; spleen [n=2, splenectomy], kidney, lung, bone [n=1 each, core needle], and stomach [n=2, esophagogastroduodenoscopy]).

The final pathology was RT in 25 (46%) patients (21 with DLBCL and four with classical Hodgkin lymphoma), CLL in 18 (33%; 15 can be classified as histologically aggressive CLL according to the World Health Organization 2016 criteria, with the presence of expanded proliferation centers that are broader than a 20x field or becoming confluent, or a Ki-67 proliferation index >40%), second malignancy in nine (17%; six with recurrent malignancy, three with new malignancy), and inflammation in two (4%) patients (Table 2).

The median SUV$_{max}$ was 11.3 (range: 4.6-24.0) for patients with RT, 6.4 (range: 1.8-12.5) for patients with progressive CLL (P<0.001 *vs.* RT; Figure 1A), and 8.9 (range: 3.1-17.4) for patients with a second malignancy (P=0.18 *vs.* RT; Figure 1A). Only 1 of 7 patients with a SUV$_{max}$ <5 had RT. In patients with a SUV$_{max}$ ≥5 but <10, 10 of 26 (38%) had RT; and in patients with a SUV$_{max}$ ≥10, 14 of 21 (67%) had RT. The sensitivity and specificity for identifying RT (*vs.* other pathology) using a threshold of SUV$_{max}$ ≥5 was 96% and 21%, respectively; and using a threshold of SUV$_{max}$ ≥10 was 56% and 76%, respectively (Figure 1B). The negative predictive value (NPV) of SUV$_{max}$ <5 in predicting RT was 86%, and the positive predictive value (PPV) of SUV$_{max}$ ≥10 in predicting RT was 67%. Using the ROC analysis, a threshold of SUV$_{max}$ ≥9 was determined to be the best discriminator for detecting RT *vs.* other pathology in all 54 patients who underwent a biopsy, with a sensitivity of 72% and specificity of 72% (Figure 1C). The PPV and NPV of this cut-off was 69% and 75%, respectively. Additional results regarding ibrutinib hold and survival after PET are available in the *Online Supplementary Materials and Methods.*

Our study confirms findings by Mato *et al.*[12] In CLL patients receiving a BCRi who underwent a PET scan for evaluation of potential disease progression, although a SUV$_{max}$ of 9 was the best cut-off to discriminate RT *versus* other pathology, the sensitivity (72%) and specificity (72%) at this cut-off were both low. The sensitivity

(96%) and NPV (86%) for identification of RT using a lower cut-off of SUV$_{max}$ ≥5 was excellent, but the specificity (76%) and PPV (67%) remained low using a higher cut-off of SUV$_{max}$ ≥10. The role of PET in detecting RT needs to be revisited in the novel agent era.

While tissue biopsy still remains the gold standard for diagnosing RT in CLL patients with suspected transformation of disease, a PET scan helps by i) determining if a biopsy should be considered if the SUV$_{max}$ exceeds a certain cut-off; and ii) identifying the area with the highest FDG uptake for an excisional or core needle biopsy. Mato *et al.*[12] reported a sensitivity of 71% and a specificity of only 4% using a cut-off of SUV$_{max}$ ≥5 and a sensitivity of 71% and a specificity of 50% using a cut-off of SUV$_{max}$ ≥10 in CLL patients who progressed after BCRi. In our study, a cut-off of SUV$_{max}$ ≥5 had a sensitivity of 96% and a specificity of 21%, while a cut-off of SUV$_{max}$ ≥10 had a sensitivity of 56% and a specificity of 76%. We propose using SUV$_{max}$ ≥5 as the cut-off to strongly consider biopsy given the high sensitivity (96%) and NPV (86%) in our study. In our cohort, only one patient with SUV$_{max}$ <5 was diagnosed with RT on excisional biopsy of a cervical lymph node that was enlarging asynchronously. In contrast, approximately 40% of the patients with a SUV$_{max}$ ≥5 but <10 and two-thirds of the patients with a SUV$_{max}$ ≥10 were diagnosed with RT, emphasizing the need to perform a tissue biopsy in patients with a SUV$_{max}$ ≥5.

CLL progression on BCRi can be associated with a relatively high SUV in a PET scan, as ibrutinib can change the metabolism of CLL cells by increasing glucose uptake,[14,15] and CLL progression developed on ibrutinib is often clinically aggressive.[9-12] It is important not to assume a diagnosis of RT even with a high SUV$_{max}$ (e.g., ≥10), and tissue biopsy is still the gold standard to make a diagnosis.

The strengths of our study include a relatively homogenous study population from a single institution (CLL patients on BCRi therapy who underwent PET scan for the evaluation of disease progression), and a central review of PET images for SUV measurement/confirmation. The limitations include the retrospective design, lack of a tissue biopsy in a subset of patients (although the majority had a low SUV$_{max}$), incomplete central pathology review, potential referral bias, and the small cohort size.

In summary, the role of a PET scan in identifying RT in the era of novel agent CLL therapy has evolved owing to the changing biology of CLL with novel targeted therapy. A biopsy should be strongly considered in patients receiving BCRi therapy with suspected RT with a SUV$_{max}$ ≥5 on PET. Prospective re-examination of the diagnostic value of PET in CLL patients with suspected transformation in the novel agent era with larger cohorts of patients and with central imaging and pathology review is warranted.

Yucai Wang,[1] Kari G. Rabe,[2] Michael S. Bold,[3] Min Shi,[4] Curtis A. Hanson,[4] Susan M. Schwager,[1] Timothy G. Call,[1] Saad S. Kenderian,[1] Eli Muchtar,[1] Suzanne R. Hayman,[1] Amber B. Koehler,[1] Amie L. Fonder,[1] Asher A. Chanan-Khan,[5] Daniel L. Van Dyke,[6] Susan L. Slager,[2] Neil E. Kay,[1] Wei Ding,[1] Jose F. Leis[7] and Sameer A. Parikh[1]

[1]Division of Hematology, Mayo Clinic, Rochester, MN; [2]Division of Biomedical Statistics and Informatics, Mayo Clinic, Rochester, MN; [3]Department of Radiology, Mayo Clinic, Rochester, MN; [4]Division of Hematopathology, Mayo Clinic, Rochester, MN; [5]Division of Hematology and Medical Oncology, Mayo Clinic, Jacksonville, FL; [6]Division of Laboratory Genetics and Genomics, Mayo Clinic, Rochester, MN and [7]Division of Hematology and Medical Oncology, Mayo Clinic, Phoenix, AZ, USA

Correspondence:
SAMEER A. PARIKH - parikh.sameer@mayo.edu

References

1. Parikh SA, Kay NE, Shanafelt TD. How we treat Richter syndrome. Blood. 2014;123(11):1647-1657.
2. Rossi D, Gaidano G. Richter syndrome: pathogenesis and management. Semin Oncol. 2016;43(2):311-319.
3. Rossi D, Spina V, Gaidano G. Biology and treatment of Richter syndrome. Blood. 2018;131(25):2761-2772.
4. Wang Y, Tschautscher MA, Rabe KG, et al. Clinical characteristics and outcomes of Richter transformation: Experience of 204 patients from a single center. Haematologica. 2020;105(3):765-773.
5. Bruzzi JF, Macapinlac H, Tsimberidou AM, et al. Detection of Richter's transformation of chronic lymphocytic leukemia by PET/CT. J Nucl Med. 2006;47(8):1267-1273.
6. Mauro FR, Chauvie S, Paoloni F, et al. Diagnostic and prognostic role of PET/CT in patients with chronic lymphocytic leukemia and progressive disease. Leukemia. 2015;29(6):1360-1365.
7. Falchi L, Keating MJ, Marom EM, et al. Correlation between FDG/PET, histology, characteristics, and survival in 332 patients with chronic lymphoid leukemia. Blood. 2014;123(18):2783-2790.
8.. Michallet AS, Sesques P, Rabe KG, et al. An 18F-FDG-PET maximum standardized uptake value > 10 represents a novel valid marker for discerning Richter's syndrome. Leuk Lymphoma. 2016;57(6):1474-1477.
9. Jain P, Keating M, Wierda W, et al. Outcomes of patients with chronic lymphocytic leukemia after discontinuing ibrutinib. Blood. 2015;125(13):2062-2067.
10. Maddocks KJ, Ruppert AS, Lozanski G, et al. Etiology of Ibrutinib therapy discontinuation and outcomes in patients with chronic lymphocytic leukemia. JAMA Oncol. 2015;1(1):80-87.
11. Jain P, Thompson PA, Keating M, et al. Long-term outcomes for patients with chronic lymphocytic leukemia who discontinue ibrutinib. Cancer. 2017;123(12):2268-2273.
12. Mato AR, Wierda WG, Davids MS, et al. Utility of PET-CT in patients with chronic lymphocytic leukemia following B-cell receptor pathway inhibitor therapy. Haematologica. 2019;104(11):2258-2264.
13. Parikh SA, Rabe KG, Call TG, et al. Diffuse large B-cell lymphoma (Richter syndrome) in patients with chronic lymphocytic leukaemia (CLL): a cohort study of newly diagnosed patients. Br J Haematol. 2013;162(6):774-782.
14. Galicia-Vazquez G, Smith S, Aloyz R. Del11q-positive CLL lymphocytes exhibit altered glutamine metabolism and differential response to GLS1 and glucose metabolism inhibition. Blood Cancer J. 2018; 8(1):13.
15. Galicia-Vazquez G, Aloyz R. Metabolic rewiring beyond Warburg in chronic lymphocytic leukemia: How much do we actually know? Crit Rev Oncol Hematol. 2019;134:65-70.

Peripheral neuropathy and monoclonal gammopathy of undetermined significance: a population-based study including 15,351 cases and 58,619 matched controls

Monoclonal gammopathy of undetermined significance (MGUS) is a common benign precursor condition of multiple myeloma (MM) and related disorders.[1,2] MGUS is considered asymptomatic but has been shown to be associated with peripheral neuropathy (PN).[3] However, the literature is unclear regarding the prevalence, clinical implications, and even the existence of MGUS-associated PN.[4] We therefore conducted a large population-based study of MGUS and PN. We found PN to be truly associated with MGUS and under-recognized in clinical practice. Furthermore, PN was associated with a 2.9-fold risk of a light-chain amyloidosis (AL).

We included individuals with MGUS diagnosed in Sweden between 1986-2013, as has been described previously.[5] Four controls that were alive and free of lymphoproliferative disease were matched to each case on the day of MGUS diagnosis by sex, year of birth, and county of residence. Data from Swedish national registries were cross-linked to participants using a unique identification number.

The primary endpoint was PN as recorded in the Swedish Patient Registry using International Classification of Diseases (ICD) codes by Swedish physicians recording their clinical diagnoses. However, underlying symptoms or diagnostic testing leading to PN diagnosis were not available. Acute inflammatory neuropathies and critical care neuropathy were excluded. Symptomatic codes were included but were excluded in a sensitivity analysis. We assessed the prevalence of PN in the full cohort and followed those who did not have PN at inclusion until PN or censoring at death as recorded in the Swedish Cause of Death Registry, lymphoproliferative disease as recorded in the Swedish Cancer Registry, or end of follow-up. We then estimated hazard ratios (HR) using Cox proportional hazard regression adjusting

for age, sex, and year of inclusion. PN is common in the general population but is often undetected.[6] Individuals with MGUS, who are under medical surveillance, might therefore have more diagnoses of a PN that might otherwise have stayed subclinical in the control population. To mitigate this bias, we also stratified the cohort by diabetes mellitus (DM) and repeated the analysis. DM patients are under regular medical surveillance, similar to that of patients with MGUS. Furthermore, PN is a well-known feature of DM, and DM patients often undergo PN screening during follow-up, presenting a more appropriate comparison group.

In a secondary analysis, we assessed the association of PN and MGUS progression and death. We included all participants with MGUS and considered PN as the exposure. We then followed them until death or the diagnosis of MM, Waldenström's macroglobulinemia (WM), and AL in four separate analyses while censoring at the other endpoints or loss to follow-up. In order to prevent immortal time bias in those participants who developed PN after MGUS diagnosis, we included PN as a time-dependent covariate in a Cox proportional hazard regression model. The models were adjusted for age, sex, and year of MGUS diagnosis, as well as for DM when assessing risk of death.

A total of 15,351 participants with MGUS and 58,619 matched controls were included in the study. The prevalence of PN was higher in participants with MGUS than controls (6.5% *vs.* 2.8%) (Table 1). The reported prevalence of PN varies widely but more recent observational studies estimate the prevalence at 15-20%.[7] Therefore, these findings, based on clinical diagnoses of PN, indicate under-recognition of PN during the clinical care of individuals with MGUS.

Individuals with MGUS had 2.7-fold risk of PN compared to matched controls (HR=2.7; 95% confidence interval [95%CI]: 2.4-3.1; *P*<0.001). After stratification for DM, we found MGUS and DM to be associated with higher risk of PN as compared to controls without MGUS and DM (MGUS alone: HR=3.0; 95%CI: 2.6-3.4; *P*<0.001 and DM alone: HR=3.6; 95%CI: 3.2-4.2; *P*<0.001).

Table 1. Baseline characteristics of study participants in the original cohort and after additional stratification for diabetes mellitus (DM) as well as results of a Cox proportional hazard regression model of risk of peripheral neuropathy (PN) for each group.

| | Original cohort | | After DM stratification | | | |
	MGUS	Control	MGUS alone	DM alone	MGUS+DM	Control
N	15,351	58,619	12,818	7,953	2,533	50,666
Median age (years)	73	72	72	74	74	72
Age range (years)	18-104	18-101	18-104	26-97	26-95	18-101
% male	51%	51%	50%	58%	58.1	50%
N by year of inclusion						
1986-1995	22%	22%	22%	23%	22%	21%
1996-2005	33%	33%	33%	35%	31%	33%
2006-2013	45%	45%	45%	42%	47%	46%
PN	996 (6.5%)	1,644 (2.8%)	681 (5.3%)	620 (7.8%)	315 (12.4%)	1024 (2.0%)
before MGUS/matching (% of PN)	549 (55%)	770 (47%)	376 (55%)	310 (50%)	173 (55%)	460 (45%)
Median follow-up (years)	4.0	6.1	4.1	6.1	3.7	6.1
Risk of PN in HR (95% CI)[1]	2.7 (2.4-3.1)***	Reference	–	–	–	–
	–	–	3.0 (2.6-3.4)***	3.6 (3.2-4.2)***	7.5 (6.3-9.1)***	Reference
	–	–	0.8 (0.7-1.0)*	Reference	2.1 (1.7-2.5)***	0.3 (0.2-0.3)***

[1]Adjusted for sex, age, and year of inclusion. **P*<0.05, ****P*<0.001, MGUS: monoclonal gammopathy of undetermined significance; HR: hazard ratio, 95% CI: 95% confidence interval; N: number.
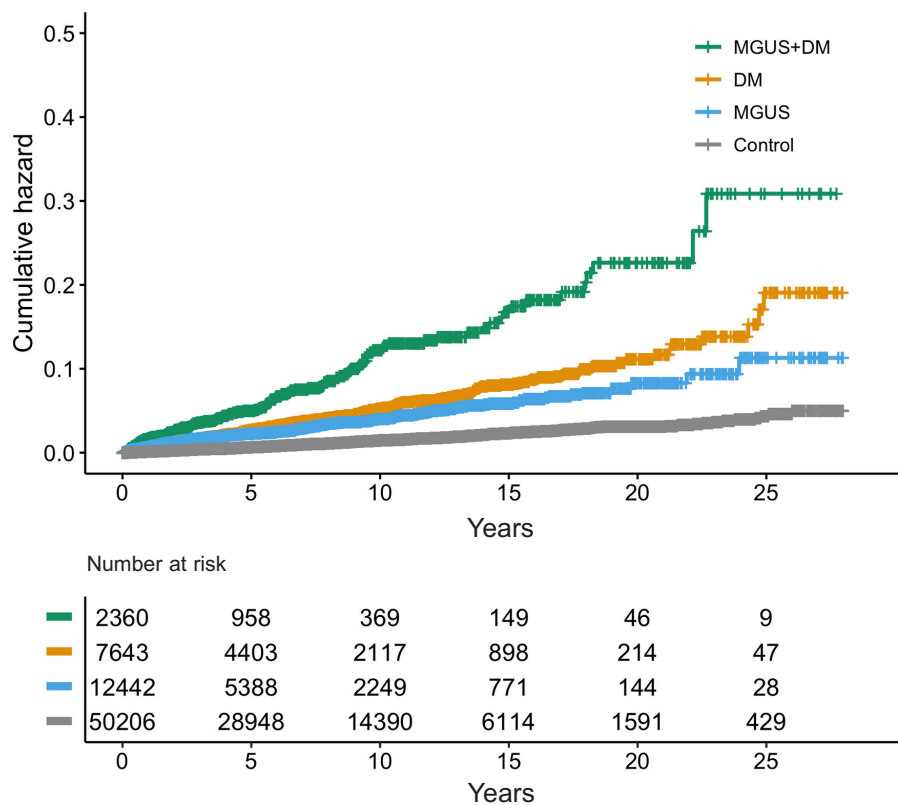
Figure 1. Kaplan-Meier graph illustrating the cumulative hazard of peripheral neuropathy (PN) throughout the study period by assigned study group. MGUS: monoclonal gammopathy of undetermined significance; DM: diabetes mellitus.

MGUS was associated with a 0.8-fold risk of PN as compared to DM (HR=0.8; 95%CI: 0.7-0.9, P=0.02). Participants with MGUS and DM had a 2.1-fold risk of PN as compared to those with DM alone (MGUS and DM: HR= 2.1; 95%CI: 1.7-2.5; P<0.001) (Table 1 and Figure 1). Although these findings could suggest a synergistic effect of MGUS and DM, it is more likely that excess PN caused by MGUS is being detected during DM or MGUS follow-up in individuals with DM and MGUS as compared to those with DM alone. These findings indicate that PN is truly associated with MGUS, contradicting previous findings that questioned this.[4]

In the secondary analysis, 1,368 participants progressed to MM, 449 progressed to WM, and 173 progressed to AL (Table 2). PN was associated with lower risk of MM (HR=0.7; 95%CI: 0.5-0.9; P=0.02) but was not associated with WM progression (HR=1.3; 95%CI: 0.9-1.9; P=0.2). PN has been shown to be more common in IgM MGUS[3] that rarely progresses to MM, but rather to WM,[8] potentially leading to selection bias. Unfortunately, isotype data are not available for this cohort making it difficult to interpret these results. However, these findings could indicate that PN is unlikely to be associated with increased risk of MM or WM, suggesting that the development of PN in MGUS might be unrelated to progression of the underlying plasma cell disorder.

Interestingly, we found PN to be associated with a 2.9-fold risk of MGUS progression to AL (HR=2.9; 95%CI: 1.8-4.6; P<0.001). Furthermore, we found that nine out of the 11 individuals (82%) with PN at diagnosis who later progressed to AL did so within a year of MGUS diagnosis. Diagnosis of AL can be difficult, leading to under-recognition and a delay in diagnosis of AL.[9] Furthermore, virtually all cases of AL are preceded by MGUS,[10] so it is likely that these participants had AL, not MGUS, at inclusion. These findings stress the importance

of a thorough evaluation for AL in individuals with MGUS and PN, especially at MGUS diagnosis.

We found PN to be associated with a 1.3-fold risk of death in MGUS (HR=1.3; 95%CI: 1.2-1.5; P<0.001). When associated with other disorders, PN can lead to falls and fractures[11-13] which might contribute to this increased risk of death. However, PN is also associated with various other diseases that might lead to increased risk of death, such as other cancers and alcohol misuse.[6] Therefore, it is unclear whether this represents a causal relationship. Further studies are needed to validate these findings.

Our study has several strengths. We included a nationwide population of 15,351 MGUS cases and 58,619 matched controls diagnosed over a 28-year period. Data were acquired with high accuracy and completeness from well-established registries. As far as we know, this is the largest study of MGUS-associated PN so far. Secondly, by including clinical data from routine care, the study provides an insight into the real-world care of individuals with MGUS. Finally, by also stratifying participants for DM, we mitigated detection bias that would otherwise have affected the results of this type of study.

The study also has important limitations. Firstly, PN diagnoses were acquired from diagnostic coding without data on the underlying symptoms or diagnostic tests, relying on detection, and accurate diagnosis of PN by physicians. By stratifying for DM, we mitigated some of the effects of any unequal detection and reporting of PN in the cohort. Secondly, study participants were not screened for MGUS, but were diagnosed during the work-up of other medical problems, leading to biased selection of participants with other medical problems into the MGUS group. Furthermore, MGUS might have been diagnosed as a result of PN. However, this applies to all real-world MGUS populations, and individuals with PN before MGUS diagnosis were excluded from analyses

Table 2. Baseline characteristics, rates and incidence of progression, and risk of progression to MM, WM, and AL as well as death for study participants with MGUS with and without PN as assessed by Cox proportional hazard regression with PN as a time dependent covariate.

	MGUS without PN	MGUS and PN
N	14,355	996
Male	51%	63%
Median age	73	69
Median follow-up (years)	4.0	3.0
Progressed to MM (incidence[1])	1,328 (1.6)	40 (1.0)
HR (95%CI)[2]	–	0.7 (0.5-0.9)*
Progressed to WM (incidence[1])	422 (0.5)	27 (0.7)
HR (95%CI)[2]	–	1.2 (0.8-1.8)
Progressed to AL (incidence[1])	153 (0.2)	21 (0.5)
HR (95%CI)[2]	–	2.3 (1.5-3.7)***
Death (mortality rate[1])	5,522 (6.8)	315 (8.0)
HR (95%CI)[3]	–	1.3 (1.2-1.5)***

[1]Incidence per 100 person-years. [2]Adjusted for sex, age, and year of inclusion. [3]Adjusted for sex, age, year of inclusion, and diabetes mellitus (DM). ***$P<0.001$, MGUS: monoclonal gammopathy of undetermined significance; PN: peripheral neuropathy; MM: multiple myeloma; WM: Waldenström's macroglobulinemia; AL: amyloid light-chain amyloidosis; HR: hazard ratio; 95%CI: 95% confidence interval.

assessing risk of PN. Thirdly, and unfortunately, immunoglobulin isotype data are not available for this cohort, and some isotypes, especially IgM, might be associated with higher risk of PN and skew the average risk for the whole cohort so that it might not be representative for each isotype. Furthermore, this limits the interpretation of analyses of progression to MM and WM. Prospective studies including screening for MGUS and PN are needed to validate these findings. We are currently conducting a population-based screening study for MGUS (*clinincaltrials.gov identifier: NCT03327597*). A substudy is ongoing assessing the prevalence, symptoms, clinical impact, and associated disease factors of MGUS-associated PN.

In conclusion, in this large population-based study, including 15,351 MGUS individuals and 58,619 matched controls, we found that a significant proportion of individuals with MGUS have clinically evident PN (6.5%) and that PN is truly associated with MGUS. In addition, our findings suggest under-recognition of PN in the real-world care of individuals with MGUS. Interestingly, we found PN to be associated with a 2.9-fold risk of AL and that PN is not associated with increased risk of MM or WM. PN was associated with increased risk of death, but multiple confounders make it impossible to establish a causal relationship. When associated with other disorders, PN leads to falls, fractures,[11-13] and lower quality of life.[14] It is, therefore, reasonable to assume that PN causes considerable morbidity in MGUS that may go unrecognized. Our findings should help increase awareness of MGUS as a cause of PN among all clinicians and promote closer monitoring of individuals with MGUS for symptoms of PN.

Sæmundur Rögnvaldsson,[1] Vilhjálmur Steingrímsson,[1] Ingemar Turesson,[2] Magnus Björkholm,[3] Ola Landgren[4] and Sigurður Yngvi Kristinsson[1,3]

[1]*Faculty of Medicine, University of Iceland, Reykjavík, Iceland;* [2]*Skåne University Hospital, Malmö/Lund, Sweden;* [3]*Department of Medicine, Karolinska University Hospital Solna and Institutet, Stockholm, Sweden and* [4]*Myeloma Service, Department of Medicine, Memorial Sloan-Kettering Cancer Center, New York, NY, USA*

Correspondence:
SAEMUNDUR ROGNVALDSSON - saer2@hi.is

References

1. Kyle RA, Therneau TM, Rajkumar SV, et al. Prevalence of monoclonal gammopathy of undetermined significance. N Engl J Med. 2006;354(13):1362-1369.
2. Dispenzieri A, Katzmann JA, Kyle RA, et al. Prevalence and risk of progression of light-chain monoclonal gammopathy of undetermined significance: a retrospective population-based cohort study. Lancet. 2010;375(9727):1721-1728.
3. Gosselin S, Kyle RA, Dyck PJ. Neuropathy associated with monoclonal gammopathies of undetermined significance. Ann Neurol. 1991;30(1):54-61.
4. Bida JP, Kyle RA, Therneau TM, et al. Disease associations with monoclonal gammopathy of undetermined significance: a population-based study of 17,398 patients. Mayo Clin Proc. 2009;84(8):685-693.
5. Kristinsson SY, Bjo M, Goldin LR, McMaster ML, Turesson I, Landgren O. Risk of lymphoproliferative disorders among first-degree relatives of lymphoplasmacytic lymphoma / Waldenström macroglobulinemia patients: a population-based study in Sweden. Blood. 2008;112(8):3052-3056.
6. Hanewinckel R, van Oijen M, Ikram MA, van Doorn PA. The epidemiology and risk factors of chronic polyneuropathy. Eur J Epidemiol. 2016;31(1):5-20.
7. Steiner N, Schwärzler A, Göbel G, Löscher W, Gunsilius E. Are neurological complications of monoclonal gammopathy of undetermined significance underestimated? Oncotarget. 2017;8(3):5081-5091.
8. Kyle RA, Therneau TM, Rajkumar SV, et al. Long-term follow-up of IgM monoclonal gammopathy of undetermined significance. Blood. 2003;102(10):3759-3764.
9. Lousada I, Comenzo RL, Landau H, Guthrie S, Merlini G. Light chain amyloidosis: patient experience survey from the Amyloidosis Research Consortium. Adv Ther. 2015;32(10):920-928.
10. Weiss BM, Hebreo J, Cordaro D, Roschewski MJ, Abbott KC, Olson SW. Monoclonal gammopathy of undetermined significance (MGUS) precedes the diagnosis of AL amyloidosis by up to 14 years. Blood. 2011;118(21):1827.
11. Strotmeyer ES, Cauley JA, Schwartz AV, et al. Nontraumatic fracture risk with diabetes mellitus and impaired fasting glucose in older white and black adults. Arch Intern Med. 2005;165(14):1612.
12. Timar B, Timar R, Gaita L, Oancea C, Levai C, Lungeanu D. The impact of diabetic neuropathy on balance and on the risk of falls in patients with type 2 diabetes mellitus: a cross-sectional study. PLoS One. 2016;11(4):e0154654.
13. Marshall TF, Zipp GP, Battaglia F, Moss R, Bryan S. Chemotherapy-induced-peripheral neuropathy, gait and fall risk in older adults following cancer treatment. J Cancer Res Pract. 2017;4(4):134-138.
14. Benbow SJ, Wallymahmed ME, MacFarlane IA. Diabetic peripheral neuropathy and quality of life. QJM. 1998;91(11):733-737.

Long-term outcomes after splenectomy in children with immune thrombocytopenia: an update on the registry data from the Intercontinental Cooperative ITP Study Group

Immune thrombocytopenic purpura (ITP) is an acquired immune-mediated disease characterized by a decrease in platelet count due to antiplatelet autoantibody-mediated increased platelet destruction and, in some cases, associated impaired platelet production.[1]

There has been a decline in the number of splenectomies performed as a second-line treatment after the introduction of new therapies, such as thrombopoietin-receptor agonists. However, the current availability of long-term data on these new second-line therapeutic options seems to suggest that splenectomy remains the more effective second-line intervention in ITP.[2] Therefore, data on long-term outcomes of splenectomy in children are relevant.

The Splenectomy Registry of the Intercontinental Cooperative ITP Study (ICIS) Group collects information regarding children who underwent splenectomy to treat ITP, including perioperative management and follow-up data. A report of the first 134 patients was published in 2007.[3] The present study aims to update the findings of the ICIS Splenectomy Registry by analyzing over a decade of new data, with a focus on long-term outcomes of children with primary ITP.

Details of the data collection forms of the Splenectomy Registry have been previously described.[3] Investigators included patients with ITP in whom splenectomy was planned. For the analysis, we excluded records in which splenectomy was not reported or no platelet counts were available at follow-up. Investigators sought local ethics approval prior to patient entry, according to the regulatory requirements of each institution. Response to splenectomy was classified as a complete response (CR: ≥60% of platelet counts performed ≥1 month post-splenectomy ≥100x10⁹/L), response (R: ≥60% of platelet counts ≥1 month post-splenectomy ≥30x10⁹/L), or no response (NR: <60% of platelet counts ≥1 month post-splenectomy ≥30x10⁹/L).[4] At least two counts after the first month post-splenectomy were required for outcome assessment. Refractoriness was defined as either the failure to achieve at least R or loss of R after splenectomy + clinically relevant bleeding.[5]

Bleeding events were classified as major and clinically relevant non-major (CRNM) according to current definitions of the International Society on Thrombosis and Haemostasis for patients on anticoagulants.[6,7]

The trajectory of platelet counts over time was investigated using generalized estimating equations (GEE) models with basic splines to accommodate for the non-linear shape of the regression line. Predictors of response to splenectomy were explored using logistic regression analysis. Predictors associated with the outcome at $P \leq 0.20$ in univariable analysis were considered for multivariable modeling. For model performance, simple bootstrap with 200 replications was used to estimate the optimism corrected (internally validated) area under the Receiver Operating Characteristic (ROC) curve. Significance was set at an alpha of 0.05. Analysis was performed in R.

A total of 267 patients were entered in the Registry between June 1997 and September 2017 by 82 investigators from 63 institutions and 26 countries. Seventeen records were excluded due to incompleteness and 11 due to secondary ITP diagnosis. Hence, 239 patients were

included in the analysis. Eighty of those patients (80 of 239, 33%) came from a single institution (The Hospital for Sick Children [SickKids], Toronto, Canada). Patients at SickKids were identified using the ICD-9-CM and ICD-10-CA codes, which explains the large number of participants identified in this institution.

The median duration of follow-up was 25 months (25th-75th percentile: 7.8-53.4 months). One hundred and thirty-five patients (135 of 250, 54%) were females. Median age at the time of ITP diagnosis was 9.2 years (25th-75th percentile: 4.8-13.0 years).

Splenectomy was performed at a median age of 11.7 years (25th-75th percentile: 7.9-15.3 years). Sixty-two of the 239 patients (26%) had their splenectomy performed <1 year after diagnosis (i.e., before reaching chronic ITP status) and ten of those 62 patients (16%) had their splenectomy performed <3 months after ITP diagnosis (i.e., before reaching persistent ITP status).

There was one intra-abdominal bleeding event documented during surgery. Eleven patients (11 of 239, 5%), including the patient with intra-abdominal bleeding, received peri-procedural red blood cell transfusions. Twenty-four patients (24 of 239, 10%) had fever at a median of 41 hours post-procedure (range: 6-99 hours). No deaths or episodes of sepsis in the immediate post-operative period were recorded.

One-hundred and eighty-six patients were followed up for >6 months. No major bleeding events were reported on those patients. Sixteen patients (16 of 184, 8.7%) had a documented CRNM bleed; all cases were classified as CRNM bleed because of the need for hospitalization. Twenty patients (20 of 186, 11%) had at least one admission due to fever or infection and five patients (5 of 186, 2.7%) were reported to have had sepsis (one viral, one due to *Streptococcus B*) on long-term follow-up. A systematic review of studies conducted between 1966 and 1996 reported an incidence of invasive infection of 2.1% among 484 patients with ITP, including adults and children.[8] In comparison, a more recent report including nearly 10,000 adults with ITP estimated the cumulative incidence of sepsis at 11.1% in splenectomized *versus* 10.1% in non-splenectomized patients.[9] Age and the number of co-morbidities and longer follow-up of these patients (median of 25 months of total observation in our study *vs.* 35 months median time from surgery to sepsis in the adult study) were also associated with higher risk of sepsis and might explain the lower frequency seen in our study.

Trend of platelet count post-surgery in the first 30 days and up to 4 years post-surgery is shown in Figure 1. The peak platelet count after surgery was 549x10⁹/L (range: 5-1,944x10⁹/L) at a median of 7 days (range: 1-35 days). The median platelet count between 30-60 days post-surgery was 337x10⁹/L (25th-75th percentile: 128-493x10⁹/L). Generalized estimating equations showed a non-statistically significant decline in platelet count over time of 0.56x10⁹/L per month, 95%CI: 1.15-0.04, $P=0.08$, after the first month post-splenectomy.

Frequency of CR/R/NR is shown in Figure 2. Overall, 93% of patients showed CR/R; this frequency is slightly higher than that reported among adult patients[10] and might be explained by the high frequency of splenectomy performed before reaching chronic ITP status (26%) and by a relatively low number of patients who received second-line therapy (51 of 239, 21%). In addition, we observed a significant difference on the median time to surgery from ITP diagnosis before and after 2009 (median time: 1.7 years, 25th-75th percentile: 0.9-3.1 years, before and including 2009, and 3.2 years, 25th-75th percentile:

2.0-4.3 years after 2009) when standardized definitions for chronic and persistent ITP were published.[4] Importantly, the higher frequency of bleeding documented as the response category decreases (Figure 2), suggesting that the classification used in this study approximates clinically relevant outcomes.

Refractoriness was 1.7% (4 of 239) among all children and 2.6% (4 of 152) in children with ≥1 year of follow-up. These estimates of refractoriness are slightly lower than those for adult patients,[5] as we did not take into account administration of platelet-enhancing therapy on follow-up since administration of platelet-enhancing therapy at the time of each platelet count was not reported in the Registry.

Results of simple logistic regression are shown in Table 1. In multivariable analysis, both age at the time of surgery and average platelet count on the first 30 days post-splenectomy predicted CR/R. For every year increase in age at the time of surgery, the odds of CR/R increased by 1.18 (95%CI: 1.02-1.40) and for every 10×10^9/L increase in the average platelet count in the first month, the odds of response increased by 1.09 (95%CI: 1.05-1.16). In terms of model performance, the optimism-corrected area under the ROC curve was estimated as 0.87.
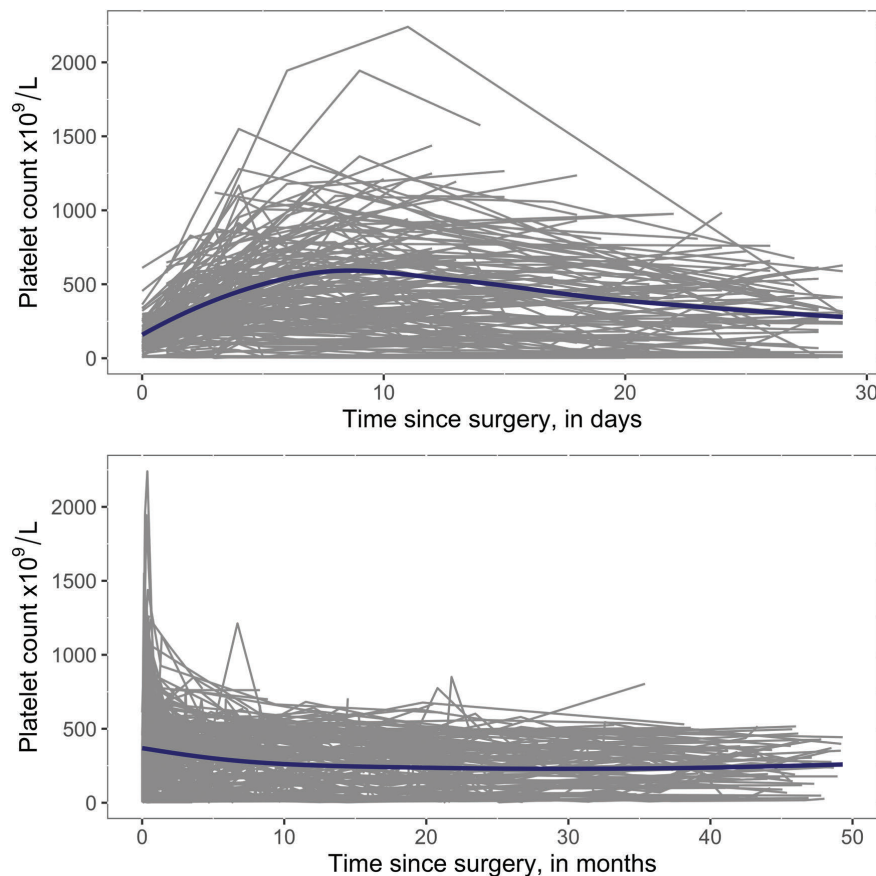

Figure 1. Spaghetti plot showing platelet counts over time. Spaghetti plots of platelet count for each individual over time after splenectomy. The upper panel shows platelet counts in the first 30 days and the lower panel shows platelet counts in the first 50 months of follow-up. The blue solid line represents the regression line (loess).

Table 1. Simple logistic regression results for complete response or response to splenectomy in primary immune thrombocytopenia (ITP).

Predictor	OR (95%CI)	P
Sex (male *vs.* female)	0.94 (0.30-3.05)	0.92
Age at time of ITP diagnosis, years	1.12 (0.99-1.29)	0.09
Age at time of surgery, years	1.15 (1.01-1.33)	0.04
Time from diagnosis to surgery, years	1.05 (0.86-1.41)	0.71
N. of previous treatment modalities	0.70 (0.41-1.24)	0.21
Second-line therapy (yes *vs.* no)	0.30 (0.09-0.97)	0.04
Steroids as part of initial therapy (yes *vs.* no)	1.02 (0.05-5.83)	0.99
IVIG as part of initial therapy (yes *vs.* no)	0.59 (0.03-3.25)	0.99
Platelet count immediately before splenectomy*	1.01 (1.01-1.03)	0.01
Average platelet count in first 30 days post-splenectomy*	1.09 (1.04-1.15)	<0.001
Any platelet count <100x10⁹/L in first 30 days post-splenectomy (no *vs.* yes)	26.32 (6.62-176.30)	<0.001
Peak platelet count in first 30 days post-splenectomy*	1.03 (1.01-1.06)	0.009

OR: odds ratio; CI: confidence interval; N: number; IVIG: intravenous immunoglobulin. *For every 10×10^9/L increase.
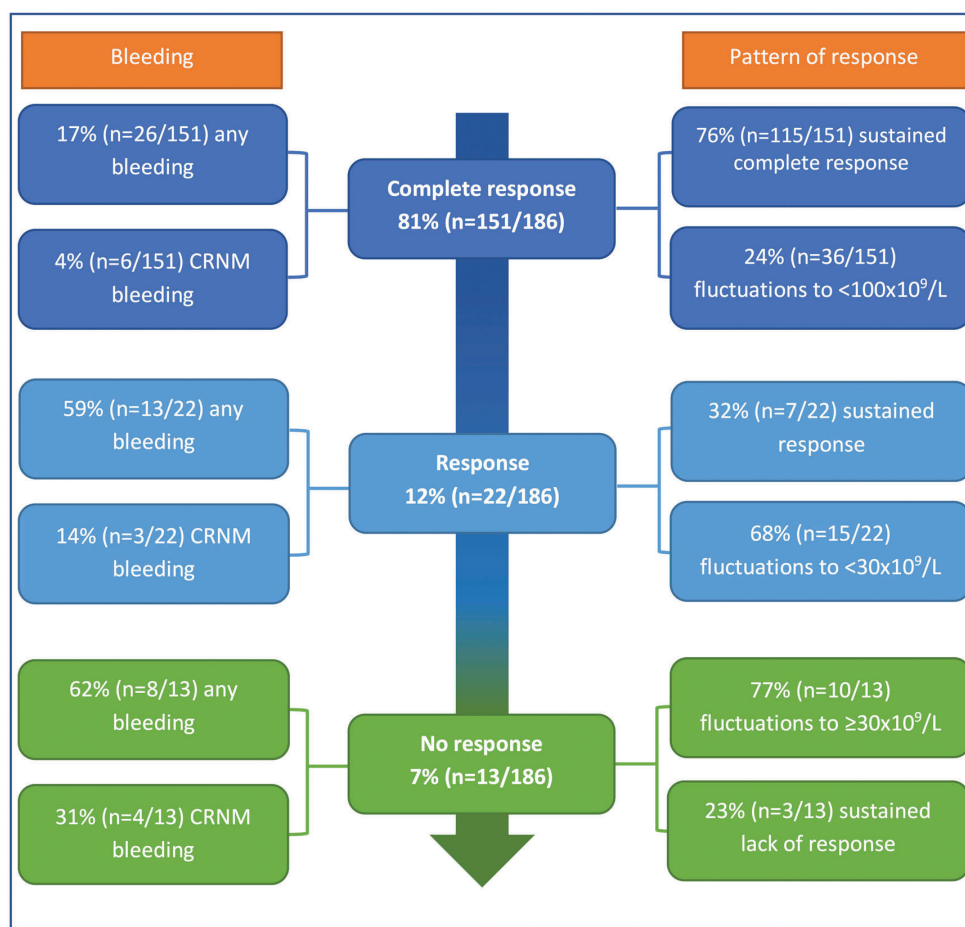
Figure 2. Frequency of response and bleeding in primary immune thrombocytopenia. Center column shows the overall response category and percentage of patients in each of them. Left column shows the frequency of bleeding and clinically relevant non-major (CRNM) bleeding according to response category. Right column shows the frequency of patterns of response in each response category depending on whether the response was sustained or there were fluctuations over time. n: number.

Older age at the time of diagnosis was reported to be an independent predictor of CR in the previous analysis of this Registry[3] and age at the time of diagnosis was highly correlated with age at the time of splenectomy in the present study. Younger age is considered a predictor of CR/R in adult patients with ITP undergoing splenectomy,[11,12] perhaps indicating that there might be a similar underlying mechanism among teenagers and young adults. Older age is also a predictor of chronic ITP in pediatrics,[13] further indicating a distinct pathophysiology in ITP affecting teenagers and young adults. It is also possible that patients who undergo splenectomy at a young age are also more refractory to treatment.

Higher platelet counts in the first month post-splenectomy was also an independent predictor of both CR/R in this population. Interestingly, higher platelet counts immediately before surgery, not having platelet counts $<100 \times 10^9$/L in the first 30 days post-splenectomy, and higher peak platelet count in the first 30 days post-splenectomy were predictors of CR/R in univariable analysis. Ahmed *et al.* reported that platelet count at the time of splenectomy was one of the predictors of CR/R in a cohort of 254 patients that included 87 children.[14] In addition, high platelet count in the first week after splenectomy has been shown to predict response in some studies conducted in adult patients, although results are

inconsistent.[10] A more recent study among 174 adults splenectomized for ITP showed that higher pre- and post-operative platelet count were predictors of response in univariable analysis.[12] Importantly, pre-surgical and early post-surgical platelet counts may be influenced by platelet enhancing therapy administered pre-operatively in addition to the thrombocytosis seen after splenectomy. Taken together, these observations indicate that individuals able to increase and sustain platelet counts in response to an intervention are more likely to show CR/R in the long term.

The present study has some limitations. For example, biases such as selection bias and information bias of an intercontinental registry cannot be ruled out. However, one-third of the patients included in the Registry come from a systematic search at a single center (SickKids) which could help, in part, overcome the issue of selection bias. In addition, the median follow-up time was 25 months, despite the fact that the registry has been open for two decades. Retention can be problematic in registries, particularly when they are voluntary. However, use of registry data can be beneficial as registries are also characterized by strong external validity in view of the heterogeneous populations included, thus better reflecting clinical practice.[15] In addition, the differential diagnosis in terms of primary or secondary ITP was left to the

decision of the treating physician, and therefore misclassification cannot be ruled out. However, the high frequency of response found herein suggests misclassification is unlikely and may not have impacted the results. Lastly, there was no specific protocol attached to the registry, and care of the patient was left to the discretion of the clinician, thus reflecting general practice.

In conclusion, splenectomy is a very effective approach for the management of selected children with primary ITP as evidenced by platelet count recovery. Although low, the risk of adverse events both peri-operative and in the long-term should be carefully considered when indicating this therapeutic modality. The only predictor of response available prior to indication of splenectomy is patient age; the older the patient, the higher the odds of response.

Maria L. Avila,[1,2] Nour Amiri,[1] Eleanor Pullenayegum,[2] Victor Blanchette,[1] Paul Imbach[3] and Thomas Kühne[4] on behalf of the Intercontinental Cooperative ITP Study Group

[1]Department of Pediatrics, University of Toronto, Division of Hematology/Oncology, The Hospital for Sick Children, Toronto, Ontario, Canada; [2]Child Health Evaluative Sciences, The Hospital for Sick Children, Toronto, Ontario, Canada; [3]Medical Faculty, University of Basel, Switzerland and [4]UKBB Universitäts-Kinderspital, Oncology/Hematology, Basel, Switzerland

Correspondence:
THOMAS KUEHNE - thomas.kuehne@ukbb.ch

References

1. Cooper N, Bussel J. The pathogenesis of immune thrombocytopaenic purpura. Br J Haematol. 2006;133(4):364-374.
2. Rodeghiero F. A critical appraisal of the evidence for the role of splenectomy in adults and children with ITP. Br J Haematol. 2018;181(2):183-195.
3. Kühne T, Blanchette V, Buchanan GR, et al. Splenectomy in children with idiopathic thrombocytopenic purpura: a prospective study of 134 children from the Intercontinental Childhood ITP Study Group. Pediatr Blood Cancer. 2007;49(6):829-834.
4. Rodeghiero F, Stasi R, Gernsheimer T, et al. Standardization of terminology, definitions and outcome criteria in immune thrombocytopenic purpura of adults and children: report from an international working group. Blood. 2009;113(11):2386-2393.
5. Rodeghiero F, Ruggeri M. ITP and international guidelines: what do we know, what do we need? Presse Med. 2014;43(4 Pt 2):e61-67.
6. Kaatz S, Ahmad D, Spyropoulos AC, Schulman S; the Subcommittee on Control of Anticoagulation. Definition of clinically relevant non-major bleeding in studies of anticoagulants in atrial fibrillation and venous thromboembolic disease in non-surgical patients: communication from the SSC of the ISTH. J Thromb Haemost. 2015; 13(11):2119-2126.
7. Schulman S, Kearon C; the Subcommittee on Control of Anticoagulation of the Scientific and Standardization Committee of the International Society on Thrombosis and Haemostasis. Definition of major bleeding in clinical investigations of antihemostatic medicinal products in non-surgical patients: definitions of major bleeding in clinical studies. J Thromb Haemost. 2005;3(4):692-694.
8. Bisharat N, Omari H, Lavi I, Raz R. Risk of infection and death among post-splenectomy patients. J Infect. 2001;43(3):182-186.
9. Boyle S, White RH, Brunson A, Wun T. Splenectomy and the incidence of venous thromboembolism and sepsis in patients with immune thrombocytopenia. Blood. 2013;121(23):4782-4790.
10. Chaturvedi S, Arnold DM, McCrae KR. Splenectomy for immune thrombocytopenia: down but not out. Blood. 2018;131(11):1172-1182.
11. Kojouri K. Splenectomy for adult patients with idiopathic thrombocytopenic purpura: a systematic review to assess long-term platelet count responses, prediction of response, and surgical complications. Blood. 2004;104(9):2623-2634.
12. Guan Y, Wang S, Xue F, et al. Long-term results of splenectomy in adult chronic immune thrombocytopenia. Eur J Haematol. 2017; 98(3):235-241.
13. Heitink-Polle KMJ, Nijsten J, Boonacker CWB, de Haas M, Bruin MCA. Clinical and laboratory predictors of chronic immune thrombocytopenia in children: a systematic review and meta-analysis. Blood. 2014;124(22):3295-3307.
14. Ahmed R, Devasia AJ, Viswabandya A, et al. Long-term outcome following splenectomy for chronic and persistent immune thrombocytopenia (ITP) in adults and children: splenectomy in ITP. Ann Hematol. 2016;95(9):1429-1434.
15. Gliklich R, Dreyer N, Leavy M, eds. Registries for evaluating patient outcomes: a user's guide. 3rd ed. Rockville (MD); Agency for Healthcare Research and Quality (US); 2014.

Decolonization of multi-drug resistant bacteria by fecal microbiota transplantation in five pediatric patients before allogeneic hematopoietic stem cell transplantation: gut microbiota profiling, infectious and clinical outcomes

Fecal microbiota transplantation (FMT) is playing a prominent role in the treatment of recurrent *Clostridium difficile* infection in adults, showing high efficacy and safety.[1] It has also been proposed for treatment of other diseases associated with alterations of intestinal microbiota, including intestinal inflammatory diseases (inflammatory bowel disease)[2] and graft-*versus*-host disease (GvHD).[3] Moreover, FMT has been proposed for decolonization of multi-drug resistant (MDR) germs from the intestinal tract, with good results in adults.[4,5] Indeed, antimicrobial resistance (AMR) is of great concern in the hemato-oncologic field, since a very high mortality rate has been demonstrated in patients infected by MDR bacteria (up to 36-95% in patients undergoing allogeneic

hematopoietic stem cell transplantation [HSCT]).[6] Moreover, up to 70% of cases of bacteremia originate from the gut in these patients.[7]

Between October 2018 and March 2019, five consecutive patients colonized by MDR bacteria underwent FMT before HSCT (see Table 1 for details), on a compassionate use basis after local ethical committee approval and informed consent of parents/legal guardians of patients. Notably, three patients had a prior history of systemic infections by a colonizing MDR pathogen, which had required intensive care unit admission. Isolated MDR pathogens were *Pseudomonas aeruginosa* and carbapenem-resistant Enterobacteriaceae (CRE) (Table 1); three patients had isolation of different species of CRE in stools (Figure 1). Real-time polymerase chain reaction (RT-PCR) targeting carbapenemases detected bla_{VIM} in three cases, bla_{NDM} in one case, and $bla_{OXA48-181-232}$ in another case.

For each subject, the same unrelated healthy volunteer adult donor was used. Donor screening was performed according to European consensus guidelines on FMT,[1] our institutional FMT protocol and Italian recommendations

Table 1. Characteristics of patients undergoing fecal microbiota transplantation (FMT) for multidrug resistant (MDR) decolonization.

	Patient 1	Patient 2	Patient 3	Patient 4	Patient 5
Age (years) at FMT	18	17	11	9	2
Gender	M	M	M	M	F
Hematologic disease	AML	AML	AML	ALL	SCID
Phase of disease	CR1	CR1	CR1	CR2	Disease present
MDR pathogen	PA	CF, KOr, EntCl	KP, EC	EC	EC, KO, KP
AMR gene	bla_{VIM}	bla_{VIM}	bla_{VIM}	$bla_{OXA48-181-232}$	bla_{NDM}
Pre-FMT relevant infections	Sepsis by Carb-R-PA	Sepsis by Carb-R-EC	None	None	Multiple sepsis and meningoencephalitis by Carb-R-EC
Donor	UD	UD	UD	UD	UD
Stool	Fresh	Frozen	Frozen	Frozen	Frozen
N. of FMT	1	1	1	1	1
Volume administered	170 mL	200 mL	150 mL	240 mL	100 mL
Preparation with oral antibiotic	N	Y	Y	Y	Y
MDR bacteria clearance at 1 week	Y	Y	N	Y	Y
MDR bacteria clearance at 1 month	N	N	Y	N	N
MDR bacteria clearance at last follow-up	N	N	Y	N	N
Last microbiological follow-up (days)	44	28	53	42	113
Time elapsing between FMT and HSCT	12 days	14 days	13 days	16 days	16 days
Type of donor and stem cell source	HLA-haploidentical relative, PBSC	HLA-haploidentical relative, PBSC	HLA-identical sibling, BM	HLA-haploidentical relative, PBSC	HLA-haploidentical relative, PBSC
Conditioning regimen	TBI + TT + LPAM + ATLG + rituximab	TBI + TT + LPAM + ATLG + rituximab	Bu + Cy + LPAM	TBI + TT + Flu + ATLG + rituximab	Treo + Flu + ATLG + rituximab
Graft manipulation	TCRαβ/CD19-depletion	TCRαβ/CD19-depletion	None	TCRαβ/CD19-depletion	TCRαβ/CD19-depletion
CD34+ infused/kg	9.6×10^6	14.4×10^6	5.2×10^6	18.2×10^6	18.0×10^6
Engraftment Y/N, days	Y, 9	Y, 12	Y, 17	Y, 16	Y, 12
Acute/chronic GvHD	N	Y, acute, grade I, +40 after HSCT	N	N	N
Follow-up (days after FMT)	302	264	204	162	120

AMR: antimicrobial resistant; ALL: acute lymphoblastic leukemia; AML: acute myeloid leukemia; ATLG: anti-T lymphocyte globulins; bla_{NDM}: New Delhi metallo-beta-lactamase; bla_{VIM}: Verona imipenenase; bla_{OXA} oxacillinase; BM: bone marrow; Bu: busulfan; CF: *Citrobacter freundii*; Carb-R: carbapenem-resistant; CR: complete remission; Cy: cyclophosphamide; EC: *Escherichia coli*; EntCl: *Enterobacter cloacae*; Flu: fludarabine; GvHD: graft-*versus*-host disease; HSCT: hematologic stem cell transplantation; KP: *Klebsiella pneumoniae*; KOr: *Klebsiella ornithinolytica*; KO: *Klebsiella oxytoca*; LPAM: melphalan; M: male; N: number; PA: *Pseudomonas aeruginosa*; PBSC: peripheral blood stem cells; SCID: severe combined immune deficiency; TBI: total body irradiation; TCR: T-cell receptor; Treo: treosulfan; TT: thiotepa; UD: universal donor.

of the National Health Authority (Consiglio Superiore Sanità) (*http://www.regione.lazio.it/binary/rl_sanita/tbl_normativa/SAN_DCA_U00111_14_03_2019.pdf*). FMT emulsion was prepared under aerobic conditions, from either frozen or fresh preparation, according to stool bank availability and clinical need. FMT infusion was performed *via* esophagogastroduodenoscopy (EGDS) in the duodenum. A naso-gastric tube was placed after FMT in order to protect the patient from vomiting/inhalation. During the week before FMT, no systemic antibiotics were administered. All patients, except one, received a 3-day course of oral colistin before FMT to improve decolonization efficacy. Stool sample collection was performed at the FMT day (T0), day 1(T1), 3(T2), 7±1(T3), 10±2(T4), 20±3(T5), 25±2(T6), 28±2(T7), according to patients' clinical condition and sample availability.

After a minimum of three days post-FMT, based on physician's evaluation, the conditioning regimen for HSCT was started. Anti-infectious prophylaxis/treatment strategy is reported in the *Online Supplementary Appendix*. Adverse events (AE) were graded according to Common Terminology Criteria for Adverse Events (CTCAE), version 4.03. MDR bacteria surveillance and gut microbiota profiling are reported in the *Online Supplementary Appendix*.

Multi-drug resistant decolonization was achieved within one week in 4 of 5 patients (80%), for whom RT-PCR for bla alleles resulted negative on stools. However, at 1-month follow-up, the only patient who was still colonized after FMT, achieved decolonization, while the four previously decolonized patients switched to a new colonization status (from the same pathogen identified before FMT) (see Figure 1 for details). At last microbio-

logical follow-up (mean time 56 days, range 28-113 days), 4 of 5 patients were colonized by MDR pathogens. Details on gut microbiota ecology are reported in Figure 2 and in the *Online Supplementary Appendix*.

Patient 1, after achieving decolonization, experienced a sepsis due to the same MDR-colonizing pathogen (Figure 1) 5 days post-HSCT (17 days after FMT). Patient 5 experienced a sepsis 24 hours after FMT from the same pathogen colonizing her stools; however, after careful clinical revision, this was attributed to contamination of the central venous line by the caregiver. Both episodes were promptly treated with targeted antibiotics, and patients fully recovered without sequelae. The remaining three patients did not present any major infective episodes. Other AE recorded were nausea (two patients with grade 1 and 2, respectively), abdominal pain (grade 1), and bloating (grade 1) in single patients.

Globally, FMT for MDR decolonization in pediatric patients has been reported only twice. The first case refers to a 14-year-old patient treated for hemophagocytic lymphohistiocytosis, experiencing recurrent carbapenem-resistant *Klebsiella pneumoniae* (CR-KP) infections, successfully decolonized by FMT, and with no recurrence of infection in the following 1.5 years.[8] The second patient described in a recent retrospective study focusing on adult hematologic patients was a 16-year-old female with acute myelogenous leukemia.[9] This patient underwent two FMT for VRE (Vancomycin-resistant Enterococci) and CP-producing bacteria colonization 98 days after HSCT, resulting in decolonization of VRE and persistence of carbapenemase (CP)-producing bacteria, with no reported AE.

In our study, FMT using samples from the same donor
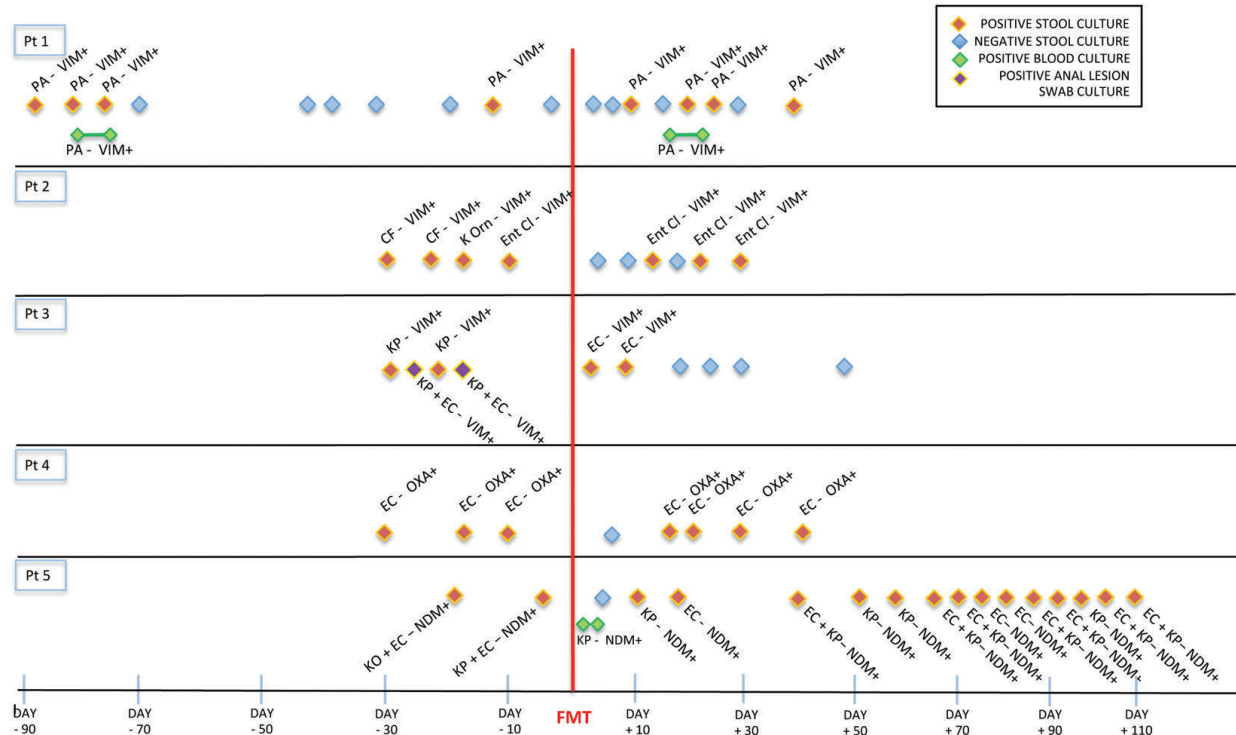
Figure 1. Distribution of multidrug resistant (MDR) pathogens isolated before and after fecal microbiota transplantation (FMT) and characterized. CF: *Citrobacter freundii*; EC: *Escherichia coli*; EntCl: *Enterobacter cloacae*; KP: *Klebsiella pneumoniae*; Kor: *Klebsiella ornithinolytica*; KO: *Klebsiella oxytoca*; NDM: New Delhi metallo-beta-lactamase; OXA: oxacillinase; PA: *Pseudomonas aeruginosa*; Pt: patient; VIM: Verona imipenenase.
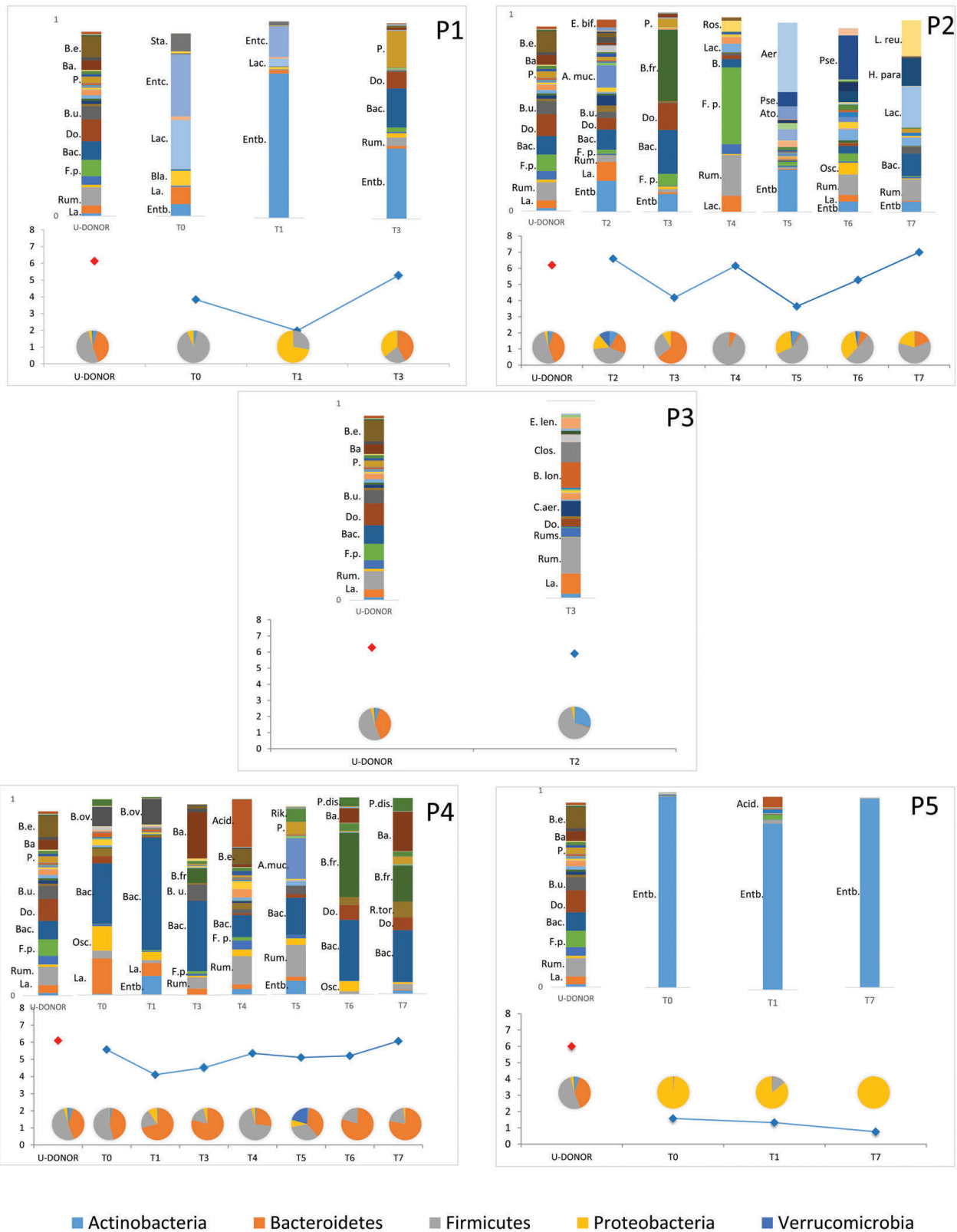
Figure 2. Targeted-metagenomics-based gut microbiota profiling. Barr plots represent operational taxonomic unit distribution of universal donor (U-DONOR) and patient follow-up time-points; line graph represents the Shannon index values for each time points; pie charts report phylum distributions for each time points. Histogram abbreviations: Acid.: *Acidaminococcus*; A.muc.: *A. muciniphila*; Aer.: *Aerococcaceae*; Ato.: *Atopobium*; B.e.: *B. eggerthii*; B.fr.: *B. fragilis*; B.lon.: *B. longum*; B.ov.: *B. ovatus*; B.u.: *B. uniformis*; Bac.: *Bacteroides*; Ba.: *Barnesiellaceae*; Bla.: *Blautia*; C.aer.: *C. aerofaciens*; Clos.: *Clostridiaceae*; Do.: *Dorea*; E.len.: *E. lenta*; E.bif.: *E.biforme*; Entb.: *Enterobacteriaceae*; Entc.: *Enterococcaceae*; F.p.: *F. prausnitzii*; H.para.: *H. parainfluenzae*; L.reu.: *L. reuteri*; La., *Lachnospiraceae*; Lt.: *Lactobacillus*; Osc.: *Oscillospira*; P., *Parabacteroides*; P. dis.: *P. distasonis*; Pse.: *Pseudomonas*; Ros.: *Roseburia*; Rum.: *Ruminococcaceae*; Rums.: *Ruminococcus*; Rik.: *Rikenellaceae*; R.tor.: *R. torques*; Sta.: *Staphylococcus*.

resulted in 80% (4 of 5) MDR decolonization within one week after the procedure. Since repeated FMT could increase the chances of durable decolonization, this protocol might be indicated for patients with a predicted long-lasting immunosuppression or in the presence of other risk factors for recurrent infections.

Our data suggest FMT safety and feasibility in pediatric patients with hematologic disorders immediately before the aplastic phase of HSCT. Four patients did not experience serious AE, while patient 1 suffered from an episode of sepsis (from the same pathogen for which he received FMT) 17 days after the procedure. In all patients, only few symptoms related to the FMT procedure were recorded, all being transient and easily controlled by symptomatic drugs. Recently, two episodes of life-threatening/fatal sepsis due to ESBL *E. coli* were reported in adults undergoing FMT in two different clinical trials.[10] However, based on the last European Consensus[11] and national recommendations, extensive MDR bacteria testing is a cornerstone of donor screening in our institution.

Antibiotic-driven decolonization is a matter of discussion in the context of FMT. Oral colistin was proposed as a treatment to decolonize gut microbiota MDR bacteria before FMT. Stoma *et al.* randomized 62 adult hematologic patients colonized by MDR bacteria to receive oral colistin or placebo for 14 days,[12] showing improved decolonization at the end of treatment not persisting 1 week later; moreover, the incidence of bloodstream infections in the case/control groups was similar. Based on these results, oral colistin was administered to four of our patients before FMT to provide an "induction" therapy followed by "consolidation" through FMT, with the idea of improving donor microbiota "engraftment". From our data, it seems that, at early time points after FMT preceded by oral colistin administration, the gut microbiota composition was more similar to that of the FMT-donor. However, more patients are needed to assess the effective role of oral colistin as FMT preparation on microbiome composition.

After the exclusion of related donors, who were not eligible because of the presence of pathogens/commensals at screening, a healthy unrelated volunteer was selected, in agreement with previous literature. Indeed, systematic reviews/meta-analysis[13] in patients receiving FMT for *C. difficile* infection did not report any difference in outcomes based on donor selection. Donor (unrelated-*versus*-related) and sample (fresh-*versus*-frozen) types are emerging topics, since availability of stool banks could widen and facilitate FMT,[14] especially under emergency regimes. We used both fresh and frozen emulsions from the Ospedale Pediatrico Bambino Gesù FMT bank. Since the screening of potential donors can require weeks, the use of frozen material can reduce the time to perform the procedure.

We administered the stool preparation during EGDS directly in the duodenum. Battipaglia *et al.* used enema as a way of administration, reporting good rate of decolonization.[9] We preferred upper gastrointestinal tract (GI) administration to extend as much as possible the effect of FMT to the whole intestine.[15] Current literature reports the administration *via* upper GI in most cases.

Results obtained in 4 of 5 patients suggest that microbiota changes following FMT occur after T1, when its composition is still similar to T0. In particular, the recipients' microbiota seems to be colonized by donor bacteria starting from one week after the procedure. These similarities are not long-lasting. Indeed, at approximately 10 days after FMT, the recipients' microbiota display a consistently different profile both from the donor and the recipient's T0. These changes could be secondary to the conditioning regimen and/or antibiotic prophylaxis. Therefore, boosts of FMT should be considered within one week after first procedure to consolidate MDR decolonization (e.g., leaving in place a naso-jejunale tube in pediatric patients).

From an ecological point of view, 1 day after FMT we recorded the overgrowth of facultative anaerobes and aerobes, as Enterobacteriaceae, probably promoted by the O_2-conditions generated during the FMT emulsion. Afterward, the slow growth of strict anaerobes from donor reduced the O_2-conditions suppressing the relative amount of Enterobacteriaceae. Thus, we suggest that future FMT emulsion preparations should be performed under anaerobic conditions to reduce the Enterobacteriaceae overgrowth favoring MDR species.

Main limitations of this report are: (i) its non-prospective nature; (ii) some heterogeneity of the FMT protocol (e.g., use of colistin, fresh/frozen material); (iii) the small number of cases, all affecting the possibility to draw firm conclusions.

In conclusion, we showed that FMT for MDR-decolonization of pediatric hematologic patients is safe, feasible, and effective in the short-term. Stool preparations from universal donors, starting from either fresh or frozen material, are readily available and safe, thus paving the way to stool banks. Further studies enrolling more populations are needed to confirm these preliminary data and to improve effectiveness of decolonization and infection clearance during the HSCT window.

Pietro Merli,[1] *Lorenza Putignani,[2]* *Annalisa Ruggeri,[1]*
Federica Del Chierico,[3] *Livia Gargiullo,[4]* *Federica Galaverna,[1]*
Stefania Gaspari,[1] *Daria Pagliara,[1]* *Alessandra Russo,[3]*
Stefania Pane,[5] *Luisa Strocchio,[1]* *Mattia Algeri,[1]*
Francesca Rea,[6] *Erminia Francesca Romeo,[6]* *Paola Bernaschi,[7]*
Andrea Onetti Muda,[8] *Bruno Dallapiccola[9]* and
Franco Locatelli[1,10]

[1]Department of Hematology/Oncology, Cellular and Gene Therapy, Bambino Gesù Children's Hospital; [2]Unit of Parasitology and Unit of Human Microbiome, Bambino Gesù Children's Hospital; [3]Unit of Human Microbiome, Bambino Gesù Children's Hospital; [4]Unit of Immunology and Infectious Diseases, University-Hospital Pediatric Department, Bambino Gesù Children's Hospital; [5]Unit of Parasitology, Bambino Gesù Children's Hospital; [6]Digestive Endoscopy and Surgery Unit, Bambino Gesù Children's Hospital; [7]Unit of Microbiology, Bambino Gesù Children's Hospital; [8]Department of Laboratories, Bambino Gesù Children's Hospital; [9]Scientific Directorate, Bambino Gesù Children's Hospital and [10]Sapienza, University of Rome, Rome, Italy

PM and LP contributed equally as co-first authors.

Correspondence:
PIETRO MERLI - pietro.merli@opbg.net

References

1. Cammarota G, Ianiro G, Tilg H, et al. European consensus conference on faecal microbiota transplantation in clinical practice. Gut.

2017;66(4):569-580.

2. Fang H, Fu L, Wang J. Protocol for fecal microbiota transplantation in inflammatory bowel disease: a systematic review and meta-analysis. BioMed Res Int. 2018;2018:8941340.

3. Spindelboeck W, Schulz E, Uhl B, et al. Repeated fecal microbiota transplantations attenuate diarrhea and lead to sustained changes in the fecal microbiota in acute, refractory gastrointestinal graft-versus-host-disease. Haematologica. 2017;102(5):e210-e213.

4. Bilinski J, Grzesiowski P, Sorensen N, et al. Fecal microbiota transplantation in patients with blood disorders inhibits gut colonization with antibiotic-resistant bacteria: results of a prospective, single-center study. Clin Infect Dis. 2017;65(3):364-370.

5. Singh R, de Groot PF, Geerlings SE, et al. Fecal microbiota transplantation against intestinal colonization by extended spectrum beta-lactamase producing Enterobacteriaceae: a proof of principle study. BMC Res Notes. 2018;11(1):190.

6. Caselli D, Cesaro S, Ziino O, et al. Multidrug resistant Pseudomonas aeruginosa infection in children undergoing chemotherapy and hematopoietic stem cell transplantation. Haematologica. 2010; 95(9):1612-1615.

7. Samet A, Sledzinska A, Krawczyk B, et al. Leukemia and risk of recurrent Escherichia coli bacteremia: genotyping implicates E. coli translocation from the colon to the bloodstream. Eur J Clin Microbiol Infect Dis. 2013;32(11):1393-1400.

8. Freedman A, Eppes S. Use of stool transplant to clear fecal colonization with carbapenem-resistant Enterobacteraciae (CRE): proof of concept. Open Forum Infect Dis. 2014;(Suppl 1):S65.

9. Battipaglia G, Malard F, Rubio MT, et al. Fecal microbiota transplantation before or after allogeneic hematopoietic transplantation in patients with hematologic malignancies carrying multidrug-resistance bacteria. Haematologica. 2019;104(8):1682-1688.

10. DeFilipp Z, Bloom PP, Torres Soto M, et al. Drug-resistant E. coli bacteremia transmitted by fecal microbiota transplant. N Engl J Med. 2019;381(21):2043-2050.

11. Cammarota G, Ianiro G, Kelly CR, et al. International consensus conference on stool banking for faecal microbiota transplantation in clinical practice. Gut. 2019;68(12):2111-2121.

12. Stoma I, Karpov I, Iskrov I, et al. Decolonization of intestinal carriage of MDR/XDR gram-negative bacteria with oral colistin in patients with hematological malignancies: results of a randomized controlled trial. Mediterr J Hematol Infect Dis. 2018;10(1):e2018030.

13. Li YT, Cai HF, Wang ZH, Xu J, Fang JY. Systematic review with meta-analysis: long-term outcomes of faecal microbiota transplantation for Clostridium difficile infection. Aliment Pharmacol Ther. 2016; 43(4):445-457.

14. Terveer EM, van Beurden YH, Goorhuis A, et al. How to: establish and run a stool bank. Clin Microbiol Infect. 2017;23(12):924-930.

15. Kamada N, Chen GY, Inohara N, Nunez G. Control of pathogens and pathobionts by the gut microbiota. Nat Immunol. 2013; 14(7):685-690.

COVID-19 in patients with sickle cell disease – a case series from a UK tertiary hospital

At the time of this manuscript going to press, Europe remains the epicenter of the COVID-19 pandemic and new cases and deaths in the UK continue to demonstrate an exponential rise.[1] London has the highest number of reported UK cases.[2] Clinical reports indicate that older adults with comorbidities such as diabetes and hypertension are most at risk of severe COVID-19.[3,4] Overwhelming inflammation and cytokine associated lung injury are potential pathological features. Secondary hemophagocytic lymphohistiocytosis-like syndrome with raised pro-inflammatory cytokines has been associated with adverse outcomes.[5]

King's College Hospital is a teaching hospital in South London, caring for approximately 500 adults and 500 children with sickle cell disease (SCD). South London currently has some of the highest numbers of confirmed cases of COVID-19 in England[2] and a large local SCD cohort. It is thought that patients with SCD might demonstrate a more severe illness if infected with SARS-CoV-2 due to associated functional hyposplenia, high prevalence of concomitant chronic respiratory disease and increased levels of inflammation.[6]

In this report we describe the clinical features of the first 10 confirmed cases of COVID-19 in patients with SCD in the King's College Hospital. At the time of this report, there were 22,141 confirmed cases of COVID-19 in the UK, of which the majority of cases were from the boroughs of Lambeth and Southward in South London.[2] All patients underwent real-time quantitative PCR assay from RNA extracted from nasopharyngeal swabs using a locally validated procedure recommended by Public Health England.[7] All patients had homozygous SCD (HbSS) and presented with symptoms such as cough, fever, coryza and associated acute sickle vaso-occlusive pain. None had any recent travel history (Table 1).

Apart from patient 9 who has severe pre-morbid disease with intensive care admission within the last 12 months due to SCD-related cerebrovascular disease, all patients had relatively mild clinical symptoms related to COVID-19 (Table 2).

In this series, seven patients were female, and the median age was 37 years (range: 25-54 years). No children were seen with SCD and COVID-19. All but two patients were on some disease modification treatment, either hydroxycarbamide (2 of 10) or transfusions (6 of 10). Patients on top-up transfusions were on a 4-weekly program with a post-transfusion hemoglobin target of 120-130 g/L. One patient was on an angiotensin converting enzyme inhibitor (patient 6), and this was not discontinued during the period of illness. Two patients had a history of overt strokes and one patient had a history of recurrent transient ischemic attacks. All patients had ongoing comorbidities, ranging from end stage renal failure to hyperhemolysis. All admitted patients received standard thromboprophylaxis with low molecular weight heparin injection as per hospital venous thromboembolism prevention guidelines.

The mean number of days from onset of symptoms to PCR testing was 2.5 days. Of the seven patients in this cohort needing hospital admission, the mean number of days from the onset of symptoms to hospital admission was two days. Nine of 10 patients made a full recovery. Two patients presenting with cough and hypoxia received early top up transfusions. See Figure 1 for the chest radiograph of patient 2 who was hypoxic on admission and received an additive transfusion. All in-patients received broad spectrum antibiotics to cover community acquired pneumonia. No COVID-19 specific treatment was given. The lymphocyte count fell significantly during infection compared to the baseline, from a median of 3.7 to 1.9 x10^9/L (P=0.037, Wilcoxon signed-rank test).

One patient died of respiratory complications following COVID-19. She had multiple comorbidities, inclu-

Table 1. Characteristics of COVID-19 positive patients with sickle cell disease.

Patient number	Genotype	Sex	Age (years)	Baseline Hb concentration (g/L)	Baseline HbF percentage	Smoker	BMI	HC	Regular transfusions	Comorbidity
1	HbSS	M	36	–	5.2	N	26.9	N	Top up	ACS in the last 12 months, chronic pain
2	HbSS	F	38	87	3.2	N	40.8	N	Top up	Recurrent leg ulcers
3	HbSS	F	34	106	0.8	N	20.9	N	ARECT	Stroke, severe cerebral vasculopathy
4	HbSS	F	46	91	1.5	N	25.7	N	Top up	ESRF, HDx, Chronic pain, asthma
5	HbSS	M	37	104	0.4	N	24	N	ARCET	Stroke
6	HbSS	F	52	115	18	N	28.3	Y	N	Chronic shoulder pain
7	HbSS	M	25	114	0.8	N	25.8	N	ARCET	Recurrent TIA
8	HbSS	F	35	97	19.6	N	–	Y	N	Chronic hip pain
9	HbSS	F	54	105	11.9	N	33.4	N	N	Hyperhemolysis, asthma, bilateral hip AVN
10	HbSS	F	44	108	0.9	N	31.5	N	ARCET	ACS in the last 12 months, stroke, iron overload

ACS: acute chest syndrome, ARCET: automated red cell exchange transfusion, AVN: avascular necrosis, Hb: hemoglobin, HbF: fetal hemoglobin, ESRF: end stage renal failure, HDx: hemodialysis, HbSS: homozygous sickle cell disease, TIA: transient ischaemic attack, HC: hydroxycarbamide.

Table 2. COVID-19 clinical features in SCD patients.

Patient number	Temp >37.8°C at presentation	Cough	Acute pain	Mode of respiratory support	Hemoglobin concentration nadir(g/L)	Lymphocyte count nadir (x10^3/L)	Platelet count nadir (x10^{*9}/L)	Maximum CRP (mg/L)	Transfused on admission	Outcome
1	Y	Y	N	None	–	2.2	243	10.7	N	Full recovery following inpatient in hospital
2	Y	N	N	Nasal canula	75	2.35	410	59.3	Top up	Full recovery following inpatient in hospital
3	Y	N	Y	None	96	1	189	5.1	N	Full recovery following inpatient in hospital
4	N	N	N	None	91	2.21	463	31.5	N	Self-limiting illness, not admitted
5	N	N	N	None	103	2.7	327	6.6	N	Self-limiting illness, not admitted
6	N	N	N	None	122	1.22	90	66.1	N	Self-limiting illness, not admitted
7	N	N	Y	None	114	1.56	261	N/A	N	Self-limiting illness, not admitted
8	Y	Y	Y	None	93	5.16	415	10.1	N	Self-limiting illness, not admitted
9	Y	Y	Y	Nasal canula	96	0.83	122	339	N	Died of severe respiratory failure and other co-existing morbidity
10	Y	Y	Y	None	79	1.41	177	3.6	Top up	Full recovery following inpatient in hospital

ding a history of brittle asthma and hyperhemolysis with multiple red cell alloantibodies, making it difficult to transfuse her. Escalation to ventilation was deemed unsuitable due to existing comorbidities.

Based on our small early cohort of 10 individuals with HbSS who have tested positive for COVID-19, patients seem to be experiencing a relatively mild course despite having significant associated comorbidities such as end stage renal failure, severe cerebral vasculopathy and recurrent painful episodes. Half were managed at home with regular telephone contact by the clinical team.

Our first (and so far) only fatality was in an individual of >50 years with poor pre-infection performance status and severe pre-existing lung disease, who had had admissions to intensive therapy unit (ITU) within the last 12 months, as well as multiple red cell alloantibodies and a previous history of severe delayed hemolytic transfusion reactions, which precluded transfusion. This patient had lymphopenia, thrombocytopenia and a high C-reactive protein (CRP), which have been identified as poor prognostic markers in patients without SCD.

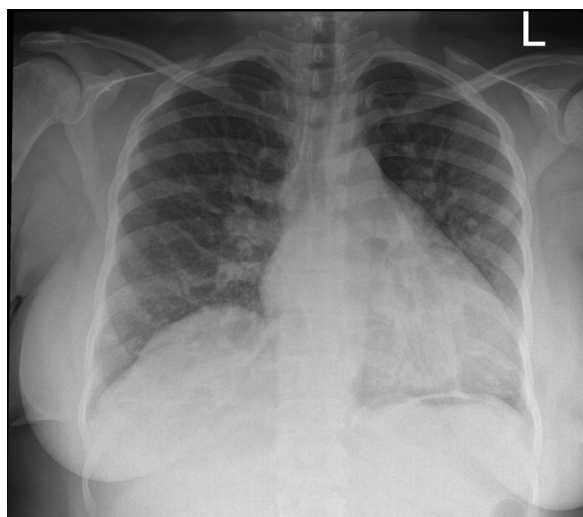Seven of 10 patients in this series were female, all patients were non-smokers and all but two were on a di-

Figure 1. Chest radiograph of patient 2 who was hypoxic on admission and received an early additive transfusion. This showed bilateral congestive changes with no additional pulmonary parenchymal pathology and was obtained on day 2 of admission.

sease modifying treatments, such as regular a blood transfusion programme or hydroxycarbamide. These demographic features may have contributed to the mild clinical course in all but one patient.

SCD is mentioned in the Public Health England list of conditions which should prompt individuals to be shielded from infection, by rigorous self-isolation. Our series shows that patients with SCD can have a relatively mild course with COVID-19. It is difficult to speculate why this might be the case, and it may be postulated that most of our patients were already on some form of disease modification, which may have helped with the host response. It is unclear whether hyposplenism has played a role in the apparent lack of a hyperimmune syndrome and this is likely to be an area of research in the future. The one patient who died was in a poor prognostic group, based on risk factors identified in the general population. So far, we have seen no children with COVID-19 and SCD, suggesting that this may be a mild condition in children with SCD, as has been found in the general population. It is not entirely clear why more women are represented in this group. It is possible that with time, this ratio may become more skewed to the male sex. The relatively low case fatality is evidence that affected individuals should not be excluded from potentially lifesaving measures including respiratory support and artificial ventilation, particularly as our well-studied cohort have a median survival of 67 years.[8]

Subarna Chakravorty, Giselle Padmore-Payne, Fester Ike, Virginia Tshibangu, Charlotte Graham, David Rees and Sara Stuart-Smith

King's College Hospital, London, UK

Correspondence:
SUBARNA CHAKRAVORTY - subarna.chakravorty@nhs.net

References

1. World Health Organisation. Coronavirus disease (COVID-19) situation summary. 2020 27/3/2020. Available from: https://experience.arcgis.com/experience/685d0ace521648f8a5beeeee1b9125cd.
2. Public Health England. Total UK COVID-19 cases update 2020 27/3/20. Available from: https://www.arcgis.com/apps/opsdashboard/index.html#/f94c3c90da5b4e9f9a0b19484dd4bb14.
3. Zhou F, Yu T, Du R, et al. Clinical course and risk factors for mortality of adult inpatients with COVID-19 in Wuhan, China: a retrospective cohort study. Lancet. 2020;395(10229):1054-1062.
4. Shi Y, Yu X, Zhao H, Wang H, Zhao R, Sheng J. Host susceptibility to severe COVID-19 and establishment of a host risk score: findings of 487 cases outside Wuhan. Crit Care. 2020;24(1):108.
5. Huang C, Wang Y, Li X, et al. Clinical features of patients infected with 2019 novel coronavirus in Wuhan, China. Lancet. 2020;395(10223):497-506.
6. Piel FB, Steinberg MH, Rees DC. Sickle cell disease. N Engl J Med. 2017;376(16):1561-1573.
7. Public Health England. Guidance and standard operating procedure COVID-19 virus testing in NHS laboratories. 2020. https://www.england.nhs.uk/coronavirus/publication/guidance-and-standard-operating-procedure-covid-19-virus-testing-in-nhs-laboratories/
8. Gardner K, Douiri A, Drasar E, et al. Survival in adults with sickle cell disease in a high-income setting. Blood. 2016;128(10):1436-1438.

Anti-C5 antibody treatment for delayed hemolytic transfusion reactions in sickle cell disease

Delayed hemolytic transfusion reaction (DHTR) is an unpredictable severe complication of transfusion in patients with sickle cell disease (SCD). It presents clinically as a vaso-occlusive crisis (VOC), often associated with the failure of one or more organs, after the transfusion of packed red blood cells (pRBC).[1,2] Hyperhemolysis is encountered in the most severe forms. Both transfused and autologous red blood cells (RBC) are lysed.

The mechanisms underlying DHTR remain unclear.

Alloantibodies against RBC antigens were initially thought to underlie the pathophysiology, but no such antibodies are detected in about a third of the cases.[3]

RBC degradation products, such as hemoglobin and heme, are released into the bloodstream during intravascular hemolysis. These elements and heme-loaded membrane microvesicles have recently been implicated in inflammation and organ injury in DHTR.[4] Complement is activated via the classical pathway, by alloantibodies, and/or via the alternative pathway, by free heme.[5] Heme-dependent complement deposits on the endothelium contribute to organ damage.[6] Due to these vascular lesions, hyperhemolysis often progresses to multiple

Table 1. Clinical and biological findings at diagnosis and during follow-up.

	This series	Habibi et al.	
Patient characteristics			
Number of patients; DHTR episodes	18; 18	69; 99	
Hb $\beta^s\beta^s$	18 (100%)	65 (94.2%)	
Sex F/M	11/7	48/21	
Age, years	24.6 ± 12.6	30 ± 9	
Number of pRBC units in transfusion episode	2 ± 1.9	2 ± 3	
Transfusion indications			
Preventive measure	5 (27.8%)	51 (51.5%)	
Vaso-occlusive complications	11 (61.1%)	48 (48.5%)	
Other	2 (11.1%)		
Timeline			
Days from transfusion to DHTR diagnosis	8 [7-12.8]	10 [8-14] (MD=19)	
Days from transfusion to anti-C5 infusion	10.5 [9-15.5]		
Biological findings in the emergency room			
Total Hb level, g/dL	63.5 [53.3-77.8] (NA=6*)	78 [69-93] (MD=5)†	P=0.03
LDH level, IU/L	1612 [825-2702] (NA=6*)	758 [554-958] (MD=16)	P<0.01
Treatment**			
EPO	17 (94.4%)	45%	
Corticosteroids	1 (5.6%)	3%	
Plasma or albumin exchange	4 (22.2%)		
IV immunoglobulins	9 (50%)	4%	
Anti-CD20 antibody	7 (38.9%)	2%	
Anti-C5 antibody	16 (100%)	2%	
Secondary pRBC transfusion	14 (77.8%)	35%	
Extreme biological findings			
Lowest total Hb level, g/dL	30.5 [25.5-42.8]	55 [45-63] (MD=5)†	P<0.01
Highest LDH level, IU/L	3337 [2573-7986]	1335 [798-2086] (MD=7)	P<0.01
Lowest reticulocyte count, 10⁹/L	46.1 [35.8-84.8] (MD=2)	180 [121-240] (MD=14)	P<0.01
Delta Hb‡, g/dL	57.5 [45.8-67.5] (MD=4)	46 [31-53] (MD=26)†	P=0.06
Outcome			
ICU admission	17 (94.4%)	41 (40%)	
ICU-stay duration, days	17.7 ± 10.2	6.2 ± 4	P<0.01
Hospital-stay duration, days	35.6 ± 25.3	15.9 ± 10	P<0.01
Transfusion-to-death interval, days	51.7 ± 47.9	10 ± 2	
Death	3 (16.7%)	6%	

Continuous variables are expressed as means ± one standard deviation (SD) or medians (MD, [interquartile range]), depending on whether they are normally or asymmetrically distributed. Categorical variables are expressed as numbers (%). For comparison with the largest published delayed hemolytic transfusion reaction (DHTR) series, the data in column 2 are reprinted from Habibi et al.1 with permission. The patients of our series, who received anti-C5 antibody, had very severe DHTR with hyperhemolysis (P-values in column 3 compare our patients with those of the historical series). *Six patients had not even been discharged, due to the severity of their DHTR, **All patients in both series also received supportive vaso-occlusive crisis (VOC) treatment, hydration, oxygenation, and analgesia. †Values were converted to g/L (from g/dL in Habibi et al.). ‡Delta hemoglobin (Hb) is the difference between the highest and lowest values available post-transfusion. F: female; M: male; pRBC: packed red blood cells, LDH: lactate dehydrogenase, EPO: erythropoietin.
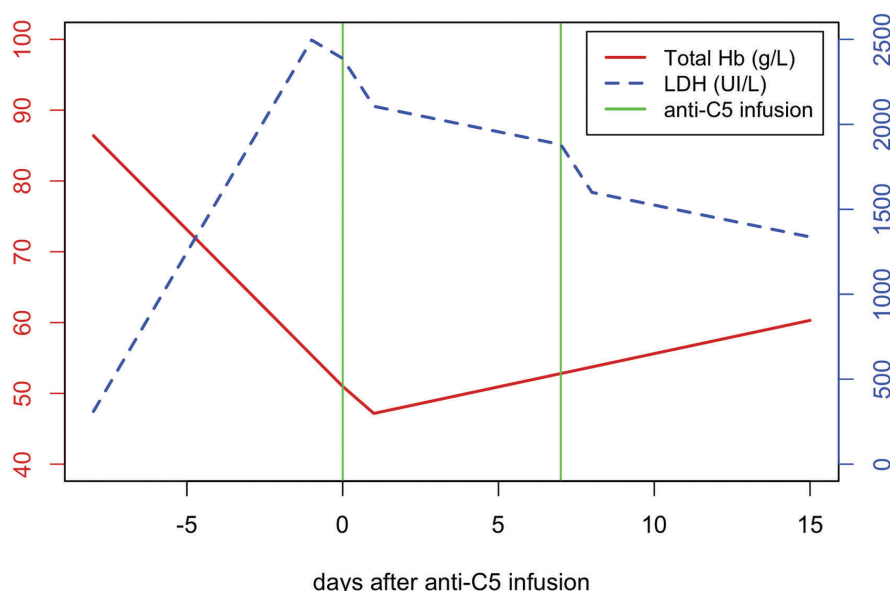
Figure 1. Best mixed-effects model for total hemoglobin and lactate dehydrogenase during delayed hemolytic transfusion reaction, before and after anti-C5 antibody infusion. Hemoglobin (Hb) levels are predicted for a "theoretical" patient receiving anti-C5 antibody infusions on days 0 and 7 and no packed red blood cell (pRBC) transfusions. Before anti-C5 antibody infusion, basal total Hb concentration in this model was 51.0 g/L (the intercept of the model), with an increase of +3.8 g/L for each pRBC unit transfused, and ongoing hemolysis at a rate of -4.4 g/L for each passing day (the fixed effects of the model). However, after anti-C5 antibody infusion, Hb levels gradually increased, with a basal Hb concentration of 46.2 g/L: the effect of each transfusion was an increase of 1.58 g/L for each pRBC unit transfused and an increase in Hb levels of 0.94 g/L.

organ failure and, in some cases, death.

These pathophysiological findings suggest that inhibitors of complement activation may be useful for treating DHTR with hyperhemolysis. Eculizumab is a monoclonal anti-C5 antibody that inhibits the cleavage of C5 into C5a by the C5 convertase, thereby preventing the late stages of the complement cascade. Anti-C5 therapy has been offered to several SCD patients for DHTR treatment at our SCD referral center in France since 2013.[1,7] Other teams have also treated DHTR in patients with and without detectable allo- or auto-antibody formation with Eculizumab, with promising results.[8-11] The American Society of Hematology (ASH) guidelines include a conditional recommendation for the use of anti-C5 antibodies in patients with SCD presenting DHTR and ongoing hyperhemolysis, based on currently very low levels of certainty.[12]

This retrospective study focuses on the biological and clinical findings and the effects of anti-C5 therapy on DHTR, for patients treated between 2013 and 2019 who experienced particularly severe DHTR.

DHTR was diagnosed[1,2] on the basis of VOC signs occurring 5-20 days after pRBC transfusion, with no other identifiable cause of intravascular hemolysis, in association with at least one of the following signs:
- rapid decrease in, or unexpectedly low, hemoglobin A (HbA) concentration (the diagnostic nomogram for DHTR diagnosis was used),[2]
- hemoglobinuria, as revealed by dark urine,
- positive direct antiglobulin test (DAT) results or new antibody formation.

The criteria for the use of anti-C5 therapy was based either on the existence, at the time anti-C5 infusion was decided, of one or more organs with dysfunction and/or very low total Hb concentration (< 50 g/L), and/or a rapidly worsening clinical state.[7]

Data were collected retrospectively from patient records. The clinical and biological findings available at transfusion, at the time of DHTR diagnosis and during follow-up were collected. We also noted patient sex, age, history of DHTR, pRBC transfusion, and antibody screens. We recorded the number of pRBC units and the indication of the transfusion(s) occurring within a timeframe compatible with DHTR (some patients had received pRBC on several occasions during the 5-20 days preceding DHTR). Clinical (hemoglobinuria, pain and VOC signs, organ failure) and biological (hemoglobin concentration, reticulocyte count, LDH, total bilirubin) findings at DHTR diagnosis were collected. The first clinical signs compatible with DHTR were noted, particularly pain indicative of VOC recurrence, and hemoglobinuria indicative of intravascular hemolysis. We collected follow-up data for biological tests, intensive care unit admission and discharge, organ failure and treatments. This study was performed in accordance with the Declaration of Helsinki.

We used R3.6.1 and lme4[13] for a linear mixed-effects model analysis of the relationship between Hb and lactate dehydrogenase (LDH) levels and anti-C5 treatment. Hb and LDH levels were modeled before and after treatment. An initial blind statistical analysis was performed, and several models were then proposed, with days and pRBC transfusions as fixed effects, and different combinations of random effects for subjects, days and pRBC transfusions. We obtained *P*-values for likelihood ratio tests of the full model with random effects against the model without additional terms, which we used to select the best model.

Eighteen SCD patients received anti-C5 treatment for DHTR with hyperhemolysis. All patients had signs of VOC 5-20 days after pRBC transfusion, with low HbA concentrations (<10 g/L) in five patients, a rapid decrease in HbA concentration in 10 patients (estimated by the nomogram[2] as a high (n=4) or intermediate (n=6) risk of

DHTR), hemoglobinuria in 11 patients, and positive DAT results or antibody formation in 12 patients (anti-MNS3, anti-KEL6, anti-RH10 + anti-RH20, anti-MNS5, anti-FY5 in one patient each, one patient developed multiple antibodies including anti-MNS3, anti-RH20 and auto-antibodies, two patients developed auto-antibodies and two patients delevopde allo-antibodies for which the specificity could not be determined and two patients had positive DAT but no new antibody was subsequently identified). A 19th patient received anti-C5 antibody for hyperhemolysis but it was impossible to determine whether this patient had DHTR due to hemolysis under extracorporeal membrane oxygenation,[14] so this patient was excluded from the analysis.

The main characteristics of the patients are presented in Table 1. Sixteen patients (89%) had risk factors for DHTR: a history of previous DHTR (n=2), a history of RBC antibodies (n=11), or the administration of fewer than 12 pRBC units before the episode leading to DHTR (n=11).15 Three patients had a history of ineffective pRBC transfusions, possibly due to previous undetected episodes of DHTR. None of the patients were enrolled in chronic transfusion programs. Five patients underwent repeat transfusions before the diagnosis of DHTR, which may have worsened their clinical presentation at diagnosis.

The findings at diagnosis and during follow-up, compared with those of a historical cohort[1] are presented in Table 1 (see *Online Supplementary Data* for individual timelines). At diagnosis, the patients had particularly severe DHTR, with parameters highly indicative of hemolysis (low Hb, high LDH concentrations), and the failure of at least one organ in 50% of cases (n=9): kidney failure (n=7), liver failure (n=4, including two with indications for liver transplantation), respiratory failure (n=5). Five patients had hemodynamic failure requiring treatment with vasoactive agents.

One to three anti-C5 doses were administered at 1-week intervals (one dose n=6, two doses n=9 and three doses n=1), in association with other treatments (Table 1). Unfortunately, complement activation measurements were not performed for most patients. The number of pRBC units transfused was restricted as much as possible, to limit exacerbations of hyperhemolysis.

Remarkably, a worsening of clinical conditions during follow-up occurred only in the hours immediately following anti-C5 infusion (i.e., due to the progression of pre-existing organ damage due to DHTR; n=2), or as a result of sepsis due to additional infectious complications (n=2). One patient suffered hemodynamic failure within a few hours of anti-C5 infusion. One patient (16P) with kidney failure, hemodynamic failure and a severe hepatic alteration before anti-C5 infusion rapidly progressed to hepatic failure a few hours after the first infusion.

The outcome was favorable in 15 patients (83%), with a complete recovery of all failing organs. Three patients died (17%). All three had acute liver failure requiring emergency transplantation (already present at DHTR diagnosis in two of these patients). Two patients improved after one and two anti-C5 infusions and were able to undergo transplantation. However, both died from infectious complications due to encapsulated bacteria unrelated to anti-C5 treatment but promoted by the immunosuppressive regimen: ventilator-associated pneumonia 11 days after transplantation in patient 8H, and digestive and urinary infection 47 days after transplantation in patient 16P. No compatible organ could be found for patient 3C, who died one day after anti-C5 antibody infusion.

Despite the heterogeneity of the data, linear mixed-effect model analysis with adjustment to produce the best model ($P<0.05$) highlighted an influence of the anti-C5 antibody treatment on total Hb and LDH levels (Figure 1). The inversion of the slope for total Hb and LDH levels before and after anti-C5 treatment indicated that hyperhemolysis was stopped, or at least greatly decreased, by treatment. The gradual increase in Hb levels may also be due to the other treatments received by the patients, especially erythropoietin (EPO) (Table 1). The stimulation of erythropoiesis improves the reticulocyte count, and proportionally increases hemoglobin S (HbS). In several patients who received secondary RBC transfusion, HbA concentration was maintained post transfusion (e.g., patients 2B, 15O, 16P, 17Q).

In conclusion, this is the largest series to date of cases of severe DHTR with hyperhemolysis in SCD patients, treated with anti-C5 antibody. It demonstrates the effect of anti-C5 therapy against hyperhemolysis in DHTR, with remarkable beneficial effects on pre-existing organ failure and additional organ failure once the effects of the treatment are established. These findings consolidate the recommendation in the ASH guidelines to use anti-C5 antibody in patients with SCD and ongoing hyperhemolysis.[12] Other anti-complement drugs may also be useful for treatment in this context. A prospective clinical trial would be required to determine whether all DHTR patients would benefit from anti-C5 therapy or whether such treatment is beneficial only for the most severe clinical presentations.

Aline Floch,[1] Alexandre Morel,[2] Fabian Zanchetta-Balint,[2] Catherine Cordonnier-Jourdin,[3] Slimane Allali,[4] Maximilien Grall,[5] Ghislaine Ithier,[6] Benjamin Carpentier,[7] Sadaf Pakdaman,[1] Jean-Claude Merle,[8] Radjiv Goulabchand,[9] Tackwa Khalifeh,[10] Ana Berceanu,[11] Cécile Helmer,[12] Christelle Chantalat-Auger,[13] Véronique Frémeaux-Bacchi,[14] Marc Michel,[15] Mariane de Montalembert,[4] Armand Mekontso-Dessap,[16] France Pirenne,[1] Anoosha Habibi[2] and Pablo Bartolucci[2]

[1]Etablissement francais du sang Ile de France, INSERM Unit 955, Laboratory of Excellence GR-Ex, Mondor Institute of Biomedical Research, Paris-Est Creteil University, Creteil; [2]French Sickle Cell Referral Center, Henri Mondor Teaching Hospital, Assistance Publique-Hopitaux de Paris, Laboratory of Excellence GR-Ex, INSERM Unit 955, Mondor Institute of Biomedical Research, Paris-Est Creteil University, Creteil; [3]Department of Pharmacy, Henri Mondor Teaching Hospital, Assistance Publique-Hopitaux de Paris; [4]Department of Pediatrics, Necker Hospital for Sick Children, Assistance Publique-Hopitaux de Paris, Laboratory of Excellence GR-Ex, Paris Descartes University, Paris; [5]Department of Internal Medicine, Rouen Teaching Hospital, Rouen; [6]Hematology Unit, Reference Center of Sickle Cell Disease, Robert Debré Hospital, Assistance Publique-Hopitaux de Paris, Paris; [7]Department of Hematology, Saint Vincent de Paul Hospital, Lille Catholic University, Lille; [8]Department of Anesthesia and Surgical Intensive Care, Liver Intensive Care Unit, Henri Mondor Teaching Hospital, Assistance Publique-Hopitaux de Paris, Creteil; [9]Department of Internal Medicine-Multiorganic Diseases, Local Referral Center for Autoimmune Diseases, Saint-Eloi Hospital, Montpellier University, Montpellier; [10]Pediatric Medical-Surgical Department, Poitiers Teaching Hospital, Poitiers, France; [11]Intensive Care Hematology Unit, Besancon Teaching Hospital, Besancon; [12]Etablissement francais du sang Auvergne-Rhône Alpes, Grenoble; [13]Department of Internal Medicine, Bicetre Teaching Hospital, Assistance Publique-Hopitaux de Paris, Universite Paris 11, Le Kremlin-Bicetre, Paris; [14]Laboratory of Immunology, European Georges Pompidou Hospital, Assistance Publique-Hopitaux de Paris, Mixed Health Research Unit INSERM

872, Cordeliers Research Center, Paris; *15Department of Internal Medicine, National Referral Center for Immune Cytopenias, Henri Mondor Teaching Hospital, Assistance Publique-Hopitaux de Paris, Creteil and *16Medical Intensive Care Unit, Henri Mondor Teaching Hospital, Assistance Publique-Hopitaux de Paris, Creteil, France*

Correspondence:
PABLO BARTOLUCCI - pablo.bartolucci@aphp.fer

References

1. Habibi A, Mekontso-Dessap A, Guillaud C, et al. Delayed hemolytic transfusion reaction in adult sickle-cell disease: presentations, outcomes, and treatments of 99 referral center episodes. Am J Hematol. 2016;91(10):989-994.
2. Mekontso Dessap A, Pirenne F, Razazi K, et al. A diagnostic nomogram for delayed hemolytic transfusion reaction in sickle cell disease. Am J Hematol. 2016;91(12):1181-1184.
3. de Montalembert M, Dumont M-D, Heilbronner C, et al. Delayed hemolytic transfusion reaction in children with sickle cell disease. Haematologica. 2011;96(6):801-807.
4. Merle NS, Grunenwald A, Rajaratnam H, et al. Intravascular hemolysis activates complement via cell-free heme and heme-loaded microvesicles. JCI Insight. 2018;3(12):96910.
5. Merle NS, Boudhabhay I, Leon J, Fremeaux-Bacchi V, Roumenina LT. Complement activation during intravascular hemolysis: Implication for sickle cell disease and hemolytic transfusion reactions. Transfus Clin Biol. 2019;26(2):116-124.
6. Merle NS, Paule R, Leon J, et al. P-selectin drives complement attack on endothelium during intravascular hemolysis in TLR-4/heme-dependent manner. Proc Natl Acad Sci USA. 2019;116(13):6280-6285.
7. Pirenne F, Yazdanbakhsh K. How I safely transfuse patients with sickle-cell disease and manage delayed hemolytic transfusion reactions. Blood. 2018;131(25):2773-2781.
8. Dumas G, Habibi A, Onimus T, et al. Eculizumab salvage therapy for delayed hemolysis transfusion reaction in sickle cell disease patients. Blood. 2016;127(8):1062-1064.
9. Chonat S, Quarmyne M-O, Bennett CM, et al. Contribution of alternative complement pathway to delayed hemolytic transfusion reaction in sickle cell disease. Haematologica. 2018;103(10):e483-e485.
10. Unnikrishnan A, Pelletier JPR, Bari S, et al. Anti-N and anti-Doa immunoglobulin G alloantibody-mediated delayed hemolytic transfusion reaction with hyperhemolysis in sickle cell disease treated with eculizumab and HBOC-201: case report and review of the literature. Transfusion. 2019;59(6):1907-1910.
11. Vlachaki E, Gavriilaki E, Kafantari K, et al. Successful outcome of hyperhemolysis in sickle cell disease following multiple lines of treatment: the role of complement inhibition. Hemoglobin. 2018;42(5-6):339-341.
12. Chou ST, Alsawas M, Fasano RM, et al. American Society of Hematology 2020 guidelines for sickle cell disease: transfusion support. Blood Adv. 2020;4(2):327-355.
13. Bates D, Mächler M, Bolker B, Walker S. Fitting linear mixed-effects models using lme4. J Stat Softw. 2015;67(1):85262.
14. Boissier F, Bagate F, Schmidt M, et al. Extracorporeal life support for severe acute chest syndrome in adult sickle cell disease: a preliminary report. Crit Care Med. 2019;47(3):e26-e265.
15. Narbey D, Habibi A, Chadebech P, et al. Incidence and predictive score for delayed hemolytic transfusion reaction in adult patients with sickle cell disease. Am J Hematol. 2017;92(12):1340-1348.

Genetic platelet depletion is superior in platelet transfusion compared to current models

Manuel Salzmann,[1] Waltraud C. Schrottmaier,[1] Julia B. Kral-Pointner,[1] Marion Mussbacher,[1] Julia Volz,[3] Bastian Hoesel,[1] Bernhard Moser,[1] Sonja Bleichert,[1,2] Susanne Morava,[1] Bernhard Nieswandt,[3] Johannes A. Schmid[1] and Alice Assinger[1]

[1]Institute of Vascular Biology and Thrombosis Research, Medical University of Vienna, Vienna, Austria, [2]Department of Surgery, General Hospital, Medical University Vienna, Vienna, Austria and [3]Institute of Experimental Biomedicine, University Hospital and Rudolf Virchow Center, University of Würzburg, Würzburg, Germany

An incorrect version of Figure 5 appeared in the June 2020 issue on page 1744.
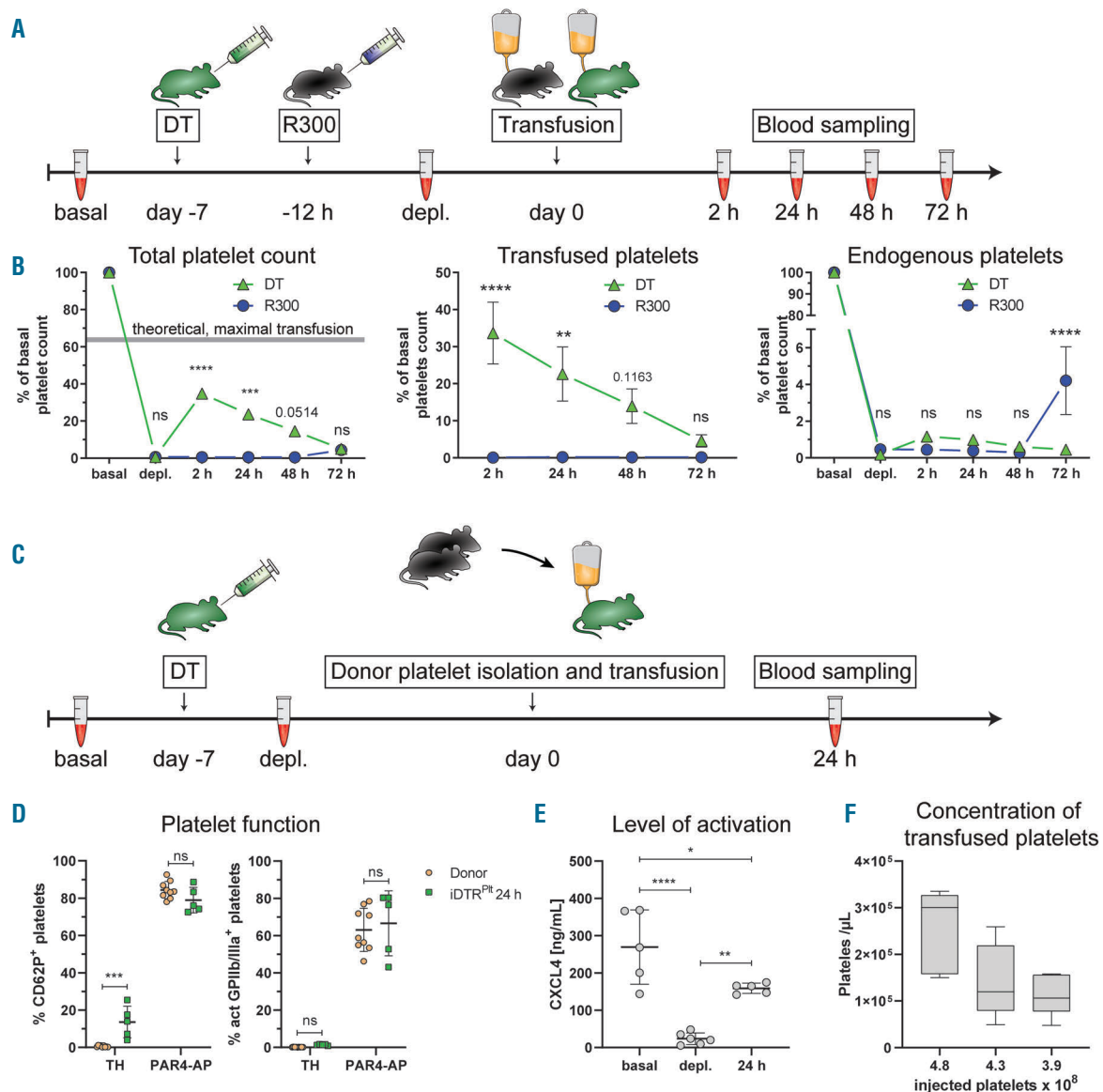*The correct version of Figure 5 is published on this page.*

Figure 5. Platelet transfusion efficacy and donor platelet function analysis of iDTR^Plt mice. (A) Graphical overview for comparison of platelet transfusion. DT treatment started 7 days prior to transfusion and R300 treatment 12 hours prior to transfusion. Blood was taken at basal and depleted state, and 2, 24, 48, and 72 hours after transfusion. (B) Percentage of total, transfused, and endogenous platelet counts, relative to initial counts. Transfused platelets were labeled with an anti-GPIbβ-Dylight649 antibody. Theoretical, maximal transfusion is depicted as grey area. n = 5. (C) Graphical overview of donor platelet function evaluation. DT treatment started 7 days prior to transfusion and blood was taken at basal and depleted state, and 24 h after transfusion. (D) Comparison of percentage of CD62P+ and activated GPIIb/IIIa+ platelets in whole blood, freshly drawn from donors and after circulating for 24 hours in iDTR^Plt mice. n = 4-9. (E) Concentration of plasma CXCL4 of iDTR^Plt mice at basal and depleted levels, and 24 h after platelet transfusion. n = 5 (F) Concentration of circulating exogenous platelets after transfusion of indicated numbers of platelets. n = 5-10.

RESEARCH, READ & CONNECT
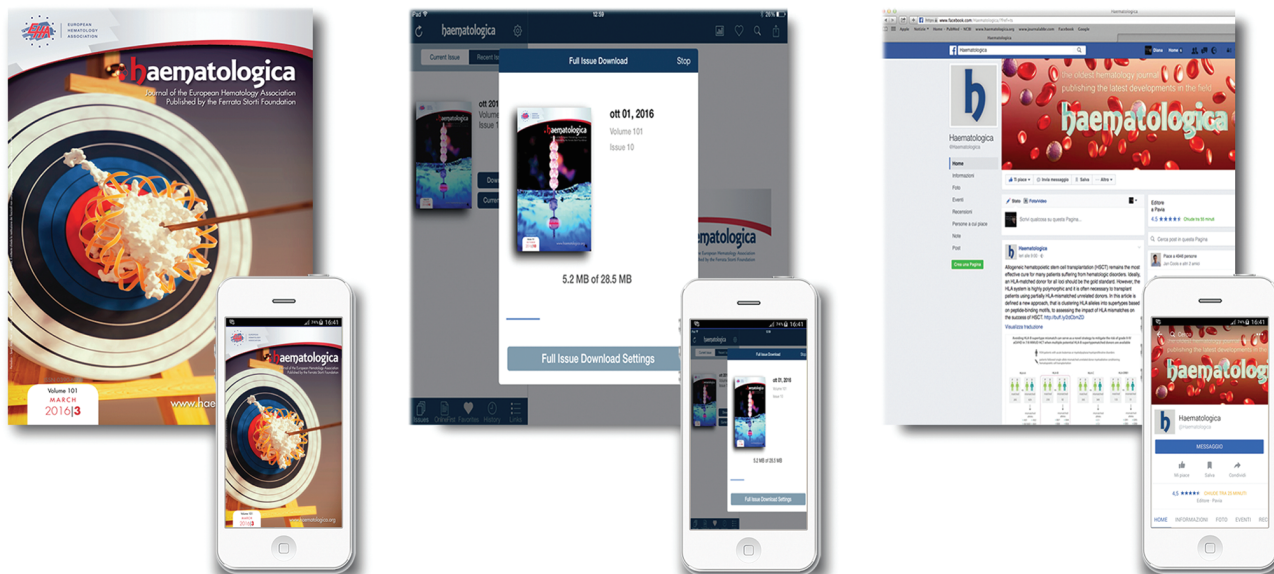
We reach more than
6 hundred thousand readers each year

The first Hematology Journal in Europe

Impressions YTD

14,171,734

Digital Readers	Total Audience
4,908	**558,982**

Worldwide rank	Impact factor	Total citations
7th	**7.116**	**10,831**